ASSESSING PHYSICAL SOIL QUALITY USING MECHANICAL INDICES FROM APPLYING INTERNAL AND EXTERNAL STRESSES TO REMOULDED AND STRUCTURALLY INTACT SOIL SAMPLES

A Thesis

Presented to

The Faculty of Graduate Studies

of

The University of Guelph

by

PAMELA JANE SHANTZ JOOSSE

In partial fulfilment of requirements

for the degree of

Doctor of Philosophy

December, 1998.

National Library of Canada
Acquisitions and Bibliographic Services
395 Wellington Street
Ottawa ON K1A 0N4
Canada

Bibliothèque nationale du Canada
Acquisitions et services bibliographiques
395, rue Wellington
Ottawa ON K1A 0N4
Canada

Your file Votre référence

Our file Notre référence

0-612-35800-3

Canada

ABSTRACT

ASSESSING PHYSICAL SOIL QUALITY USING MECHANICAL INDICES FROM APPLYING INTERNAL AND EXTERNAL STRESSES TO REMOULDED AND STRUCTURALLY INTACT SOIL SAMPLES

Pamela Jane Shantz Joosse
University of Guelph, 1998

Advisor:
Professor R.A. McBride

This thesis investigates the application of existing pedotransfer functions, based on the compression characteristics of structurally intact and remoulded samples, for southwestern Ontario to soils outside this physiographic region and attempts to devise analogous indicators using shrinkage tests. Structurally intact and bulk samples were collected from the diagnostic A, B and C horizons of natural, agricultural and pipeline workspace areas from plastic soil series in Texas, Alberta, Ottawa region and southwestern Ontario. Remoulded samples were compressed by a slurry consolidometer and intact samples by static uniaxial compression. Shrinkage characteristic curves were constructed using prescribed matric potentials in both $v(w)$ and $e(\sigma')$ co-ordinates and fit with a 3 straight line segment model.

Both compression and shrinkage testing indicated convergence of the remoulded and structured curves in $e(\sigma')$ co-ordinates. Overconsolidation, as indicated by the displacement of the structured curve below the remoulded curve, often occurred for B, C and clay rich (>36% clay content) horizons. Regardless of mineralogy or land use, a threshold of 0.40 for $(e^*_{1kPa}-e_0)$ and 0.25 for $(e_{\alpha R}-e_{\alpha S})$ indicated overconsolidation and severe plant growth limitations as indicated by macroporosity, plant available water-holding capacity and saturated hydraulic conductivity. In covariate analysis using clay or organic carbon content, significant treatment differences in relative

mechanical indices (remoulded minus structured values) often persisted, suggesting that structure in addition to constitutive properties influenced the mechanical responses. The mechanical response to internal stresses was divided into 2 groups of soils based on clay and organic matter contents. Soils with ≤27% clay and >4%organic carbon exhibited no "normal" shrinkage stage when remoulded but often did exhibit a "normal" stage when structured, which was opposite for the other group of soils (>27%clay and ≤4% organic carbon).

The relative displacement of the structured compression or shrinkage curves below the remoulded curves was not entirely explained by the amount of area occupied by optically anisotropic material in the matrix. Clay orientation was an indicator of previous stress history in the soil depending on the inclusion of coarse fragments in the matrix, mineralogy and drainage conditions, but was not a causative factor in the present mechanical behaviour of the soil.

ACKNOWLEDGEMENTS

There are many people who deserve appreciation and acknowledgement for their contributions to this thesis. Thank you to Tony Vadlja of Union Gas Ltd. for permitting access and sending crews to locate pipeline workspace sites. Ed Mozuraitis of Ecological Services Group Intl. and Chris Shrive of CH2M-Gore and Storrie aided in identifying southern Ontario sites and providing pipeline reports. Dr. Larry Wilding and Clement Couloumbe of Texas A & M helped in classifying and sampling the Texas site. Dr. Steven Dudas and Mike Rutherford of the University of Alberta located and sampled the Alberta site. Dr. Edward Gregorich of Agriculture Canada helped secure the Ottawa region site. Patrice Joliceour of Agriculture Canada also aided in finding alternative sites and sending shrinkage equipment.

I also received a lot of physical and moral support from the various technical staff and summer students of the University of Guelph who worked on this project over the years. Thank you to Don Irvine, Carolyn Miller, Glen Wilson, William Matthes-Sears and Peter von Bertoldi for your input of technical expertise. Thank you to Wilma Veenhof and Kathy Howe for your hard days in the sun. Melissa Dumbrell, Sandra van Osch and Pete Presant put in countless tedious hours of lab and computer work. Fellow grad students, in particular Dave Fallow and Derek Veenhof, provided advice, personal and technical, and a sounding board for frustrations. I couldn't have made it without you. It was a privilege to work with people of integrity who I now count as good friends.

A special thanks needs to be extended to the Soil Science Department and Agriculture Canada staff at the University of Manitoba where I sojourned for 2 years. They provided lab space and technical support even though I was not a paying graduate student. Special thanks to Bob Eilers, Dr. Geza Racz, Dr. Tee Boon Goh and Dr. David Burton for their co-operation and advice. The Geology Department's microscopy lab was also accessible thanks to the aid of Sergio

Mejia and Dr. Norman Halden. I will fondly remember my prairie learning experience.

Gratitude is also expressed to the members of my advisory committee, Dr. Pieter Groenevelt and Dr. Richard Protz, University of Guelph, Dr. Graeme Spiers, and Dr. Denis Angers, Agriculture Canada. You helped make this thesis a true learning experience. Dr. Des McGarry, CSIRO, Queensland also supplied insight as a "shrinker".

The Natural Sciences and Engineering Research Council provided the majority of funding to make this research possible. Scholarships through the University of Guelph, OAC Alumni and the LRS department also provided ample incentive to continue the hard work.

I received a lot of encouragement from my main mentor and role model, Dr. Ray McBride. You have taught me independence, thoroughness and discipline, and I only hope I can continue to work up to your standards.

To my husband, Dennis, thank you for your patience and encouragement as this has not been an easy career path. Here's to a new and improved life!

I would like to dedicate this thesis to my grandmothers and parents who taught me to love myself and the world.

Table of Contents

List of Tables

List of Figures

Notation for Symbols

e- void ratio, volume voids/volume solids $= \frac{\rho_p}{\rho_b} - 1$

e_0 - precompression (initial) void ratio for structurally intact, saturated soils

e^*_{1kPa} - void ratio at unit stress (σ=1kPa) of the equation describing the NCL

$e_{\sigma c}$ - void ratio at $\sigma=\sigma_c$ on the VCL

$e^*_{\sigma c}$ - void ratio at $\sigma=\sigma_c$ on the NCL

w - gravimetric water content (kg kg^{-1})

w_L - liquid limit, expressed as w * 100%

w_P - plastic limit, expressed as w * 100%

I_P - plasticity index, where $I_P = w_L - w_P$

I_L - liquidity index, where $I_L = (w - w_P)/ I_P$

activity - ratio of I_P to percent clay content

OC - organic carbon content (%)

ρ_b -dry bulk density (Mg m^{-3})

ρ_0 - precompression (initial, saturated) dry bulk density (Mg m^{-3})

ρ_p - particle density (Mg m^{-3})

ρ_w - density of water (Mg m^{-3})

σ - total stress (kPa)

σ' - effective stress (kPa)

σ_c -preconsolidation stress (MPa) expressed in terms of total stress based on intersection with C_C

σ_{c0}' -preconsolidation stress (MPa) expressed in terms of effective stress based on intersection with C_{C0}'

VCL - virgin compression line, or the linear portion of the $e(\log\sigma)$ function for an overconsolidated, structured soil

NCL - normal compression line, or the linear $e(\log\sigma')$ function for the normally consolidated soil slurry

C_C - compression index, or slope of the VCL, where $C_C = (e_1 - e_2)/(\log(\sigma_2/\sigma_1))$ based on 10 point regression

C_C' - compression index, or slope of the VCL, where $C_C = (e_1 - e_2)/(\log(\sigma'_2/\sigma'_1))$ based on 10 point regression and effective stresses

C_{C0} - compression index, or slope of the VCL, where $C_C = (e_1 - e_2)/(\log(\sigma_2/\sigma_1))$ based on tangent to VCL where second derivative = 0

C^*_C - compression index, or slope of the NCL, where $C^*_C = (e_1 - e_2)/(\log(\sigma_2/\sigma_1))$

A - parameter coefficient form the Bailey et al. (1986) equation (dimensionless)

B - parameter coefficient from the Bailey et al. (1986) equation (MPa^{-1})

C - parameter coefficient from the Bailey et al. (1986) equation (MPa^{-1})

r^2 (or R^2) - coefficient of simple (or multiple) determination

R - correlation coefficient

n - sample size

SEE - standard error of estimate

σ'_{wL} - effective stress at the liquid limit interpolated from a normally consolidated $e(\log\sigma')$ function, kPa

σ'_{wP} - effective stress at the plastic limit interpolated from a normally consolidated $e(\log\sigma')$ function, kPa

e_{wL} - void ratio at the liquid limit = $w_L \frac{\rho_p}{\rho_w}$

e_{wP} - void ratio at the plastic limit = $w_P \frac{\rho_p}{\rho_w}$

b_0 - parameter coefficient representing the intercept of a function fitted by least squares regression

b_{1-n} - parameter coefficients representing the independent partial regression slopes of a function fitted by least squares regression

SEb0 - standard error of intercept parameter estimate

SEb1-n - standard error of slope parameter estimate

$v_{\alpha R}$, $v_{\alpha S}$ Intercept of $v(w)$ plot, 0% water content (structured [S] and remoulded [R])

w_{AR}, w_{BS}, w_{CS} Gravimetric water contents of shrinkage limit, end of structural shrinkage, and maximum water content respectively in $v(w)$ plot

v_{AR}, v_{BS}, v_{CS} Specific volume at shrinkage limit, structural shrinkage and maximum gravimetric water contents

P_{AR}, P_{BS} Air-filled specific volume at shrinkage limit and structural shrinkage limit, e.g. $P_{AR} = v_{AR} - w_{AR} \cdot 1/\rho_p$

$r_{vS \text{ or } eR \text{ or } vS \text{ or } vR}$, n, s Slopes of first, second or third line segments from origin for various

structural conditions and coordinates

$e_{\alpha R}$, $e_{\alpha S}$ Intercept of $e(\sigma')$ plot at $\log_{10}(1\ kPa)=0$

e_{AR}, e_{BS}, e_{CR} Void ratios (V_{voids}/V_{solids}) at structural shrinkage, shrinkage limit and pF7 (oven dry) stresses

σ_{AR}, σ_{BS} Effective stresses at end of structural shrinkage and the shrinkage limit, respectively.

Abbreviations for Samples

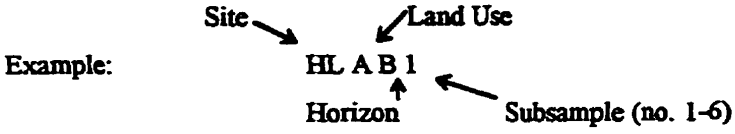

Site	Location	Soil Series
AB	Alberta	Malmo
HL	Halton	Chinguacousy
LB	Lambton	Brookston
MD	Middlesex	Tavistock
TX	Texas	Houston Black
WA	Waterloo	Maplewood

Land Use

A	Agricultural
N	Natural
W	Workspace (pipeline)

Horizon

A	Ah or Ap horizons
B	Bt, Bg, Bm or Bk horizons
C	Ck, Ckg, Ccag or Cg horizons

1. Introduction and Literature Review

1.1 Introduction

This thesis contributes to the search for suitable physical soil quality indicators initiated over the past decade as society became increasingly concerned about the impact of human land management practices on environmental quality (Indicators Task Force, 1991; Acton, 1992; CLBRR, 1995). In particular, the rapid and current assessment of regional and national soil quality changes is needed to evaluate the effectiveness of government policies and to aid in the allocation of scarce public funds for sustainability of our land resources (Papendick and Parr, 1992). The success of soil conservation efforts and management to maintain soil quality depends on an understanding of how soils respond to agricultural use and practice over time (Gregorich et al., 1994; CLBRR, 1995). Utilization of existing soil survey databases, in conjunction with updated land use change patterns and an understanding of soil dynamics under various land use systems, form the basis for this type of regional assessment.

An understanding of physical soil quality dynamics is related to an understanding of soil mechanics which has been historically used for geotechnical engineering purposes but recently has been adapted to surface and near surface agricultural soils (Hettiarachi, 1987; Kirby, 1991; Petersen, 1993). Both anthropogenic (tillage, wheel and livestock traffic, utility corridor construction) and natural (overburden, desiccation) stresses are exerted on the soil, the stresses varying in magnitude and duration (Papendick and Parr, 1992). The response of the soil depends on soil properties, such as water content, particle-size distribution, pore-size distribution, soil strength and organic matter content, which vary depending on the spatial and temporal scale chosen for soil quality assessment. In addition to predicting the response, it is also necessary to have a reference against which to compare improving or degrading soil quality measurements (Granatstein

and Bezdicek, 1992).

The following literature review investigates compression and shrinkage measurements on remoulded and structurally intact soil samples as potential indicators of physical soil quality. The potential for using microscopic image analysis to elucidate reasons for differences between mechanical responses of remoulded and structured soils is also reviewed.

1.2 Literature Review

1.2.1 Assessing Physical Soil Quality

Soil quality has been defined broadly as "the degree of fitness of a soil for a specific use" (Gregorich et al., 1994, p. 367), and more specifically as "the soil's ability to function as a medium for plant growth (productivity), in the partitioning and regulation of water flow in the environment, and as an environmental buffer" (Pierce and Larson, 1993, p. 7; Doran and Parkin, 1994). The capacity of a soil to function can be inherent, but is usually defined with reference to a particular set of uses or functions to narrow the range of potential parameters used to measure and monitor soil quality (Karlen et al., 1997). Soil quality is the key to establishing sustainable land management (Pierce and Larson, 1993). Physical soil quality is necessarily linked to the form, strength and resiliency of soil structure as it affects these functions (Kay, 1990). Soil compaction in agricultural systems has been linked to degradation of physical soil quality through increases in soil strength and decreases in pore space and continuity (Monnier and Goss, 1987; Baumgartl and Horn, 1991). Thus soil compaction affects water, nutrient, heat and gas exchange, as well as root penetration and consequently crop production (Wolkowski, 1990; Lipiec and Stepniewski, 1995). Soil compaction can also have environmental consequences in increased runoff, increased denitrification, increased nitrate to groundwater, increased energy consumption due to extra fuel required to cultivate compacted soils and increased microbiological production of greenhouse

gases, all of which could affect the health of the ecosystem (Malicki et al., 1991; Soane and van Ouwerkerk, 1995; Lipiec and Stepniewski, 1995). Because of the serious consequences of soil compaction, it is advisable to have its severity and extent included in global surveys of soil degradation (Soane and van Ouwerkerk, 1995).

There are many indicators which could be chosen to represent physical soil quality. Texture, plant-available water-holding capacity, organic carbon content, dry bulk density, saturated hydraulic conductivity and penetration resistance have all been suggested as part of a minimum data set for monitoring physical soil quality (Larson and Pierce, 1994). The choice of indicators is based on their sensitivity to a specific function and the provision of available methodology, including ease of duplication, and facility for accuracy and speed (Boone, 1986; Gregorich et al., 1994). Indicators are not static qualities of the soil but are dynamic in that they respond to different management practices. This allows the use of a dynamic assessment approach and statistical quality control theory to monitor the natural variance and "in or out of control" behaviour of land use systems (Pierce and Larson, 1993).

Analyzing the mechanical properties of soil may be one way to assess the susceptibility to, and variability of, changes in soil structure when under external (mechanical) or internal (effective) stresses. The mechanical behaviour of soil can be quantified by the changes brought about in the pore space of the soil in response to applied stresses (Hettiaratchi and O'Callaghan, 1980; Hettiaratchi, 1987). To describe the dynamics of soil, the state of compaction must not only refer to the form of the soil (pore space) but also how the soil persists against further stresses (soil strength) for use in predicting soil and crop responses (Schafer and Johnson, 1990; Taylor and Brar, 1991). Compaction sensitivity of the land is increasingly being presented using precompaction or preconsolidation stress (Koolen and Kuipers, 1989). The state of compaction can then be described as the resulting soil condition from previous stresses which loosen or

compact the soil (Schafer and Johnson, 1990). There are established mechanical indices used to describe the rate of change in strain with change in stress (eg. compression index) and to indicate the previous stress history of the soil and its susceptibility to further change (eg. preconsolidation stress).

1.2.1.1 The use of baseline or reference states

Most measures of changes in soil quality are comparative and made with reference to a baseline level which may be a treatment (such as the virgin state) or may be a threshold value (Gregorich et al., 1994; Snakin et al., 1996). These indicators are relative in the sense that different management and land use practices can be compared to the base state for that soil type. Comparisons of an artificially derived reference state to a structurally intact sample of the same soil have also been done. Håkansson (1988, 1990) achieved a reference dry bulk density by sieving field moist soils to 25 mm, wetting to beyond field capacity and then compressing (static, uniaxial, drained) in an oedometer to 200 kPa for 1 week. The optimum ratio of the structured to reference state dry bulk density (D_{opt}=87%) was similar for all soil textures and has been related to crop productivity in Europe. This indicator gives a good sense of the current condition of the soil independent of soil texture (Jones, 1983) but not how it might behave in the future under additional stresses. To extrapolate these findings without employing extensive field and laboratory work requires modelling of the compression of the reference state so that it could be derived elsewhere.

Carter (1990) used both the concepts of a standard compaction state and equilibrium bulk density (Heinonen, 1977, 1979) to arrive at relative measures of soil bulk density on fine sandy loam soils. Equilibrium or "normal" bulk density values have been found to be largely dependent on soil texture and organic carbon content for which significant regression equations have been developed (Heinonen, 1979). Carter (1990) used the Proctor test (dynamic, 597 kJm^{-3}) to obtain

the maximum reference dry bulk density. The equilibrium bulk density was considered to be the maximum dry bulk density achieved after one growing season when the soil had been exposed to numerous wetting/drying cycles and consolidation processes (Carter, 1990). A close relationship was found between relative compaction and macroporosity (r^2=.849). A relative compaction range of 84-89% was found to be the equilibrium soil density which corresponded to a macropore volume of 13.5-10% which was adequate for permeability but possibly inadequate for optimum aeration or grain yield (77-84% relative compaction associated with ≥95% relative grain yield) (Carter, 1990).

Hartge (1986) used soil mechanics theory to establish a concept of "normal" compaction, finding a linear relationship between void ratio and overburden stresses for virgin soils and non-linear overconsolidated portions for agricultural land uses. The steepness of the slope was related to the amount of loosening by bio- and cryoturbation (Hartge, 1986). He also found for virgin soils that the slope of the regression lines increase as the void ratio at 1 kPa increased (Hartge, 1986). The linear relationship was only found for in-situ soils which had undergone strong drying at some earlier time as the void ratios observed in the field were much lower than those obtained in laboratory tests, where only mechanical stress of this magnitude (1 and 10 kPa approximate overburden pressures for B and C horizons) were applied (Hartge, 1986). Hartge (1986) hypothesized that the soil started from a maximal density due to drying (desiccation stresses 10^4 times greater than overburden stresses) and was then loosened to one that was stable under the load of the covering soil layers.

It is apparent that reference states against which to compare soil quality measurements are necessary. The above methods often require extensive field or laboratory measurements on various soil types. Regression equations have been developed for critical and equilibrium bulk densities based primarily on the clay content; the relationships of these indices with other physical properties to indicate the degree of compactness, however, differ over a complete range of clay contents

(Heinonen, 1979; Canarache, 1991). A reference state which has not been widely explored in agricultural research is a remoulded, saturated condition which has been widely used for geotechnical comparisons. The mechanical behaviour of this reference state is determined only by the physicochemical properties of the colloidal and clastic particles and the pore water.

1.2.2 Compression Testing

Uniaxial compression in oedometers or Rowe cells has been used for compaction (unsaturated conditions; volume change largely due to reduction in air-filled porosity and rearrangement of soil particles) and consolidation (saturated conditions; volume change dependent on drainage of excess pore water pressure and permeability of soil) tests (McBride, 1989; Dawidowski and Lerink, 1990; Craig, 1992). These tests simplify stress-strain relationships by utilizing only the perpendicular normal stress and not lateral deviatoric stresses as in traditional triaxial tests to determine soil shear strength and critical state parameters (Hettiaratchi, 1987; Petersen, 1993). Uniaxial compression is used to represent compaction in the field because the soil volume is confined laterally for the periods of time considered in trafficking (Koolen and Kuipers, 1983). These tests allow the collection of large quantities of data to test models which often form the foundation for more advanced compression models (McNabb and Boersma, 1996; Grisso et al., 1987; Raper et al., 1994). Compression testing also integrates characteristics of interest in assessing structural quality, such as soil and aggregate shear strength and pore continuity/ permeability (Baumgartl and Horn, 1991; Lebert and Horn, 1991; Craig, 1992).

The variables used to quantify and describe compression behaviour in this thesis for remoulded and structurally intact samples are illustrated in Figure 1.1. Of principal importance in assessing the structural quality of the soil and its susceptibility to change are the remoulded and structured compression indices, C_C^* and C_C, respectively, and the preconsolidation stress (σ'_c).

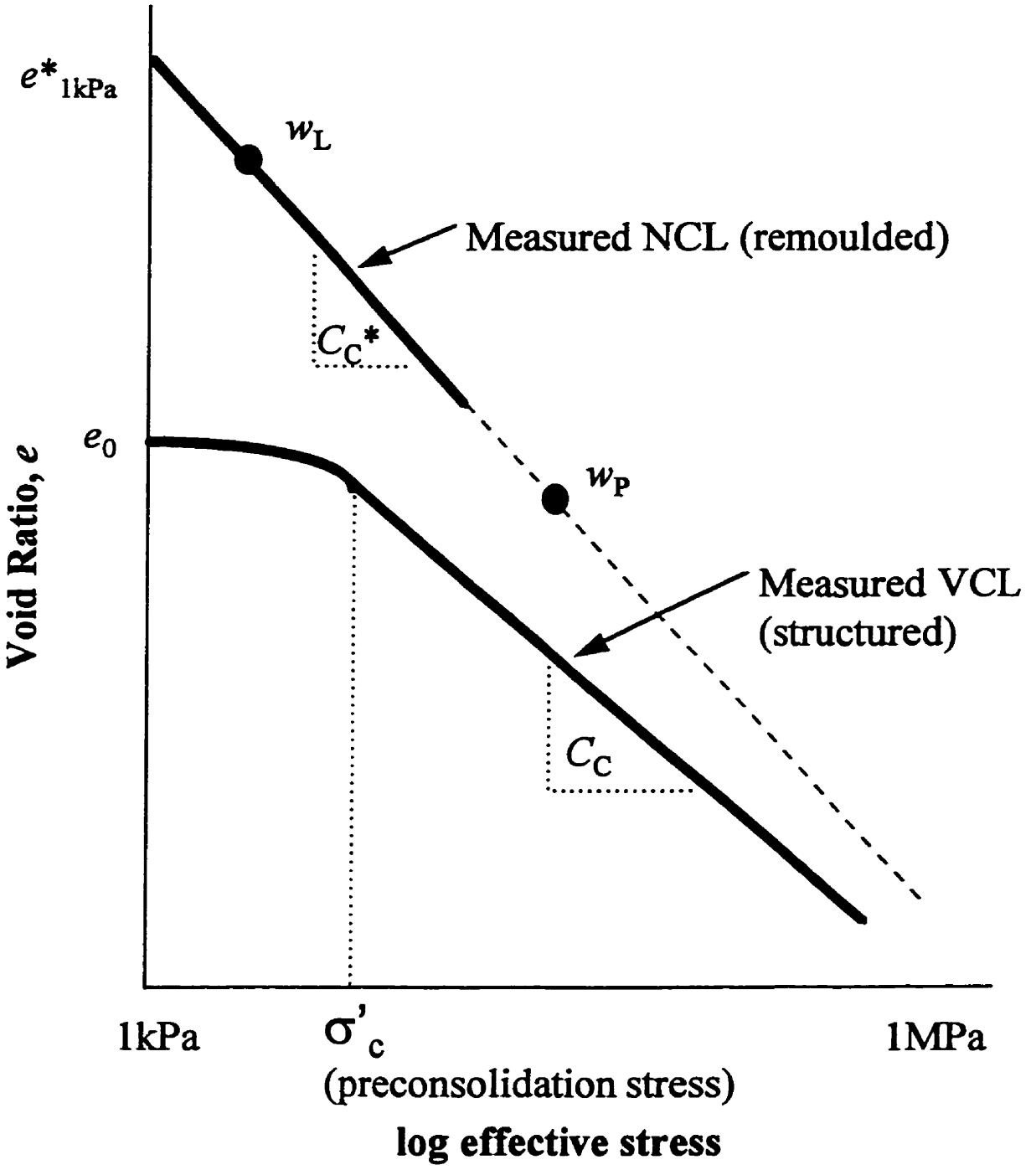

Figure 1.1 Illustration of compression variables used to describe remoulded and structurally intact samples.

1.2.2.1 Compression index

Soil compressibility is the ease with which a soil decreases in volume when subjected to a mechanical load (Bradford and Gupta, 1986). The structured compression index (C_C) is the slope of the virgin compression line (VCL) in void ratio-log stress co-ordinates. The remoulded counterpart is the normal consolidation line (NCL), the slope of which is the C_C*. Irreversible compression of the soil occurs along the VCL or NCL when the present state of stress in the soil is the greatest it has ever been subjected to in the past (Craig, 1992). A more theoretically correct representation for comparing the compressibility of soils at a particular stress is the compression ratio ($C_C/(1+e_0)$), so that the additional compressibility of a sample because of its higher void ratio is standardized (Wesley, 1988).

Factors which affect the steepness of the C_C or C_C* include the clay content, particle thickness or size and mineralogy (Larson et al., 1980; Assouline et al., 1997); amount and type of exchangeable cations (Dexter and Chan, 1991); moisture content at time of stress (Leeson and Campbell, 1983; Kirby, 1989; McNabb and Boersma, 1996; Petersen, 1993); initial void ratio (Culley and Larson, 1987; Angers et al., 1987; Veenhof and McBride, 1996; Al-Khafaji and Andersland, 1992); duration of stress (Crawford, 1965; Guérif, 1982); and, content and nature of organic matter (Soane, 1990; O'Sullivan, 1992). The soil pH can affect the compactibility of strongly weathered soils such as oxisols where kaolinite and oxides are dominant (Assouline et al., 1997). It can be seen that compaction behaviour is determined by properties which determine the nature of the resulting cohesive forces between the soil constituents (Assouline et al., 1997).

It is not surprising then that compressibility is linked to the plasticity index of the soil (Hardin, 1989; Nakase et al., 1988; Carrier and Beckman, 1984). This is the range in water content between the liquid and plastic limits where the magnitude of net interparticle forces is such

that the soil particles can slide freely relative to each other while still maintaining some degree of cohesion (Craig, 1992). The compression characteristics have been related to the plasticity index, and although not sufficiently precise to avoid the need to undertake consolidation tests, are adequate for preliminary design purposes (Carrier and Beckman, 1984). Since the liquid limit and plastic limit represent continually remoulded samples, it follows that they would represent points on the critical state line (CSL) since it describes all conditions under which a soil will undergo continuous remoulding without a change in volume (Campbell, 1991). The ratio of the shear strengths at the liquid and plastic limits is known to be about 100 times; thus, it is possible to define the slope of the critical state line on a plot of the logarithm of the spherical pressure versus the specific volume in terms of the plasticity index (Schofield and Wroth, 1968; Wroth and Wood, 1978).

Graham and Li (1985) found the normal consolidation and critical state lines for both remoulded and natural, structured plastic clay samples to be parallel, with structured values at higher specific volumes than remoulded samples. Hettiaratchi (1987) and Nakase et al. (1988) also point out that similarities exist between the mechanical behaviour of soils in the remoulded and critical state condition. Petersen (1993), however, found that the slope of the CSL and NCL were parallel at water contents near the liquid limit but that they differed for other moisture contents. The compression index for unsaturated soil was not related to the Atterberg limits, whereas in saturated soil it was (Kirby, 1991). The availability of Atterberg limit data in existing soil surveys and the possibility of positioning them in e(log stress) co-ordinates presents the possibility of acquiring reasonable estimation of soil behaviour along the NCL (McBride and Baumgartner, 1992; Veenhof and McBride, 1996).

Studies utilizing disturbed, sieved soil aggregates have found almost parallel NCL or VCL with desaturation, with the VCL displaced in a linear manner towards higher e at a given stress

(Larson et al., 1980, Guérif, 1982, Angers, 1990; O'Sullivan, 1992). On the other hand, studies on structurally intact soil have illustrated that the initial e can have a dominant effect on the C_C of a sample, masking the effect of matric potential (Veenhof and McBride, 1996; McNabb and Boersma, 1993, 1996) and resulting in a converging rather than parallel behaviour for strongly structured soils. It is also important to ascertain the overconsolidated portion of a structured soil so that compression along the VCL is not overestimated (Culley and Larson, 1987).

1.2.2.2 Preconsolidation stress

The preconsolidation stress is defined as the maximum vertical effective stress which has previously been placed on the soil (Craig, 1992). Soils often exist in an overconsolidated state in which the current stress is less than the preconsolidation stress. This can occur by erosion or glaciation removing overburden pressures, or secondary compression, or changes in pore water pressure due to changes in water table elevation (Holtz and Kovacs, 1981). In agricultural soils, the σ'_c is regarded more as the transition between elastic (reversible) and plastic (irreversible) mechanical behaviour (Kirby, 1991; Jakobsen and Dexter, 1989) since additional structural strength factors come into play caused by freezing, drying, stabilizing organic and inorganic materials, age-hardening and hard setting behaviour (Kay, 1990). If an overconsolidated soil is loaded at stresses smaller than the preconsolidation stress, soil deformation is small, elastic and reversible as aggregates are not destroyed (Lebert and Horn, 1991; Baumgartl and Horn, 1991). If stresses exceed the preconsolidation stress, plastic and irreversible deformation takes place along the VCL causing changes in soil hydraulic conductivity and air permeability because aggregates are deformed (Lebert et al., 1989; Kirby and Blunden, 1991; Baumgartl and Horn, 1991: Ball and Robertson, 1994).

The σ'_c of deep sediments can be estimated based on the overburden pressures and a

generalized soil state parameter that accounts for soil plasticity (Nagaraj and Srinivasa Murthy, 1986). The dry bulk density/degree of aggregation and water content are important in determining the σ'_c of agricultural soils (Lebert and Horn, 1991; Horn, 1988; Kirby 1991). Salire et al. (1994) investigated intact subsoils (45 cm) of varying clay content (14-27%) at different matric potentials and also found the σ'_c to increase with increased dry bulk density and matric potential. No correlation was found between plasticity index or clay content and C_C or σ'_c, implying that structural characteristics and matric potential exert a greater influence on mechanical properties than do textural characteristics under short-duration loading (Salire et al., 1994). The σ'_c of agricultural soils at two water potentials was predicted with $r^2>0.75$ by multiple regression when the angle of internal friction and cohesion were included for structured, clay soils (Lebert and Horn, 1991).

The preconsolidation stress is an important parameter because it helps define the stress history of the soil and determine the type of failure and potential amount of degradation under further shear or compactive stresses (Hettiaratchi, 1987). In soils where the ratio of current normal stress to maximum previous normal stress (σ'_c) is high (>0.5, inverse of overconsolidation ratio), the behaviour is 'loose of critical' or normally consolidated and the soil compacts on shear; at lower stress ratios (<0.5) the behaviour is 'dense of critical' or overconsolidated and the soil expands on shear to approach the critical state (Kirby, 1989). Petersen (1993) similarly found that a sandy loam and loam failed in a ductile (compressive) manner when the (p/p_{max}) ratio was larger than ≈0.5 and that in a wet range (>20% $kg.kg^{-1}$) soils can still fail in a ductile manner even at (p/p_{max}) as low as 0.25 to 0.30. To avoid the risk of compaction, the stresses exerted by vehicles in the subsoil should not be allowed to exceed the internal soil strength or preconsolidation pressure (Håkansson and Medvedev, 1995). Preconsolidation pressure increased exponentially with saturated liquidity index further supporting the proposition that the Atterberg limits might be used

as a basis for guidelines for the avoidance of compaction by traffic or for tillage (Baver, 1930; Kirby, 1991).

1.2.2.3 Relationships between remoulded and structured samples

Burland (1990) showed that the intrinsic properties of a clay (one that has been reconstituted at between 1-1.5 times the liquid limit and consolidated one-dimensionally) provide a robust frame of reference against which to assess the in situ state of the soil, its structure and the measured mechanical properties of undisturbed samples. He demonstrated that the intrinsic compression line (ICL) is a valuable reference line for studying the compression characteristics of natural normally and overconsolidated sedimentary clays (Burland, 1990). Provided the Atterberg limits lie above the A line (CL or CH soils) (Figure 2.4), there was good correlation between the constants of intrinsic compressibility, C_C^* and e^*_{100}, and the void ratio at the liquid limit. Burland (1990) normalized the ICL by defining the void index I_v :

$$I_v = \frac{e - e^*_{100}}{e^*_{100} - e^*_{1000}} = \frac{e - e^*_{100}}{C_c^*}$$

which is analogous to the I_L but contrastingly is defined in terms of two directly measured mechanical properties derived from a one-dimensional compression test. His analysis is based, for robustness, on an ICL defined for pressures equal to or greater than 100 kPa. He then compares a void index I_{vo} substituting the natural e_0 for e to give a sedimentation compression curve (SCL). Over the range 10 to 1000 kPa, the ICL and SCL for normally consolidated clays were approximately parallel. For a given void ratio, the effective overburden pressure carried by the natural clay was approximately five times that carried by the equivalent reconstituted clay (Burland, 1990). This is a measure of the enhanced resistance of a naturally deposited clay over a reconstituted one and results from difference in the fabric and bonding of the soil skeleton. At pressures in excess of 1000 kPa, the ICL and SCL tended to converge. Burland (1990) found the

ratio for the intrinsic swelling index to the natural swelling index to be a sensitive indicator of fabric and interparticle bonding in the natural soil for the overconsolidated situation.

Bradford (1981) conducted consolidated, drained direct shear tests on natural and remoulded samples of a silty clay loam B horizon of a Typic Hapludalf. Comparison of both remoulded and structured sample results provided insight into the influence of macrostructure on stress-deformation properties of a structured soil. The denser, remoulded sample would be stronger if strength differences were accounted for only in terms of void ratio, but the opposite in strength was indicated when looking at shear strength. This study showed that remoulded soil samples with the same initial porosity and under equal normal stresses as the structurally intact soil samples have different volume change and strength characteristics, and as a result have limited field application. The remoulded samples, however, were overconsolidated due to sample preparation at 550 kPa while the maximum normal stress during shear tests was 145 kPa which influenced the volume change results (Bradford, 1981).

Although similarities appear between remoulded and structured behaviour for normally consolidated soils, there are definite differences for overconsolidated soils where significant macrostructure exists. Tests on remoulded soils can indicate the major differences in behaviour between soil types but undisturbed samples would be required for investigations in the effects of soil structure or management (O'Sullivan et al., 1994). Thus the difference between the two states could provide an index of structural quality.

1.2.3 Shrinkage Tests

Soil shrinkage, the decrease in soil volume with decrease in soil water content, is a common measure used by agriculturalists and engineers in land inventories and soil classification systems (McGarry, 1995). In agriculture, their principal application has been in the

characterization and classification of soils containing clay, as the degree of shrinkage and swelling largely determines the potential for soil structure development (Dasog et al., 1987; Reeve et al., 1980). Other studies have made use of the shrink-swell capacity of clay soils to re-develop structure in compacted soils as a key component of structure repair in degraded agricultural soils (Reeve and Hall, 1978; Kuznetsova and Davilova, 1988; Bullock et al., 1985). In engineering, soil shrinkage is regarded as a key determinant of material stability for building and soil conservation structures (Grossman et al., 1968; McCormack and Wilding, 1975).

Shrinkage measurements have been made in the field, often with lysimeters because of the difficulty in finding a true anchor point (Yule and Ritchie, 1980b; Bronswijk, 1991a,b; Mitchell and van Genuchten, 1992). Laboratory measurements are more commonly done to make inferences about behaviour in the field and to reveal differences between soil types (Warkentin, 1993; McGarry, 1995). Physical dimensions have been taken of intact cores of relatively large size (Yule and Ritchie, 1980a), sometimes using a travelling microscope (Chang and Warkentin, 1968) or a series of pins for accuracy (Wires et al., 1987). The irregular shape of most natural soil clods or aggregates has led to the use of various coatings or fluids for volume displacement measurement techniques. Paraffin wax (Lauritzen and Stewart, 1941) and Saran (Brasher et al., 1966) have been used as coatings for fairly large samples (>100 cm^3) where error due to the volume of the coating is negligible and capturing the interaggregate porosity of the field is important. Mercury (Haines, 1923), toluene (Sibley and Williams, 1989; Pellissier, 1991) and kerosene (McIntyre and Stirk, 1954; Monnier et al., 1973) have been used to assess volume because of their immiscibility in water and negligible layer thickness for smaller clods (<10 cm^3). Concern over the toxicity of many of these substances has led to a method which places the sample in a rubber membrane to which a vacuum is applied before displacing in water (Tariq and Durnford, 1993b). Of these measurements, the Saran method is probably the most popular for tracing the volume change with

water loss curve (shrinkage characteristic curve) on structurally intact samples.

For soil classification, one of the parameters derived from the dry bulk density (ρ) change of Saran-coated, intact natural clods from - 33kPa to oven dry is the coefficient of linear extensibility ($COLE_{std}$) (Eq. [1]) (Grossman et al., 1968)

$$COLE_{std} = \sqrt[3]{\frac{\rho_{o.d.}}{\rho_{33}}} - 1 \qquad [1]$$

where $\rho_{o.d.}$ is the bulk density when oven dry and ρ_{33} is the bulk density at -33 kPa tension. The use of $COLE_{std}$ values for threshold values to remove subjectivity for soil classification has received attention mainly in Canada and South Africa (McGarry, 1995).

Shrinkage measurement techniques have also been developed for sieved (McKenzie et al., 1994) or remoulded samples ($COLE_{rod}$, Schafer and Singer, 1976) to avoid the collecting and maintaining of structurally intact samples. Generally in these methods, the linear shrinkage (one dimension) is measured on an extruded sample at two matric potentials (Schafer and Singer, 1976). These have been correlated with $COLE_{std}$ but often there is not a 1:1 relationship or considerable variability cannot be explained (McGarry, 1995). This high variability is likely due to the loss of soil fabric in $COLE_{rod}$,for soils with inherently strong structure, that is lost in grinding (Simon et al., 1987).

1.2.3.1 Shrinkage process

The change in volume with change in water content is portrayed in reciprocal dry bulk density(water content) (McGarry and Malafant, 1987), or void ratio (moisture ratio) (Bronswijk, and Evers-Vermeer, 1990; Tariq and Durnford, 1993a), co-ordinates as the shrinkage characteristic curve. Four shrinkage characteristic curve stages have now been identified, although the terminology varies and all 4 stages are not always present (Reeve and Hall, 1978; McGarry

and Malafant, 1987; Tariq and Durnford, 1993a). The 4 ranges can generally be described as:

1. Structural- occurs over the wettest part of the moisture range where the volume change is less than the volume of water removed, arising from the draining of large pores and entry of some air into the pores
2. Normal - volume decrease of the soil is equal to the volume of water lost and the volume of the air remains constant
3. Residual - the water loss exceeds the soil volume change, resulting in an increase in air-filled pores
4. Zero - no change in volume and moisture loss is due to pore drainage

An analytical model to describe all 4 portions has been described by Tariq and Durnford (1993a) which utilizes straight lines for the zero and normal shrinkage ranges, a second degree polynomial for the structural range and a third-degree polynomial for the residual range. It is an extension of the three straight lines model proposed by McGarry and Malafant (1987) who use a single straight line for the residual and zero shrinkage zones combined and a straight line to describe the structural shrinkage (Figure 1.2). The Tariq and Durnford (1993a) model provides a smoother transition in slope between the shrinkage zones and fits the measured data in the residual shrinkage zone better than the McGarry and Malafant (1987) model but its increased complexity does not necessarily aid in defining structural states.

The shrinkage process is a combination of pore drainage and aggregate/pore contraction under effective stress, which intuitively suggests a smooth or curvilinear transition between shrinkage stages (McGarry and Malafant, 1987). Several researchers have provided evidence, however, that the stage changes occur at either distinct w or over a very restricted range of w values both in the lab (McGarry, 1988; Newman and Thomasson, 1979; Yule and Ritchie, 1980a) and in the field (Mitchell and van Genuchten, 1992; Bronswijk, 1991b) so that a straight line segment model is appropriate.

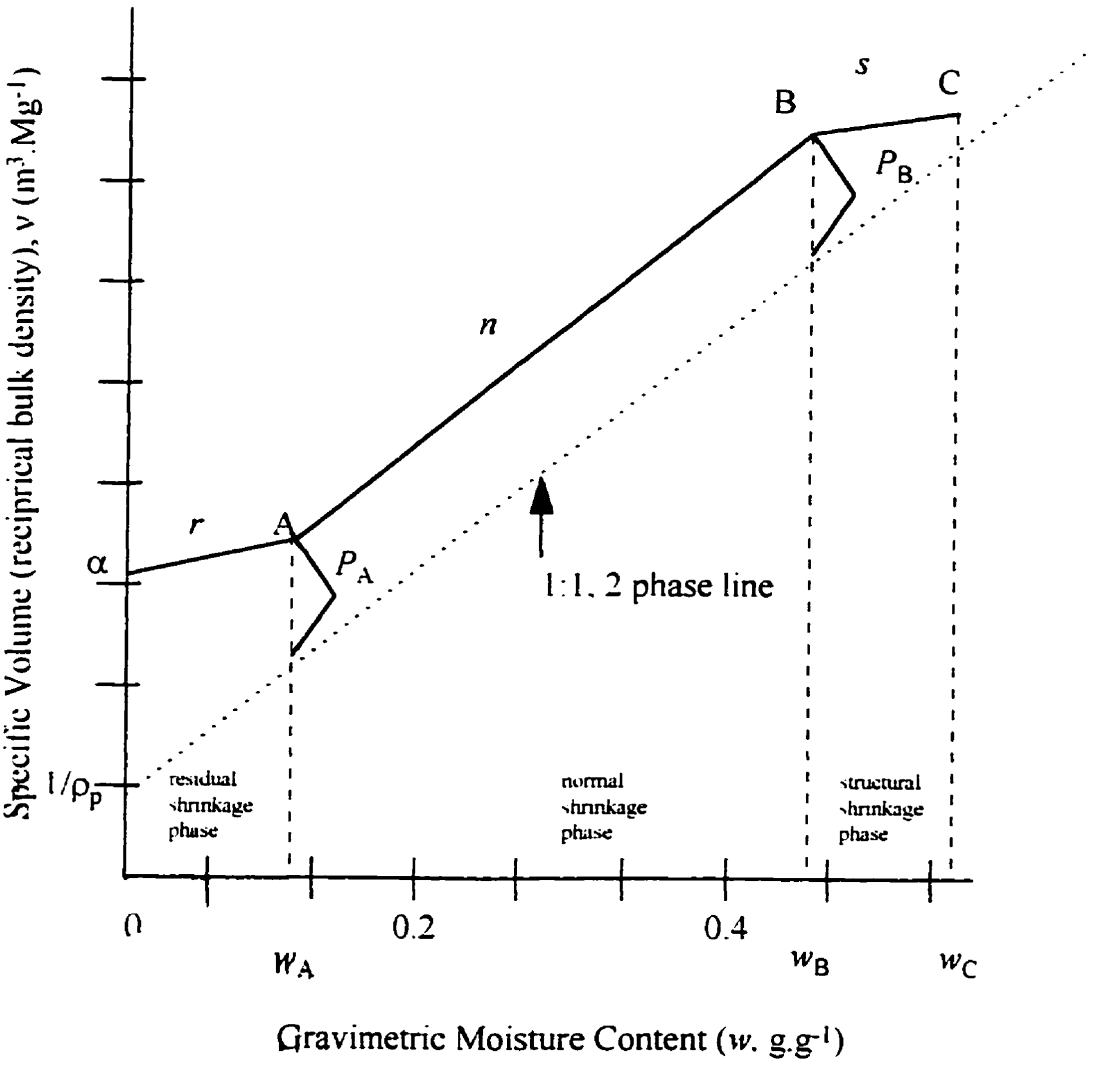

Figure 1.2. The shrinkage characteristic curve and variables used to describe the 3 line model of McGarry and Malafant (1987).

1.2.3.2 Relationships of shrinkage stages to soil properties

"Normal" shrinkage, where the slope of the shrinkage characteristic curve =1, is the dominant process in remoulded soils or small aggregates (Stirk, 1954; Chang and Warkentin, 1968). The complete collapse of pores typifies "normal" or unitary shrinkage which is plastic deformation in response to decreasing matric potential (Haines, 1923; Greene-Kelly, 1974; Newman and Thomasson, 1979). In structured soils, it is probable that a soil with pores 10-200 nm that contract on drying, and unstable pores 200 nm-30 μm that collapse on drying, will show strict normal shrinkage during drying; the lack of stable porosity delays air-entry until contraction pores are small and the soil dries to dense intractable aggregates (Newman and Thomasson, 1979; Guillame and Cabidoche, 1998). The greater the proportion of pores in the size range below 200 nm the greater is the proportion of normal shrinkage (Newman and Thomasson, 1979).

Improved structure is associated with reducing total shrinkage for the soil; the contribution of structural and residual shrinkage to total shrinkage increases with structural development (Stirk, 1954; Reeve and Hall, 1978). Structural shrinkage is difficult to measure in practice (D. McGarry, personal communication) and exists by virtue of structural development of larger pores in the soil (Stirk, 1954) and thus depends on the relationship of clod size to the size of structural aggregates (Reeve and Hall, 1978). Residual shrinkage has been described both as air entry into voids (Haines, 1923) or the point at which air enters a different set or type of pores (Bruand and Prost, 1987; Mitchell and van Genuchten, 1992). Residual shrinkage commences when the soil particles or units are brought into close contact and shrinkage is retarded (Stirk, 1954). Probably structure development influences this stage to some extent also, as it will determine the size of the units and therefore the interval before they come into contact (Stirk, 1954).

1.2.3.2.1 Air-entry point (Shrinkage limit)

Some authors have emphasized water content or suctions corresponding to the limits of shrinkage zones to characterize structural degradation. The presence of stable pores 200 nm-30 μm allows air entry at an earlier stage of drying (Newman and Thomasson, 1979). A relatively low water content at the 'air entry' point at the onset of residual shrinkage was related to poor structure (Chang and Warkentin, 1968). Conversely, structured clods have been found to have lower residual shrinkage limits (10%) than remoulded samples; however a well structured treatment had a structured shrinkage zone but the degraded irrigated one had a higher structural shrinkage limit indicating a lower volume of structural pores (Chan, 1982). Physical ripening (structural development) was accompanied by a prominent reduction of the total shrinkage from saturation to oven dry due to i) the relatively large decrease of the void ratio at saturation compared to the void ratio at oven dry, ii) the movement of the air entry point toward a higher moisture ratio, and iii) a slight increase of the air volume for a given moisture ratio in the normal and residual shrinkage zone (Kim et al., 1992).

The air entry point is not only influenced by structure but also by texture and organic matter content. Kim et al. (1992) found that the air entry point, which also determines the degree of approach to the saturation line, seemed to be influenced much more by the amount of clay than by structural ripening. The air entry occurred at higher moisture ratio for the samples having a lower clay percentage. When the coarse fraction of the soil is large, the character of the shrinkage is altered and residual shrinkage is the main mechanism as these particles provide a rigid framework within the soil (Stirk, 1954). Normal shrinkage occurred over a limited range of water content near saturation and the residual shrinkage rapidly commenced for coarse and medium-textured (<25% clay content) surface soils from Spain (Paz, 1998). Lauritzen (1948) found organic matter to raise the water content of the air entry point for a Houston black clay and lower

it for an Oasis silt loam. The residual shrinkage phase has been found to initiate at stresses around -50 kPa (Bronswijk and Evers-Vermeer, 1990) to below the wilting point (-1500 kPa) (Stirk, 1954; Yule and Ritchie, 1980a; Reeve and Hall, 1978).

1.2.3.2.2 Slope of "normal" shrinkage stage

Another way to assess structural development is that soils with stable pores will not have strictly normal shrinkage (slope =1). Lauritzen (1948) found that normal shrinkage hardly applies to clods compared to remoulded samples. Allbrook (1992) found the slope in the "normal" shrinkage zone to be an important indicator of the stability of soil pores. Stable pores (200 nm-30 μm) may act as surfaces of weakness that allow development of new pores in the size range 200nm-2 μm as the soil matrix contracts; shrinkage in such soils will not be strictly normal because a small amount of air entry occurs as the planes of weakness are opened, although full development will occur only when residual shrinkage begins (Newman and Thomasson, 1979). Remoulded clods showed no structural shrinkage and lay closely to the 45° line until residual shrinkage commenced (Chan, 1982) while the shrinkage curve deviated from the saturation line with ripening (Kim et al., 1992). Again, however, factors other than structure affect the slope. Sand in quantities of 25 per cent or more resulted in elimination of a moisture range in which the reduction in volume was equal to the volume of water lost (normal shrinkage) (Lauritzen, 1948). High organic matter contents also tended to eliminate normal shrinkage (Lauritzen, 1948), however, Reeve et al. (1980) and Paz (1998) found the amount of shrinkage (COLE) to be positively correlated with organic matter.

Where normal shrinkage (n_v=1) has been measured on structured soils, it has usually been on soils containing smectites and/or of clay content > 60% or organic carbon content <1% (Bronswijk and Evers-Vermeer, 1990; Cabidoche and Voltz, 1995; Bronswijk, 1991a). Cabidoche

and Voltz (1995) sampled large (50 to 500 cm^3) undisturbed clods over time at various water contents and found the slope not significantly different than 1 between the shrinkage and swelling limits for B horizons with > 80% smectitic clay and less than <1% organic carbon. The A horizon with 78% clay and 1.85% organic carbon exhibited residual shrinkage over most of the range of water content encountered in the field and was excluded because the model only accounted for normal shrinkage. Allbrook (1992) conducted shrinkage tests on the A and B horizons of soils with mineralogies other than smectite; soils dominated by either halloysite, allophane or kaolinite/vermiculite were studied. Three different sized aggregates (10, 20 and 40 mm) were tested to construct one shrinkage curve. It was the lowest clay (28%) but highest carbon (6-14%) content soils which had normal shrinkage slopes approaching 1 (.84-.87) and which had all three shrinkage stages. Soils of other clay mineralogies had normal slopes less than 1. The only soil with significant residual shrinkage was the halloysite sample which would have interlamellar water like smectite (Allbrook, 1992). Similarly in mica-dominant samples, the normal slope was different than 1 because the volume of air-filled voids at 15 bar was found to be less than the volume of air-filled voids at 1/3 bar tension but this result was considered untenable (McCormack and Wilding, 1976). Soils showing little change in the volume of air over a range of matric potential (-.05 bar to -15 bar (30 μm to100 nm)) (i.e. normal shrinkage) can have few pores in this size range and therefore have poor aeration (Reeve and Hall, 1978; Newman and Thomasson, 1979). Wires et al. (1987) found the influence of soil structure on soil shrinkage inconclusive because there appeared to be a complex interaction between ped size and the scale of measurement for shrinkage.

1.2.3.3 Relationship between structured and remoulded samples

Shrinkage between pF 2 and 4 correlated significantly with the expansive clay mineral

content for remoulded but not for dried and rewetted specimens (overconsolidated); shrinkage between pF 4 and pF 6 was strongly correlated with expansive clay mineral content for both kinds of specimens for clayey (40-64% clay) B and BC horizons (sieved to <0.4 mm)(Greene-Kelly, 1974).

The difference between $COLE_{rod,wet}$ and $COLE_{clod,wet}$ (from saturation) decreased as the clay content increased, whereas the difference persisted for the $COLE_{rod}$ and $COLE_{clod}$ samples equilibrated at -33 kPa (De Jong et al., 1992). The dependence of the COLE on clay content suggested that mixing of the samples had created more micropores (diameter $<10^{-5}$ m) at all clay contents; at low clay contents mixing had increased total porosity, but at high clay contents total porosity was little affected by the mixing (De Jong et al., 1992). It is possible that the relatively poor correlation between $COLE_{std}$ and $COLE_{rod,wet}$, $COLE_{rod,33}$ or plasticity index is due to differences in soil structure. However, plots of $COLE_{clod}$ vs. $COLE_{rod}$ did not reveal any pattern that could be related to the soil horizons (De Jong et al.,1992). These were similar to results of Simon et al. (1987) who found poor explanation of structured COLE values using remoulded COLE values (r^2=0.55) due to differences in soil fabric.

The normal shrinkage concept was established using clay paste which, suggested by Bronswijk (1993), could be used for reference to compare natural clayey soils. Various relative structural quality indices using shrinkage parameters have been suggested but have not been used widely in structural studies. Lauritzen (1948) notes that the apparent specific volume of structured samples at oven dry was always larger than the volume of remoulded samples. The ratio of these two specific volumes would represent a measure of the porosity which exists in the soil by virtue of structural development greater than that which would exist under conditions of minimum apparent specific volume (Lauritzen,1948). Stirk (1954) suggests that this difference in pore volume and the nature of the shrinkage characteristic between structured and remoulded samples could be

exploited at other pF values. Greene-Kelly (1974) found remoulding not only accentuated differences in shrinkage but also in the amount of water held at pF 2 (-10 kPa); this suggested that other properties related to the void ratio at pF 2 would also be more differentiated on remoulding (Greene-Kelly, 1974). Bullock et al. (1985) calculated the amount of air-filled pores within clods due to soil morphological structure by subtracting the systematic soil volume components (solid volume + liquid volume + intergranular air-filled pore volume, represented by remoulded soil volume at similar moisture contents) from the total volume of a clod retaining internal structure.

1.2.4 Image Analysis of Soil Fabric

The various compression and shrinkage studies on remoulded and structured samples suggest that soil fabric or clay fabric (microfabric) is often responsible for observed differences in mechanical behaviour. Clay fabric is defined as the orientation and arrangement or spatial distribution of the solid particles and the particle-to-particle relationships (Bennett et al., 1991). Numerous authors have put forward the concept of increased orientation of clay with various indices of soil structural degradation (eg. increased massive structure, decreased water-holding capacity, increased dry bulk density, decreased porosity and decreased soil shrinkage) (Aitchison and Holmes, 1953; Stirk, 1954; Chang and Warkentin, 1968). It has been shown that the variation in aggregate stability of soils with similar texture and mineralogy can be related to additional factors such as the degree of particle orientation (Cagauan and Uehara, 1965 in Assouline et al., 1997).

Studies which investigate the pattern or fabric of the matrix are not common in the soil science literature (McGarry, 1989; Terrible and Fitzpatrick, 1995), and are found mostly in geological/ sedimentary literature where it has long been recognized that particle orientation plays a key role in defining depositional and stress patterns as well as influencing the engineering properties of the soil (Collins and McGown, 1974; Bennett et al., 1991). Important properties such as porosity, permeability

and stress-strain behaviour are intimately tied to the microfabric and physicochemical characteristics (Bennett et al., 1991). In unsaturated soils, the fabric can be of even greater importance than in saturated soils. In uncemented, saturated soils the initial fabric will be destroyed by shear or compression to higher stresses. In unsaturated soils, the fabric is supported by the suction and may be maintained even under the application of shear or compressive stresses (Toll, 1990).

It is likely that the proportion/dominance of a microfabric feature in any one structural condition influences the physical behaviour. This hypothesis is supported by Collins and McGown (1974) who found that the dominance of particular microfabric features could be associated with certain types of engineering/mechanical behaviour (sensitivity, collapse and expansion) but that there was little evidence of unique relationships between microfabric features and depositional environment. Most of the studies involving image analysis of clay orientation have involved monomineralic (kaolin), saturated (de-aired water) clays in carefully controlled stress conditions in triaxial apparatus or shear boxes (McKeyes and Yong, 1971; McConnachie, 1974; Morgenstern and Tchalanko, 1976; Tovey et al., 1989; Smart and Leng, 1993). Collins and McGown (1974) found that natural soil microfabric was much more complex than previously reported. The inherent assumption of previous models was that the dominant factors in the determination of the particle arrangement were the mode of deposition and the electrochemistry of the pore fluid at the time of deposition. In fact, many other factors are also known to influence the depositional arrangement of particles, among which are particle size, shape and gradation; clay mineralogy; exchangeable cations; pH; organic carbon content; concentration of sediment and rate of deposition; state of agitation and depth of water; seasonal drying out (Collins and McGown, 1974; Mitchell, 1976; Dalrymple and Jim, 1984). Many of the elementary particle arrangements described by Lambe (1958) and Barden and Sides (1971) were not unique in natural soils and were found to exist side by side in any one soil; therefore, soils with different modes of deposition and depositional environments can contain similar arrangements. Single clay platelet arrangements of any form were rarely seen

whereas groups of clay platelets interacting in various forms and multi-level assemblages were commonly found (Collins and McGown, 1974; McConnachie, 1974). Collins and McGown (1974) developed a fabric characterization scheme which divided fabric into three levels: the elemental, the assemblage and the composite levels.

Clay particles tend to become oriented against grains and pores in soils due to surface tension pulling them out of suspension into parallel formation as the soil dries. Domains are groups of particles in which contiguous particles have approximately the same orientation, and which cannot be broken down into smaller groups on the basis of differences in the orientations of its constituent particles (McConnachie, 1974). The anisotropy of a clay is due mainly to these domains which appear to behave as a single anisotropic unit (Morgenstern and Tchalanko, 1976) because of parallel orientation of the component individual grains. As stresses are applied, domains orient themselves perpendicular to the major principle stress and become more closely packed, suggesting rotations rather than rupture at points of contact (Quigley and Thompson, 1966; McConnachie, 1974; Sposito and Giraldez, 1976; Groenevelt and Parlange, 1974). Dalrymple and Jim (1984) found that medium clay content (20-40%) and a high sand:silt ratio favoured clay orientation and the formation of a coarse matrix under drying conditions.

1.2.4.1 Image analysis and orientation measurement techniques

The use of image analysis techniques in studying soil micromorpohology has largely been directed towards describing the pore/void space characteristics of a soil after various crop/tillage management practices (Murphy et al., 1977; Bullock et al., 1985; Bui and Mermut, 1988; Koppi et al., 1992; Mermut et al., 1992; Oleschko et al., 1993; Fiès and Bruand, 1990; Bruand et al., 1993). Image analysis is widely used in quantifying the size and orientation of pores in binary images where the pore and solid interface is clearly defined, often using ultraviolet dyes(Moran and McBratney, 1992; McBratney et al., 1992; Koppi et al., 1992; Mermut et al., 1992).

A variety of techniques have been used to visualize the orientation of the clay fabric. The small dimension of clay particles (< 2 μm) makes the resolution of individual particles impossible with an optical light microscope. Development of the scanning electron microscope (SEM), transmission electron microscope (TEM) and backscatter collection electron microscope (BSEM) in the last 40 years has improved the resolution of clay particle images and elucidated many features qualitatively (Smart and Tovey, 1982). X-ray diffraction and birefringent techniques have also been applied to the study of clay orientation.

Quigley and Thompson (1966) used X-ray diffraction techniques to measure particle parallelism. The principle is based on the knowledge that as the clay platelets become more and more orientated in a given plane, the intensity of the basal X-ray reflections increases (ie. high degrees of particle parallelism will produce strong (00l) peaks). A clay with an initially random fabric should be forced into a state of semi-parallelism as a result of uniaxial consolidation. "Undisturbed" Leda clay samples cut from a block and remoulded samples were consolidated and impregnated with Carbowax 600. Areas of 3/8" by 1/2" were exposed to X-rays with successive surfaces prepared by grinding. The degree of particle parallelism was inferred from the measurement of the amplitude of the (001) illite peaks, and corrected with reference to background radiation. Quigley and Thompson (1966) concluded that the void ratio was directly related to induced parallelism, this parallelism increasing as the void ratio decreased. The remoulding process had little effect on the fabric-void ratio relationship despite its great effect on the pressure-void ratio relationship (Quigley and Thompson, 1966). Greater clay platelet parallelism was produced at much lower pressures when the clays were remoulded, proving that sample disturbance caused a marked breakdown of the interparticle bond so that the clay platelets were able to rotate more easily under a given load and the soil consolidated to a lower void ratio.

McKeyes and Yong (1971) compared three techniques to view the fabric of saturated kaolin clay after shearing in a triaxial apparatus. The first method used was polarized transmitted light

microscopy of a resin impregnated sample. This method takes advantage of the birefringence of the kaolinite mineral, which causes the incoming polarized light to be split into components parallel to the mineral optical axes. The resultant light intensity observed in the polarizing microscope is a maximum when the *c* axes of kaolinite particles are oriented at an angle of about 45° to the direction of incoming polarized light and a minimum when the axes are parallel to the direction of light travel (McKeyes and Yong, 1971). Observation of this extinction phenomenon allows for the determination of the orientation of individual clay particles as well as groups or aggregates of oriented clay particles which can exhibit various patterns (McKeyes and Yong, 1971; McGarry, 1989). Scanning electron microscopy and transmission electron microscopy were also employed using cleaved vacuum desiccated samples. Once a composite of micrographs was assembled it was found that the width of shear zones where there was increased parallelism and the fabric pattern were the same using all methods. Replica TEM provided the best resolution of clay particles, while scanning electron microscopy allowed for a three dimensional view of a cleavage surface through a shear zone. Polarized light microscopy yielded the best integral view of the zone and its surroundings, and may be the best method to use for determining the direction of the shear movement or other large scale features of the phenomenon (McKeyes and Yong, 1971).

Recently, McGarry (1989) used a stereo microscope with polarizer to observe zones of striated clay (Brewer, 1964) in vertisols in cultivated and undisturbed states. A magnification of 5X was used which provided a resolution of 0.2 X 0.2 mm. Zones of striated clay were drawn 2.5X actual size onto graph paper using intersections of the zone (etched on a cover slip) with the grid graticule in the eyepiece (McGarry, 1989). Only one variable, area fraction (%) of striated clay in total area, was generated. The orientation pattern was said to be strongly-, moderately, or weakly-striated when, respectively, > 60%, 20-60 % and < 20% of the material exhibited striation (Brewer, 1964). In the surface layers (0-10 cm) of all soils tested, the zones of striated clay were dominantly single discrete units, surrounded by pore space. No striated clay zones were found beneath 0.54 m in any profile, and none below 0.4-0.45 m in

most; there were no zones of striated clay in the profiles from the 'never'-cultivated stock routes. The main finding was that cultivation of this vertisol when wet had led to major increases in the area fraction of zones of striated clay, the difference being at a maximum in the 0.05-0.2m layer in the soil. Soils cultivated dry had on average < 1% of the area composed of zones of striated clay, whereas soil cultivated wet had up to 17% area having strongly striated clay. The main difference in parallelism being in the 0.05-0.2 m layer is not surprising knowing that tillage implements have high shearing forces which could induce orientation of particles.

McConnachie (1974) used a transmission electron microscope on ultrathin sections at 2500-16000 X magnification to distinguish clay particles of kaolin. A pure kaolin was consolidated at various pressures and samples were extracted, water was replaced by acetone and the samples were resin impregnated. McConnachie (1974) was the first to devise an arithmetic, quantitative means of describing particles and voids in TEM micrographs. Size, breadth, shape (breadth/size), orientation of the longest axis and packing were all calculated after selecting features visually and measuring them with a drafting machine.

Virtually all of the electron microscope observations of structures of clay soils are now made using the back-scattered mode of scanning electron microscopy (BSEM) (Smart and Leng, 1993). Contrast in the back-scattered mode arises primarily from atomic number contrast, so that particles appear bright against a dark background of resin-filled pores (Smart and Leng, 1993). The incident electrons penetrate some distance into the sample, and there is some spreading of electrons within the sample. Thus, some particles which are actually below the true surface may be seen more or less faintly and there is some softening of the contrast (Smart and Leng, 1993).

In natural soils, dispersion of particles will likely not occur and intra-aggregate void and domain spacing will be very small. At this scale the separation of voids and aggregates is not discernible by simple image analysis techniques because of the massive nature of the aggregate. Tovey et al. (1989,

1992) have proposed an intensity gradient technique for determining the orientation pattern in BSEM micrographs. Petruk (1989) has described several techniques for routine analysis of percentage of inclusion in host, mineral associations, grain separations, grain boundary reconstruction, separating interconnected grains, grain clustering analysis, and erosion-dilation for fractal analysis from BSEM (energy dispersive X-ray analyzer) images but does not deal with orientation of particles or the fabric which is dealt with here.

The intensity gradient technique is essentially an edge detection method, in which the changes in intensity are of importance (Tovey et al., 1989). Since absolute values of intensity are not required, the problems of thresholding do not arise, and direct image analysis with little or no intervening processing is possible (Tovey et al., 1989, 1992). A further advantage is that the orientation of features evaluated by this method is directly related to the size and shape of the feature, rather than the specification of a single orientation given by other methods (Tovey et al., 1989). In its most simple form, the intensity gradient technique for orientation analysis considers the rate at which the intensity is changing in two orthogonal directions across a micrograph. If there is a linear feature in the micrograph, then this intensity will vary in a direction orthogonal to the alignment of that feature and this is readily evaluated once the intensity gradient is known in the two orthogonal directions. Studies of natural soils and sediments using the intensity gradient technique have been few, including the study of marine soils (Tovey and Sokolov, 1981; Tovey, 1990) and the surface microtexture of sand grains (Tovey and Krinsley, 1990).

There are alternative image analysis routines to analyze the orientation of clay fabric but which are more complex than intensity gradient analysis. Luo et al. (1992) devised a method in which the edges of the particles are followed and recorded as chain code; then, for each particle in turn, the chain code is reduced to provide a measure of the orientation of that particle. Luo et al. (1992) went on to analyse the particles by superimposing the convex hull (ie. the figure formed by the enveloping tangents, from which he took the longest diameter as an indicator of orientation).

Thus there is the ability to measure clay or microfabric orientation at many levels of resolution using image analysis techniques to determine if orientation is related to structured soil behaviour. Measurements on natural soils in relation to applied stress conditions are relatively rare.

1.3 Information Needs and Proposed Research

Many authors have pointed out that differences exist between structurally disrupted and structurally intact soil mechanical behaviour, which prevents using laboratory measurements on disturbed samples to directly predict behaviour in the field. Few studies have used the mechanical parameters of both structural states to determine if there are systematic differences in behaviour which could be used to assess soil structural quality. In terms of a reference state, the remoulded (saturated, slurried) state has not been widely studied for agricultural soils. Studies which have compared structured and remoulded soils are often limited to one dominant mineralogy and few soil types or initial structural conditions. Shrinkage studies have not used common model parameters for describing the shrinkage characteristic curve and so comparisons have mainly been made between the apparent specific volume at a particular moisture content or pF value. It is also not known to what extent microfabric orientation varies with structural quality and to what degree it will influence mechanical behaviour of natural soils. In addition there has been little attempt to provide evidence or models to assess soil structural quality using relative mechanical indices on a regional basis using pedotransfer functions and soil survey information, rather than conducting extensive laboratory mechanical tests.

These gaps in knowledge led to this PhD research project. This study attempts to devise structural quality indices based on compression (external stress) and shrinkage (internal stress) tests of structurally intact samples in relation to remoulded reference soils to deduce if there are

systematic responses based on extremes in land use treatment, clay mineralogy or soil properties such as clay or organic carbon content. Various differences or ratios between structured and remoulded mechanical parameters would need to be assessed for their sensitivity and systematic response to soil characteristics to see if unique quality criteria values could be found. Sampling a range of textures, mineralogy, and land use variables of classification (treatments) could aid in developing pedotransfer functions for soil quality. A quantitative examination of clay orientation could help explain the relative placement of structured and remoulded compression or shrinkage curves. This research is an approach to devising dynamic indicators of physical soil quality so that systematic and predictable mechanical response based on soil properties and land use may lead to the improved use of soil survey information for assessing physical soil quality regionally.

The specific objectives, methods and results for each of the three areas of study, compression, shrinkage and image analysis, are presented as independent chapters in paper style in this dissertation. Comparison and concluding chapters help to bridge information among the three main bodies of work, summarize the knowledge gained, and point out future research needs.

1.4 References

Acton, D.F. 1992. Development of a framework for soil quality evaluation in Canada (Draft). National Soil Quality Evaluation Program. Agriculture Canada, August.

Aitchison, G.D. and J.W. Holmes. 1953. Aspects of swelling in the soil profile. Aust. J. Appl. Sci. 4:244-259.

Al-Khafaji, A.W.N. and O.B. Andersland. 1992. Equations for compression index approximation. J. Geotech. Eng. 118(1):148-153.

Allbrook, R.F. 1992. Shrinkage of some New Zealand soils and its implications for soil physics. Aust. J. Soil Res. 31:111-118.

Angers, D.A. 1990. Compression of agricultural soils from Quebec. Soil & Tillage Res. 18:357-365.

Angers, D.A., B.D. Kay and P.H. Groenevelt. 1987. Compaction characteristics of a soil cropped to corn and bromegrass. Soil Sci. Soc. Am. J. 51:779-783.

Assouline, S., J. Tavares-Filho, and D. Tessier. 1997. Effect of compaction on soil physical and hydraulic properties: Experimental results and modelling. Soil Sci. Soc. Am. J. 61:390-398.

Ball, B.C. and E.A.G. Robertson. 1994. Effects of uniaxial compaction on aeration and structure of ploughed or direct drilled soils. Soil & Tillage Res. 31:135-148.

Barden, L. and G. Sides. 1971. Sample disturbance in the investigation of clay structure. Géotechnique. 21 (3)211-222.

Baumgartl, Th. and R. Horn. 1991. Effect of aggregate stability on soil compaction. Soil & Tillage Res. 19:203-213.

Baver, L.D. 1930. The Atterberg consistency constants: Factors affecting their values and a new concept of their significance. J. Am. Soc. Agron. 22:935-948.

Bennett, R.H., N.R. O'Brien and M.H. Hulbert. 1991. Determinants of clay and shale microfabric signatures: Processes and mechanisms. pp. 5-32 *In* R.H. Bennett, W.R. Bryant and M.H. Hulbert (eds.) Microstructure of Fine-Grained Sediments: From Mud to Shale. Springer Verlag: New York. 582 pp.

Boone, F.R. 1986. Towards soil compaction limits for crop growth. Neth. J Agr. Sci. 34:349-360.

Bradford, J.M. 1981. The shear strength of a moderately well-structured soil in its natural and remolded states. Soil Sci. Soc. Am. J. 45:9-12.

Bradford, J.M. and S.C. Gupta. 1986. Compressibility. p. 479-492 *In* Methods of Soil Analysis Part 1. Physical and Mineralogical Methods. ASA, Agronomy Monograph no. 9 (2nd ed.)

Brasher, B.R., D.P. Granzmeier, V. Valassis and S.E. Davidson. 1966. Use of Saran resin to coat natural soil clods for bulk-density and water-retention measurements. Soil Sci. 101(2):108.

Brewer, R. 1964. Fabric and Mineral Analysis of Soils. John Wiley & Sons, Inc.: Sydney. 470 pp.

Bronswijk, J.J.B. 1991a. Drying, cracking and subsidence of a clay soil in a lysimeter. Soil Sci. 152(2):92-99.

Bronswijk, J.J.B. 1991b. Relation between vertical soil movements and water-content changes in cracking clays. Soil Sci. Soc. Am. J. 55:1120-1226.

Bronswijk, J.J.B. 1993. Comments on "Shrinkage terminology: escape from normalcy". Soil Sci. Soc. Am. J. 57(2):558-559.

Bronswijk, J.J.B. and J.J. Evers-Vermeer. 1990. Shrinkage of Dutch clay soil aggregates. Neth. J. Agric. Sci. 38:175-194.

Bruand, A. and R. Prost. 1987. Effect of water content on the fabric of a soil material: an experimental approach. J. Soil Sci. 38:461-472.

Bruand, A., L.P. D'Acqui, P. Nyamugafata, R. Darthout and G.G. Ristori. 1993. Analysis of porosity in a tilled "crusting soil" in Zimbabwe. Geoderma 59:235-248.

Bui, E.N. and A.R. Mermut. 1988. Orientation of planar voids in Vertisols and soils with vertic properties. Soil Sci. Soc. Am. J. 52:171-178.

Bullock, P., A.C.D. Newman and A.J. Thomasson. 1985. Porosity aspects of the regeneration of soil structure after compaction. Soil & Tillage Res. 5:325-341.

Burland, J.G. 1990. On the compressibility and shear strength of natural clays. Géotechnique. 40(3):329-378.

Cabidoche, Y.-M. and M. Voltz. 1995. Non-uniform volume and water content changes in swelling clay soil: II. A field study on a Vertisol. Eur. J. Soil Sci. 46:345-355.

Campbell, D.J. 1991. Liquid and plastic limits pp. 367-398 *In* K.A. Smith and C.E. Mullins (eds.) Soil analysis: Physical methods. Books in soils, plants and the environment. Marcel Dekker, New York.

Canarache, A. 1991. Factors and indices regarding excessive compactness of agricultural soils. Soil & Tillage Res. 19:145-164.

Carrier, W.D. and J.F. Beckman. 1984. Correlations between index test and the properties of remoulded clay. Géotechnique. 34:211-228.

Carter, M.R. 1990. Relative measures of soil bulk density to characterize compaction in tillage studies on fine sandy loams. Can. J. Soil. Sci. 70:425-433.

Centre for Land and Biological Resources Research (CLBRR). 1995. The health of our soils: Toward sustainable agriculture in Canada. D.F. Acton and E.J. Gregorich (eds.) Research Branch, Agriculture and Agri-food Canada. Publication A53-1906/E.

Chan, K.Y. 1982. Shrinkage characteristics of soil clods from a grey clay under intensive cultivation. Aust. J. Soil Res. 20:65-68.

Chang, R.K. and B.P. Warkentin. 1968. Volume change of compacted clay soil aggregates. Soil Sci. 105(2):106-111.

Collins, K. and A. McGown. 1974. The form and function of microfabric features in a variety of natural soils. Géotechnique. 24(2):223-254.

Craig, R.F. 1992. Soil Mechanics. Fifth Ed. Chapman and Hall: London.

Crawford, C.B. 1965. The resistance of soil structure to consolidation. Can. Geotech. J. 11(2):90-97.

Culley, J.L.B. and W.E. Larson. 1987. Susceptibility to compression of a clay loam Haplaquoll. Soil Sci. Soc. Am. J. 51:562-567.

Dalrymple, J.B. and C.Y. Jim. 1984. Experimental study of soil microfabrics induced by isotropic stresses of wetting and drying. Geoderma 34:43-68.

Dasog, G.S., D.F. Acton and A.R. Mermut. 1987. Genesis and classification of clay soils with vertic properties in Saskatchewan. Soil Sci. Soc. Am. J. 51:1243-1250.

Dawidowski, J.B. and P. Lerink. 1990. Laboratory simulation of the effects of traffic during seedbed preparation on soil physical properties using a quick uni-axial compression test. Soil & Tillage Res. 17:31-45.

De Jong, E., L.M. Kozak and H.B. Stonehouse. 1992. Comparison of shrink-swell indices of some Saskatchewan soils and their relationships to standard soil characteristics. Can. J. Soil Sci. 72:429-439.

Dexter, A.R. and K.Y. Chan. 1991. Soil mechanical properties as influenced by exchangeable cations. J. Soil Sci. 42:219-226.

Doran, J.W. and T.B. Parkin. 1994. Defining and assessing soil quality. p. 3-21 *In* J.W. Doran et al. (ed) Defining soil quality for a sustainable environment. SSSA Special Publication no. 35. SSSA and ASA, Madison, WI.

Fiès, J.C. and A. Bruand. 1990. Textural porosity analysis of a silty clay soil using pore volume balance estimation, mercury porosimetry and quantified backscattered electron scanning image (BESI). Geoderma 47:209-219.

Graham, J. and E.C.C. Li. 1985. Comparison of natural and remolded plastic clay. J. Geotech. Eng. 111(7):865-881.

Granatstein, D. and D.R. Bezdicek. 1992. The need for a soil quality index: local and regional perspectives. Am. J. Alt. Agr. 7(1/2):12-16.

Greene-Kelly, R. 1974. Shrinkage of clay soils: a statistical correlation with other soil properties. Geoderma 11:243-257.

Gregorich, E.G., M.R. Carter, D.A. Angers, C.M. Monreal and B.H. Ellert. 1994. Towards a minimum data set to assess soil organic matter quality in agricultural soils. Can. J. Soil Sci. 74:367-385.

Grisso, R.D., C.E. Johnson and A.C. Bailey. 1987. Soil compaction by continuous deviatoric stress. Trans. of the ASAE. 30:1293-1301.

Groenevelt, P.H. and J.Y. Parlange. 1974. Thermodynamic stability of swelling soils. Soil Sci. 118:1-5.

Grossman, R.B., B.R. Brasher, D.P. Franzmeier and J.C. Walker. 1968. Linear extensibility as calculated from natural clod bulk density measurements. Soil Sci. Soc. Am. Proc. 32:570-573.

Guérif, J. 1982. Compactage d'un massif d'agrégats: effet de la teneur en eau et de la pression appliquée. Agonomie 2(3):287-294.

Guillame, P. and Y. Cabidoche. 1998. Casting of structural pores in vertisols: relation between shapes and water availability for plants. Paper presented at the 16th World Conference of Soil Science, Aug. 20-26, 1998, Montpellier, France. ISSS and AFES. No. 5745. Symp. 1.

Haines, W.B. 1923. The volume change associated with variations of water content in soil. J. Agric. Sci. 13:296-310.

Håkansson, I. 1988. A method for characterizing the state of compactness of an arable soil. Catena Supplement 11:101-105.

Håkansson, I. 1990. A method for characterizing the state of compactness of the plough layer. Soil & Tillage Res. 16:105-120.

Håkansson, I., and V.W. Medvedev. 1995. Protection of soils from mechanical overloading by establishing limits for stresses caused by heavy vehicles. Soil & Tillage Res. 35:85-97.

Hardin, B.O. 1989. 1-D strain in normally consolidated cohesive soils. J. Geotech. Eng. 115(5):689-709.

Hartge, K.H. 1986. A concept of compaction. Z. Pflanzenernaehr. Bodenk. 149:361-370.

Heinonen, R. 1977. Towards "normal" soil bulk density. Soil Sci. Soc. Am. J. 41:1214-1215.

Heinonen, R. 1979. The notion of "normal bulk density" in arable soils. p 87-90 *In* 8th Conference of the International Soil Tillage Research Organization, ISTRO, Bundesrepublik Deutschland.

Hettiaratchi, D.R.P. 1987. A critical state soil mechanics model for agricultural soils. Soil Use and Management 3:94-105.

Hettiaratchi, D.R.P. and J.R. O'Callaghan. 1980. Mechanical behaviour of agricultural soils. J. Agr. Eng. Res. 25:239-259.

Holtz, R.D. and W.D. Kovacs. 1981. An Introduction to Geotechnical Engineering. Prentice-Hall, Inc., Englewood, NJ.

Horn, R. 1988. Compressibility of arable land. p. 53-71 *In* J. Drescher et al. (ed) Impact of water and external forces on soil structure. Catena Supplement 11. Catena-Verlag, Cremlingen-Destedt, Germany.

Indicators Task Force and State of the Environment Reporting. 1991. A report on Canada's progress towards a national set of environmental indicators. A state of the environment report No. 91-1. Environment Canada, Minister of Supply and Services, Ottawa, ON.

Jakobsen, B.F. and A.R. Dexter. 1989. Prediction of soil compaction under pneumatic tyres. J. Terramech. 26(2):107-119.

Jones, C.A. 1983. Effect of soil texture on critical bulk densities for root growth. Soil Sci. Soc. Am. J. 47:1208-1211.

Karlen, D.L., M.J. Mausbach, J.W. Doran, R.G. Cline, R.F. Harris and G.E. Schuman. 1997. Soil quality: A concept, definition, and framework for evaluation (A guest editorial). Soil Sci. Soc. Am. J. 61:4-10.

Kay, B.D. 1990. Rates of change of soil structure under different cropping systems. p1-52 *In* B.A. Stewart (ed) Advances in Soil Science Vol 12. Springer-Verlag, New York, NY.

Kim, D.J., H. Vereecken, J. Feyen, D. Boels and J.J.B. Bronswijk. 1992. On the characterization of properties of an unripe marine clay soil: I. Shrinkage processes of an unripe marine clay soil in relation to physical ripening. Soil Sci. 153(6):471-481.

Kirby, J.M. 1989. Measurements of the yield surfaces and critical state of some unsaturated agricultural soils. J. Soil Sci. 40:167-182.

Kirby, J.M. 1991. Critical-state soil mechanics parameters and their variation for vertisols in eastern Australia. J. Soil Sci. 42:487-499.

Kirby, J.M., and B.G. Blunden. 1992. Interaction of soil deformations, structure and permeability. Aust. J. Soil Res. 29:891-904.

Koolen, A.J. and H. Kuipers. 1983. Agricultural Soil Mechanics. Advanced Series in Agricultural Sciences 13. Springer Verlag: Heidelberg.

Koolen, A.J. and H. Kuipers. 1989. Soil deformation under compressive forces. p. 37-52 *In* Larson et al. (eds) Mechanics and Related Processes in Structured Agricultural Soils.

Proceedings of the NATO Advanced Research Workshop, St. Paul, MN, Sept. 13-16, 1988. Kluwer Academic Publishers:Dordecht.

Koppi, A.J., J.T. Douglas and C.J. Moran. 1992. An image analysis evaluation of soil compaction in grassland. J. Soil Sci. 43:15-25.

Kuznetsova, I.V. and V.I. Danilova. 1988. Loosening of soils by swelling and shrinkage. Sov. Soil Sci. (Engl. Transl.) 6:59-70.

Lambe, T.W. 1958. The structure of compacted clay. Proc. Am. Soc. Civ Eng. 84:1-34.

Larson, W.E., S.C. Gupta and R.A. Uesche. 1980. Compression of agricultural soils from eight soil orders. Soil Sci. Soc. Am. J. 44:450-457.

Larson, W.E. and F.J. Pierce. 1994. The dynamics of soil quality as a measure of sustainable management. pp. 37-51 *In* Defining soil quality for a sustainable environment. SSSA Special Publication no. 35. SSSA, Madison, WI.

Lauritzen, C.W. 1948. Apparent specific volume and shrinkage characteristics of soil materials. Soil Sci. 65:155-179.

Lauritzen, C.W. and A.J. Stewart. 1941. Soil volume changes and accompanying moisture and pore size relationships. Soil Sci. Am. Proc. 6:113-116.

Lebert, M. and R. Horn. 1991. A method to predict the mechanical strength of agricultural soils. Soil & Tillage Res. 19:275-286.

Lebert, M., N. Burger and R. Horn. 1989. Effects of dynamic and static loading on compaction of structured soils. pp. 73-80 *In* W.E. Larson et al. (eds) Mechanics and Related Processes in Structured Agricultural Soils. Kluwer Academic Publishers.

Leeson, J.J. and D.J. Campbell. 1983. The variation of soil critical state parameters with water content and its relevance to the compaction of two agricultural soils. J. Soil Sci. 34:33-44.

Lipiec, J., and W. Stepniewski. 1995. Effects of soil compaction and tillage systems on uptake and losses of nutrients. Soil & Tillage Res. 35:37-52.

Luo, D., J.E.S. Macleod, X. Leng and P. Smart. 1992. Automatic orientation analysis of particles of soil microstructures. Géotechnique. 42(1):97-107.

Malicki, J., A. Bieganowski and M. Dabek-Szerniawska. 1991. Mathematical modelling of biological activity in differently compacted soil. Soil & Tillage Res. 13:383-397.

McBride, R.A. 1989. Estimation of density-moisture-stress functions from uniaxial compression of unsaturated, structured soils. Soil & Tillage Res. 13:383-397.

McBride, R.A. and N. Baumgartner. 1992. A simple slurry consolidometer design for determination of the consistency limits of soils. J. Terramech. 29(2):223-238.

McBratney, A.B., C.J. Moran, J.B. Stewart, S.R. Cattle and A.J. Koppi. 1992. Modifications to a method of rapid assessment of soil macropore structure by image analysis. Geoderma 53:255-274.

McConnachie, I. 1974. Fabric changes in consolidated kaolin. Géotechnique. 24(2):207-222.

McCormack, D.E. and L.P. Wilding. 1975. Soil properties influencing swelling in Canfield and Geeburg soils. Soil Sci. Soc. Am. Proc. 39:496-502.

McGarry, D. 1988. Quantification of the effects of zero and mechanical tillage on a Vertisol by using shrinkage curve indices. Aust. J. Soil Res. 26:537-542.

McGarry, D. 1989. The effect of wet cultivation on the structure and fabric of a Vertisol. J. Soil Sci. 40:199-207.

McGarry, D. 1995. Soil Shrinkage. pp. 1-22. *In* Coughlan, K.J., McKenzie, N.J. and H.P. Cresswell. (eds.) Soil physical measurement and interpretation for land evaluation. Australian soil and land survey handbook series. Volume 5. Australian Collaborative Land Evaluation Program, CSIRO, Canberra, Australia.

McGarry, D. and K.W.J. Malafant. 1987. The analysis of volume change in unconfined units of soil. Soil Sci. Soc. Am. J. 51(2):290-297.

McIntyre, D.S. and G.B. Stirk. 1954. Method for determination of apparent density of soil aggregates. Aust. J. Agr. Res. 5:291-296.

McKenzie, D.J. Jacquier and A.J. Ringrose-Voase. 1994. A rapid method for estimating soil shrinkage. Aust. J. Soil Res. 32:931-938.

McKeyes, E. and R.N. Yong. 1971. Three techniques for fabric viewing as applied to shear distortion of a clay. Clay and Clay Minerals. 19:289-293.

McNabb, D.H. and L. Boersma. 1993. Evaluation of the relationship between compressibility and shear strength of Andisols. Soil Sci. Soc. Am. J. 57:923-929.

McNabb, D.H., and L. Boersma. 1996. Non-linear model for compressibility of partly saturated soils. Soil Sci. Soc. Am. J. 60:333-341.

Mermut, A.R., M.C.J. Grevers and E. De Jong. 1992. Evaluation of pores under different management systems by image analysis of clay soils in Saskatchewan, Canada. Geoderma 53:357-372.

Mitchell, J.K. 1976. Fundamentals of Soil Behaviour. Series in soil engineering. John Wiley & Sons, Inc. New York.

Mitchell, A.R. and M. Th. van Genuchten. 1992. Shrinkage of bare and cultivated soil. Soil Sci. Soc. Am. J. 56:1036-1042.

Monnier, G., P. Stengel and J.C. Fiès. 1973. Une méthode de mesure de la densité apparente de petits agglomérats terreux: Application à l'analyse des systèmes de porosité du sol. Ann.

Agron. 24(5):533-545.

Monnier, G. and M.J. Goss. 1987. Concluding session. pp. 157-163 *In* G. Monnier and M.J. Goss (eds). Soil Compaction and Regeneration. Proceedings of the Workshop on Soil Compaction: Consequences and Structural Regeneration Processes. Avigon, 17-18 September, 1985. Commission of the European Communities: Rotterdam.

Moran, C.J. and A.B. McBratney. 1992. Acquisition and analysis of three-component digital images of soil pore structure. I. Method. J. Soil Sci. 43:541-549.

Morgenstern, N.R. and J.S. Tchalenko. 1967. The optical determination of preferred orientation in clays and its application to the study of microstructure in consolidated kaolin. Proc. Royal Soc. London. A300:214-250.

Murphy, C.P., P. Bullock and R.H. Turner. 1977. The measurement and characterization of voids in soil thin section by image analysis. Part I. Principles and techniques. J. Soil Sci. 28:498-508.

Nagaraj, T.S. and B.R. Srinivasa Murthy. 1986. Prediction of compressibility of overconsolidated uncemented soil. J. Geotech. Eng. 112:484-488.

Nakase, A., T. Kamei and O. Kusakabe. 1988. Constitutive parameters estimated by plasticity index. J. Geotech. Eng. 114(7):844-857.

Newman, A.C.D. and A.J. Thomasson. 1979. Rothamsted studies of soil structure III: Pore size distribution and shrinkage processes. J. Soil Sci. 30:415-439.

Oleschko, K., J.E. Etchevers and L. Osorio. 1993. Pedological features as indicators of the tillage effectiveness in Vertisols. Soil & Tillage Res. 26:11-31.

O'Sullivan, M.F. 1992. Uniaxial compaction effects on soil physical properties in relation to soil type and cultivation. Soil & Tillage Res. 24:257-269.

O'Sullivan, M.F., D.J. Campbell and D.R.P. Hettiaratchi. 1994. Critical state parameters derived from constant cell volume triaxial tests. Eur. J. Soil Sci. 45:249-256.

Papendick, R.I. and J.F. Parr. 1992. Soil quality-the key to a sustainable agriculture. Am. J. Alt. Agr. 7(1/2):2-3.

Paz, A. 1998. Shrinkage characteristics of aggregates from soils with limited amounts of swelling materials. Paper presented at the 16th World Conference of Soil Science, Aug. 20-26, 1998, Montpellier, France. ISSS and AFES. No. 904. Symp. 2.

Pellissier, J.P. 1991. The toluene and wax-freezing method of determining volumetric free swell. ASTM Geotech. Test. J. 14(3):309-314.

Petersen, C.T. 1993. The variation of critical-state parameters with water content for two agricultural soils. J. Soil Sci. 44:397-410.

Petruk, W. 1989. Techniques for performing image analysis routines. pp. 19-34 *In* Short Course on

Image Analysis Applied to Mineral and Earth Sciences. Mineralogical Association of Canada. Volume 16 Ottawa, May 1989. 156 pp.

Pierce, F.J. and W.E. Larson. 1993. Developing criteria to evaluate sustainable land management. pp. 7-14 *In* J.M. Kimble (ed.) Proceedings of the Eighth International Soil Management Workshop: Utilization of soil survey information for sustainable land use. May 1993. USDA, Soil Conservation Service, National Soil Survey Centre.

Quigley, R.M. and C.D. Thompson. 1966. The fabric of anisotropically consolidated sensitive marine clay. Can. Geotech. J. 3(2):61-73.

Raper, R.L., C.E. Johnson and A.C. Bailey. 1994. Coupling normal and shearing stresses to use in finite element analysis of soil compaction. Trans. ASAE 37:1417-1422.

Reeve, M.J. and D.G. Hall. 1978. Shrinkage in clayey subsoils of contrasting structure. J. Soil Sci. 29:315-323.

Reeve, M.J., D.G.M. Hall and P. Bullock. 1980. The effect of soil composition and environmental factors on the shrinkage of some clayey British soils. J. Soil Sci. 31:429-442.

Salire, E.V., J.E. Hammel and J.H. Hardcastle. 1994. Compression of intact subsoils under short-duration loading. Soil & Tillage Res. 31:235-248.

Schafer, R.L. and C.E. Johnson. 1990. Soil dynamics and cropping systems. Soil & Tillage Res. 16:143-152.

Schafer, W.M. and M.J. Singer. 1976. A new method of measuring shrink-swell potential using soil pastes. Soil Sci. Soc. Am. J. 40:805-806.

Schofield, A. and P. Wroth. 1968. Critical State Soil Mechanics. McGraw-Hill, London.

Sibley, J.W. and D.J. Williams. 1989. A procedure for determining volumetric shrinkage of an unsaturated soil. ASTM Geotech. Test. J. 12(3):181-187.

Simon, J.J., L. Oosterhuis and R.B. Reneau. 1987. Comparison of shrink-swell potential of seven ultisols and one alfisol using two different COLE techniques. Soil Sci. 143(1):50-55.

Smart, P. and X. Leng. 1993. Present developments in image analysis. Scanning Micro. 7(1):5-16.

Smart, P. and N.K. Tovey. 1982. Electon microscopy of soils and sediments: techniqes. Oxford University Press, Oxford, UK.

Snakin, V.V., P.P. Krechetov, T.A. Kuzovnikova, I.O. Alyabina, A.F. Gurov and A.V. Stepichev. 1996. The system of assessment of soil degradation. Soil Tech. 8:331-343.

Soane, B.D. 1990. The role of organic matter in soil compactibility: a review of some practical aspects. Soil & Tillage Res. 16:179-201.

Soane, B.D., and C. van Ouwerkerk. 1995. Implication of soil compaction in crop production for the quality of the environment. Soil & Tillage Res. 35:5-22.

Sposito, G. and J.V. Giraldez. 1976. Thermodynamic stability and the law of corresponding states in swelling soils. Soil Sci. Soc. Am. J. 40:352-358.

Stirk, G.B. 1954. Some aspects of soil shrinkage and the effect of cracking upon water entry into the soil. Aust. J. Agr. Res. 5:279-290.

Tariq, A, and D.S. Durnford. 1993a. Analytical volume change model for swelling clay soils. Soil Sci. Soc. Am. J. 57:1183-1187.

Tariq, A. and D.S. Durnford. 1993b. Soil volumetric shrinkage measurements: a simple method. Soil Science 155(5):325-330.

Taylor, H.M. and G.S. Brar. 1991. Effect of soil compaction on root development. Soil & Tillage Res. 19:111-119.

Terrible, F. and E.A. Fitzpatrick. 1995. The application of some image-analysis techniques to recognition of soil micromorphological features. Eur. J. Soil Sci. 46:29-45.

Toll, D.G. 1990. A framework for unsaturated soil behaviour. Géotechnique. 40(1):31-44.

Tovey, N.K. 1990. The microfabric of some Hong Kong marine soils. pp 519-530. In Microstructure of Fine Grained Sediments . From mud to shale. R.H. Bennett, W.R. Bryant and M.H. Hulbert (eds). Springer, New York.

Tovey, N.K. and V.N. Sokolov. 1981. Quantitative SEM methods for soil fabric analysis. Scanning Electron Microsc. 1:536-554.

Tovey, N.K., P. Smart, M.W. Hounslow and X.L. Leng. 1989. Practical aspects of automatic orientation analysis of micrographs. Scanning Microscopy. 3(3):771-784.

Tovey, N.K. and D.H. Krinsley. 1991. Mineralogical mapping of scanning electron micrographs. Sediment. Geol. 75:109-123.

Tovey, N.K., P. Smart, M.W. Hounslow and X.L. Leng. 1992. Automatic orientation mapping of some types of soil fabric. Geoderma. 53:179-200.

Veenhof , D.W. and R.A. McBride. 1996. Overconsolidation in agricultural soils: I. Compression and consolidation behavior of remolded and structured soils. Soil Sci. Soc. Am. J. 60:362-373.

Warkentin, B.P. 1993. Soil Shrinkage. pp. 513-518. *In* M.R. Carter (ed.) Soil Sampling and Methods of Analysis. Canadian Society of Soil Science. Lewis Publishers: Boca Raton.

Wesley, L.D. 1988. Compression index: Misleading parameter? J. Geotech. Eng. 114:718-723.

Wires, K.C., W.D. Zebchuk and G.C. Topp. 1987. Pore volume changes in a structured silt-loam

soil during drying. Can. J. Soil Sci. 67:905-917.

Wolkowski, R.P. 1990. Relationship between wheel-traffic-induced soil compaction, nutrient availability, and crop growth: a review. J. Prod. Agr. 3:460-469.

Wroth, C.P. and D.M. Wood. 1978. The correlation of index properties with some basic engineering properties of soil. Can. Geotech. J. 15:137-145.

Yule, D.F. and J.T. Ritchie. 1980a. Soil shrinkage relationships of Texas vertisols: I. Small cores. Soil Sci. Soc. Am. J. 44:1285-1291.

Yule, D.R. and J.T. Ritchie. 1980b. Soil shrinkage relationships of Texas vertisols: II. Large cores. Soil Sci. Soc. Am. J. 44:1291-1295.

2. Mechanical Compression Parameters of Intact and Remoulded Samples

2.1 Introduction

Soil compaction is noted as a prevalent problem in many agricultural cropping systems around the world and has even been considered "practically inevitable in modern agronomy" (Assouline et al., 1997). Soil compaction on agricultural land is also a prevalent problem following resource delivery system construction (Culley et al., 1982; Naeth et al., 1987; Landsburg, 1989; McKague et al., 1993). The reduction in pore space and increase in soil strength caused by soil compaction can lead to reduced crop productivity as well as environmental problems such as increased use of fossil fuels, increased greenhouse gas production and increased run off (Soane and van Ouwerkerk, 1995; Lipiec and Stepniewski, 1995). Although topsoil compaction can generally be alleviated within 5 years through tillage and natural processes, subsoil compaction is a particular concern because it can persist for decades (Håkansson and Medvedev, 1995). Because of the serious consequences of soil compaction and the limited reliability of current global areal estimates, compaction should receive more widespread and detailed attention in future global surveys of soil degradation (Soane and van Ouwerkerk, 1995).

There are many indicators which could be chosen to represent physical soil quality to aid in the monitoring of soil compaction and the development of sustainable land managed systems. Soil texture, plant-available water-holding capacity, dry bulk density, maximum rooting depth, cone penetration resistance and hydraulic conductivity are all measurements proposed in a minimum data set for monitoring soil physical quality (Larson and Pierce, 1994). In addition to routinely collecting these measurements, it was recognized that many soil properties are interrelated and can be predicted from other properties using pedotransfer functions (PTFs). A PTF is described by Bouma (1989) as a mathematical function that relates different soil

characteristics and properties (continuous or class variables) to one another or to land qualities. PTFs can be used to extend the utility of minimum data sets used to monitor soil quality and to estimate parameters which are too costly or difficult to measure routinely (Larson and Pierce, 1994; Van den Akker, 1998; Wösten and Lilly, 1998).

Dry bulk density and cone penetration resistance would be likely candidates from the above list for monitoring or assessing soil compaction on a regional basis. Dry bulk density is more routinely measured but is limited in universality when comparing sites or land uses because of particle size, organic carbon, and climatic differences which influence dry bulk density (Jones, 1983; Carter, 1990). The dry bulk density also reveals nothing of the pore-size distribution or continuity or the susceptibility to compression (McNabb and Boersma, 1996). Cone penetration resistance is a good indicator of soil strength but is highly dependent on soil moisture, is spatially variable and is not routinely collected (Okello, 1991; Meshalkina et al., 1995). Kay (1990) suggests that our definition of soil structure should not only include the form and strength, as the dry bulk density and cone penetration resistance measure, but also some measure of the resiliency of the soil's structure and its ability to rejuvenate or be maintained under changes in management practices. Following this dynamic rather than static assessment of soil structure, Pierce and Larson (1993) promote the use of an approach to soil quality monitoring based on statistical quality control theory. In this theory, the dynamic range of soil quality measurements are the basis for determining sustainability of the system. These approaches recognize that there are natural fluctuations in measured parameters within sustainably managed systems, but that there can be forces, such as change in land management, which alter soil attributes beyond threshold values or control limits such that they no longer represent "sustainable" systems but are rather "out of control"(Pierce and Larson, 1993).

New methods based on soil mechanical principles are needed to improve the understanding

of the extent and severity of the soil compaction problem (Veenhof and McBride, 1996; Van den Akker, 1998) and to aid in understanding the dynamics of the parameters used for monitoring soil quality. Soil mechanics is the study of change in strain under change in stress and thus provides a frame-work to study the dynamics of soil structural quality. Methods based on soil mechanics have the additional benefit of contributing to the information used for many compaction models which use soil mechanics principles, such as critical state soil mechanics, to describe soil behaviour under stress. The mechanical terms and parameters used throughout this chapter are illustrated in Figure 2.1.

One mechanical parameter which could be potentially useful as a soil quality indicator is the preconsolidation stress (σ_c') (Figure 2.1). In geotechnical terms, σ_c' is defined as the maximum effective vertical stress which has acted on a saturated, plastic soil in the past (Craig, 1992). A preconsolidation stress is measurable, and a soil is overconsolidated, if the current effective stress is less than stresses applied in the past. In unsaturated agricultural soils, σ_c' is an important measure of internal soil strength as it divides elastic from plastic behaviour under applied stresses (Kirby and Blunden, 1991). If an applied stress is below the σ_c', the soil reacts elastically within an "equilibrium" dry bulk density range where normal force and shear resistance are large enough to compensate for the applied forces (Kirby, 1989; Lebert and Horn, 1991) and soil aggregates remain largely intact (Baumgartl and Horn, 1991). If the applied stress exceeds the σ_c', plastic and irreversible deformation takes place in cohesive soils because soil aggregates are destroyed (Lebert and Horn, 1991; Horn et al., 1995) which often results in decreased permeability for air and water (Kirby and Blunden, 1991). Increases in σ_c', therefore, indicate the level of stress experienced by the soil and when irreversible changes have occurred. Under the same climatic conditions and soil use, the σ_c' values vary owing to differences in soil texture, degree of aggregation and matric potential (Horn et al., 1995). Veenhof and McBride (1996) also found the σ_c' to vary with

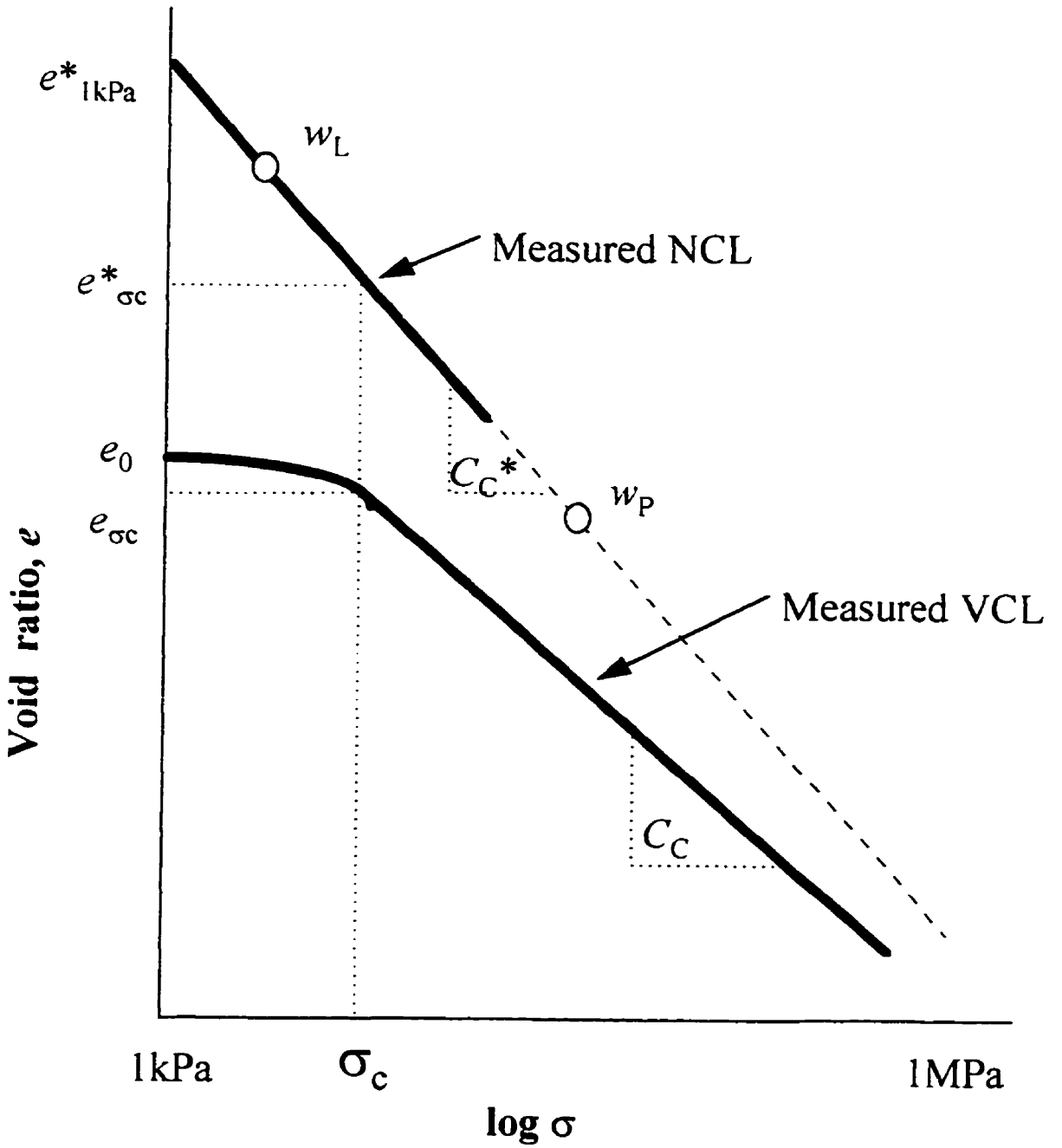

Figure 2.1. Illustration of mechanical parameters used for describing remoulded and structured consolidation.

the initial void ratio (e_0) and to influence the steepness of the virgin compression line (VCL).

The preconsolidation stress is determined graphically after Casagrande (1936) from a void ratio (e) (log stress (σ)) plot based on data from uniaxial compression or oedometer tests (Figure 2.2). The σ_c' has been determined from intersection of straight line estimates (Culley and Larson, 1987; Lebert and Horn, 1991; Dias Junior and Pierce, 1995) as well as from computer generated functions and derivatives (McBride, 1988; Dawidowski and Koolen, 1994) to overcome error associated with visually estimating tangents to the compression curve. These methods require extensive laboratory testing of undisturbed soil cores to produce the compression curves.

Alternatively, McBride and Joosse (1996) proposed a pedotransfer function (PTF2) to estimate a minimum possible preconsolidation stress (Holtz and Kovacs, 1981) for saturated, plastic soils. In PTF2, the NCL determined under saturated, remoulded conditions is substituted for the tangent to the VCL (saturated, structured). The NCL equation is estimated by the liquid and plastic limits (expressed as void ratios) represented by discrete points on the NCL and the associated stresses estimated by equations and values proposed by McBride and Baumgartner (1992). Veenhof and McBride (1996) also found that structured, untilled subsoil horizons (30 cm sample depth) did not have parallel NCLs and VCLs but that the lines tended to converge for overconsolidated soils which limited application of PTF2 to soils with saturated liquidity indexes (I_L) > 0.25 to ensure a conservative estimate of the σ_c'. Additionally, a relative variable (e^*_{1kPa}-e_0) was found to be significantly related to the preconsolidation stress (Veenhof and McBride, 1996) and used as a pedotransfer function (PTF1). PTF1 was found to have similar results to PTF2 (McBride and Joosse, 1996). These PTFs have minimum soil survey data requirements of dry bulk density, particle density, organic matter content, and the Atterberg consistency limits (liquid and plastic limits) (McBride and Joosse, 1996).

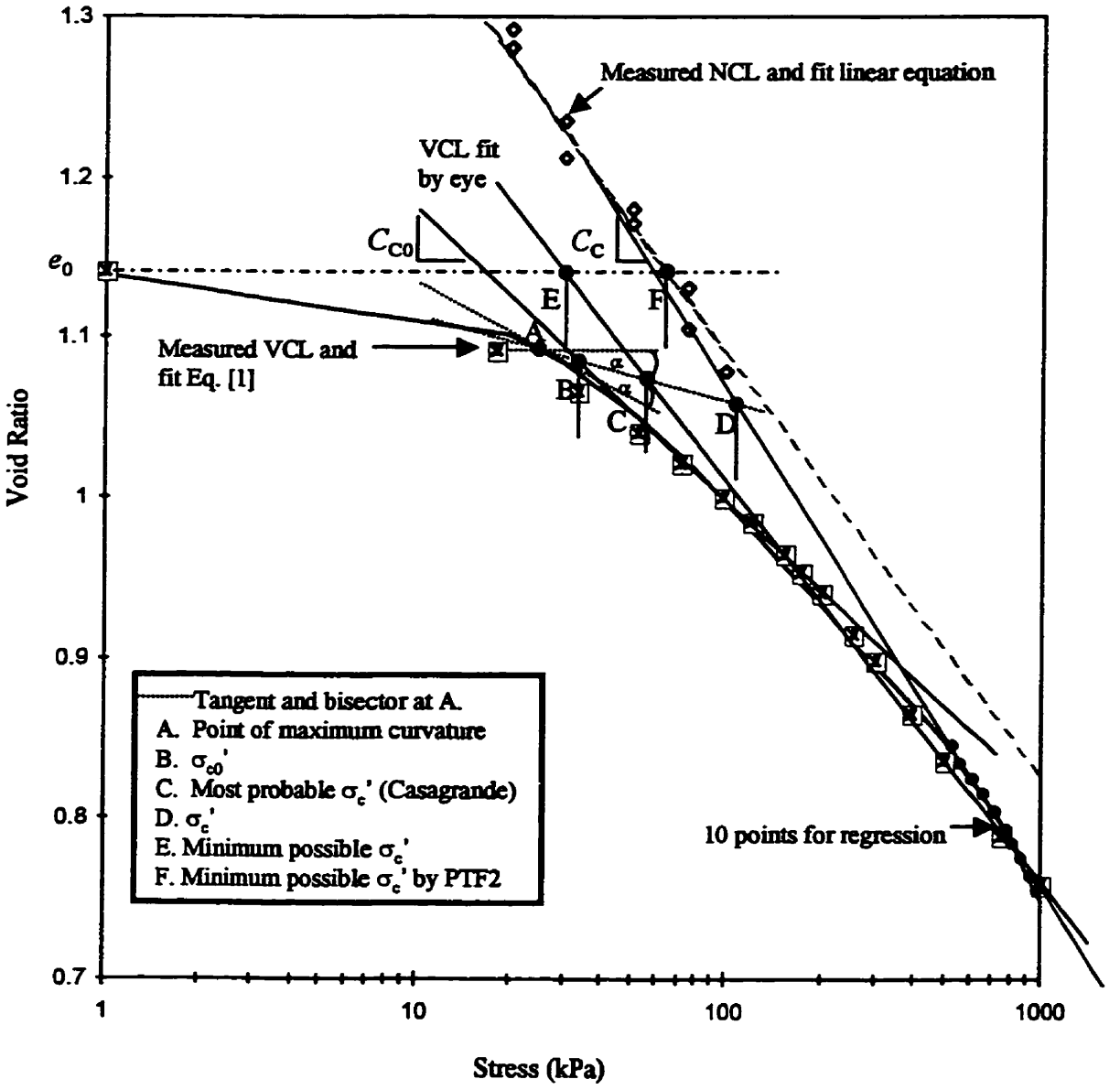

Figure 2.2. Illustration of calculating preconsolidation stress (σ_c') using Casagrande (1936) method, C_{C0} and C_C, and by PTF2. Example Brookston (LB) natural B horizon.

Pedotransfer functions to estimate the less commonly measured particle density and Atterberg limit variables have also been developed empirically for soils in southern Ontario where these PTFs were developed (Watson, 1996). To date these PTFs have been successfully used to describe the structural quality of soils in a 5 county region in southwestern Ontario (McBride and Joosse, 1996), to estimate the potential for further structural degradation under various land use scenarios for eastern Canada (McBride et al., 1997) and to estimate the apparent stress associated with the Proctor test maximum bulk density (R.A. McBride, per. comm.) where the dominant mineralogy is Ca-saturated clay mica (illite) and vermiculite.

The first objective of this study was to validate the concepts used for developing PTF1 and PTF2 by assessing if the existing equations for estimating the stresses at the liquid and plastic limit for saturated, plastic soils were valid for soils outside of the physiographic region of southern Ontario and of different clay mineralogies. This required the construction of remoulded, saturated compression lines (NCL) and structured, saturated compression lines (VCL) in $e(\log\sigma)$ co-ordinates to compare the relative placement and alignment of the curves and to measure the preconsolidation stress from a range of soil textures and mineralogies. From the NCL, the stresses associated with the w_L and w_P needed to be corroborated with the present equations to expand the use of PTF1 and PTF2. Behaviour of the remoulded soils serves as a frame of reference (benchmark) for the different soil types and structures, as well as offering the potential for inference of behavioural properties from soil survey and land use databases.

The second objective was to determine if there were unique values of "relative soil quality indicators" derived from the comparison of mechanical parameters from remoulded and structurally intact compression curves, which were indicative of soil structural quality and independent of clay content, clay mineralogy, and organic carbon content. These soil attributes are known to influence mechanical and structural properties. Veenhof and McBride (1996) found a

unique value of $(e^*_{1kPa}-e_0) \approx 0.36$ to separate saturated, normally consolidated, or near parallel NCL and VCL, from significantly overconsolidated soils. A saturated liquidity index below (I_L) ≈0.5 was also found to indicate highly overconsolidated soils with elevated preconsolidation stresses (>200 kPa) (Veenhof and McBride, 1996; Veenhof, 1993). These and other potential "relative indicators", such as $(C_C^*-C_C)$ and $(e^*_{\sigma c} - e_{\sigma c})$, needed to be tested for their sensitivity and independence across a range of soil mineralogies and constituent properties. Comparison of these parameters to established physical soil quality parameters such as plant available water-holding capacity, saturated hydraulic conductivity and macroporosity would also provide an indication of their utility and sensitivity for monitoring soil quality.

The third objective was to examine if the relative displacement of the VCL below the NCL, which demonstrates severe overconsolidation, was due to particle alignment from secondary consolidation due to natural processes as hypothesized by Veenhof and McBride (1996). To date, only soils under agricultural land use have been studied to develop the PTFs for southern Ontario. To achieve this objective, soil profiles were sampled from natural, agricultural and gas pipeline installation (workspace) land use locations at each site in southern Ontario. This would enable comparison of differences in structural characteristics and mechanical behaviour arising by natural pedogenic processes as opposed to the impact of prolonged agricultural practice or a brief yet intense impact by pipeline construction. Using the natural condition as a frame of reference (benchmark) for an "impact assessment" would provide some indication of the utility and sensitivity of the mechanical parameters proposed here for monitoring soil quality.

The fulfilment of these objectives would allow the development of more widely applicable pedotransfer functions aimed at improving the currently limited information on physical indicators of soil quality (Doran and Parkin, 1994).

2.2 Materials and Methods

Seven sites were investigated in this study. All sites were selected based on having a soil clay content sufficient enough to make them plastic. Four sites were selected in southern Ontario which had a natural gas pipeline installed. The soil series sampled were Tavistock from Middlesex County (MD), Chinguacousy from the Regional Municipality (R.M.) of Halton (HL), Brookston from Lambton County (LB) and Maplewood from the R.M. of Waterloo (WA). Sites were selected which had close proximity between agricultural (A), pipeline workspace (W) and natural (N) land use conditions to minimize variation in drainage, soil texture and soil development processes between profiles. The pipeline workspace is an area 8-10 m from the centre and parallel to the pipeline which is not excavated during construction but is heavily trafficked by large, industrial equipment. At three of the sites, pipeline construction had last occurred during the summer of 1991 which was a relatively dry year. On the fourth site in Lambton County, pipeline installation had last occurred in 1975 but crop production limitations were persistent due to extensive soil structural damage. These sites were samples from July to October 1993.

Three sites were selected outside of this physiographic area to test soils of different mineralogic origin and pedogenic development. At these three sites both natural and agricultural land use conditions were sampled. Again close proximity and similarity between profiles was a basis for profile selection. Soils from Alberta, Texas and the Ottawa area were sampled. The Malmo soil was an Eluviated Black Chernozem (Typic Agrialboll), sampled from the Ellerslie Research Station of the University of Alberta (AB) in June 1994. A Houston Black clay was sampled from the USDA Grasslands Research Centre at Riesel, Texas (TX) during August 1993. A North Gower soil was sampled from the Winchester Agronomy Station of Kemptville College near Ottawa, Ontario (OT) in August 1993. The location of the 7 sites on the North American continent are illustrated in Figure 2.3.

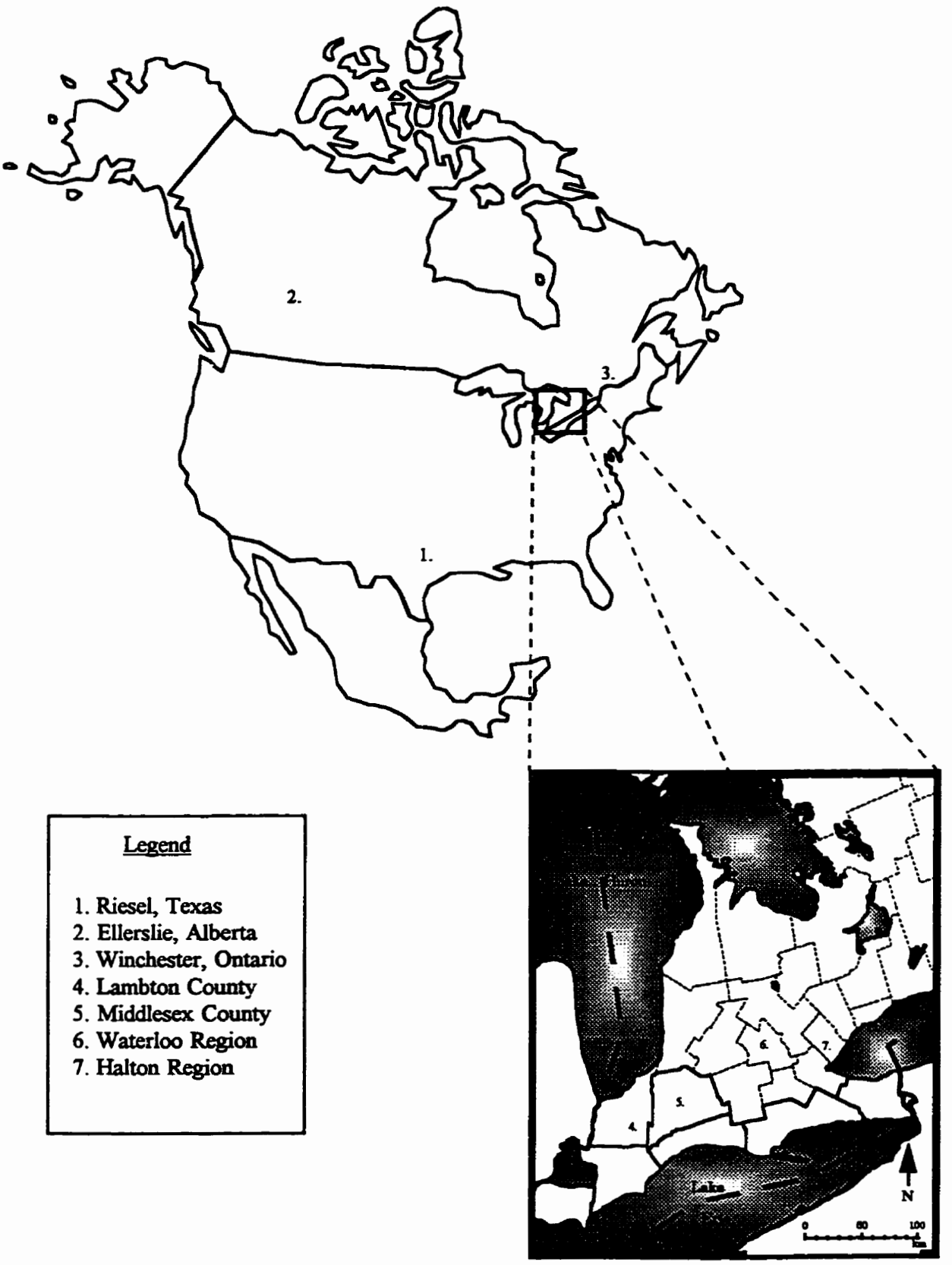

Figure 2.3. Location of 7 study sites on the North American Continent and in Southern Ontario (inset)

At each site, one soil profile was sampled in each of the available land use treatments. The distance between 2 profiles was never more than 100 m except for OT where a site in a natural condition was found 2 km away. A pedon-sized (1 m^2) sampling area was excavated from which intact soil cores and bulk soil samples could be taken. The depth of sampling was determined by the depth of the major diagnostic (A, B and C) horizons in each profile. Organic matter content was used to differentiate the A from the B horizons. The appearance of free carbonates was used to distinguish between the B and C horizons. Once the boundary was distinguished, an additional 2-3 cm depth was excavated to ensure sampling from within the horizon. Where free carbonates were present throughout the entire profile or were absent altogether, lack of significant pedogenic development was used to distinguish the C horizon.

Structurally intact soil cores (8.25 cm diam. x 3.0 cm height) and bulk soil samples (≅2 kg) were taken at each depth (horizon) in the profile. Eight intact soil cores were taken from each horizon. Intact samples were kept at 4°C prior to testing. The bulk samples were air-dried and sieved to <2 mm allowing for determination of percentage gravel. Soil and physical chemical analyses consisted of particle-size distribution with the pipette method (Sheldrick and Wang, 1993), particle density by the pycnometer method (Blake and Hartge, 1986), carbonate content by the gravimetric technique (Goh et al., 1993), organic C content by LECO induction furnace (Nelson and Sommers, 1982) and soil pH (0.01 *M* $CaCl_2$) by glass-calomel electrode pH meter (Henderschott et al., 1993). Sub-samples of the bulk soils were further sieved to <0.425 mm for determination of the Atterberg limits with the ASTM D423-72 and ASTM D424-71 procedures (McBride, 1993).

Field saturated hydraulic conductivity (K_{fs}) measurements were taken in these same pits using the Guelph Pressure Infiltrometer (Reynolds, 1993b) or a modified clay permeameter (Fallow et al., 1993, Groenevelt et al., 1996). Where field measurements were not possible, intact soil

cores were taken for laboratory determination of saturated hydraulic conductivity (K_s) (Reynolds, 1993a). Three intact cores (47 mm diam. x 25 mm height) were also taken from each depth for soil water retention determination (Topp et al., 1993). Samples were trimmed and wrapped on the bottom with a polyester cloth. Cores were saturated with deaired Guelph tap water for 1 week and then massed for saturated water contents. The cores were equilibrated on pressure plates after Topp et al. (1993) but modified for 25 mm high cores using the times and contact media shown in Table 2.1.

Table 2.1 Moisture retention methods.

Potential (kPa)	Time to Equilibration	Contact medium
0	7 days	
-2	2 days	silica flour
-5	2 days	silica flour
-10	3 days	silica flour
-33	4 days	silica flour
-100	10 days	silica flour
-500	10 days	aluminum oxide
-1500	2 weeks	aluminum oxide

Three height measurements were determined on each core after each equilibration to determine changes in volume. Both constant volume and variable volume available water content (between -33 kPa and -1500 kPa) and macroporosity (between saturation and -5 kPa) were calculated.

Mineralogy of the <2μm fraction was determined from horizons sampled from the natural profiles. The clay fraction was separated from the whole soil sample using sonification energy of 300 J/mL (Gregorich et al., 1988; de Kimpe, 1993). Slides were prepared (Table 2.2) using the methods of de Kimpe (1993) but there was no pre-treatment to remove carbonates or organic matter on the suggestion of Dr. Graeme Spiers (personal communication). X-ray diffraction was carried out using .02° step widths and 4 sec counts between 3-40° for K 0%RH and Mg 54%RH slides and 3-15° for the remaining slides.

Table 2.2 Clay mineralogy slide pre-treatments.

K saturated	Mg Saturated
0% Relative humidity 54% Relative humidity 300°C 550°C HCl digestion	54% Relative Humidity Ethylene Glycol Glycerol

Structurally intact soil cores were trimmed in the lab to 7.2 cm diam. and 2.9 mm height. The cores were wrapped with acetate film held in place with a hose clamp and with a cloth across the bottom face. The cores were then saturated in deaired, distilled water for 2 weeks at 4 °C. Cores were massed for saturated water content and degree of saturation prior to compression testing.

To measure the VCL, two ELE Rowe Consolidation cells (ELE International Limited, Hemel Hempstead, Hertfordshire, England; sample chamber 7.3 cm diam x 3.5 mm height) were equipped with an automated, regulated pressure system for "fast" uniaxial compression testing. A ring of porous stainless steel (Mott Porous Metal, Farmington, CT) lined with porous plastic was substituted for the solid Rowe cell chamber to allow rapid and complete dissipation of pore water pressure. A Lucifer/Honeywell pressure regulator (EPP 3 JC 21 U/I 600 10; Honeywell Ltd, North York, Ontario) controlled with a Motorola programmable RISC microprocessor chip was used to apply pressure in steps of 20, 30, 50, 75, 100, 125, 150, 175, 200, 250, 300, 400, 500, 750, and 1000 kPa. Applied pressure was monitored with an inline pressure transducer (Brainard-Kilman,model E-124, Stone Mountain, Georgia, USA). A loading time of 85 minutes was used throughout for each incremental stress level. Pore water pressure was measured with Sensotec (Columbus, OH) A-10 and LM pressure transducers. Height displacement was measured with calibrated electronic displacement transducers (MPE HS-25B, APEK Design and Developments Ltd., Wimborne, Dorset, England). Height and pore water measurements were recorded using a Campbell Scientific 21X Datalogger (Logan, UT) at 1 minute intervals. The sample was allowed

to rebound for 85 minutes before disassembling the cell for measurements. The final height of the sample (6 measurements) was taken with callipers. The samples were massed for final water content and oven dried for 48 hours at 105 °C.

The compression curves for saturated, remoulded conditions (NCL) were constructed using the slurry consolidometer and procedures described by McBride and Baumgartner (1992). Maximum disruption of aggregates was achieved by instantaneous wetting of air-dried aggregates with distilled water. The compression of occluded air compressed and the differential swelling of the clay fraction induces the "explosion" of aggregates, causing slaking and dispersion the soil particles (Emerson, 1977; Grant and Dexter, 1990). Physical moulding and the presence of free water over 48 hours also increases the amount of dispersion (Kay and Dexter, 1990). Soils used for remoulded consolidation were sieved to <2 mm rather than <.425 mm used by McBride and Baumgartner (1992) for direct comparison to structurally intact samples. It was also suggested by Veenhof (1993) that it may be possible to eliminate the need to sieve soil materials to <0.425 mm as the slurry consolidation NCL may not be significantly affected by the presence of clastic particles in the 0.425-2.00 mm range. Stresses of 5, 7.5, 10, 15, 20, 30, 50, 75 and 100 kPa were applied until the pore water pressure dissipated (measured 0 kPa) which usually required 6-12 hours. Tests for a given soil were duplicated at each stress. Soil water content (w) and drop cone measurements (BS1377, 1975 in McBride, 1993) were taken after equilibrium (zero pore water pressure) was achieved for each stress.

All compression data from intact and remoulded samples was plotted as $e(\log\sigma)$ or $e(\log\sigma')$ functions as information was available for applied and effective stresses, respectively. To determine the preconsolidation stress (σ_c or σ'_c) of the structurally intact cores, the $\rho_b(\sigma)$ or the $\rho_b(\sigma')$ functions were first fitted to the three-parameter Bailey et al. (1986) equation (Eq. [1]) by non-linear regression using the Marquardt procedure in Mathcad.

$$\ln(\rho_b) = \ln(\rho_0) - (A + B\sigma)(1 - e^{-C\sigma}) \qquad [1]$$

Start values for solving the least squares equations were determined by visually fitting the function in Mathcad before initiating iterations. The σ_c or σ'_c were calculated from the three regression coefficients (A, B and C) with a Fortran computer program, PCP1.2 (McBride, 1988), which numerically determines the first and second derivatives along the fitted Eq.[1], but with the function transformed to $e(\log\sigma)$ or $e(\log\sigma')$ co-ordinates. The PCP1.2 model finds a tangent to the VCL by 2 methods: i) by taking the tangent (first derivative) of the point at which the second derivative first becomes 0 (C_{C0}), and ii) by linear regression through 10 points between 500 and 1000 kPa calculated by the Bailey et al. (1986) equation parameters (C_C) (Figure 2.2).

To examine the effects of mineralogy, treatment, horizon and organic matter, Analysis of Variance (ANOVA) and Analysis of Covariance (ANCOVA) were conducted (Cochran and Cox, 1957). The ANOVA and ANCOVA were carried out in SAS (SAS Institute, 1996) following the design and procedure outlined in the Appendix. Correlation, simple regression and forward stepwise multiple regression analysis were conducted in Statistica (Statsoft, 1995).

2.3 Results and Discussion

2.3.1 General Soil Properties

Detailed physical and chemical data for all horizons sampled are shown in Table 2.3. The range and distribution of several of the characteristics are displayed in Table 2.4. The uniformity in soil texture between profiles at a given site was relatively good except for the WA and OT site where there were significant differences in the WAAC and WAWB, and the OTNB and OTNC from the corresponding horizons. The WA and MD sites had the coarsest textured soils which in some cases bordered on being marginally plastic. Plastic limits and liquid limits were able to be

Table 2.3. Physical and chemical properties by soil horizon.

Soil Series Location	Land Use	Drainage	Sampling Depth	Texture	Sand	Silt	Clay	Gravel	Particle Density	Organic Carbon	$CaCO_3$	w_L	w_P	pH	Activity	ALINE Category
			(cm)		——%kg kg^{-1}——				Mg m^{-3}		——% kg kg^{-1}——					
Brookston (LB)	Natural	Poor	3	Silty clay	6.2	47.8	46.0	0.59	2.493	6.8	0.6	74.2	51.8	5.3	0.49	MH
Enniskillen Twp	woodlot		22	Silty clay	5.0	50.7	44.4	1.12	2.701	1.7	1.2	50.1	31.2	5.3	0.43	MH
Lot 5 Con VI			52	Silty clay	7.6	50.7	47.0	2.77	2.746	0.9	0.4	45.5	25.6	6.3	0.42	CL
Water reworked	Agricultural		3	Silty clay	6.1	51.7	42.2	0.72	2.516	2.6	0.1	47.0	32.7	4.5	0.34	ML
Glacial Till	corn		22	Silty clay	5.3	46.7	48.0	0.81	2.622	1.1	0.3	48.2	29.3	4.8	0.39	ML
			52	Silty clay	7.6	44.3	48.1	1.20	2.669	0.8	0.3	46.9	25.4	6.5	0.45	CL
Orthic Humic	Workspace		5	Silty clay loam	13.1	52.0	34.9	4.54	2.599	2.3	1.2	43.6	29	7.3	0.42	ML
Gleysol	soybean		23	Silty clay	9.1	45.0	45.9	3.37	2.707	1.0	0.9	44.4	26	5.8	0.40	CL
			47	Silty clay	13.5	43.0	43.4	8.09	2.703	1.3	1.1	45.3	25.5	7.0	0.46	CL
Chinguacousy	Natural	Imperfect	3	Clay loam	20.1	46.0	33.9	5.34	2.59	4.3	0.7	51.9	35.9	6.1	0.47	MH
(HL)	fencerow		20	Silty clay	14.0	42.4	43.6	2.66	2.691	0.9	0.6	42.3	23.4	4.8	0.43	CL
Milton Twp			53	Silty clay loam	18.1	48.4	33.5	10.38	2.657	0.4	16.4	32.1	20.5	7.5	0.35	CL
Lot 9, Con 5E	Agricultural		7	Clay loam	21.5	49.5	29.0	1.25	2.548	2.7	0.5	40.4	28.4	6.2	0.41	ML
Glacial Till	soybean		17	Silty clay	17.1	42.6	40.4	4.01	2.71	0.7	0.5	39.1	22.4	6.6	0.41	CL
			45	Silty clay loam	19.9	50.1	30.0	11.50	2.717	0.5	13.2	32.0	19.9	4.6	0.40	CL
Gleyed Gray	Workspace		3	Clay loam	21.1	48.8	30.1	1.36	2.648	2.6	1.1	42.4	28.3	6.8	0.47	ML
Brown Luvisol	soybean		18	Silty clay	14.4	40.4	45.1	1.37	2.686	0.7	0.5	46.5	24.2	6.3	0.50	CL
			41	Clay loam	20.1	49.6	30.3	8.68	2.676	1.1	15.4	32.9	20.1	7.6	0.42	CL
Tavistock (MD)	Natural	Imperfect	2	Silt loam	12.0	69.5	18.6	0.58	2.485	7.0	0.8	64.5	50.1	6.4	0.77	MH
Lobo Twp	woodlot		20	Silty clay loam	13.1	51.6	35.3	5.36	2.67	1.5	2.0	41.3	25	7.1	0.46	CL
Lot 16, Con VII			30	Clay loam	20.1	44.3	35.6	16.74	2.713	0.6	31.2	34.8	20	7.6	0.42	CL
	Agricultural		3	Silt loam	26.5	56.0	17.5	0.57	2.374	8.2	1.0	56.4	53.5	6.8	0.17	MH
Till Phase	corn		20	Silt loam	16.3	58.6	25.1	1.54	2.64	0.8	3.6	33.5	21.4	7.4	0.48	CL
			30	Silt loam	26.0	60.8	13.2	17.00	2.685	0.5	31.2	22.4	20.2	7.6	0.17	ML
Gleyed Brunisolic	Workspace		2	Silt loam	19.9	61.0	19.2	2.30	2.614	2.5	1.0	39.5	29.5	7.4	0.52	ML
Gray Brown	corn		30	Silt loam	18.1	57.0	24.9	0.56	2.7	0.5	1.6	33.5	20.7	7.1	0.51	CL
Luvisol			40	Silt loam	24.9	59.6	15.5	11.55	2.721	0.1	23.6	27.6	20.4	7.6	0.46	CL

Soil Series Location	Land Use	Drainage	Sampling Depth	Texture	Sand	Silt	Clay	Gravel	Particle Density	Organic Carbon	$CaCO_3$	w_L	w_P	pH	Activity	ALINE Category
			(cm)		——%kg kg^{-1}——				Mg m^{-3}	——% kg kg^{-1}——						
Maplewood (WA)	Natural	Poor	5	Loam	36.9	38.8	24.3	0.85	2.596	3.4	0.5	40.8	30.1	6.8	0.44	ML
Woolwich Twp	fencerow		30	Loam	45.1	34.6	20.4	2.51	2.62	1.3	0.8	28.4	20	6.9	0.41	CL
Lot 11			60	Clay	8.8	34.6	56.6	0.00	2.714	0.4	6.8	50.5	26.6	7.4	0.42	CH
German Co. Tract	Agricultural		5	Loam	35.5	42.0	22.5	0.55	2.608	3.2	1.0	39.3	27.5	6.7	0.52	ML
	alfalfa		30	Loam	25.6	48.0	26.3	0.37	2.72	0.5	1.0	29.8	18.5	6.9	0.43	CL
Glaciolacustrine			55	Silty clay	6.3	50.3	43.4	0.37	2.748	0.3	4.1	38.0	19.7	7.4	0.42	CL
Gleyed Brunisolic	Workspace		5	Loam	51.8	31.4	16.8	1.29	2.643	1.9	3.3	29.2	22.8	7.2	0.38	ML
Gray Brown	alfalfa		30	Clay	23.4	24.7	41.9	0.97	2.673	0.5	5.5	40.6	20.4	7.4	0.48	CL
Luvisol			50	Heavy clay	2.7	36.3	61.0	0.15	2.708	0.3	28.7	44.1	23.4	7.7	0.34	CL
Houston Black	Natural	Mod. Well	12	Silty clay	9.8	43.2	47.1	1.21	2.651	2.4	40.0	57.1	25.9	7.4	0.66	CH
(TX)	grassland		35	Silty clay	7.8	45.7	46.5	0.54	2.669	1.6	44.8	50.8	21.9	7.5	0.62	CH
			150	Silty clay	3.6	45.0	51.5	1.10	2.737	0.0	32.2	64.5	19.6	7.5	0.87	CH
	Agricultural		13	Silty clay	11.2	40.2	48.6	0.81	2.68	1.4	18.2	56.5	20.5	7.5	0.74	CH
	corn		40	Silty clay	7.6	42.3	50.2	0.30	2.701	1.0	23.3	57.6	22.3	7.6	0.70	CH
Typic Haplustert			150	Silty clay	7.6	42.3	50.1	0.28	2.724	0.4	20.7	67.2	19.9	7.6	0.94	CH
North Gower (OT)	Natural	Poor	5	Silty clay	15.6	40.2	44.1	0.00	2.311	13.2	0.4	90.1	69.1	5.8	0.48	MH
	woodlot		25	Clay loam	26.0	34.8	39.2	1.27	2.726	0.6	0.6	42.9	21.2	6.4	0.55	CL
Marine			80	Heavy clay	1.6	32.8	65.6	0.00	2.751	0.8	1.9	60.6	23.8	6.9	0.56	CH
	Agricultural		5	Clay loam	20.7	41.0	38.3	0.45	2.576	2.0	0.2	40.9	24.9	6.4	0.42	CL
Orthic Humic	corn		30	Clay	5.3	37.3	57.3	0.18	2.712	0.5	0.4	56.8	28.6	6.8	0.49	CH
Gleysol			85	Silty clay loam	3.7	59.2	37.1	0.15	2.722	0.2	0.6	39.1	23.3	7.1	0.43	CL
Malmo (AB)	Natural	Well	6	Loam	24.4	48.6	27.0	0.70	2.56	4.5	0.6	45.5	30	6.0	0.57	ML
	grassland		43	Clay loam	30.1	32.2	37.7	1.46	2.689	0.6	0.8	44.2	17.7	6.1	0.70	CL
Glaciolacustrine			130	Clay loam	25.9	42.6	31.5	1.26	2.686	0.4	6.2	36.2	18.9	7.6	0.55	CL
	Agricultural		6	Clay loam	25.9	46.6	27.6	1.52	2.511	6.3	0.5	47.4	39.4	5.8	0.29	ML
Eluviated Black	barley		43	Clay loam	32.3	30.7	37.0	1.66	2.636	0.5	0.7	42.7	18.4	6.3	0.66	CL
Chernozem			130	Clay loam	26.1	39.9	34.0	1.32	2.698	0.3	3.0	39.4	18.9	7.4	0.60	CL

Table 2.4. Descriptive statistics of general soil properties.

	Valid N	Mean	Median	Minimum	Maximum	Std. Dev.	Skewness	Kurtosis	Distribution (p<.05)
% sand	54	17.4	16.7	1.59	51.8	10.9	.882	.940	lognormal
% silt	54	45.5	45.0	30.7	69.5	8.41	.477	.215	normal
% clay	54	37.1	37.4	13.2	65.6	12.2	.0004	-.516	normal
% organic carbon	54	1.90	.952	0.00	13.2	2.43	2.71	8.77	lognormal
ρ_P	54	2.65	2.68	2.31	2.75	.090	-1.79	3.74	-
w_L	54	45.2	43.2	22.4	90.1	12.3	1.15	2.44	lognormal
w_P	54	26.6	23.6	17.7	69.1	9.85	2.51	7.17	lognormal
pH	54	6.77	6.90	4.50	7.70	.815	-1.03	.469	normal
$CaCO_3$	54	7.37	1.05	.100	44.8	11.7	1.76	2.05	exponential
% gravel	54	2.73	1.23	0.00	17.0	4.00	2.32	4.96	exponential
VCS	54	1.26	1.03	0.20	3.80	.850	1.34	1.68	lognormal
CS	54	1.54	1.51	0.30	3.40	.753	.402	-.336	normal
MS	54	2.69	1.98	0.32	7.90	1.90	1.28	.956	lognormal
FS	54	4.92	3.55	0.32	20.6	4.46	1.56	2.47	lognormal
VFS	54	6.96	6.05	0.32	22.7	5.68	.738	-.315	exponential
FC	54	14.0	13.0	3.90	31.4	6.09	.841	.699	lognormal
CC	54	23.2	23.1	7.70	48.6	8.67	.826	1.29	normal
FSI	54	31.3	32.0	16.8	50.9	7.43	.252	.0588	normal
CSI	54	14.2	11.7	3.10	34.4	7.21	1.26	.977	lognormal

VCS=very coarse sand, CS=coarse sand, MS=medium sand, FS=fine sand, VFS=very fine sand, FC=fine clay, CC=coarse clay, FSI=fine silt, CSI=coarse silt

determined on all horizons, although difficulty was noted for some of the soils of low plasticity (I_P<4 for MDAC and MDAA).

A wide range in organic carbon (OC) contents was sampled, from the low organic matter content vertisols of TX to the high OC content of the natural horizons. The OTNA horizon had an OC content of 13.2% which is approaching the threshold of 17% used to classify organic soils in the Canadian system of soil taxonomy (Agriculture Canada Expert Committee on Soil Survey, 1987). The TXNC horizon had a 0% organic carbon content which was reported as 0.1% for calculating log values and which is the minimal detection and error level of the induction furnace. Values for pH tended to increase with depth. Elevated pH values in the workspace A horizons are indicative of deposition and/or mixing of subsoil/calcareous parent material during pipeline installation even though mitigation had been taken in recent excavations to stockpile subsoil materials on the opposite side of the trench. Of further note is that the ON and OT soil profiles

occur under imperfectly and poorly drained moisture regimes while the smectitic AB and TX sites have well and moderately well drained profiles, respectively.

Several of the soil properties were not normally distributed (Table 2.4). The significance of the distributions was tested using a combination of the Shapiro-Wilks W test, Chi-square, Kolmogorov-Smirnov D and Lilliefors probability estimate of D (Statistica, Statsoft, 1995). The variety of distributions, in addition to normal, is not surprising considering that one third of the samples are A horizons which will have much higher organic carbons, and one third are C horizons which will naturally have more carbonates than the A and B horizons, due to pedogenic processes. The range in soil particle size is narrower than that used by Veenhof and McBride (1996) but the range in OC, $CaCO_3$, pH, w_L and w_P are larger. OC did have a significant MNR*TRT*HOR 3-way interaction, largely dominated by differences between the OTNA horizon and other A horizons. There was a slightly significant variation in clay content by MNR ($p=.0585$) and TRT*HOR ($p=.1096$) as determined by ANOVA analysis. The TX soils had a higher clay content than the AB and ON soils ($p<0.05$) and the Natural C horizons had higher clay contents than the A horizons and Agr C, and the Workspace B horizons had higher clay contents than the Workspace A horizons.

The A-line category was assigned from the position on the plasticity chart using the Unified Classification System (Howard, 1984) (Figure 2.4). There were 6 MH horizons (inorganic silts of high plasticity), 9 CH horizons (inorganic clays of high plasticity), 27 CL horizons (inorganic clays, silty clays, sandy clays of low plasticity) and 12 ML horizons (inorganic silts, silty clays or clayey fine sands of low plasticity). The determination of the w_L before and after removing organic carbon was not done to determine OH or OL (organic clay or silt) classifications; however, 5 of the 6 MH horizons were A horizons with greater than 4% organic carbon and 10 of the 12 ML horizons were A horizons with greater than 1.9% organic carbon suggesting that these

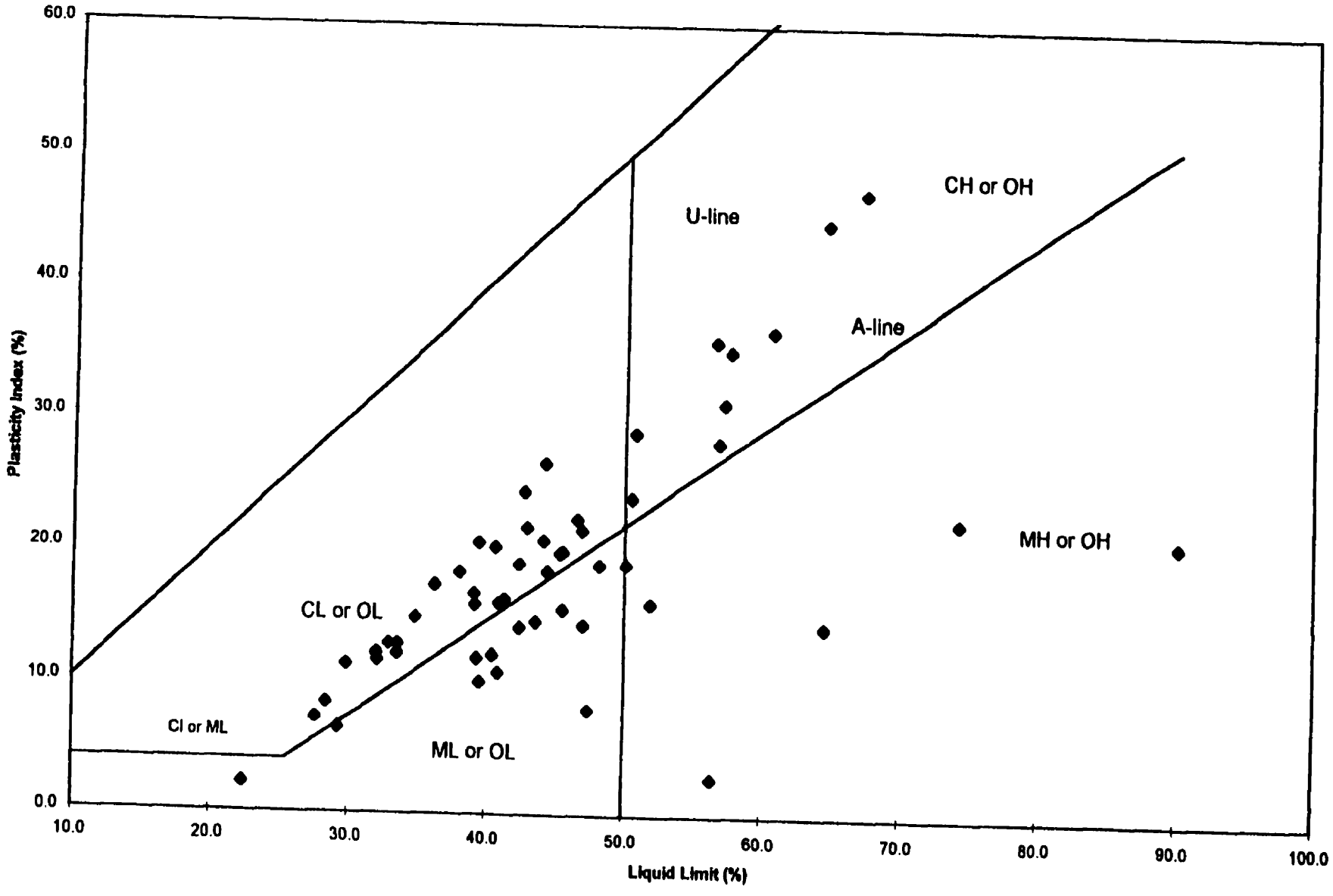

Figure 2.4. Position of soil horizon samples in Unified Classification Plasticity Chart.

may be OH and OL horizons, respectively.

The clay fraction mineralogy of these different sites are summarized in Table 2.5. No quantitative determinations were made, but a semi-quantitative analysis describing the dominant and relative amounts of minerals is presented. Notable differences in mineralogy occur for the Texas and Alberta soils which both have the swelling 2:1 mineral smectite as the dominant mineral. The Texas soils are also dominated by calcite as evident by the high $CaCO_3$ contents (Table 2.3) and the pedogenic formation of white carbonate nodules through all horizons due to the evaporative climate while the other soils have significantly less calcite. On the other hand the Alberta soils have clay mica and quartz present in significant amounts of which the Texas soils have none or trace amounts.

The southern Ontario soils are dominated by clay mica and/or vermiculite and also have significant amounts of quartz in the clay fraction. The dispersion between 1.0 and 1.4 nm in the X-ray diffraction traces indicates significant weathering of the clay mica to vermiculite and perhaps the incomplete expansion or contraction because of the presence of oxides and organic matter. Clay mica (illite) is a 1:1 non-expansive mineral while vermiculite is a 2:1 phyllosilicate with a lower layer charge than smectite. Of note is the presence of small amounts of clay-sized feldspars in all horizons of the North Gower soil and in the C horizon of the Maplewood soil. The presence of feldspars in the North Gower soil may be due to its marine lacustrine origin which differs from that of the southern Ontario soils which are largely derived from glacial till and glaciolacustrine deposits. The origin of the feldspars in the Maplewood soil is not known but note was made of the dense, virtually gravel-free, pinkish clay found in the C horizon at this site which differed from that at the other southern Ontario sites. Chlorite occurs in small to trace amounts for 3 of the southern Ontario soils from till parent material. Kaolinite is present in significant and small amounts in the Alberta and Texas soils, respectively, while it is absent or in trace amounts for many of the other

Table 2.5. Clay fraction (< 2μm) mineralogy.

Soil Series	Sampling Depth										
	cm	Vermiculite	Smectite	Clay Mica	Kaolinite	Chlorite	Quartz	Calcite	Dolomite	Feldspars	Lepidocrocite
Southern Ontario	3	2		1	3		1				
Brookston	22	2		1	4		2				3
	52	2		1	4		1				
Chinguacousy	3	2		1	4	4	2				
	20	2		1		4	1				
	53	2		1		3	1	2			
Tavistock	2	1		1	4	3	1				
	20	1		1	4	3	2				
	30	2		1		3	1	2			
Maplewood	5	1		2	3	3	2				
	30	1		2	3	3	2				
	60	1		1	4	3	1	3		3	
Texas	12		1		3		4	1			
Houston Black Clay	35		1		3		4	1			
	150		1		3		3	1			
Ottawa	5	1		2	3		2			3	
North Gower	25	1		2	4		2			3	
	80	1		2			2			3	
Alberta	6		1	2	3		2				
Ellerslie	43		1	2	2		2				
	130	3	1	2	2		2	4	4		

Relative abundance of mineral: 1. Dominant 2. Significant Amount 3. Small Amount 4. Trace

soils. A peak between 6.25 and 6.27 nm in the Brookston B horizon is thought to possibly represent lepidocrocite, an iron oxide polymorph of goethite. Although this diagnosis is based on only 1 peak, it is supported by the fact that the horizon was from a poorly drained Gleysol and had bright orange mottling as is indicative of this mineral (Allen and Hajck, 1989).

The activity values for the southern Ontario soils vary from 0.17 -0.52 (Table 2.3), lower than expected values for soil dominated by Ca-illite (0.5-1.3, Holtz and Kovacs, 1981) which may be due to the relatively high amount of quartz in the clay fraction of these samples (quartz activity =0). One horizon (MDNA) had exceptionally higher activity (0.77) due to a higher liquid limit which cannot be explained by clay mineralogy or organic matter content. For the Texas soil, the activity values range from 0.62-0.94 which is lower than would be expected from soils dominated by Ca saturated smectite mineralogy (1.5, Holtz and Kovacs, 1981). This low activity may be because of the high amount of calcite in these samples which only has an activity of 0.2 (Holtz and Kovacs, 1981). Similarly the Alberta soils' activity values range from 0.55 to 0.7 , lower than the Texas soil , which may be because of the significant amounts of clay mica. One exceptionally low value of 0.29 occurred for the ABAA horizon. There is a high plastic limit for ABAA which may be due to the higher organic matter levels that decreases the activity. A second determination of the plastic limit was 36.4 % which would result in an activity of 0.40. The Ottawa soils have activities similar to the southern Ontario soils (0.42-0.56). Lower than expected activities may have generally resulted from organic and inorganic C in the samples reducing the active surface area available for interactions (De Jong et al., 1990).

2.3.2 Remoulded Compression Results

The consolidation of the remoulded soils was plotted in $e(\log\sigma')$ co-ordinates from which a slope (C_C^*) and intercept (e^*_{1kPa}) for the normal consolidation line (NCL) were computed. The least squares fits for the remoulded line were $r^2 > 0.90$ except for 4 horizons. The Alberta Natural B horizon had the poorest fit at $r^2=0.577$. Note was made during the experiment of the difficulty of remoulding and mixing both the natural and agricultural B horizons from this site. The samples tended to settle, clump and stick to the bottom of the mixing container. It was also noted that these samples often required >36 hours to reach less than 5 kPa pore water pressure at pressures greater than 50 kPa. The AB Agricultural B horizon had an r^2 of .940 and parallels the natural horizon, i.e. the slopes are not significantly different but intercepts are significantly different at $p<.05$. No laboratory notes were made about the poor fits (.829-.889) for the other 3 horizons (ABNA, MDWA and MDAB). Observation of the graphs (in Appendix) indicates that the MDAB ($r^2=.861$) horizon has a concave curve which can also be seen in the MDAC plot ($r^2=.905$). Nothing precludes retaining these 4 horizons in the analysis. Another visual observation from these graphs is that there is a slight curvature in the NCL at stresses below 10 kPa for the HL B and C, MDWA and WAWB horizons which has also been noted by Veenhof and McBride (1996). Coleman et al. (1964) found that particularly stable aggregates only break down with prolonged and repeated remoulding.

The C_C^* and e^*_{1kPa} values were converted to values in $w(\log\sigma')$ co-ordinates after McBride and Baumgartner (1992) by dividing the parameters by the particle density and multiplying by 100%. Figure 2.5 shows a plot of the C_C^* values from both e and w plots against clay content. Similar to McBride and Baumgartner (1992) there is a relationship where values of -5 in w co-ordinates corresponding to values of -.1325 in e co-ordinates and 13% clay content, mark the

margin between marginally plastic and plastic soils. The marginally plastic horizon MDAC, I_P=2.2, has the least compressibility and approaches this boundary (slope of -5.18 % kg/kg or -.1391 and 13.2% clay).

The w_L and w_P were assumed to represent discrete points on the normal consolidation line plotted in $e(\log\sigma')$ co-ordinates. The stresses and drop cone depth associated with these points were calculated and are summarized in Table 2.6. There is a lot of variability at these stresses as evident by the high CV values which is likely associated with the wide range of organic carbon contents and textures. Of note is that the w_L stress (σ'_{wL}) for the Texas soils (4 kPa), all of which are CH soils, and for the CH soils (7.4 kPa) was lower than that for the Canadian soils. This is consistent with σ'_{wL} of about 5 kPa found by R. McBride (personal communication) for Australian smectitic vertisols. In addition these soils have a higher drop cone penetration, 21.0 and 20.4 mm, respectively, than the Ontario soils. It has been noted previously (Veenhof, 1993; McBride and Baumgartner, 1992; McBride, 1993) that a depth of 13 mm is more appropriate for Ontario soils than the BS standard of 20 mm based on British soils which are presumed to be smectite rich. The 13 mm drop cone depth would be appropriate here for the ML, CL and MH soils (average=13.16 mm) which include the Ottawa and Alberta soils.

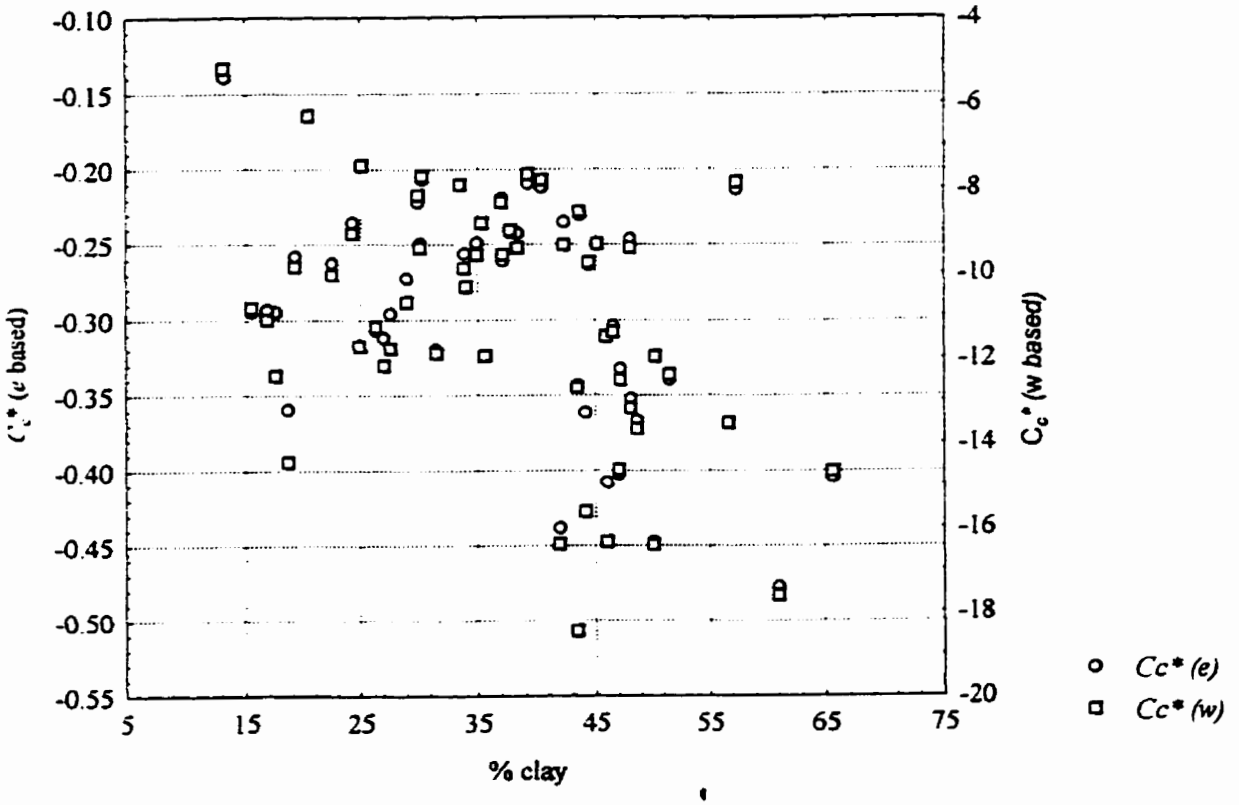

Figure 2.5. Slope of NCL (*e* and *w* based) vs. clay content.

Table 2.6. Liquid limit and plastic limit stress values from slurry consolidometer results.

		Drop cone	σ'_{wL}					σ'_{wP}				
Site	**n**	**mm**	**mean**	**std**	**CV%**	**min.**	**max.**	**mean**	**std**	**CV%**	**min.**	**max.**
LB	9	15.8	14.9	5.5	36.91	9.7	25.5	657.1	339.6	51.68	226.8	1349.0
HL	9	15.7	17.4	12.0	68.97	6.4	40.4	1032.2	659.2	63.86	170.3	1851.8
MD	9	11.9	29.7	8.6	28.96	16.3	46.2	527.0	621.7	117.97	48.1	1949.3
WA	9	12.3	31.0	18.0	58.06	7.1	60.3	535.5	462.6	86.39	104.4	1469.6
TX	6	21.0	4.0	2.0	50.00	1.2	7.2	2828.4	1491.7	52.74	1180.1	4984.5
OT	6	15.8	15.3	13.9	90.85	2.7	42.2	4102.9	4018.0	97.93	117.6	10681.7
AB	6	14.7	11.7	10.4	88.89	2.5	31.7	1340.9	1375.8	102.6	51.1	3712.0
Aline												
CH	9	20.4	7.4	7.7	104.05	1.2	25.1	3759.9	2966.6	78.9	1180.1	10681.7
MH	6	11.2	13.1	8.1	61.83	6.4	28.1	291.8	293.1	100.45	48.1	870.8
CL	27	14.8	25.4	14.6	57.48	2.5	60.3	1306.9	1268.0	97.02	143.0	6420.3
ML	12	13.5	16.1	11.3	70.19	7.1	46.2	293.6	347.4	118.32	51.1	1349.0
Horizon												
A	18	13.0	12.7	7.1	55.91	3.8	28.1	439.3	710.5	161.73	48.1	3070.5
B	18	16.9	16.6	14.2	85.54	2.5	52.6	2325.6	2586.7	111.23	352.1	10681.7
C	18	15.1	27.6	15.2	55.07	1.2	60.3	1368.4	1371.9	100.26	122.7	4984.5

2.3.2.1 Prediction of w_L and w_P from soil survey information

The current pedotransfer function concept requires construction of the NCL for which measurements or estimates of the liquid and plastic limits are needed. Forward stepwise regression was used to estimate the w_L and w_P from this thesis data. Particle density (ρ_p) was highly correlated to other variables, particularly organic carbon. Equations to predict the particle density from soil survey information are:

$\rho_p = 2.574 - 0.031\%organic\ carbon + 0.001\%\ clay + 0.013pH$ R^2=0.877 SEE=0.0325 [2]

$\rho_p = 2.675 - 0.033\%organic\ carbon + 0.001\%\ clay$ R^2=0.866 SEE=0.0337 [3]

To preserve the integrity of the "independence of variables" requirement in regression analysis, ρ_p was not included as a variable in stepwise multiple regression procedures. Regression equations were developed for two cases depending on the detail of soil survey information available: i) sand, silt and clay particle-size fractions, or ii) individual sand fractions, coarse and fine clay, and coarse and fine silt particle sizes as defined by Sheldrick and Wang (1993) for the Canadian system of taxonomy. The various sand fractions were not determined when the % sand was less than 10% (Ontario Institute of Pedology lab, personal communication) so values of % sand÷5 were entered for the 5 sand fractions for 19 horizons which may affect the interpretation of these regression equations. Only one particle size case was used at a time in forward stepwise regression to prevent multicollinearity.

Equations to estimate the w_L and w_P from this thesis data are as follows:

$w_L = 11.81 + 0.7037\%clay + 3.793\%OC$ [4]

F=119.7 SEE=5.274 R^2=0.824 P<0.001

$w_L = 3.851\%OC + 0.9394pH + 1.210\%fine\ clay + 0.3707\%coarse\ clay + 0.1936\%fine\ silt$ [5]

F=103.44 SEE=3.78 R^2=0.913 P<0.001

$w_P = 23.43+3.818\%OC-0.1982\%sand-0.0970\%CaCO_3$ [6]

F=348.7 SEE=2.166 R^2=0.954 P<0.001

$w_P = 25.93+3.769\%OC-0.6670\%medium\ sand-0.0959\%CaCO_3-0.2686\%very\ fine\ sand-0.1847\%fine\ clay$ F=283.7 SEE=1.872 R^2=0.967 P<0.001 [7]

All of these equations include % organic carbon as a variable. Smith et al. (1985) found organic matter to increase the liquid and plastic limit due to the effect of reducing compaction and to the strong attraction of water to humus so that greater amounts of water must be taken up before plasticity can be attained. This is similar to studies from as early as Baver (1930).

These equations can be compared to equations developed by other researchers (Watson, 1996; DeJong et al, 1990; Odell et al, 1960) to predict the consistency limits for different geographic areas, southern Ontario, Saskatchewan and Illinois, respectively.

Watson: $w_L = 16.5+3.2\%organic\ carbon+.54\%clay$ [8]

DeJong et al.: $w_L = 13.75+2.937\%organic\ carbon+.637\%clay$ [9]

Odell et al.: $w_L = 11.14+4.93\%organic\ carbon+.669\%clay$ [10]

Equation [4] is similar to Eq. [10] which has the component for % montmorillonite in the clay fraction removed. The authors noted that reasonably accurate estimates could be made of the w_L and w_P without the percent of montmorillonite as the amounts of clay and organic carbon are the most important determinants of Atterberg limits in soils dominated by montmorillonite and illite (2:1 lattice clays) (Odell et al., 1960).

There was a 1:1 relationship of the measured w_L to the w_L predicted by the Odell and DeJong equations, r^2=.919 and .800, SEE=2.99 and 4.69, respectively, for the 36 southern Ontario horizons. It is surprising there is such a good relationship for these w_L equations as they were developed on soils with smectite/montmorillonite mineralogy of which there are none in the ON soils. For the Watson equation there was a 1:1 relationship for southern Ontario once soils with

greater than 6.74% organic carbon were removed (r^2=.886, SEE=2.57). This is the organic carbon threshold of the pedotransfer function developed by McBride and Baumgartner (1992). The Watson (1996) equation is generally not used for soils with OC> 5% (R.A. McBride, personal communication).

There was not a 1:1 relationship between the w_L and the w_L predicted by the DeJong equation (Eq. [9]) for the Alberta soils. This is surprising as this equation was developed for the neighbouring province, Saskatchewan. There appeared to be a curvilinear relationship in which the w_L was overestimated for the A horizons in particular. Using the equation developed for the B and C horizons greatly underestimated the w_L (b1=2.9) but the relationship was more linear. When the AB and TX soils were combined there was a 1:1 relationship (r^2=.572, SEE=6.75, p=.0043), but there was a clustering of the TX soils due to their fairly uniform clay content throughout the profile. There was also a 1:1 relationship for the Watson equation for AB and TX w_L (r^2=.388, SEE=8.08,p=.0305).

There was a 1:1 relationship for the 6 OT horizon w_L and those predicted by the Watson and DeJong equations. When combined with the Ontario soils however there was not quite a 1:1 relationship (>6.74% organic carbon removed for the Watson equation). Lower confidence limits for the slope were 1.010 and 1.018, respectively, showing that the equations slightly underestimated the measured w_L.

The corresponding equations for the w_P from the 3 sources are:

Watson: w_P =15+3.67*%organic carbon*+.1*%clay* R^2=.614 [11]

DeJong et al.: w_P =10.95+1.156*%organic carbon*+.239*%clay* R^2=.35 [12]

Odell et al.: w_P =14.78+3.73*%organic carbon*+.101*%clay* R^2=.74 [13]

Again there is remarkable similarity between two equations, Eq. 11 and Eq. 13. The R^2 for these three equations are much poorer than those derived by equations [6] and [7]. It is interesting to

note that DeJong et al. (1990) chose to remove the sand variable to eliminate multicollinearity yet it is sand which is significant in the equations with the higher R^2. Derdour and Angers (1992) found w_P to be related to fine sand and organic matter content and w_L to be related to the clay and fine silt content of 16 soil horizons from Algeria which is similar to the results here.

There was a 1:1 relationship for all 54 soils for the Watson and Odell w_P equations (r^2=.922, SEE=2.78 for both). There is also a 1:1 relationship for the AB and TX soils alone for these 2 equations (r^2=.960, SEE=1.32). Similar to the Watson w_L equation, there is only a 1:1 relationship for the w_P of southern Ontario soils when those with >6.74% organic carbon are removed (n=33). There is also a 1:1 relationship for the Ontario and Ottawa soils combined when soils with >6.74% organic carbon are removed (Eq. 11).

In summary, there appear to be good existing equations, verified by regression analysis, to predict the w_L of southern Ontario and Ottawa soils, and the w_P of all 54 soils. The Illinois study in particular parallels the equations developed here. The soils from Illinois were calcareous to acid in reaction and from dominantly illitic glacial till to montmorillonitic loess (Odell et al., 1960). No existing equation was able to predict the w_L of the smectitic soils measured here. This may be due, especially for the Texas soils, to the high percentage of calcium carbonate (18.2-44.8%) which exceeded the range used to establish the existing prediction equations. The best predictive equations for the w_L for AB and TX from the existing data are:

$$w_L = 54.954 - 1.1655\%sand - 12.3765 log(\%CaCO_3) + .6355\%clay \quad [14]$$

R^2=.9254 SEE=3.1535 F=33.088 p=.00007 n=12

$$w_L = .4592\%organic\ carbon^2 + 1.4315\%fine\ clay + .6676\%fine\ silt \quad [15]$$

R^2=.9275 F=38.385 p=.000019 SEE=2.9311 n=12

2.3.2.2 Estimation of stresses at the w_L and w_P using the measured NCL

Validating the theory for the existing pedotransfer functions required independent predictions of the stresses associated with the Atterberg limits. This was done assuming that the liquid and plastic limit occupy discrete locations on the NCL in $e(\log\sigma)$ co-ordinates. Both ANOVA/ANCOVA and forward stepwise regression modelling procedures were used. ANOVA/ANCOVA are more suited to testing the significance of non-continuous, class variables such as horizon, land use and mineralogy but become too complex for testing more than one covariate (continuous) variable at a time for which the regression approach is more suitable.

a) ANOVA/ANCOVA approach

The predictive equations generated by the ANOVA/ANCOVA approach have one mean square error (MSE) and correlation coefficient (R) for either a single equation or a series of equations (numbered as one equation) depending on the form of the model. The MSE is the residual error term estimated via restricted maximum likelihood iterations in PROC MIXED; there may be additional error terms in the model used to test higher order factors in the split plot design. The R value is derived from a simple correlation using PROC CORR, comparing the predicted and observed values. Asymptotic standard errors (SEE) for the equation parameters and variance estimates are estimated from the first derivative found during the Newton-Raphson iterations (SAS Institute, 1997; W. Matthes-Sears, personal communication).

The ANOVA analysis for the measured liquid limit stress indicated a significant MNR*TRT*HOR interaction. The 3-way interaction represents single horizons without replication (except ON) which indicates significant differences between individual horizons but makes systematic explanation very difficult. When the log(% organic carbon content) (logOC) was included as a covariate, the model was simplified to only having mineralogy as a factor. There were differences in the intercepts and slopes depending on the mineralogy. The difference in

slopes means that the organic carbon level must be considered when comparing 2 mineralogies (Cochran and Cox, 1957). The following equations describe the model (n=54, MSE=.06095, R=.9681):

i) AB: $\ln(\sigma'_{wL}$ kPa +3)=2.506916+.219106*logOC SEb0=.2922, SEb1=.50718 [16]

ii) ON: $\ln(\sigma'_{wL}$ kPa +3)=3.177840-.6232798*logOC SEb0=.1399, SEb1=.22900

iii) OT: $\ln(\sigma'_{wL}$ kPa +3)=2.72364002-.805525*logOC SEb0=.2922, SEb1=.34084

iv) TX: $\ln(\sigma'_{wL}$ kPa +3)=1.94428+.299845*logOC SEb0=.2952, SEb1=.39534

The intercepts for the smectite-rich soils (AB&TX) are significantly different than the other mineralogies (ON&OT) (p=.0155). Similarly the slopes for the smectite-rich soils are significantly different than those for the other mineralogies and are opposite in sign (p=.0200); however the slopes for AB and TX are not significantly different than 0. The above equation set Eq.[16, i-iv] was used to predict the σ'_{wL} for the different mineralogies and compared to the measured σ'_{wL}. When the untransformed σ'_{wL} values were compared there was a significant 1:1 relationship (SEE=.4536, F=61.46, p<.001) for the ANOVA results but not much of the variability was explained (r^2=.5417). When the values were back transformed, there remained a 1:1 relationship and the r^2 remained low (r^2=.5105, SEE=9.8795).

The σ'_{wL} predicted from the equations of the ANCOVA analysis, Eq. [16, i-iv], gave a good prediction of the measured w_L when inserted into the measured NCL, in that there was a significant 1:1 relationship.

w_L =2.09525+.949079 *pred*w_L [17]

r^2=.9557, SEE=2.6245, SEb0=1.3348, SEb1=.02835

For the plastic limit stress there was a simpler ANOVA model with significant MNR and HOR factors for $\ln(\sigma'_{wP})$ (Table 2.7). There was a significant difference (p=9.30e-4) between the average of AB and ON sites (back transformed mean (BTM)=551.7 kPa) and the TX and OT sites

Table 2.7. LSmeans separation pdiff and LSmean values for ln(σ'_{wP} (kPa)).

Factor	MNR						HOR		
	AB vs ON	AB vs OT	AB vs TX	ON vs OT	ON vs TX	OT vs TX	A. vs. B.	A vs. C	B vs. C
p-value	.4620	.0491*	.0253*	.0033*	.0013*	.7365	5.97e-5*	.0012*	.1498
	AB	ON	OT	TX			A	B	C
LSmean	6.4733	6.1529	7.6358	7.8219			5.9327	7.8258	7.3044
LSmean Back Transformed (kPa)	647.6	470.1	2071.0	2494.6			377.2	2504.3	1486.8

(BTM=2272.9 kPa), as well as between the A (BTM=377.2 kPa) and the average of the B and C horizons (BTM=2241.9 kPa) (p=6.24e-5). The A horizon mean and Alberta and Ontario means are not significantly different than the average of 420 kPa used by McBride and Baumgartner (1992). The w_P predicted from the average 550 kPa for ON and AB and 2270 kPa for AB and TX determined by ANOVA analysis had a significant 1:1 relationship (r^2=.7446, SEE=5.0241) with a better r^2 and slightly smaller SEE than when a simple average of 420 kPa was used. These values are used later in calculating slopes and intercepts of the NCL. Although this was a significant ANOVA model with or without an outlier, the residuals were not always reliably normal (p=.007-.07).

When organic carbon was added as a covariate, the residuals were normally distributed and there were no outliers. The model was more complicated in that there were significant TRT and OC*MNR factors. Essentially the mean σ'_{wP} for the Natural treatment (BTM=1207.1kPa) is consistently higher than the average of the Agricultural and Workspace (BTM=839.7 kPa, p=.0147) treatments. The differences between mineralogies will depend on the level of organic matter they are compared at because of the significant OC*MNR factor. The model for the Agricultural treatment will be (n=54, MSE=.20835, R=.9639): [18]

i) AB: ln(σ'_{wP} kPa)=7.55454-.569633**%organic carbon* SEb0=.5989, SEb1=.1633

ii) ON: ln(σ'_{wP} kPa)=6.453527-.252913**%organic carbon* SEb0=.26086, SEb1=.07073

iii) OT: $\ln(\sigma'_{wP}$ kPa)=7.98645-.2001002**%organic carbon* SEb0=.45739, SEb1=.06256

iv) TX: $\ln(\sigma'_{wP}$ kPa)=8.747037-.806167**%organic carbon* SEb0=.60055, SEb1=.42298

These models are shifted rigidly in the intercept from the Agricultural model by +.36102 for the Natural Treatment (p=0.0173) and -.00406 for the Workspace treatment, although the Workspace is not significantly different (p=.9817) than the Agricultural treatment. The Ontario intercept is significantly different than the average of the other mineralogies and the slope of the smectite mineralogies is again different than the average of the slopes for the other 2 mineralogies. The TX slope is not significantly different from 0 (p=.0687).

The σ'_{wP} predicted from these ANCOVA equations Eq. [18, i-iv] (no adjustment between Workspace from Agricultural) has a 1:1 relationship when untransformed (r^2=.800, SEE=.1443) with the measured σ'_{wP} but not when back transformed values are compared. The w_P predicted using the NCL and the σ'_{wP} predicted from Eq. [18, i-iv] gave a significant 1:1 relationship (r^2=.912, SEE=2.948, n=54).

Both ANCOVA models indicate the significance of organic carbon and mineralogy in determining the stresses associated with the consistency limits, and the additional variation for predicting the σ'_{wP} in the natural land use condition. In terms of mineralogy, it can be seen from the above models that Ontario and/or Ottawa are differentiated from the Alberta and Texas soils to varying degrees which is likely related to the smectitic mineralogy of these two soils.

The ANCOVA analysis showed that there was an opposite in sign and statistically insignificant relationship for AB and TX soils and logOC when predicting σ'_{wL} which the McBride and Baumgartner (1992) pedotransfer equation is based upon. Given that the AB and TX soil σ'_{wL} did not have a significant relationship with logOC, the simple arithmetic means of the σ'_{wL}, , 11.7 and 4.0 kPa, respectively, and a regression for OT and ON soils with logOC were used to predict the σ'_{wL} and w_L. Equation [19] was derived in Statistica for the ON and OT soils.

σ'_{wL} (kPa)=23.1-17.6*logOC [19]

F=19.6, p<.001, r^2=.329, SEE=11.388 n=42, SEb0=1.771, SEb1=3.978

This equation for Ontario and Ottawa takes the same form as the McBride and Baumgartner (1992) equation but with a poorer fit. The new equation could go up to 20.56% organic carbon before σ'_{wL} becomes negative. The w_L for ON and OT predicted using equation [19] do not have a 1:1 relationship with the measured w_L. When all 54 soil horizons were analyzed together using the means and Eq [19] there were significant 1:1 relationships for the predicted σ'_{wL} (r^2=.445, SEE=10.516) and w_L (r^2=.943, SEE=2.954).

b) Regression approach

The corresponding stresses at the liquid limit and plastic limit were estimated by forward stepwise regression. Including activity (I_P÷%clay) as a variable tended to increase the r^2 (or R^2) of the regression equations by 5 to 30%. Activity would aid in explaining differences in mineralogy between the sites. It was decided, however, not to include activity in the forward stepwise procedures because it is a variable determined a posteriori, i.e. after the w_L and w_P are known, and therefore would not be useful in predictive equations for the Atterberg limits or the corresponding stresses.

Equations to predict log(σ'_{wL}) and σ'_{wL} are presented in Table 2.8. The r^2 (or R^2) values improved by using information from the more detailed particle size analysis although the R^2 rarely went above 0.70. Many of the relationships derived include the percentage sand (or some sand fraction) as a parameter. The difficulty in deriving relationships of high predictive ability (r^2>0.80) for the liquid limit stress may be related to the inclusion of the coarser sand fractions (i.e. not sieved to <0.425 mm) for slurry consolidation. Although of lower predictive capability, the greater significance of these equations over that proposed by McBride and Baumgartner (1992) (R.A. McBride, personal communication) is encouraging .

Table 2.8. Equations to estimate liquid limit stress divided by A-Line category.

No.	Soil Group		Equation (σ' in kPa)	n	SEE	r^2 (R^2)	*P*<
i	All	fractions	$\log_{10}(\sigma'_{wL})$=2.0196-0.2453log(*%oc*)-0.0601*%med. sand* -0.0507*%fine clay*	54	.2465	.598	0.00000
ii	All		$\log_{10}(\sigma'_{wL})$=2.060-0.0169*%clay*-.0128*%sand*-.0268% $CaCO_3$ +.427 log(*%*$CaCO_3$)	54	.3266	.309	0.00101
iii	All	fractions	σ'_{wL}= 49.37-1.654*%fine clay* - 11.58log(*%oc*)-5.606*coarse sand* + 5.535log(*%*$CaCO_3$)	54	9.091	.609	0.00000
iv	All		σ'_{wL}= -35.14+4.729 *pH* +.492*%silt*-8.80*%oc*	54	12.006	.305	0.00037
v	CL,ML, MH	fractions	$\log_{10}(\sigma'_{wL})$=1.922 -0.0507 *%med. sand* -.2059 log*%oc* -0.09857*%coarse sand* - 0.03245*%fine clay*+.16481.log(*%*$CaCO_3$)	45	.1791	.699	0.00000
vi	CL,ML, MH		$\log_{10}(\sigma'_{wL})$=-0.0101*%sand* + 0.2155*pH*	45	.2221	.489	0.00000
vii	CL,ML, MH	fractions	σ'_{wL}= -9.0208+6.302 *pH* +10.67log(*%*$CaCO_3$)-6.0067*coarse sand* -.6413*fine sand*	45	8.277	.678	0.00000
viii	CL,ML, MH		σ'_{wL}= 4.037 *pH* +11.75log(*%*$CaCO_3$)-0.3727 *sand*	45	9.242	.575	0.00000
ix	CL,ML	fractions	$\log_{10}(\sigma'_{wL})$=2.468 -0.2426 *%coarse sand* +0.1678 log% $CaCO_3$ -0.0217*%very fine sand* -0.0482*%fine clay* -.06608*%organic carbon*	39	.1618	.765	0.00000
x	CL,ML		$\log_{10}(\sigma'_{wL})$=-0.0109*%sand* + 0.2194*pH*	39	.2269	.482	0.00000
xi	CL,ML	fractions	σ'_{wL}= 34.30+17.51log(*%*$CaCO_3$)-9.603*coarse sand*	39	8.413	.667	0.00000
xii	CL,ML		σ'_{wL}= 4.326 *pH* +11.07log(*%*$CaCO_3$)-0.4370 *sand*	39	9.386	.586	0.00000
xiii	CH,MH	fractions	$\log_{10}(\sigma'_{wL})$=1.482-0.0345*%fine clay*	15	.2714	.526	0.00220
xiv	CL	fractions	$\log_{10}(\sigma'_{wL})$=1.505 - 0.0444 *medium sand*-0.05567*%fine clay* +.0198*%coarse clay*+ .01497*%coarse silt*	27	.1746	.763	0.00000
xv	CL		$\log_{10}(\sigma'_{wL})$=-0.0152*%sand* + 0.2316*pH*	27	.2221	.564	0.00000
xvi	CL	fractions	σ'_{wL}=-12.29+ 8.090 *pH* +9.187log(*%*$CaCO_3$)-10.16*coarse sand*-.7134*%very fine sand*	27	8.312	.726	0.00001
xvii	CL		σ'_{wL}= -61.08+ 14.13 *pH* -.5964% *sand*	27	9.726	.591	0.00002
xviii	CH		$\log_{10}(\sigma'_{wL})$=2.925-0.0724*%fine silt*	9	.2551	.644	0.00927
xix	CH	fractions	σ'_{wL}= 51.13 -1.422% *fine silt*	9	4.805	.662	0.00761

No.	Soil Group		Equation (σ' in kPa)	n	SEE	$r^2(R^2)$	$P<$
xx	CH		$\log_{10}(\sigma'_{wL})$=5.093-0.1210% *silt* +0.4705 log(%$CaCO_3$)	9	.1958	.820	0.00583
xxi	CH		σ'_{wL}= 92.06 -2.326% *silt* +8.861 log(%$CaCO_3$)	9	3.819	.817	0.00612
xxii	MH	fractions	σ'_{wL}= 32.54-.8795%*coarse clay*	6	5.238	.663	0.04859
xxiii	ML	fractions	$\log_{10}(\sigma'_{wL})$=1.174+0.5068% log(%$CaCO_3$) -0.2474%*coarse sand*+.01313%*fine silt*	12	.0911	.890	0.00035
xxiv	ML		$\log_{10}(\sigma'_{wL})$=1.650-0.5451 log(%*oc*) -0.0110%*clay*	12	.1289	.752	0.00189
xxv	ML	fractions	σ'_{wL}= 50.39-1.611%*fine clay* - 7.242%*coarse sand* + 1.478%$CaCO_3$ - .6599%*coarse silt*	12	3.213	.948	0.00014
xxvi	ML		σ'_{wL}= 42.87-0.5838%*clay* - 27.92log(%*oc*)	12	4.459	.872	0.00010
xxvii	S. Ont	fractions	$\log_{10}(\sigma'_{wL})$=1.381+0.2725% log(%$CaCO_3$) -0.0991%*very coarse sand* - 0.1882 log(%*oc*)	36	.1658	.642	0.00000
xxviii	S. Ont		$\log_{10}(\sigma'_{wL})$= -0.2058log(%*oc*) + 0.1938*pH*	36	.1802	.550	0.00000
xxix	S. Ont	fractions	σ'_{wL}= 23.46 - 5.692%*very coarse sand* + 14.858log(%$CaCO_3$)-9.537log(%*organic carbon*)	36	7.778	.699	0.00000
xxx	S. Ont		σ'_{wL}= 21.09-9.607*log(%oc)* + 11.26log(%$CaCO_3$)	36	9.087	.577	0.00000

The r^2 (and R^2) values above and through much of this dissertation are relatively low, even though the relationships are highly significant ($p<0.001$ unless otherwise stated). The amount of variability generally accepted in the soil science literature is $r^2>0.7$-0.8 for predictions made for soil water retention data or bulk density for example. In contrast, the geotechnical literature provides few, if any, statistics regarding "universally accepted" predictive equations relating soil constitutive properties and mechanical behaviour. The coefficients of determination can be particularly low when comparing soils with origins from around the globe as is typically done to arrive at general equations. For example, one of the most widely adopted equations for predicting the compression index based on the liquid limit is Equation [20] which has a reliability range of about ±30% (Holtz and Kovacs, 1981).

$$C_C=.009(w_L-10) \qquad [20]$$

When applied to this thesis data, it results in a significant 1:1 relationship but an r^2 of only 0.38. According to the geotechnical literature, in which much more extensive work relating soil constituent properties and mechanical behaviour has been done, equations with r^2 (or R^2) values in the range 0.40-0.60 appear to be justified in their use, especially across widely varying soil properties. Therefore, equations with low r^2 (and R^2) (i.e. those <0.70) will continue to be reported, as long as they are significant, to provide insight into factors controlling mechanical behaviour in this rather exploratory work.

The pH and log($CaCO_3$) variables were significant in many regression equations and they are also correlated to each other (R=0.763) . The liquid limit of highly calcareous (25-61% $CaCO_3$), attapulgite soils from Egypt increased with increasing $CaCO_3$ up to 35%; the plastic limit stayed rather constant, so the plasticity index showed the same tendency as the liquid limit (Stakman and Bishay, 1976). The same trend occurred for clay up to 30-40% so it is difficult to separate the effects of clay and carbonate (Stakman and Bishay, 1976). De Jong et al. (1992)

found the opposite effect, with increased levels of inorganic C reducing the Atterberg limits and the plasticity index of the B and C horizons and having no effect on the A horizons. De Jong et al (1992) also had lower than expected activities due to the organic and inorganic C in the samples reducing the extent of the surface area available for interactions. Smith et al. (1985) found that $CaCO_3$ had little influence on the Atterberg limits of calcareous Israeli soils compared to clay content and CEC. Stakman and Bishay (1976) found that not only the total amount of $CaCO_3$, but also the distribution of $CaCO_3$ over the particle size fractions influenced the plasticity limits. In the Egyptian soils, 88-100% of the $CaCO_3$ was present in the clay and silt fraction. The higher amount of $CaCO_3$ does not need to imply a greater surface area; Holfod and Mattingly (1975 in Stakman and Bishay, 1976) found that surface area of $CaCO_3$ was an inverse function of the $CaCO_3$ percentage. The $CaCO_3$ could also affect the plasticity due to the predominance of Ca on the exchange sites which favours electrostatic attraction between positive edges and negative clay faces leading to a flocculated particle arrangement which increases the Atterberg limits and the I_P (Baver, 1930; Dexter and Chan, 1991; Sridharan et al., 1988). Rimmer and Greenland (1974) and Desphande et al. (1964) found calcium carbonate to suppress the swelling of sieved and compacted soils by suppression of the diffuse layer and because it acted as a cement or coating which prevented access to parts of the external surface. Organic carbon and clay contents were often significant variables but not as frequently as sand, $CaCO_3$ content and pH in predicting the liquid limit stress. These relationships are unlike the previous relationship derived by McBride and Baumgartner (1992) which found the stress at the liquid limit to be independent of texture but significantly related to the logarithm of organic carbon.

When divided by A-line group, the R^2 values for the liquid limit stress determination improved (Table 2.8). The best relationships, R^2 from 0.66 to 0.95, were determined for the MH and ML groups which are the high and low plasticity silts and organic soils, respectively. The

relationships describing the least amount of variability, surprisingly were for the CL soils which would be most similar in terms of mineralogy and behaviour to the soils used for the slurry consolidometer development.

The w_L predicted by substituting the regression predicted σ'_{wL} (Table 2.8, Equation iii) into the measured NCL did not result in a significant 1:1 relationship but it did have a high r^2 =.919.

w_L =6.6633+.85024*pred* w_L [21]

SEb0=1.657, SEb1=.03501, F=589.7, p<.001

Eq. [21] had a SEE=3.548 which was considerably higher than that found by Veenhof (1993; SEE=0.089) when using the McBride and Baumgartner (1992) equation for southern Ontario soils. This SEE is also higher than the one with the predicted σ'_{wL} from ANCOVA equations (Eq. 16).

The σ'_{wP} could be determined by the following equations.

For all horizons (n=54):

$\log_{10}(\sigma'_{wP}$ kPa)=2.069+0.0260*%clay*-0.1010*%oc* SEE=0.3121, R^2=0.675 [22]

$\log_{10}(\sigma'_{wP}$ kPa)=2.849+0.0375*%fine clay*-0.1057 *%oc* -0.0232 *%coarse silt* SEE=0.286 R^2=0.732 [23]

For southern Ontario (n=36):

$\log_{10}(\sigma'_{wP}$ kPa)=2.226+0.0182*%clay*-0.0972*%oc* SEE=0.2579, R^2=0.639 [24]

$\log_{10}(\sigma'_{wP}$ kPa)=1.939+0.0429*%fine clay*-0.1215*%oc* + 0.0142 *%fine silt* SEE=0.2494 R^2=0.673 [25]

There were no significant relationships for σ'_{wP} with normally distributed residuals without a log transformation. There was no improvement in R^2 by segregating into A-line categories. Again these relationships are highly significant but have limited predictive capability and the inclusion of the sand fraction may have given inconsistent results. The σ'_{wP} estimated by Eq. [23] resulted in a strong 1:1 relationship in log(log) co-ordinates (r^2=.7318, SEE=.2860). There remained a 1:1 relationship with the back transformed values but the residuals were not normally distributed, the r^2

was low(r^2=.32686) and the standard error of estimate was unacceptably high (SEE=1553.2 kPa).

Although not a 1:1 relationship, the w_P values computed using Eq. [23] had the following equation.

w_P =3.189+0.8876**pred* w_P [26]

SEb0=1.0114, SEb1=.03566, r^2=0.9225, SEE=2.7667

Equation [27] was developed by Veenhof (1993) for estimating the σ'_{wP} for soil horizons from Middlesex County and Haldimand-Norfolk Region.

σ'_{wP} kPa =(16.5*%clay)-(13*%clay*log(%organic carbon)) [27]

r^2=.66, SEE=202.1 kPa, p<.001

Eq. [27] was used to estimate the stress at the plastic limit and substituted into the measured NCL . This substitution resulted in a 1:1 relationship for w_P:

w_P =1.332+.9069**pred* w_P [28]

F=342.7 r^2=.8682 SEE=3.6085 SEb0=1.448 SEb1=.0490

The standard error is of the order found by Veenhof (1993; SEE=2.24) and is an improvement over the average 420 kPa used by McBride and Baumgartner (1992). The SEE and r^2 for the w_P derived from Eq. [27] are not as good as those derived from Eq. [18, i-iv] in the ANCOVA approach, likely due to combining mineralogy's and/or exclusion of activity as a parameter.

Stepwise regression was then undertaken for AB and TX soils separately from ON and OT soils as the ANCOVA analysis tended to find significant differences between these 2 groups. Results are displayed in Table 2.9. The sample size was small (n=12) so care was taken not to overparameterize the model. Significant improvements in the models were made for $\log(\sigma'_{wL})$ with AB and TX combined over CH soils alone for the equations with the subdivided fractions. The R^2 were also high for the $\log(\sigma'_{wP})$ models for AB and TX compared to the equations for all horizons. This may be partially attributed to the smaller n available relative to the number of parameters

Table 2.9. Equations to estimate liquid limit stress and plastic limit stress grouped by mineralogy.

No.	Soil Group		Equation (σ' in kPa)	n	SEE	r^2 (R^2)	$P<$
i	AB,TX	fractions	$\log_{10}(\sigma'_{wL})$=-.61037+.26836log(*%oc*) -0.04728%*fine clay*-.06191%*coarse clay* +.51173*pH*	12	.1660	.875	0.00283
ii	AB,TX		$\log_{10}(\sigma'_{wL})$=-0.049773 %*clay* +.39392*pH*	12	.18726	.772	0.00061
iii	AB,TX	fractions	σ'_{wL}=-22.2243-1.0747%*fine clay* +11.932*pH*-1.5489%*coarse clay*	12	4.2662	.804	0.00337
iv	AB,TX		σ'_{wL}= -22.7657-1.1105%*clay*+10.7995 *pH*	12	4.1367	.792	0.00085
v	ON,OT	fractions	σ'_{wL}=26.3378-9.0787log%*organic carbon* +14..643log(%$CaCO_3$)-4.6678% *very coarse sand*	42	8.819	.618	0.00000
vi	ON,OT		σ'_{wL}= 20.699-9.3688log(%*organic carbon)* +11.41log(%$CaCO_3$)	42	9.53	.542	0.00000
vii	AB,TX	fractions	$\log_{10}(\sigma'_{wP})$=2.806+0.0260%*fine clay*-.0352%*organic carbon*^{2}	12	.17616	.925	0.00001
viii	AB,TX		$\log_{10}(\sigma'_{wP})$= 1.728-.0344%*organic carbon*^{2} +.0448%*clay*-.3155log(%$CaCO_3$)	12	.12543	.966	0.00000
ix	AB,TX	fractions	σ'_{wP}=111.01%*fine clay*	12	1121.9	.492	0.00759
x	AB,TX		σ'_{wP}=-5566+213.6%*clay*-65.90%$CaCO_3$	12	971.9	.688	.00531
xi	ON,OT	fractions	$\log_{10}(\sigma'_{wP})$=2.030+0.04020%*fine clay*-.08663%*organic carbon* +.01729%*coarse clay*	42	.3104	.649	0.00000
xii	ON,OT		$\log_{10}(\sigma'_{wP})$= 2.0776-.0852%*organic carbon* +.0237%*clay*	42	.3122	.636	0.00000
xiii	ON,OT	fractions	σ'_{wP}=55.15%*coarse clay*	42	1750	.170	0.00595
xiv	ON,OT		σ'_{wP}=36.72%*clay*	42	1757	.164	.00708

used to fit the model. The combining of ON and OT soils generally reduced the predictive capability relative to the ON soils alone for both the plastic and liquid limit stresses.

When grouped by mineralogy (Table 2.9), the role of organic carbon and clay content on the σ'_{wL} and σ'_{wP} became more evident rather than the various sand fractions. The pH and the $CaCO_3$ content continued to play important roles. Of note is that OC or logOC are important in the ON and OT equations for σ'_{wL}, $\log\sigma'_{wL}$, and $\log\sigma'_{wP}$, but only $\log\sigma'_{wP}$ for the AB and TX horizons.

Eq. [iv and vi] (Table 2.9) were used to predict the σ'_{wL} which was then inserted into the measured NCL to arrive at significant 1:1 relationships between the predicted and measured σ'_{wL} (r^2=.644, SEE=8.431, b0=.01245, SEb0=2.267, b1=.9995, SEb1=.10315, $p<0.001$) and w_L (r^2=.967, SEE=2.277, b0=1.602, SEb0=1.164, b1=.9669, SEb1=.0249, $p<0.001$). Use of the separate regression equations for smectite-rich vs. non-smectitic soils gave significant improvements over using Eq. [19] for ON and OT and the means for AB and TX from the ANOVA analysis (page 78), or Eq. [iii](Table 2.8) for all soils combined. This analysis confirmed that the liquid and plastic limits occupy discrete positions on the NCL, the stresses which can be predicted reasonably well from soil survey information.

2.3.2.3 Comparison to existing PTF2 equations

Testing of the PTF derived by McBride and Baumgartner (1992), for estimating σ'_{wL} Eq. [29], was undertaken with this independent dataset to validate the equation's application to southern Ontario soils and determine if it was appropriate for use outside this region.

σ'_{wL} =26.6-32.1*log(%Organic Carbon) [29]

r^2=.835, SEE=6.1kPa, n=25

(58.7 kPa for soils with 0% organic carbon). There was not a 1:1 relationship between the σ'_{wL} predicted by Eq. [29] and the measured σ'_{wL} (r^2=.1435, SEE=13.068, n=54).

Calculating the w_L from the predicted σ'_{wL} and inserted into the measured NCL also did not result in a 1:1 relationship. It could be seen that 4 of the MH soils clearly did not follow the 1:1 line (Figure 2.6). These horizons had an organic carbon content greater than the upper limit for Eq. [29] (>6.74%) which resulted in calculation of a negative stress value for which either 1 kPa or 5 kPa was substituted. When the 6 MH horizons were removed, a significant 1:1 relationship between the predicted and observed liquid limit occurred (Eq. [30]).

w_L =.4683+1.0506*pred* w_L [30]

F=104.9, r^2=.6951, p<.001, SEE=5.3775, SEb0=4.199, SEb1=.10258, n=48

Substituting the mean stress (15.6 kPa) for the 4 MH horizons into the NCL also resulted in a significant 1:1 relationship for the predicted and observed w_L (Figure 2.7) suggesting that this may be an appropriate stress value to use when the organic carbon content exceeds 6.74%. When the clustered TX (CH) soils were removed the 1:1 relationship also improved (r^2=.9114, SEE=3.5701, n=48).

There is a significant 1:1 relationship between the predicted and observed σ'_{wL} for just the Ontario soils when Eq. 29 is used and the 15.6 kPa mean is substituted for soils with OC>6.74% (r^2=.47358, SEE=9.981, n=36). When the Ottawa horizons were included, there was also a 1:1 relationship (r^2=.3988, SEE=10.78, n=42). There was also a 1:1 relationship with Eq.[29] and 15.6 kPa substituted for the negative stresses and the means for TX and AB for the w_L (r^2=.955, SEE=2.63) but not the σ'_{wL}.

The prediction of the σ'_{wL} from Eq. 29 was, thus, only valid for non-smectitic soils and confirms the results of the ANCOVA analysis (Eq. [16]). When predictions of w_L are made, however, the 1:1 relationship supports the use of Eq. 29 to predict the w_L from a measured NCL

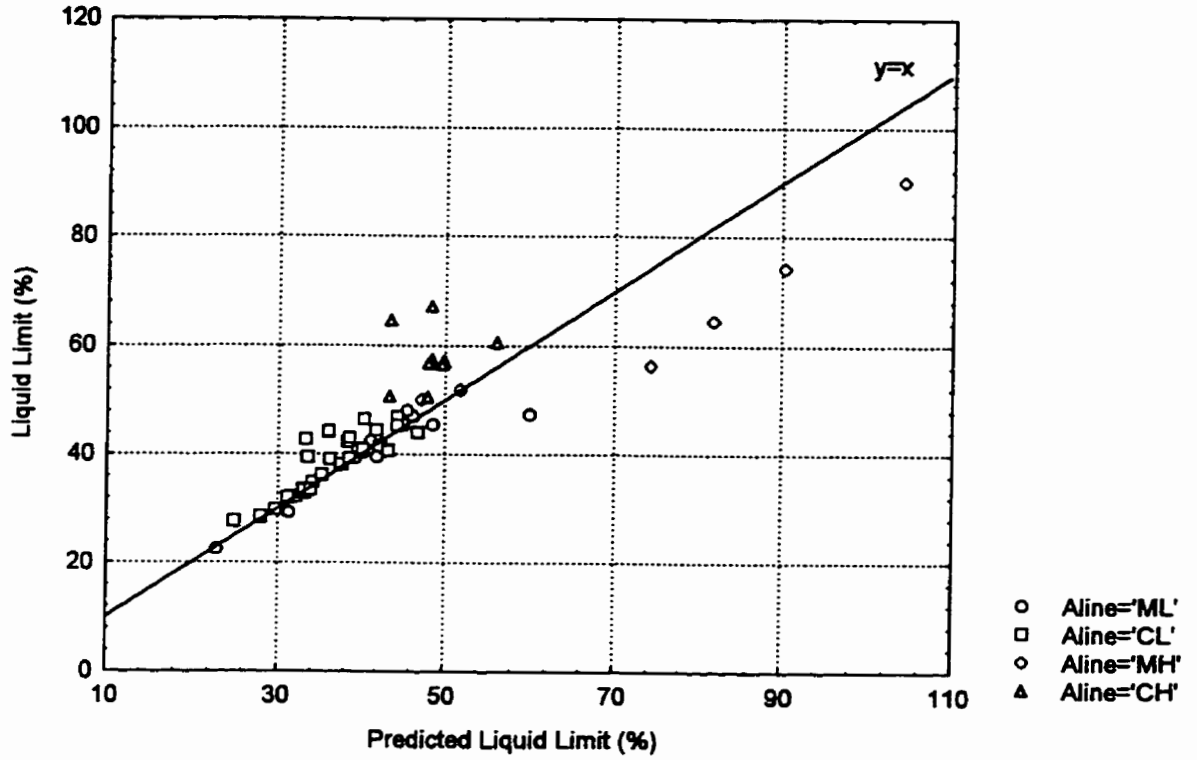

Figure 2.6. Comparison of w_L predicted using Equation of McBride and Baumgartner (1992).

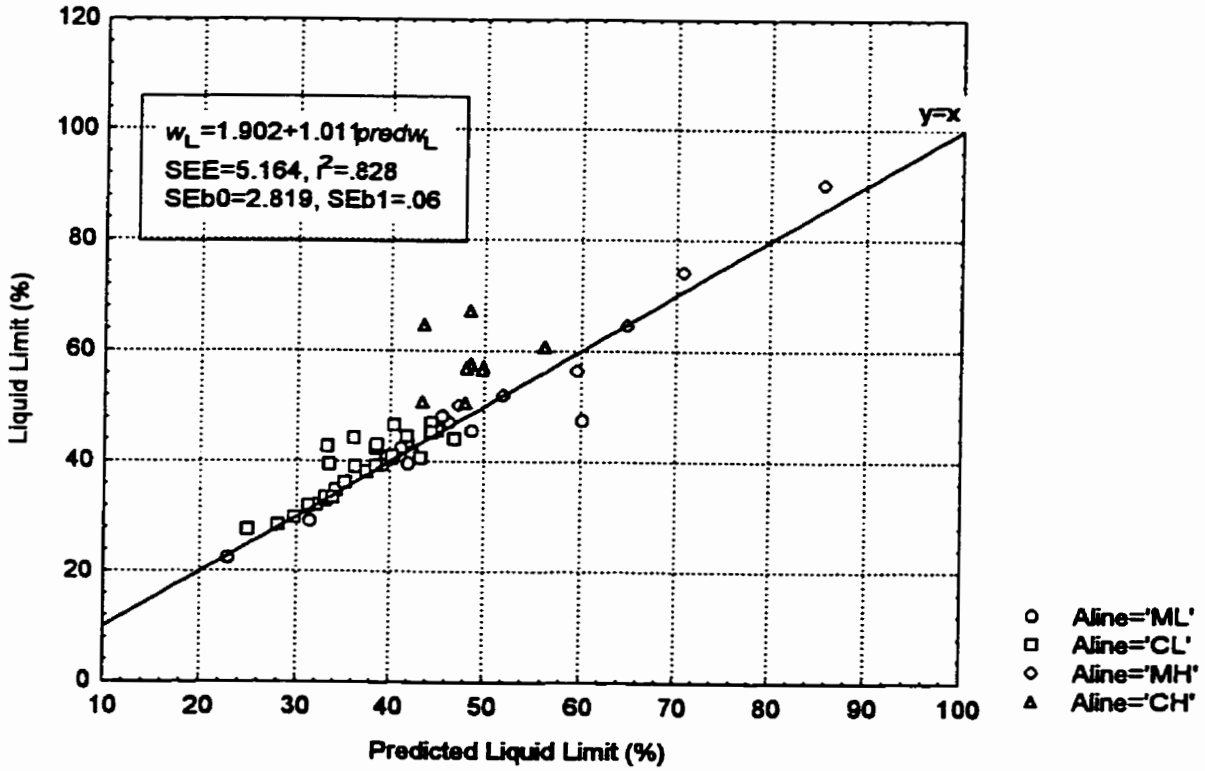

Figure 2.7. Figure comparing w_L predicted using Eq. [29] and 15.6 kPa for >6.74% OC.

for soils of smectitic and feldspar mineralogies as long as the organic carbon content is < 6.74%, although TXNC, TXAC and ABAA were outliers and there was a clustering of CH horizons.

The w_P predicted by the average stress 420 kPa determined by McBride and Baumgartner (1992) inserted into the measured NCL had a significant 1:1 relationship (r^2=.6365, SEE=5.993, n=54). The measured σ'_{wP} varied widely from 420 kPa (Table 2.6) but the 1:1 relationship for w_P arose partially due to the semi-logarithmic scale used in presenting the NCL.

2.3.2.4 Predicting the slope and intercept of the NCL

The concept of pedotransfer functions was further tested by reconstructing the NCL using the existing PTF2 equations and the relationships developed independently using this thesis data.

There was not a significant 1:1 relationship between the PTF2 C_C* , determined using Eq[29] (15.6 kPa if > 6.74% OC) for the σ'_{wL} and an average of 420 kPa for the σ'_{wP} (McBride and Baumgartner, 1992), and the measured C_C* for all 54 horizons and there was a significant amount of unexplained variability (r^2=.1817, p=.00131, SEE=.07135). There was also not a 1:1 relationship for the measured and PTF2 e^*_{1kPa} (r^2=.4653, p=.00000, SEE=.23604). The source of the unexplained variability could be due to the average 420 kPa used for the σ'_{wP} and the combination of the mineralogies as indicated by the ANCOVA analysis.

Table 2.6 illustrated the range and variability of the measured σ'_{wP} and the ANOVA analysis indicated there were significant mineralogy and horizon effects. An average σ'_{wP} of 550 kPa was substituted into the predicted NCL equation for the Alberta and Ontario soils and an average of 2270 kPa was substituted into the TX and OT soils. Again there was not a 1:1 relationship for the slope or intercept. There was also not a significant relationship between the NCL predicted by Eq. [29] and Eq. [27] combined. Predicting the NCL slopes or intercepts

entirely from the ANCOVA equations, Eq. [16] and Eq. [18] for both the plastic and limit stresses did not result in 1:1 relationships with the measured slopes or intercepts but the r^2 and SEE were improved. Predicting the NCL slope and intercept from regression equations Eq. [22] and Eq. [iv and vi] from Table 2.9 resulted in an non-1:1 relationship with the C_C^* (r^2=.295, SEE=.06621) but a highly significant 1:1 relationship for the e^*_{1kPa} (r^2=.817, SEE=.138, b0=.1643, SEb0=.0915, b1=.8989, SEb1=.0590). This difference in ability to predict the intercept versus the slope is interesting in that the intercept of the NCL seems to be more highly related to the void ratio at the liquid limit, forcing the predicted NCL towards the measured intercept, than the stresses associated the w_L or w_P.

Forward stepwise regression was used to determine equations for predicting the slope and intercept of the NCL directly from soil survey data as an alternative to predicting the liquid and plastic limit stresses.

$$C_C^* = .02446 + .000051 clay^2 + .01162 organic\ carbon + .0323 pH \quad [31]$$

F=10.78, R^2=.3923, SEE=.0627, p<.001

$$C_C^* = -.1863 + .1364 e_{wL} + .0229 pH + .0044 coarse\ clay + .0042 coarse\ silt \quad [32]$$

F=10.418 R^2=.460 SEE=.0597 p<.001

Although significant, neither of these equations explain very much of the variation in C_C^* by general soil properties. One of the reasons it may be difficult to predict the slope of the NCL is that the ANOVA analysis found a significant TRT*HOR interaction for ln(C_C^*). The MDAC horizon was removed as an outlier which resulted in the best distribution of residuals. It is reasonable to remove this horizon from the analysis because it is marginally plastic (C_C^* = -.139, I_P=2.2). The TRT*HOR interaction of the back transformed means is illustrated in Figure 2.8 . There are no significant differences of C_C^* within or between the A and C horizons of any of the treatments. The Agr B and Nat B horizons are not significantly different from each other. There

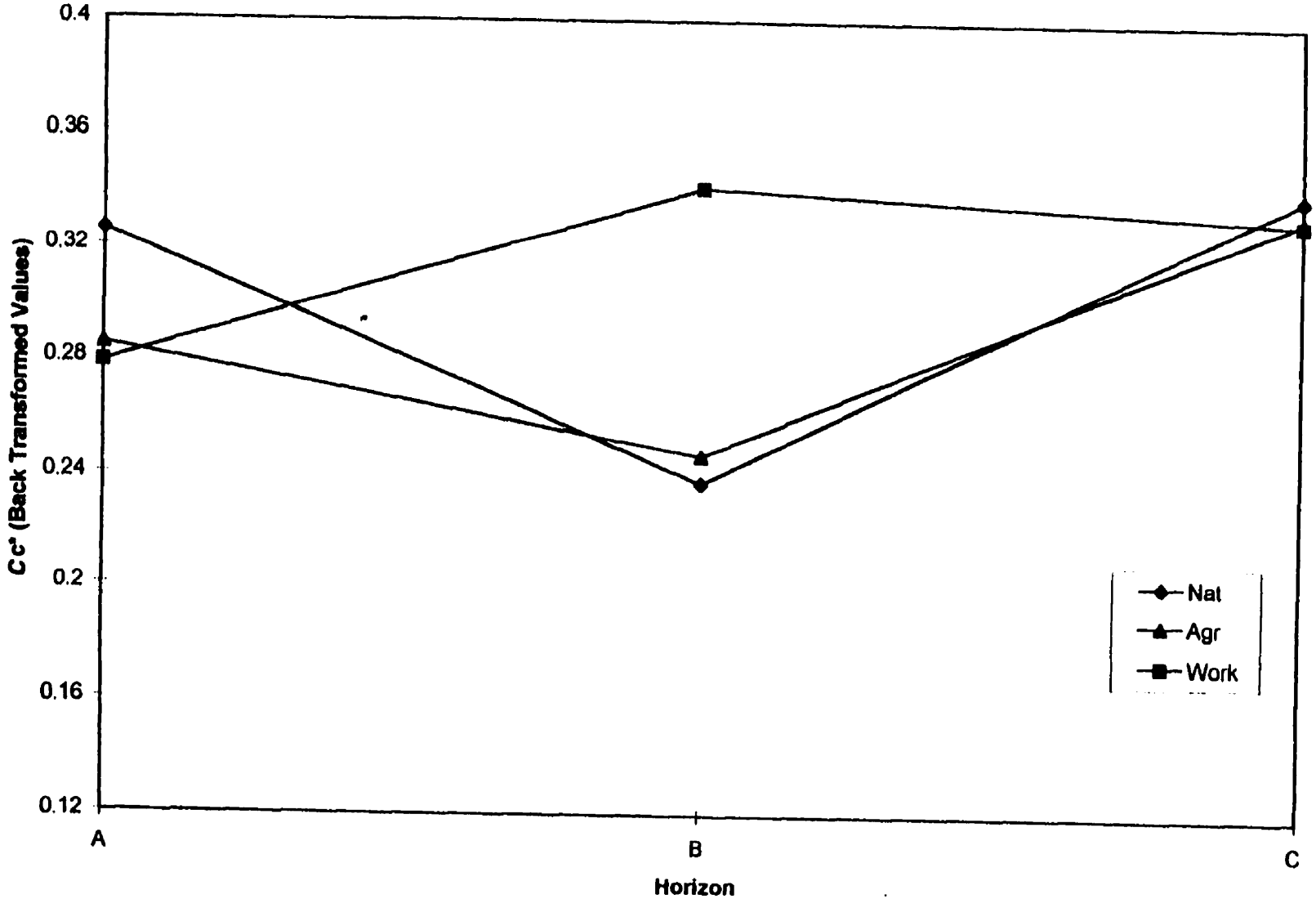

Figure 2.8. Cc* TRT*HOR interaction. Back transformed LSmean values.

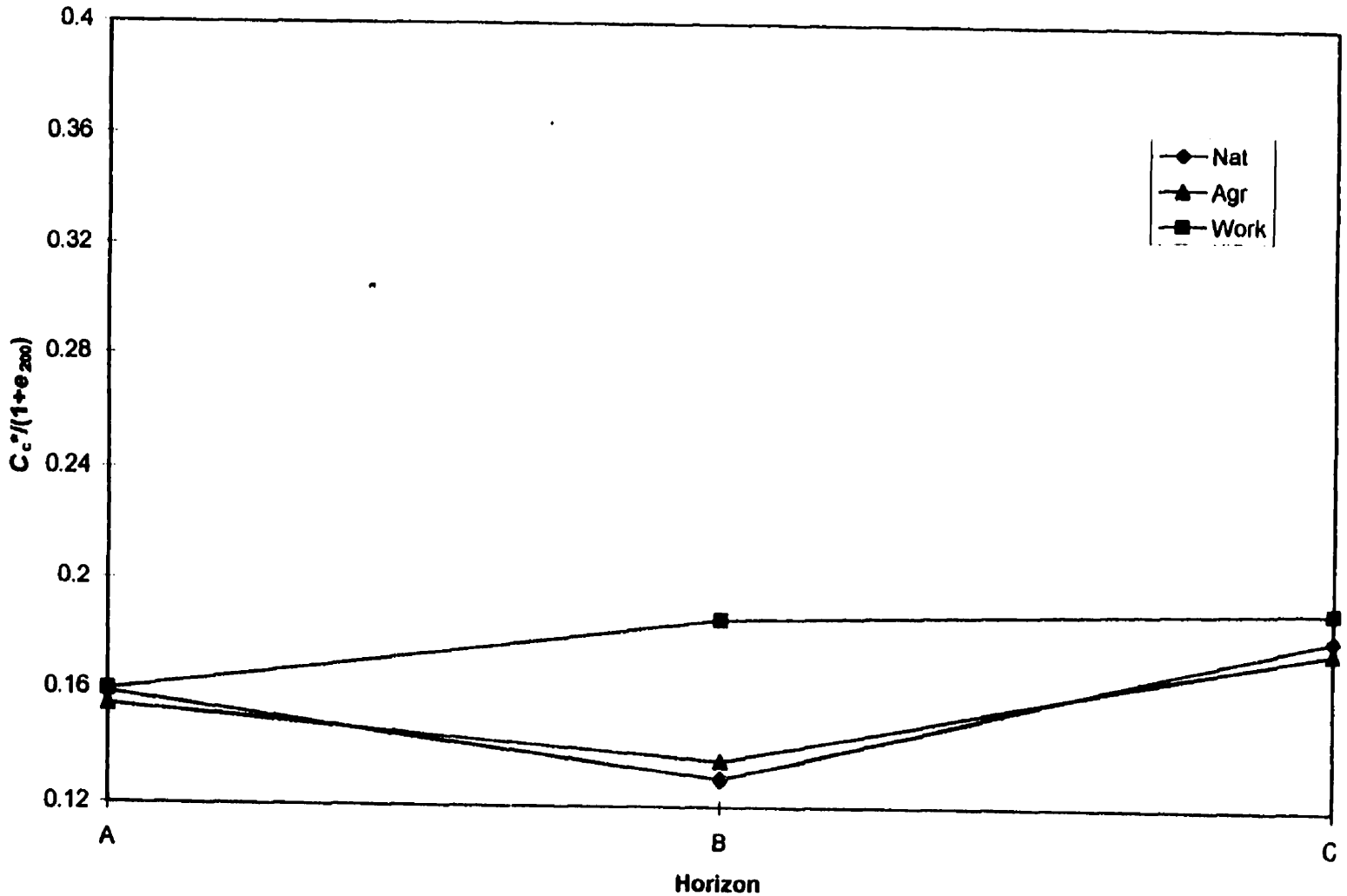

Figure 2.9. Compression Ratio interaction for the remoulded state.

are significant differences ($p<.05$) between these 2 horizons and the C horizons and the Workspace B and Natural A horizons.

An analysis was also undertaken using the Compression Ratio (CR) of Wesley (1988) where the additional compressibility of a sample because of its higher void ratio is standardized by dividing the compression index by the void ratio at a particular stress ($CR^*=C_C^*/(1+e_{200})$). This provides an idea of the true "compressibility" of the sample compared to other soils. A stress of 200 kPa was selected so that comparisons to the structured curve could also be undertaken at a sufficiently high enough stress that the point would be along the C_C. A similar figure (Figure 2.9) and significant differences to C_C^* resulted, with a TRT*HOR interaction for CR* when MDAC and WAAC outliers were removed. The interaction shows that Workspace B and all C horizons are significantly more compressible than the Agr and Nat B horizons. When all the data were included, the TRT*HOR interaction significance was reduced to $p=0.08$ and there were 2 differences in pdiff values. A significant HOR term remained showing the C horizon to have higher compressibility in the remoulded condition than the A or B horizons. The B horizons have the lowest compressibility which may be due to a lack of organic matter and or calcium carbonate compared to the A and C horizons which increase the steepness of the NCL because they absorb greater amounts of water and therefore can lose more water over equivalent ranges in stress.

It is interesting to note that the Workspace B horizon is more compressible in the remoulded state than the other B horizons. It has been suggested that some micro-aggregate and clay domain structure could remain intact even after intense remoulding (Veenhof and McBride, 1996). This may impart more strength in the agricultural and natural slurries, or may actually allow the particles to slide more easily past each other if they are severely degraded with clay particles oriented towards each other in the workspace condition. The Natural treatment is the only one with the A, B and C horizons all with significantly different compressibility. Increasing

$CaCO_3$ up to 35% has also been shown to be correlated to an increased plasticity index (Stakman and Bishay, 1976) which is directly related to the compressibility of a soil.

An ANCOVA for C_C* was undertaken with organic carbon; the difference between treatments remained with a significant OC*TRT interaction. This interaction and several ANOVA factors were only significant at the 10% level (p=.0641) which was considered sufficient to retain them in this exploratory modelling. Both MDAC and WANB were outliers as they have the lowest C_C* values and border on being non-plastic soils, but it made no difference to the model if they were included or excluded. The model equations are (MSE=0.00796762, R=.92808, n=54):

[33]

i) Nat: $\ln(C_C^*+.2)$=-.74163894+.01429195**%organic carbon*, SEb0=.046324, SEb1=.00854

ii) Agr: $\ln(C_C^*+.2)$=-.76498656+.01125524**%organic carbon*, SEb0=.046232, SEb1=.01306

iii) Work: $\ln(C_C^*+.2)$=-.5893356-.0798102**%organic carbon*, SEb0=.0715517, SEb1=.03894

The Workspace intercept and slope are significantly different from the averages of the Agr and Nat intercept and slope, p=.0275 and p=.0208 respectively. Also the slopes for Agr and Nat treatments are not significantly different from 0. It has been found that changes in organic carbon tend to shift the Atterberg limits simultaneously without changing the absolute value of the plasticity index so we would not expect OC to affect the prediction of the C_C* (Baver, 1930; Smith et al, 1985). It is interesting, therefore, that it is the workspace horizons' C_C* which should be affected by organic carbon.

The plasticity index is known to be dependent on the clay content. When clay content is included as a covariate for C_C* the significance of all class variables is removed. The $\ln(C_C^*)$ transform is required. The resulting equation is (MSE=0.02555604, n=54, R=0.90381): [34]

$\ln(C_C^*)$=-1.67168+.01108295**%clay* SEb0=.11849, SEb1=.00292

Eq [34] regressed against the measured C_C* resulted in a significant 1:1 relationship but with poor

predictive capability (r^2=.239, SEE=.0688).

There were much better predictive equations for the intercept of the NCL. Since activity and plasticity index are correlated they could not be included at the same time in regression analysis without exceeding tolerance levels, therefore there are three equations for e^*_{1kPa}.

e^*_{1kPa}=-.3468+.000216%*clay*^{2}+.08564*pH*+1.016e_{wP}+.5338*activity* [35]

F=68.61, r^2=.8485, SEE=.1294, p<.000000

e^*_{1kPa}=-.2193+1.0781e_{wL}+.08412*pH*+.000146%*clay*^{2}-.01761I_P [36]

F=63.7 r^2=.8387 SEE=.1335, p<.00000

e^*_{1kPa}=.852138e_{wL}+.01465*coarse clay*+.01238*coarse silt* [37]

F=90.121 r^2=.8413, SEE=.12985 p=.00000

The e^*_{1kPa} is also related to the void ratio at the liquid limit by the simple equation:

e^*_{1kPa}=.44375+.9111e_{wL} [38]

SEE=.1633 r^2=.7441

The ANOVA analysis of e^*_{1kPa} produced results similar to C_C* with a significant TRT*HOR interaction and an identical pattern (Figure 2.10), although with not as many significant differences. No transform was able to improve the distribution of the residuals. The Agr and Workspace treatment horizons have similar LSmean e^*_{1kPa} within and between them. The Workspace B and C horizons cannot be distinguished from the other horizons. The Nat A horizon is significantly different than the Agr A and Work A horizons. The Nat B horizon is significantly different than the Nat C and Nat A horizons. There is a significant correlation (R=.814) between e^*_{1kPa} and C_C* indicating that those horizons with the steeper NCL tend to have the greater e^*_{1kPa} values which would explain the similar pattern of TRT*HOR for C_C* and e^*_{1kPa}. There is a correlation, although not as strong, between CR* and e^*_{1kPa} (R=.508). Petersen (1993) and Hettiaratchi (1987) found a linear dependency between C_C* and e^*_{1kPa} which could lead to the

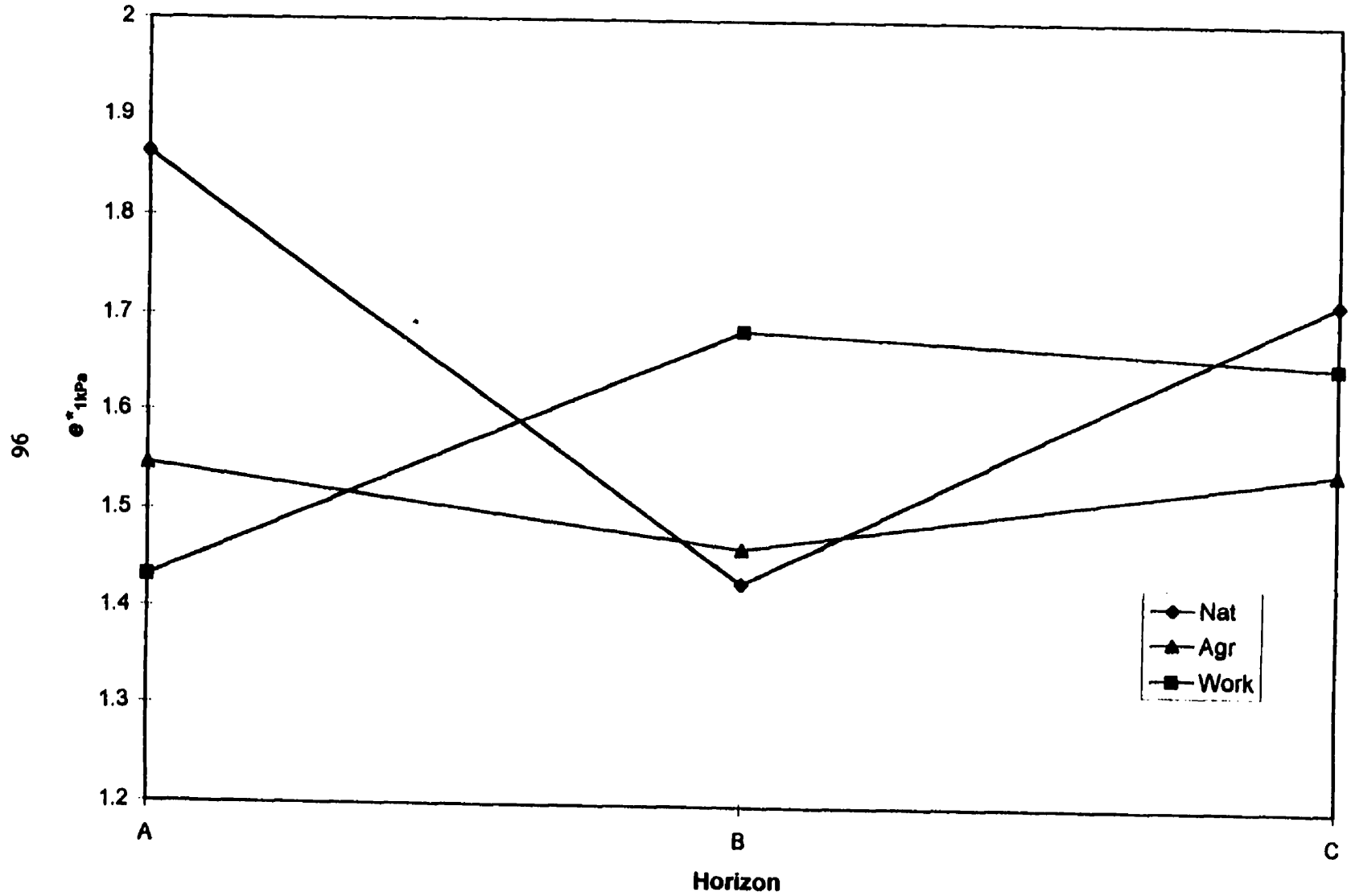

Figure 2.10. NCL intercept (e^*_{1kPa}) TRT*HOR interaction.

existence of a pivot point in the ln(p)-v plane for rotation of the NCL with changing moisture content.

2.3.2.5 Summary of remoulded compression results

There is no satisfactory, single method of predicting the entire equation of the NCL for all of the soils studied. The slope is affected by the clay content and plasticity index of the soil but not with any significant predictive capability. The workspace horizons' C_C* are somewhat affected by organic carbon content while the other treatments are not. The workspace B horizons are more compressible and conversely the Nat and Agr B horizons are less compressible which could be affecting the prediction from soil survey data alone. It is possible to satisfactorily predict the e^*_{1kPa} of the NCL if the w_L, w_P, pH and clay content are known. The significance of the e^*_{1kPa} rather than the entire NCL will become apparent in further sections.

If a measured NCL is constructed, the w_L and w_P can be predicted through the stresses predicted at these points based on the % organic carbon or log %organic carbon. The w_L and w_P predicted from the regression equations did not produce 1:1 relationships. Eq. 29 can be used for predicting the w_L for soils with less than 6.74% OC and is best for Ontario soils. The TX soils in particular affect the fit of the 1:1 relation when Eq. 29 is used. The use of the Veenhof equation (Eq. 27] for the σ'_{wP} is an improvement over the averages from McBride or from the ANOVA analysis. The best predictions were given by the ANCOVA equations because the differences in mineralogy were accounted for by 4 separate equations (8 equations for σ'_{wP} because of the difference for natural horizons). The ANCOVA equations also involved log transforms of the y variable to obtain normal residuals which was not undertaken in the regression approach as variables other than organic carbon helped to create normal residuals. The ANCOVA equations are similar in form to the McBride and Baumgartner (1992) equation, involving simply %organic

carbon as a variable.

2.3.3 Structured Compression Results

Structured compression data results are presented for 2 data sets; that for the total stress (σ) and that for the effective stress (σ') measurements. There were high correlations between the Bailey parameters (Eq. [1]) and the C_C and σ'_c measurements between the 2 sets of data (Table 2.10). There are two C_C and σ'_c measurements. The C_{C0} refers to the slope of the VCL when the second derivative first equals 0, i.e. becomes a straight line. The σ'_{c0} refers to the preconsolidation stress determined using C_{C0} for the slope for the VCL. The C_C refers to the slope of the VCL calculated from a regression of 10 points between .5 and 1 MPa and the σ'_c refers to the preconsolidation pressure determined using this slope of the VCL (Figure 2.2).

There were compression curves flagged by the PCP1.2 program in both data sets. FLAG3 indicated a 0 second derivative was not found and the PCP1.2 program then assigned values for the compression index (C_{C0}) equal to the tangent at 1 MPa . This default setting overestimated the C_{C0} and σ'_{c0} values (i.e. 300+ kPa). It was also found that up to 24 σ'_c values were below the point of maximum curvature as determined by the PCP1.2 computer model; by the Casagrande method this theoretically cannot occur. The configuration causing this underestimation could be identified graphically as compression curves having a "sigmoidal shape" with a strongly convex shape at stresses lower than 100 kPa and then asymptotically approaching a minimum void ratio at stresses higher than 500 kPa. This led to intersection of the bisector and a compression index, determined by the fitting of a 10 point regression, lower than the point of maximum curvature. This asymptotic behaviour of the compression curve may be due to the extended time (1 1/2 hours) between stress increments or the porous nature of the compression chamber allowing for more complete compression. Mostly A and B horizons from natural and agricultural treatments had this

configuration so it is not that the soils were so severely degraded structurally that they could not be compressed (i.e. had low C_C values) . In these two cases, the stress at the point of maximum curvature (x co-ordinate) was substituted for the spurious σ'_c values which aided in meeting the normality and homoscedasticity assumptions in some cases. It is known that the Bailey et al. (1987) equation tends to be sigmoidal at higher stresses and has bulk density approaching ∞ as stress increases which is not a physical possibility. A new model proposed by Assouline et al. (1997), has a boundary condition in which there is a finite maximal bulk density to which the soil can be compressed, depending on the specific soil and its initial water content. It is multiplicative like the Bailey et al. equation but only has 2 fitting parameters (1 if the maximum bulk density is well known or estimable) and avoids natural log representation. This model may overcome underestimation of the preconsolidation stress and would require further study.

Individual analysis of the Bailey coefficients will not be discussed because of the correlation between many of these coefficients and the VCL parameters (Table 2.10). Also the ANOVA analysis indicated many MNR*TRT*HOR interactions, outliers, and transforms for the individual Bailey coefficients which could not be systematically explained . In particular the A parameter was highly correlated to the initial bulk density (D) and the C_{C0}. The B parameter was used to fit the end portion of the compression curve and is highly correlated to the C_C values. The C parameter is used to fit the curved portion of the compression curve and is correlated to the σ'_{c0} and the points of maximum curvature values. These correlations were similar to those found by Veenhof (1993). The D parameter, i.e. initial bulk density, is related to both compression indices, C_{C0} and C_C. Similar outliers, transforms and models occurred for the Bailey coefficients and the corresponding C_C and σ'_c values. McNabb and Boersma (1996) also found the Bailey coefficients highly correlated and suggested that Multivariate Analysis be undertaken of the Bailey coefficients simultaneously as a function of several soil parameters to derive universal compression equations.

Table 2.10 Correlation matrix of Bailey and compression parameters for applied and effective stress data sets.

	A	B	C	D	C_{C0}	C_C	A′	B′	C′	D′	C_{C0}'	C_C'	σ_{v0}	σ_c	σ'_{v0}	σ'_c
A		.595	.452	.808	.897	.740	.994	.518	.486	.808	.878	.712	-.311	.784	-.367	.762
B	.595			.825	.751	.931	.550	.972		.825	.740	.923	.196	.215	.156	.210
C	.452			.330	.398	.171	.474		.957	.330	.416		-.865	.454	-.847	.437
D	.808	.825	.330		.902	.921	.786	.776	.354		.892	.906	-.168	.449	-.218	.427
C_{C0}	.897	.751	.398	.902		.906	.877	.698	.424	.902	.987	.890	-.247	.545	-.293	.521
C_C	.740	.931	.171	.921	.906		.708	.893	.203	.921	.895	.992		.303		.286
A′	.994	.550	.474	.786	.877	.708		.454	.517	.786	.859	.672	-.351	.786	-.420	.771
B′	.518	.972		.776	.698	.893	.454			.776	.691	.912	.267		.260	
C′	.486		.957	.354	.424	.203	.517			.354	.445	.155	-.830	.471	-.860	.502
D′	.808	.825	.330		.902	.921	.786	.776	.354		.892	.906	-.168	.449	-.218	.427
C_{C0}'	.878	.740	.416	.892	.987	.895	.859	.691	.445	.892		.882	-.274	.516	-.313	.487
C_C 3	.712	.923		.906	.890	.992	.672	.912	.155	.906	.882			.274		.234
σ_{v0}	-.311	.196	-.865	-.168	-.247		-.351	.267	-.830	-.168	-.274			-.249	.975	-.237
σ_c	.784	.215	.454	.449	.545	.303	.786		.471	.449	.516	.274	-.249		-.295	.972
σ'_{v0}	-.367	.156	-.847	-.218	-.293		-.420	.260	-.860	-.218	-.313		.975	-.295		-.307
σ'_c	.762	.210	.437	.427	.521	.286	.771		.502	.427	.487	.234	-.237	.972	-.307	

Shaded correlation coefficients are not significant at $p<.05$

σ'_{v0} and σ'_c values are corrected for flagged and underestimated values by substituting the stress corresponding to the point of maximum curvature.

Since this study looks at the compressive behaviour rather than the model itself, only the C_C and σ'_c variables will be discussed in detail.

2.3.3.1 Compression results for total stress

There is a straightforward relationship between C_{c0} and Trt and Hor (Table 2.11) once the 5 flagged cores where C_{c0} would be overestimated are removed. Essentially the Natural treatment has the steepest slope followed by the Agricultural and then Workspace treatment and occurs independent of mineralogy. Similarly the A horizons are more steep than the B and C horizons which are not significantly different from each other.

The C_C ANOVA analysis is more complicated in that C_C has a significant TRT*HOR interaction which is illustrated in Figure 2.11. In any one land use treatment, the B and C horizon C_C are not significantly different and the A horizon is different than both. The Workspace B and C horizons have significantly lower slopes than the other horizons; the one exception is that the Agr B and Wrk C horizons are not significantly different. The Natural A horizon is steeper than all the other horizons. The ANCOVA models for C_C and C_{c0} using organic carbon were fairly complicated with OC*OC*MNR*TRT and OC*MNR*TRT interactions and will not be presented. The ANCOVA models for C_C and C_{c0} using clay had CLAY*CLAY*MNR and CLAY*MNR*TRT interactions which complicated the analysis but only ON and OT had slope parameters significantly different than 0 because the % clay ranges for AB and TX were narrow.

As the compression index is not directly related to compressibility (stress/strain increment), the C_C was converted to a Compression Ratio (CR) (Wesley, 1988) at 200 kPa. The ANOVA was not straightforward as there was a significant MNR*TRT *HOR interaction. A ln(CR-.045) transformation was required to approach normally distributed residuals, or if 2 outliers, TXNA3 and MDAC3, were removed no transform was required. A significant 3-way interaction resulted in either case and the interaction for all data is shown. Figure 2.12 illustrates

Table 2.11. LSmeans Separation pdiff and LSmean values for ln(C_{C0}) (5 flagged cores removed).

	TRT			HOR		
Parameter	Ag. vs. Nat.	Agr. vs. Work	Nat. vs. Work	A vs. B	A vs. C	B vs. C
pdiff	3.41e-4*	0.0278*	2.49e-6*	5.97e-9*	5.04e-10*	0.4696
	Agr	Nat	Work	A	B	C
LSmean	-1.47657695	-1.13131008	-1.72903716	-0.96563199	-1.65051332	-1.72077888
Back Transformed Mean	0.228418239	0.322610334	0.1774551887	0.38074250	0.19195135	0.17892673

Table 2.12. LSmeans Separation pdiff and LSmean values for ln(C_{C0}'-.05) (8 flagged cores removed).

Factor	TRT			HOR		
	Agr vs. Nat	Agr vs. Work	Nat. vs. Work	A vs B	A vs C	B vs C
pdiff	3.99e-5*	.0052*	1.11e-7*	1.81e-5*	2.46e-6*	.2576
	Agr	Nat	Work	A	B	C
LSmean	-1.70739	-1.27622	-2.04300	-1.07282	-1.89810	-2.05569
Back Transformed Means	0.231338	0.329090	0.179639	0.392043	0.199853	0.178004

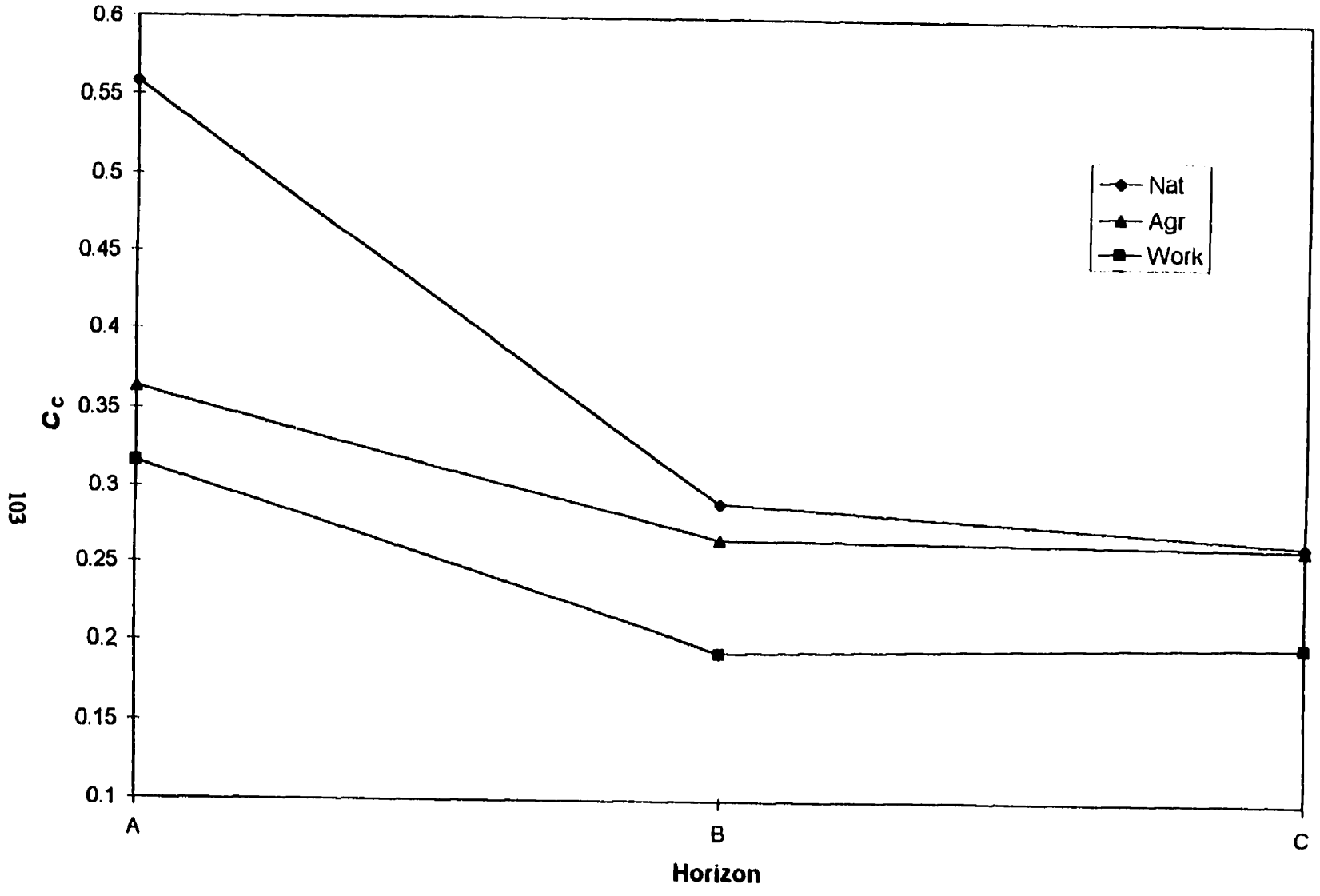

Figure 2.11. Compression index based on 10 point regression and total stress (C_c) TRT*HOR interaction

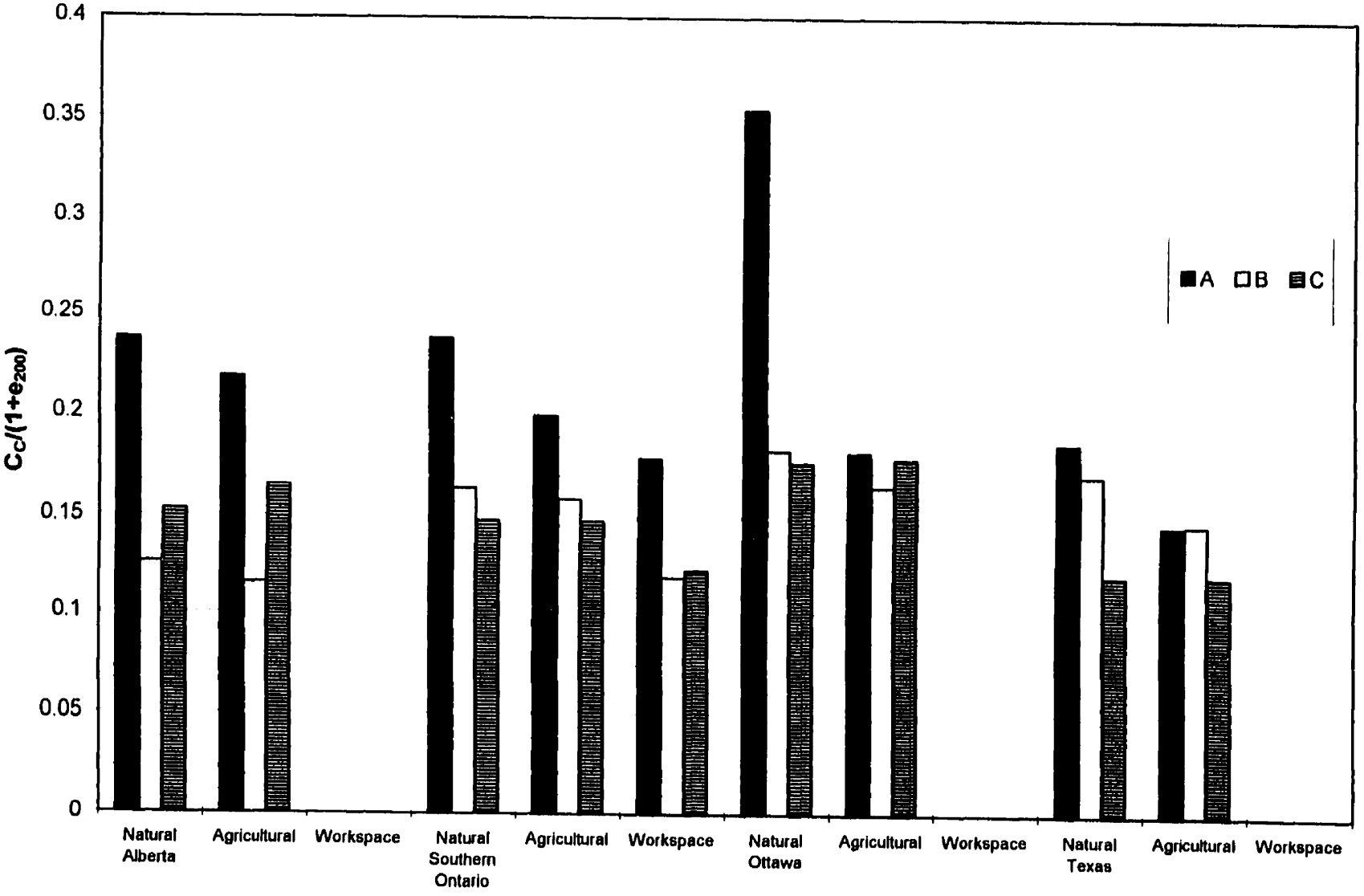

Figure 2.12. CR MNR*TRT*HOR interaction. Back transformed values.

that the OTNA horizon is more compressible than all the other horizons except for ABAA and ABNA. Otherwise most of the A horizons are not significantly different from each other; TXAA is less compressible than ABNA and ONNA, and ONWA is less compressible than ONNA. The A horizon in a given profile is more compressible than the B and C horizons from the same profile except for ABAA/ABAC, OTAA/OTAB/OTAC, TXAA/TXAB/TXAC and TXNA/TXNB. Some horizons of significantly lower compressibility for many combinations, particularly with the A horizons, are TXNC, TXAC, ABAB, ONWB and ONWC. The ONWB and ONWC horizons are less compressible than all the Ottawa horizons, the TXNA, TXNB, ABAA, ABNA, ONAA, ONAB, ONNA, ONNB and ONWA horizons. In addition, ONWB is significantly less compressible than ABAC, ONAC, and ONNC. In general, the same pattern as Figure 2.11 with highly compressible Nat A horizons and least compressible Work B and C horizons, resulted.

The σ_{c0} values had significant MNR*TRT*HOR interactions with or without the TXNA3 outlier. The TXNA3 core had the poorest r^2 fit for all of the Bailey equations (r^2=0.96) which would have affected subsequent calculations of the C_C and σ'_c since this core did not fit the model well compared to the other cores. The ANOVA results for $\log\sigma_{c0}$ are illustrated in Figure 2.13. Overall the σ_{c0} values seem to be relatively low compared to what would be expected in the field, particularly for some of the B and C horizons, and high for A horizons. ABAB and TXNA had significantly higher σ_{c0} than all the ON and OT horizons. Generally the TX and AB σ_{c0} are larger than for ON or OT. ABNA had a higher σ_{c0} than all the ON and OT horizons but ONNB and OTAA. The ON Agricultural and Workspace B and C horizons had lower σ_{c0} values than AB natural horizons, ABAA, ABAB, Ontario natural horizons, ONAA and TXNA.

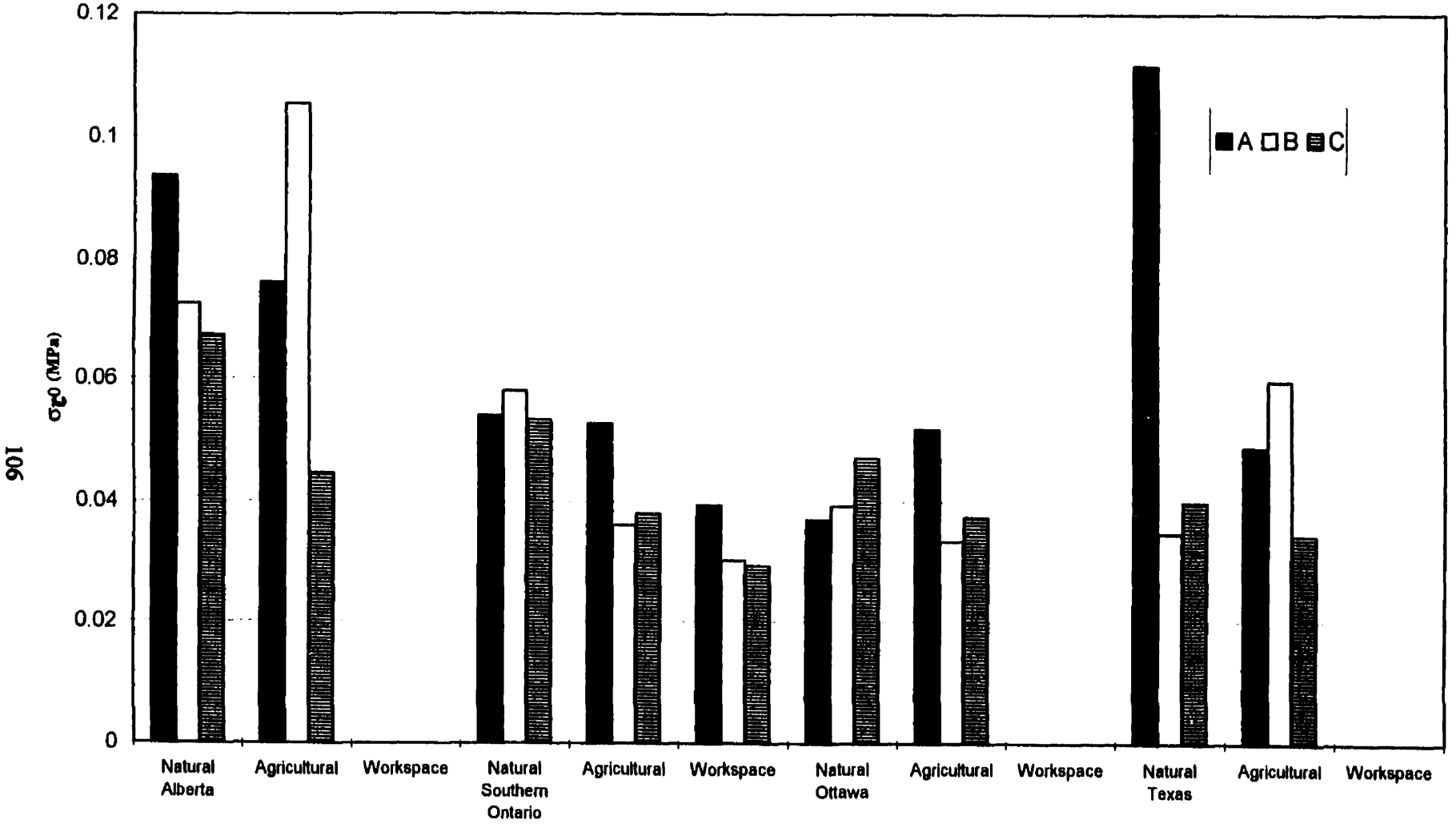

Figure 2.13. σ_{c0} MNR*TRT*HOR interation. Back transformed values. TXNA3 removed.

When an ANCOVA was conducted with organic carbon as a covariate, a simplified model resulted with OC, OC*OC, TRT and MNR factors for $\ln(\sigma_{c0})$. Since there are no interactions there are 7 separate equations for each scenario. The best residuals were obtained when the outlier TXNA3 was removed and these are the model estimates presented. There is not a significant change in the model with or without the outlier. The linear OC coefficient estimate is 0.11480671 (SEb1=.03907421) and the quadratic OC*OC estimate is -.01054232 (SEb2=.00337237) (MSE=.08845, n=161, R=.7546) The corresponding estimates of the intercepts are:

Intercept LSMean $\ln(\sigma_{c0})$	SEb0	Back Transformed Mean σ_{c0} (MPa)
AB =-3.10092505	0.16578268	0.04501
ON=-3.53885202	0.09453395	0.02905
OT=-3.57753719	0.16338719	0.02794
TX=-3.49501083	0.16415504	0.03035
Agr=-3.22498586	0.10309665	0.03976
Nat=-3.04447777	0.10456348	0.04762
Work=-3.49501083	0.16415504	0.03035

The AB intercept is significantly different than the other mineralogies (p=.0118) and the average of the smectites is significantly different than the average of ON and OT (p=.0502), although TX is not significantly different than ON or OT alone. The Treatments are all significantly different from each other and it is surprising that the natural treatment is higher than the other σ_{c0} values. The model indicates parallel responses to organic carbon due to common slope parameters with increasing back transformed σ_{c0} with increasing OC. There remain significant TRT and MNR effects separated by intercept differences. As state previously, the σ_{c0} was closely associated with the point of maximum curvature and likely does not represent the σ'_c as determined by the Casagrande method. The small intercept values and increase in σ_{c0} with organic carbon are

opposite to what would be expected in the field if the σ_{co} is taken as an indicator of soil strength or resistance to compaction. If on the other hand, σ_{co} is taken as the separation between elastic and plastic behaviour (Kirby and Blunden, 1991), its increase with increasing organic matter content makes more sense. The σ_{co} values had a similar ANOVA model to the C values from Eq[1]. When fitting the Bailey equations it was noted that the C parameter (and hence the σ_{co}) changed drastically between treatments and horizons and this may be a more distinguishing characteristic of the compression behaviour than the σ'_c.

The σ_c values had a MNR*TRT*HOR interaction when 2 outliers were removed (WAAA2 and OTAA1) . There were significant differences between some of the AB horizons and the ON AA horizon with the other mineralogies, in particular ONAA and ABNB with the OT horizons. There was no justification for removal of the outliers except for improving the normality of the residuals.

When all the data were considered, a $\ln(\sigma_c + .025)$ transformation was required and there was a significant MNR*HOR interaction. There was no treatment effect for the σ_c values (Figure 2.14) unlike the σ_{co} values. The σ_c values are in a range more expected in the field with back transformed means ranging from 0.0735 MPa to 0.1836 MPa. The Alberta B horizons are significantly different than the B horizons of the other mineralogies. The ON and OT A horizons are different than the corresponding B and C horizon while the TX and AB A horizons are not significantly different than the B and C horizons. Alberta is the only mineralogy where the B horizon σ_c is lower than the A horizon although it is not significantly different.

One of the reasons this may occur is that Alberta was sampled earlier in the year (June '94) when the soils were still moist from spring thaw and rains and had little plant growth and desiccation of the soils, while the other sites were sampled later in the growing season (July-Oct. '93) when significant drying had occurred through the profile. This difference should have been

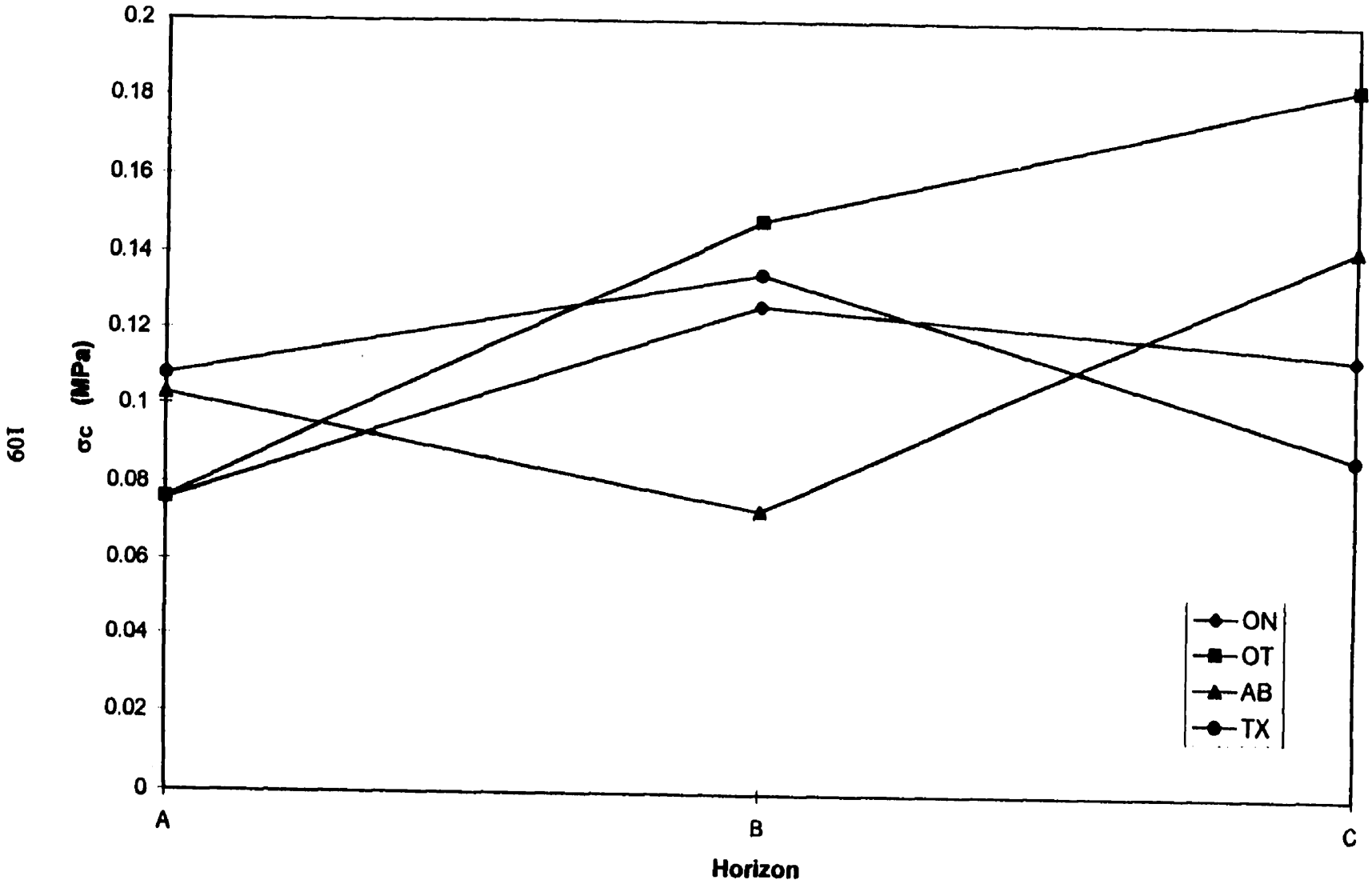

Figure 2.14 Preconsolidation stress MNR*HOR interaction. Back transfromed values.

overcome by saturation prior to compression. There were, however, significant differences between the Natural and A horizons and the other horizons in the degree of saturation prior to compression (Table 2.13) which may have influenced the compression curves (McNabb and Boersma, 1993). This difference is likely due to the drainage of macropores while moving the cores from the balance to the Rowe cells. The A horizon degree of saturation was significantly lower than the average of the B and C horizons (p=.0048), and the Natural horizons' degree of saturation was lower than the average of the Agr and Work horizons (p=1.11e-4).

Table 2.13. LSmeans Separation pdiff values for degree of saturation.

	Trt (Land Use)			Horizons		
Degree of Saturation (%)	Ag. vs. Nat.	Agr. vs. Work	Nat. vs. Work	A vs. B	A vs. C	B vs. C
Pdiff	5.86e-4**	0.2916	4.32e-4*	.0273*	.0061*	0.5419
	Agr	Nat	Work	A	B	C
LSmean	0.95067	0.88124	0.97138	0.91102	0.94200	0.95028

When organic carbon is included as a covariate for σ_c, only OC is significant (n=54, R=.863, MSE=.03674) and the equation is: [39]

$\ln(\sigma_c + .03) = -1.87408903 - 0.05746529 * \%\text{organic carbon}$

SEb0=0.05050062, SEb1=0.01435929

This means that the back transformed σ_c values decrease as the amount of organic carbon increases which is opposite from the σ_{c0} values which have a positive slope term. Eq. [39] explains more of the variability than the model for σ_{c0} and suggests that only organic carbon, or the degree of saturation since the Natural and A horizons have the most organic carbon, are controlling the σ_c. Lower degrees of saturation however, would tend to increase the σ_c (Kirby, 1991) rather than lower it.

2.3.3.2 Compression results for effective stress

It would be expected that the compression curves computed using the effective stress would have steeper compression indices (C_C' and C_{c0}') since the effective stresses could be lower than the total stresses due to positive pore water pressures remaining in the sample. Usually the pore water pressures at the end of 85 minutes were low (20-30 kPa) or even negative for some A horizons, even though the Rowe cell had been wrapped in plastic to avoid evaporation. There were 13 horizons, mostly from TX, OT and WA, which had pore water pressures >100 kPa at 1000 kPa total stress and so analysis using effective stresses was deemed necessary.

There was a high correlation between C_{c0}' and C_{c0} (R=.9867) and the C_{c0}' values were significantly greater by a paired t-test (p= 0.003553, t=2.95, df=161). There were an additional 3 flagged cores for this data set giving a total of 8 outliers removed for analysis. The ANOVA model and LSmeans for C_{c0} and C_{c0}' were very similar (Table 2.12). Using OC as a covariate, there were significant OC*TRT and OC*OC*TRT factors for C_{c0}'. The model equations are (MSE=.0186,R=.9519, n=154): [40]

i) Agr: $\ln(C_{c0}'+.1)=-1.2640+.13510OC-.0057(OC^2)$

SEb0=.06563, SEb1=.04771, SEb2=.005687

ii) Nat: $\ln(C_{c0}'+.1)=-1.1616+.16963OC-.00427(OC^2)$

SEb0=.06360, SEb1=.028556, SEb2=.002273

iii) Work: $\ln(C_{c0}'+.1)=-1.7822+.77121OC-.182992(OC^2)$

SEb0=.11579, SEb1=.184156, SEb2=.06220

Neither of the quadratic terms are significant at p=.05 for the Agr or Nat equations and application of the quadratic term is limited to the narrow range of OC in the Workspace treatment (Range .0135-2.63 %oc). The intercept, linear term and quadratic coefficients are not significantly different between the Agr and Nat treatments but the 2 equations are not coincident. The

Workspace intercept, linear term and quadratic term are significantly different from those for the Nat and Agr treatments, all at p<.01. Essentially for each treatment the slope of the tangent at second derivative =0 becomes steeper with an increase in organic carbon although the relationships with OC are not the same for each treatment. The Work treatment responds more to changes in organic carbon. This is similar to the results for C_C* and OC where the Workspace treatment was the only one affected by organic carbon differences (page 94).

The ANOVA model for the C_C' values was like the C_C values having a TRT*HOR interaction. A paired t-test shows that the C_C' values are consistently steeper (dif=.01296, SD=.02415, t=6.828). In the pdiff comparison there are 2 instances that differ in that the Wrk B C_C' values do not differ from those for Agr C and Nat C while they do differ for C_C (Figure 2.11).

The ANOVA model and LSmean for the ln(CR') based on C_C' and e_{200}, was very similar to that for CR (Figure 2.12) with ONAC, OTAB, OTNB and TXAB horizons being more compressible when measured using effective stresses. OTNA becomes more compressible than all horizons; the rest of the A horizons are not significantly different from each other except ABNA is more compressible than TXAA. ABAB and ABNB became less compressible than all the OT horizons. The ONWB and ONWC horizons are less compressible than all the ON horizons except ONNC. All the OT horizons except OTNC become more compressible than TXAC. Otherwise, the pdiff results for CR and CR' are similar.

Likewise the σ'_{co} model is similar to the σ_{co} model as there is a MNR*TRT*HOR interaction. There were no significant differences between the σ'_{co} and σ_{co} values (t=-.056731, p=.9548) as determined by a paired t-test. This is not surprising since the σ'_{co} values are largely determined by the point of maximum curvature which is also related to the Bailey C parameter . The point of maximum curvature would not be affected very much by positive pore water pressures as these generally did not occur until the applied stress was >500 kPa and confirms that

there was good drainage through the initial compression stages. The models differ when the covariate OC is introduced as there is no simplification of the model for σ'_{c0} as OC*OC*MNR and OC*MNR*TRT interactions are retained.

The σ'_c ANOVA model with or without outliers is similar. Although the MNR*TRT*HOR interaction is not significant it is retained since the MNR*TRT and MNR*HOR interactions are significant. There is no simple summary of the pdiff table and again there are only a few significant differences. The σ'_c and σ_c values are highly correlated (R=.9716) and the σ'_c are significantly greater by a paired t-test (mean diff=.005646, SD=.01085, t=6.60315). When the covariate OC is included in the model there is a relatively simple solution in which MNR and OC*MNR are significant. The model equations are (MSE=.04011, R=.85677,n=162): [41]

i) AB: $\ln(\sigma'_c MPa+.03)$=-1.95647-.013925OC SEb0=.15538, SEb1=.0479

ii) ON: $\ln(\sigma'_c MPa +.03)$=-1.86864-.06064OC SEb0=.06885, SEb1=.02331

iii) OT: $\ln(\sigma'_c MPa +.03)$=-1.3782-.31394OC SEb0=.17336, SEb1=.10405

iv) TX: $\ln(\sigma'_c MPa +.03)$=-2.24612+.26544OC SEb0=.1922, SEb1=.13405

The ON equation is similar to the overall equation for σ_c (Eq.[39]). The Alberta slope is not significant and the Texas slope is just significant (p=.0503). The smectite-rich, AB and TX intercept and slope averages are significantly different than the averages for the other 2 mineralogies. In addition, the OT intercept and slope is significantly different from the averages of the other 3. ON and OT σ'_c values decrease with organic carbon increases while AB and TX σ'_c values are not affected or increase, respectively. There is a lot of scatter around the fitted lines but essentially it seems that the σ'_c of the smectite-rich soils is not affected by organic carbon additions the same way that ON and OT soils are. This was similar to predicting the σ'_{wL} and σ'_{wP} in that AB and TX did not have significant relationships with logOC (Section 2.3.2).

2.3.3.3 Estimation of structured compression parameters

The compression index and void ratio at the preconsolidation stress for the structured samples are largely controlled by the initial, saturated void ratio (e_0). From the graphs in the Appendix it is obvious for the A and B horizons that the initial void ratio influences the steepness of the C_C and the amount of curvature in the VCL leading to determination of the σ'_c. There is often visual separation by land use because of differences in initial void ratio. The C horizons of AB, TX, and HL show rather parallel VCL and the e_0 are fairly confined within a narrow range. This dependency of C_C on e_0 is similar to that shown by Veenhof and McBride (1996) and Kirby (1991) and reported in the geotechnical literature by Al-Khafaji and Andersland (1992) and Rendon-Herrero (1980). A larger amount of interaggregate porosity provides more space to accommodate fracturing aggregates with each increment of pressure which results in larger values of C_C and also decreases the angle of internal friction and cohesion further augmenting soil compressibility (Angers et al., 1987; Komandi, 1992).

The correlation coefficients between e_0 and C_{C0} and C_{C0}' are .95 and .94, respectively, and between C_C or C_C' is .96, indicating that as the initial void ratio increases, the compression index (at 0 second derivative or using a 10 pt regression) becomes steeper. The correlation coefficient for the void ratio at the preconsolidation stress ($e_{\sigma c}$), whether determined using total or effective stress, was 1.00 for the point determined by the 0 second derivative and 0.99 for the 10 pt regression.

The equations were not significantly different between total and effective stresses and the values for the total stress are reported. All equations are significant at $p<0.001$, $n=162$.

$C_{C0}=-.1765+.4177e_0$ SEb0=.0132, SEb1=.0107, $r^2=.9035$, SEE=.0638 [42]

$C_C=-.0505+.3303e_0$ SEb0=.0091, SEb1=.0074, $r^2=.9256$, SEE=.0438 [43]

$e_{\sigma c0}=.0767+.8203e_0$ SEb0=.0058, SEb1=.0047, $r^2=.99467$, SEE=.0289 [44]

$e_{\sigma c}$=-.00682+.8354e_0 SEb0=.00875, SEb1=.00713, r^2=.98849, SEE=.0422 [45]

The intercept is not significant for the last equation and the equation becomes:

$e_{\sigma c}$ =.8303e_0 SEb1=.0027 r^2=.9884, SEE=.0412 [46]

This is similar to the 0.865 slope determined by Veenhof and McBride (1996) for soils at different initial pore water potentials. Eq. [43] parameter estimates are also very similar to those derived by Veenhof and McBride (1996) (Table 2, Eq[II]) and Hough (1957). The r^2 for the above equations is higher than those reported by Veenhof and McBride (1996) which may be due to only analyzing saturated soils but the SEE is higher which may be due to the wider range of initial void ratios sampled particularly for the natural A horizons.

The prediction of these VCL parameters can be improved by multiple regression and variables in addition to e_0 .

C_C=.03087+.31102e_0 +.01306*%organic carbon*-.00196w_L +.00057*%*$CaCO_3$ [47]

SEE= .0377, R^2=.946, n=162

C_C'=.3403e_0+.00704*%organic carbon*-.05233e_{wL} SEE=.0459, R^2=.9289,n=162 [48]

C_{C0}'=-.1124+.4384e_0-+0046*%sand*+0026*%*$CaCO_3$-0258*pH*-00896I_L [49]

SEE=.0489, R^2=.9470, n=154

C_{C0}=-0918+4645e_0+0038*%sand*+0021*%CaCO3*-0213*pH*-.00997*LI*-.0015*LL* [50]

SEE=.0451, R^2=.9534, n=157

O'Sullivan (1992) found that organic matter did not influence the relative change in specific volume with stress for 2 soils types. Larson et al. (1980) found the compression index to increase linearly as the clay content increased up to about 33%. Angers (1990) found significant relationships between C_C and clay and sand content for low clay content soils (<35%) and clay and organic matter for high clay content soils (>35%). No division was made here as the soils used were largely clay-rich (plastic) and the prediction equations were deemed to have sufficient

predictive capability.

The $e_{\sigma c}$ estimate can be improved slightly to R^2=.989 by the addition of -.0013*%silt*, and the $e_{\sigma c0}$ estimate can be improved slightly to .997 by additions of sand, pH and CaCO3 multiplied by parameters representing less than 1% of the content. Essentially e_0 is the controlling factor in determining the slope of the VCL and the positioning of the $e_{\sigma c0}$.

There were significant regression equations for estimating σ'_c and σ'_{c0} directly but none which explained greater than 32% of the variability.

2.3.3.4 Summary of structured compression results

There were very similar ANOVA and ANCOVA results whether C_C and CR were calculated using effective or total stresses, indicating that the primary consolidation phase had been effectively completed for all soils. The C_{C0} values could distinguish Natural and A horizons, while the C_C values were better at distinguishing these and the Workspace B and C horizons. The CR values had the same trend of A>B>C but the differences between land uses were not as clear. The ONWB, ONWC, AB B and TX C horizons were the least compressible. The σ'_{c0} results showed differences between land use and mineralogy more clearly than the σ'_c results. There were quadratic relations for organic carbon as a covariate for σ'_{c0} which were free of interactions for the σ_{c0} values but there were still significant MNR and TRT factors. Increasing organic matter tended to increase the σ'_{c0}. There were no treatment effects for σ_c and there was a MNR*TRT*HOR interaction for σ'_c. As a covariate, OC explained the variability for σ_c and MNR*OC for σ'_c. The σ'_c values get smaller with increasing organic carbon. This contradictory behaviour of the two preconsolidation measurements is likely because they do not physically measure or represent the same thing. The σ'_{c0} is closely related to the point of maximum curvature and therefore divides elastic from plastic behaviour. The σ'_c is more dependent on the intersection of the tangent bisector

with the C_C which is increased with increases in organic carbon (Eq. 47 and 48) which is opposite that found by Angers (1990) and from what the relationship with σ'_c would suggest. It is more likely these values are linked to the extent of potential void volume change with low σ'_c indicating a high potential for volume change and vice versa for the high values, but give no indication of the recoverability of that void ratio when the stress is removed. The σ'_c values are not completely accurate because of the substitutions necessary when there was underestimation.

There appear to be 2 sets of behaviour when comparing Figure 2.12, Figure 2.13 and the graphs in the Appendix. Firstly, there is the configuration for horizons, such as ABNB and ABAB, which have low compressibility (CR) and a correspondingly high σ_{c0} (but low σ_c) and conversely for OTNA which has high compressibility and a relatively low σ_{c0}. These horizons' VCL tend to be above and/or parallel to the NCL within the pressure range applied by the Rowe cell (i.e. up to 1 MPa). On the other hand there is a group of soils for which both the compressibility and the σ_{c0} are low, such as for the ONWB, ONWC, TXAC and TXNC which is counterintuitive to what would be expected for the strength of these soils given that they are structurally degraded (dense) or have little structural development. These soils tend to have the VCL lying below the NCL and the NCL may never be reached in the pressure range applied. It is hypothesized, as suggested by Biarez and Hicher (1994), that some soils may have undergone consolidation stresses greater than 1MPa in the past, particularly given the negative pressure potential surface soils can be exposed to through desiccation (> 1.5 MPa), such that tests in the lab underestimate the C_C because the σ'_c is never reached at the stresses in the oedometer. There may be small radii of curvature which can be distinguished at low stresses but these "lead in practice to a considerable underestimation of σ'_c and false evaluation of C_C" (Biarez and Hicher, 1994).

The analysis of the structured compression parameters alone allowed some insight into the structural quality of the soils sampled. The C_C parameter gave a clear picture of the behaviour and

strength of the different soils in terms of TRT and HOR factors while the σ'_c was more ambiguous. The structured compression curves also exhibited a converging pattern controlled by e_0 (Rendon-Herrero, 1988; Veenhof and McBride, 1996). These parameters were not particularly sensitive for distinguishing between the different structural states and land uses, amalgamating several horizons together and having only 1-3 horizons which were different than all the others. An approach utilizing relative indicators was attempted to determine if using a remoulded reference state could provide more distinction.

2.3.4 Comparison of Remoulded and Structured Compression

There were 21 graphs generated illustrating the positioning of the VCL and NCL for each of the horizons at each of the locations (in Appendix). A constant range in the e_0 co-ordinate from 0.4-2.2 allowed visual comparison between all the horizons except for LBNA and OTNA, the 2 wooded profiles, which had $e_0 > 2.5$. In general, there is convergence of the NCL and VCL compression lines. Figure 2.15 illustrates this by comparing the differences in the slopes (C_C *- C_{C0}) and the void ratio at the preconsolidation stress ($e^*_{\sigma c0} - e_{\sigma c0}$) between the remoulded and structured samples. The pattern is the same whether the applied or effective stresses are used or the σ'_c and C_C values using the 0 second derivative or regression on 10 points are used. The r^2 and SEE are best for values obtained from the σ'_{c0} and C_{C0} values. Figure 2.15 is similar to the plot produced by Veenhof and McBride (1996). The majority of the compression curves fall into quadrants I or III which exhibit convergent behaviour between the VCL and NCL. The soils which tend to have the VCL above the NCL (quadrant III) tend to be from the less plastic/clayey ML or MH soils and also tend to be A horizons. For (C_C *- C_C) as the y co-ordinate, the ML and MH soils all had the VCL slopes steeper than the NCL slope. There is a significant intercept, unlike Veenhof and McBride (1996) which becomes not significantly different from 0 if the MH soils are

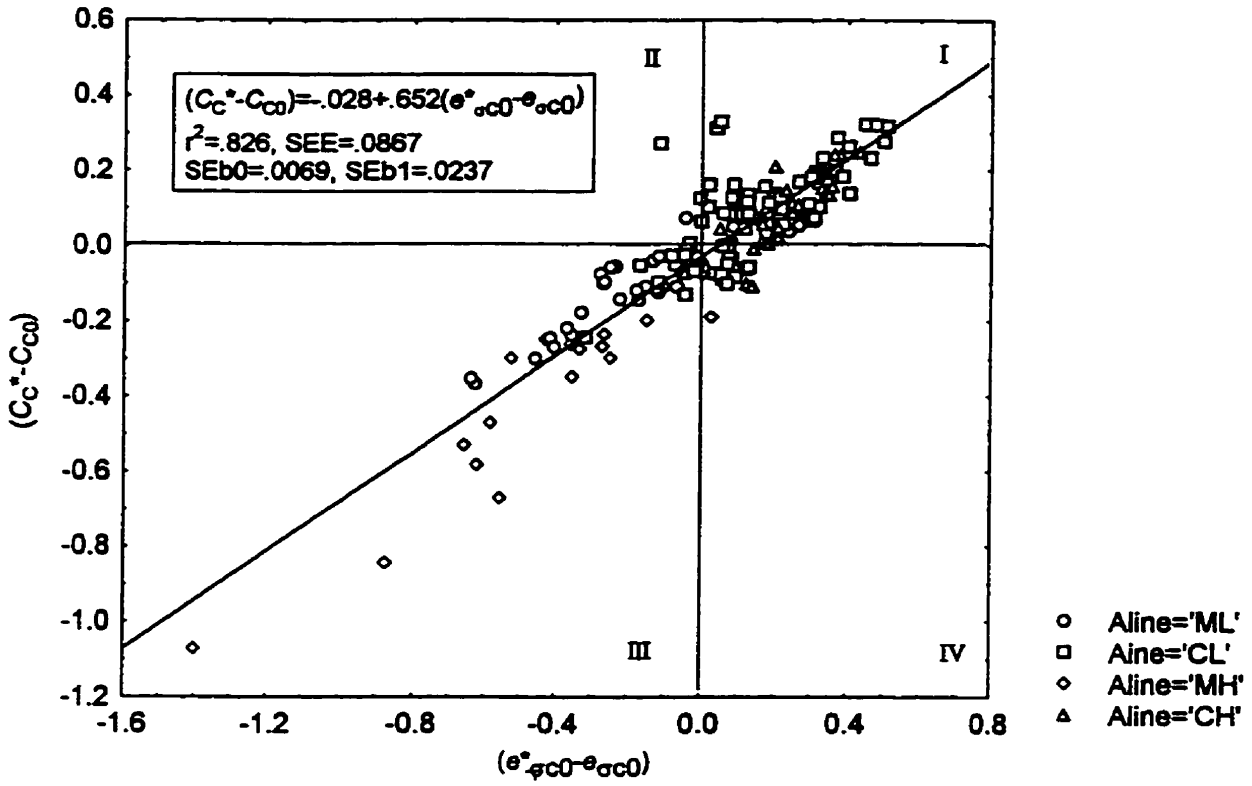

Figure 2.15. Measured difference in slope and in void ratio at σ'_{c0} between the VCL and the corresponding NCL.

removed. The significant intercept means, however, that when the straight line portion of the VCL and NCL parallel each other, the void ratio at the σ'_{c0} on the remoulded curve is above that on the structured curve. This makes sense considering how the σ'_c is determined by the Casagrande method such that it would be on the extrapolated VCL. There are always 3 distinct outliers from the Waterloo Agricultural C horizon which are divergent because the NCL is very steep and cuts across the VCL unlike any other horizon. This NCL was based on only 5 pressures and note was made of the difficulty in remoulding this sample for slurry consolidation so there may be some experimental error.

Given this dominantly convergent behaviour, it would be expected that the intercept of the NCL and initial void ratio would be related to the slopes. Graphs and equations were constructed for $(e^*_{1kPa}-e_0)$ on the y-axis versus either $(e^*_{\sigma c0} - e_{\sigma c0})$ or $(C_C{}^* - C_C)$ on the x-axis to obtain a value and confidence limit for the y (eg. Figure 2.16). The y intercepts were 0.34 (95% CI .329-.367) for $(e^*_{\sigma c0} - e_{\sigma c0})$ and 0.40 (95% CI .376-.427) for $(e^*_{\sigma c} - e_{\sigma c})$ for the applied or effective stresses which are similar to the 0.36 determined by Veenhof and McBride (1996) for distinguishing between over- and underconsolidated structured soils. Since there was a significant intercept (Figure 2.15), a comparison to $(C_C{}^* - C_C)$ could be potentially more informative/conservative for distinguishing between over- and underconsolidation. The y intercept for $(C_C{}^* - C_{C0})$ was 0.40 (95% CI .378-.423) and for $(C_C{}^* - C_{C0}')$ was .41 (95% CI .388-.439). The intercept for $(C_C{}^* - C_C)$ was .46 (95% CI .435-.481) and for $(C_C{}^* - C_C')$ was 0.48 (95% CI .452-.505) (Figure 2.16). The r^2 and SEE were again better for the values based on the 0 second derivative C_{C0}. Regardless of whether applied or effective stresses, or slope or $e_{\sigma c}$ differences are used, a cut-off around 0.40 for $(e^*_{1kPa}-e_0)$ to distinguish between overconsolidated (>0.40) and normally or underconsolidated (<0.40) soils seemed to apply universally regardless of mineralogy, horizon, texture or land use.

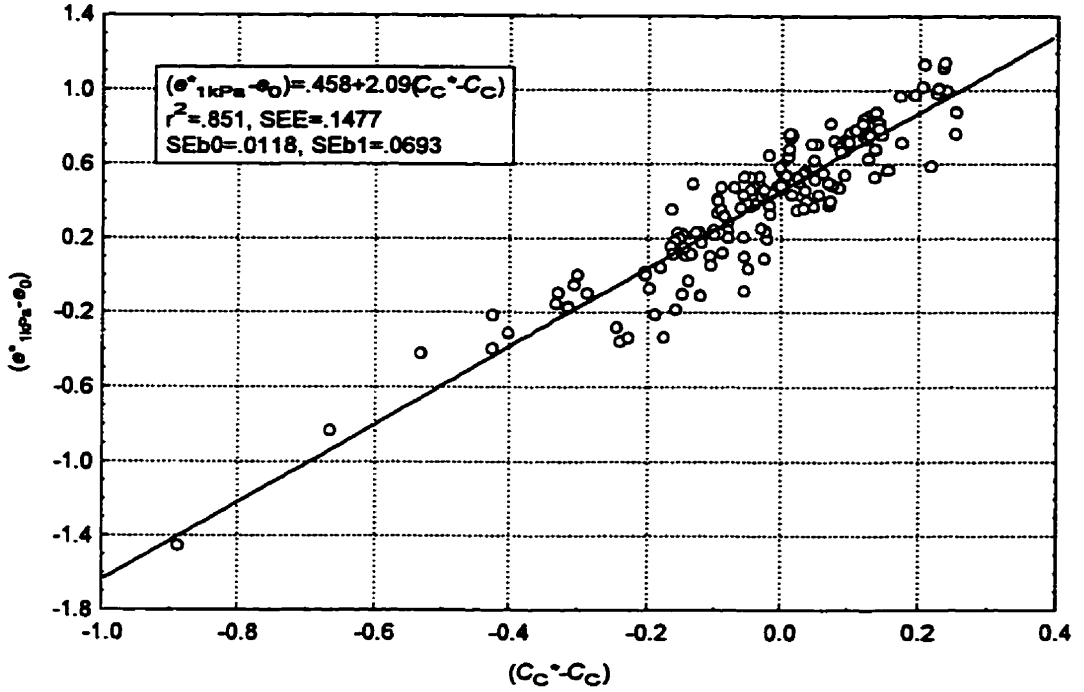

Figure 2.16. Measured difference in void ratio at unit stress and slopes between the structured and corresponding remoulded compression lines. Based on 10 point regressions C_C.

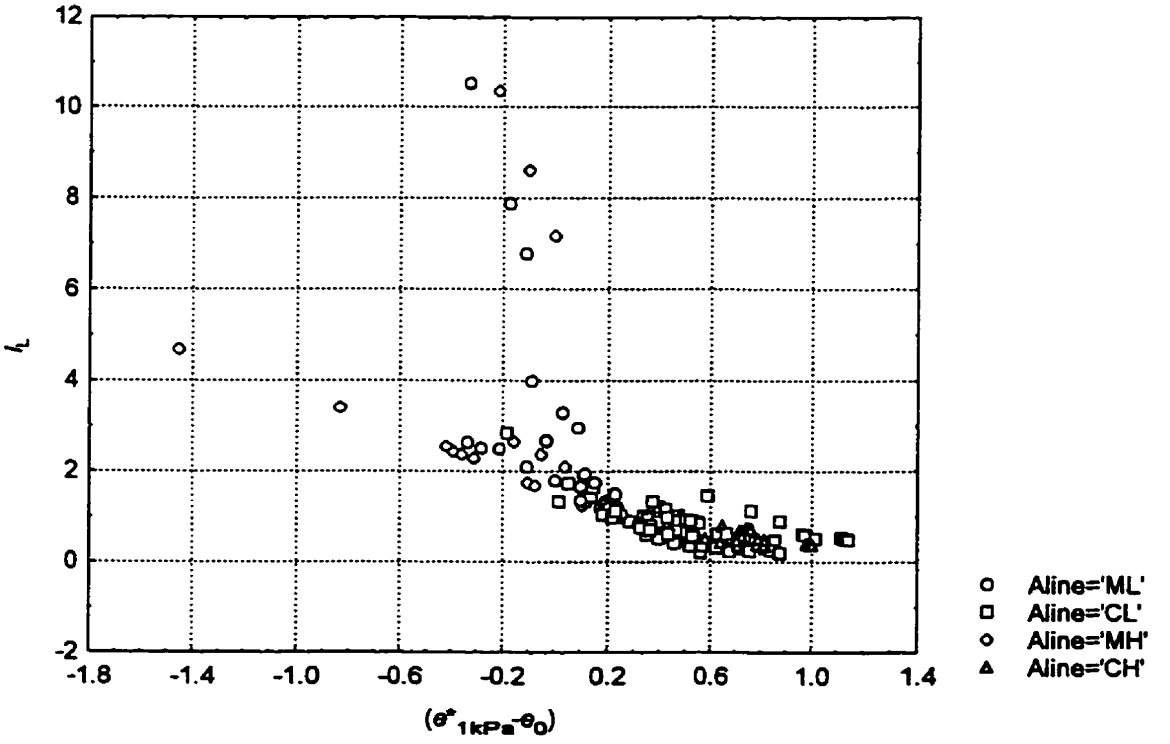

Figure 2.17. Correlation of saturated liquidity index vs. the (e^*_{1kPa}-e_0) variable.

This threshold also continued to correspond to a saturated liquidity index less than 1 (Figure 2.17) similar to that found by Veenhof and McBride (1996) and McBride and Joosse (1996) for PTF1. All the MH and ML soils are below a cut-off of 0.4 and all the CH soils are above a cut-off of 0.4. The 3 WAAC cores are outliers and this may be due to their divergent behaviour and potential overestimation of the C_C*.

When an ANOVA analysis was conducted on the (e^*_{1kPa} -e_0) variable, some fairly clear trends emerged which verified the visual observations of the graphs. There was a significant MNR effect (Table 2.14) and a TRT*HOR interaction (Figure 2.18). The model and significant differences remained the same whether two OTNA outliers were removed or not. The MNR factor indicates that the TX soils are different from the average of the others (p=.0024) by a factor of .4837. Essentially Figure 2.18 holds for the AB, OT and ON soils and a factor of .4837 is added to the means to produce the diagram of the interaction for TX. This confirms the absence of negative (e^*_{1kPa}-e_0) values for TX and the observation that it is the only MNR where the e_0 is always below the e^*_{1kPa} and that there is a substantially greater difference between the NCL and VCL for this site. Addition of the MNR factor difference would mean the TXNA horizon would be positive and would be the only TX horizon below the cut-off of 0.40 for overconsolidation.

Table 2.14. LSmeans separation pdiff and LSmean values for e^*_{1kPa}-e_0 (all data).

Factor	MNR					
	AB vs ON	AB vs OT	AB vs TX	ON vs OT	ON vsTX	OT vs TX
pdiff	.9646	.5321	.0154*	.4071	.0042*	.0047*
	AB	ON	OT	TX		
LSmean	0.3817580	0.3874871	0.2788582	0.8330885		

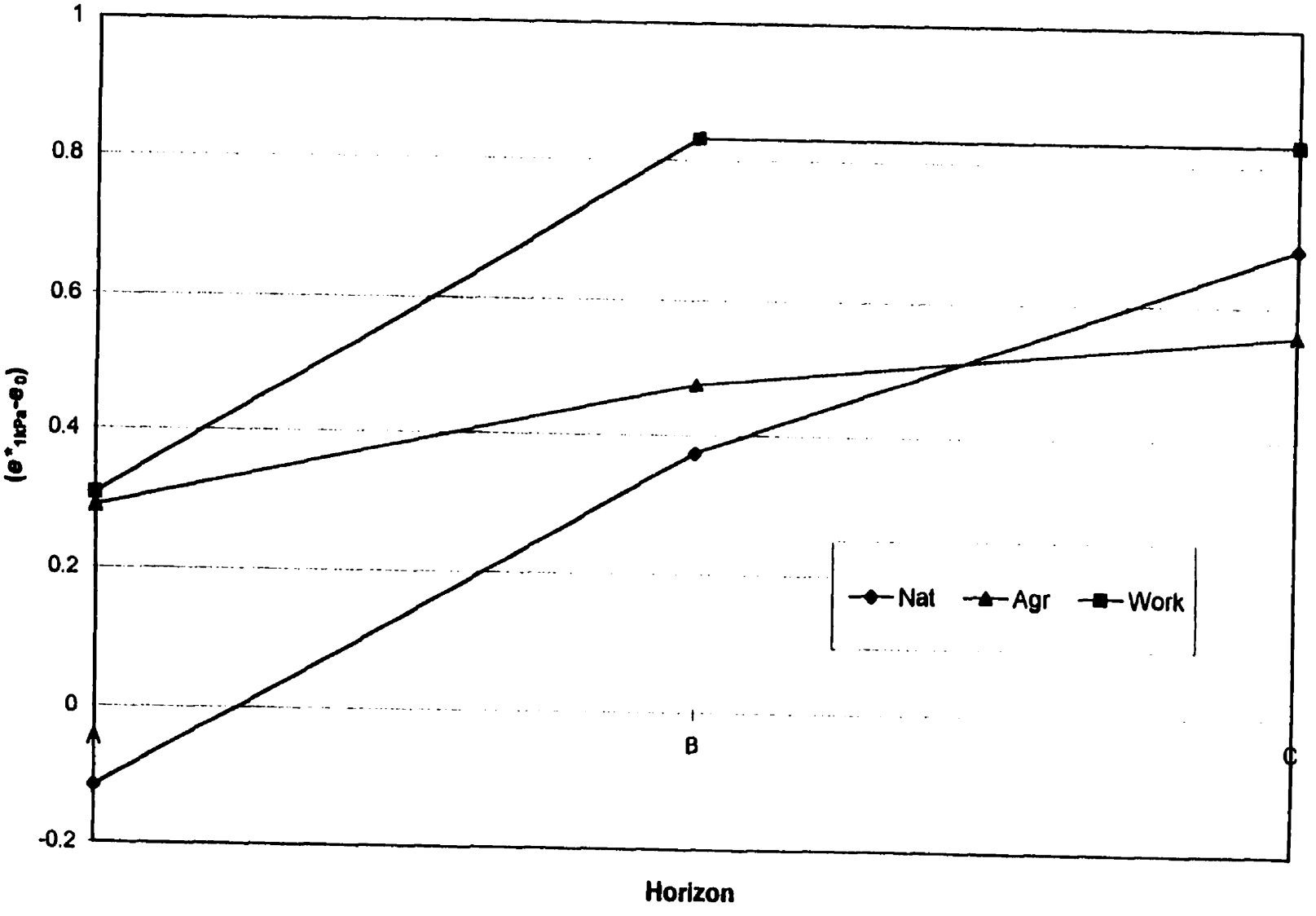

Figure 2.18. Illustration of TRT*HOR interaction for $(e^*_{1kPa}-e_0)$ variable.

The actual (e^*_{1kPa}-e_0) mean for the TXNA horizon is 0.542. The remoulding and wetting to 3-6 times the w_L of these smectitic soils must have allowed substantial swelling for construction of the NCL. Also the structured Texas soils were sampled in a relatively dense state in August after severe drought and even 2 weeks saturation may not have been adequate to allow swelling to increase the structurally intact void ratios (Reeve and Hall, 1979). The Texas A horizons also have the lowest organic matter contents compared to the A horizons of the other sites sampled. The Alberta smectites did not behave in this way. One possibility is that they did not have sufficient clay content to induce swelling to the same degree in the remoulded condition as the TX soils. The coarser texture of the AB horizons was noted when trying to construct the NCL. The AB soils are loam and clay loam (24-32%sand, 27-38% clay) while the TX soils are silty clays (4-11% sand, 47-52% clay).

The TRT*HOR interaction (Figure 2.18) verifies the observation that it is the Natural A horizons which have initial void ratios (e_0) greater than the intercept of the NCL (e^*_{1kPa}) resulting in negative values for (e^*_{1kPa}-e_0) (except for TX as noted). The Nat A horizons are significantly different than all other horizons. The Workspace B and C horizons are also distinguished as being severely overconsolidated from all but the Nat and Agr C horizons. The Agr and Nat B's and C's are not significantly different. If a threshold of 0.40 is used, all the A horizons and the Natural B horizon are normally or underconsolidated while the C horizons and the Workspace and Agricultural B horizons are overconsolidated. The one horizon which does not fit this model is MDAC for all three cores. It is the only C horizon which has negative (e^*_{1kPa}-e_0) values, meaning it is highly underconsolidated. This indicates that this horizon is very likely non-plastic as suspected by the clay content (≈13%) and the remoulded analysis. Veenhof and McBride (1996) found that non-plastic soils never exceeded their 0.36 threshold. Excluding the MDAC horizon raises the mean of the Agr C horizons closer to that of the Nat C horizon.

The differences in the remoulded and structured compression slopes and void ratios at the σ'_c can be looked at separately to look at mechanical reasons for the above differences. Table 2.15 and Table 2.16 illustrate that the relative difference between the compression index of the NCL and VCL (C_C *- C_C) distinguishes A and Natural horizons having the structured compression index steeper than the remoulded (negative differences). The (C_C *- C_{C0}) difference can also distinguish between the Natural and Agricultural horizons but the horizon order is opposite with the A horizons having the greatest difference between the remoulded and structured slopes. MNR was significant at $p<0.10$ with TX being significantly larger than the average of the other horizons. Looking at Figure 2.8 and Figure 2.11 the C_C TRT*HOR interaction is almost opposite that for the C_C * TRT*HOR interaction in that the Workspace B and C horizons go from being the most compressible in the remoulded state to the least compressible in the structured state. The A horizon compressibility is distinguished from the C horizon in the structured state but not in the remoulded state. The range in compressibility is greater for the structured soils and encompasses the Cc* values for the remoulded soils.

For the ($e^*_{\sigma c}$ - $e_{\sigma c}$) and ($e^*_{\sigma c0}$ - $e_{\sigma c0}$) variables there is a significant TRT*HOR interaction which is very similar to the (e^*_{1kPa}-e_0) interaction except that there are more significant differences. The MNR model factor had $p=0.17$ but TX was significantly higher at $p=.05$ by a contrast statement. The complex MNR*TRT*HOR and/or lack of TRT response for the σ'_c stress values was simplified by using the relative indicator.

ANCOVA analyses with OC as a covariate were conducted for these relative variables. They all had very similar models and had R values around 0.97. The OTNA cores were outliers for all the relative variables whether clay or organic carbon was used as a covariate. This horizon borders on being an organic horizon, (i.e. 13% vs the taxonomic 17% OC requirement), and is likely outside the application to mineral soils, although it follows the same converging behaviour.

Table 2.15. LSmeans separation pdiff and LSmean values for ln(-(C_C *- C_C)+.3) (all data).

	Trt (Land Use)			Horizons		
Parameter	Ag. vs. Nat.	Agr. vs. Work	Nat. vs. Work	A vs. B	A vs. C	B vs. C
pdiff	.1662	.0645	.0074*	.0079*	4.85e-5*	.0115*
	Agr	Nat	Work	A	B	C
LSmean	-1.27164643	-1.06643248	-1.62578399	-0.92841521	-1.32995625	-1.70549144
Back Transformed Mean	0.0196303674	-0.044234393	0.1032426411	-0.095179491	0.035511168	0.118316922

Table 2.16. LSmeans separation pdiff and LSmean values for ln(-(C_C *- C_{C9})+.7) (5 flagged cores removed).

Factor	TRT			HOR		
	Agr vs. Nat	Agr vs. Work	Nat. vs. Work	A vs B	A vs C	B vs C
pdiff	.0266*	.0682	.0017*	9.78e-6*	5.15e-9*	.0150*
	Agr	Nat	Work	A	B	C
LSmean	-0.44133478	-0.29279602	-0.58838318	-0.21604347	-0.486382	-0.62009
Back Transformed Mean	0.05682265	-0.04617433	0.144775743	0.392043	0.199853	0.178004

The ($e^*_{\sigma c}$ - $e_{\sigma c}$) and (C_C *- C_C) variables required log transformations while those based on the 0 second derivative did not. There were always significant TRT and OC*TRT factors. The MNR factor could be significant at the 10% level; even at higher p-values there was a significant TX vs other mineralogies ($p<.05$) contrast but this may not be valid with a protected LSD given that many contrasts between TX and individual horizons were not significant. The Workspace intercepts and slopes were always significantly different than the average of the Agr and Natural land uses. The ($e^*_{\sigma c0}$ - $e_{\sigma c0}$), (C_C *- C_{C0}) and (e^*_{1kPa}-e_0) variables had negative slopes with organic carbon while ($e^*_{\sigma c}$ - $e_{\sigma c}$) and (C_C *- C_C) had positive slopes; workspace land use had the steepest slope in either case. The ANCOVA with organic carbon does not necessarily make interpretation any easier but it points out that there is little mineralogical effect (i.e. not at $p<0.05$) using relative terms for Canadian soils but that TX might need to be considered separately ($p<0.10$). It also indicates that the workspace treatment responds in the same direction but to a greater degree to additions of organic carbon than the agricultural and natural land uses.

An ANCOVA was also conducted using %clay as a covariate for the relative variables. This time a much simpler model resulted for ($e^*_{\sigma c0}$ - $e_{\sigma c0}$), (C_C *- C_{C0}), (e^*_{1kPa}-e_0), and ($e^*_{\sigma c}$ - $e_{\sigma c}$) which all had common positive slopes and a TRT factor with Nat<Agr<Work. No transformations were required when the 3 OTNA outliers were again removed which greatly improved the normality of the residuals. The (C_C *- C_C) variable required a log transformation and there was a positive quadratic term and a negative linear value for the clay covariate.

The e^*_{1kPa}-e_0 variable model can be used as an example of the clay covariate results since the relative variables are all interrelated (MSE=.007155, R=.97782, n=159): [51]

i) Agr: e^*_{1kPa}-e_0 =-.27324565+.01860597*%clay* SEb0=.0589966, SEb1=.00280343

ii) Nat: e^*_{1kPa}-e_0 =-.39528867+.01860597*%clay* SEb0=.0597668

iii) Work: e^*_{1kPa}-e_0 =-.05343999+.01860597*%clay* SEb0=.1183179

The Workspace intercept is not significantly different than 0 (p=.656). All intercepts, and therefore means, are significantly different from each other such that there is a constant separation between treatments at each clay content (Figure 2.19).

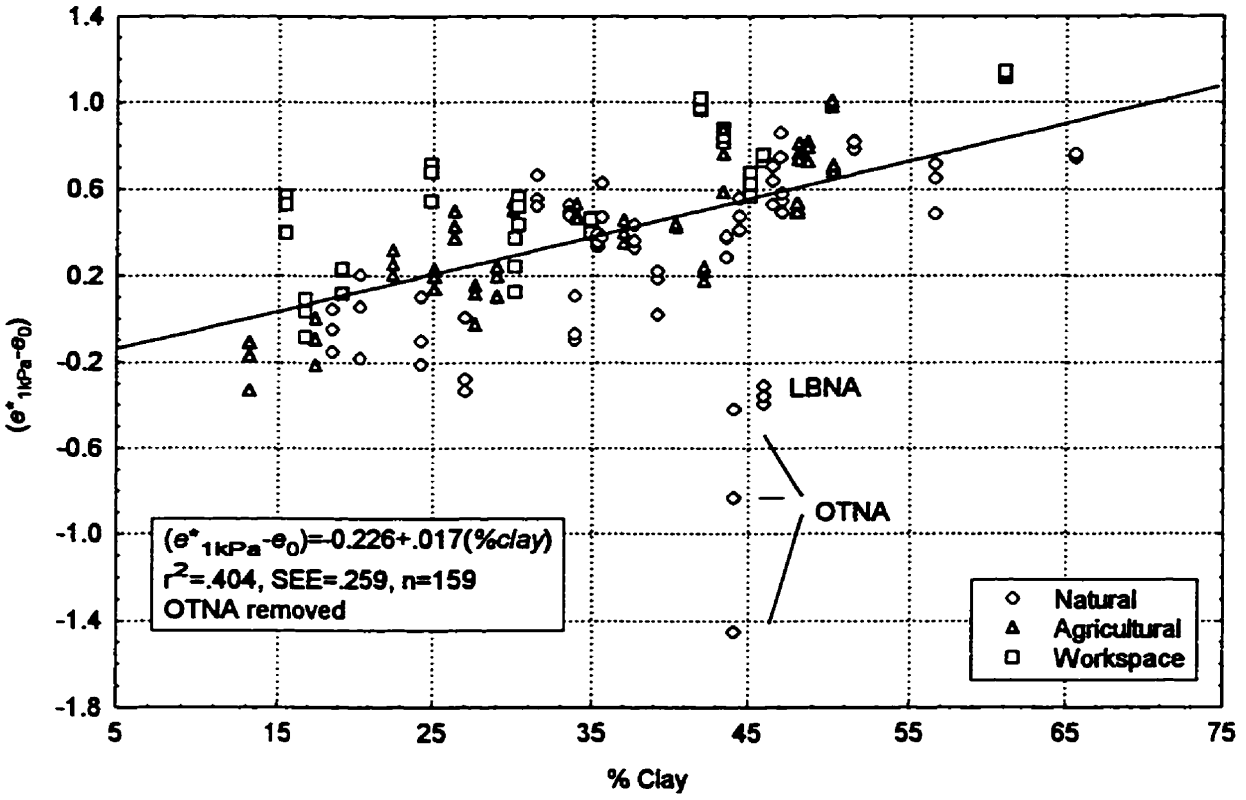

Figure 2.19. Covariance between e^*_{1kPa}-e_0 variable and % clay content.

2.3.5 Implications for Assessing Structural Quality

The relative compression variables had the capability to distinguish structural states and past land use history better than the remoulded and structured compression parameters alone. This sensitivity could be compared to other indicators of structural quality. All the relative variables showed linear relationships with plant available water content (AWC), macroporosity (-5kPa) and log saturated hydraulic conductivity. The ($e^*_{\sigma c} - e_{\sigma c}$) variables gave the highest correlations, the ($C_C{}^* - C_{C0}$) the lowest and the ($e^*_{1kPa}-e_0$) were intermediate; the ($e^*_{1kPa}-e_0$) results will be presented here since they are the easiest to conceptualize and determine in the lab or by predictive equations, and essentially synthesize the other relative variables into one parameter. There were significant linear relationships for the horizon averages (n=54) of the ($e^*_{1kPa}-e_0$) variable with both AWC (r^2=.51) and macroporosity (r^2=.64) (Figure 2.20 and Figure 2.21). Substituting an overconsolidation threshold of 0.40 produced an AWC of 0.0883 (SEE=.01814) and a macroporosity of .0742 (SEE=.0325) which ensures the value of 0.40 will be a conservative classification of severely overconsolidated and structurally impaired soils. These aeration restrictions could also lead to a change in the soil drainage class. It should be noted that many of the soils sampled would be classified as having some kind of structural limitation because of their low AWC (<16%). With respect to the Canada Land Inventory, soils with AWC <10% would be classified as 3d and have a corresponding productivity index 70% that of a class 1 soil (McBride and Mackintosh, 1984). A combination of sampling higher clay content soils and subsoils may have contributed to the relatively low values of AWC and macroporosity represented here.

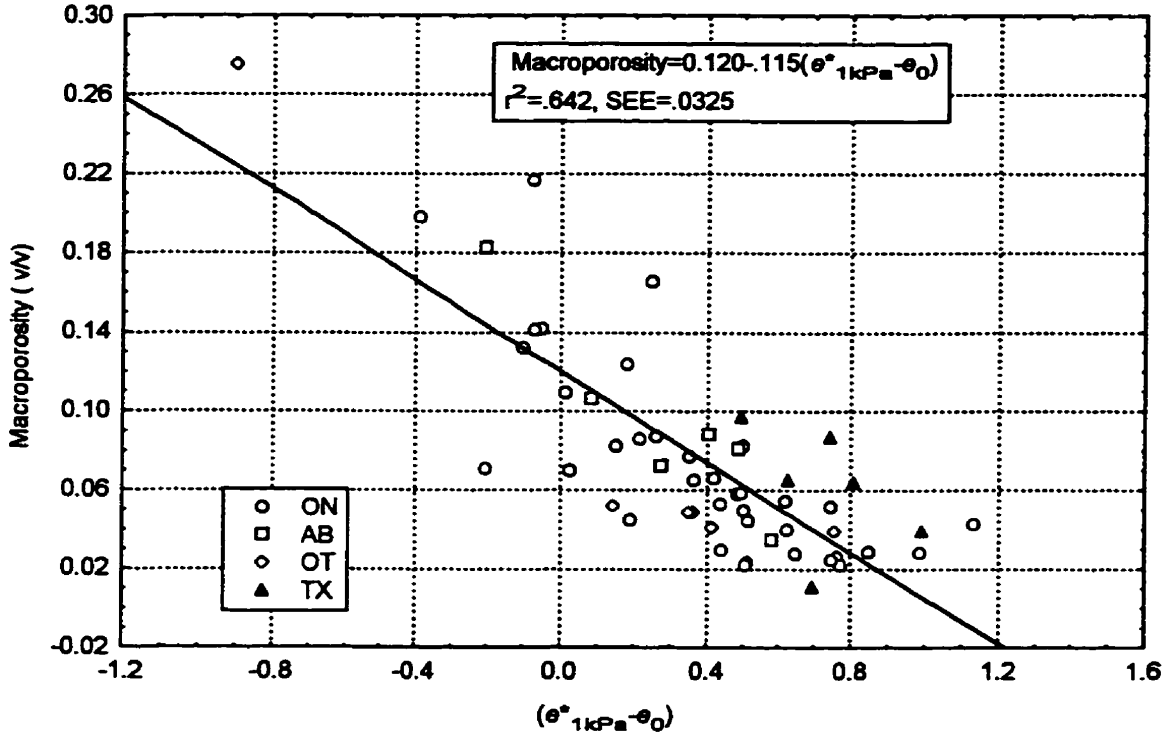

Figure 2.20. Relationship between e^*_{1kPa}-e_0 variable and macroporosity (0 to -5kPa)

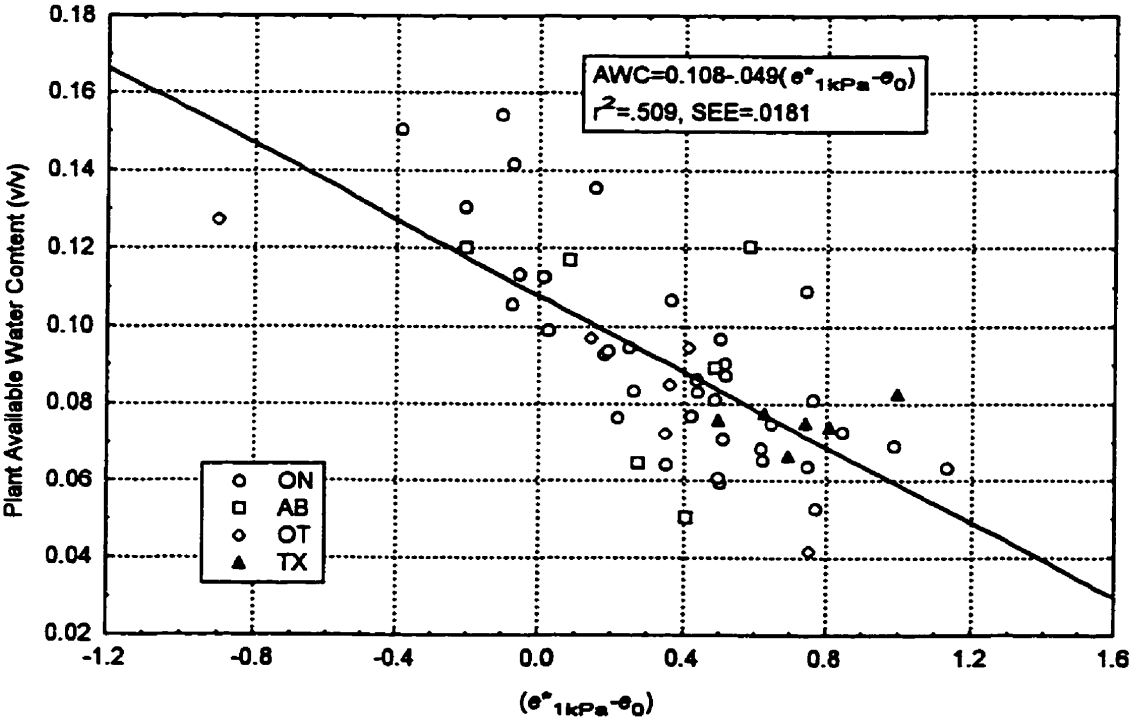

Figure 2.21. Relationship between (e^*_{1kPa}-e_0) and plant available water content (-33 to -1500 kPa).

Similarly, there was a significant linear relationship between the log(K_{sat}) and the e^*_{1kPa}-e_0 variable but the amount of variability explained was low (r^2=.249, SEE=1.10, n=49, p<.001) (Figure 2.22). There were 5 horizons for which either a field saturated or laboratory K_{sat} determination were not made. McKeague et al. (1982) use 8 classes of K_{sat} values for general conductivity guidelines which can be separated into High, Medium and Low by boundaries of 4.63 x 10^{-5} m/s and 1.16 x 10^{-6} m/s, respectively. The corresponding log values are -4.33 and -5.93. A wide range of values is represented in Figure 2.22. Substituting a value of 0.40 results in a logK_{sat} of 5.00 which is in the middle of the Medium conductivity class and again ensures a conservative estimate of structurally degraded soils.

The relationship between e^*_{1kPa}-e_0 and clay or organic carbon content creates implications for using a threshold of 0.40 universally. For horizons having greater than 3% organic carbon, the e^*_{1kPa}-e_0 variable was less than 0.40. Similarly, looking at all treatments simultaneously with OTNA removed, the mean e^*_{1kPa}-e_0 was greater than 0.40 when the clay content was greater than 36.0% which is essentially the lower boundary for the fine clay family particle size class (Agriculture Canada Expert Committee on Soil Survey, 1987). When analyzing the treatments individually, the threshold of 0.4 represents 24.4% clay for the Workspace, 36.1% clay for the Agricultural and 42.7% clay for the Natural treatments indicating that higher clay contents do not necessarily mean more overconsolidation and can be overcome when there is sufficient bioturbation in a land use system. Conversely, the stresses induced in the workspace treatment can create overconsolidated soils at clay contents as low as 24% (i.e. loam and silt loam particle size classes). If (C_C *- C_C) is used as the relative variable, the clay content when the difference is 0 is equal to 40.7%. Therefore, somewhere around 36-40% clay content the compressibility (slope) of the saturated NCL and VCL will be similar but greater than 42% clay the VCL will show an overconsolidated state and below 36% clay the VCL will show a normally or underconsolidated

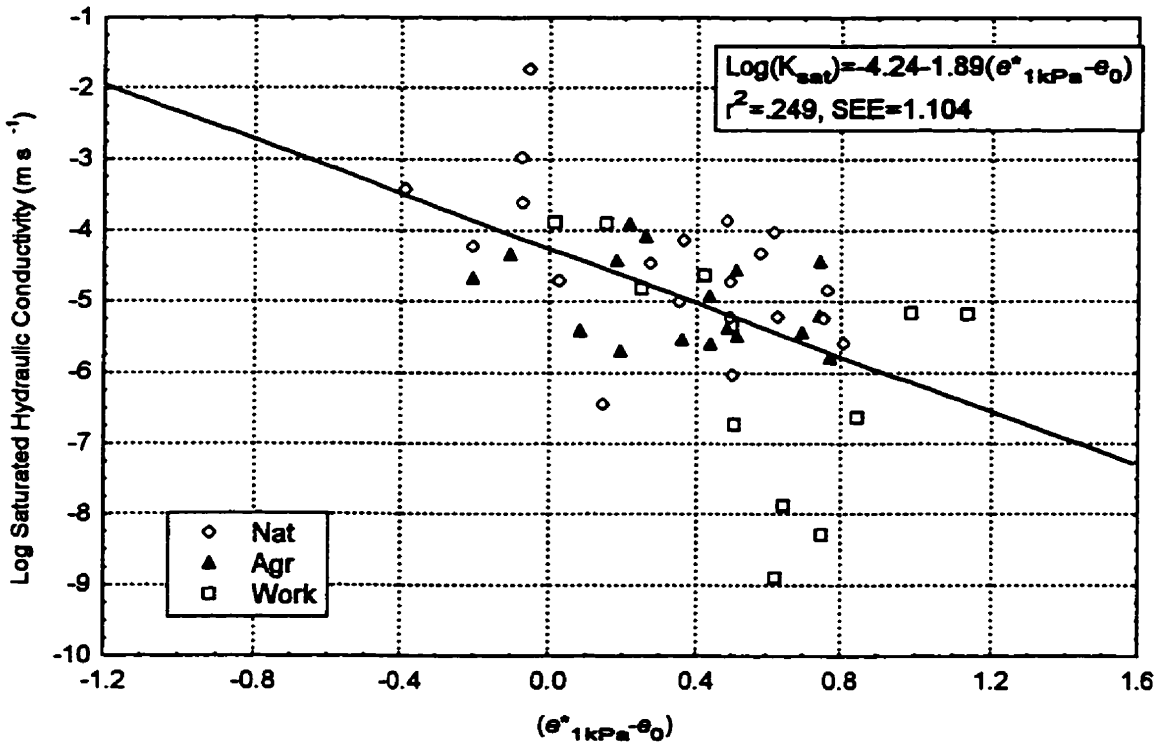

Figure 2.22. Relationship between saturated hydraulic conductivity and e^*_{1kPa}-e_0.

state for structurally intact samples.

Increased organic carbon works to raise the VCL above the NCL and increased clay works to raise the NCL above the VCL as shown by the preceding ANCOVAs and the following regressions (OTNA removed, n=159, $p<0.001$):

$e^*_{1kPa}-e_0=.014751\%clay-.079177\%organic\ carbon$ SEE=.2114, $r^2=.6036$ [52]

$e^*_{1kPa}-e_0=.01611\%clay-.003197\%organic\ carbon x\%clay$ SEE=.1957, $r^2=.6602$ [53]

When estimating an e^*_{1kPa} value, both equations [36] and [38] were used. When the $(e^*_{1kPa}-e_0)$ variable is estimated on a core by core basis (n=162), equation [36] does not produce a 1:1 relationship with the measured $(e^*_{1kPa}-e_0)$ variable and there was separation of the TX and OT soils from a 1:1 line (Figure 2.23). Equation [36 did produce a 1:1 relationship based on the average e_0 and $(e^*_{1kPa}-e_0)$ by horizon (n=54). The much simpler equation [38], based solely on the void ratio at the liquid limit, did produce a 1:1 relationship with all 162 cores ($r^2=.8251$, SEE=.160) and with averages for 54 cores ($r^2=.816$, SEE=.162) and there was no distinction based on mineralogy but the residuals were not normally distributed. The WAAC, WAWB and WAWC cores were all outliers with the prediction underestimating the measured $e^*_{1kPa}-e_0$ variable (Figure 2.24). When these cores were removed, a 1:1 relationship did not result for 153 cores (b0=.0038, SEb0=.0133, b1=.9212, SEb1=.0248, $r^2=.902$, SEE=.1144) but remained for the n=51 cores ($r^2=.896$, SEE=.116).

There was a significant ($p<0.001$) positive relationship (normally distributed residuals with the OTNA cores removed) which did not explain much of the variability between the $e^*_{1kPa}-e_0$ variable and the σ'_c values ($r^2=.19$, SEE=.038) and a negative relationship with the $\log\sigma'_{c0}$ values ($r^2=.12$, SEE=.176). Similarly there was a positive trend between the σ'_c estimated using PTF2 (McBride and Joosse, 1996) ($r^2=.11$) and the measured σ'_c values and a negative trend with the $\log\sigma'_{c0}$ values ($r^2=.10$). This confirms the relationship of the σ'_{c0} values to the point of maximum

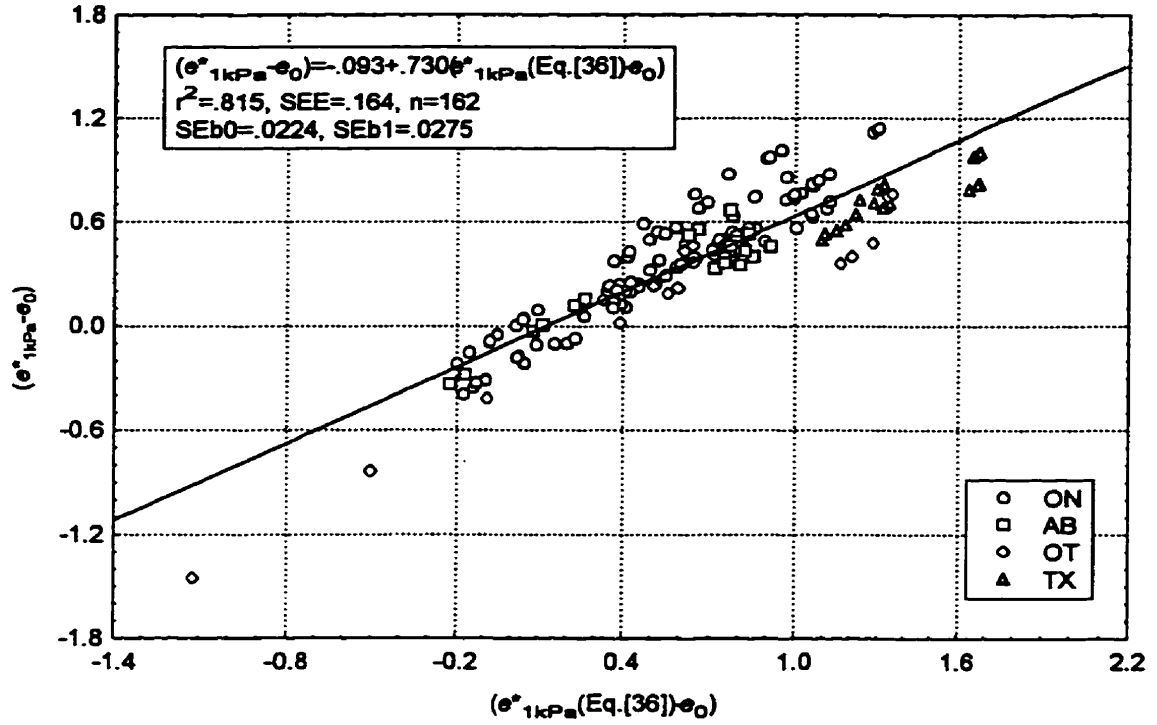

Figure 2.23. Comparison of measured e^*_{1kPa}-e_0 versus predicted difference using Eq. [36].

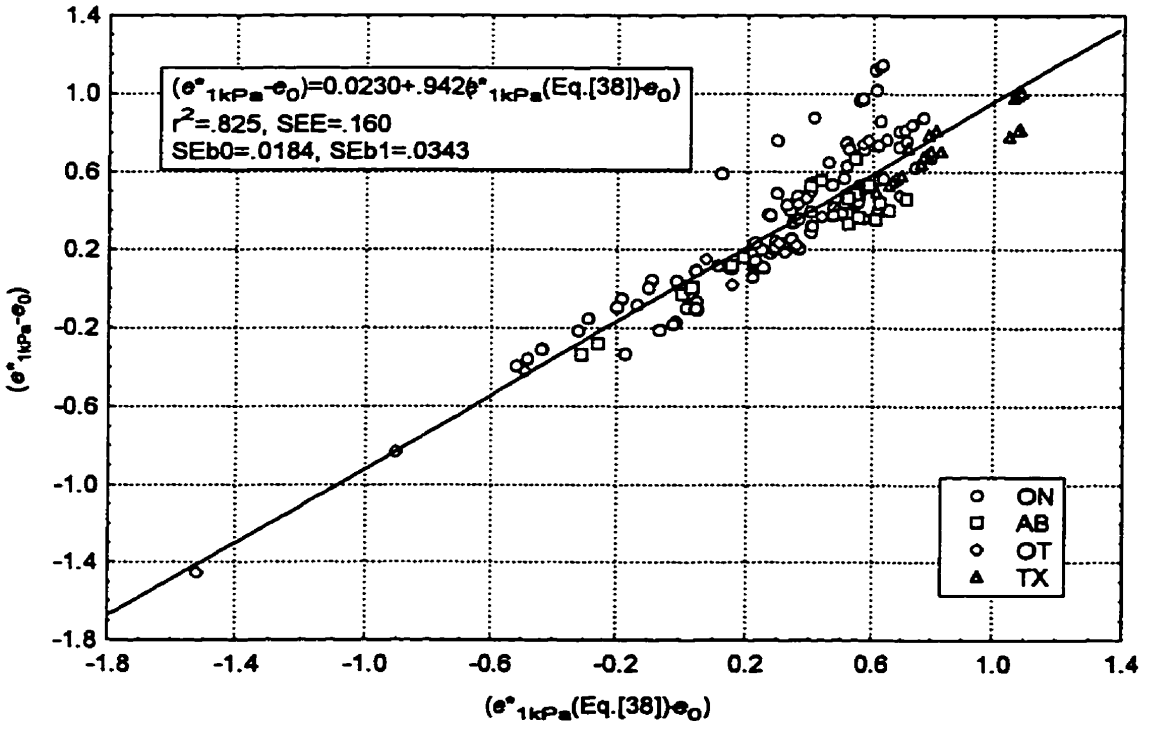

Figure 2.24. Comparison of measured e^*_{1kPa}-e_0 versus predicted difference using Eq. [38]

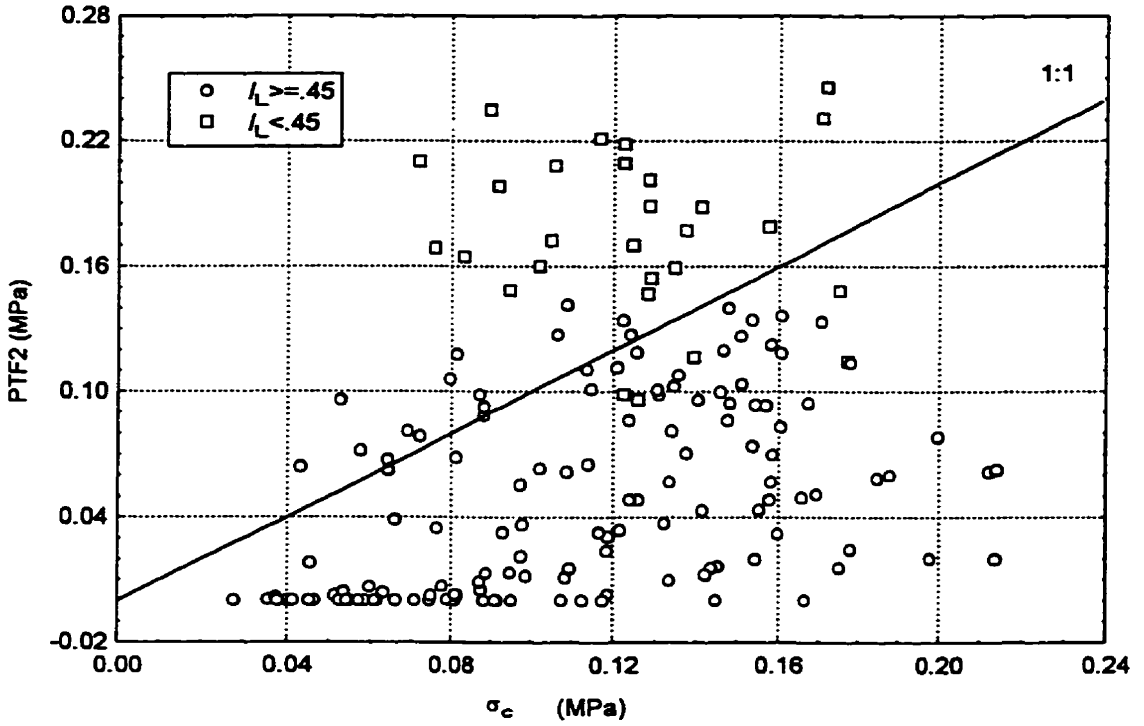

Figure 2.25. I_L = 0.45 cutoff for comparing PTF2 estimated and measured σ_c.

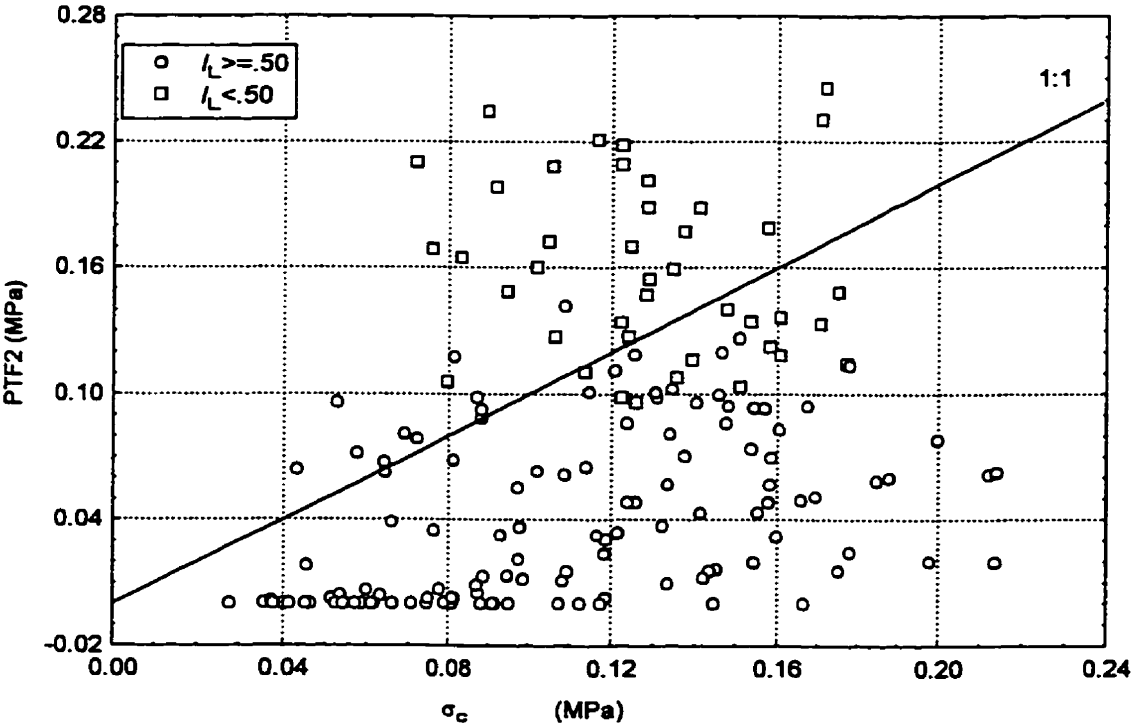

Figure 2.26. I_L = 0. 50 cutoff for comparing PTF2 estimated and measured σ_c.

curvature (i.e. at higher stresses for the more loose and compressible soils) rather than the σ'_c values determined by the Casagrande method. Using PTF2 on soils with a structured saturated liquidity index greater than 0.45-0.5 prevents overestimation of the σ'_c values for overconsolidated soils (Figure 2.25 and Figure 2.26). The horizons for which PTF2 overestimates the σ'_c are the TXA A and the AB B horizons even though the I_L>0.5. This may be due to the distinction that the smectite soils did not have a significant relationship with organic carbon with the σ'_{wL} which PTF2 is based upon. The values are not overestimated by more than 40 kPa when a threshold of 0.45 is used.

The estimated σ'_c values via PTF2 for all cores (n=162) were subjected to an ANOVA analysis using the split plot design of the experiment rather than a completely randomized design. No threshold I_L value was used at this point and a square root transformation was required; an attempt using I_L <.25 did not improve the distribution of the residuals. There were significant TRT and HOR effects (Table 2.17); MNR was not significant (p=.36) and TRT*HOR had p=.08. Two MDWC and a HLWC core were outliers but the model did not change so the results are presented with all the data . Table 2.17 resembles the results of Table 2.15 for the (C_C *- C_C) variable.

Table 2.17. LSmeans separation pdiff and LSmean values for sqrt(PTF2) (n=162).

	Trt (Land Use)			Horizons		
Parameter	Ag. vs. Nat.	Agr. vs. Work	Nat. vs. Work	A vs. B	A vs. C	B vs. C
pdiff	.1469	4.45e-5*	1.05e-6*	4.23e-11*	1.65e-12*	.2673
	Agr	Nat	Work	A	B	C
LSmean	0.23901	0.20948	0.35357	0.12473	0.32611	0.35121
Back Transformed Mean (MPa)	0.057	0.042	0.125	0.016	0.106	0.123

When the PTF2 values were calculated using the average e_0 for a horizon (n=54), no transform was required if the marginally plastic horizon, MDAC, was removed. There was again no MNR effect and there was a significant TRT*HOR interaction illustrated in Figure 2.27. Figure 2.27 resembles Figure 2.18 for the e^*_{1kPa}-e_0 variable. Figure 2.27 represents the concept of "normal" bulk density described by Hartge (1986); the stresses determined by the corresponding e_0 of the natural horizons increase linearly with depth due to overburden pressures. The A horizon stresses are not significantly different from each other; except for Work A and Nat B. The A horizons are significantly different from the other horizons. The agricultural and workspace B horizons represent stresses higher than what would result from a linear relationship with overburden pressure alone and are not significantly different from the corresponding C horizons; conversely, the Nat B horizon is different from the Nat C horizon. The workspace B and C horizons are significantly different ($p<.001$) from all the other horizons indicating that even the C horizon has endured stresses higher than "normal" overburden pressures; conversely, the Agricultural and Natural C are not significantly different nor are the Agr B and Nat B. The maximum overburden pressure calculated from saturated bulk densities for overlying horizons is 0.0274 MPa for the 150 cm deep TX C horizons. Most overburden pressures are < 0.001 MPa for the A horizons, around 0.001 MPa for the B horizons and around .010 MPa for the C horizons. The estimated PTF2 values are higher than this and the measured σ'_c are even higher supporting the hypothesis that factors such as desiccation and trafficking contribute greater consolidation pressures than overburden pressures alone.

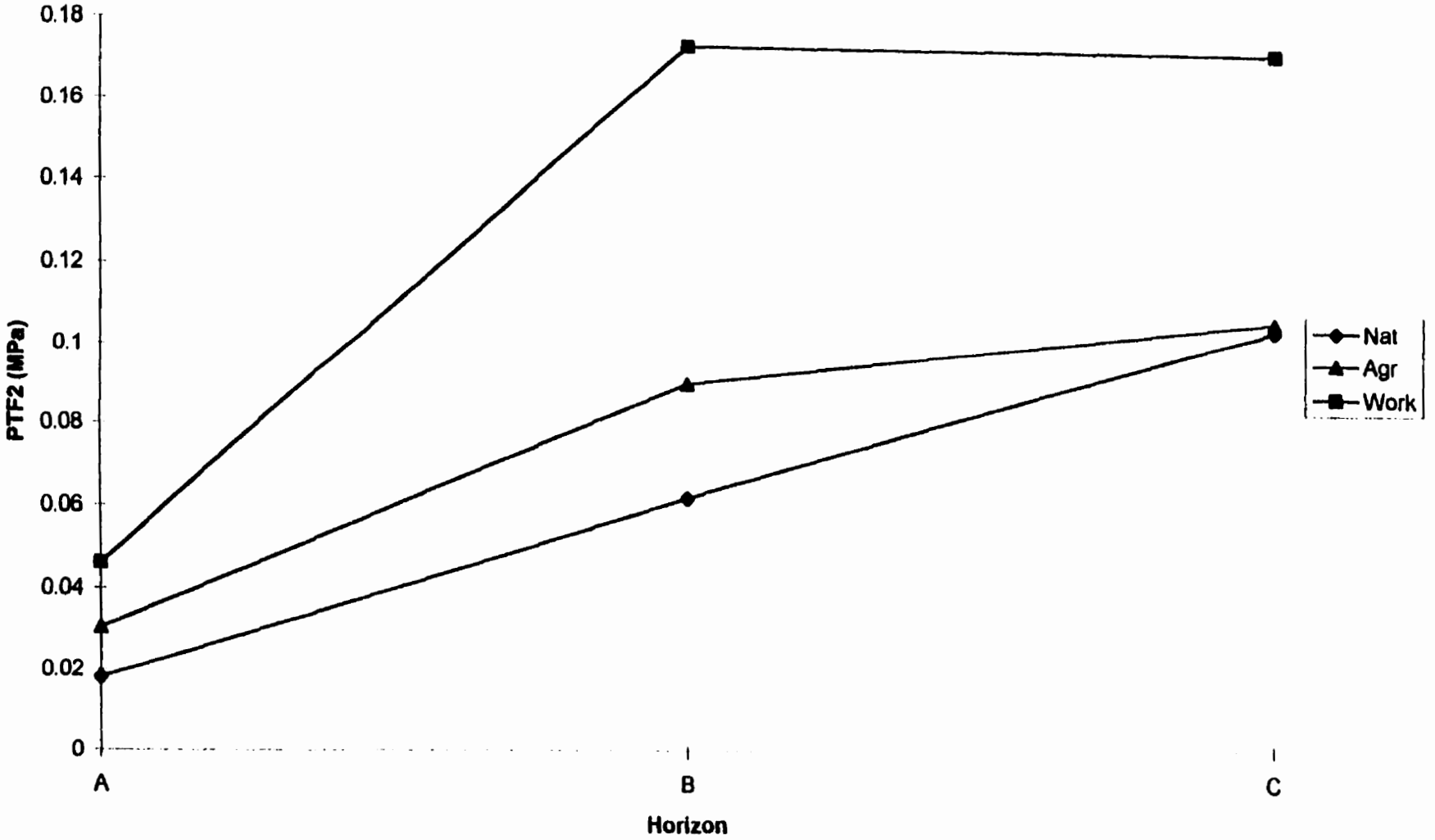

Figure 2.27. PTF2 TRT*HOR interaction. MDAC removed.

2.4 Conclusions

In regards to the first objective, the existing equations for predicting the σ'_{wL} by PTF2, and used in PTF1, do not apply to soils of smectitic mineralogy. Both TX and AB soils had no significant relationship between the σ'_{wL} and organic carbon. Three models to estimate σ'_{wL} produced equally good estimates of w_L (1:1 relationships, r^2>.95) when inserted into the measured NCL. These were i) Eq.[29] and a simple average for AB and TX sites and for soils with > 6.74% organic carbon, ii) an ANCOVA with logOC and transformed y values for each mineralogy separately, Eq.[16], or iii) separate regression equations for smectitic and non-smectitic mineralogy (Eq. [iv and vi], Table 2.9). Testing indicated that ANCOVA and regression models which included % clay and/or % organic carbon were more appropriate to approximate the σ'_{wP} than an average value. Both i) the ANCOVA with $\ln(\sigma'_{wP})$ and OC*MNR and TRT factors, Eq.[18], and ii) the equation of Veenhof (1993), Eq.[27], gave 1:1 relationships with w_P ($r^2 > 0.87$) when inserted into measured NCL equations. Only sieving to <2 mm rather than the accepted <.425 mm may have complicated the prediction of the stresses from soil survey data as existing equations fit the data well for most cases.

Estimating the NCL slope and intercept using measured Atterberg limits and these equations for the stresses at the Atterberg limits did not produce good results. The only significant 1:1 relationship was found between the measured e^*_{1kPa} and that estimated using Eq. [22] and Eq. [iv and vi] from Table 2.9. Similarly, regression equations with suitable predictive capability (r^2 > 0.74) were only found for the intercept and not the slope of the NCL. The inability to predict the C_C* may be related to the TRT*HOR interaction which found the A and C horizon slopes to be similar and Agr and Nat B horizons to be significantly less compressible in the remoulded state than Work B and all the C horizons. The interaction was partially removed with % organic carbon

as a covariate, leaving only a OC*TRT factor with Work horizons having a significant relationship, and completely removed for %clay as a covariate but not very much of the variability was explained by the resulting equation. Thus in addition to clay and organic carbon contents, which are predominantly thought to influence the colloidal and cohesive properties of the soil, other factors such as $CaCO_3$ content and microaggregate structure may influence the compressibility of soil which can be affected by land use even in the remoulded state. This is not thought to be a large enough concern to preclude using remoulded conditions as a reference state as the chemical properties between samples are maintained and the majority of the biologically important structure is destroyed. The results do, however, question the validity of using the positioning of the liquid and plastic limit alone to reconstruct the NCL and more research is required to confirm this concept.

In regard to the second objective, the relative soil quality indicator (e^*_{1kPa}-e_0) threshold of 0.40 universally divides those samples with the configuration of the structured VCL above the NCL from those with the structured VCL below the NCL, independent of clay mineralogy or land use. The converging pattern of the VCL and NCL means that other relative indicators, ($e^*_{\sigma c0}$ - $e_{\sigma c0}$), (C_C *- C_{C0}), ($e^*_{\sigma c}$ - $e_{\sigma c}$) and (C_C *- C_C), are interrelated and the simpler intercept difference, which is more easily estimated, is a surrogate for all the others. Because of the geometry, (e^*_{1kPa}-e_0) is an expression of the overconsolidation ratio as suggested by Bard (1993) (in Biarez and Hicher, 1994, p. 105).

$$e_{NC} - e_{OC} = (C_C - C_S)\log(\frac{p'_C}{p'})$$

Using the threshold value of 0.40 for e_{NC}-e_{OC}, 0.286 for C_C (the median value for C_C*, C_C and C_C') and assuming the swelling index C_S =0, the overconsolidation ratio p'_c/p' is 25 which would indicate a highly overconsolidated soil.

Individually, the C_C , C_C', CR and CR′ parameters are more informative of differences between treatments than the σ'_c. The Workspace treatment C_C* and C_C' respond more to changes in organic carbon than the Natural or Agricultural treatments which shows the value of using a remoulded sample from that same treatment as the reference state but also that more disruptive remoulding may be required to destroy all structural differences. The C_C are also dependent on the e_0 of the saturated, structured samples. The σ_c and σ'_c variables had no treatment effect and the AB and TX site values were not affected by organic matter content.

The difference of the TX soils in the displacement of the VCL from the NCL may have indicated a threshold value of $(e^*_{1kPa}-e_0)$=0.88 to be more appropriate, but comparison of the AWC, macroporosity and K_{sat} data indicate that a threshold of 0.40 is a conservative indicator of structural quality for all mineralogies. The low r^2 for many of the relationships indicates that $(e^*_{1kPa}-e_0)$ may not be the most sensitive indicator of structural quality for treatment differences but its applicability for regional soil survey interpretation is promising.

In regard to the third objective, it has been shown that much of the overconsolidation in surface soils (< 1m depth) is due to natural processes as displacement of the VCL below the NCL was evident in all natural land use profiles. In particular, those soils with greater than 36% clay content ("fine" family particle size class) had the tendency to be overconsolidated. It is only in land uses with significant bioturbation that natural processes, in particular desiccation, have been overcome. All A horizons (except TX) had sufficient biological activity to be normally or under-consolidated while the C horizons (except the marginally plastic MDAC) were overconsolidated. The B horizon characteristics were most sensitive to land use treatments. The natural land use served as a frame of reference with index values decreasing linearly with depth. The Natural B horizons, on average, were normally consolidated (except TX) while the workspace and agricultural B horizons were overconsolidated and had index values similar to the C horizons.

PTF2, (e^*_{1kPa}-e_0), ($e^*_{\sigma c}$ - $e_{\sigma c}$) and ($e^*_{\sigma c0}$ - $e_{\sigma c0}$) were all structural indices which had similar TRT*HOR results and could be considered suitable indicators for regional physical soil quality monitoring. PTF2 can then be regarded as a relative indicator as well, since it combines the compressibility of a remoulded sample with the current intact void ratio to estimate a conservative ("minimum possible") preconsolidation pressure.

2.5 References

Agriculture Canada Expert Committee on Soil Survey. 1987. The Canadian system of soil classification. 2nd ed. Agric. Can. Pub. 1646. Supply and Services Canada, Ottawa, ON.

Al-Khafaji, A.W.N. and O.B. Andersland. 1992. Equations for compression index approximation. J. Geotech. Eng. 118(1):148-153.

Allen, B.L. and B.F. Hajck. 1989. Mineral occurrence in soil environments. p. 199-278 *In* J.B. Dixon and S.B. Weed (eds). Minerals in Soil Environments. Soil Science Society of America Book Series No. 1. SSSA, Madison, WI.

American Society for Testing and Materials. 1981. 1981 Annual book of A.S.T.M. standards, Part 190. ASTM, Philadelphia, PA.

Angers, D.A., B.D. Kay and P.H. Groenevelt. 1987. Compaction characteristics of a soil cropped to corn and bromegrass. Soil. Sci. Soc. Am. J. 51:779-783.

Angers, D.A. 1990. Compression of agricultural soils from Quebec. Soil & Tillage Res. 18:357-365.

Assouline, S., J. Tavares-Filho, and D. Tessier. 1997. Effect of compaction on soil physical and hydraulic properties: Experimental results and modelling. Soil Sci. Soc. Am. J. 61:390-398.

Biarez, J. and P. Hicher. 1994. Elementary mechanics of soil behaviour: saturated remoulded soils. A.A. Balkema, Rotterdam, NL.

Bailey, A.C., C.E. Johnson, and R.L. Schafer. 1986. A model for agricultural soil compaction. J. Agric. Eng. Res. 33:237-262.

Baver, L.D. 1930. The Atterberg consistency constants: factors affecting their value and a new concept of their significance. J. Am. Soc. Agron. 22:935-948.

Blake, G.R. and K.H. Hartge. 1986. Particle density. p. 377-382. *In* A. Klute (ed.) Methods of soil analysis. Part 1. 2nd ed. Agron. Monogr. 9 ASA and SSSA, Madison, WI.

Bouma, J. 1989. Using soil survey data for quantitative land evaluation. Adv. Soil Sci. 9:177-213.

Carter, M.R. 1990. Relative measures of soil bulk density to characterize compaction in tillage studies on fine sandy loams. Can. J. Soil. Sci. 70:425-433.

Casagrande, A. 1936. Determination of the preconsolidation load and its practical significance. Proc. of the Int. Cong. on Soil Mechanics and Foundation Engineering. Vol III, No.D-34.

Cochran, W.G. and G.M. Cox. 1957. Experimental Designs. 2nd ed. 1992 . John Wiley & Sons, Inc.: Toronto. 611 pp.

Coleman, J.D., D.M. Farrar, and A.D. Marsh. 1964. The moisture characteristics, composition and structural analysis of a red clay soil from Nyeri, Kenya. Géotechnique. 14:262-276.

Craig, R.F. 1992. Soil Mechanics. Fifth Ed. Chapman and Hall: London.

Culley, J.L.B., B.K. Dow, E.W. Presant and A.J. MacLean. 1982. Recovery of productivity of Ontario soils disturbed by an oil pipeline installation. Can. J. Soil Sci. 62:267-279.

Culley, J.L.B. and W.E. Larson. 1987. Susceptibility to compression of a clay loam Haplaquoll. Soil Sci. Soc. Am. J. 51:562-567.

Dawidowski, J.B. and A.J. Koolen. 1994. Computerized determination of the preconsolidation stress in compaction testing of field core samples. Soil & Tillage Res. 31:277-282.

De Jong, E., D.F. Acton and H.B. Stonehouse. 1990. Estimating the Atterberg limits of southern Saskatchewan soils from texture and carbon contents. Can. J. Soil Sci. 70:543-554.

De Kimpe, C.R. 1993. Soil separation for mineralogical analysis. p. 711-717. *In* M.R. Carter (ed.) Soil Sampling and Methods of Analysis. Canadian Society of Soil Science. Lewis Publishers: Boca Raton.

Derdour, H. and D.A. Angers. 1992. Influence on salinity and other constituents on the mechanical behaviour of clay soils. Soil Tech. 5:39-46.

Dexter, A.R. and K.Y. Chan. 1991. Soil mechanical properties as influenced by exchangeable cations. J. Soil Sci. 42:219-226.

Dias Junior, M.F. and F.J. Pierce. 1995. A simple procedure for estimating preconsolidation pressure from soil compression curves. Soil Tech. 8:139-151.

Doran, J.W. and T.B. Parkin. 1994. Defining and assessing soil quality. p. 3-21 *In* J.W. Doran et al. (ed) Defining soil quality for a sustainable environment. SSSA Special Publication no. 35. SSSA and ASA, Madison, WI.

Emerson, W.W. 1977. Physical properties and structure. pp. 78-104 *In* J.S. Russell and E.L. Greacen (eds.) Soil Factors in Crop Production in a Semi-arid Environment. Univ.

Queensland Press: St. Lucia, Queensland.

Fallow, D.J., D.E. Elrick, W.D. Reynolds, N. Baumgartner and G.W. Parkin. 1993. Field measurement of hydraulic conductivity in slowly permeable materials using early-time infiltration measurements in unsaturated media. *In* D.E. Daniel and S.J. Trautwein (eds).Hydraulic conductivity and waste containment transport in soils. ASTM STP 1142. American Society for Testing and Materials, Philadelphia, PN.

Grant, C.D. and A.R. Dexter. 1990. Air entrapment and differential swelling as factors in the mellowing of moulded soil during rapid wetting. Aust. J. Soil Sci. 28:361-369.

Gregorich, E.G., R.G. Kachanoski and R.P. Voroney. 1988. Ultrasonic dispersion of aggregates: distribution of organic matter in size fractions. Can. J. Soil Sci. 68:395-403.

Groenevelt, P.H., B.P. Odell and D.E. Elrick. 1996. Time domains for early-time and steady-state pressure infiltrometer data. Soil Sci. Soc. Am. J. 60:1713-1717.

Håkansson, I., and V.W. Medvedev. 1995. Protection of soils from mechanical overloading by establishing limits for stresses caused by heavy vehicles. Soil & Till Res. 35:85-97.

Hartge, K.H. 1986. A concept of compaction. Z.Pflanzenernaehr. Bodenk. 149:361-370

Henderschott, W.H., H. Lalande and M. Duqutte. 1993. Soil reaction and exchangeable acidity. p. 141-145. *In* M.R. Carter (ed.) Soil Sampling and Methods of Analysis. Canadian Society of Soil Science. Lewis Publishers: Boca Raton.

Holtz, R.D. and W.D. Kovacs. 1981. An introduction to geotechnical engineering. Prentice-Hall Inc., Englewood Cliffs, NJ.

Horn, R., H. Domzal, Anna Slowinska-Jurkiewicz, and C. van Ouwerkerk. 1995. Soil compaction processes and their effects on the structure of arable soils and the environment. Soil & Tillage Res. 35:23-36.

Howard, A.K. 1984. The revised ASTM standard on the Unified Soil Classification System. Geotechnical Testing Journal. GTJODF, 7(4):216-222.

Jones, C.A. 1983. Effect of soil texture on critical bulk densities for root growth. Soil Sci. Soc. Am. J. 47:1208-1211.

Kay, B.D. and A.R. Dexter. 1990. Influence of aggregate diameter, surface area and antecedent water content on the dispersibility of clay. Can. J. Soil Sci. 70:655-671.

Komandi, G. 1992. On the mechanical properties of soil as they affect traction. J. Terra. 29(4/5):373-380.

Landsburg, S. 1989. Effects of pipeline construction on chernozemic and solonetzic A and B horizons in central Alberta. Can J. Soil Sci. 69:327-336.

Larson, W.E. and F.J. Pierce. 1994. The dynamics of soil quality as a measure of sustainable

management p.37-51 *In* J.W. Doran et al. (ed) Defining soil quality for a sustainable environment. SSSA Special Publication no. 35. SSSA and ASA, Madison, WI.

Larson, W.E., S.C. Gupta and R.A. Uesche. 1980. Compression of agricultural soils from eight soil orders. Soil Sci. Soc. Am. J. 44:450-457.

Lipiec, J. and W. Stepniewski. 1995. Effects of soil compaction and tillage systems on uptake and losses of nutrients. Soil & Tillage Res. 35:37-52.

McBride, R.A. 1988. Estimation of compactibility and overconsolidation in unsaturated, structured soils. p. 281 *In* Agronomy abstracts, ASA, Madison, WI.

McBride, R.A. and N. Baumgartner. 1992. A simple slurry consolidometer designed for the estimation of the consistency limits of soils. J. of Terramechanics 29:223-238.

McBride, R.A. 1993. Soil consistency limits. p. 519-528 *In* M.R. Carter (ed.) Soil Sampling and Methods of Analysis. Canadian Society of Soil Science. Lewis Publishers: Boca Raton.

McBride, R.A. and P.J. Joosse. 1996. Overconsolidation in agricultural soils. II. Pedotransfer functions for estimating the preconsolidation stress. Soil Sci. Soc. Am. J. 60:373-380.

McBride, R.A. and E.E. Mackintosh. 1984. Soil survey interpretations from water retention data: I. Development and validation of a water retention model. Soil Sci. Soc. Am. J. 48:1338-1343.

McBride, R.A., G.C. Watson and G. Wall. 1997. Feasibility study on the development and testing of agri-environmental indicators of soil compaction risk (eastern Canada). Report No. 23 of the Agri-environental Indicator Project. Soil degradation risk indicator: soil compaction component. Agriculture and Agri-Food Canada, Ottawa, ON. 40 pp.

McKague, K.J., R.A. McBride, S. Rimmer and W.S. Scott. 1993. Soil compaction along transmission line rights-of-way and its effect on the agronomic productivity of selected soils. Proceedings of the Fifth International Symposium on Environmental Concerns in Rights-of Way Management, Montreal, PQ.

McKeague, J.A., C.Wang and G.C. Topp. 1982. Estimating saturated hydraulic conductivity from soil morphology. Soil Sci. Soc. Am. J. 46:1239-1244.

McNabb, D.H. and L. Boersma. 1996. Nonlinear model for compressibility of partly saturated soils. Soil Sci. Soc. Am. J. 60:333-341.

Meshalkina, J.A., A. Stein and Ye. A. Dmitriev. 1995. Spatial variability of penetration data on Russian plots in different land use. Soil Tech. 8:43-59.

Naeth, M.A., W.B. McGill and A.W. Bailey. 1987. Persistence of changes in selected soil chemical and physical properties after pipeline installation in solonetzic native rangeland. Can. J. Soil Sci. 67:747-763.

Nelson, D.W. and L.E. Sommers. 1982. Total carbon, organic carbon and organic matter. p. 539-579 *In* A.L. Page et al. (ed.) Methods of soil analysis. Part 2. 2nd ed. Agron. Monogr. 9. ASA and SSSA, Madison, WI.

Odell, R.T., T.H. Thornburn and L.J. McKenzie. 1960. Relationships of Atterberg limits to some other properties of Illinois soils. Soil Sci. Soc. Am. Proc. 24:297-300.

Okello, J.A. 1991. A review of soil strength measurement techniques for prediction of terrain vehicle performance. J. Agr. Eng. Res. 50:129-155.

O'Sullivan, M.F. 1992. Uniaxial compaction effects on soil physical properties in relation to soil type and cultivation. Soil & Tillage Res. 24:257-269.

Petersen, C.T. 1993. The variation of critical-state parameters with water content for two agricultural soils. J. Soil Sci. 44:397-410.

Pierce, F.J. and W.E. Larson. 1993. Developing criteria to evaluate sustainable land management. p. 7-14 *In* J.M. Kimble (ed.) Proceedings of the Eighth International Soil Management Workshop: Utilization of Soil Survey Information for Sustainable Land Use. May 1993. USDA, Soil Conservation Service, National Soil Survey Centre.

Rendon-Herrero, O. 1980. Universal compression index equation. J. Geotech. Eng. 106:1179-1200.

Reynolds, W.D. 1993a. Saturated hydraulic conductivity: Laboratory measurement p. 589-598 *In* M.R. Carter (ed.) Soil Sampling and Methods of Analysis. Canadian Society of Soil Science. Lewis Publishers: Boca Raton.

Reynolds, W.D. 1993b. Saturated hydraulic conductivity: Field measurement p. 599-613 *In* M.R. Carter (ed.) Soil Sampling and Methods of Analysis. Canadian Society of Soil Science. Lewis Publishers: Boca Raton.

SAS Institute. 1996. SAS System for Windows. Version 6.12, SAS Inst. Inc., Cary , NC.

Sheldrick, B.H. and C. Wang. 1993. Chapter 47. Particle size distribution. p.499-511. *In* M.R. Carter (ed.) Soil Sampling and Methods of Analysis. Canadian Society of Soil Science. Lewis Publishers: Boca Raton.

Smith, C.W., A. Hadas, J. Dan and H. Koyumdjisky. 1985. Shrinkage and Atterberg limits in relation to other properties of principal soil types in Israel. Geoderma. 35:47-65.

Soane, B.D., and C. van Ouwerkerk. 1995. Implication of soil compaction in crop production for the quality of the environment. Soil & Tillage Res. 35:5-22.

Sridharan, A. S.M. Rao and N.S. Murthy. 1988. Liquid limit of kaolinitic soils. Géotechnique. 38(2);191-198.

Stakman, W.P. and B.G. Bishay. 1976. Moisture retention and plasticity of highly calcareous

soils in Egypt. Neth. J. Agric. Sci. 24:43-57.

Statsoft. 1995. Statistica for Windows, Version 5.0. Statsoft, Inc., Tulsa, OK.

Tee Boon Goh, R.J. St. Arnoud and A.R. Mermut. 1993. Carbonates. p. 177-185. *In* M.R. Carter (ed.) Soil Sampling and Methods of Analysis. Canadian Society of Soil Science. Lewis Publishers: Boca Raton.

Topp, G.C., Y.T. Galgavon, B.C. Ball, and M.R. Carter. 1993. Soil water desorption curves. p. 569-580. *In* M.R. Carter (ed.) Soil Sampling and Methods of Analysis. Canadian Society of Soil Science. Lewis Publishers: Boca Raton.

Van den Akker, J.H. 1998. Requirements to construct a wheel load bearing capacity map as a tool to prevent subsoil compaction. Paper presented at the 16th World Conference of Soil Science, Aug. 20-26, 1998, Montpellier, France. ISSS and AFES. No. 1100. Symp. 20.

Veenhof, D.W. 1993. The compression characteristics and susceptibility to compaction of soils from the regional municipality of Haldimand-Norfolk. M.Sc. Thesis. University of Guelph, Guelph, ON. 433 pp.

Veenhof , D.W. and R.A. McBride. 1996. Overconsolidation in agricultural soils: I. Compression and consolidation behavior of remolded and structured soils. Soil Sci. Soc. Am. J. 60:362-373.

Watson, G.C. 1996. The development of a standardized approach for describing and organizing data generated through land resource field research. Unpublished thesis. University of Guelph. 202 pp.

Wesley, L.D. 1988. Compression index: Misleading parameter? J. Geotech. Eng. 114:718-723.

Wösten, H. and A. Lilly. 1998. Use of soil hydraulic pedotransfer functions for the assessment of soil quality on a European scale. Paper presented at the 16th World Conference of Soil Science, Aug. 20-26, 1998, Montpellier, France. ISSS and AFES. No. 843. Symp. 1.

3. Shrinkage of Intact and Remoulded Samples

3.1 Introduction

Many studies have investigated the shrinkage of soils as a potential hazard to engineering practices (Grossman et al., 1968; McCormack and Wilding, 1975), as a pedogenic process used in the classification of soils (Dasog et al., 1987; Wilding and Tessier, 1988; Reeve et al., 1980), or as an agent in the rejuvenation of soil structure (Reeve and Hall, 1978; Shiel et al., 1988; Kuznetsova and Davilova, 1988; Makeyeva, 1988). Very few studies (McGarry and Daniells, 1987; McGarry, 1988; Lauritzen, 1948; Paz, 1998) have looked at the shrinkage characteristic curve and its fitting parameters to potentially distinguish different structural states or treatment effects, even though it is often stated that the inherent fabric of structured samples affects the amount of linear normal shrinkage and positioning of the shrinkage characteristic curve as compared to remoulded samples (Chan, 1982; Stirk, 1954; Simon et al., 1987; Lauritzen, 1948).

Four shrinkage characteristic curve stages have now been identified, although the terminology varies and all 4 ranges are not always present (Reeve and Hall, 1978; McGarry and Malafant, 1987; Tariq and Durnford, 1993a). The 4 ranges can generally be described as:

1. Structural- occurs over the wettest part of the moisture range where the volume change is less than the volume of water removed, arising from the draining of large pores and entry of some air into the pores
2. Normal - volume decrease of the soil is equal to the volume of water lost and the volume of the air remains constant
3. Residual - the water loss exceeds the soil volume change, resulting in an increase in air-filled pores
4. Zero - no change in volume and moisture loss is due to pore drainage

The shrinkage characteristic curve is portrayed in reciprocal dry bulk density(water content) or void ratio (moisture ratio) coordinates.

Several studies have found the shrinkage characteristic of sieved and/or remoulded samples

to exhibit a large water content range over which 'normal' shrinkage (n_v =1) occurs for soils of smectitic mineralogy, relatively high fine particle-size content (>50%) and/or low organic carbon content (<1%) (Haines, 1923; Tariq and Durnford, 1993b; Derdour et al, 1994; Chang and Warkentin, 1968). The shrinkage characteristic for a remoulded soil often lies on top of the 2 phase 1:1 line until "air-entry" occurs at the shrinkage limit, indicating complete saturation for the "normal" stage (Chan, 1982; Tariq and Durnford, 1993b). It has even been suggested that "clay paste be the norm used for reference to compare natural clayey soils" (Bronswijk, 1993, p. 558).

The amount of shrinkage and particularly normal shrinkage in the remoulded state is largely dependent on the existence of contracting fine pores (<.2 μm) which is primarily related to the clay content (Haines, 1923; Newman and Thomasson, 1979; De Jong et al., 1992; Bruand and Prost, 1987). In geotechnical terms, "normal" refers to isotropic consolidation (equal all-round pressure) of a saturated clay specimen in which the present effective stress is the maximum to which the clay has ever been subjected (Craig, 1992). "Presumably during normal shrinkage, plastic deformation of the soil occurs in response to the decreasing water potential" (Newman and Thomasson, 1979, p. 429). Thus if we want to apply the term "normal" to shrinkage terminology, the conditions should be such that the stress is equally applied throughout the sample and it should have no stress history. The condition of equally distributed stress would only apply when the pores are of equal size and saturated, which is likely only to occur in the remoulded state where pore-size distribution has been homogenized.

It is surprising then that structured clods have exhibited "normal" shrinkage zones (Bronswijk and Evers-Vermeer, 1990; Cabidoche and Voltz, 1995; Bronswijk, 1991) except that these have usually been high clay content (>80%), low organic matter (< 1%) smectitic soils. This confirms that either there is a large proportion of the pore-size distribution within a relatively narrow range or that there is a relatively uniform particle size throughout the clod. The amount of

residual shrinkage depends on the organic matter content (Haines, 1923).

In structured clods (McGarry and Daniells, 1987; Lauritzen, 1948; Wu et al., 1997) and in field conditions (Mitchell and van Genuchten, 1992; Jayawardane and Greacen, 1987; Lauritzen and Stewart, 1941) where there has been a stress history, n_v has deviated to values above or below 1. Very few natural clods resemble the theoretical picture which can be ascribed to the presence of silt and sand particles which may locally restrict shrinkage and induce air entry (n_v<1) (Bronswijk and Evers-Vermeer, 1990) or to soils of high porosity which have the volume of air contract in proportion to the total clod shrinkage(n_v>1) (McGarry, 1988).

In structured soils, shrinkage is a combination of three processes: i) drainage of stable pores (.2-30 μm) which resist surface tension stresses (largely over the plant available water content range), ii) collapse of unstable pores in this size range, rearrangement of aggregates and the contraction of micropores <0.2 μm (shrinkage), and iii) formation of new pores (.2-2 μm) on drying (Newman and Thomasson, 1979; Chang and Warkentin, 1968). Thus, both the pore-size distribution and the stability of the pores/aggregates determine the amount of air entry into the clod and the amount/rate of shrinkage/contraction. The shrinkage characteristic in structured clods is usually under partially saturated conditions; the gap between the shrinkage characteristic and the saturation line (1:1 line) represents stable air-filled pores which are biological in origin (Newman and Thomasson, 1979; Cabidoche and Voltz, 1995). The shrinkage will only be strictly "normal", i.e. constant volume of air , if there are few pores in the clod between two sizes, i.e. between two associated tensions (Newman and Thomasson, 1979) or if unstable water-filled pores collapse, either of which is undesirable for optimal plant growth. The slope in the normal shrinkage zone is important as it indicates the stability of the soil pores (Allbrook, 1992). "Aeration should not be a problem in soils in which so-called normal shrinkage is absent" (Lauritzen, 1948, p.173). In addition, the sample size influences the shape of the shrinkage characteristic because of the

inclusion of various pore sizes (Bruand and Prost, 1987; Hartmann, 1998). To avoid confusion in terminology, Bruand and Prost (1987) refer to stage I, II and III of their shrinkage characteristics curve as it represented water entering different sets of pores (Mitchell and van Genuchten, 1992).

These differences between the remoulded and structured shrinkage process could be exploited to derive indices of physical soil quality. A 3-straight line model proposed by McGarry and Malafant (1987) represents structural, normal and residual shrinkage zones by straight line segments whose parameters have direct physical significance (Figure 3.1a). In terms of structural quality, at least 4 parameters from the 3-line model have been found useful in distinguishing treatment effects of wet versus dry cultivation, and zero versus conventional tillage; the apparent specific volume at zero water content (v_α), the slope of the line in the normal shrinkage zone (n_v), and the specific volume of air-filled pores at both the onset of normal and residual shrinkage (P_B, P_A) (McGarry and Daniells, 1987). Additional work also found the specific volumes at the ends of the three stages (v_A, v_B ,v_C), the range of water content in the structural zone (w_C -w_B), and the air-filled porosity at the intercept (P_α) could distinguish treatments (McGarry, 1988). An extension of this model proposed by Tariq and Durnford (1993a) which uses 4 shrinkage stages and polynomial equations, better fits experimental data for individual clods, particularly in the residual shrinkage zone. None of the structural indices above require definition of the residual zone with any accuracy or with this increased complexity and the 3-line segment model was considered adequate for this exploratory analysis.

The line segment model fitting parameters allow a standard comparison of structured and remoulded soils. Plots of $v(w)$ have been widely used to portray volume change in soils but the volume ratio ($\delta v/\delta w$) does not truly represent a soil mechanics response in which a strain increment is related to a stress increment. Any given w is associated with an effective stress (σ') (negative pore water potential in this case) such that the volume changes could be plotted in $e(\sigma')$

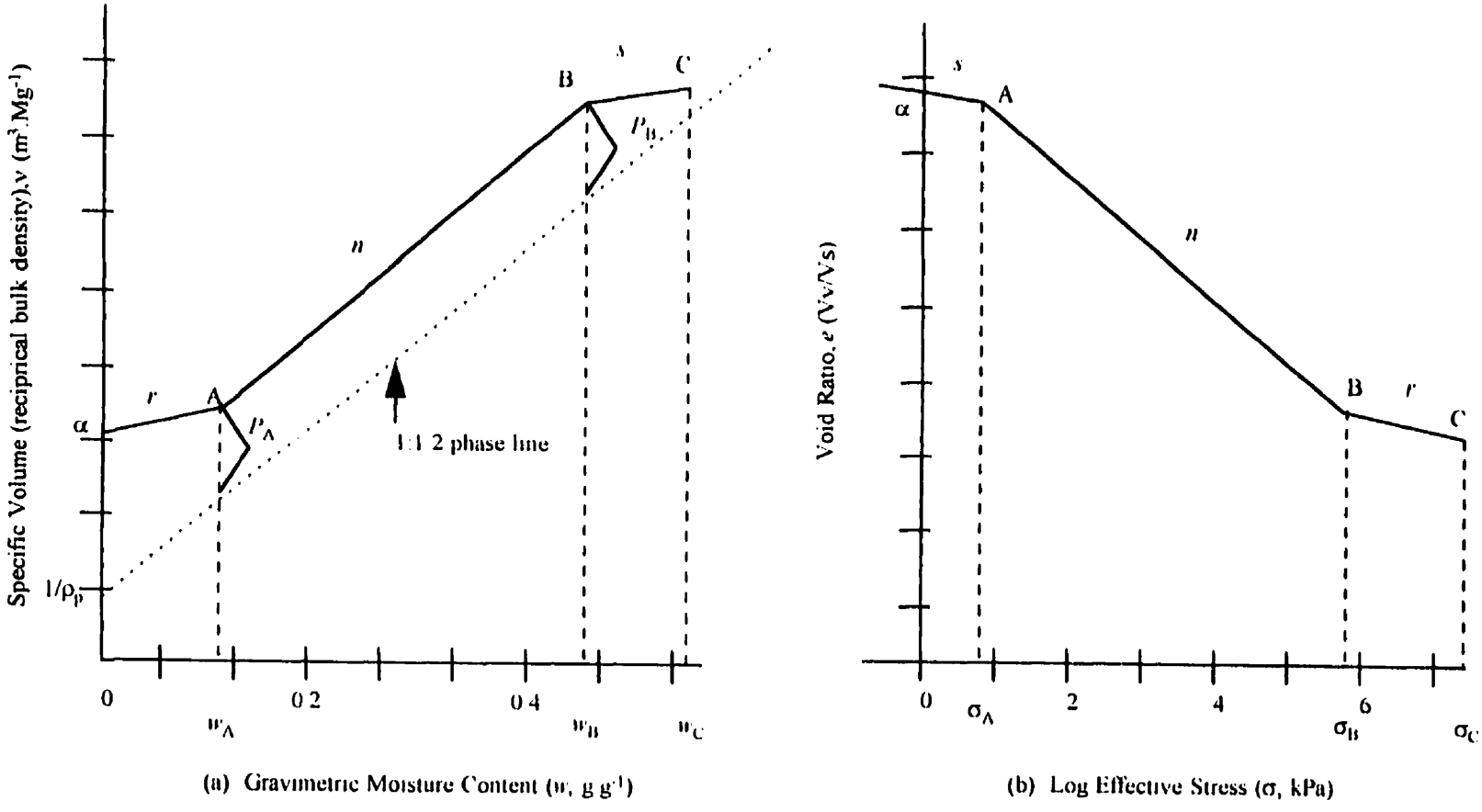

Figure 3.1. Illustration of variables used to describe the shrinkage characteristic curve (after McGarry and Daniells, 1987) and the shrinkage-stress curve.

coordinates, or a shrinkage-stress curve. This plot would be a mirror image of the $v(w)$ plots (Figure 3.1b) where: i) the void ratio changes little up to a certain tension as there is drainage, ii) there are large changes in volume as capillary binding, aggregate rearrangement and pore contracting occur, and iii) then there is a tension beyond which there is little change in volume because the strength or interference of the aggregates exceeds the capillary forces and the inter-aggregate menisci are broken (Chang and Warkentin, 1968). Stirk (1954) plots volume ratio ($\delta v/\delta w$) between successive values of soil suction (pF) against a coordinate of pF, Ho et al. (1992) portray e against $\log(u_a - u_w)$ and Baumgartl (1998) plots e against log matric potential which are the only strain/stress portrayals of shrinkage in the literature. This portrayal would allow an understanding of structural dynamics in terms of soil mechanics and provide potentially more transferability/ interpretation by a reader at a later date to provide alternate data on soil physical condition (McGarry and Malafant, 1987).

The first objective of this study was to measure the shrinkage of remoulded and structured soil clods with a variety of physical, chemical, mineralogical and structural properties to determine the response to effective stress and fit a functionally based 3 line segment model of soil shrinkage in $v(w)$ and $e(\sigma)$ co-ordinates. Soils vary in their shrink-swell potential due to many factors including clay mineralogy, dry bulk density, clay content, organic matter content, CEC, adsorbed cations, and surface area (Reeve et al., 1980; De Jong et al., 1992; Ross, 1978). Most shrinkage studies have been conducted on soils of high clay content and smectitic mineralogy which exhibit the most dramatic and potentially destructive volume change, but it is known that soils of coarser texture and/or considered to have non-expansive minerals can exhibit significant shrinkage (Reeve et al., 1980; Ross, 1978; Allbrook, 1992). Soils of almost any textural class will show volume changes associated with changes of water content (Stirk, 1954). Volume decreases of 15-20% have been shown in clods with clay contents of only 15-16% (Bronswijk and Evers-Vermeer, 1990)

where the clay consists mainly of illite (30-40%) and smectite (20-40%). Shrinkage experiments are not routinely carried out on soils from Canada and the potential for vertic soil properties is also of interest (Dasog et al., 1987).

The second objective of this study was to test if model fitting parameters from the shrinkage characteristic or shrinkage-stress curve could be used as indicators of soil structural quality. In particular, using remoulded samples as a reference base to which structured samples could be compared has not been widely attempted even though references to soil structure/fabric influencing shrinkage have been made. Laurtizen (1948) provides the only reference and results of using the ratio of the structured shrinkage characteristic intercept (v_o) to the remoulded intercept of the same material as a measure of the porosity which exists by virtue of structural development. This ratio offered a measure of degree to which structural development had progressed or deteriorated relative to a minimum apparent specific volume (remoulded conditions). There was little correlation between organic matter and sand and this ratio (Lauritzen, 1948). Thus relative shrinkage parameters (remoulded versus structured) may provide a means of comparing structural quality independent of soil properties which influence shrinkage as outlined above.

3.2 Materials and Methods

3.2.1 Soil Sampling

The location and physical and chemical characteristics of the soils sampled are documented in Chapter 2. Samples for shrinkage analysis were collected at the same time as samples for compression testing. An intact layer of soil (≈ 25 cm wide x 36 cm high x 10 cm deep) was excavated, wrapped in a polyethylene bag, placed inside a rigid plastic container and stored at 4°C until sample preparation. This provided an adequate number of secondary structural clods to sample and minimized disturbance. Ample amounts of bulk soil were collected at the same time

for soil characterization as well as for creating remoulded "clods".

3.2.2 Sample Preparation

The methodology used was similar to that of Stirk (1954). For structurally intact samples, 5 peds of 5-30 mm diameter were carefully separated along natural lines of structural weakness which essentially represented the secondary structure of the soil horizon. Samples were massed and placed in desiccators fitted with filter paper (Whatman No. 1) for water uptake. Samples were first placed under a vacuum (-65 kPa) for 12 hours in the desiccator. De-aired, distilled water was gradually added to the desiccator until water covered the end of the filter paper overhangs. A slight vacuum (-4kPa) was left on the samples for another 24 hours and then they were left to equilibrate at -0.3 kPa for 5 days. Once saturated, samples were equilibrated to the following pressure potentials using various contact materials (Table 3.1)

Table 3.1. Methods for establishing pressure potentials in structurally intact samples.

Pressure potential	Apparatus	Contact Material	Days to Equilibrium
Saturated (-0.3 kPa)	Desiccator		5 days
-1 kPa (pF 1)	Ultrafiltration cell (Tessier and Berrier, 1979)	Kaolinite	4 days
-10 kPa (pF 2)	Ultrafiltration cell (Tessier and Berrier, 1979)	Kaolinite	4 days
-100 kPa (pF 3)	Pressure plate	Silica flour	9 days
-500 kPa (pF 3.7)	Pressure plate	Aluminum oxide	10 days
-1500 kPa (pF 4.2)	Pressure plate	Aluminum oxide	14 days
-10000 kPa (pF 5)	Relative humidity 92%, saturated solution K_2HPO_4		21 days
-100000 kPa (pF 6)	Relative humidity 45%, saturated solution K_2NO_2		21 days
-1000000 kPa (pF 7)	Oven at 105°C		48 hours

For the remoulded samples, 300-400 g of soil sieved to < 2 mm was combined with enough distilled water such that w was at least 2 times the w_L . The slurries were left to equilibrate for 5 days in a refrigerator at 4°C. Maximum disruption of aggregates was achieved by instantaneous

wetting of air-dried aggregates with distilled water, which induces the "explosion" of aggregates as occluded air is compressed and the differential swelling of the clay fraction, causing slaking and dispersion the soil particles (Emerson, 1977; Grant and Dexter, 1990). Physical moulding and the presence of free water over several days also increases the amount of dispersion (Kay and Dexter, 1990).

A suction filter apparatus using 11 cm diameter porcelain filter holders on top of glass beakers was used to prepare the samples. Whatman No. 50 Filter paper was placed in the holder and wet with distilled water. A 1.5 cm thick layer of slurry was poured on the filter paper and the holders were covered with plastic to avoid desiccation. The vacuum pump was set to -10 kPa and the slurries were allowed to equilibrate until no water was being removed and the slurry could be sampled/cut (approximately 4 hours). Sometimes the soils were difficult to consolidate and were subjected to slightly higher vacuums (up to -20 kPa) for a short period of time at the end of the procedure. The end of a 60 mL syringe was removed to provide a 2.5 cm diameter cutting tool which was pushed into the layer of remoulded soil. Six subsamples were taken from each filter device; three subsamples were assigned to each tension. The syringe could be used to move the sample to the appropriate apparatus and slight depression of the syringe pushed the sample out of the tube with minimal disturbance. Prepared samples were placed in each of the desiccation apparati and equilibrated to the selected pressure potentials without using contact materials as the procedure produced a sample with a flat surface in contact with the tension media (Table 3.2). A cellulose membrane type pressure plate was used which had minimal clearance (depth) and limited the height of the samples but gave good contact.

Table 3.2. Equilibration methods for remoulded samples.

Pressure potential	Apparatus	Min. Time to Equilibrium
-33 kPa	Ultrafiltration cell (Tessier and Berrier, 1979)	4 days
-100 kPa (pF 3)	Pressure plate (ceramic plate)	10 days
-500 kPa	Pressure plate (cellulose membrane)	10 days
-1500 kPa	Pressure plate (cellulose membrane)	14 days
-10000 kPa (pF 5)	Relative humidity K_2HPO_4	21 days
-100000 kPa (pF 6)	Relative humidity K_2NO_2	21 days
-1000000 kPa (pF 7)	Oven dry at 105 oC	48 hours

3.2.3 Volume Determination

Volume determination was made using a kerosene immersion method adopted from Monnier et al. (1973). This method minimized water loss after removal of samples from tension apparati and allowed volume determination on fragile/non-cohesive clods. Once equilibrated, both structured and remoulded samples were cleaned of contact material if necessary and massed for water content. The samples were then placed in a plexiglass ring (3 cm diam. x 2 cm high) covered with fine nylon mesh on the bottom and immersed in kerosene. The samples were allowed to saturate in kerosene for 1-2 hours. The three or five subsamples per tension were removed at one time and placed on Whatman No 42 filter paper briefly to allow excess kerosene to drain away until the clods were no longer shiny (max. 10 minutes). A metal clip was used to pick up the basket containing the sample and suspend them from a Mettler hanging balance. The sample and basket were massed in the air and then massed again while suspended in kerosene. The empty baskets were massed similarly in air and kerosene at the beginning of the study. The volume of the clod was then determined using Archimedes' Principle (Eq. [1]). The density of the kerosene was determined independently to be 0.794 $g.cm^{-3}$ for the remoulded samples and 0.784 for the structured samples (Aldrich and Fischer suppliers, respectively).

$$volume_{clod} = \frac{mass_{air} - mass_{kerosene}}{\rho_{kerosene}} - volume_{basket} \quad [1]$$

The level of kerosene in the container was maintained by massing and adjusting as necessary after every set of subsamples. The samples were oven dried for 48 hours at 105°C to determine the mass of soil from which dry bulk density, apparent specific volume (reciprocal of dry bulk density) and void ratio were calculated.

3.2.4 Statistical Analysis

Shrinkage results were plotted in specific volume vs. gravimetric water content co-ordinates, $v(w)$, after McGarry and Daniells (1987). The plot is referred to as the shrinkage characteristic curve. The specific volume portrayed is actually the reciprocal of dry bulk density ($1/\rho_b$; $cm^3\ g^{-1}$) rather than the true specific volume given by volume total/volume solids ($=1+e$). The reciprocal of dry bulk density allows a common denominator of mass solids for both axes so that a 1:1, 2 phase line can be drawn. This is analogous to the void ratio vs. moisture ratio (V_w/V_s) representation of Tariq and Durnford (1993), where volume solids is the denominator for both axes and is obtained by multiplying each by the particle density. Identical line segment parameter values result for both representations. The measured data were also plotted in void ratio vs. log effective stress $e(\sigma')$ co-ordinates to correspond to the compression data and soil mechanics theory.

The SAS Proc REG and Proc NLIN procedures were used to fit 1, 2 and 3 line segment models to the data. Start values were estimated visually and changed if necessary based on the initial parameter estimates and convergence of the model. The parameters were allowed to deviate from "theoretical" values to produce the best fit to the data by statistical iteration rather than visually which has been done for most shrinkage data. In some cases, convergence criteria were met but the Jacobian/Hessian estimate was singular (i.e. 0 variance) for a parameter indicating that

there was insufficient data to fit the fuller model and perhaps only one point was being used to estimate the parameter (Matthes-Sears, personal communication). This indicated that 2 and/or 3 line models were not always appropriate to describe the data. F-tests were conducted based on the extra sums of squares to determine the most appropriate number of line segments for the model. Depending on the shape of the shrinkage curve and the portion represented, parameters were extracted to an Excel file and used to calculate other variables. The equations and parameters are listed below (Table 3.3) and correspond to Figure 3.1.

Table 3.3. Variables used for describing 3 line segment model.

Model	v vs. w	e vs. σ'
1 line (only normal shrinkage)	$v_\alpha + n * w$	$e_\alpha + n_e * \log\sigma'$
2 line (with residual shrinkage only)	$v_\alpha + r_v * w_A + n_v * (w - w_A)$	$e_\alpha + n_e * \sigma_B + r_e * (\log\sigma' - \log\sigma_B)$
2 line (with structural shrinkage only)	$v_\alpha + n_v * w_B + s_v * (w - w_B)$	$e_\alpha + s_e * \sigma_A + n_e * (\log\sigma' - \log\sigma_A)$
3 line	$v_\alpha + r_v * w_A + n_v * (w_B - w_A) + s_v * (w - w_B)$	$e_\alpha + s_e * \sigma_A + n_e * (\log\sigma_B - \log\sigma_A) + r_e * (\log\sigma' - \log\sigma_B)$

The shrinkage parameters were analyzed by simple and forward stepwise regression and ANOVA/ANCOVA analysis to determine effects of mineralogy (MNR), land use (TRT) and horizon (HOR) class factors as well as continuous soil properties. The split plot model used for ANOVA/ANCOVA analysis and its interpretation are described in the Appendix.

3.3 Results and Discussion

There were 4 sets of data based on whether the samples were remoulded (R) vs. structured (S) or specific volume (v) vs. void ratio (e) coordinates. These 4 sets of data and their parameters are designated by v S , v R, e R, and e S regarding coordinates and structural condition, respectively.

3.3.1 Remoulded Shrinkage Data

3.3.1.1 Representation in v(*w*) coordinates

For the remoulded samples in v(*w*) coordinates, there was always a residual shrinkage zone (2 line model) and for 19 of the 54 horizons there was also a structural shrinkage zone (3 line model) as determined by statistical line segment fitting. The r^2 values were the highest for the v(*w*) coordinates of the 4 data sets (mean .978, median 0.986). While conducting statistical analysis, it was noted that many of the outliers were from 3 line shrinkage characteristic curves and that theoretically there should not be a structural shrinkage zone for remoulded samples. In addition, the shape of the curve was such that the second line segment would have occurred over a relatively small portion of the change in water content or one of the change points or slopes was not significantly different from 0. The original data were re-examined to extract the 2 line parameters for the 19 horizons. It was found that 4 of the horizons did not have significant 2 line models (WANA, WANB, MDWC, OTNA). These 4 horizons also had the poorest fits (r^2=.626-.835) to the straight line model (Figure 3.2). It is likely that these horizons did not contain enough cohesive material to exhibit 2 stages of shrinkage or that there was a high variability between sample clods. These spurious data sets were removed in statistical analysis if they were found to be outliers.

The coefficient of variation (% CV) was determined on the void ratio at each tension and the number of samples required to estimate the mean within 10% calculated. Usually only 1 sample was required to estimate the mean within 10% (CV<5%) at a given tension. The 3 remoulded subsamples were quite adequate to portray the shrinkage characteristic curve and explains the high degree of fit.

The intercept for the shrinkage characteristic curve (v_{aR}) had a significant MNR*TRT *HOR interaction whether the 4 single line segment curves were removed or included. ANCOVA

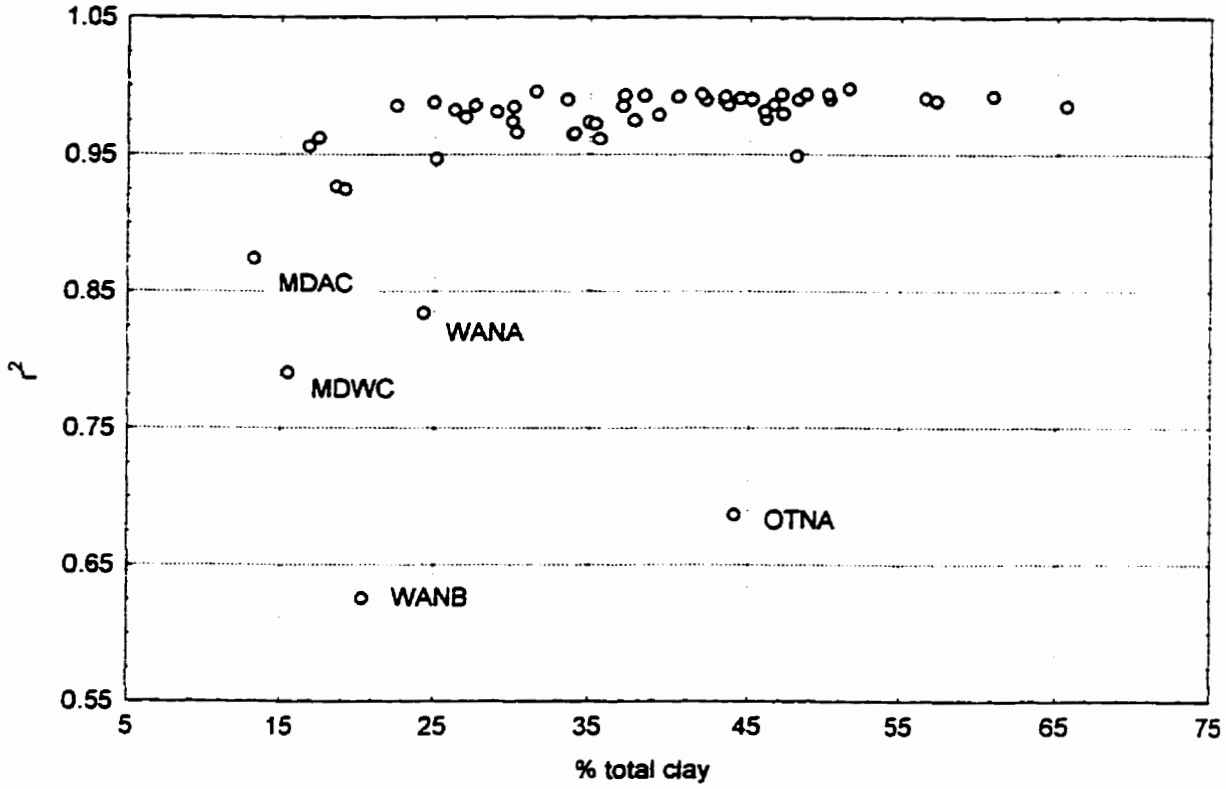

Figure 3.2. Correlation of simple determination for remolded data fit to straight line models.

analysis showed that % organic carbon (OC) removed any significant MNR or TRT factors when the 4 outliers were removed.

$\ln(v_{\alpha R})$=-.684504+.0563733*%organic carbon* [2]

SEb0=.01889, SEb1=.00290, R=.962, MSE=.0013, n=50

There was a significant clay*TRT interaction where only the relationship for the Agricultural soils was significant, but the residuals were not normally distributed so the model could not be verified.

The e_{wP} was converted into a reciprocal dry bulk density at the plastic limit calculated assuming 100% saturation with water by equation 3.

$$v_{wP} = \frac{e_{wP} + 1}{\rho_p} \quad [3]$$

There was a significant relationship with this and the $v_{\alpha R}$ variable.

$v_{\alpha R}$ =.0491+.805977v_{wP} [4]

r^2=.893, SEE=.0256, n=50, p<.001

The specific volume at the plastic limit was greater than the final oven dry specific volume except for OTNB. Equation [4] was very similar to the equation comparing the specific volume at the shrinkage limit.

v_{AR}=.0585+.802886 v_{wP} [5]

r^2=.909, SEE=.0233, n=50, p<0.001

These 2 equations indicated the close relationship between the specific volumes at the plastic and shrinkage limits and the oven dry state.

The ANOVA for the shrinkage limit (w_{AR}) had a TRT*HOR interaction when LBNA and MDAA outliers were removed (Figure 3.3). LBNA and MDAA both have organic carbon contents >6.8% and high shrinkage limits, .35 and .38, respectively. The next highest w_{AR} value was 0.26 and the mean was 0.159 (95% CI=0.140 -0.179). The Natural A horizons had significantly lower

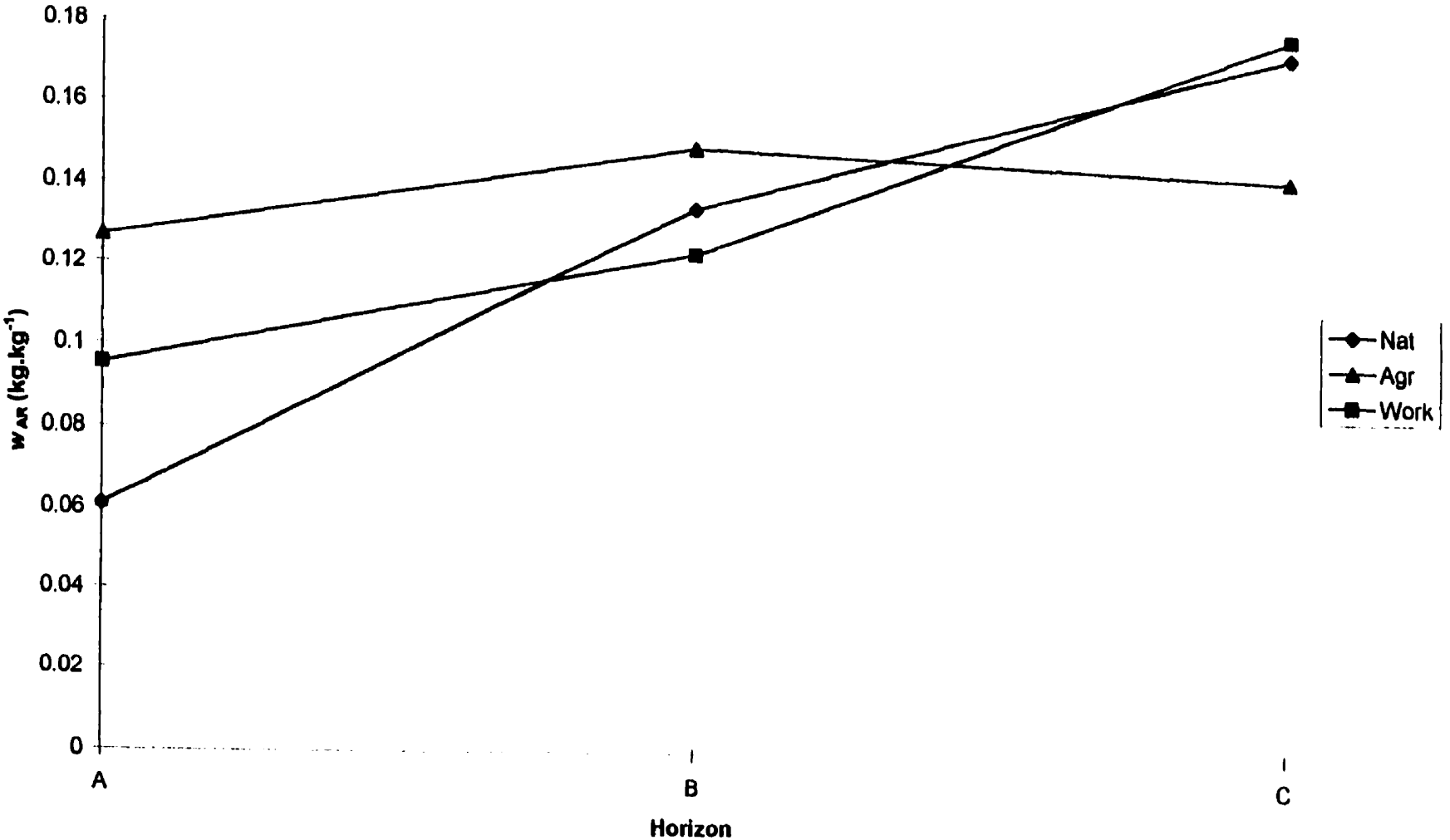

Figure 3.3 w_{AR} TRT*HOR interaction.

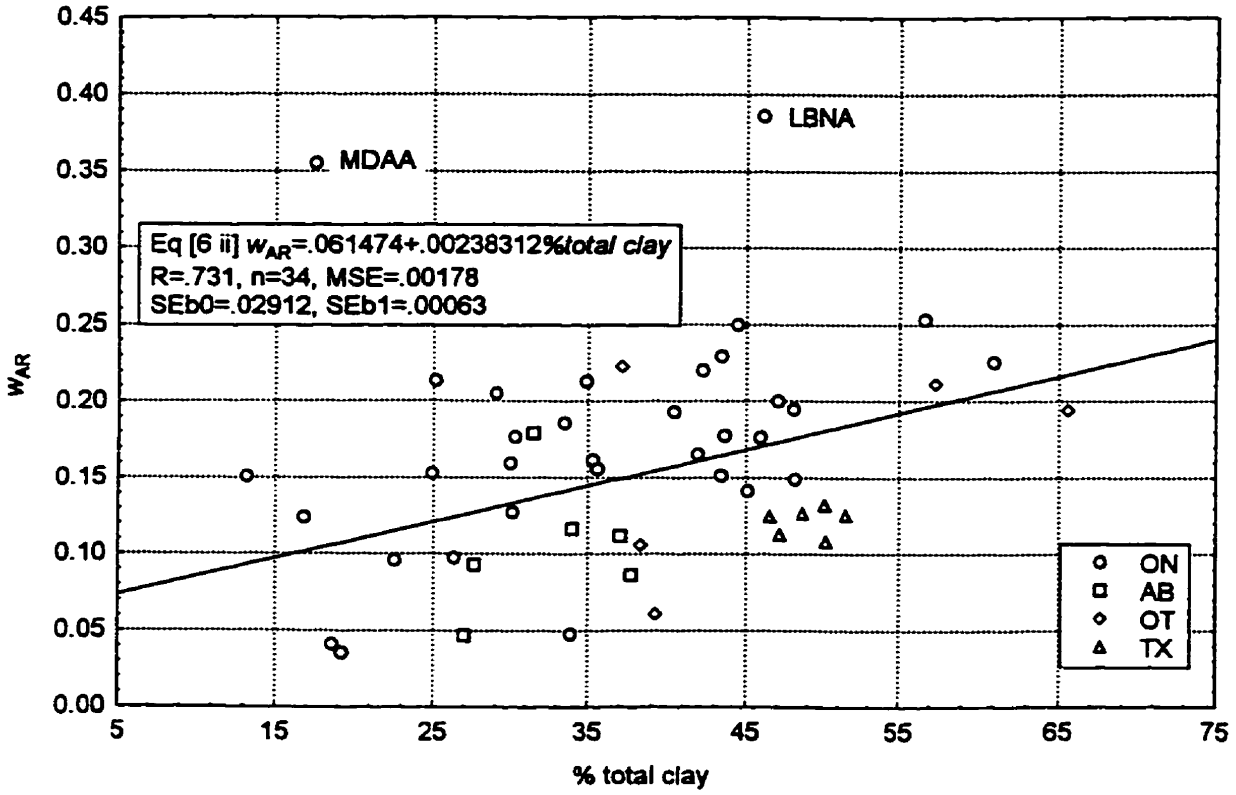

Figure 3.4. Covariance of w_{AR} with clay content.

shrinkage limits than all horizons but the Workspace A and B horizons. The Workspace A horizons were also significantly lower than the Natural and Workspace C horizons. When the outliers were included only a HOR factor was significant, with the A horizons having significantly lower w_{AR} than the C horizons.

The shrinkage limit did have a fairly straightforward relationship with clay content as a covariate (Figure 3.4). The same general model with clay was reached whether the 2 outliers MDAA and LBNA were included or not, but the p-value of the MNR term changed from .0052 to .0779 when they were included (MSE=.001776, R=.731, n=48). [6]

i)AB: w_{AR} =.0122811+.00238312*%clay* SEb0=.02912, SEb1=.000635

ii)ON: w_{AR} =.0614740+.00238312*%clay* SEb0=.02443, "

iii)OT: w_{AR} =.0206036+.00238312*%clay* SEb0=.03746, "

iv) TX: w_{AR} =-.0188417+.00238312*%clay* SEb0=.02912, "

The only intercept which is significantly different from 0 is for the southwestern Ontario soils. There are significant differences between ON and TX, and ON and AB intercepts.

The relationship with w_{AR} and organic carbon was more complex. When the outliers LBNA and MDAA were removed (n=48) there were significant OC*MNR*TRT interactions and the R value was less than when all horizons with a shrinkage limit were included. This is a misleading OC*MNR*TRT interaction since one of the most significantly different equations is for OT Nat for which there are only 2 points and has a positive slope. There were significant OC*TRT and OC*OC terms when all 50 horizons were analyzed.(MSE=.094503, R=.919, n=50) (Figure 3.5)

i)Agr: $\ln(w_{AR})$=-1.77412-.24604*%organic carbon*+.043465(*%organic carbon*)^2 [7]

SEb0=.17557, SEb1=.13478, SEb2=.016649

ii) Nat: $\ln(w_{AR})$=-1.608897-.408087*%organic carbon*+.043465(*%organic carbon*)^2

SEb0=.18661, SEb1=.126897, "

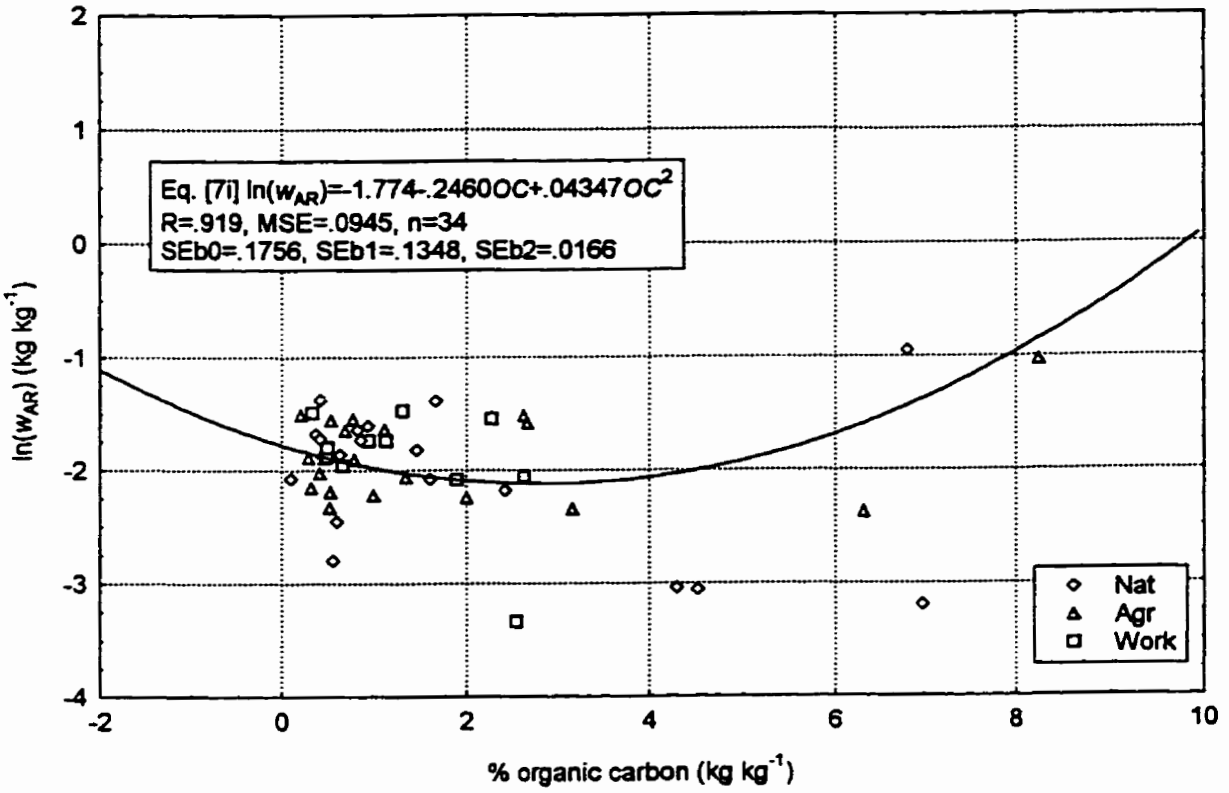

Figure 3.5. Covariance of w_{AR} with organic carbon content.

iii) Work: $\ln(w_{AR})=-1.58825-.386659\%organic\ carbon+.043465(\%organic\ carbon)^2$

SEb0=.25896, SEb1=.15694, "

None of the intercepts are significantly different from each other and only the Agricultural slope is significantly different from the Natural slope (p=.0075). Eqns. [6] and [7] show the generally negative relationship between w_{AR} and organic carbon up to about a limit of 6%, and the positive relationship with clay content.

It is surprising that the shrinkage limit of the A horizons should be so much lower than for the B and C horizons given that organic carbon tends to stiffen the soil fabric, thereby allowing fissuring and air entry at higher water contents (Reeve and Hall, 1978). Generally, a relatively lower water content at the 'air entry' point at the onset of residual shrinkage is associated with poor structure (Chang and Warkentin, 1968). This would generally cause the shrinkage limit to occur at higher rather than lower water contents for the A horizons.

There were other indications that the measured data were not behaving according to the 3-line model of McGarry and Malafant (1987). Twenty-nine of the first line segment slopes (r_{vR}) were not significantly different than 0 suggesting that the residual shrinkage segment was not significant enough to be measured and that zero shrinkage was actually being measured. This is a fourth shrinkage zone according to Tariq and Durnford (1993) and Bronswijk and Evers-Vermeer (1990). There were also 16 negative r_{vR} values which does not fit the McGarry shrinkage model. This may be due to the lack of points between the shrinkage limit and the final specific volume since assigned tensions rather than gradual water contents were used for constructing the curve. In addition there is a potential for increase in soil volume from air dryness to oven dryness which has been noted in previous studies by De Jong et al. (1992). Increases in soil volume may be due to the release of surface tension when all water is driven from the soil particles or the creation of micrometric cracks on drying beyond that experienced in the field (Haines, 1923; Bruand and

Prost, 1987). There is an average increase in void ratio in this study of 3.5% from air dryness to oven dryness but this is not normally distributed with a median of 0.6%, a minimum of -12.6% and a maximum of 29.8%. This increase in void ratio is particularly evident for the high organic matter content and coarser textured horizons which may have increased in volume due to loss of mass/organic carbon on oven drying or due to handling during weighing (Topp, 1993). Therefore, the r_{vR} variable ANOVA is not reported because the residuals were never normally distributed due to the variability in values around 0 and a reliable model could not be found.

In terms of fitting the theoretical models, the remoulded second line segment. or "normal" shrinkage slope (n_{vR}), was not significantly different or greater than 1, for 27 or 50% of the horizons. These soils tended to be C horizons, have a I_P>20 and a clay content >30% (Figure 3.6 and Figure 3.7). Half of the horizons had second line segment slopes less than 1. Soils with n_{vR} < 0.6 tended to be from the ML and MH A-line categories.

An ANOVA analysis with the 4 spurious data sets (i.e. 1 line segment models) removed showed that there was a significant difference of n_{vR} between the A and the B and C horizons (Table 3.4).

Table 3.4. LSmeans separation pdiff and LSmean values for ln(n_{vR} +.2).

	HOR		
	A. vs. B.	A vs. C	B vs. C
pdiff	3.71E-04*	3.40E-05*	0.1456
	A	B	C
LSmean	-0.2608677	0.06166751	0.16337512
Back Transformed Mean	0.5704	0.8636	0.9775
Confidence Interval	.4615-.6971	.7160-1.0349	.8127-1.1691

Both the B and C horizon n_{vR} confidence intervals for the mean encompass 1 which is the theoretical "normal" shrinkage slope.

An ANCOVA revealed significant relationships between n_{vR} and clay and log organic

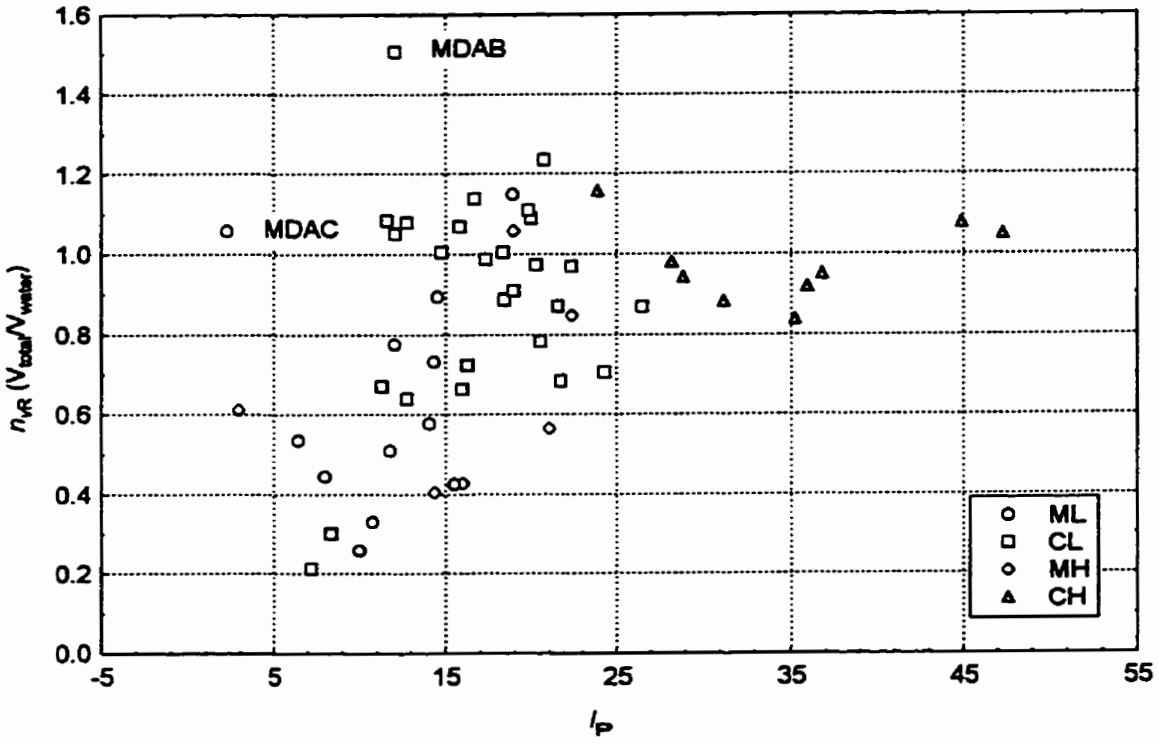

Figure 3.6. n_{vR} versus plasticity index.

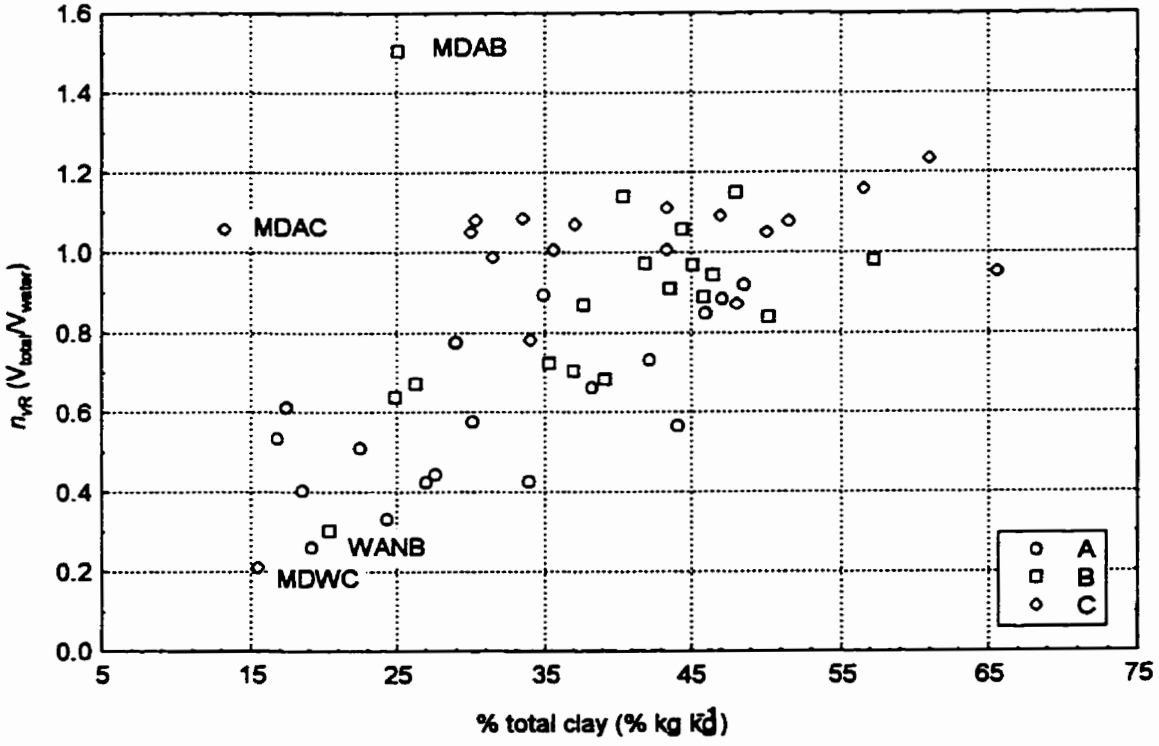

Figure 3.7. n_{vR} versus clay content.

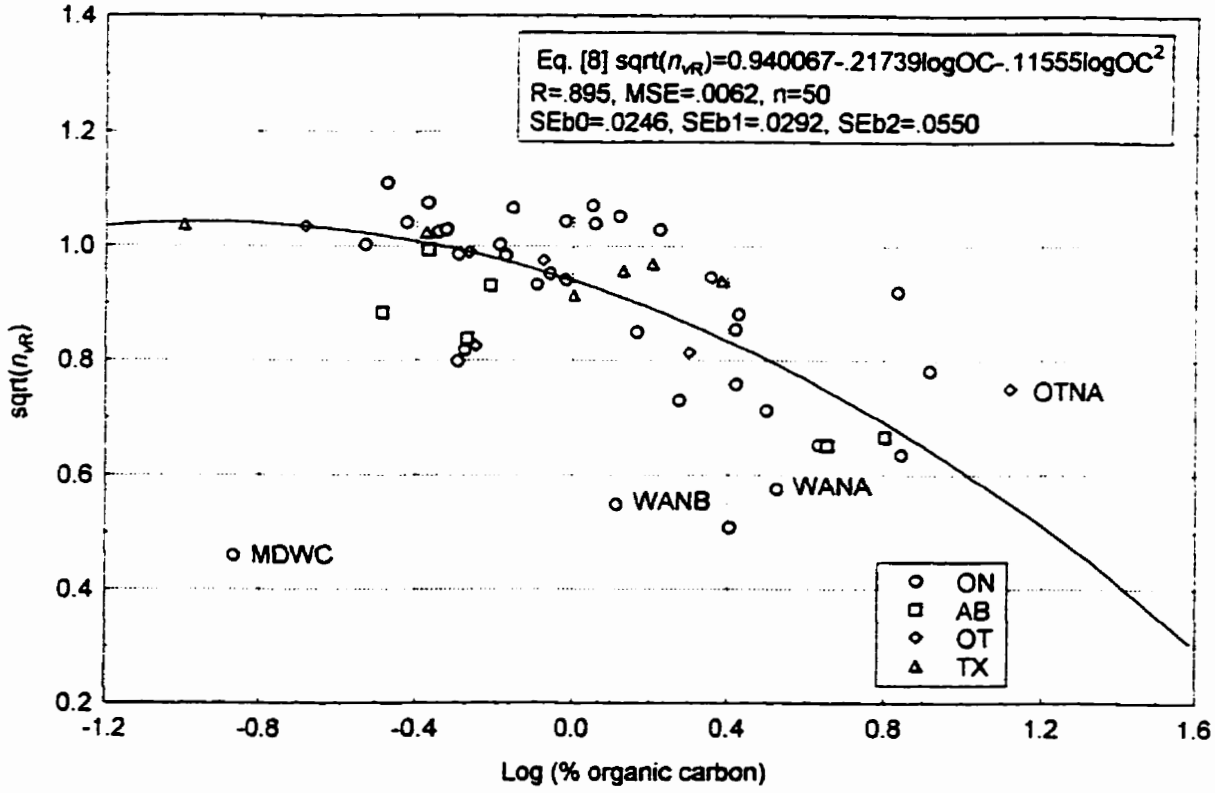

Figure 3.8. Sqrt(n_{vR}) versus log (% organic carbon).

carbon covariates when the 4 spurious data sets were removed (n=50). No significant mineralogy or treatment effects remained (Figure 3.7 and Figure 3.8).

$\text{sqrt}(n_{vR})=0.940067-.21739\text{logOC}-.11555(\text{logOC})^2$ [8]

R=.8948, MSE=.0062, SEb0=.02458, SEb1=.02921, SEb2=.05503

$\ln(n_{vR}+.2)=-.30884+.00861\%\text{clay}$ [9]

MSE=.0134, R=.9592, SEb0=.1176, SEb1=.0028

When all data were considered, the residuals were not as well distributed and there were additional covariate by TRT interactions largely due to the 3 Natural horizons in the outliers.

It was surprising that the A horizon n_{vR} were so much <1 and that n_{vR} varied with clay and organic carbon content, given that theoretically the slope in the normal shrinkage zone should be equal to 1. It was considered a possibility that the soils with high organic matter content were already past the air entry point and in a state of "residual" shrinkage at -33 kPa, the starting tension for the remoulded samples, and that the measured "shrinkage limits" were actually the transition between residual and zero shrinkage as defined by Tariq and Durnford (1993).

Another trend in the remoulded state was for a steeper n_{vR} as the water content at the shrinkage limit (w_{AR}) increased. Two horizons did not conform to this trend, LBNA and MDAA, outliers for the w_{AR} , and even though they have high shrinkage limits (.35 and .38, respectively), they do not have correspondingly high slopes (Figure 3.9). When these 2 horizons are left out, along with the 4 horizons which do not have w_{AR} values because they are single lines, a significant relationship results.

The possibility of residual rather than normal shrinkage for several horizons was also indicated by the high air filled porosity (P_{AR}) at the shrinkage limit for those soils of high organic matter content and low n_{RS} values (Figure 3.10). The P_{AR} was close to 0 (i.e. on the 1:1 line, saturated) for remoulded soils with slopes approaching 1. The P_{AR} was > 5% for the soils with a

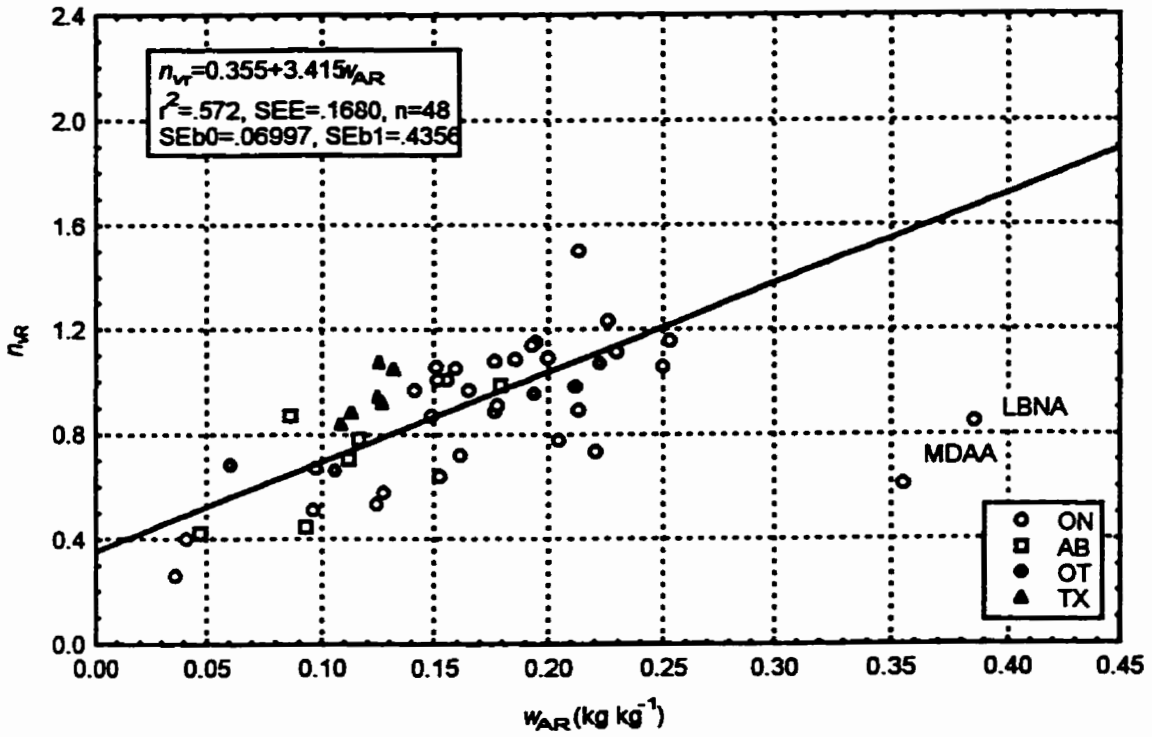

Figure 3.9. Illustration of increasing slope (n_{vR}) with increasing water content at the shrinkage limit (w_{AR}) for remoulded samples.

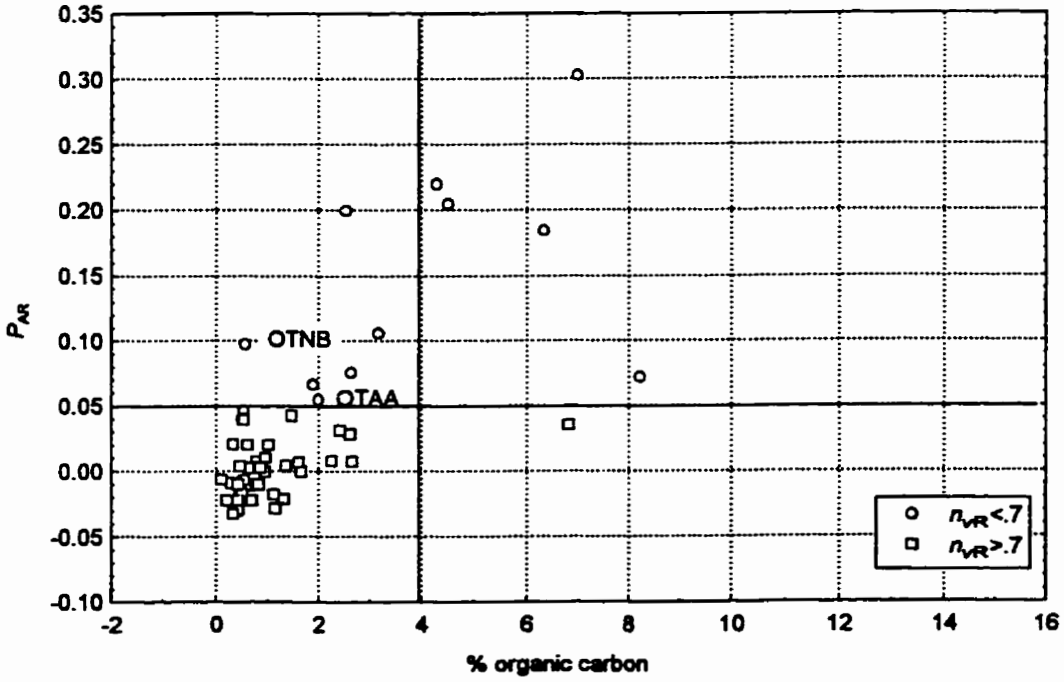

Figure 3.10. Relationship between air-filled porosity (P_{AR}), organic carbon and slope (n_{vR}).

n_{vR} < 0.7. These included 12 of the 18 A horizons, all of the loam textured soils, 5 of 7 silt loam soils (soils with ≤ 27% clay) and soils with greater than 4% organic carbon content. Two soils which deviate from these textural or organic carbon criteria but which had low n_{vR} and high P_{AR} are the OTAA and OTNB horizons which were both clay loam in texture and have 2.00 and 0.56 % organic carbon content, respectively. Therefore, although linear shrinkage was measured on all samples and a 2-line segment model fit for 50 horizons, the portion of the shrinkage curve represented is more likely the zero and residual portions for these 17 horizons (includes the 4 horizons with only a significant 1 line model).

The division of soils by n_{vR} and P_{AR} could also be discerned visually. The shrinkage characteristic graphs in the Appendix show that 9 of these 17 horizons have the maximum w at the 1:1 line with the n_{vR} approaching the 1:1 line at an oblique angle so that there is no opportunity for paralleling the 1:1 line and having a slope of 1. The v_{AR} and entire shrinkage characteristic curve was positioned well above the 1:1 line. The soils were therefore divided into 2 groups; Group 1 had normal and residual shrinkage (n=37) and Group 2 had residual and zero shrinkage (%clay≤27, %oc>4%) (n=17). The 27% clay content threshold corresponds to a division on the textural triangle between silt loam/loam and silty clay loam/clay loam soils (ACECSS, 1987). Similarly, Paz (1998) found that for coarse textured materials (<21% clay content) there was largely residual shrinkage and normal shrinkage only occurred close to saturation. Of the 18 horizons with n_{vR} <0.7, 14 were from the Group 2 soils. Many of the Group 2 soils were of the MH or ML A-line classification. Similar threshold values were proposed by Kuznetsova and Davilova (1988) (20-35% clay; > 4% humus) when predicting the loosening capacity of soils during shrinking and swelling. This confirms the work of Haines (1923) who found that total and normal shrinkage depended on the clay content whose effect on shrinkage would only be shown when present in large enough quantities to act as a general matrix for the larger particles and that

residual shrinkage depended on organic matter content. Lauritzen (1948) also found that the addition of sand >25% to clay fractions resulted in the elimination of the normal shrinkage region. Also organic matter additions caused the residual shrinkage to begin at a higher moisture content in Houston black clay blocks and at lower moisture content in Oasis silt loam blocks and eliminated normal shrinkage in the silt loam soil (Lauritzen, 1948). WA and MD soils represent 10 of the 17 Group 2 horizons and these were the most coarse textured sites sampled. This suggests that there may be a threshold slope value of 0.7 for distinguishing residual from "normal" shrinkage or, low from high shrink-swell potential soils, similar to the slope threshold between plastic and non-plastic compression (5% or 0.13) for remoulded soils. Stirk (1954) and Reeve and Hall (1978) defined 'normal shrinkage' if the ratio of volume change to water loss was greater than 0.9, residual and structural shrinkage if the volume ratio is 0.05-0.9 and no shrinkage if the ratio is less than 0.05.

It is noted that there were negative values for some of the air-filled porosity values which may be due to four reasons. Firstly, a correction was done on all horizons when there was a gain in oven dry mass because of residual kerosene. This correction was subtracted as a percentage of the soil mass. The correction was less than 1% for all soils and less than 0.5% for most. For some of the soils, A horizons and coarser textured soils in particular, there was a loss of mass on oven drying which may have been due to losses of organic matter (Topp, 1993) or to some soil being lost when transferring to weigh boats. No correction was made for soils with a weight loss; the loss of mass was less than 0.2% for the remoulded and less than 0.4% for the structured oven dry samples. The uniform application of this correction to all tension levels may have resulted in lowering the values below the 1:1 2 phase line, resulting in negative values. Secondly, the P_{AR} value is calculated from the calculated specific volume using the fit $v_{\alpha R}$, r_{vR} and w_{AR} values. These values could converge below the 1:1 line since no boundary conditions were supplied to the model, only simple non-linear regression. Thirdly, there may be experimental error in massing and

determining the volume of the samples particularly due to the mass of the clip and baskets used relative to the size of the sample. Since, especially in the remoulded condition, the air-filled porosity would be very close to 0 along the shrinkage characteristic curve, slight negative values should not be surprising from experimental error alone. The negative P_{AR} values are not large (Range -.0327 to -.0004, n=20). Fourthly, most shrinkage curves in the literature have been constructed for single clods where the mass and structure are carefully controlled, while in this experiment the natural variability within 45 clods to construct the curve may lead to less internally consistent results. Since most of the negative P_{AR} values are from B and C horizons it is assumed that it is the correction factor or natural or experimental variability producing the negative values.

A direct way to look at the mechanism of remoulded shrinkage is to look at the amount of water loss between saturation and the shrinkage limit ($w_{BR} - w_{AR}$). The n_{vR} is fairly independent of change in water content if the 17 Group 2 soils in residual shrinkage are removed, which it should be as the value should tend towards 1. The ANOVA analysis shows that the amount of water loss during normal shrinkage is dependent on the horizon (Table 3.5), with the A horizons losing the most water over ($w_{BR} - w_{AR}$). There is a significant difference between the A horizon and the average of the B and C horizons (p=.011).

Table 3.5. LSmeans pdiff separation for ln ($w_{BR} - w_{AR}$) (1 lines removed).

Factor	HOR		
	A. vs. B.	A vs. C	B vs. C
pdiff	0.0995	0.0051*	0.1217
	A	B	C
LSmean	-1.23803139	-1.55949345	-1.85969444
Back Transformed Mean	0.28995	0.21025	0.15572

Covariate analysis indicated that the change in water content ($\ln(w_{BR} - w_{AR})$) was independent of the amount of clay (Figure 3.11) in the sample but was related to the amount of organic carbon (Figure 3.12) when the 4 single line segment models were removed. Analyzing the Group 1 soils

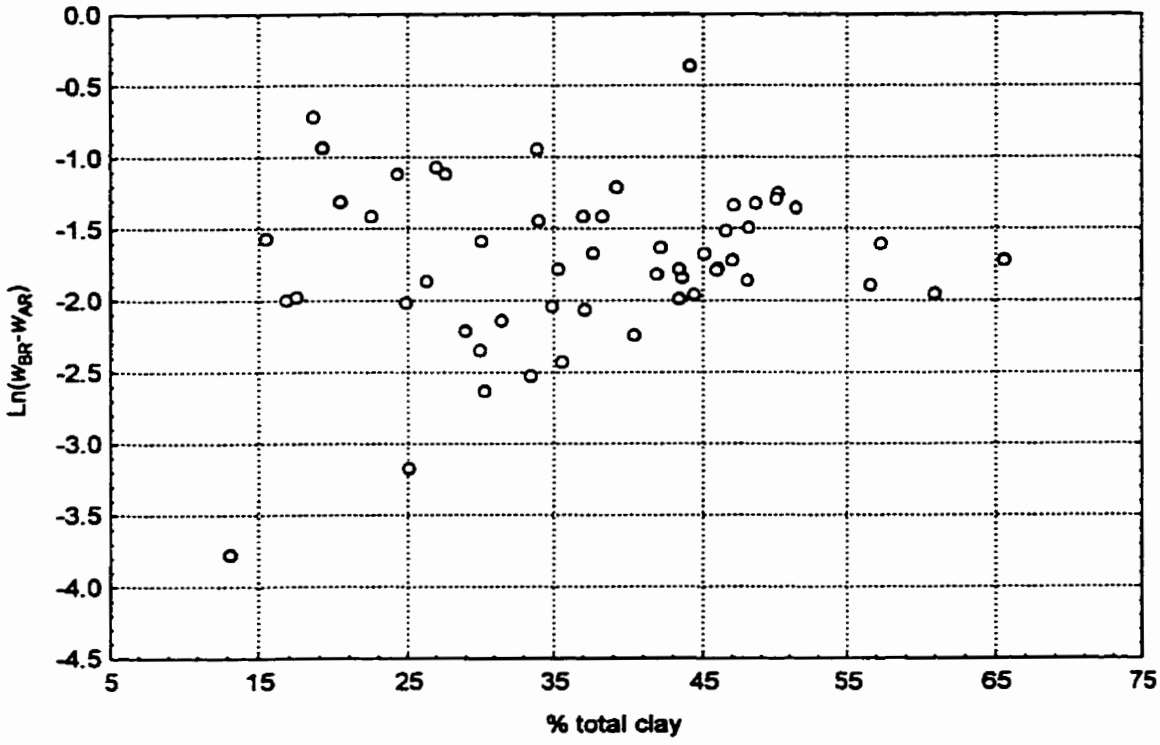

Figure 3.11. Independence of $\ln(w_{BR} - w_{AR})$ from %clay content.

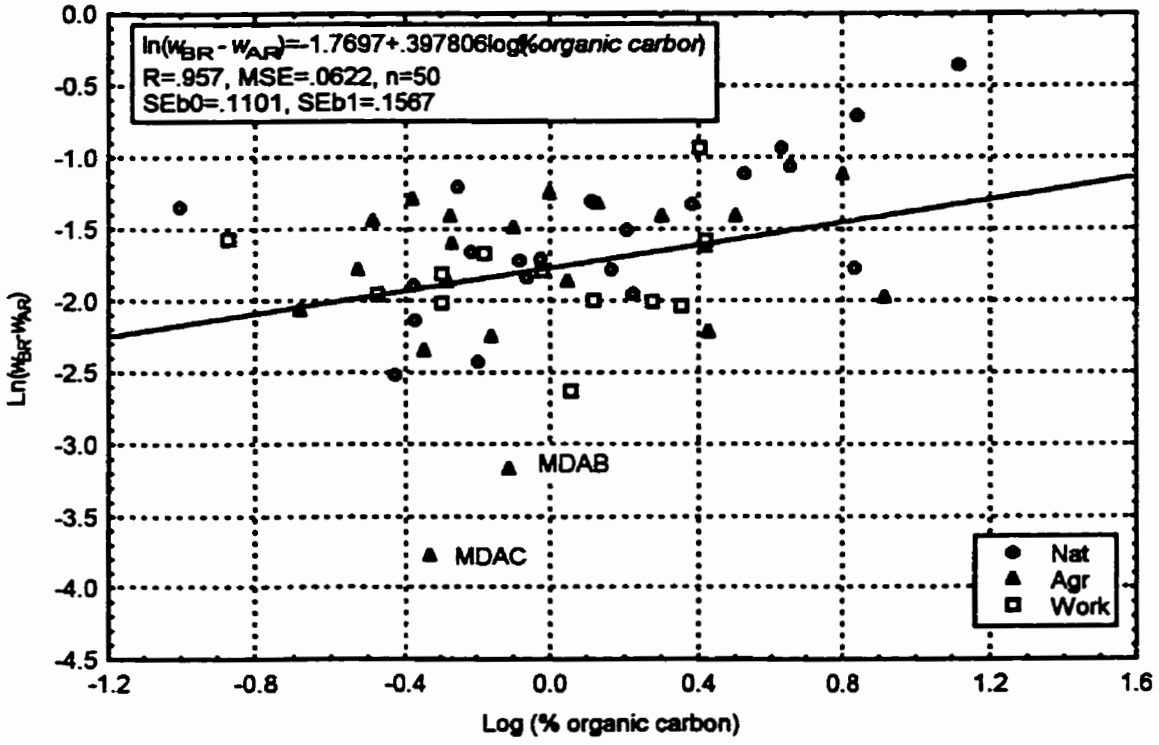

Figure 3.12. Covariance of $\ln(w_{BR} - w_{AR})$ with % organic carbon.

alone showed that there was not a significant relationship between the (w_{BR} - w_{AR}) variable and %organic carbon (p=.73, SEE=.06238, r^2=.003, n=37). This shows the high influence of organic carbon on water loss during the residual shrinkage stage for the Group 2 soils even though there was relatively little volume change. Haines (1923) found that the percentage of residual shrinkage (expressed relative to oven dry volume) was greatest for a peaty soil and least for kaolin. It was proposed that the organic colloid material was concentrated at points of contact between the solid particles which only lost water once air began to replace water in the soil pores (Haines, 1923).

A standard parameter for estimating the shrink-swell potential of soils is the coefficient of linear extensibility (COLE). Since the shrinkage measurements were made in 3 dimensional volume units, the equation of Grossman et al. (1968) was used to determine both $COLE_{rem}$ for remoulded samples and $COLE_{clod}$ for structured samples.

$$COLE = \sqrt[3]{\frac{\rho_{o.d.}}{\rho_{33}}} - 1 \qquad [10]$$

Equation [10] was slightly modified, as the average void ratio at the two pressure potentials was recorded, to determine the same value.

$$COLE_{ClodorRem} = \sqrt[3]{\frac{\frac{\rho_p}{(e_{o.d.}+1)}}{\frac{\rho_p}{(e_{33}+1)}}} - 1 = \sqrt[3]{\frac{(e_{33}+1)}{(e_{o.d.}+1)}} - 1 \qquad [11]$$

Since the void ratio at -33 kPa was not measured directly for the structured samples, it was interpolated from the structured $e(\sigma')$ model parameters.

There was a weak relationship between $COLE_{rem}$ and all the n_{vR} for all horizons (F=10.221, r^2=.164, SEE=.0319, p<0.01, n=54). $COLE_{rem}$ was not related to n_{vR} once the Group 2 soils were removed (Figure 3.13). The graph of $COLE_{rem}$ vs. (w_{BR} - w_{AR}) (Figure 3.14) was one of the best indications that there were two groups of soils in terms of shrinkage characteristics and

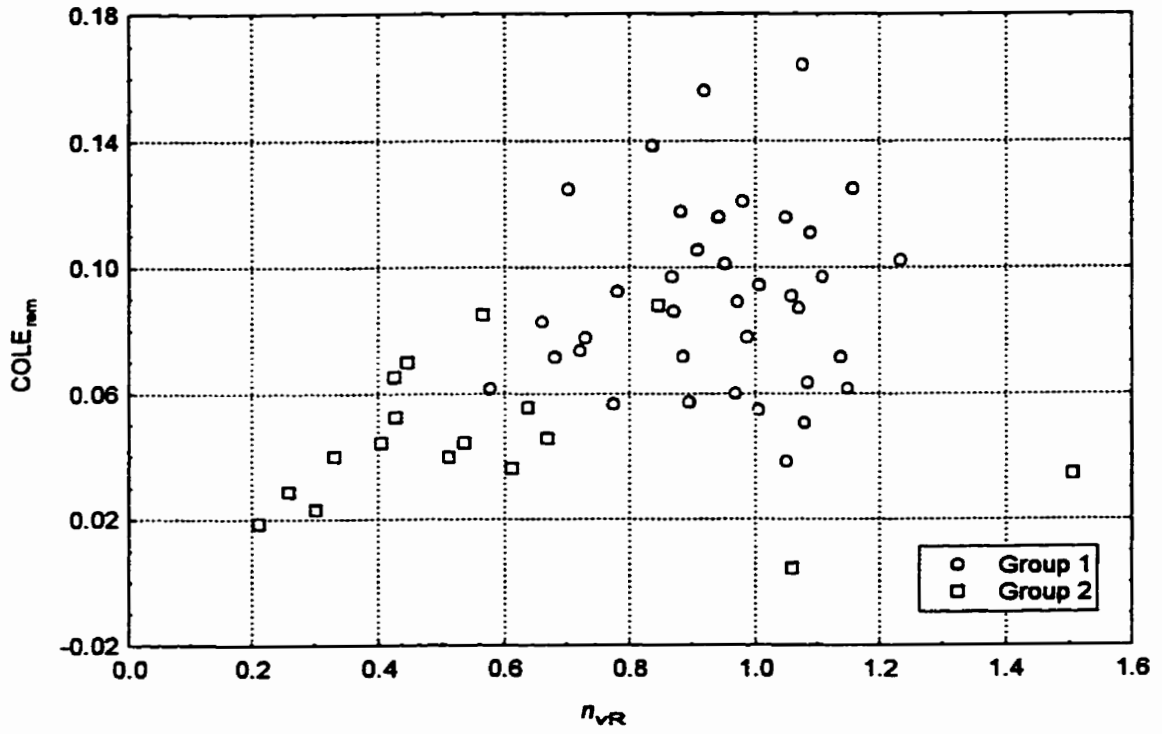

Figure 3.13. $COLE_{rem}$ versus n_{vR}.

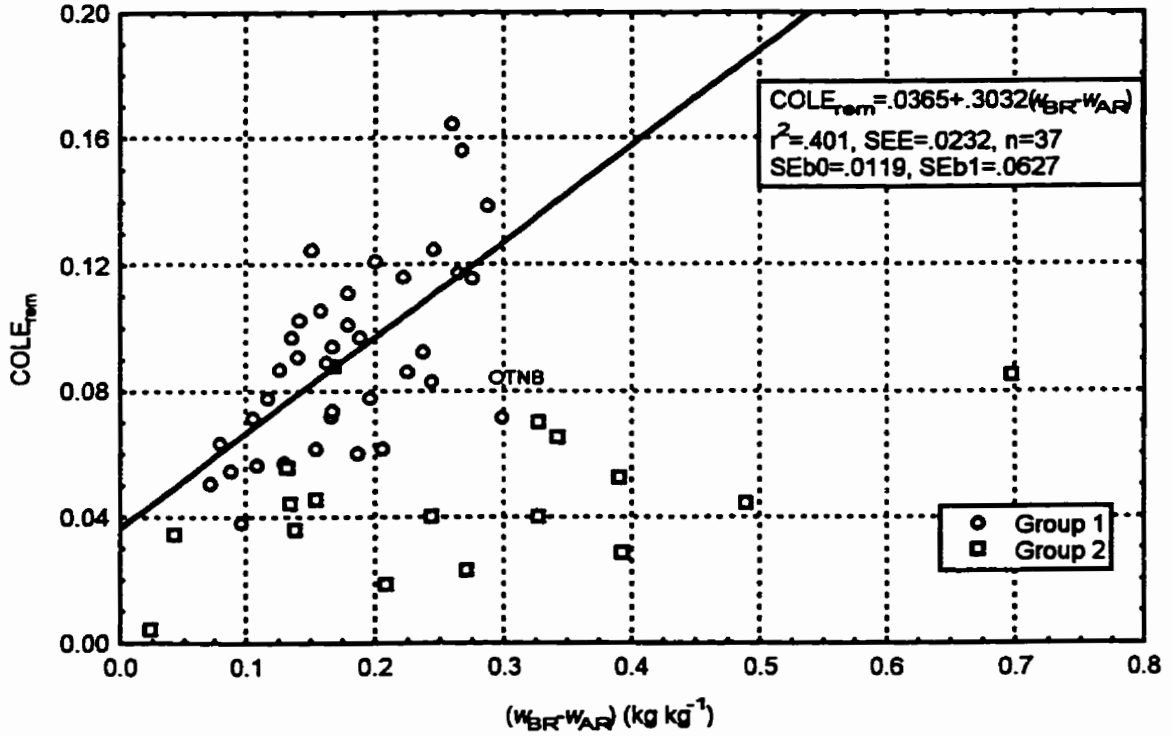

Figure 3.14. $COLE_{rem}$ versus (w_{BR} - w_{AR}) for all data.

was used for discerning the boundary conditions. There was a significant linear relationship between $COLE_{rem}$ and the (w_{BR} - w_{AR}) variable when the Group 2 soils were removed. When the outlier OTNB was removed the intercept became 0.0282 (SEb0=.0112) and the r^2 improved (.509). The positive intercept is curious since with no change in water content we would expect no volume change. As (w_{BR} - w_{AR}) is essentially the water change over "normal shrinkage", this relationship marks the lower boundary for shrink swell potential, similar to the 0.03 value suggested by Dasog et al. (1988).

Both the %fine clay (<0.2 μm) and the % total clay (<2 μm) predict the $COLE_{rem}$ equally well (Figure 3.15 and Figure 3.16). Neither intercept is significantly different than zero. For the % total clay there seems to be a separation of the smectitic and micaceous mineralogies. The percentage coarse clay (<2 μm and >0.2 μm) does not predict the $COLE_{rem}$ particularly well (r^2=.3297) and the residuals are not normally distributed (Figure 3.17). This is due to 2 groups of soils. One group is 4 Texas soils, TXAA, TXAB, TXAC and TXNC where the % fine clay is greater than the % coarse clay (~10% more) and the other group is 4 soils from the feldspar containing mineralogy where the % coarse clay is considerably greater (~20-30%) than the % fine clay (OTAB, OTNC, WANC, WAWC). The remaining soils have 5-10% more coarse clay than fine clay in the clay fraction (Figure 3.18). When the 17 Group 2 soils are removed, the %fine clay equation drops in r^2 to .591 but the SEE becomes slightly smaller (Eq.[12]), while the % total clay equation becomes much less significant (Eq.[13]).

$COLE_{rem}$=.02986+.003806*%fine clay* [12]

SEb0=.00968, SEb1=.00057, SEE=.0198, r^2=.591, n=37

$COLE_{rem}$=.002176+.002074*%clay* [13]

SEb0=.0190, SEb1=.00044, SEE=.0233, r^2=.392, n=37

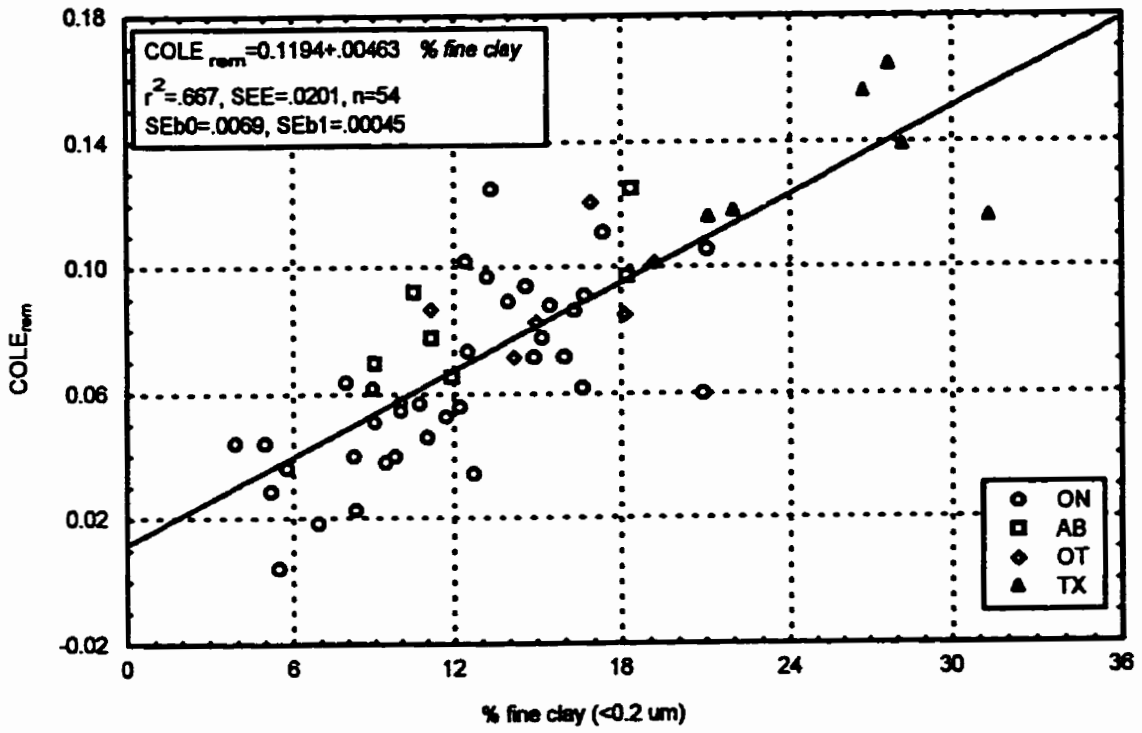

Figure 3.15. $COLE_{rem}$ versus % fine clay.

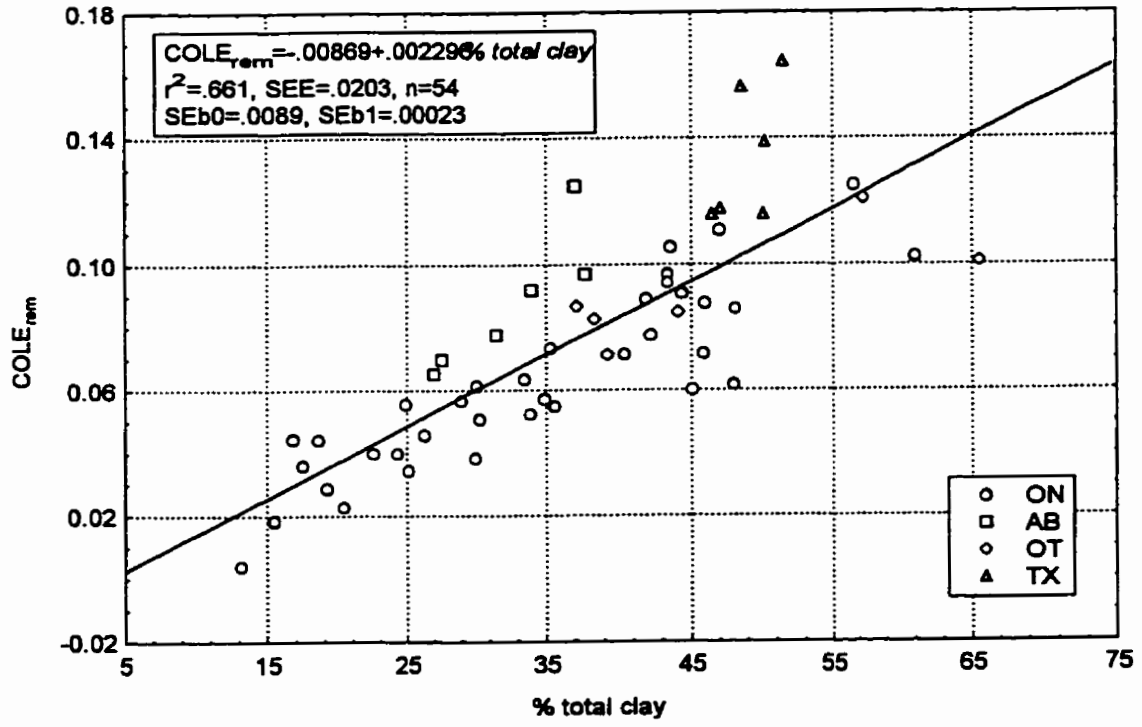

Figure 3.16. $COLE_{rem}$ versus % total clay.

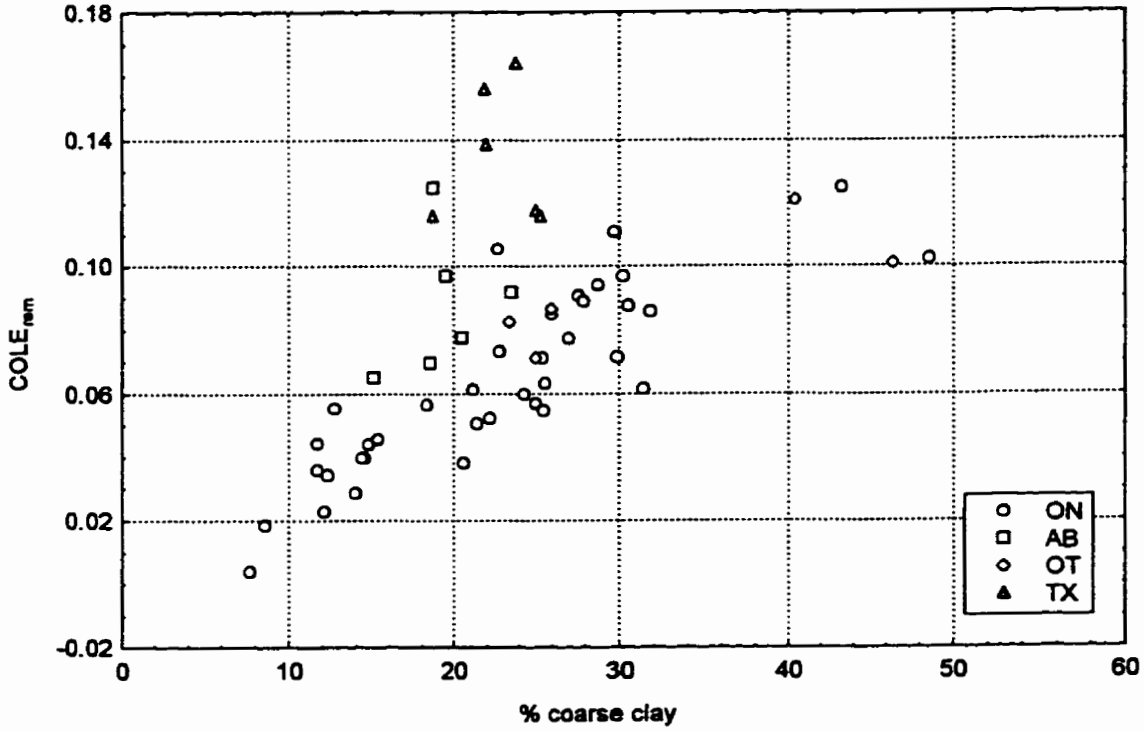

Figure 3.17. COLE$_{rem}$ versus % coarse clay.

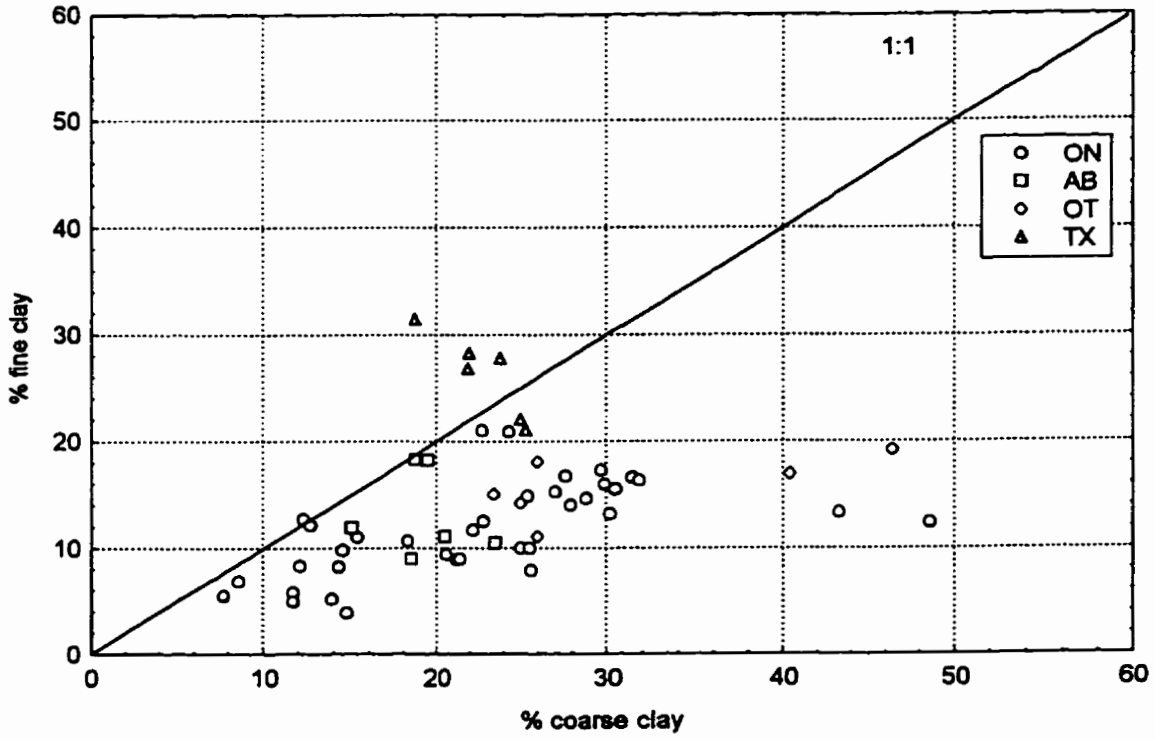

Figure 3.18. % fine clay versus % coarse clay.

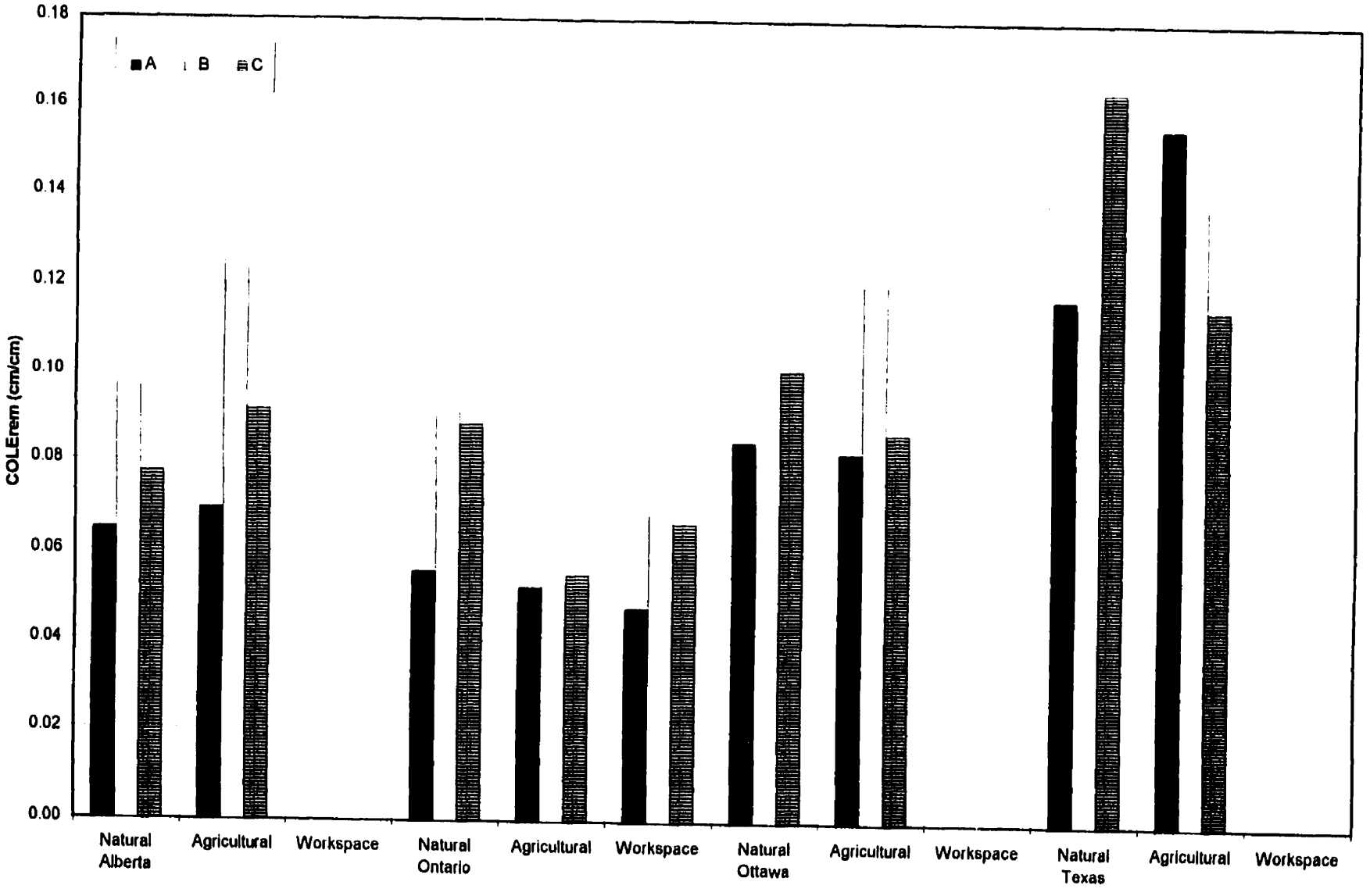

Figure 3.19. $COLE_{rem}$ MNR*TRT*HOR interaction (WANC removed).

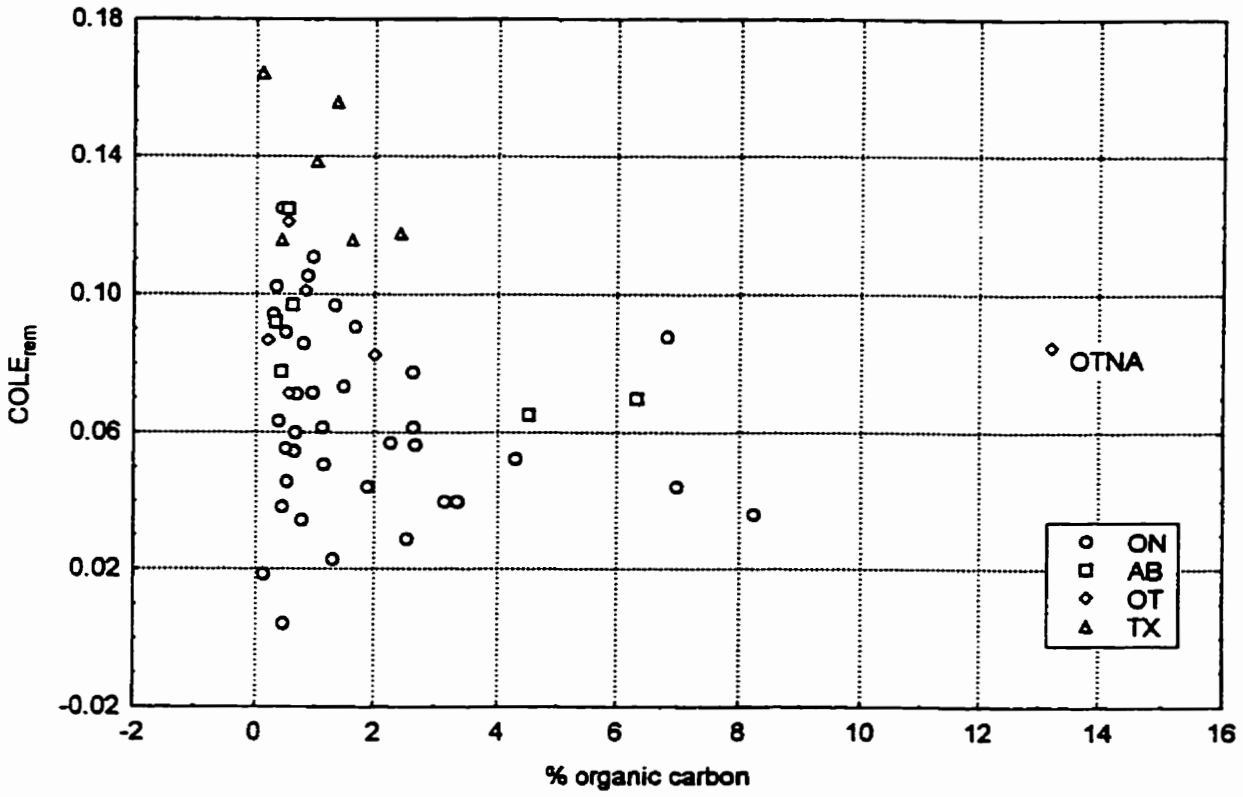

Figure 3.20. COLE$_{rem}$ vs. % organic carbon.

An ANOVA analysis for $COLE_{rem}$ indicated a significant MNR*TRT*HOR factor. The Texas soils, ABAB, OTAB and OTNC had $COLE_{rem}$ values greater than 0.10 and Ontario Agricultural, ONNA and ONWA soils had $COLE_{rem}$ less than 0.06 but it was difficult to make conclusions from pdiff values alone (Figure 3.19). ANCOVA analysis revealed there was no significant relationship between $COLE_{rem}$ and organic carbon except for Ottawa soils which was due to the one extreme value for OTNA (Figure 3.20). There were significant ANCOVA relationships for both % total clay and % fine clay. The significant clay*MNR*TRT term for the slopes with % total clay were misleading because of the similar clay contents for the Texas horizons giving very steep slopes of the opposite sign from the other mineralogies (Figure 3.16). The % fine clay was independent of mineralogy when the outlier WANC was removed. This horizon had the highest $COLE_{rem}$ for the Ontario soils. The effect of retaining WANC was to give a positive MNR*TRT interaction for the intercepts; a significant intercept for ON Agr resulted which was significantly different than the other Agr intercepts which weren't significantly different from zero. The overall relationships with % fine clay remained the same and the equations without WANC are presented here (MSE=.00011, R=.9775, n=53). [14]

i) Agr: $COLE_{rem}$ =-.021443+.009516*%fine clay*-.0001549*%fineclay*^{2}

SEb0=.0195, SEb1=.0024, SEb2=.00007

ii) Nat: $COLE_{rem}$ =.03224+.0009122*%fine clay*+.0001412*%fineclay*^{2}

SEb0=.0202, SEb1=.0026, SEb2=.00008

iii) Work: $COLE_{rem}$ =-.03830+.015386*%fine clay*-.0004909*%fineclay*^{2}

SEb0=.0240, SEb1=.0039, SEb2=.00015

None of the intercepts are significant and none of the Natural slope parameters are significantly different from zero. The Natural parameters are significantly different from the Agricultural and Workspace parameters. The Workspace and Agricultural parameters are not significantly different

but they are also not coincident upon each other. It is of note that the Natural horizon $COLE_{rem}$ values are statistically independent of % fine clay content and that the intercept and quadratic parameter are opposite in sign from the agricultural and workspace treatments which is likely related to the higher organic matter contents in these horizons.

There are 2 existing equations in the literature for predicting $COLE_{rem}$ from % total clay.

Ross (1978): $COLE_{Ross}$=-.0047+.0018*%clay* r^2=.81 [15]

Simon et al. (1987) $COLE_{Simon}$=.013+.0025*%clay* r^2=0.71 [16]

Eq. [15] does not have a 1:1 relationship with all measured $COLE_{Rem}$ values. When the Alberta and Texas soils are removed (smectitic mineralogy), a significant 1:1 relationship results (r^2=.791, SEE=.01319, n=42). This is not surprising since the equation is for soils of micaceous mineralogy from S. Ontario and Quebec and kaolinitic mineralogy from Tanzania. Also the S. Ontario and Quebec soils had roughly the same amounts of coarse and fine clay which is similar to the majority of the soils tested but not for the TX soils. When the 17 Group 2 soils are removed there is a 1:1 relationship with the remaining soils including the smectites (r^2=.392, SEE=.0233, n=37) but the standard error of estimation is doubled.

Simon et al. (1987) used a combination of micaceous and montmorillinic soils. A comparison of the $COLE_{Simon}$ values to measured $COLE_{rem}$ values shows a significant negative intercept (-.02) but the slope is not significantly different from 1 (r^2=.6614, SEE=.0203, n=54). The same relationship remains if the Group2 soils are removed (r^2=.3921, SEE=.023). Their equation is based on saturated to air dry conditions and this may result in the overestimation of $COLE_{rem}$ since it is known that the initial water content is correlated to shrink swell parameters (DeJong et al., 1992; McGarry, 1995). Saturated water content is often essentially the same as the liquid limit (DeJong et al., 1992) but in this study the maximum water content at -33 kPa is significantly less than the liquid limit which may explain the overestimation.

w_{BR}=.068483+.6308w_L [17]

SEb0=.0205, SEb1=.04388, SEE=.0394 , r^2=.799

The amount of variability explained is improved (r^2=.871) if the 6 Texas horizons are removed but the initial water content remains considerably less than the LL. There is not a 1:1 relationship with Eq. [16] when the AB and TX soils are removed suggesting it only applies over mixed mineralogies including montmorillonite/smectite.

The plasticity index is better at predicting $COLE_{rem}$ than clay content (Figure 3.21). The prediction and residuals are improved if log (% clay) is also included.

$COLE_{rem}$=-.08833+.00210I_P+.08151log(*%clay)* [18]

SEb0=.0278, SEb1=.00037, SEb2=.02117 SEE=.01582, r^2=.798, n=54

An equation of DeJong et al. (1992) uses the plasticity index to predict COLE of structured clods. When compared to $COLE_{rem}$ there is a significant relationship with a significant positive intercept (0.02) and the slope is not significantly different than 1(F=147.2, SEE=.0178, r^2=.7390, n=54). The underestimation might be due to the more free swelling and shrinking able to occur in a remoulded state but the close relationship for both states to the plasticity index is noteworthy.

The A-line classification divides predicted shrink-swell potential values broadly using the proposed ratings of Dasog et al. (1988) for structured soils (Figure 3.21). All the CH soils could be classified as Very High in the remoulded condition ($COLE_{rem}$ > 0.09). All of the ML and all but one of the MH soils have $COLE_{rem}$<0.09. The CL soils cross all shrink-swell potential categories. All the soils with a $COLE_{rem}$ greater than 0.06 have a clay content >27%. The soils with a Very High shrink swell potential also have I_P >17. There are some soils with I_P >17 where the shrink-swell potential is only High ($COLE_{rem}$ 0.06 to 0.09). The classification that Dasog et al. (1988) use for % fine clay in conjunction with COLE does not seem to fit the remoulded data. There are only 6 horizons with a fine clay percentage greater than 20% which they use as a boundary

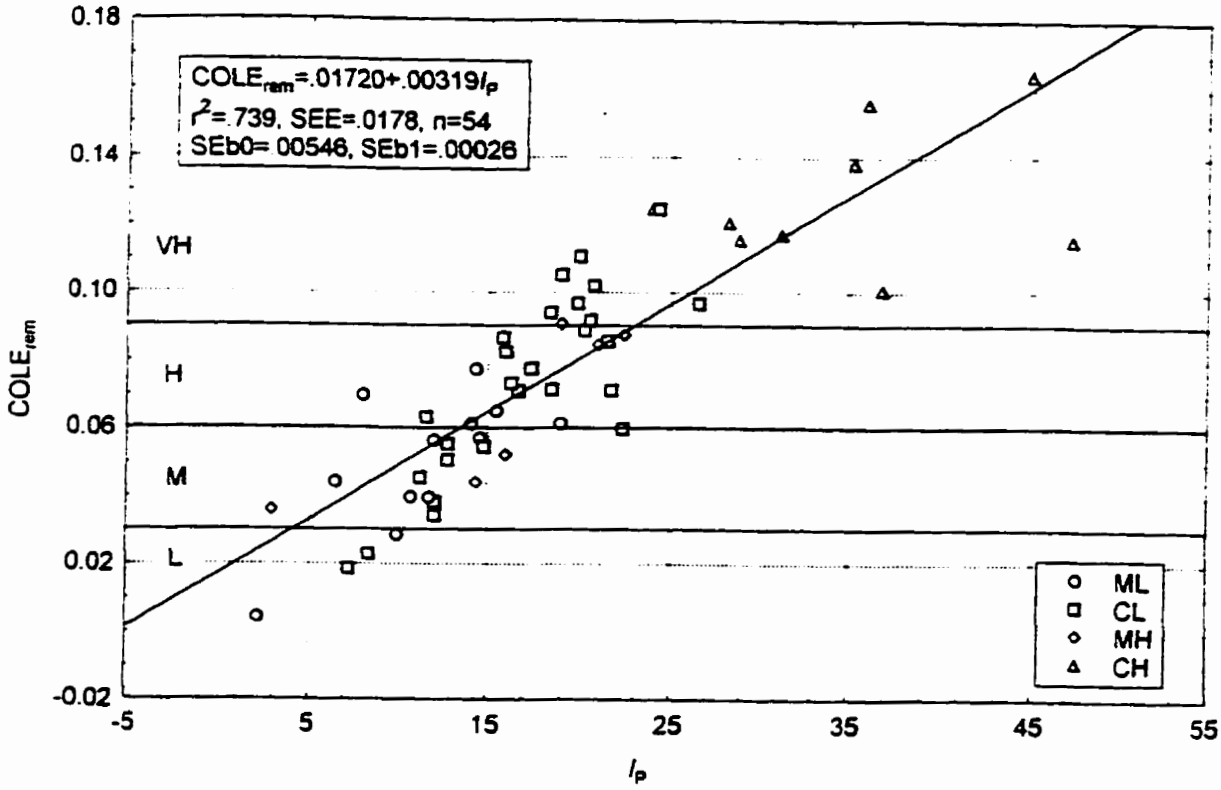

Figure 3.21. COLE$_{rem}$ versus I_P.

between Low and Medium shrink-swell potential. In the remoulded conditions these thresholds seem to apply better to % total clay rather than % fine clay. The VH soils have > 33-35% clay , the H soils have >27-28% clay and the L soils have < 20-21% clay. McCormack and Wilding (1976), Schafer and Singer (1976), Reeve et al. (1980) and De Jong et al. (1992) found the total clay to be correlated to shrinkage for Ohio, California, British and Saskatchewan soils, respectively. Other researchers have found the surface area (Ross, 1978; Smith et al., 1985) or percentage fine clay (Dasog et al., 1988) to better predict $COLE_{std}$.

3.3.1.2 Representation in $e(\sigma')$ coordinates

The remoulded data fit (r^2) for the $e(\sigma')$ coordinates was also good (mean 0.954, median 0.983). There was one $e(\sigma')$ model which was insignificant (MDAC r^2=0.006), 41 horizons with a residual shrinkage portion, and 12 horizons with a structural shrinkage portion as well. Similar to the $v(w)$ analysis, there were a significant number of outliers and it was assumed that there should be no structural line segment in the remoulded state, so only 2 line segment models were analyzed. With the MDAC horizon removed the mean of the r^2 was .967 and the median was .979. It was also the MDAC horizon which showed potentially non-plastic behavior for the NCL representation indicating a lack of shrinkage behavior for non-plastic soils. The $COLE_{rem}$ for MDAC at 0.0041 was the lowest of all the soils.

There is a 1:1 relationship between v_{aR} converted to a void ratio and e_{CR} when MDAC and OTNA horizons are removed (r^2=.9925, SEE=.0139) (Figure 3.22). The residuals are more normally distributed when MDWC, WANA and WANB (the additional 1 line segment models in $v(w)$ co-ordinates) are also removed (r^2=.9982, SEE=.00699). This makes sense since both endpoints represent the oven dry volume and will match when a 2 line segment model is fit in both coordinates. Any ANOVA, ANCOVA, and regression relationships developed for v_{aR} therefore

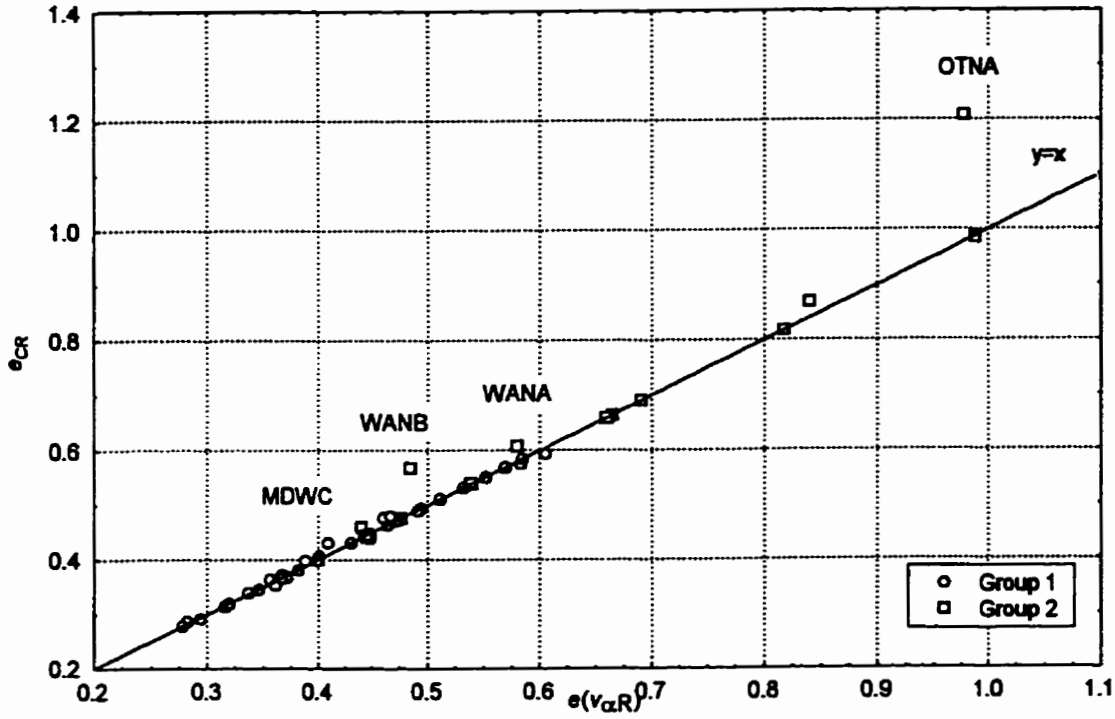

Figure 3.22. e_{CR} **versus** $v_{\alpha R}$ **converted to a void ratio.**

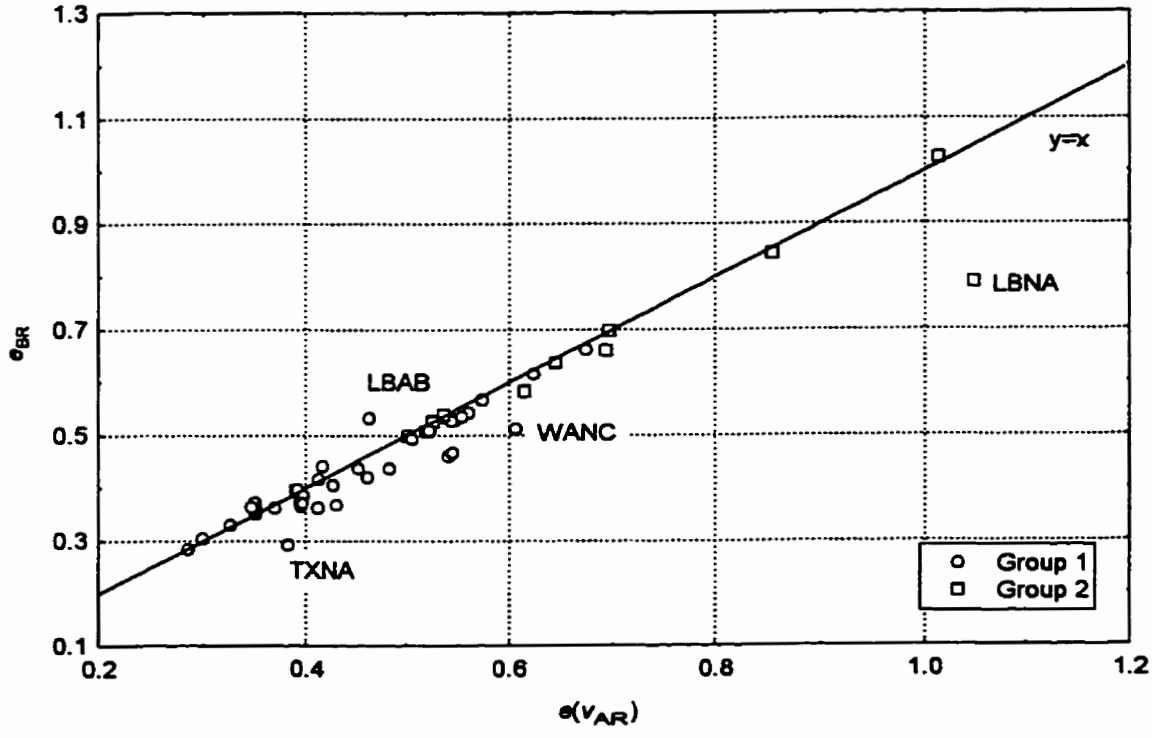

Figure 3.23. e_{BR} **versus** v_{AR} **converted to a void ratio.**

will apply for e_{CR}.

The void ratio at the shrinkage limit e_{BR} was compared to the void ratio calculated from the v_A from the $v(w)$ plots (Figure 3.23). There was a 1:1 relationship for the Group 1 soils alone but not when the Group 2 soils were included, or if the Groups 2 soils were analyzed alone. The residuals were also not normally distributed when the Group 2 soils were analyzed. The single line segment models were not included because they had no shrinkage limit. The v_A tended to be larger than e_{BR}. This may have occurred because the $e(\sigma')$ plots had greater variability than the $v(w)$ plots and used prescribed tension levels which caused the model to converge at higher stress/lower void ratio values.

The void ratio at the shrinkage limit, e_{BR}, had a significant MNR*TRT *HOR term even when the MDAA, MDAC and OTNA outliers were removed. There was a clay*MNR and MNR*TRT factors for clay as covariate with MDAA, MDAC and OTNA removed but the interpretation was complicated by the narrow clay ranges represented by the different mineralogies. A simpler relationship occurred for the covariate logOC with the OTNA outlier removed (Figure 3.24).

The e_{wL} was closely related to intercept of the $e(\sigma')$ plot (e_{aR}) (Figure 3.25). There is a 1:1 relationship for all 54 horizons but not when the OTNA horizon is removed. It is assumed that this horizon is a reasonable outlier because of its high organic carbon content. An obvious division seems to occur for soils according to their A-line categorization (w_L=50 translated into ~ e_{wL} =1.32). There is a significant 1:1 relationship between the e_{wL} and e_{aR} for the CL and ML soils.

e_{aR}=-.032323+1.0424 e_{wL} [20]

SEb0=.12297, SEb1=.1165, SEE=.1188, r^2=.684, F=79.998, n=39

This relationship indicates that at -1 kPa pressure potential, these soils in the remoulded state equilibrate close to the w_L (log10(1)=0). On the other hand, there is no significant relationship

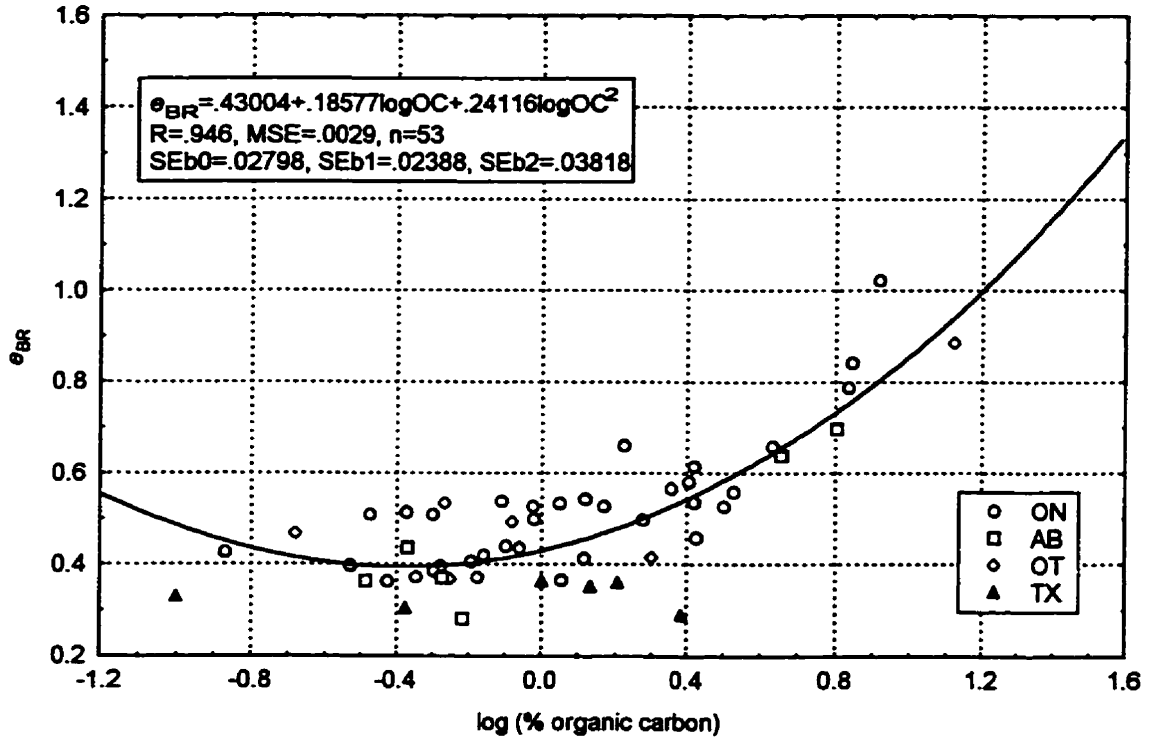

Figure 3.24. Covariance of e_{BR} with log (% organic carbon).

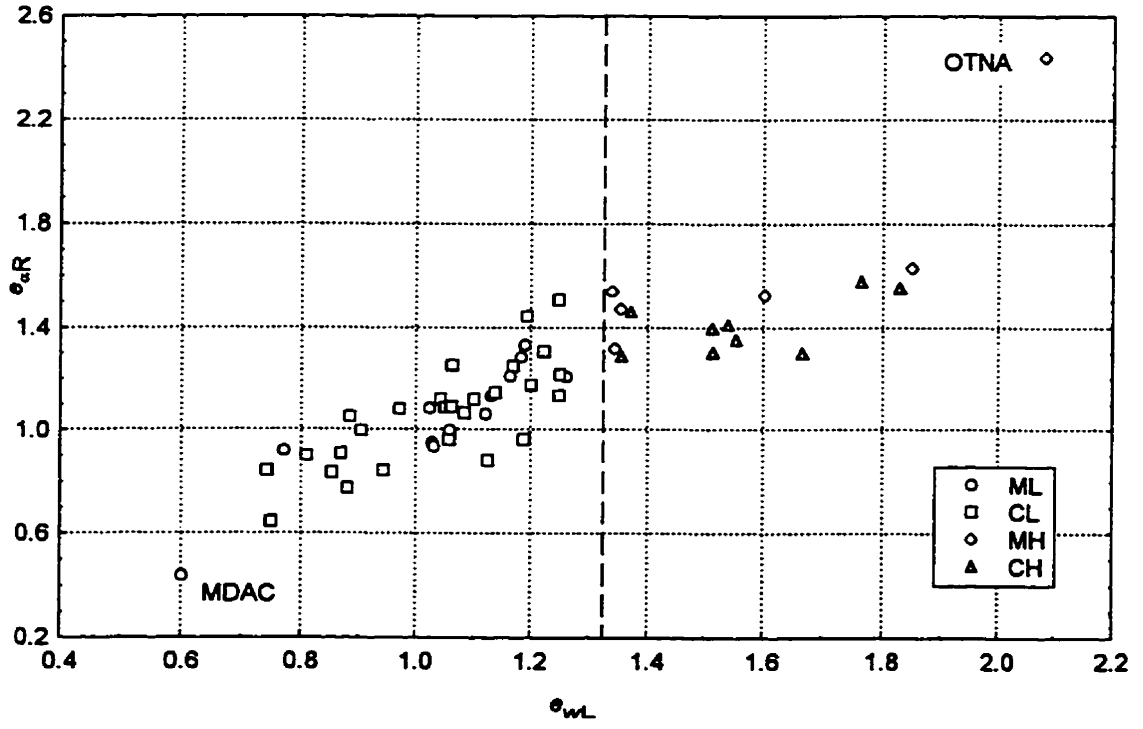

Figure 3.25. $e_{\alpha R}$ compared to e_{wL}.

(p=.0681) with the CH and MH soils (when OTNA is removed); the mean $e_{\alpha R}$ is 1.43 ±.1153. The e_{wL} is generally greater than $e_{\alpha R}$ for these soils indicating that the w_L stress must be closer to saturation (0 kPa) or that the swelling pressures are greater than the effective stresses at these water contents. The pore water pressure potential at the liquid limit has been found to vary from about -0.3 to - 15 kPa (reviewed by McBride, 1989).

There is a significant MNR*TRT*HOR interaction when all horizons are considered together for $e_{\alpha R}$. When OTNA and MDAC outliers are removed a significant TRT effect remains. The Natural intercept is largest and also significantly different than the average of the Agr and Work intercepts (p=.0182) (Table 3.6).

Table 3.6. LSmeans pdiff separation for $e_{\alpha R}$ TRT (MDAC, OTNA removed).

Factor	TRT		
	Agr vs. Nat	Agr vs. Work	Nat vs. Work
pdiff	0.1374	0.2159	.0161*
	Agr	Nat	Work
LSmean	1.19284	1.263489	1.12078

Using the covariate organic carbon and outliers WANB and OTNA removed, there is a significant MNR*TRT and quadratic term (b2=.00927379, SEb2=.00159173, MSE=.00936963, n=52) for $e_{\alpha R}$. The significant differences between intercepts are for On Agr vs. TX Agr and ON Work vs. ON Nat. When % clay is the covariate and OTNA, MDAA and MDNA are removed there is a clay*MNR effect. The only slope term significantly different from 0 is for Ontario. There are significant differences between Ontario and AB and OT for slope and intercept.

The shrinkage limit stress, σ_{BR} is unrelated to the steepness of the second line segment ($n_{\alpha R}$). There is a significant TRT*HOR interaction for all horizons considered together where the Nat A horizon is significantly different from everything else (Figure 3.26). The shrinkage limits in the remoulded condition for the Natural A horizon is the highest at 36.4 MPa, then 5.7 MPa for the Natural B horizons with rest of the horizons falling between 1.8 and 3 MPa, just above permanent

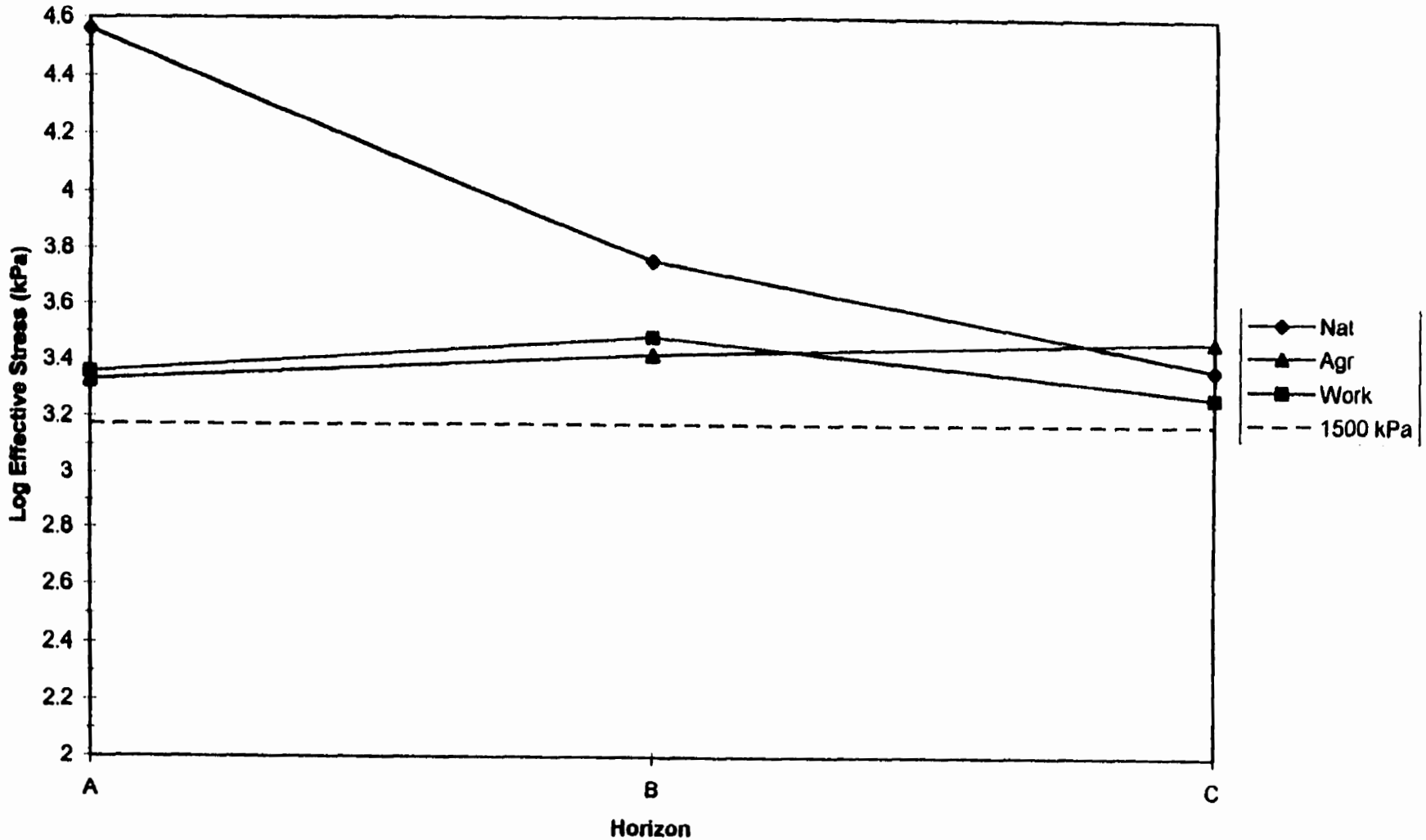

Figure 3.26. σ_{BR} TRT*HOR interaction. Back transformed means.

wilting point of 1.5 MPa. When log%organic carbon is the covariate there is an oc*TRT interaction; only the Natural horizons have a significant slope which is significantly different from both Agricultural and Workspace horizons. The R is low for this relationships (R=.7481, MSE=.1986)) as the variation is large. With %clay as the covariate for $\ln(\sigma_{BR})$, there is a clay*TRT interaction with Agr and Nat having significant and oppositely signed slopes while the Work slope in not significant (R=.7057, MSE=.0174).

The steepness of n_{aR} is correlated to the % total clay (R=.742, SEE= .0475, n=54) or % fine clay (R=.657, SEE=.0459, n=54) which is similar to the NCL but opposite from n_{vR} . The ANOVA revealed MNR and HOR factors for $n_{e\,R}$ when outliers were removed (Table 3.7). The slope is steepest for the C horizons and TX is steeper than the average of the other 3 mineralogies (p=.0125).

Table 3.7. LSmeans pdiff Separation for $n_{e\,R}$ MNR and HOR (MDAC, MDWC, WANB, OTNA removed).

Factor	MNR					
	AB vs. ON	AB vs. OT	AB vs. TX	ON vs. OT.	ON vs. TX	OT vs. TX
pdiff	.6992	.3356	.0168*	.4036	.0092*	.1118
	AB	ON	OT	TX		
LSmean	-.172819	-.184402	-.211243	-.2774842		
Factor	HOR					
	A. vs. B.	A vs. C	B vs. C			
pdiff	0.1654	0.0083*	0.1130			
	A	B	C			
LSmean	-.183311	-.209937	-.240988			

The ANCOVA with %fine clay revealed a simple correlation relationship (Figure 3.27) similar to that above. With %clay as covariate there is a clay*TRT effect. Mineralogy is also significant at the 10% level (p=.0819) and independent of any interactions. The resulting ANCOVA equations, with MDAC and OTNA removed, are (MSE=.001518, R=.9011): [21]

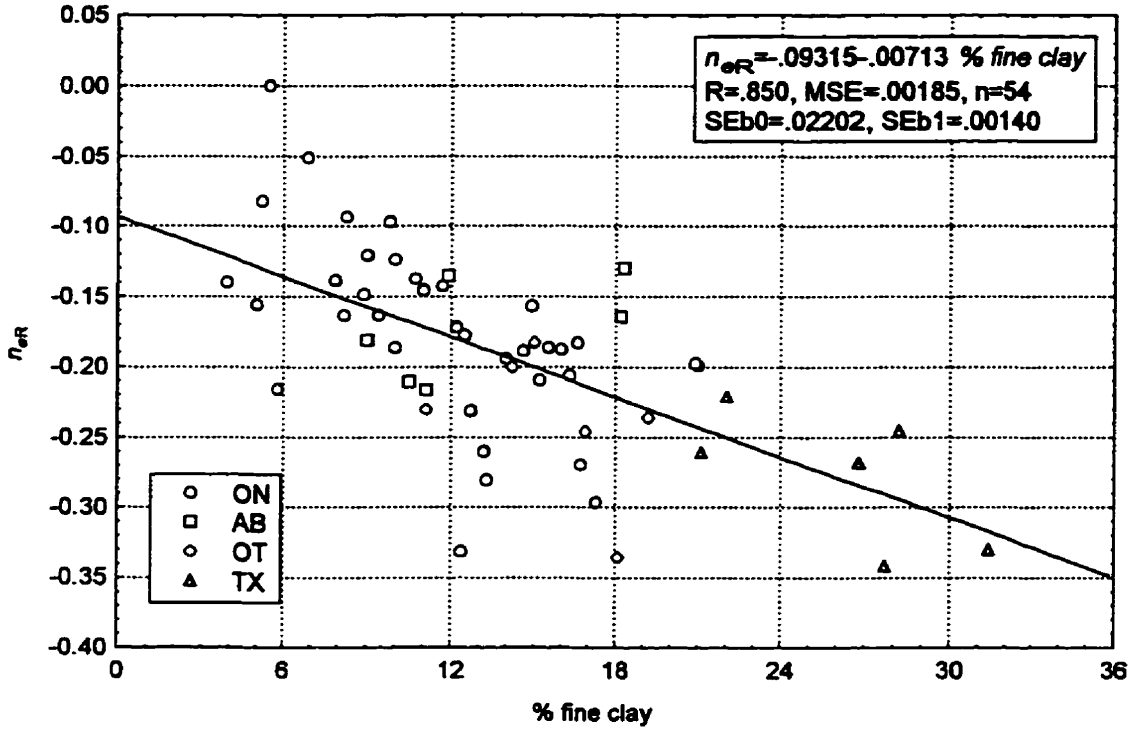

Figure 3.27. Covariance of $n_{e\,R}$ with % fine clay.

i) Agr AB: sqrt($-n_{eR}$)=.39964963 + .00094460*%clay* SEb0=.04156192, SEb1=.00104723

ii) ON: sqrt($-n_{eR}$)=.39473941 + .00094460*%clay* SEb0=.03553262

iii) OT: sqrt($-n_{eR}$)=.40795946 +.00094460*%clay* SEb0=.04530361

iv) TX: sqrt($-n_{eR}$)=.46913804 +.00094460*%clay* SEb0=.04517963

Nat Difference from above in intercepts: -.13706993 slope:.00420241

SEb0=.04586579 SEb1=.00094398

Work Difference from above in intercepts: -.17286538 slope:.00544952

SEb0=.04786975 SEb1=.00096560

The Agr slope is not significantly different from 0 and is different from the other two, while the Work and Nat slopes are not significantly different (p=.318). Similarly the TRT intercepts have Agr different than the Work and Nat intercepts. The TX mineralogy is significantly different than the average of the other 3 (p=.0169) or individually (AB .0524, ON. 0127, OT .0699).

When only the Group 1 soils are considered no transformation is required, the TRT effects are removed and the mineralogy effects remain (MSE=.001046, R=.8673, n=37). [23]

i) AB: $n_{e\,R}$ =-.6107402+.0122785*%clay* SEb0=.22948588, SEb1=.00653111

ii) ON: $n_{e\,R}$ =.0320864-.00556710*%clay* SEb0=.03518626, SEb1=.00083443

iii) OT: $n_{e\,R}$ =-.153409-.00138056*%clay* SEb0=.06044809, SEb1=.00123561

iv) TX: $n_{e\,R}$ =.5855497-.01762384*%clay* SEb0=.36463299, SEb1=.00743661

At the 5% level, the intercepts for Ontario and Texas are not significant and the slopes for Alberta and Ottawa are not significant. One of the difficulties analyzing %clay as a covariate is that the Alberta and Texas soils have a narrow range (~10%) of clay content over which to test the significance of the regression while %fine clay is more widely distributed for all mineralogies. The relationship for the Texas soils had a very high intercept and steep slope which is significantly different from the rest (p=.0433 and p=.0246)) which is likely due to this reason (Figure 3.28).

The ON intercept and slope are different from both AB and OT and the AB equation parameters are different than those for TX at the 5% level.

For the % organic carbon covariate, there is either a straight line relationship with OC*MNR and OC*TRT factors or a quadratic relationship with only MNR as a factor. The quadratic relationship is simplest because the straight and quadratic slopes are shared by all mineralogies and only the intercepts vary (n=54, MNE=.00105737, R=.9367): [24]

i) AB: $n_{e\,R}$ =-.1940259+.02102995*%organic carbon*-.00231714*%organic carbon*^{2}

SEb0=.032015, SEb1=.008902, SEb2=.00073349

ii) ON: $n_{e\,R}$ =-.19929635+.02102995*%organic carbon*-.00231714*%organic carbon*^{2}

SEb0=.0309034

iii) OT: $n_{e\,R}$ =-.22970618+.02102995*%organic carbon*-.00231714*%organic carbon*^{2}

SEb0=.03090338

iv) TX: $n_{e\,R}$ =-.29782991+.02102995*%organic carbon*-.00231714*%organic carbon*^{2}

SEb0=.03097630

There are significant differences between TX and the ON and AB intercepts (Figure 3.29). It is above 4% OC that the quadratic term really begins to have influence. If only the Group 1 soils are considered there are no MNR or TRT effects but the correlation coefficient is lower (Figure 3.30).

Similarly to the NCL, the greater the intercept ($e_{\alpha R}$) the steeper the slope $n_{e\,R}$ (Figure 3.31). There seems to be division between the CH and CL soils and MH and ML soils (and Group 1 and Group 2 soils) in terms of linearity of the relationship. A cutoff slope value of -.11 separates the non-significant and 3, 1-line remoulded shrinkage curves similar to the -.13 value separating plastic and non-plastic compression.

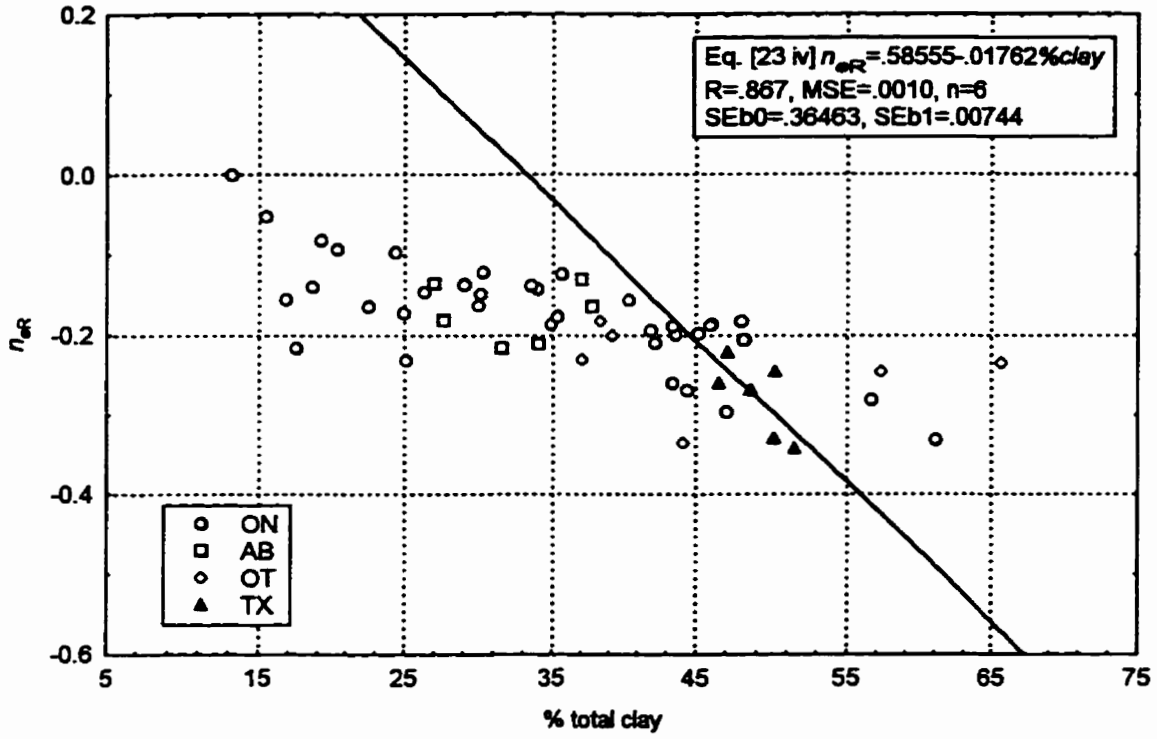

Figure 3.28. Covariance of $n_{e\,R}$ with % total clay.

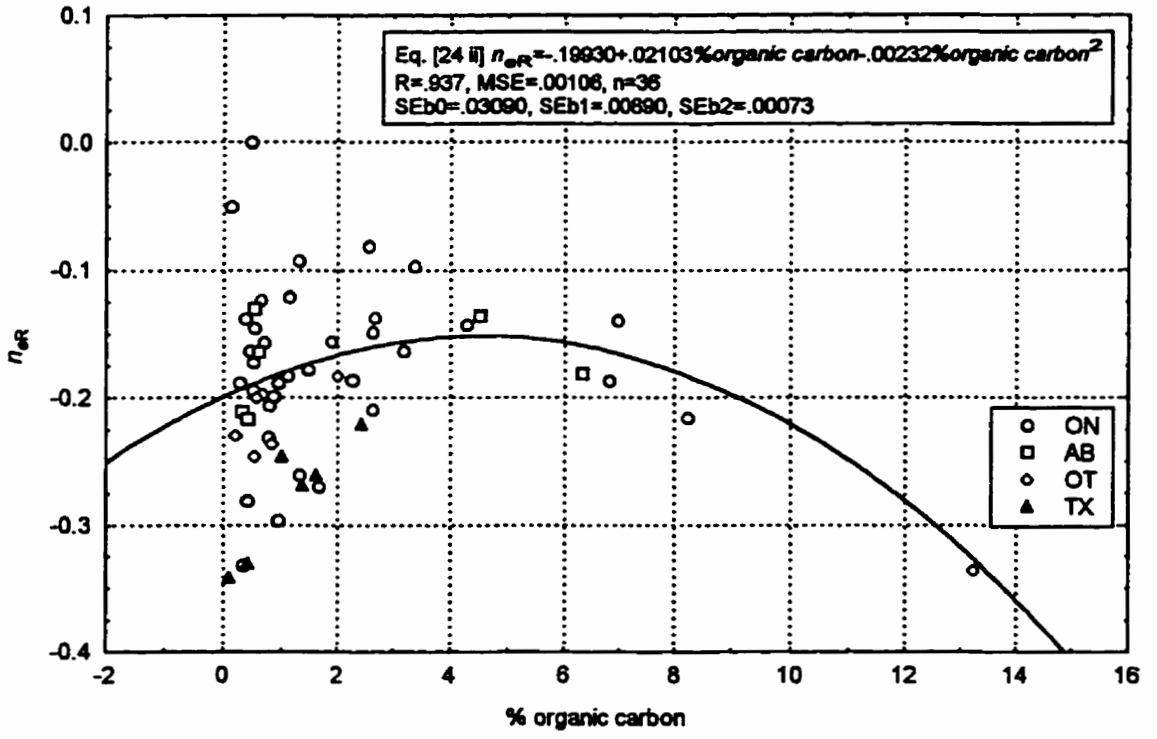

Figure 3.29. $n_{e\,R}$ versus log (% organic carbon)

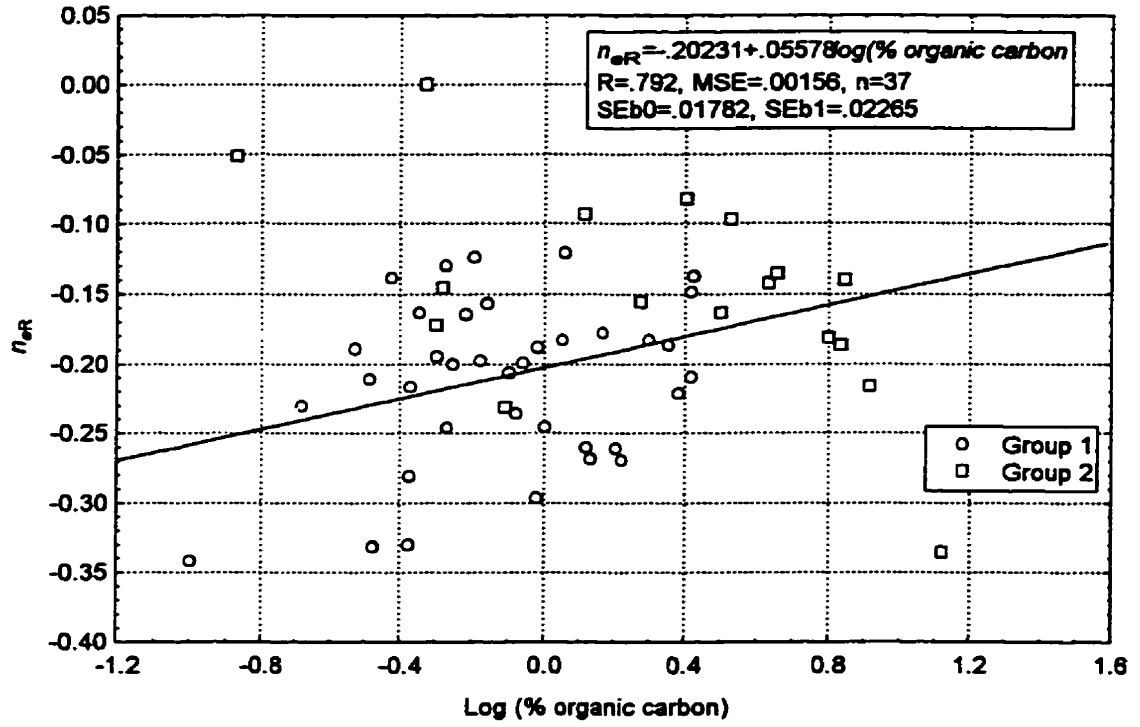

Figure 3.30. $n_{e\,R}$ **versus % organic carbon. Group 1 equation.**

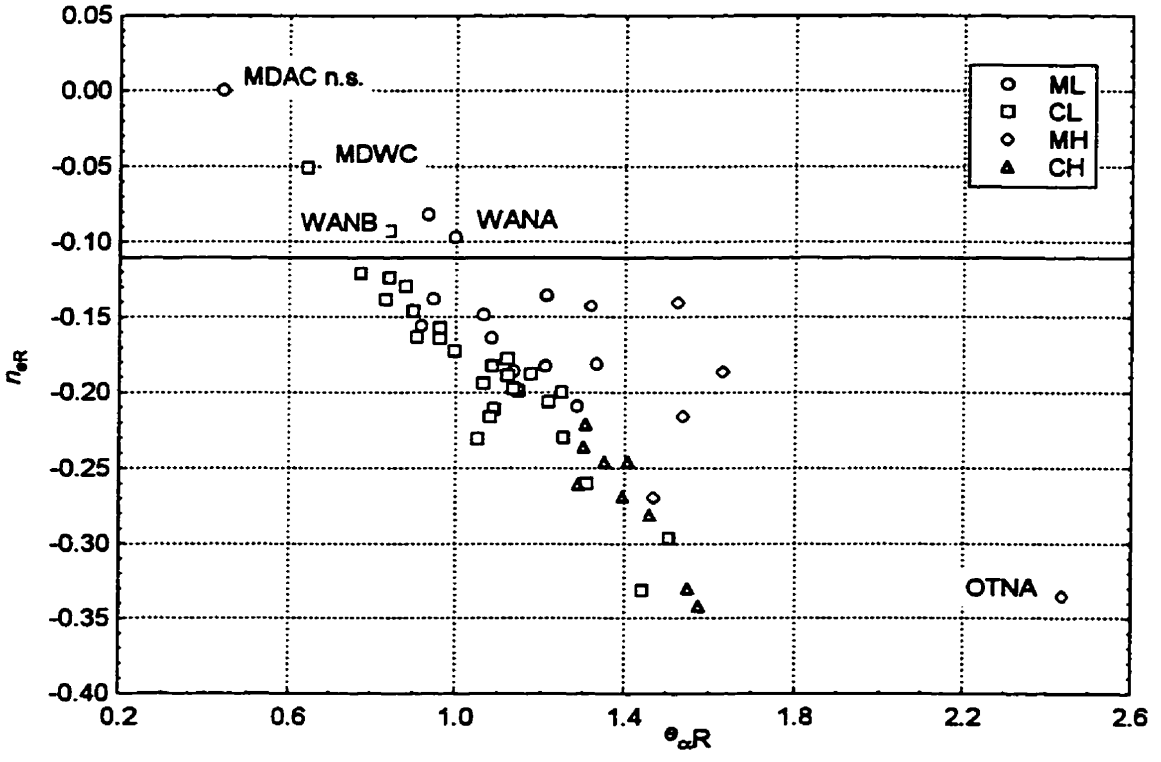

Figure 3.31. $n_{e\,R}$ **versus** e_{aR}

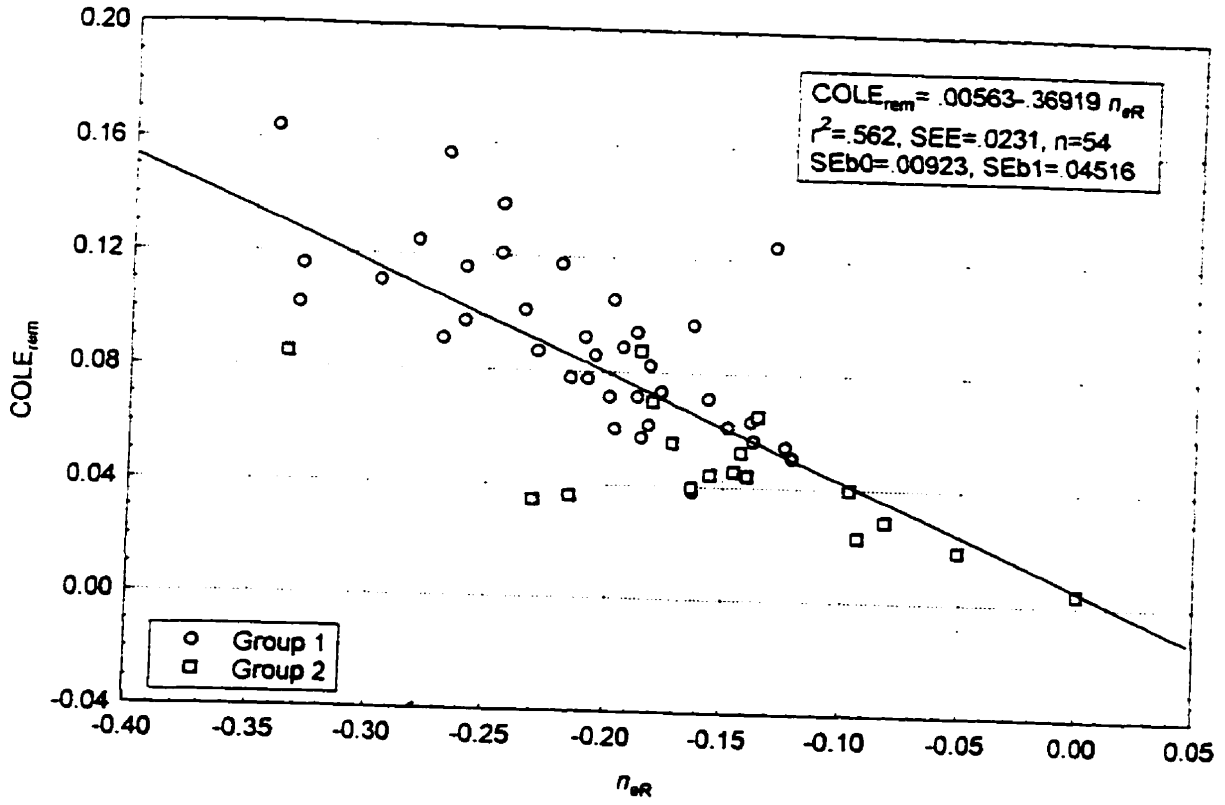

Figure 3.32. $COLE_{rem}$ versus n_{eR}

Also $COLE_{Rem}$ is related to the magnitude of n_{eR} whether the two groups of soils are looked at together or individually. The best r^2 is for all soils considered together (Figure 3.32).

3.3.1.3 Summary of remoulded shrinkage

Volume ratios (n_{vR}) less than 1 suggest that the air-entry point has already been passed or air-entry began as soon as tension was applied. Since the slope increases with clay content (and decreases from 1 as the sand content increases) it would seem that the silt and sand particles create a skeletal matrix causing the volume change to be less than the volume of water lost. Generally soils which shrink and swell include those with about 35 percent or more clay, and removal of pore water causes an equivalent contraction of the soil matrix (Newman and Thomasson, 1979). This is a higher clay content threshold than that proposed here (27%). Increasing clay content contributes to the ability of the porous matrix to deform linearly with changes in water content. Organic carbon similarly reduces the slope of the remoulded shrinkage line and increases the amount of air entry suggesting it behaves as a semi-rigid matrix, even in the remoulded state (Reeve and Hall, 1978). This may be due to hydrogen bonding or the hydrophobic nature of some organic materials or to the influence of organic matter on a wider and more stable pore size distribution. Thus the division of the data into 2 groups based on clay (27%) and organic carbon content (4%) thresholds seems to separate those soils which lose substantial amounts of water related to their organic matter content (Group 2) and those soils in which water loss and volume change are more closely related (Group 1) as there is plastic deformation of the void space due to clay content. Paz (1998) found the total amount of shrinkage from saturated to oven dry on 2-3 mm aggregates to be influenced by the organic matter content on coarse textured materials (<21% clay content). Slopes less negative than -0.70 for n_{vR} and -0.11 for n_{eR} separate residual, marginally plastic and non-significant straight line segment shrinkage characteristics from those segments with "normal"

shrinkage. Thus slope thresholds may be better definitions of plastic deformation than strictly "normal" shrinkage ($n_{vR} = 1$).

The n_{eR} is independent of the pivot point σ_{BR} while the n_{vR} slope is dependent on the moisture content at the shrinkage limit w_{AR}. This is partially due to the use of a straight line model. The n_{vR} was dependent on clay and organic carbon content for the Group 2 soils but independent of these soil properties for the Group 1 soils with n_{vR} tending towards 1. The n_{eR} systematically varied with clay, organic carbon content and $COLE_{rem}$ suggesting it may be better able to be predicted from soil survey data although there were significant MNR factors.

There are MNR effects when % total clay is the covariate for n_{eR} or $COLE_{rem}$ but not for % fine clay. This is related to the predominance of montmorillonite in the fine clay fraction and mica, kaolinite and feldspars in the coarse clay fraction of soils (Mitchell, 1976) and to the wider distribution of %fine clay in the different mineralogies. Thus the shrink swell potential in the remoulded continues to be related to the % fine clay (smectite) or surface area of colloidal particles.

3.3.2 Structured Shrinkage Data

3.3.2.1 Representation in $v(w)$ coordinates

Compared to the remoulded shrinkage data, the structured samples had poorer fits to the straight line segment model. McGarry (1988) achieved $r^2 > 99\%$ when fitting 3-line segment models to single clods but large between-clod variability of fitting indices (relative to between-block variability for a single soil type) in the order of 5-fold greater was found. Given this large variability between natural clods, the current methodology which used 5 different peds for each of 9 tensions, should better capture the variability of the horizon which was important when comparing different soil taxonomies, but some precision in fitting a "theoretical" model may be

lost. In addition, no standardization of the size of aggregate/clod sampled was done which could cause variation in the ratio of inter- to intra-aggregate porosities even between clods in a soil horizon. Inter-aggregate porosity was minimized because of the relatively small size of the clods.

The CV's were calculated for the structured void ratio at each tension and the sample size needed to estimate the mean within 10% was determined. There were 30 horizons for which a CV > 10% and 14 for which CV >15% occurred for one tension. There were only 13 horizons where a second tension had a CV> 10% for which greater than 5 samples should have been taken. These tended to be A horizons with high organic carbon and coarse textured, till subsoil horizons where there was the potential for particles > 2 mm in the peds. In a similar study which utilized the Monnier et al. (1973) kerosene technique, 15 replicates were used for 3 cm^3 samples (Bruand and Prost, 1987). Given this potential for variation, the r^2 values for the $v(w)$ plots were relatively high with mean = 0.817 (median = 0.905); 18 horizons had $r^2<0.800$, the majority of which were from Group 2 and had $I_P<15$ (Figure 3.33). The $e(\sigma')$ plot r^2 values were lower (mean 0.683, median 0.750) with 31 horizons having $r^2<0.8$. The AB and MD soils all had $e(\sigma')$ fits less than 0.800. The WANB horizon had a non-significant model for both $v(w)$ and $e(\sigma')$ plots.

For the structured $v(w)$ data there were 5 horizons for which the one line model fit best and no shrinkage limit was found (WANB, ABNA, MDAA, MDAC, HLAA); 43 fit a 2 line segment model and only 6 horizons (TXNA, TXNC, TXAA, TXAB, TXAC, OTNA) fit a 3 line model. The horizons with only 1 line were from the Group 2 soils. For 30 horizons the r_{vs} was not significantly different from zero. Twelve of the horizons had n_{vs} not significantly different than 1, and 2 horizons had n_{vs} significantly greater than 1 (OTNA, HLNA); n_{vs} >1 have been found by Lauritzen and Stewart (1941), Lauritzen (1948), McGarry (1988), and McGarry and Daniells (1987) for soils with large values of porosity at the onset of 'normal' shrinkage, where the air-filled pores shrink in proportion to the total clod shrinkage rather than remaining constant. Seven of

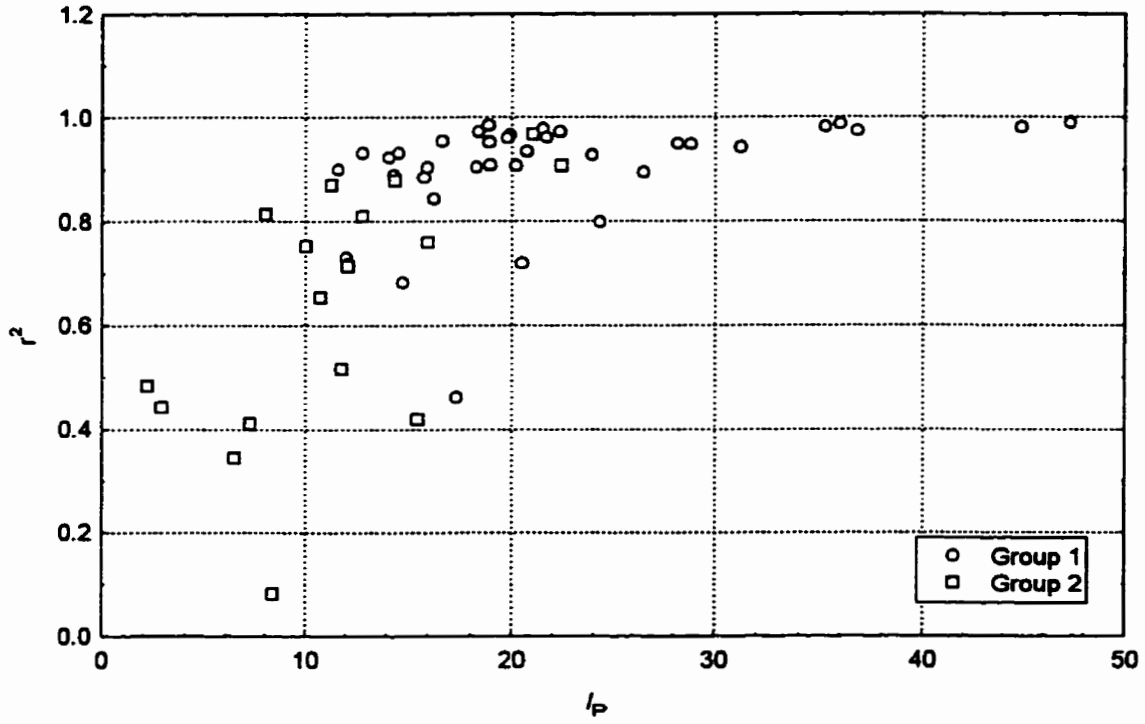

Figure 3.33. Coefficient of simple determination against I_P.

these 14 were from the Group 2 soils and 4 were from TX. Eight of these 14 horizons with "normal" shrinkage were A horizons which is opposite from the remoulded soils. Twenty horizons had n_{vS} <0.7 of which 10 were from the Group 2 soils. Lauritzen (1948) found the volume change ratio to deviate widely from the general trend, with deviation being more common in clods than blocks and in the more porous, higher organic matter soils.

For the structured $e(\sigma')$ data there were 22 horizons which fit a one-line model, 16 which fit a 2-line model and 11 which fit a 3-line model (OTAC, TXNA, TXNC, WAWB, WAWC, HLAB, HLWB, LBWB, LBWC, LBNB, LBNC). In addition there were 5 horizons for which there was a structural and normal shrinkage but no residual shrinkage (MDAA, TXAA, TXAB, TXAC, OTNC). Of the 27 horizons with a significant residual shrinkage segment, 22 had $r_{e\,S}$ values not significantly different than zero.

In terms of reliability of the model fits, the specific volume data will be more reliable since it is based on w and a straight line model for the shrinkage characteristic curve has been validated (McGarry and Malafant, 1987). The structured $e(\sigma')$ data is less reliable because of the natural variation indicated by the CV values at any particular tension; as well a straight line "shrinkage-stress" curve has not been used in the literature previously. Although not validated, the rationale for doing this was for comparison to compression data in Chapter 2 which fortuitously produced the more interesting results for remoulded and structured conditions. The variability of the number of line segments fit creates an unequal number of comparisons for several parameters (n<54).

The n_{vS} slope of the structured curve is not highly explained by clay (r^2=.194) although the correlation is significant for all data (not normal residuals) or the Groups 1 soils alone (p=.006) (Figure 3.34). There is also no relationship with organic carbon (Figure 3.35), so similarly the n_{vS} slope is independent of clay and organic carbon and should tend towards 1 as with n_{vR}. Similar to the remoulded soils, the n_{vS} increases as the w_{AS} increases, but this relationship disappears when

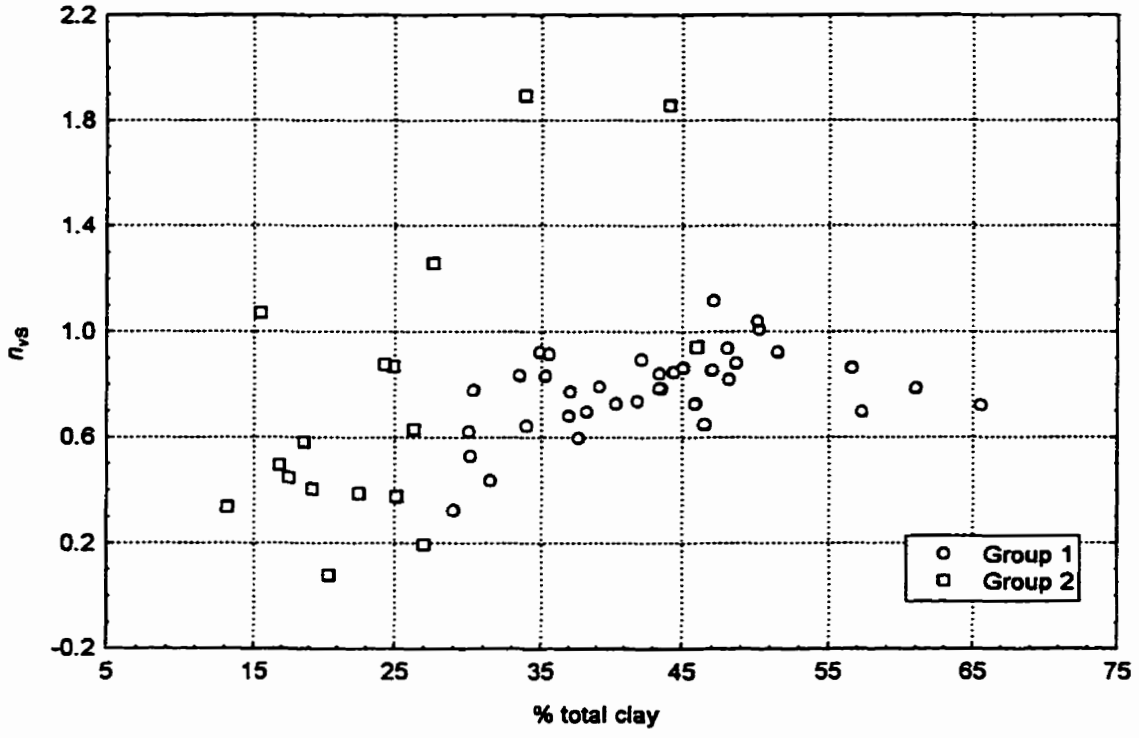

Figure 3.34. n_{vS} **versus clay content.**

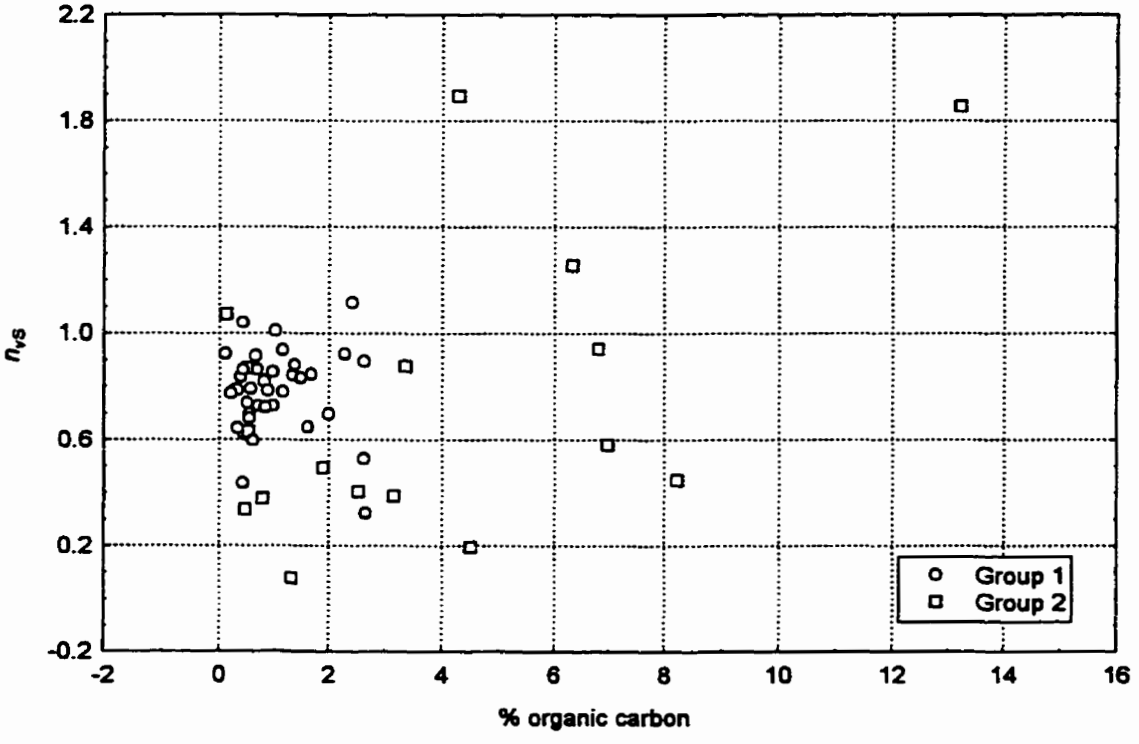

Figure 3.35. n_{vS} **versus organic carbon content.**

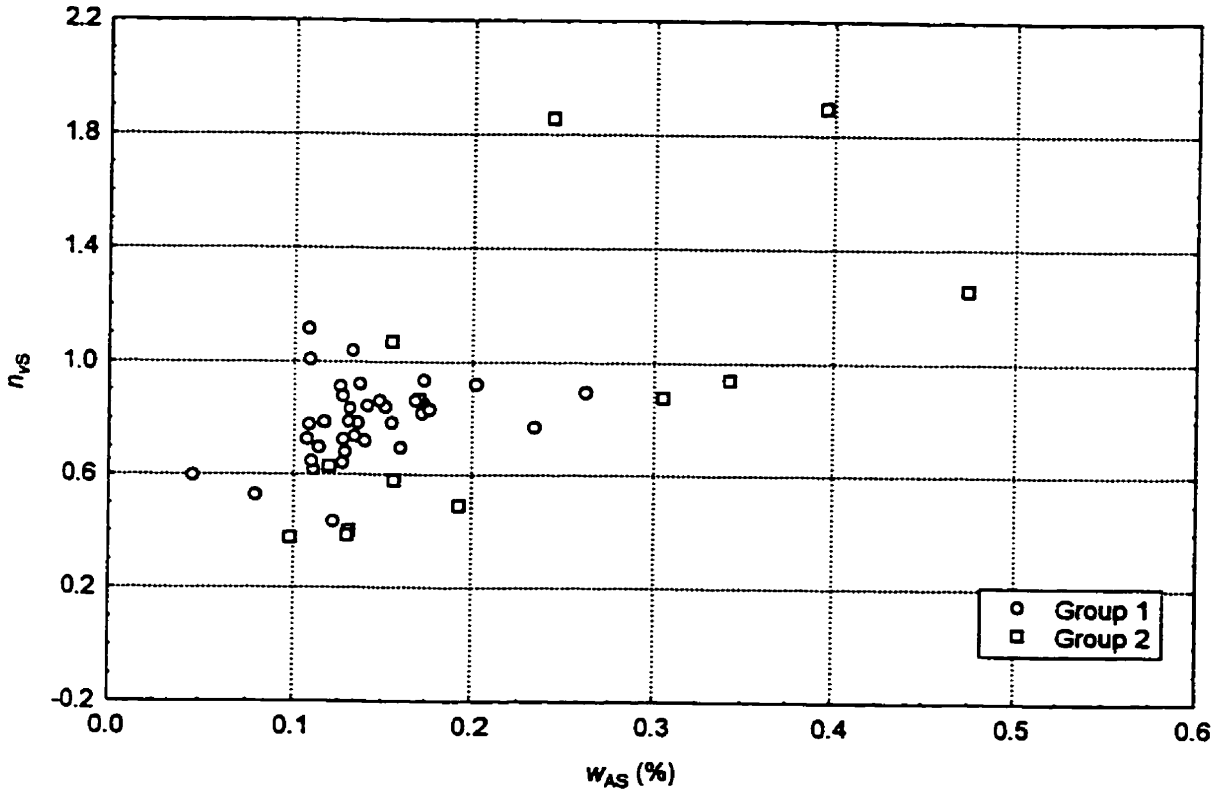

Figure 3.36. n_{VS} **versus** w_{AS}.

the Group 2 soils are removed (Figure 3.36). An ANCOVA revealed that there was a quadratic relationship between n_{vS} and total clay when the Group 1 soils were considered alone which was an improvement over the simple correlation.

n_{vS}=-1.060151+.0776313130%*clay*-.00077523%*clay*^{2} [25]

SEb0=.0454999, SEb1=.02019259, SEb2=.00021745, MSE=.01071696, R=.8332

The intercept v_{aS} is related to the organic carbon content similarly to v_{aR} (Figure 3.37). The residuals are normally distributed once the 1-line models and OTNA are removed.

The shrinkage limit in the structured condition w_{AS} is related to the plastic limit (w_P) and specific volume at the plastic limit (v_{wP}) but not as confidently as the remoulded shrinkage limit . There is no w_{AS} for 5 horizons and the residuals are normally distributed if OTNA is removed as well. The resulting relationship for v_{AS} and v_{wP} is 1:1 but encompasses 1 largely because of the large standard error of estimate (r^2=.635, SEE=.0513, b1=.8398, SEb1=.09385, n=48). The relationship between the water contents at the structural shrinkage limit and the plastic limit is not 1:1.

w_{AS} =-.0153+.6939(w_P /100) [26]

SEb0=.0325, SEb1=.1237, SEE=.0692, r^2=.4061

There is a 1:1 relationship between the specific volume at the maximum water content (v_B) and the specific volume of the w_L once the 3-line segment models with structural shrinkage are removed (r^2=.558, SEE=.0890, b1=.961, SEb1=.126, n=48). These 6 horizons all have the v_{wL} at higher values than v_B. There is a weak 1:1 relationship between the w_L and the w_{BS} which suggests that at saturation (-0.3kPa), the moisture content of a structured soil is below but could be close to the liquid limit (r^2 =.453, SEE=.0830, b1=.783, SEb1=.127, n=48).

The P_{BS} ranged from -.070 to.238 (max. = .136 if six 3-line segment models removed) indicating the various degrees of saturation and pore-size distributions in the structured soils so the

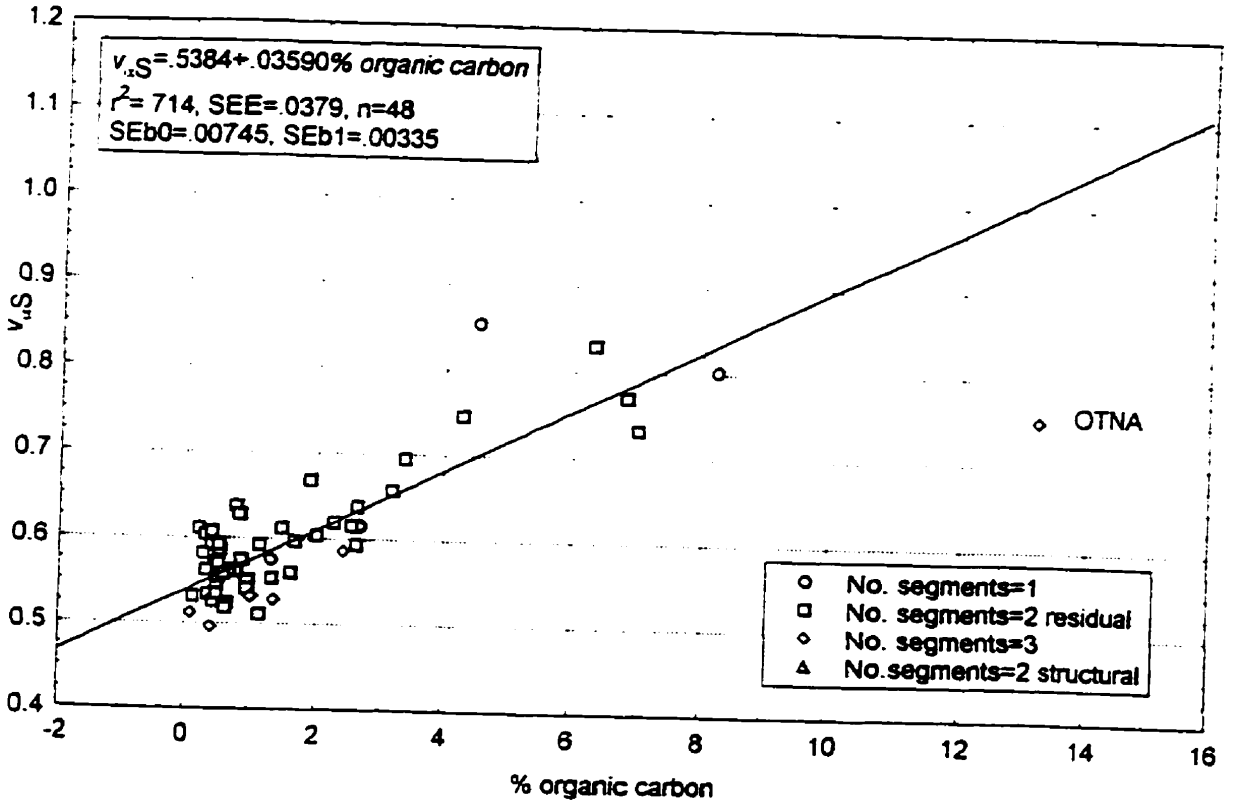

Figure 3.37. $v_{\alpha S}$ versus % organic carbon.

close association with the w_L is remarkable.

The P_{AS} did not have any significant factors when analyzed by ANOVA. When log %organic carbon is a covariate there is a significant oc*MNR term when MDNC is removed but only Ontario has a significant slope term and none of the intercepts are significantly different.

3.3.2.2 Representation in $e(\sigma')$ coordinates

The $e_{\alpha S}$ is related to the e_{wL} (Figure 3.38) but it is significantly less than a 1:1 relationship, although the intercept is not significantly different than zero. When broken down by groups, the Group 2 soils have a significant 1:1 relationship.

$e_{\alpha S}$=-.1614+1.072 e_{wL} [27]

SEb0=.1532, SEb1=.1282, SEE=.2100, r^2=.823, n=17

The Group 1 soils have a significant but poorly explained relationship.

$e_{\alpha S}$=.3426+3955 e_{wL} [28]

SEb0=.1118, SEb1=.0899, SEE=.1294, r^2=.356, n=37

This is likely because the Group 1 soils have no relationship between $e_{\alpha S}$ and organic carbon, while the Group 2 soils have a highly significant relationship because organic carbon influences and dominates their liquid limit and moisture holding capacity and subsequent void ratio on swelling (Figure 3.39).

An ANOVA revealed MNR, TRT and HOR factors for $e_{\alpha S}$ (Table 3.8). When an additional outlier (MDNC) is removed and the data is further transformed by subtracting -.4 then the MNR term disappears and TRT pdiff for Ag vs. Work also becomes significant. OT has the highest intercept, significant from all the others at a 10% significance level; the others are indistinguishable from each other. Also at a 10% level all the TRT are distinguished from each other, decreasing from Nat>Agr>Work. The A horizons are different from the B and C horizons.

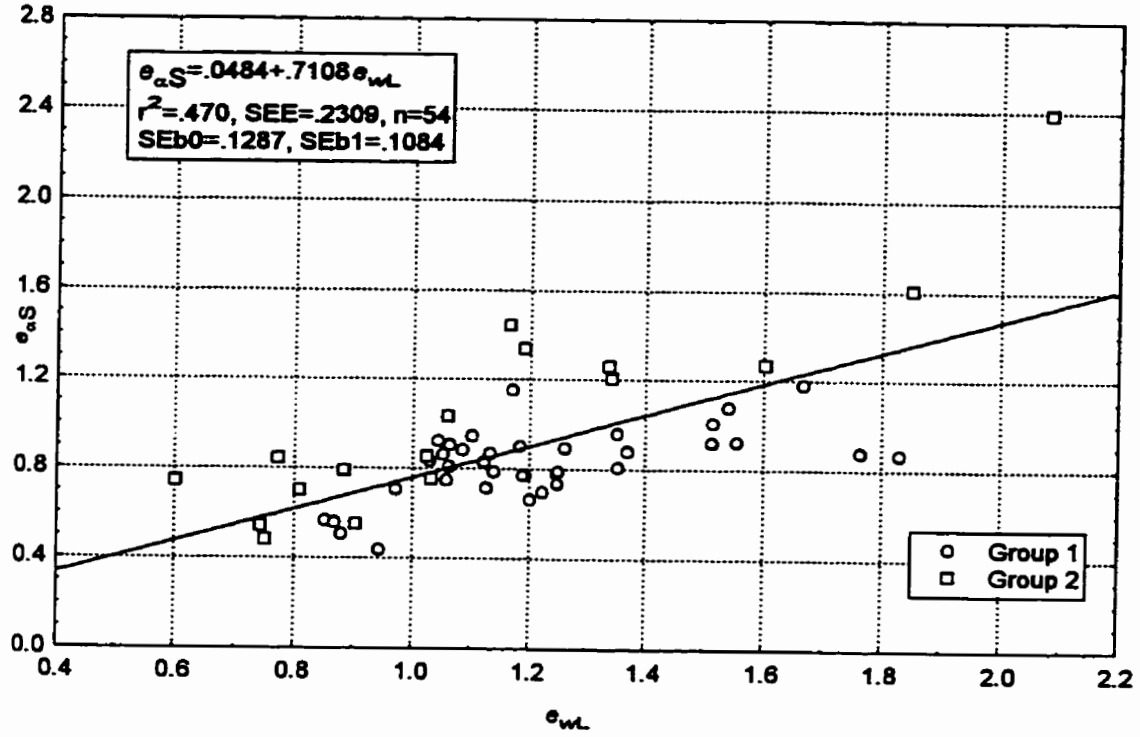

Figure 3.38. $e_{\alpha S}$ **related to the** e_{wL}

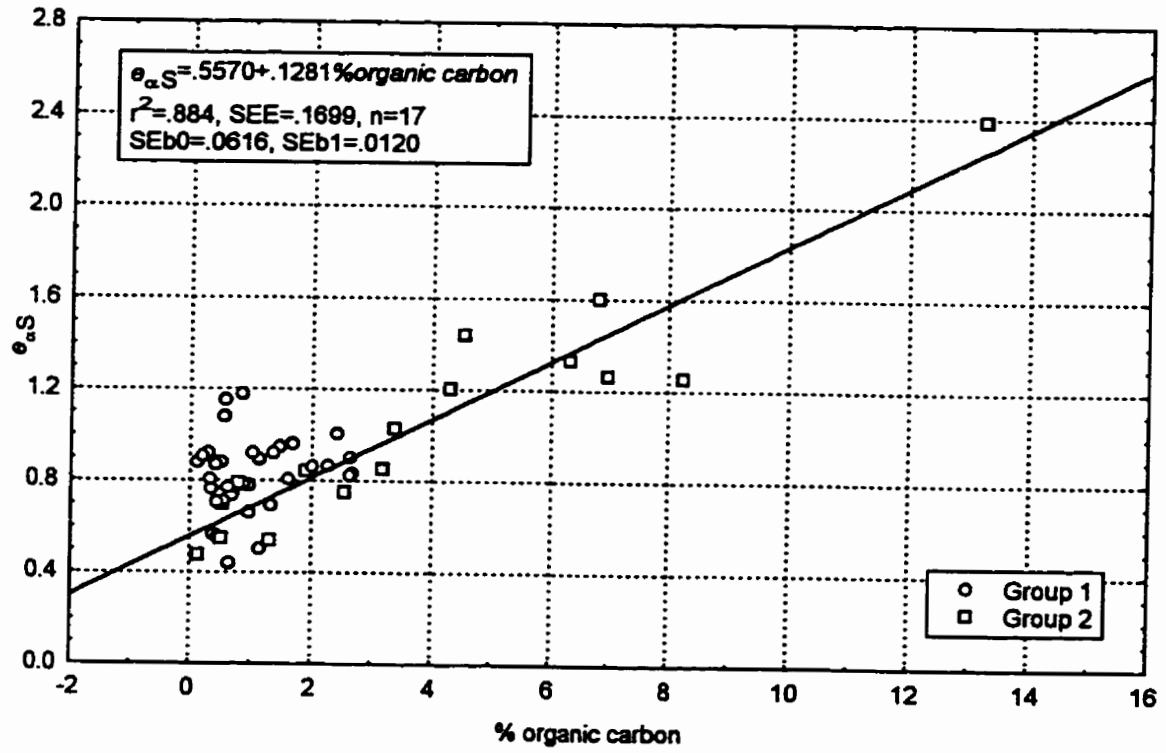

Figure 3.39. $e_{\alpha S}$ **versus % organic carbon.**

Table 3.8. LSmeans pdiff separation for ln($e_{\alpha s}$) MNR, TRT and HOR (WANB removed).

Factor	MNR					
	AB vs. ON	AB vs. OT	AB vs. TX	ON vs. OT.	ON vs. TX	OT vs. TX
pdiff	.5089	.0744	.8724	.0074*	.6445	.0550
	AB	ON	OT	TX		
LSmean	-.15059	-.22106	.10105	-.17203		
Back Transformed Mean	0.86020	0.80167	1.26196	0.67293		
Factor	TRT					
	Ag vs. Nat	Ag vs. Work	Nat vs. Work			
pdiff	.0609	.0625	.0017*			
	Agr	Nat	Work			
LSmean	-.10190	.01462	-.24470			
Back Transformed Mean	0.90312	1.01472	0.80921			
Factor	HOR					
	A. vs. B.	A vs. C	B vs. C			
pdiff	.0042*	1.94e-4*	.1613			
	A	B	C			
LSmean	.10863	-.16135	-.27927			
Back Transformed Mean	1.11476	0.85100	0.75634			

The intercept reflects both the initial void ratio of the sample and the ability of the sample to swell during saturation in the structured state which is influenced by previous stress history (Kuznetsova and Danilova, 1988).

The ANCOVA for $e_{\alpha s}$ with organic carbon has MNR, TRT and oc*TRT factors for n=52 horizons (WANB and MDNC removed) and a TRT factor for the Group 1 soils. In both cases the intercept for Workspace is less than the Agricultural or Natural intercepts. With the Group 1 soils there is a common slope, while for n=52 soils the Natural slope is significantly different from the Agricultural but not the Workspace slope. The ANCOVA model for Group 1 and OC is presented

(MSE=.00472979, R=.9541, n=37). [29]

i)Agr $e_{\alpha S}$ = 0.77287+.06282306*%organic carbon* SEb0=.03443694, SEb1=.03479518

ii)Nat $e_{\alpha S}$ = 0.79093+.06282306*%organic carbon* SEb0=.03443694, "

iii)Work $e_{\alpha S}$ =0.68742+.06282306*%organic carbon* SEb0=.06473515, "

The stress at the shrinkage limit (σ_{BS}) had significant MNR and TRT effects (Table 3.9).

Table 3.9. LSmeans pdiff separation for σ_{BS} - MNR and TRT (HLNA and MDNC removed).

Factor	MNR					
	AB vs. ON	AB vs. OT	AB vs. TX	ON vs. OT.	ON vs. TX	OT vs. TX
pdiff	.0237*	.0434*	.0028*	.8735	.0695	.1013
	AB	ON	OT	TX		
LSmean	2.25009959	4.13759376	4.04530157	5.13957109		
Factor	TRT					
	Ag vs. Nat	Ag vs. Work	Nat vs. Work			
pdiff	.3355	.0082*	.0589			
	Agr	Nat	Work			
LSmean	4.47808521	4.08762926	3.11371004			

HLNA and MDNC were removed because of their extremely low stresses at the shrinkage limit (<-2 kPa) while the average of the soils with shrinkage limits is -10000kPa (pF5). This forms a very steep shrinkage index from the intercept and not much change thereafter. MDNC also has a negative $COLE_{struc}$ value due to the low shrink-swell potential, formation of microcracks and/or variability of the clods being greater than the response to changes in stress. Surprisingly there was no TRT*HOR effect as there was for the remoulded condition, given that organic carbon influenced the σ_{BR} for the Natural horizons. A value of 3.176 represents 1.5 MPa or permanent wilting point. AB had significantly lower σ_{BS} than all the other mineralogies at the 5% level and TX is higher than all the other mineralogies at the 10% level. The AB soils were fairly coarse in texture and had low shrink-swell potential ($COLE_{struc}$ values) compared to the other clayey soils. The high shrink-swell potential of the TX soil probably allows it to continue to change in volume down to much lower tensions. The Workspace horizons have linear shrinkage stop at a higher

tension (above the wilting point) than the Agr or Nat horizons at the 10% level. This is likely due to the initial structural quality and particle alignment of these horizons which do not allow the aggregates to swell or contract significantly even at higher stresses. This comparison is a bit confounded because only the ON soils have a Workspace treatment. The parameter is not sensitive enough to distinguish between Agricultural and Natural conditions at any of the other sites.

Similar to the compression and remoulded data, the slope n_{eS} steepness is related to the initial void ratio e_{oS} (r^2=.267, SEE=.0335), but only if 3 outliers (OTNA, MDNC, HLNA) are removed (Figure 3.40). There is no relationship for the Group 2 soils alone. n_{eS} is slightly related to clay (r^2=.251, SEE=.0338) but not %organic carbon when the 3 outliers are removed. Justifying OTNA as an outlier is reasonable due to the high organic carbon content and the other outliers have been described. There were no significant MNR, TRT or HOR ANOVA factors for n_{eS}.

There are negative $COLE_{struc}$ values for MDNC and WAWA due to the low shrink-swell potential (lack of clay content), formation of microcracks and/or variability of the clods being greater than the response to changes in stress. WAWA and WANB have the two highest sand contents (51.8% and 45.1% respectively) of all the horizons. In addition there are 2 horizons, MDWC and WANB, with $COLE_{Struc}$ values < 0.005 of which WANB also had a non-significant 1-line model (Figure 3.41). MDWC only had an r^2 of only .1197 for the $e(\sigma')$ plot. MDAA and OTNA are the only MH horizons with $COLE_{Struc}$ values>0.06 and have the 2 highest organic carbon contents at 8.2 and 13.2%, respectively. These high organic carbon soils have high COLE values apparently not due to the same factors as the other soils. The rest of the MH horizons and the ML horizons all have $COLE_{struc}$ <0.06. Seven of the 9 CH horizons have $COLE_{Struc}$ >0.06.

$COLE_{Struc}$ is related to the steepness of the $n_{e\ s}$ when OTNA, HLNA and MDNC outliers are removed (Figure 3.42). There were significant relationships of $COLE_{Struc}$ with plasticity index,

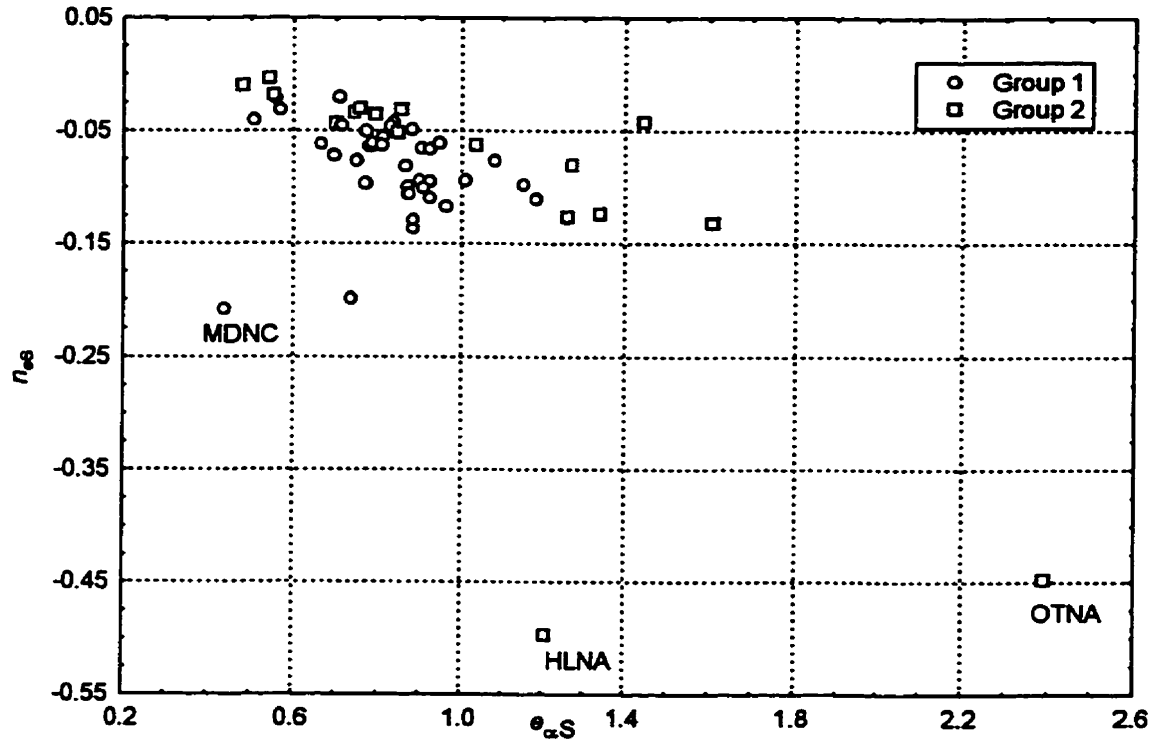

Figure 3.40. $n_{\sigma S}$ **versus** $e_{\sigma S}$.

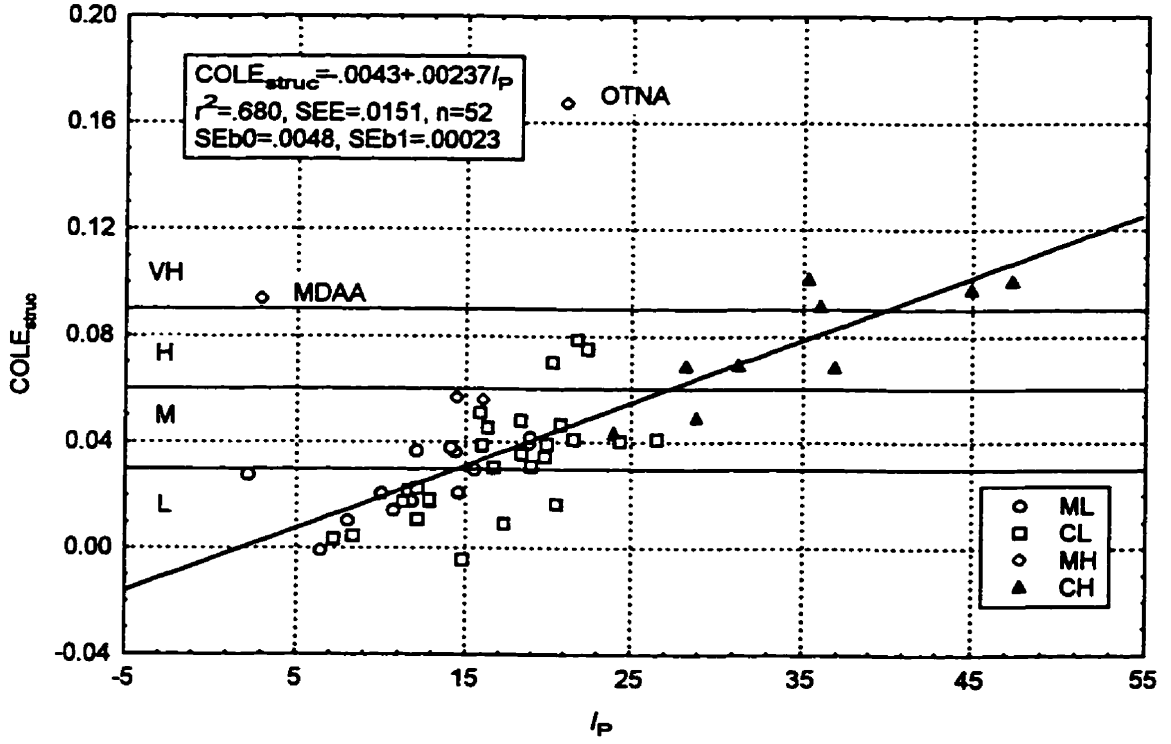

Figure 3.41. $COLE_{struc}$ **versus** I_P.

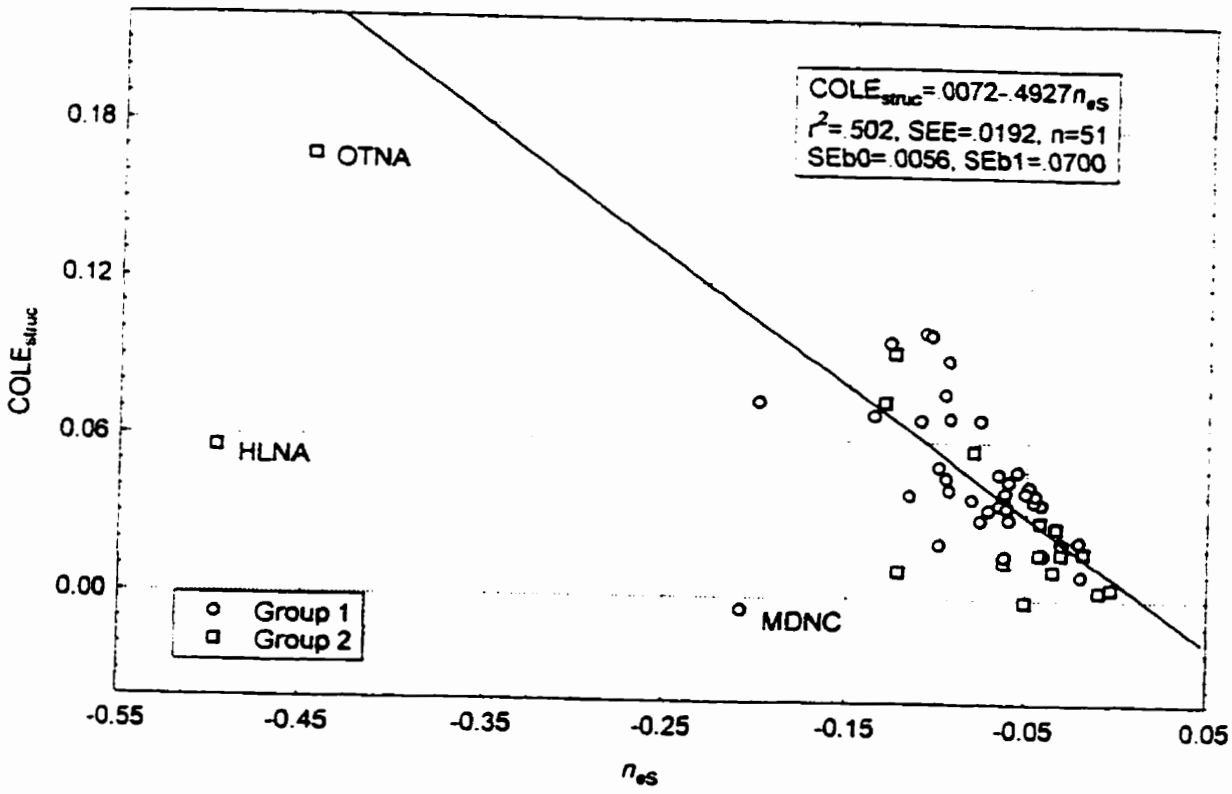

Figure 3.42. $COLE_{struc}$ versus n_{eS}.

clay and fine clay; none of these had normally distributed residuals unless 2 outliers, MDAA and OTNA were removed. The best relationship was with plasticity index (Figure 3.41). Forward stepwise regression produced only one variable, the void ratio at the w_L to give the best relationship for all horizons.

$COLE_{Struc}$=-.06147+.008828e_{wL} [30]

SEb0=.00987, SEb1=.00803, F=120.7, SEE=.0177, r^2=.699, n=54.

If MDAA and OTNA were removed a different model resulted which explained more variability.

$COLE_{Struc}$=-.0307+.00245 I_p +.0372 e_{wP} [31]

SEb0=.00944, SEb1=.000213, SEb2=.0117, SEE=.0139, r^2=.735, n=52.

The e_{wP} was highly correlated (R=.904, b1=1.86, SEb1=.122) to the initial void ratio for the core samples e_0 and the intercepts for the structured $e(\sigma')$ plots ($e_{\alpha S}$, R=.824, b1=1.17, SEE=.111); neither intercept is significantly different from 0. Equation [31] essentially combines the plasticity/compressibility and the initial structural state to predict the structured shrinkage behavior. The parameter for I_P is not significantly different from that for $COLE_{rem}$ (Eq.[18]).

The ANOVA with $COLE_{struc}$ revealed a significant mineralogy factor once 5 outliers were removed, with all MNR being different from each other at the 10% level except OT and TX (Table 3.10).

Table 3.10. LSmeans pdiff separation for ln($COLE_{struc}$) MNR (WANB, MDWC, MDNC, OTNA, WAWA removed).

Factor	MNR					
	AB vs. ON	AB vs. OT	AB vs. TX	ON vs. OT.	ON vs. TX	OT vs. TX
pdiff	0.0844	0.0099*	0.0010*	0.0781	0.0052*	0.3473
	AB	ON	OT	TX		
LSmean	-3.89502	-3.39823	-2.85998	-2.51985		
Back Transformed Mean	0.02034	0.033432	0.057270	0.080472		

Covariate analysis was difficult with $COLE_{struc}$ and % clay and % fine clay content as the

normality of residuals and the outliers kept varying with different transformations (Figure 3.43 and Figure 3.44). Attempts were made to remove several outlier groups. The best two models were:

1. TRT, clay*TRT, clay*clay*TRT - WAWA, MDNC and MDAB removed [32]

(MSE=.104106, R=.9642, n=51)

i) Agr: $\ln(COLE_{struc})$=-3.91534-.0052368*%clay*+.000576*%clay*^{2}

SEb0=1.06258, SEb1=.060385, SEb2=.0008139

ii) Nat: $\ln(COLE_{struc})$=-6.85876+.161629*%clay*-.0016126*%clay*^{2}

SEb0=1.0125, SEb1=.050538, SEb2=.000608

iii) Work: $\ln(COLE_{struc})$=-9.715557+.297215*%clay*-.0031168*%clay*^{2}

SEb0=1.02068, SEb1=.06355, SEb2=.0007909

The Natural and Workspace equations were concurrent (i.e. not significantly different, p=.3112).

2. MNR, clay*TRT terms significant at p=0.06 , Group 1 soils only [33]

(MSE=.03535001, R=.9709, n=37)

AB: i) Agr $\ln(COLE_{struc})$=-4.49309+.05097117*%fine clay* SEb1=.01519344

ii) Nat $\ln(COLE_{struc})$=-4.587813 +.05252179*%fine clay* SEb1=.01962477

ON: iii) Agr $\ln(COLE_{struc})$=-3.955318 + as for Agr

iv) Nat $\ln(COLE_{struc})$=-4.05004667 +as for Nat

v) Work $\ln(COLE_{struc})$=-4.6784819+.10946985*%fine clay* SEb1=.02289298

OT: vi) Agr lnCOLEstruc=-3.63199 + as for Agr

vii) Nat $\ln(COLE_{struc})$=-3.72669094 + as for Nat

TX: viii) Agr $\ln(COLE_{struc})$=-3.8014+ as for Agr

ix) Nat $\ln(COLE_{struc})$=-3.89612523 + as for Nat

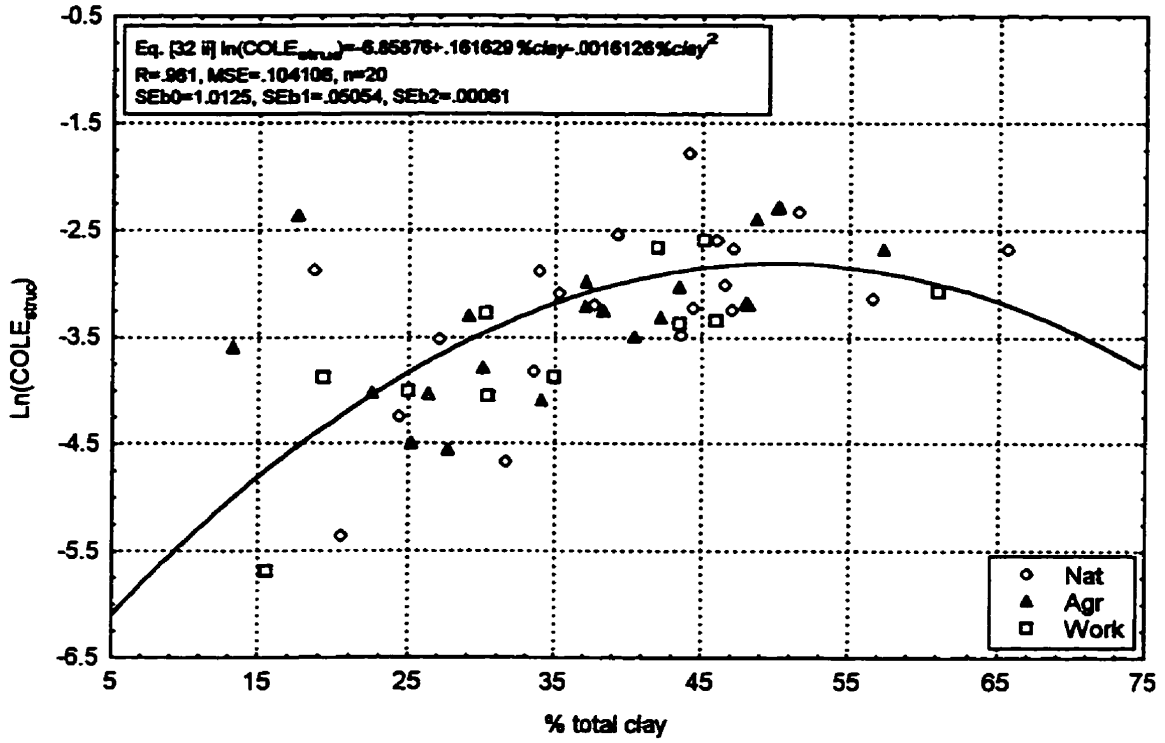

Figure 3.43. COLE$_{struc}$ versus % clay.

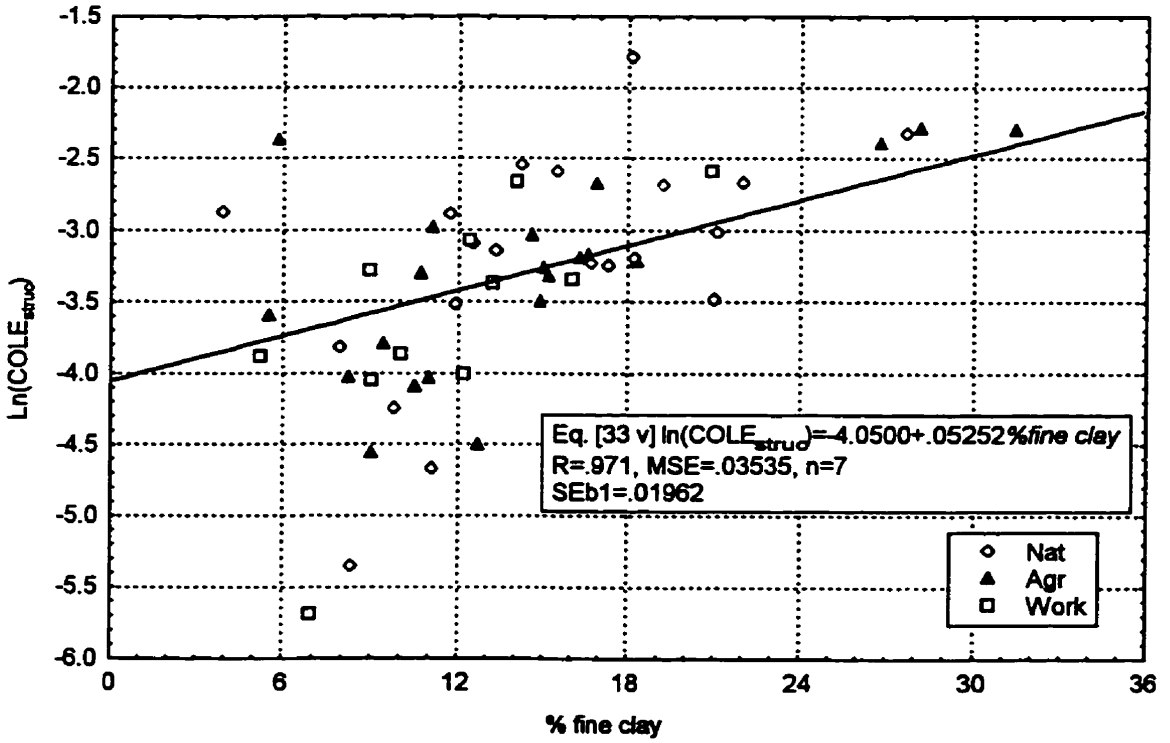

Figure 3.44. COLE$_{struc}$ versus % fine clay.

The AB mineralogy was significantly lower in the intercept for the $COLE_{struc}$ relationship than all the other mineralogies as was the case for the ANOVA. The clay*TRT factor revealed a steeper relationship for the Workspace horizons and %fine clay than either Agricultural (p=.0235)or Natural (p=.0359) which were not significantly different (p=.9128). This may be a result of the smaller and less stable pores in the degraded clay textured soils which allowed greater swelling and shrinkage to occur because of greater water uptake and rearrangement of aggregates. If the clay*TRT factor was considered not significant at the 5% level, the MNR factor remained significant with a common slope of .06395012 (SEb1=.01510296); the AB horizons had a significantly lower intercept than all other horizons and the OT horizons had a significantly higher intercept. The smectitic mineralogies also had significantly lower intercepts than the other mineralogies (p=.0335). This is curious because it means the non-smectite soils had higher $COLE_{struc}$ values at a given clay content than the smectitic soils; this may be due to the larger amount of organic matter in these soil or incomplete swelling of the smectitic soils in the structured state.

There are existing predictive equations for $COLE_{Struc}$ from Dasog et al. (1988) and De Jong et al. (1992). The residuals were not normally distributed with all 54 horizons. Two different sets of outliers were employed; i) MDAA and OTNA, n=52,and ii) 1-line segment $v(w)$ models (ABNA, WANB, MDAC, MDAA, HLAA)+negative $COLE_{Struc}$ (MDNC, WAWA) +OTNA, n=46. The basic relationships did not depend on which set of outliers was removed.

A 1:1 relationship resulted with the De Jong et al. (1992) equation based on %total clay but it had the highest SEE (0.020) and lowest r^2 (=0.42). The best "fit" was with the De Jong et al. (1992) equation based on the I_P, having the highest r^2 (=0.70) and lowest SEE (=0.014) but this was not a 1:1 relationship with the intercept not significant but the slope significantly less than 1 (b1=.825, SEb1=0.0816). This was the same equation which had a slope of 1 with the $COLE_{rem}$

measurements. The Dasog et al. (1988) equation based on the % fine clay resulted in a slope not significantly different than 1 but there was a positive intercept of 0.03 which essentially underestimates the shrinkage potential by an entire shrinkage potential class. This is not surprising given that their structured samples were 10 times the mass of the structured clods here, which may have represented larger and more stable pores or may have been restricted in shrinkage by the Saran coating (Tunney, 1970).

3.3.2.3 Summary of structured shrinkage

Structural shrinkage was measured in very few horizons. It was measured only in the high shrink-swell potential soils from TX and OTNA. Therefore the possibility to use structural shrinkage stage parameters to assess physical soil quality in soils of relatively low clay content or low shrink-swell mineralogies does not seem likely at least using this methodology. Similarly, Paz (1998) found that alternative indices from shrinkage curves (i.e. slopes or change points) were not as useful as simply specific volume as indicators of cultivation effects on coarse textured soils (<21% clay content).

Opposite from the remoulded samples, "normal" shrinkage tended to occur in the Group 2 soils and A horizons for the structured samples; the majority of the Group 2 soils still had n_{vs}<0.7. Structured "normal" shrinkage also occurred for 4 TX horizons. Four A horizons also had larger $COLE_{struc}$ than $COLE_{rem}$ values. The structured A horizons having significant linear shrinkage is similar to the results of Wires et al. (1987) who found the Ap of a Brookston soil to have the widest range of density variations (1.26-1.63) associated with the larger volume change, while the Bg horizon had the highest density in situ and showed the least range (1.52-1.63). The Ap horizon was the only horizon which followed an expected pattern, in that three phases of shrinkage could be identified (Wires et al., 1987). This may be because many of these A horizons were normally

consolidated and could have substantial swelling while, many of the B and C horizons were overconsolidated and possibly past the critical threshold of compaction where spontaneous swelling is restricted (Kuznetsova and Davilova, 1988).

The only structured shrinkage characteristic parameters able to distinguish any TRT effects were $e_{\alpha S}$ and σ_{BS} for the e (σ') plots. The AB and Work horizons had the shrinkage limit earlier (at lower stresses) than the other horizons and the $e_{\alpha S}$ was highest for the OT, Nat and A horizons so that not one single parameter distinguishes structural states well.

Existing $COLE_{struc}$ equations using %total clay or % fine clay for Saskatchewan soils had significant relationships with this data; a 1:1 relationship and a slope of 1, respectively. The existence of negative $COLE_{struc}$ values highlights the variability in structured samples, especially of low plasticity, which can mask the potential for volume change when only measured at 2 tensions. $COLE_{struc}$ was able to distinguish some treatment differences when % total clay (n=54) or %fine clay (Group 1) are used as covariates.

3.3.3 Comparison of Relative (Remoulded vs. Structured) Shrinkage Parameters

3.3.3.1 Specific volume(grav. moisture content) $v(w)$ coordinates

Significant correlations ($p<0.05$) for v_α (R=0.8283), w_B (0.5872), v_A (0.7945), v_B (0.7751) and P_A (0.4681) exist between the remoulded and structured conditions. The relationship for v_α does not have normally distributed residuals. The relationship for the Group 1 soils is shown in Figure 3.45. There are 7 horizons where the $v_{\alpha R}$ is larger than $v_{\alpha S}$ (OTNA, MDNA, MDAA, MDWA, MDWB, LBWB, LBAB) but essentially the oven dry specific volume is larger for the structured than the remoulded samples. This is similar to the results of Lauritzen (1948).

There is a MNR*TRT*HOR interaction term for the ($v_{\alpha R}$ - $v_{\alpha S}$) variable which is reduced to a TRT term significant at 10% when WANB and OTNA are removed (Table 3.11).

Table 3.11. LSmeans pdiff separation for ($v_{\alpha R}$ - $v_{\alpha S}$) TRT (WANB and OTNA removed).

Factor	TRT		
	Ag vs. Nat	Ag vs. Work	Nat vs. Work
pdiff	0.6490	0.0781	0.0389*
	Agr	Nat	Work
LSmean	-0.04625024	-0.04925963	-0.03187775

These mean values show the structured intercept is above the remoulded intercepts and that the Natural (p=5%) and Agricultural (p=10%) intercepts are significantly higher above the remoulded oven-dry specific volume than the workspace horizons. When log%organic carbon is a covariate, there are mineralogical differences and no treatment differences with WANB removed.

There is a 1:1 relationship between the specific volume at the shrinkage limit v_A for the remoulded and structured samples but the residuals are not normally distributed. The relationship for Group 1 soils is not 1:1 and is shown in Figure 3.46. There are horizons where either the remoulded or the structured sample's specific volumes are larger than the other. The ANOVA for (v_{AR} - v_{AS}) with HLNA and the eight 1-line segment models removed has significant MNR (p=.0124) and TRT (p=.0714) factors (Table 3.12). The specific volume at the shrinkage limit is larger for Alberta than ON and the difference is larger for the Agr than Workspace or Nat (p<.10) horizons. The similarity in difference between the Workspace and Natural condition may be because the Natural v_{AR} are larger due to more organic matter content raising v_{AR} closer to the structured values while the structured Workspace condition is so degraded and lacks a significant stable pore structure that the structured shrinkage limit is lowered towards the remoulded.

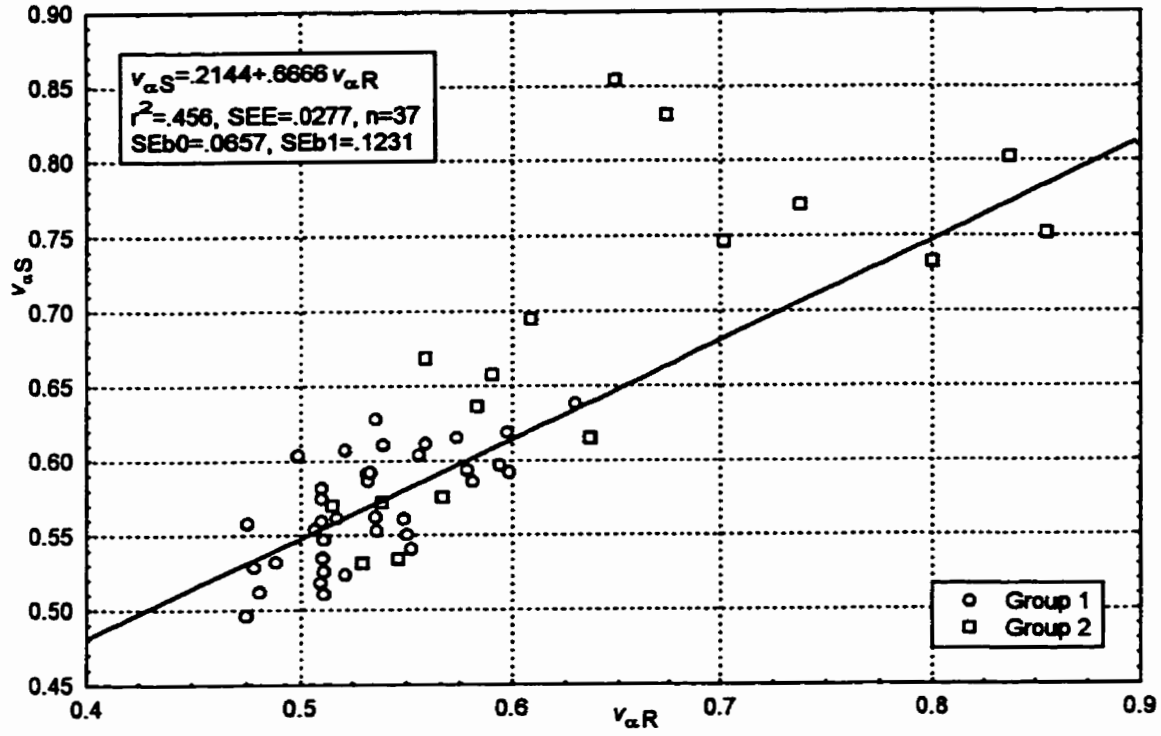

Figure 3.45. $v_{\alpha S}$ **versus** $v_{\alpha R}$.

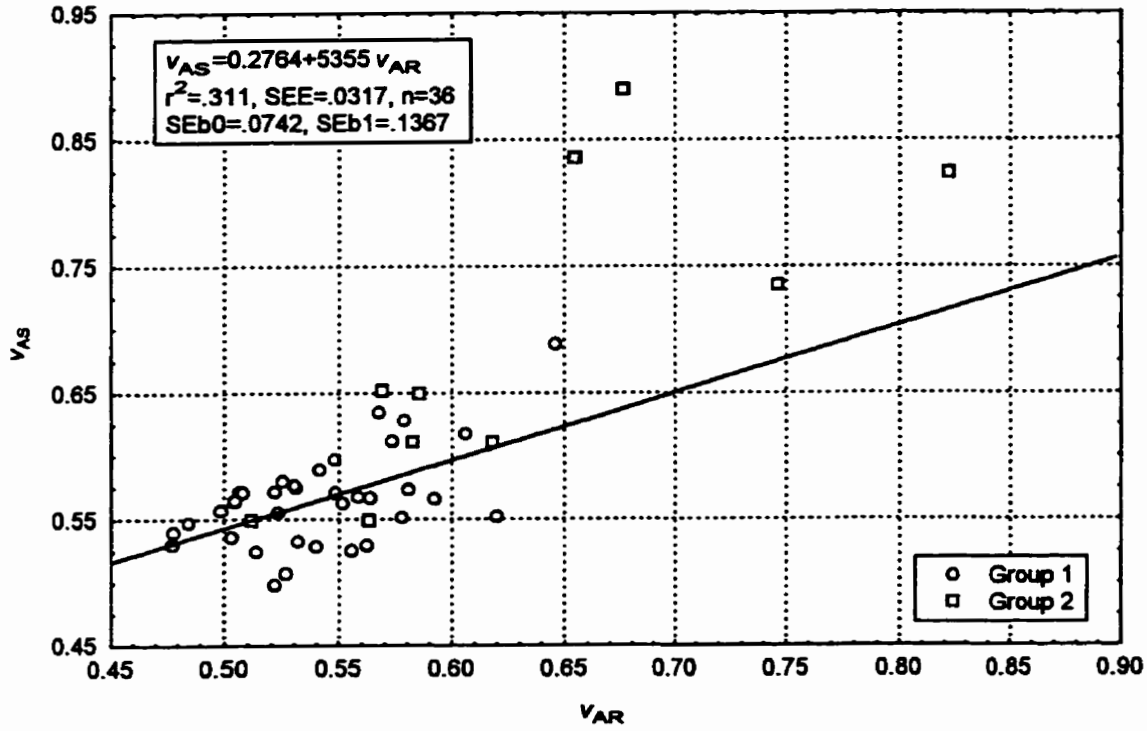

Figure 3.46. v_{AR} **versus** v_{AS}.

Table 3.12. LSmeans pdiff separation for (v_{AR} - v_{AS}) - MNR and TRT (HLNA and 1 line segment models removed).

Factor	MNR					
	AB vs. ON	AB vs. OT	AB vs. TX	ON vs. OT.	ON vs. TX	OT vs. TX
pdiff	0.0021*	0.0712	0.1729	0.2242	0.0627	0.5921
	AB	ON	OT	TX		
LSmean	-0.09263	-0.01103	-0.03896	-0.05381		
Factor	TRT					
	Ag vs. Nat	Ag vs. Work	Nat vs. Work			
pdiff	0.0739	0.0407*	0.5609			
	Agr	Nat	Work			
LSmean	-0.06315	-0.04547	-0.03869			

The P_A is more clear in that only 6 horizons have an air-filled specific volume greater in the remoulded condition than in the structured (MDNA, MDWA, OTNB, MDWB, ABAA, HLNA). There are 8 horizons not included because of a lack of shrinkage limit in either the remoulded or structured state (both for WANB).

There is a 1:1 relationship between the w_B when all horizons are considered together (r^2=.345, SEE=.0925, n=54). There is no relationship at all when only the Group 1 soils are considered which may be due to some soils having a third line segment up to higher moisture contents or the ability of these soils to swell and absorb more water in the structured condition. This makes sense since the two states had two different starting tensions and the high organic matter, low clay content soils must behave differently under tension than the Group 1 soils.

Similarly there is a 1:1 relationship for the v_B when all horizons are considered together (r^2=.640, SEE=.0835, n=54) but not when the Group 2 soils are removed.

There was no relationship between the remoulded and structured w_A or n_v slopes with being about 16 horizons which had larger structured values than remoulded values. Therefore, to compare the shape of the remoulded and structured characteristic curves, a point on the remoulded line was found using the change point at the shrinkage limit (w_{AR}) substituted into the structured

line equation (v_{AS}*). The remoulded value was chosen as the reference since the r^2 was better and assumed to be the baseline from which to compare the structure of the soil. There was a significant 1:1 relationship between v_{ARS} and v_{ASS}* (r^2=.812, SEE=.0401) but the residuals were not normally distributed. When the Group 1 soils alone were analyzed the intercept became positive and the slope was still not significantly different than 1.

v_{AS}* =.1392+.8342v_{AR} [34]

SEb0=.0450, SEb1=.08264, SEE=.0198, r^2=.7443, F=101.9, n=37

This means that at the remoulded shrinkage limit (w_{ARS}) the specific volume of the structured soil is consistently above the remoulded value by 0.14 for the Group 1 soils.

The difference in the points (v_{AR} -v_{AS}*) and the difference in slopes (n_{vR}-n_{vS}) between the remoulded and structured conditions were plotted against each other. Figure 3.47 showed that the majority of horizons (n=37, quadrant II) had the remoulded n_{vR} steeper than the n_{vS} and the structured specific volume above the remoulded specific volume. Observation of the shrinkage graphs showed most shrinkage curves to be divergent for these soils. There were 3 horizons in quadrant IV which had the remoulded specific volume above the structured at the shrinkage limit. There were 10 horizons which had the structured slope steeper than the remoulded slope and showed a convergent behavior. An ANOVA for the relative variable (n_{vR}-n_{vS}) could not be conducted because the residuals never fit a normal distribution.

The (w_{AR}- w_{AS}) relative variable had a MNR*HOR interaction but it was confounded because one of the significant horizons AB A was represented by only 1 horizon because ABNA did not have a structured shrinkage limit. There were only 3 MNR*HOR combinations which had differences significantly different than 0; LSmean values were AB A =-.369, ON B =+.0368 and ON C =+.0473. AB A was significantly different than all other horizons and ON B and ON C were different than ON A.

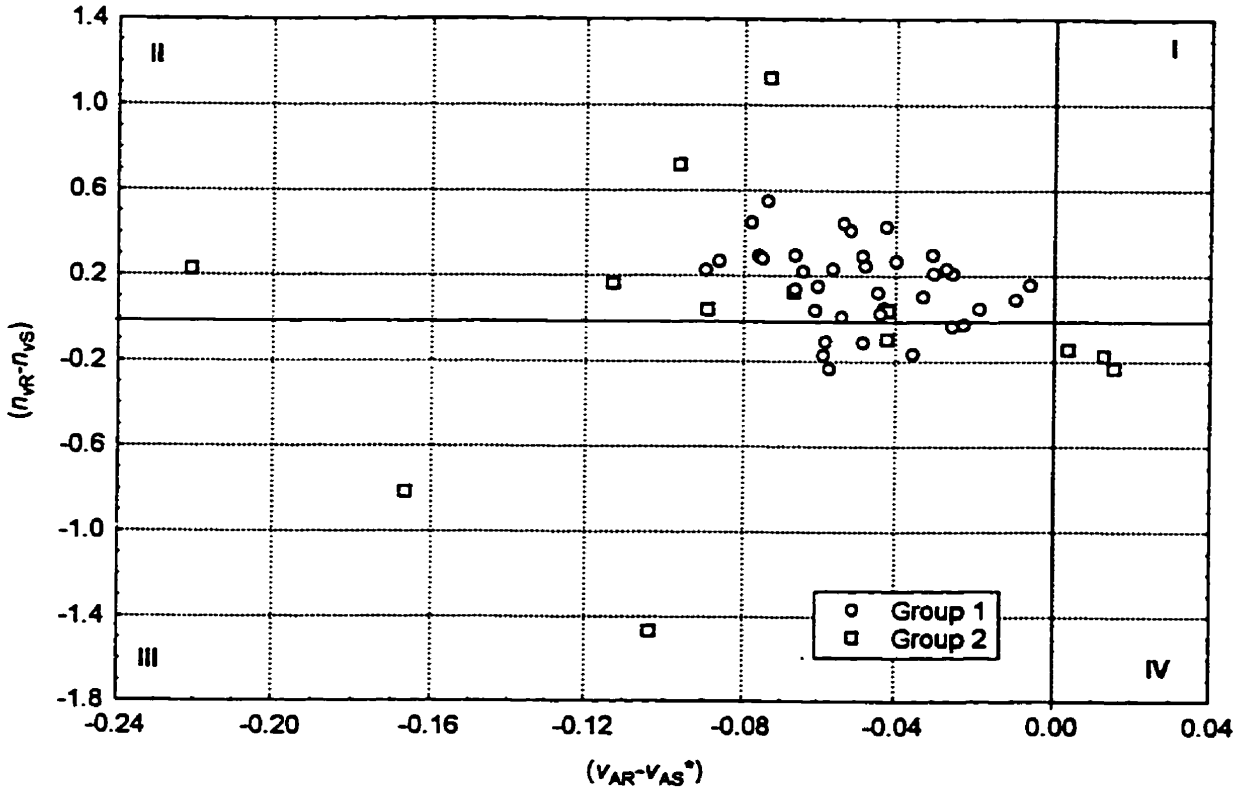

Figure 3.47. $(n_{vR}-n_{vS})$ **versus** $(v_{AR}-v_{AS}^*)$.

3.3.3.2 Void ratio (effective stress) $e(\sigma')$ coordinates

Significant correlations ($p<.05$) between the remoulded and structured parameters occurred for e_α (R=.766), n_s (.4525), e_B (.7249), and e_C (.5296).

The relationships between the void ratio intercepts in the remoulded and structured conditions is shown in Figure 3.48. The relationship is considerably different for the 2 groups of soil. Group 2 has a significant 1:1 relationship ($r^2=.843$, SEE=.1987, n=17) with 4 horizons having larger void ratios at -1kPa in the structured than the remoulded condition. Less variation is described for the Group 1 soils ($p=.00011$, $r^2=.3514$, SEE=.1299) and the remoulded intercept is always larger than the structured intercept.

The ANOVA for ($e_{\alpha R}$- $e_{\alpha S}$) revealed a MNR and TRT*HOR interaction when the marginally plastic soil MDAC was removed. The interaction is illustrated in Figure 3.49. This response is very similar to that for the (e^*_{1kPa}-e_0) compression variable except that there are no negative means, i.e. the structured intercept always tends to be below the remoulded intercept. The Natural A horizons are different from every horizon except Workspace A. Workspace A is different from all the C horizons and Workspace B. Agr B and Nat B are different from Nat C. The Natural A difference is not significantly different from 0 ($p=.2568$). The MNR factor rigidly shifts the interaction for the different mineralogies (Table 3.13). Similar to the compression data, the TX mineralogy is different from all the others ($p<.001$) in that it has the greatest displacement at the intercept between the remoulded and structured condition and that the TRT*HOR graph must be shifted by average .305 to achieve the comparison for TX.

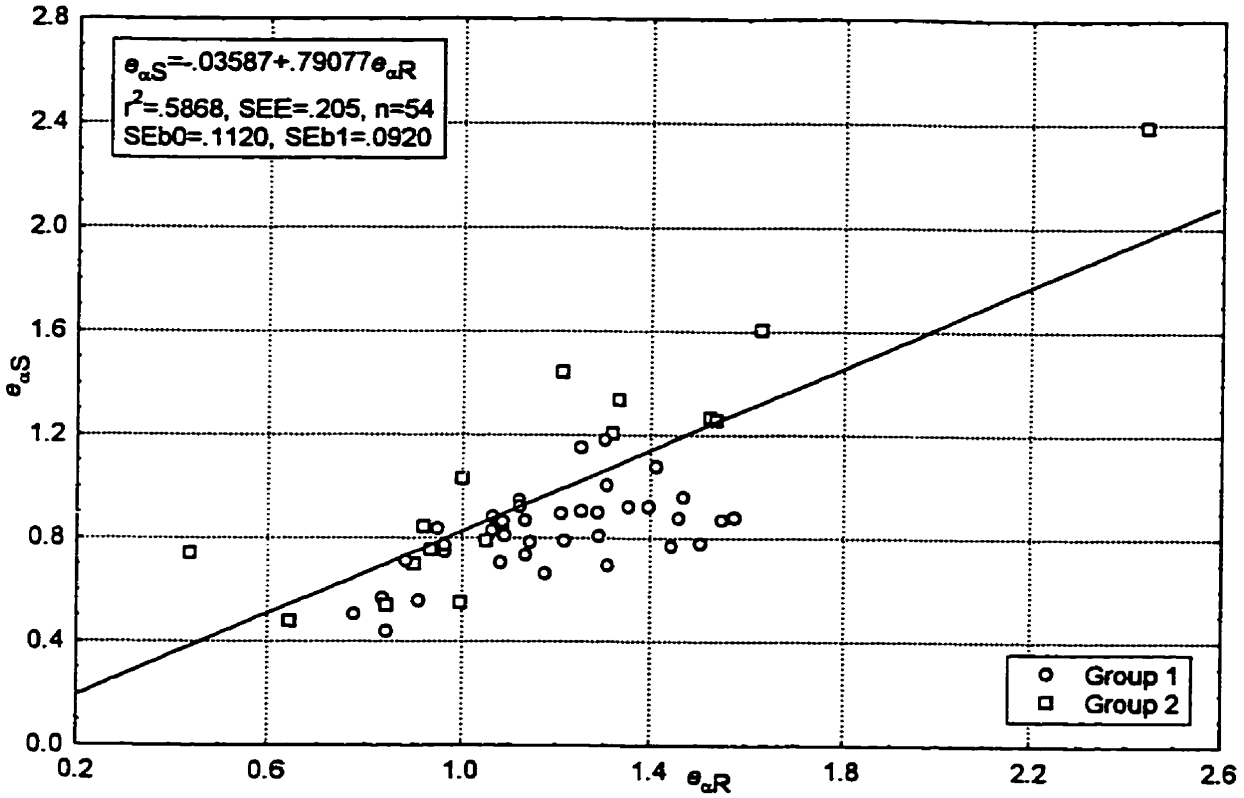

Figure 3.48. $e_{\alpha S}$ **versus** $e_{\alpha R}$.

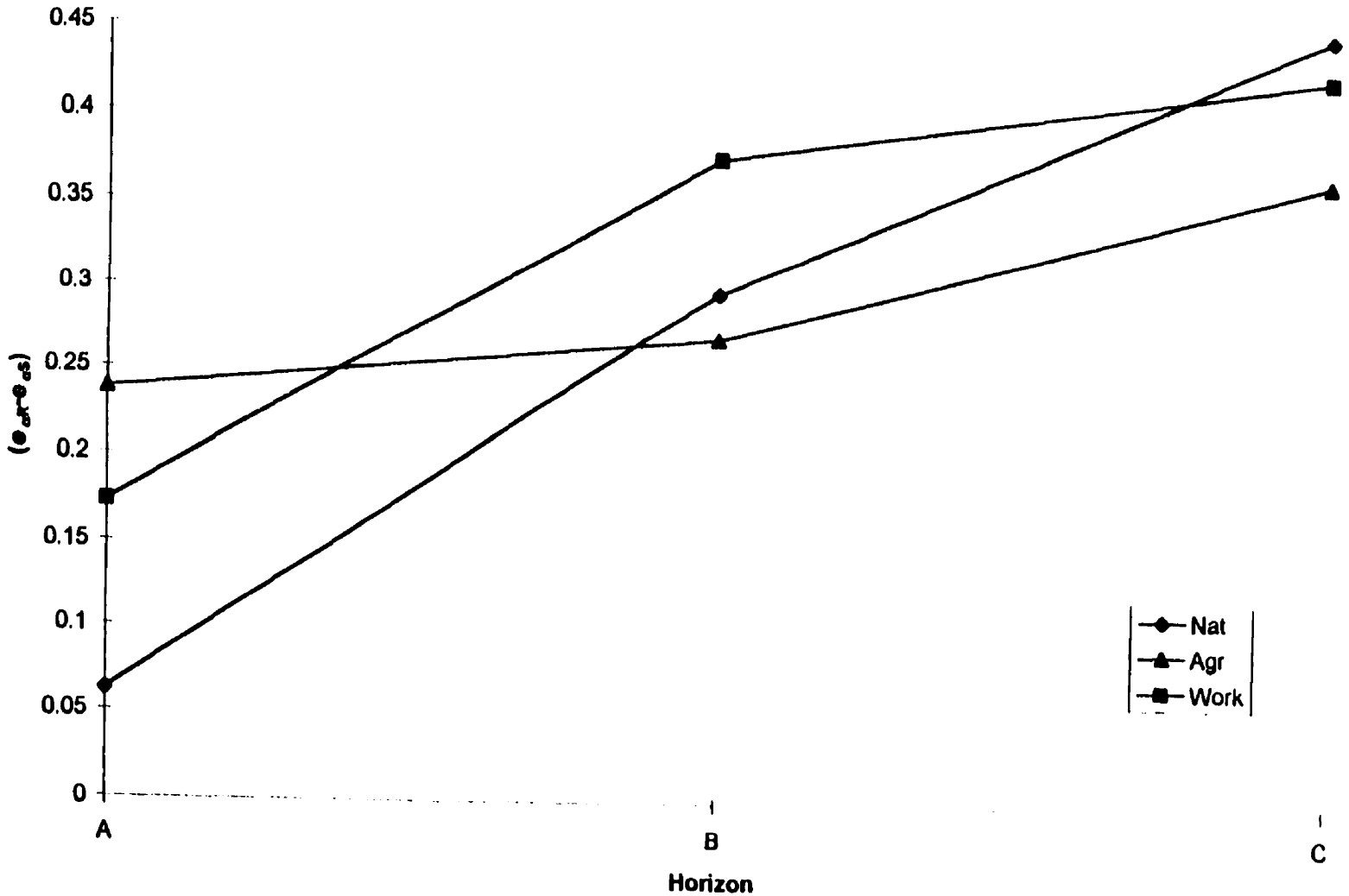

Figure 3.49. (e_{aR}- e_{as}) TRT*HOR interaction.

Table 3.13. LSmeans pdiff separation for ($e_{\alpha R}$- $e_{\alpha S}$) MNR (MDAC removed).

Factor	MNR					
	AB vs. ON	AB vs. OT	AB vs. TX	ON vs. OT.	ON vs. TX	OT vs. TX
pdiff	0.0380*	0.4815	6.71E-04*	0.1921	0.0072*	0.0029*
	AB	ON	OT	TX		
LSmean	0.143604	0.304289	0.207848	0.523655		

For the ANCOVA for ($e_{\alpha R}$- $e_{\alpha S}$) with %clay there are MNR and clay*MNR terms when LBNA and MDAA are removed (MSE=.02156345, R=.7674, n=52). None of the intercepts are significantly different from 0 or from each other. The OT and TX slopes are not significantly different than zero. AB and ON slopes are significantly different from the OT slope. Not a large amount of variability is explained by this model.

When the Group 2 horizons are removed, clay*TRT effects are revealed as well as a MNR*TRT term and much more of the variability is explained (Figure 3.50).

(MSE=.0065766, R=.9569, n=37) [35]

Agr: i) AB: ($e_{\alpha R}$- $e_{\alpha S}$)=.28289252-.00163959%*clay* SEb1=.00423324

ii) ON: ($e_{\alpha R}$- $e_{\alpha S}$)=.32122976-.00163959%*clay*

iii) OT: ($e_{\alpha R}$- $e_{\alpha S}$)=.37153129-.00163959%*clay*

iv) TX: ($e_{\alpha R}$- $e_{\alpha S}$)=.60936376-.00163959%*clay*

Nat v) AB: ($e_{\alpha R}$- $e_{\alpha S}$)=-.04417979+.00943592%*clay* SEb1=.00381174

vi) ON: ($e_{\alpha R}$- $e_{\alpha S}$)=.00985138+.00943592%*clay*

vii) OT: ($e_{\alpha R}$- $e_{\alpha S}$)=-.41504039+.00943592%*clay*

viii) TX: ($e_{\alpha R}$- $e_{\alpha S}$)=.03359239+.00943592%*clay*

Work ix) ON: ($e_{\alpha R}$- $e_{\alpha S}$)=-.17728+.01348710%*clay* SEb1=.00387272

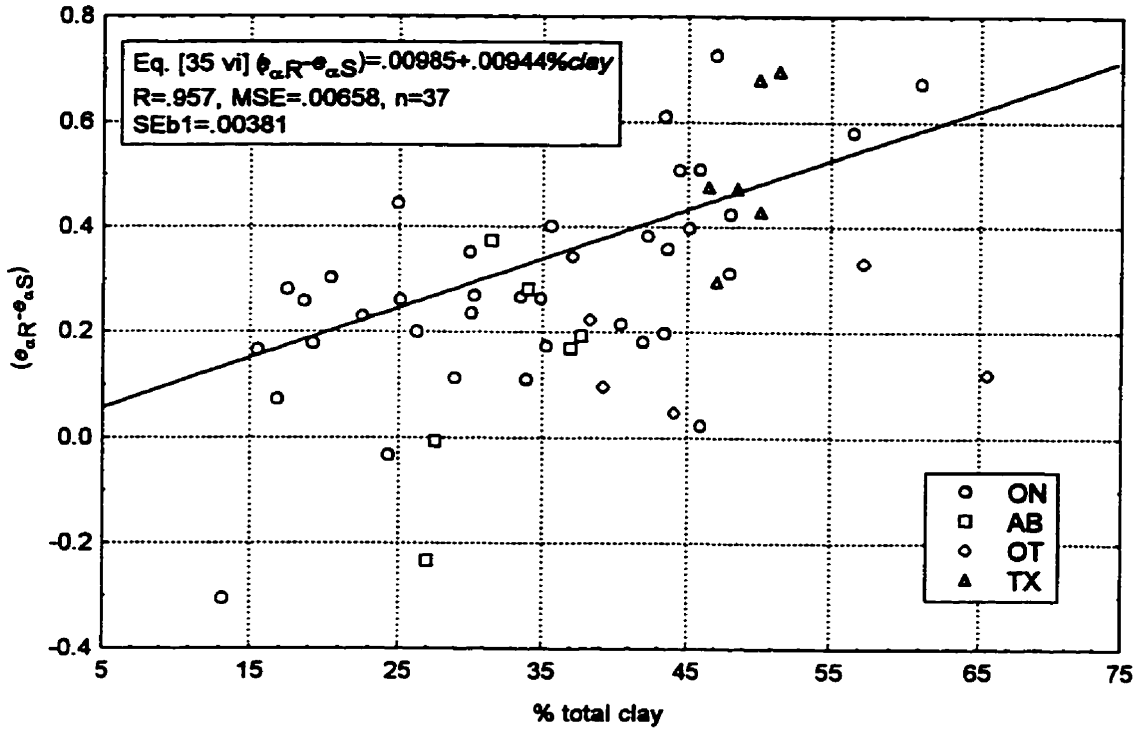

Figure 3.50. ($e_{\alpha R}$- $e_{\alpha S}$) covariance with % clay.

The OT Nat intercept is significantly different than all the other Natural intercepts. The TX Agr intercept is the only one significantly different than 0 of all the intercepts and is different from the ON and AB Agr intercepts. In addition, the ON Agr intercept is different from the ON Work intercept. The TX intercepts are still the highest for any treatment. The Natural and Workspace intercepts are lower than the Agricultural intercepts which may be due to Agricultural horizons not having any significant relationship with %clay while the Natural and Workspace horizons do. The Agricultural slope is significantly different from the Natural (p=.0860) and Workspace (p=.0117) slopes.

With %organic carbon as a covariate and MDAC removed there are MNR*TRT, oc*TRT and oc*oc terms (Figure 3.51). The TX intercepts are again larger than the other intercepts and the agricultural slope is significantly less than the natural slope (MSE=.01319201, R=.8978). When only the Group 1 soils are considered only a significant OC term remains.

$(e_{\alpha R} - e_{\alpha S})$=.43721186-.09251480*%organic carbon* [36]

SEb0=.06012104, SEb1=.00381174, MSE=.01662191, R=.74365, n=37

There was a MNR*TRT term at p=.0590 level but the only differences were OT Nat from Tx and ON Natural horizons which may have been due to only 2 horizons in the OT Nat category.

The residuals were not normally distributed for the comparison between the slopes $n_{\alpha R}$ and $n_{\alpha S}$ primarily due to 5 outliers (OTNA, HLNA, MDNC, HLWB and MDAC) which when removed showed the relationship in Figure 3.52. The ANOVA for $(n_{\alpha R} - n_{\alpha S})$revealed a significant HOR factor (p=.0057) with the A horizons significantly different than the C horizons; the C horizons had a larger difference in slope between the remoulded and structured state than the A horizons. All horizons were significantly different at the 10% level with the B horizons intermediate in value between the A and C horizons.

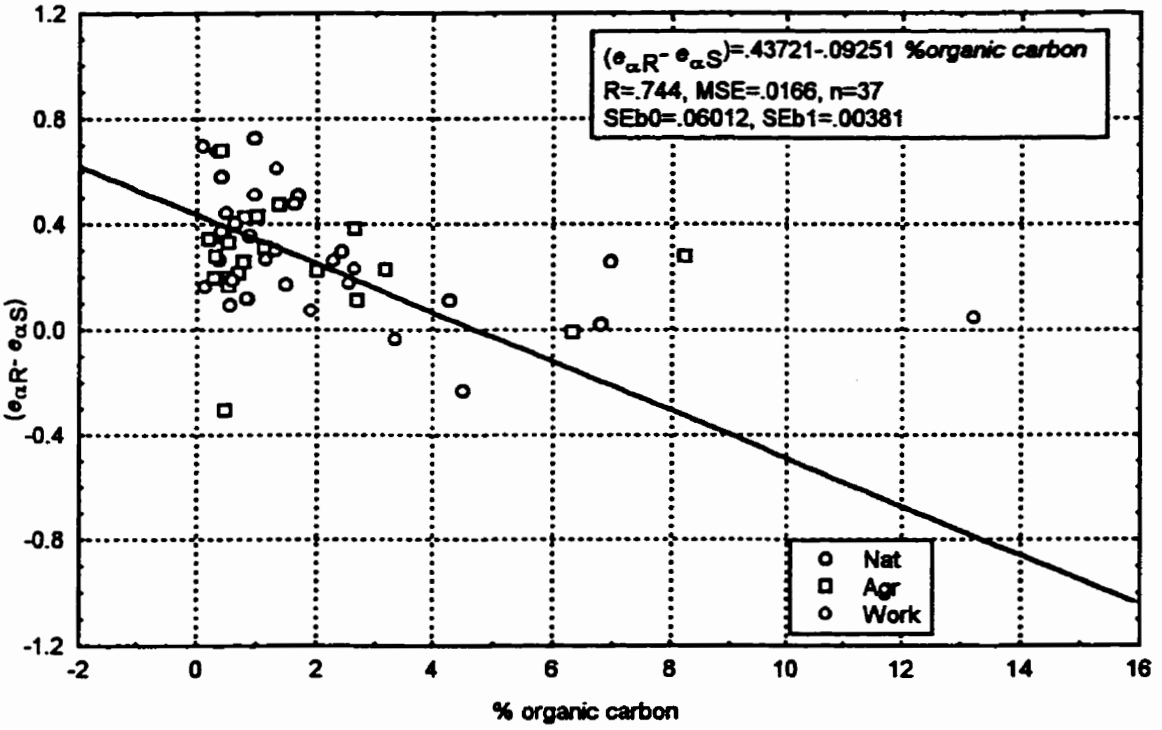

Figure 3.51. ($e_{\alpha R}$- $e_{\alpha S}$) covariance with % organic carbon.

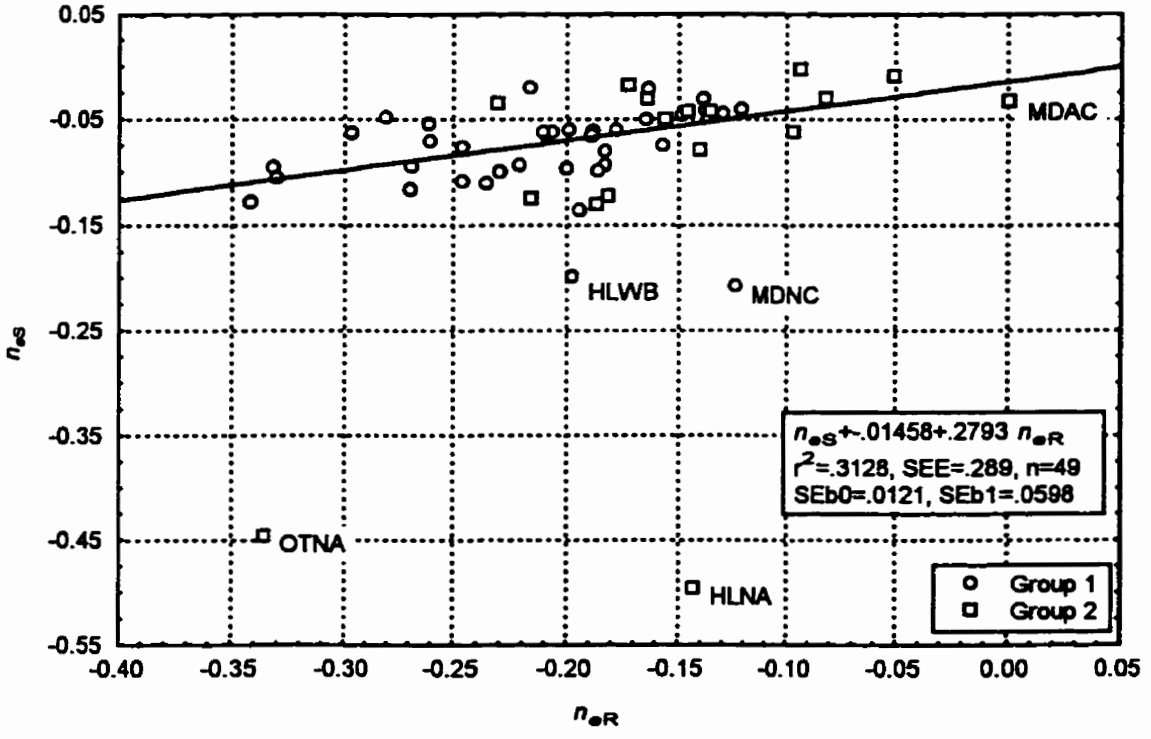

Figure 3.52. $n_{\epsilon R}$ versus $n_{\epsilon S}$.

The ANCOVA for (n_{eR}- n_{eS}) with % organic carbon had a significant OC term when all horizons but HLNA and MDNC were considered which was largely due to the natural horizons (p=.1027) with >4% organic carbon. When the Group 2 soils were removed there was no significant factors with % organic carbon as a covariate.

The ANCOVA with % clay for (n_{eR}- n_{eS}) was complicated due to outliers. The same general model resulted whether the Group 2 soils were removed or the soils with a single line segment for the $v(w)$ plots were removed. In addition, HLNA, LBNA, MDNC or HLWB had to be removed as outliers to achieve normality. The general model in either case had MNR*TRT for the intercepts and clay*TRT for the slopes. For both, the Agr intercepts were more negative than the Nat and Work intercepts and this may be due to no significant slope for Agricultural horizons. The Workspace slope is also significantly different from the Agricultural for both cases. The set which utilizes the most horizons but has a larger MSE is for the removal of the 1 line segment horizons (8) plus, HLNA, HLWB and LBNA (n=43, MSE=.00099418, R=.9482): [37]

Agr: i) AB: n_{eR}- n_{eS}=-.15328768+.00170104*%clay* SEb1=.00127040

ii) ON: n_{eR}- n_{eS}=-.17577072+.00170104*%clay*

iii) OT: n_{eR}- n_{eS}=-.20918289+.00170104*%clay*

iv) TX: n_{eR}- n_{eS}=-.26284520+.00170104*%clay*

Nat: v) AB: n_{eR}- n_{eS}=-.00545456-.00381997*%clay* SEb1=.00122587

vi) ON: n_{eR}- n_{eS}=0.03090347-.00381997*%clay*

vii) OT: n_{eR}- n_{eS}=.010122711-.00381997*%clay*

viii) TX: n_{eR}- n_{eS}=.00259256-.00381997*%clay*

Work: ix) ON: n_{eR}- n_{eS}=-.01753598-.00248882*%clay* SEb1=.00109686

The only intercepts significantly different than 0 are the Agricultural and the only difference is between ON Work and ON Agr. The Agr slope is significantly different from the Natural

(p=.0103) and Workspace (p=.0171) in this case.

There is a 1:1 relationship between the void ratio (e_B) at the shrinkage limit when all soils are considered together (Figure 3.53). The relationship disappears for the Group 2 soils alone and becomes very poor for the Group 1 soils alone (r^2=.2197, SEE=.0800, p=.02086). Most of the measured void ratios at the shrinkage limit are larger for the structured than the remoulded. HLWC, LBNB, MDNC, OTNA, MDAA, LBWB, LBNC, and LBAB all have larger remoulded than structured void ratios at the shrinkage limits.

The final void ratio (e_C) comparison between structured and remoulded has no normally distributed residuals. There is no relationship for the Group 2 soils but there is for the Group 1 soils.

e_{CS} =.2755+.5637 e_{CR} [38]

SEb0=.0638, SEb1=.1432, p=.00044, r^2=.333, SEE=.0665, n=33

The shrinkage limits in the remoulded and structured conditions did not occur at the same stresses. Of the 27 horizons which had a structured shrinkage point in e(σ) coordinates, 7 had the remoulded shrinkage stresses larger than the structured (OTNA, LBWA, HLWB, ABAA, MDNC, HLNA, WANA). Since the shrinkage points didn't occur at the same stresses, points on the structured $e(\sigma')$ curve were not directly comparable to the remoulded $e(\sigma')$ curve. Point e_{BS}* at the residual shrinkage change point was computed using σ_{BR} substituted into the structured $e(\sigma')$ equation. There was a significant relationship between theses 2 points with the slope not being significantly different than 1 so that the estimated e_{BS}* was larger than e_{BR} at the remoulded shrinkage limit by 0.187.

e_{BS}*=.18728+.9834 e_{BR} [39]

SEb0=.0685, SEb1=.1328, SEE=.1450, r^2=.5183, F=54.87, n=53

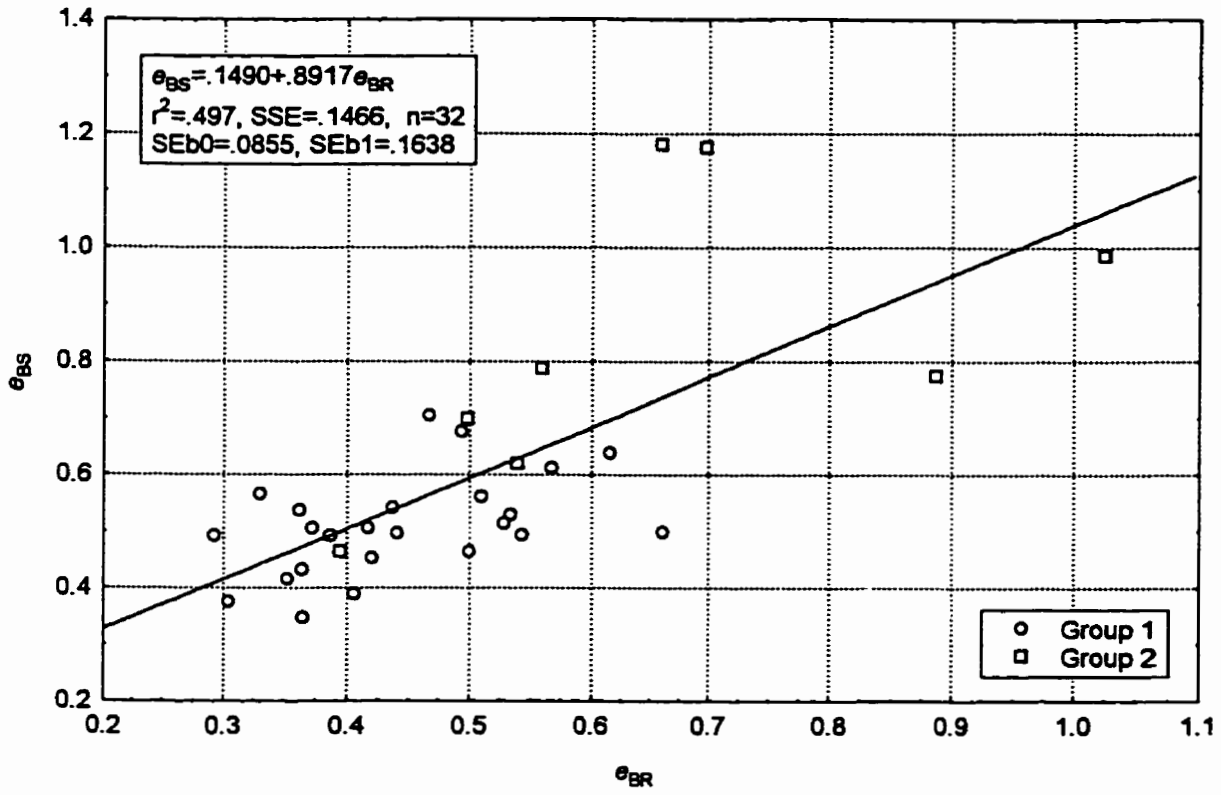

Figure 3.53. e_{BR} **versus** e_{BS}.

The only horizons which had the structured e_{BS}* below the remoulded e_{BR} were OTNA (difference =0.1264), MDNC, LBWB, and MDWB although the latter 3 were just slightly below (0.0056-0.0089).

The plot of ($n_{\alpha R}$-$n_{\alpha S}$) vs. (e_{BR}- e_{BS}*) showed no significant relationship (Figure 3.54). Even so, the majority (except for 6 horizons) were in quadrant III where the configuration was for the remoulded slope to be steeper and the shrinkage point below that on the structured curve so that the lines would cross at some stress and tended to converge. HLNA, HLWB, OTNA and MDNC all had structured slopes steeper than the remoulded. MDNA, OTNA, LBWB and MDWB had the structured void ratio below the remoulded.

A plot of ($n_{\alpha R}$-$n_{\alpha S}$) vs. ($e_{\alpha R}$- $e_{\alpha S}$) showed a significant relationship between the structured and remoulded shrinkage curves. The residuals only became normally distributed when the 3 outliers (OTNA, HLNA, MDNC) were removed (Figure 3.55). Most often (n=46) the horizons plotted in quadrant IV. The remoulded slope and intercept were larger in absolute terms than the structured values showing some kind of convergence and possibly intersection at some stress especially if considered in conjunction with the shrinkage point data. The difference between $e_{\alpha R}$ and $e_{\alpha S}$ can be predicted by Eq. [40].

$$(e_{\alpha R}- e_{\alpha S}) = .2126+.8174e_{LL} -.5150e_0 -.0055sand -.0120I_P \quad [40]$$

(F=18.6, p<.00000, r^2=.613, SEE=.1287, n=52) MDAC and WANB removed.

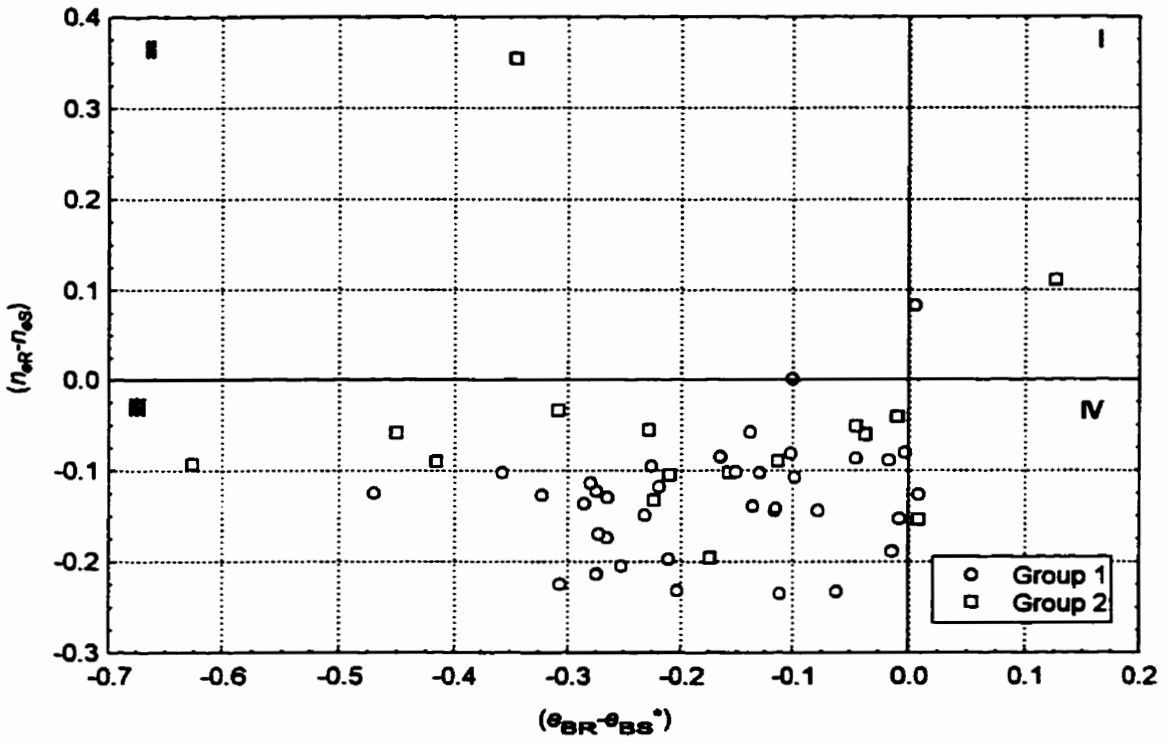

Figure 3.54. $(n_{\alpha R}-n_{\alpha S})$ **vs.** $(e_{BR}-e_{BS}^{*})$.

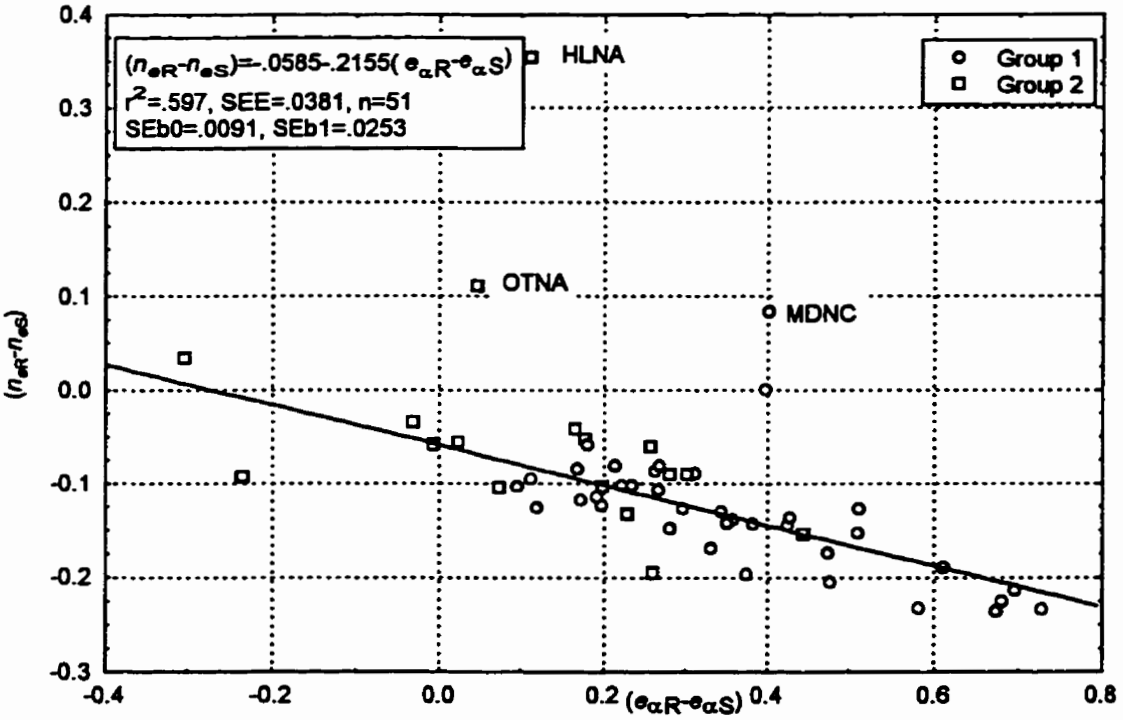

Figure 3.55. $(n_{\alpha R}-n_{\alpha S})$ **vs.** $(e_{\alpha R}-e_{\alpha S})$.

3.3.3.3 COLE values

The $COLE_{struc}$ values were generally lower than the $COLE_{rem}$ values and the regression indicated there was about half as much linear shrinkage in the structured as in the remoulded state (Figure 3.56). Two outliers, OTNA and MDAA were removed to achieve normally distributed residuals for this equation; there were 7 horizons for which the structured $COLE_{struc}$ values were larger than $COLE_{rem}$ (OTNA, MDAA, HLWB, OTNB, MDNA, HLNA, MDAC). These tended to be high organic matter or low plasticity soils except for HLWB and OTNB which are curiosities. De Jong et al. (1992) also found $COLE_{rem}$ underestimated $COLE_{clod}$ for Melfort soils which had 4.92 % OC in the Ap horizon (highest for the study) but with high (> 63%) clay content (also highest for the study).

This relationship between COLE structured and remoulded is different from the relationship parameters found by De Jong et al. (1992) where their equivalent measurements, $COLE_{std}$ and $COLE_{Rem}$, encompassed a 1:1 relationship:

-.010 (±0.007) +.822((±0.098)*$COLE_{Rod,33}$, r^2=.73, SEE=0.013,n=27,

The equations of Ross (1978) and Schafer and Singer (1976) also do not have significant 1:1 relationships with the experimental data.

$COLE_{std}$=-.033 +.784$COLE_{rem}$ r^2=.98, n=6

$COLE_{std}$=.0148 +.7075$COLE_{rem}$ r^2=.866, n=14

Both of these equations were based on individual/separate clay mineralogies and a narrow range of organic matter content soils. There was a 1:1 relationship for the equation of Schafer and Singer (1976) between COLE measured at saturation and oven dry, rather than 1/3 bar and oven dry, when OTNA and MDAA are removed to obtain normally distributed residuals.

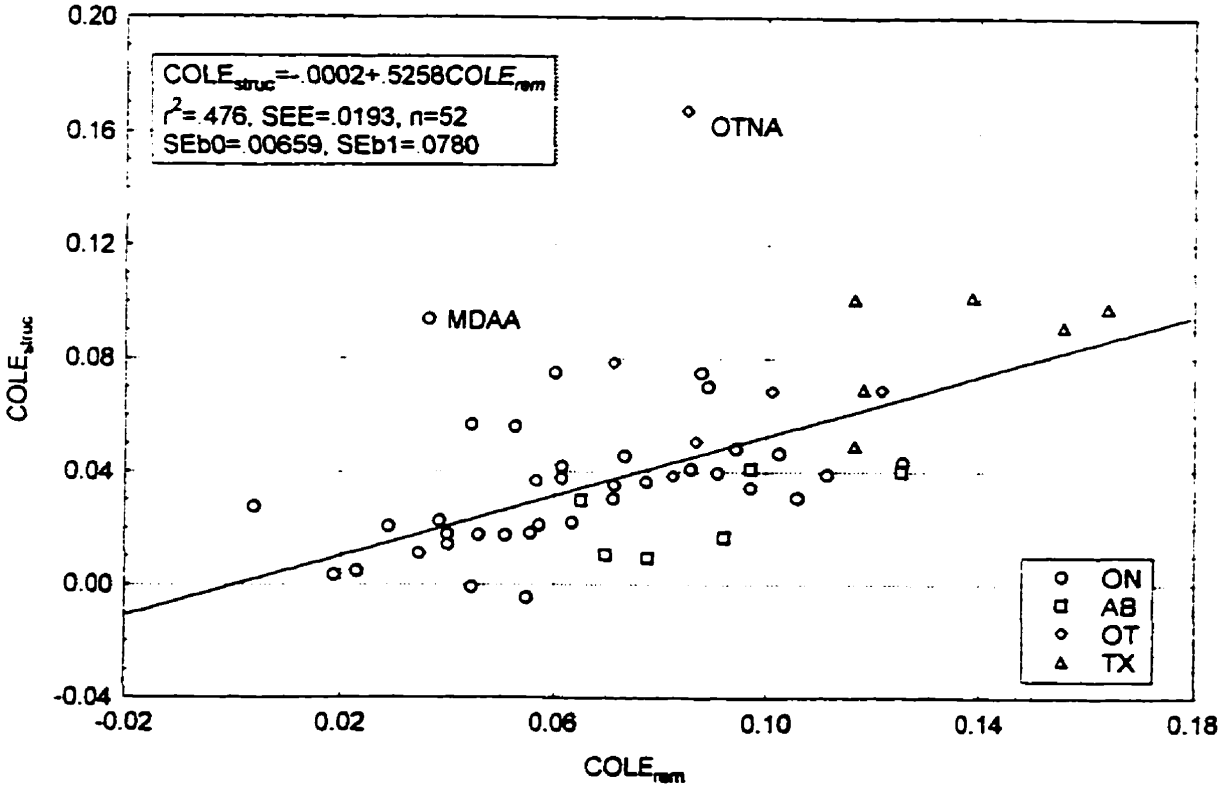

Figure 3.56. $COLE_{struc}$ versus $COLE_{rem}$.

The parameter estimates are more similar to that found by Simon et al (1987) who used only B and C horizons but from a variety of mineralogies.

$COLE_{Std}=0.475COLE_{Rod}$ $r^2=.55$

There is not a 1:1 relationship between the COLE values predicted by this equation and measured values. The large amount of unexplained variability was attributed to the destruction of soil structure in the $COLE_{Rod}$ technique and differences in soil fabric beyond differences in the amounts of montmorillonite (Simon et al., 1987).

3.3.4 Implications for Assessing Physical Soil Quality

Similar to the compression data, there are significant relationships with a low amount of variability explained, between the relative intercept variable ($e_{\alpha R}$- $e_{\alpha S}$) and available water content, macroporosity, log K_{sat} values for the horizons. To achieve normally distributed residuals a logarithmic function was used for the macroporosity data (Figure 3.57). This equation excludes the outlier MDAC which did not have a significant remoulded e(σ') equation. Although only a small part of the variability is explained it can be seen that for macroporosity values above 10% a threshold around 0.25 occurs.

The relationship for available water content is significant for all soils considered together but not significant for either Group of soils analyzed alone (Figure 3.58). An ($e_{\alpha R}$- $e_{\alpha S}$) value of 0.25 would produce an AWC around 9% which would represent structurally degraded soils.

The relationship between ($e_{\alpha R}$- $e_{\alpha S}$) and log(K_{sat}) is significant but does not explain much of the variability (Figure 3.59). A threshold around 0.25 would again aid in separating highly degraded soils, similar to the compression data where -5 is the midpoint of the medium hydraulic conductivity class.

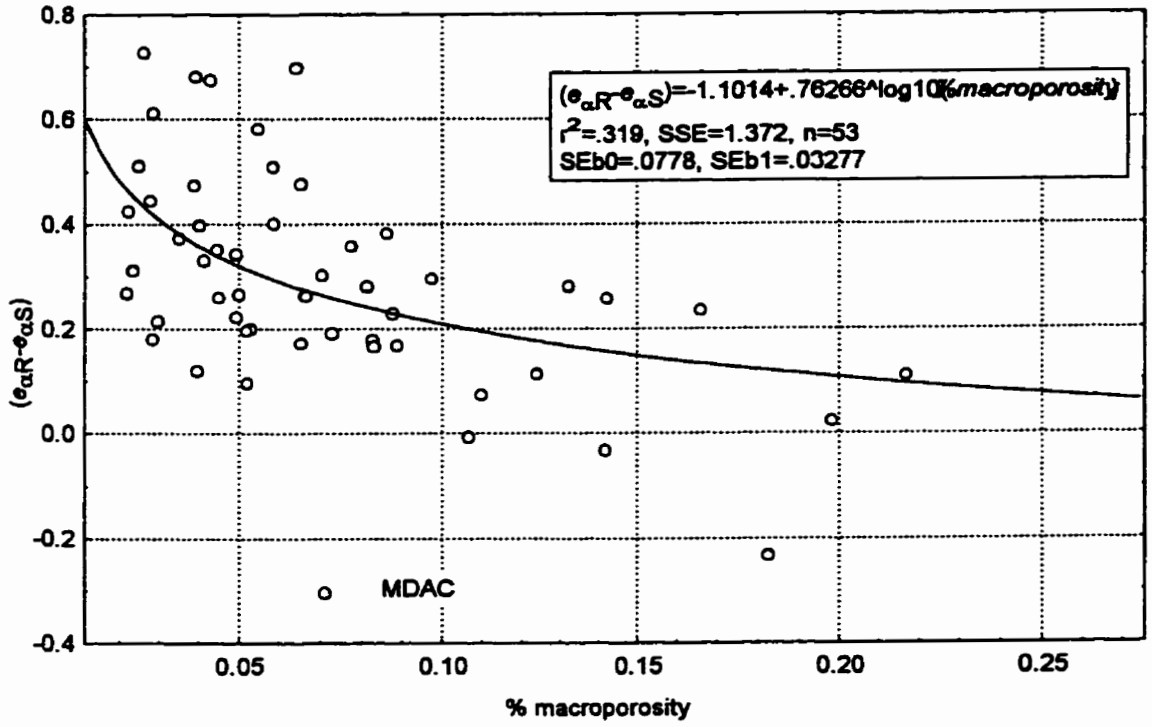

Figure 3.57. Macroporosity vs. ($e_{\alpha R}$- $e_{\alpha S}$).

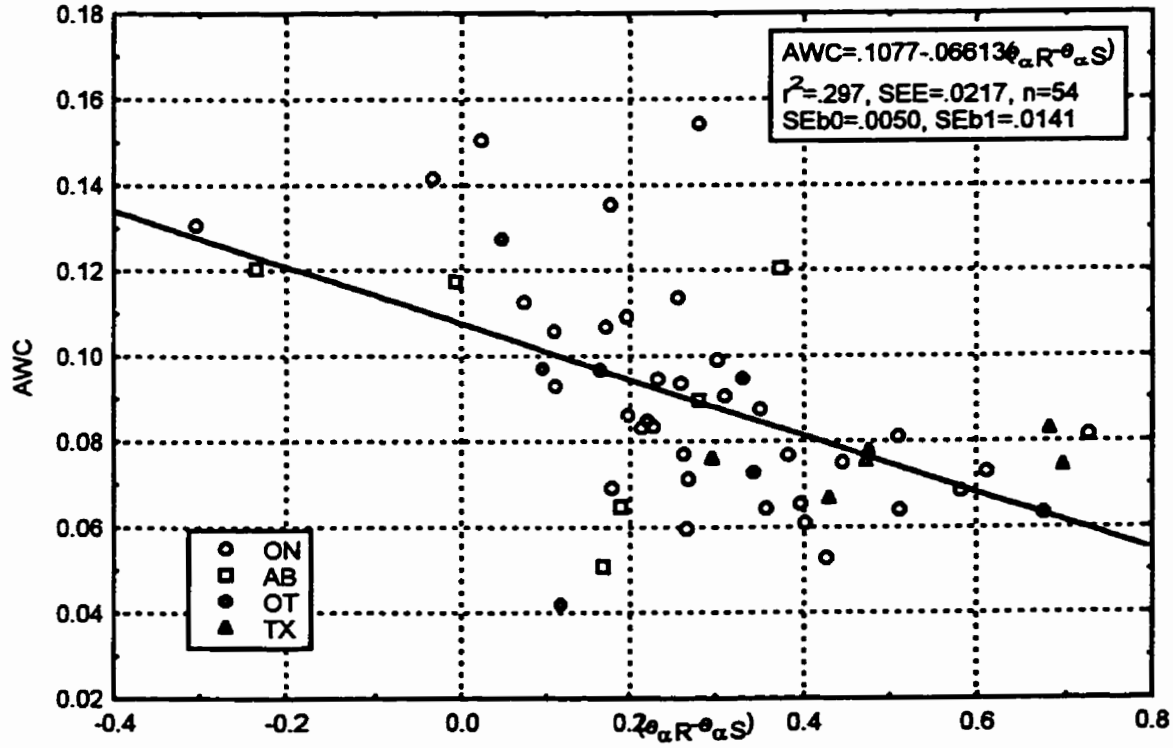

Figure 3.58. Plant available water content vs. ($e_{\alpha R}$- $e_{\alpha S}$).

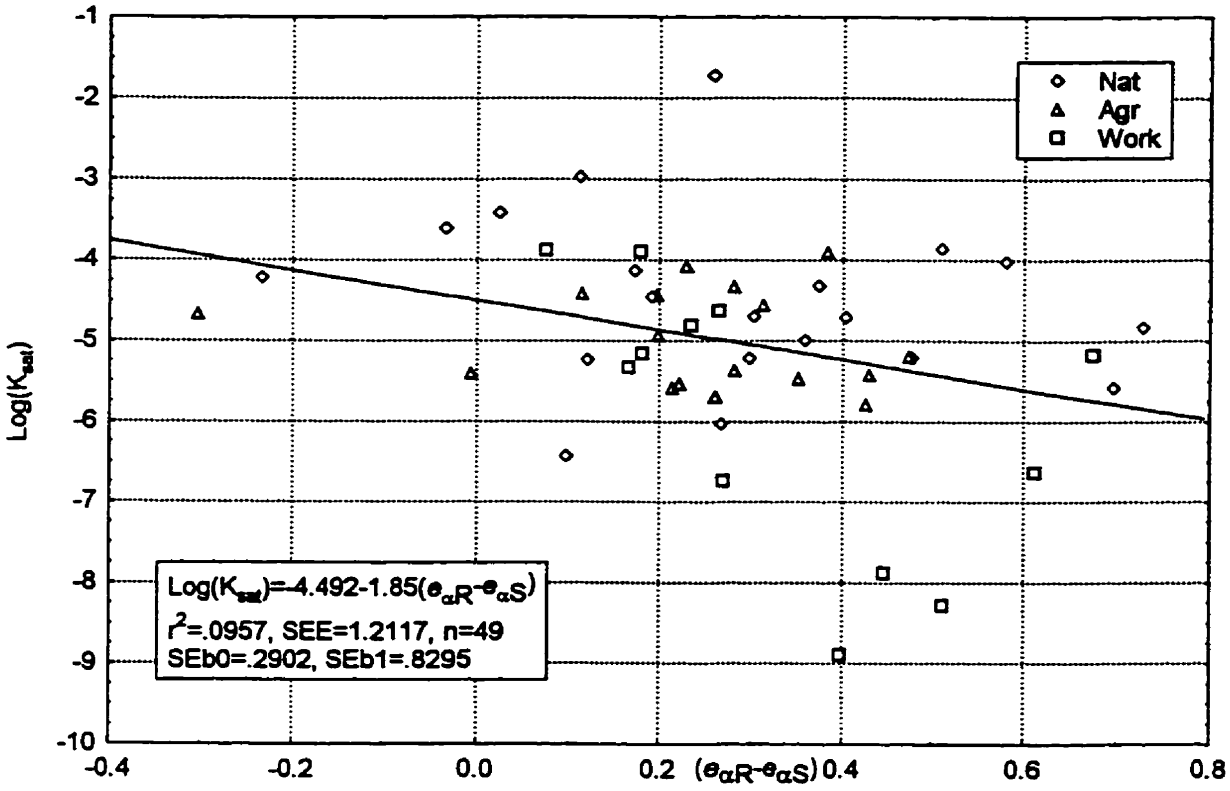

Figure 3.59. Log(K_{sat}) versus ($e_{\alpha R}$- $e_{\alpha S}$).

3.4 Conclusions

In regard to the first objective, volume change was measured on soils with a variety of particle sizes and mineralogies. A straight line model fit remoulded sample data in both $v(w)$ and $e(\sigma')$ co-ordinates well with $r^2>.90$ for most soils and the e CV<5% for all tensions. Even in the remoulded state 4 soils exhibited only 1 shrinkage phase. The difficulty in using a completely objective approach to allow straight lines to be fit statistically and tested for their significance, is that it must later be decided which line segment represents each shrinkage stage. The data was divided into 2 groups based on the remoulded results; Group 1 had >27%clay content or ≤4% organic carbon content, and Group 2 had ≤27% clay content or >4 % organic carbon. The Group 2 soils showed no "normal" shrinkage with generally $n_{vR}<0.7$ and substantial air entry beginning with the initial tension either because of the interparticle contact of sand and silt particles or the rigidity of organic matter. The Group 1 soils showed both "normal" and residual/zero shrinkage where the samples were essentially saturated and roughly paralleled the 1:1 saturation line for a significant portion of the shrinkage characteristic.

The structured samples did not fit a 3 straight line segment model as well, with a much wider range in r^2 and CV; the CV was >10% for several tensions and $r^2<0.80$ for several horizons. A wide range in the number of significant line segments was found making direct comparisons difficult. There were fewer structured n_{vs} (n=14) slopes ≥1 than remoulded (n=27) confirming a wider pore size distribution with a combination of drainage and contraction of pores during volume change in structured soils. In the structured $e(\sigma')$ plots more soil horizons had only 1 statistically significant line segment models but also more had 3-line segment models than in the remoulded plots.

In regard to the second objective, the $e(\sigma')$ plots were more consistent in being able to

distinguish soil quality or treatment effects than the $v(w)$ plots. The $e(\sigma')$ plots were also better at indicating marginally plastic, low shrink-swell potential soils. It is therefore suggested that shrinkage parameters from $e(\sigma')$ plots may better represent "normal" shrinkage in which there is plastic deformation related to a particular change in isotropic stress and residual and structural phases relate to pore water drainage over particular stress ranges, rather than simply equal volume change with equal loss of water. The $e(\sigma')$ plots showed a significant relationship between (e_{aR}- e_{aS}) and (n_{eR}- n_{eS}) indicating a dominant converging behaviour while the $v(w)$ plots varied in diverging or converging behaviour. In particular the (e_{aR}- e_{aS}) parameter was useful and similar to the compression results, in discerning MNR and TRT*HOR factors. TRT and MNR effects remained even when clay or organic carbon content were covariates. Kuznetsova and Davilova (1988) showed that well-developed soil structure affects the swelling and shrinkage properties; they found a critical threshold of compaction above which the soil loses its ability to spontaneously gain optimal tilth. Consolidation should have the effect of reducing the maximum attainable water content (and void ratio) with swelling according to Kuznetsova and Davilova (1988). This could explain variability in addition to that explained by organic matter for the (e_{aR}- e_{aS}) variable.

The (v_{aR} - v_{aS}) in $v(w)$ plots as suggested by Lauritzen (1948) showed a difference for the Workspace from the Natural treatments which was removed by organic carbon as a covariate, as both intercepts were highly related to organic matter content. Neither the difference in remoulded and structured COLE or n_v , which have routinely been used to describe shrinkage characteristics, could be used to establish useful models for assessing structural quality because of non-normal distribution of residuals.

Opposite from the remoulded samples where normal shrinkage occurred for Group 1 and B and C horizons, "normal" shrinkage tended to occur in the Group 2 soils and A horizons for the structured samples. Also the (n_{eR}- n_{eS}) difference was less for A horizons than C horizons. These

result were opposite from what was anticipated, in that those soils with a limited range in porosity were expected to be most similar to the remoulded shrinkage slopes. Structurally damaged soils compacted "wet of optimum" were expected to have the highest axial shrinkage because the fabric is more oriented or dispersed (Holtz and Kovacs, 1981). The soils with a wider range of well structured pore sizes were expected to have shrinkage slopes most dissimilar from the remoulded counterparts. However, the opposite seemed to exist for some horizons with the C horizon slopes being most different and the A horizons being most similar.

These inconsistencies in the data raise question as to the possibility of using a simple difference in shrinkage characteristic slope (Stage 2) as an index of soil structural quality although this initially seemed the logical choice. Likely there would need to be two sets of slope indices, related to the two Groups of soils and their different responses in volume change with water loss. The indices for n_v versus n_e for the 2 groups of soils would also likely be different since n_v is independent of clay and organic carbon content for the Group 1 but not Group 2 soils, while n_e is related to clay content (plasticity) and COLE for all soils. It is hypothesized that pore space contributes to the volumetric swelling in structured Group 2 soils where there is sufficient organic matter and pore space to allow a high amount of water uptake which increases the size of the pores and aggregates present. In Group 1 soils conversely, the restricted pore space and lack of organic matter in dense structured soils lessens the potential uptake of water and does not contribute to the volumetric change. The pores may actually constrict as the soil aggregates swell. Alignment of soil particles in these soil may also restrict potential swelling. On remoulding, Group 2 soils lose this "elastic" pore space and therefore do not have any normal shrinkage as the clastic particles come into close contact with each other and organic bonds are broken. For the Group 1 soils, remoulding increases the pore space and surface area of clay particles exposed for greater water uptake, leading to more normal shrinkage in the remoulded state. There is not a complete enough

set of data to test MNR, TRT and HOR effects completely for both groups.

There is much variability and confounding of shrinkage parameters with soil properties, such as the Natural and Workspace treatments not having significantly different ANCOVA responses to clay or organic matter for structured and relative shrinkage parameters, which create difficulties for deriving definitive soil quality indices from this shrinkage data set.

3.5 References

Agriculture Canada Expert Committee on Soil Survey. 1987. The Canadian System of Soil Classification. Research Branch, Agriculture Canada. Publication 1646.

Allbrook, R.F. 1992. Shrinkage of some New Zealand soils and its implications for soil physics. Aust. J. Soil Res. 31:111-118.

Baumgartl, Th. 1998. Physical soil properties in specific fields of application especially in anthropogenic soils. Soil & Tillage Res. 47:51-59.

Bronswijk, J.J.B. 1989. Prediction of actual cracking and subsidence in clay soils. Soil Science 148:87-93.

Bronswijk, J.J.B. 1991. Drying, cracking and subsidence of a clay soil in a lysimeter. Soil Sci. 152(2):92-99.

Bronswijk, J.J.B. and J.J. Evers-Vermeer. 1990. Shrinkage of Dutch clay soil aggregates. Neth. J. Agric. Sci. 38:175-194.

Bronswijk, J.J.B. 1993. Comments on "Shrinkage terminology: escape from normalcy". Soil Sci. Soc. Am. J. 57(2):558-559.

Bruand, A. and R. Prost. 1987. Effect of water content on the fabric of a soil material: an experimental approach. J. Soil Sci. 38:461-472.

Cabidoche, Y.-M. and M. Voltz. 1995. Non-uniform volume and water content changes in swelling clay soil: II. A field study on a Vertisol. Eur. J. Soil Sci. 46:345-355.

Chan, K.Y. 1982. Shrinkage characteristics of soil clods from a grey clay under intensive cultivation. Aust. J. Soil Res. 20:65-68.

Chang, R.K. and B.P. Warkentin. 1968. Volume change of compacted clay soil aggregates. Soil Sci. 105(2):106-111.

Dasog, G.S., D.F. Acton and A.R. Mermut. 1987. Genesis and classification of clay soils with vertic properties in Saskatchewan. Soil Sci. Soc. Am. J. 51:1243-1250.

Dasog, G.S., D.F. Acton, A.R. Mermut and E. De Jong. 1988. Shrink-swell potential and cracking in clay soils of Saskatchewan. Can. J. Soil Sci. 68:251-260.

De Jong, E., L.M. Kozak and H.B. Stonehouse. 1992. Comparison of shrink-swell indices of some Saskatchewan soils and their relationships to standard soil characteristics. Can. J. Soil Sci. 72:429-439.

Derdour, H. 1993. Etude des modifications de l-etat structural du sol par les pratiques culturales: consequences sur la repartition de l'espace poral d'un sol argileux. Unpublished PhD. dissertation. Universite Laval, Quebec, PQ.

Emerson, W.W. 1977. Physical properties and structure. pp. 78-104 *In* J.S. Russell and E.L. Greacen (eds.) Soil Factors in Crop Production in a Semi-arid Environment. Univ. Queensland Press: St. Lucia, Queensland.

Grant, C.D. and A.R. Dexter. 1990. Air entrapment and differential swelling as factors in the mellowing of moulded soil during rapid wetting. Aust. J. Soil Sci. 28:361-369.

Haines, W.B. 1923. The volume change associated with variations of water content in soil. J. Agric. Sci. 13:296-310.

Hartmann, C., E. Blandchart, J. Louri, L. Rangon and J. Bernard. 1998. Rehabilitation processes under fallow and pasture of a compacted Vertisol in Martinique (FWI). Paper presented at the 16th World Conference of Soil Science, Aug. 20-26, 1998, Montpellier, France. ISSS and AFES. No. 700. Symp. 2.

Jayawardane, N.S. and E.L. Greacen. 1987. The nature of swelling in soils. Aust. J. Soil Res. 25:107-133.

Kay, B.D. and A.R. Dexter. 1990. Influence of aggregate diameter, surface area and antecedent water content on the dispersibility of clay. Can. J. Soil Sci. 70:655-671.

Kuznetsova, I.V. and V.I. Danilova. 1988. Loosening of soils by swelling and shrinkage. Sov. Soil Sci. (Engl. Transl.) 6:59-70.

Lauritzen, C.W. 1948. Apparent specific volume and shrinkage characteristics of soil materials. Soil Sci. 65:155-179.

Lauritzen, C.W. and A.J. Stewart. 1941. Soil volume changes and accompanying moisture and pore size relationships. Soil Sci. Am. Proc. 6:113-116.

Makeyeva, V.I. 1988. Effect of wetting and drying on the soil structure. Engl. transl. from Pochvovedeniye. 12:80-88.

McBride, R.A. 1989. A re-examination of alternative test procedures for soil consistency limit determination: II. A simulated desorption procedure. Soil Sci. Am. J. 53(1):184-191.

McCormack, D.E. and L.P. Wilding. 1975. Soil properties influencing swelling in Canfield and Geeburg soil. Soil Sci. Soc. Am. J. 39:496-502.

McGarry, D. and I.G. Daniells. 1987. Shrinkage curve indices to quantify cultivation effects on soil structure of a Vertisol. Soil Sci. Soc. Am. J. 51:1575-1580.

McGarry, D. and K.W.J. Malafant. 1987. The analysis of volume change in unconfined units of soil. Soil Sci. Soc. Am. J. 51(2):290-297.

McGarry, D. 1988. Quantification of the effects of zero and mechanical tillage on a Vertisol by using shrinkage curve indices. Aust. J. Soil Res. 26:537-542.

Mitchell, A.R. and M. Th. van Genuchten. 1992. Shrinkage of bare and cultivated soil. Soil Sci. Soc. Am. J. 56:1036-1042.

Monnier, G., P. Stengel and J.C. Fiès. 1973. Une méthode de mesure de la densité apparente de petits aggomérats terreux: Application à l'analyse des systèmes de porosité. Ann. Agron. 24(5):533-545.

Newman, A.C.D. and A.J. Thomasson. 1979. Rothamsted studies of soil structure III: Pore size distribution and shrinkage processes. J. Soil Sci. 30:415-439.

Paz, A. 1998. Shrinkage characteristics of aggregates from soils with limited amounts of swelling material.. Paper presented at the 16th World Conference of Soil Science, Aug. 20-26, 1998, Montpellier, France. ISSS and AFES. No. 904. Symp. 2.

Reeve, M.J. and D.G.M. Hall. 1978. Shrinkage in clayey subsoils of contrasting structure. J. Soil Sci. 29:315-323.

Reeve, M.J., D.G.M. Hall and P. Bullock. 1980. The effect of soil composition and environmental factors on the shrinkage of some clayey British soil. J. Soil Sci. 1980. 31:429-442.

Ross, G.J. 1978. Relationships of specific surface area and clay content to shrink-swell potential of soils having different clay mineralogical compositions. Can. J. Soil Sci. 58:159-166.

Schafer, W.M. and M.J. Singer. 1976. A new method of measuring shrink-swell potential using soil pastes. Soil Sci. Soc. Am. Proc. 40:805-806.

Searle, W.M. and M.J. Singer. 1959. The chemistry and physics of clays and other ceramic materials. Interscience Publishers, Inc., New York, NY.

Shiel, R.S. M.A. Adey and M. Lodder. 1988. The effect of successive wet/dry cycles on aggregate size distribution in a clay texture soil. J. Soil Sci. 39(1);71-79.

Simon, J.J., L. Oosterhuis and R.B. Reneau. 1987. Comparison of shrink-swell potential of seven ultisols and one alfisol using two different COLE techniques. Soil Science 143(1):50-55.

Stirk, G.B. 1954. Some aspects of soil shrinkage and the effect of cracking upon water entry into soil. Aust. J. Agr. Res. 5:279-290.

Tariq, A, and D.S. Durnford. 1993a. Analytical volume change model for swelling clay soils. Soil Sci. Soc. Am. J. 57:1183-1187.

Tariq, A. and D.S. Durnford. 1993b. Soil volumetric shrinkage measurements: a simple method. Soil Science 155(5):325-330.

Tessier, D. and J. Berrier. 1979. Utilisation de la microscopie électronique à balayage dans l'étude des sols: Observation de sols humides soumis à différents pF. Science du Sol 1:67-82.

Topp, G.C. 1993. Soil water content. pp. 541-557. *In* M.R. Carter (ed.) Soil Sampling and Methods of Analysis. Canadian Society of Soil Science. Lewis Publishers: Boca Raton.

Tunny, J. 1970. The influence of saran resin coatings on swelling of natural soil clods. Soil Sci. 109:254-256.

Wilding, L.P. and D. Tessier. 1988. Genesis of vertisols: shrink-swell phenomena. pp 55-81 *In* L.P. Wilding and R. Puentes (eds.) Vertisols: Their distribution, properties, classification and management. Technical monograph No. 18. Soil Management Support Services, Texas A&M, College Station, TX.

Wu, L., R.R. Allmaras, D. Gimenez and D.M. Huggins. 1997. Shrinkage and water retention characteristic in a fine-textured mollisol compacted under different axle loads. Soil & Tillage Res. 44:179-194.

4. Comparison between Compression and Shrinkage Data

4.1 Introduction

Conducting both compression and shrinkage tests on remoulded and structurally intact samples allowed the unique opportunity to investigate the relationship between mechanical stresses imposed externally (via compression) and internally (via negative pore water potentials). This would determine if soil structure resisted change originating from effective internal stresses similar to external mechanical (compressive) stresses and if the parameters could be analogous to those derived from compression studies on the same soil.

The comparison of the two tests directly seems impractical since the compression tests occur under saturated conditions while the shrinkage tests occur under partially saturated soil conditions. The two stress states are linked by the concept of effective stress (σ'), the stress transmitted through the soil skeleton (Craig, 1992). Effective stress accounts for the pore space in partly saturated soil being occupied by both gas and liquid phases. Effective stress (σ') in partly saturated soils is given by:

$$\sigma' = \sigma - u_a + \chi(u_a - u_w) \qquad [1]$$

where σ equals total applied stress, u_a is pore air pressure, u_w is the pore water pressure and χ is a function of water content and wetting and drying history (Hettiaratchi and O'Callaghan, 1980). Eq. [1] is often simplified by assuming that air can escape to the atmosphere to give (Towner, 1983; Kirby, 1989):

$$\sigma' = \sigma - \chi u_w \qquad [2]$$

The parameter χ is the area the pore water pressure acts over in the water phase and is thus related to the degree of saturation of the soil but not perfectly; an additional term is required that

represents the contribution made by the surface tension forces at the air/water/solid interface (Towner, 1983). Thus under saturated compression conditions, $\chi=1$, u_w is ≥ 0 and the effective stress is less than the total stress until pore water drains and reaches 0. Under partially saturated conditions, $0<\chi<1$ and due to the curvature of the liquid menisci within the soil fabric, the pore water pressure is below atmospheric ($u_w \leq 0$) (Hettiaratchi and O'Callaghan, 1980). Thus Eq. [2] shows that the effective stresses are now greater than the total stress. This has led to the assumption that deformation of the soil in response to a change in applied stress (external isotropic) is the same as deformation in response to the factor $\chi\, u_w$ (Hettiaratchi and O'Callaghan, 1980; Towner, 1983; Kirby, 1989).

This assumption has been criticized for 2 reasons. Firstly, results by Aitchison (1961) and Towner and Childs (1972) (reported in Towner, 1983) showed that $\chi\, u_w$ increased with increasing u to a maximum and then decreased rather than increasing indefinitely as suggested by Hettiaratchi and O'Callaghan (1980). Further testing of unconfined shear strength of remoulded samples as a function of suction for a range of soil textures (very fine sand to a clay), found the effective stress component to increase with suction to some value (which was larger for the clayey soils) and thereafter change only slightly (Towner, 1983). The effective stress may actually decrease, with cementation bonds developing which obscure this effect (Towner, 1983; Hettiaratchi and O'Callaghan, 1980). Toll (1990), using a gravel with only 9% clay, found that at degrees of saturation below 55%, the suction no longer had any effect on the deviator stress or overall volume change. The water phase had retracted into the fine pores within the soil aggregates and no longer affected the particle contacts where shear was taking place (Toll, 1990). In the shrinkage characteristic context presented here, rather than triaxial tests used in these mechanical studies, this point would correspond to air entry or the shrinkage limit, and so it is not surprising that there is a limit to deformation caused by tension effective stresses.

Secondly, violations of the effective stress principle occur because applied loads and pore suctions act differently at grain contacts; only the former can introduce a shear force at a contact (Burland, 1965 in Kirby, 1989). There has, however, been suggestion of some rearrangement of aggregates (if there is sufficient pore space) on shrinkage (Chang and Warkentin, 1968) which would imply some sort of shearing; most studies only refer to pore volume change accounting for the total volume shrinkage (Wires et al., 1987; McGarry, 1988; Greene-Kelly, 1974).

Despite these difficulties when using an effective stress equation, the concept of effective stress has continued to be used in the development of critical state models for unsaturated soils using 2 approaches. One approach has been to separate stresses into 2 stress state variables (Toll, 1990; Ho et al., 1992; Rahardjo and Fredlund, 1995). The second has been to allow the contribution of effective stress (pore water tension) to manifest itself in the apparent strength parameters and nature of the shapes of the measured state boundaries (Hettiaratchi, 1987; Kirby, 1989; Petersen, 1993). Most studies have found systematic variation in the critical state parameters with moisture content (Leeson and Campbell, 1983; Horn, 1988; Kirby, 1991; Hettiaratchi, 1987; O'Sullivan et al.,1994; Petersen, 1993).

Very few studies have compared compression and shrinkage results directly. Derdour et al. (1994) conducted both compression and shrinkage tests on Kamouraska clay (58% clay, 30 %silt, 12% sand, 2.5% OC) surface soil aggregates sieved to 2-3.4 mm. The compaction sensitivity threshold water content, after Guérif (1982), was about .20-.22 kg kg^{-1} at compression loads less than 200 kPa which corresponded to the threshold water content (air entry point, shrinkage limit) marking the end of normal shrinkage. Essentially there was resistance to compaction when the degree of saturation of the aggregates was < 0.80. Ho et al. (1992) used a combination of one-dimensional consolidation, pressure-plate moisture extraction and shrinkage tests to present void ratio (e) and moisture ratio (wG_s) constitutive surfaces in (σ-u_a) and (u_a-u_w) planes, respectively,

to present volume change indices for an unsaturated silt and glacial till which had been remoulded and compacted at water contents either dry of optimum or at optimum. They found that the lower the water content or the degree of saturation at the beginning of the test, the greater the distance of the shrinkage test curve from the saturation (consolidation) line. The slope of the shrinkage line (e vs. $(\sigma\text{-}u_a)$) was considerably less than the compression line.

The objective of this study was to compare the compression and shrinkage mechanical parameters to determine if they were analogous in that soil structure resisted strain similarly whether stresses were applied internally or externally.

4.2 Results and Discussion

The materials and methods from Chapters 2 and 3 were used to measure the compression and shrinkage curves and mechanical parameters presented here. A representation similar to Ho et al. (1992) was attempted in this study to unify the volume change and moisture change indices against effective stress (either applied or suction) as represented by 2 stress state variables. It became evident quite quickly that the plots would not correspond directly as the void ratios were taken on samples with different proportions (73 mm, 47 mm and 30 mm diam. for compression, soil water retention and shrinkage experiments, respectively) rather than a consistent sample used for all tests as in Ho et al. (1992); thus the initial void ratios were different. Two examples of different structural conditions (i.e. normally and underconsolidated (LBAA, LBNA) versus overconsolidated (LBWB, WAWC) (Figures 4.1-4.4) illustrate this separation of void ratios. These figures show, however, there is some continuation/joining of the compression and shrinkage curves at stresses above 1000 kPa which is evident for both the remoulded and structured phases.

This configuration may indicate that the compression reflected a combination of inter- and

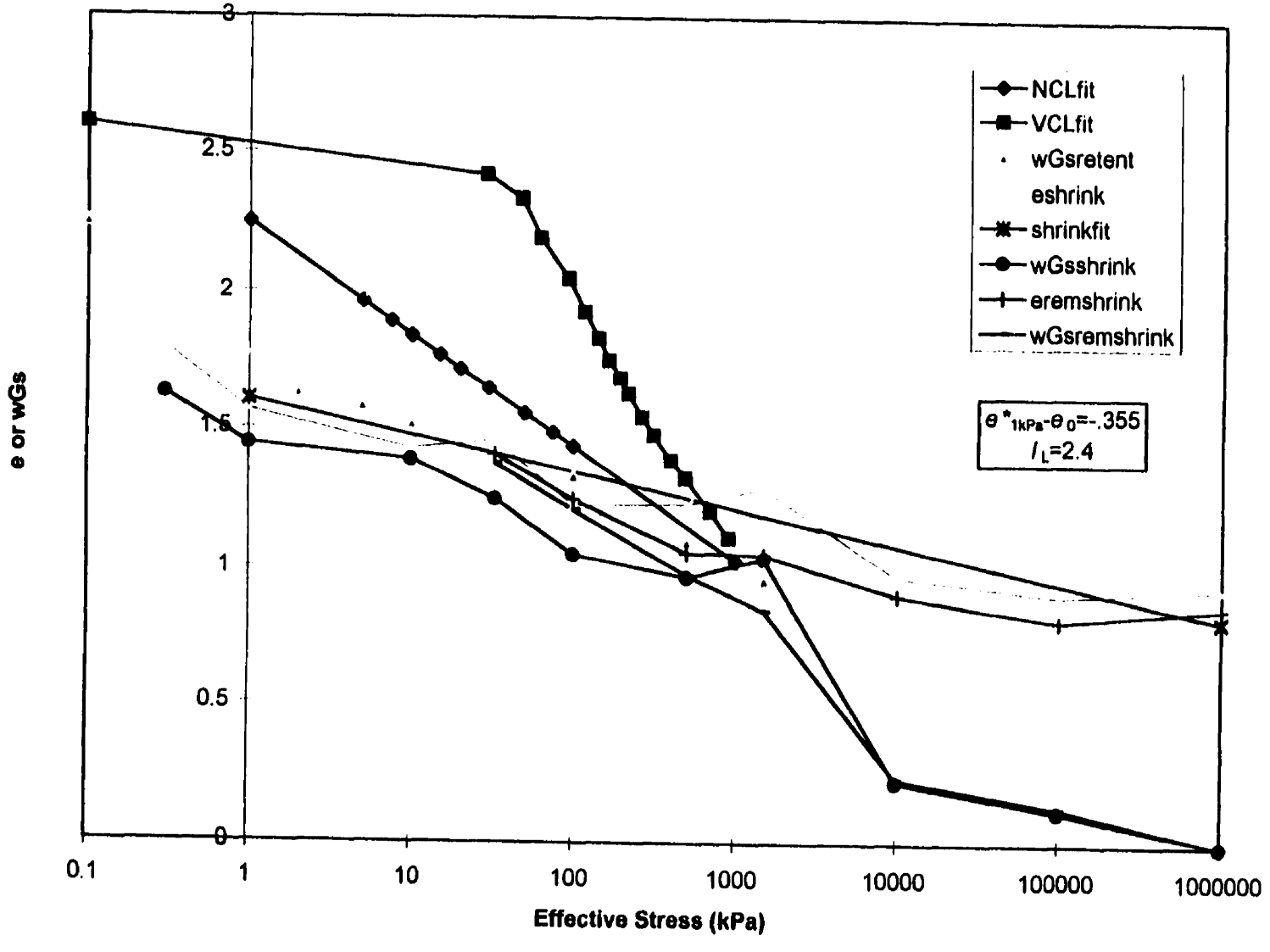

Figure 4.1 Combined mechanical test results for LBNA

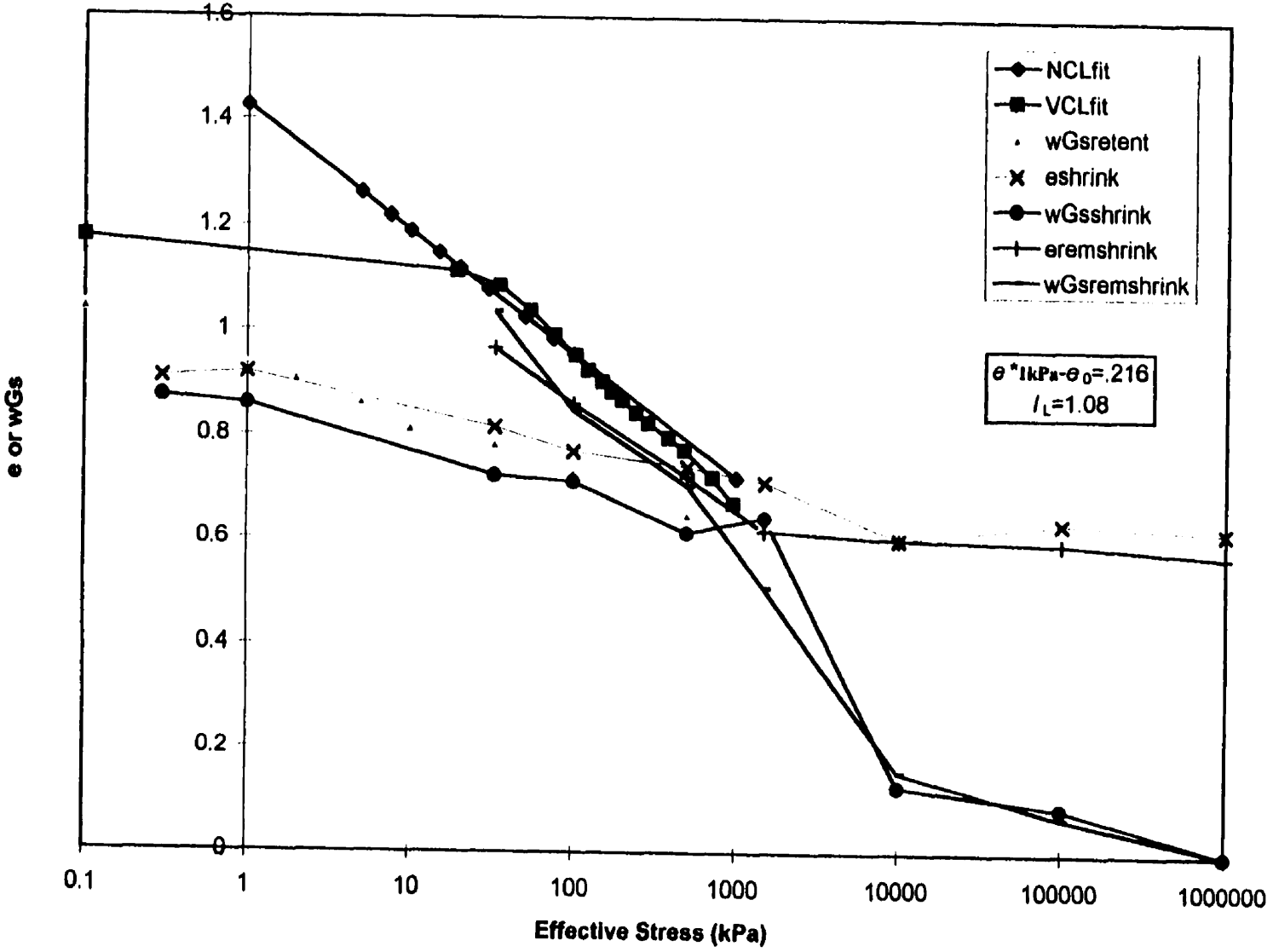

Figure 4.2 Combined mechanical test results for LBAA.

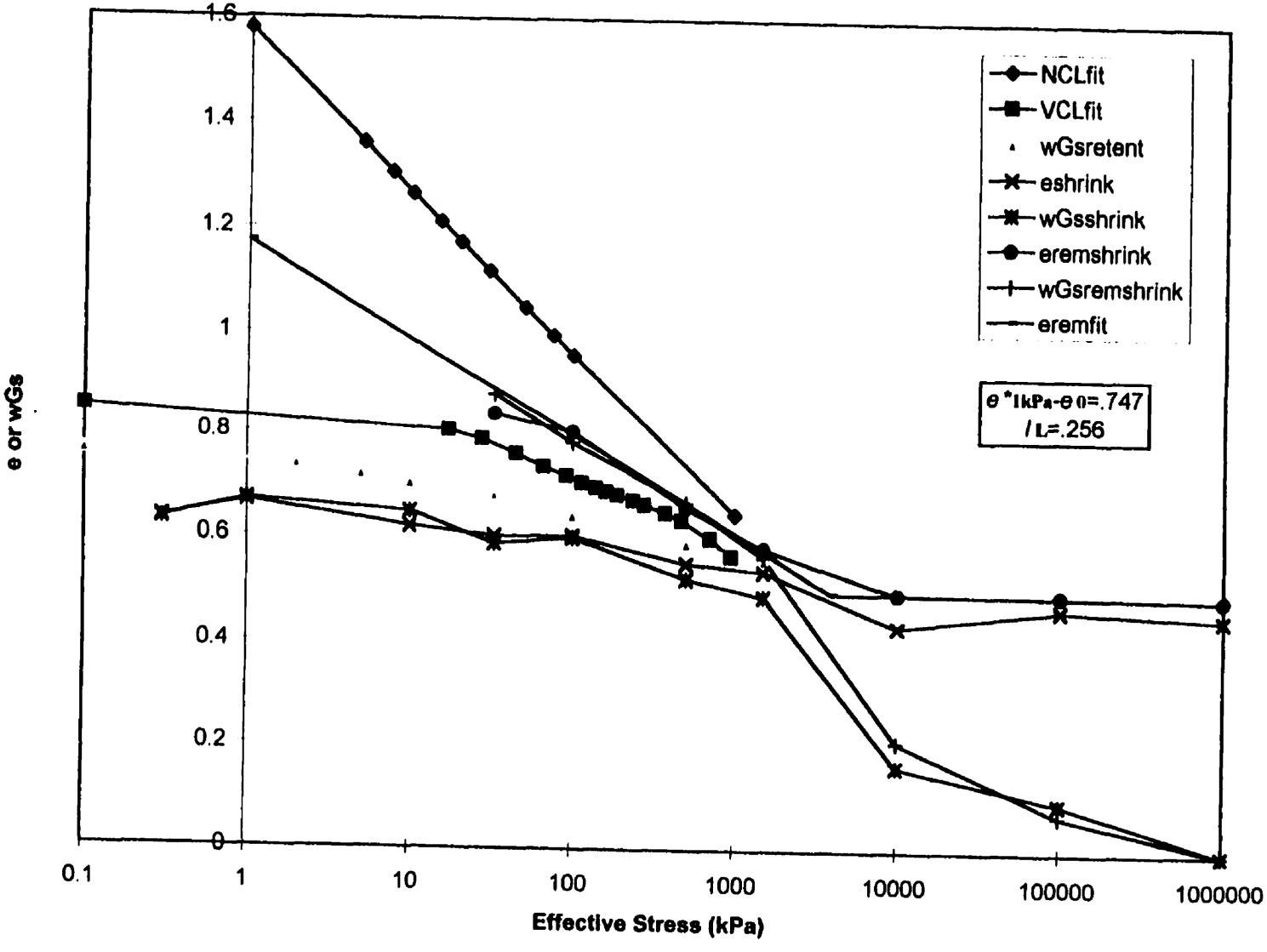

Figure 4.3 Combined mechanical test results for LBWB

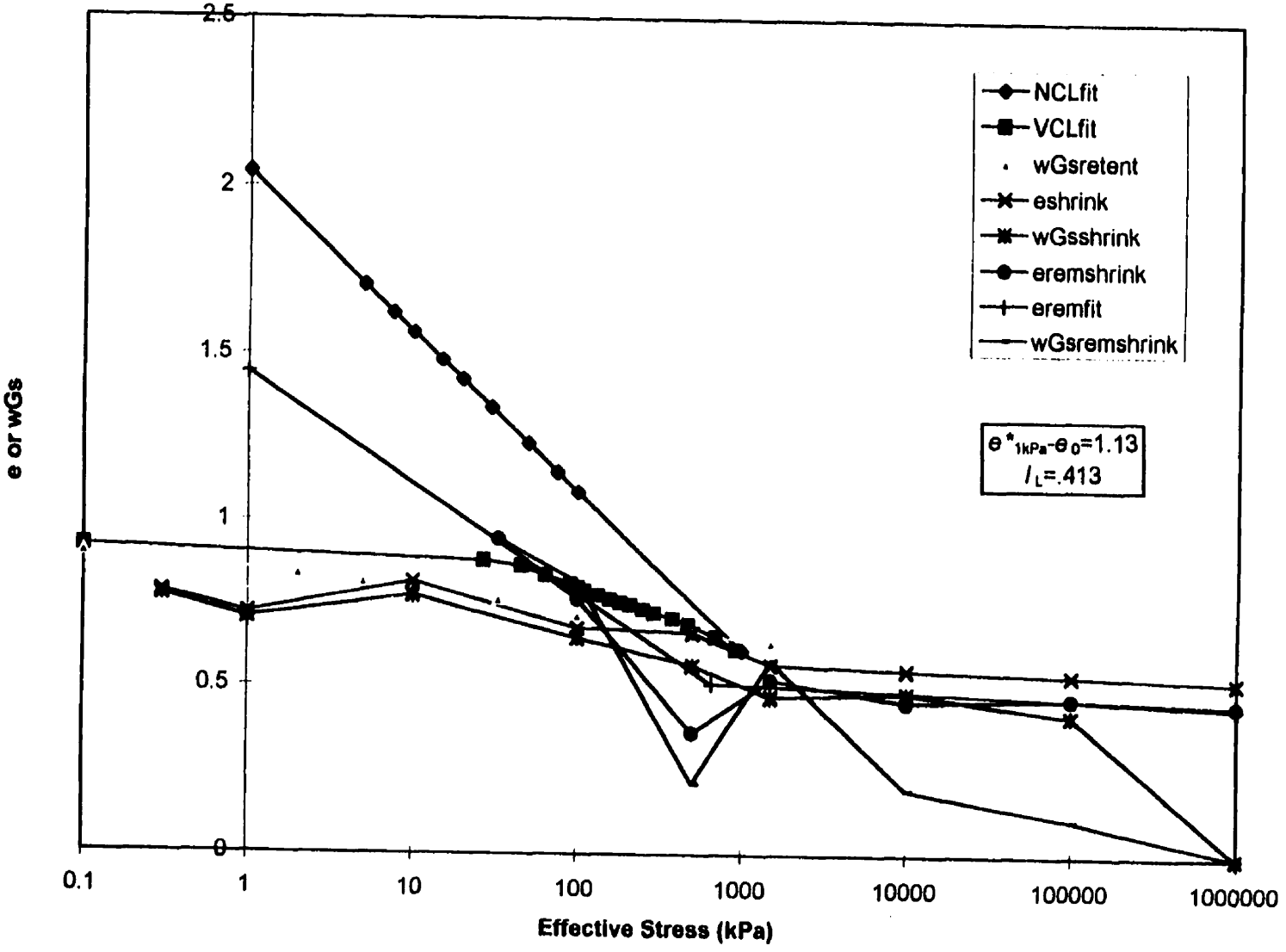

Figure 4.4 Combined mechanical test results for WAWC.

intra-aggregate porosities due to the large size of the sample, and the shrinkage represented intra-aggregate porosities due to the smaller size of clods and use of the kerosene method, with the differences disappearing once a sufficiently high stress was achieved to amalgamate aggregates (Chang and Warkentin, 1968). Bruand and Cousin (1995) looked at porosity changes in clay loam aggregates (3-4 mm diam.) during compaction. They found that at near saturated conditions (-1kPa), compaction at 50 and 200 kPa decreased structural porosity (pores > 18-50 μm diam.) and increased textural porosity (0.3-0.6 μm diam.) because of distortion (crushing) of structural pores. At a pressure of 600 kPa all structural porosity disappeared and only textural porosity remained (Bruand and Cousin, 1995).

In general, the remoulded shrinkage and compression indices (representing textural characteristics) seem to parallel each other due to the lack of any structural strength or bonding in either test. The main difference is the significant separation of the structured compression and shrinkage curves for the normally and under consolidated soils versus the closer (and almost overlapping for WAWC) alignment for the overconsolidated soils. The overconsolidated soils are saturated for a large part of the shrinkage curve. These trends appear despite the wide variability within the horizon subsamples. This portrayal of all tests in e or wG_s versus effective stress co-ordinates indicates that those soils with $(e^*_{1kPa}-e_0)>0.4$ or $I_L<0.5$ have little inter-aggregate porosity representing stable soil structure for microbial and plant root development since the compression and shrinkage curves nearly overlap; most of the porosity for these soils is intra-aggregate which does not contribute greatly to plant available water content or air-filled porosity (Bruand and Prost, 1987; Newman and Thomasson, 1979).

Other comparisons can be made directly comparing the statistical parameters derived for the compression and shrinkage curves. The remoulded shrinkage intercept, $e_{\alpha R}$ is significantly correlated to the intercept for the NCL equation (e^*_{1kPa}) (Figure 4.5). Several different groupings

of the horizons were analyzed based on A-line (Figure 4.6) and shrinkage grouping (Figure 4.5). The combination of horizons which gave normally distributed residuals for this comparison were the Group 1 soils, all soils but OTNA, CL & ML, or CH & CL horizons. For these combinations the intercepts were not significantly different from 0, but were around 0.1, and the slopes were always less than 1 (Range: b1=.63-.71, r^2=.593-.706, SEE=.133-.140). This indicates that the void ratio intercept for the remoulded shrinkage was always less than the void ratio intercept for the remoulded compression by about 65%. Both values are extrapolated from values below the range of the applied stresses on semi-logarithmic plots so there is the possibility for extrapolation errors. It is surprising the values are not closer given the similar sample size. It is also not known if the volume change response to tension is linear in this range and it is possible that the remoulded shrinkage curve meets the NCL with swelling. The remoulded shrinkage samples, however, are saturated through the lower stresses so the possibility of drainage of kerosene out of air-filled pores is quite low. The only other explanation is that the desorption allows deposition of particle bridging materials and volumetric shrinkage (rearrangement) in the sample while compression does not. There is additional water present in the compression sample compared to the shrinkage sample.

The larger intercept for the compression procedure (e^*_{1kPa}) is also linked to the larger absolute values for the slope of the NCL. The equation comparing $-C_C^*$ and n_{aR} is shown in Figure 4.7; this is the equation with the 5 single line segment models removed. The r^2 is slightly improved (r^2=.2969) if all 54 horizons are considered together but the SEE is larger. This relationship indicates that the tension stresses induce about 1/3 of the volume change as compared to equivalent applied stresses even under saturated (χ=1) and remoulded conditions. This is very likely because of the lack of shear stresses at points of contact (Burland, 1965 in Kirby, 1989). The additional water in the sample during compression may aid in lubrication and the sliding of particles past each other while the formation of particle bridges in the shrinkage samples may limit

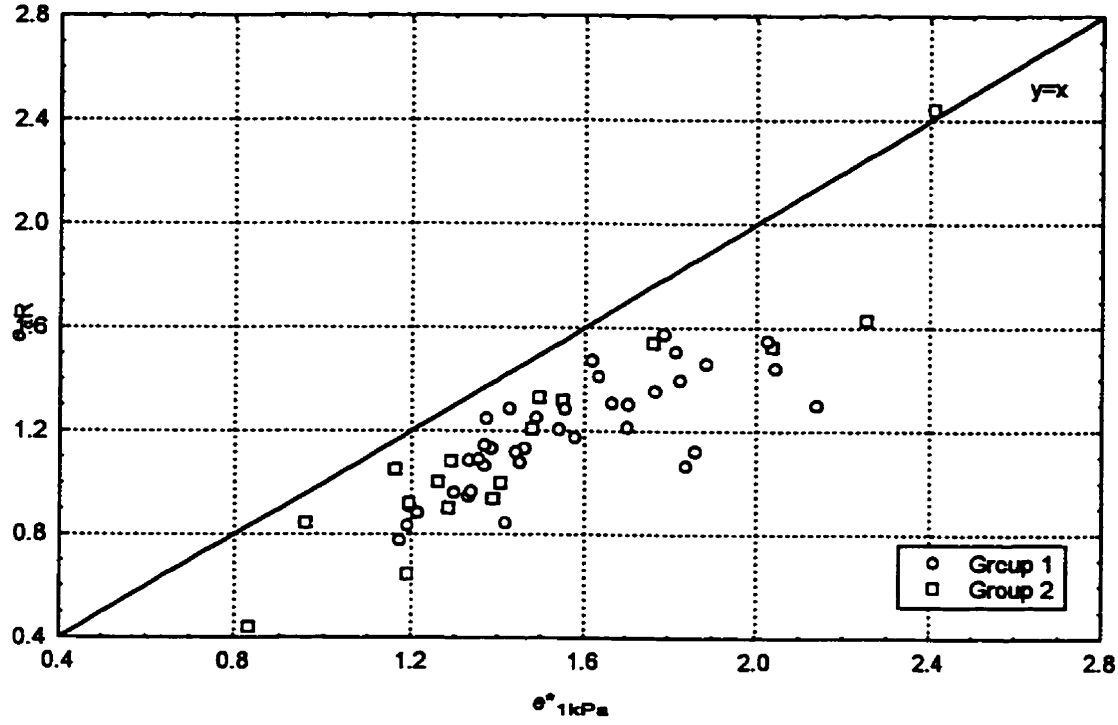

Figure 4.5. $e_{\alpha R}$ versus e^*_{1kPa} (Group 1 and 2).

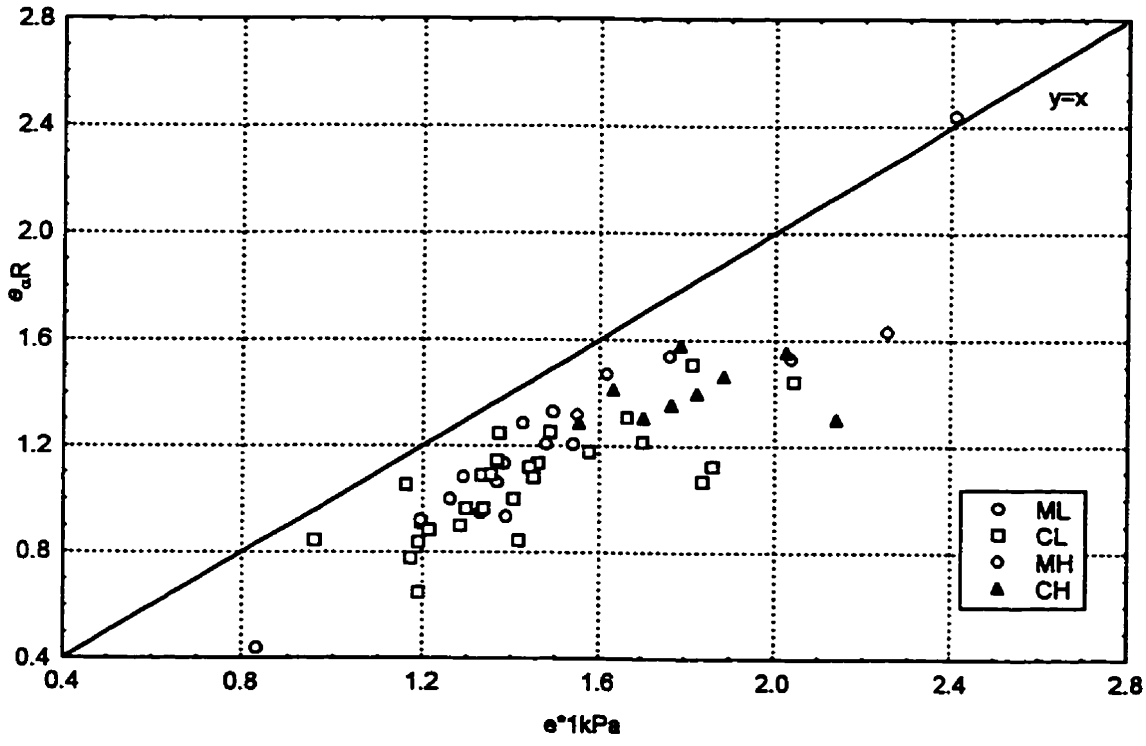

Figure 4.6. $e_{\alpha R}$ versus e^*_{1kPa} (A-line categories).

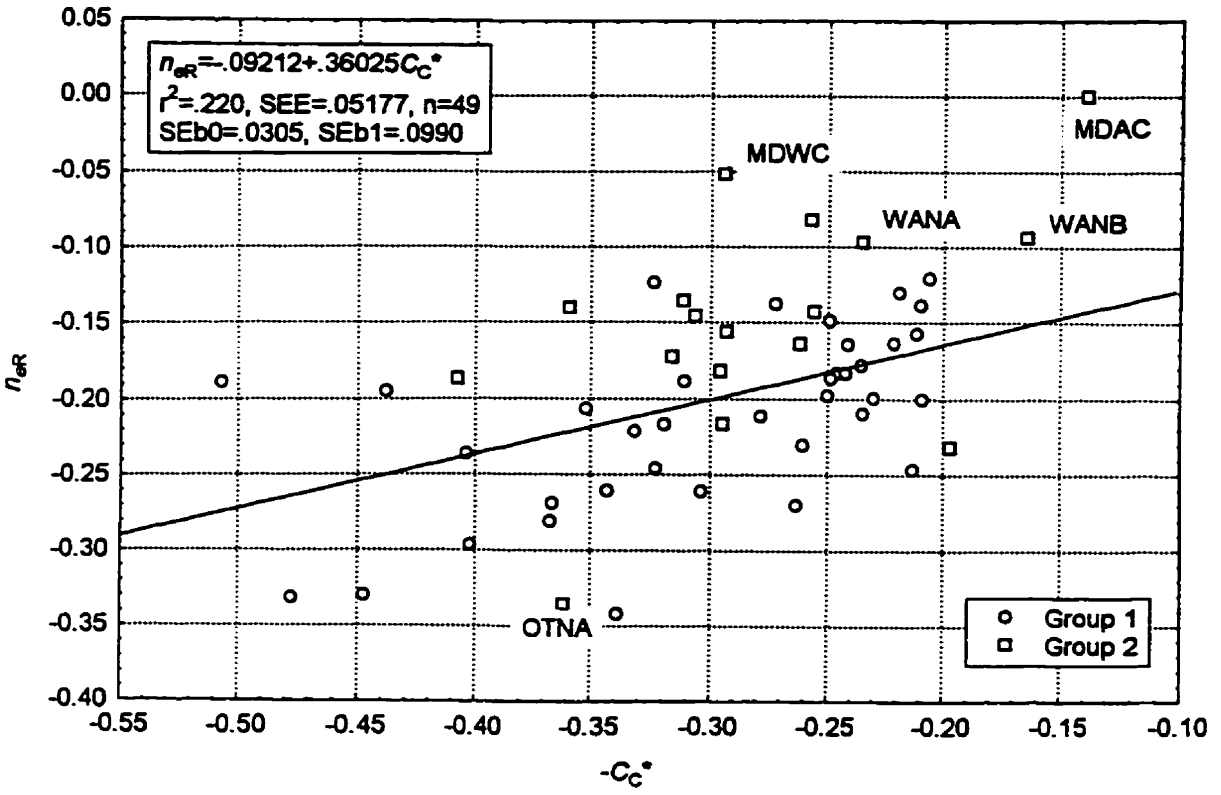

Figure 4.7. n_{eR} **versus** $-C_C^*$.

their volume change (Craig, 1992). Rahardjo and Fredlund (1995) found the coefficient of consolidation to be higher for the consolidation process (i.e. faster pore-water pressure dissipation) than for an increasing matric suction process. The consolidation process caused by an increase in total stress was not as effective as the increasing matric suction process in expelling water from an unsaturated soil (Rahardjo and Fredlund, 1995).

There are only10 horizons which approach a 1:1 relationship between the remoulded shrinkage and compression curves: OTNA, TXNC, TXNB, LBNB, LBAA, MDAB, HLNB, OTNB, OTAC, OTAB. Several of these horizons occurred as "outliers" in the data; though theoretically correct they do not represent what happens for the majority of the soils. The remoulded shrinkage and compression slope results are similar in that the presence of organic carbon acts to lessen the steepness of the normal portion, while larger clay contents increase the slope.

The stress at the w_L was derived from the $e(\sigma')$ remoulded model parameters. There was no relationship between the σ'_{wL} derived from the remoulded shrinkage and compression tests likely due to the close relationship between the e_{wL} and the $e_{\alpha R}$ at -1 kPa described in the remoulded shrinkage results; a 1:1 relationship for CL and ML soils (Section 3.3.1.2, Figure 3.26). This was true for the remoulded compression results as well, i.e. the e^*_{1kPa} was closely related to the e_{wL} (Section 2.3.2.4). In [Eq. 2.38] there was a slope not significantly different than 1 (0.91) but a positive intercept such that the intercept was always larger than the e_{wL} by 0.44. This is similar to the $(e^*_{1kPa}-e_0)$ threshold of 0.4 and explains why a difference >0.4 corresponds to a liquidity index <1.0. Thus for the remoulded samples at +1kPa the void ratio is larger than e_{wL} and at -1kPa the void ratio is at the e_{wL} or a constant for CH and MH soils.

The $e_{\alpha S}$ is closely related to the e_0 from the compression tests with the void ratios from the shrinkage significantly less than from the compression measurements (Figure 4.8). The effect of

analyzing the 2 groups separately is for the intercept to become not significantly different than 0 and the slopes to increase but the residuals become non-normal for the Group 1 soils alone. It makes sense for the void ratios in the compression chambers to be larger since larger inter-ped pores would be included in the total volume measurement and a fixed total diameter is assumed while smaller units and pores are sampled for shrinkage. The $e_{\alpha S}$ is essentially smaller than e_0 by 65%.

There is a significant relationship between the structured C_C' and the n_{eS} when 4 outliers are removed (OTNA, HLWB, HLNA and MDNC) (Figure 4.9). The specific reasons for HLWB being an outlier could not be discerned except statistically. There was no significant relationship for the Group 1 soils if they were analyzed alone, but there was a significant relationship for the Group 2 soils.

n_{eS}=.02139+.18602(C_C') [3]

SEb0=.0160, SEb1=.0359, r2=.673, SEE=.0248, n=15

There is a significant relationship between the relative intercept variables in the compression (e^*_{1kPa}- e_0) and shrinkage tests ($e_{\alpha R}$- $e_{\alpha S}$) (Figure 4.10). If the Group 1 soils are analyzed alone, the intercept becomes not significantly different from 0, the slope increases and the SEE improves slightly. If just those soils with % organic carbon > 4 are removed (n=7), the r^2 also improves and the relationship becomes:

($e_{\alpha R}$- $e_{\alpha S}$)=.0664+.5143(e^*_{1kPa}- e_0) [4]

SEb0=.0401, SEb1=.0718, r^2=.533, SEE=.1371, n=47

Essentially the relative intercept variable magnitude for the shrinkage test is half that of the compression test. This is due to the shrinkage void ratio intercepts being about .65 that of their compression counterparts. Therefore, below a ($e_{\alpha R}$- $e_{\alpha S}$) value of 0.20-0.26 (50-65% that of the 0.4 value suggested for compression), the saturated liquidity index starts to exponentially increase

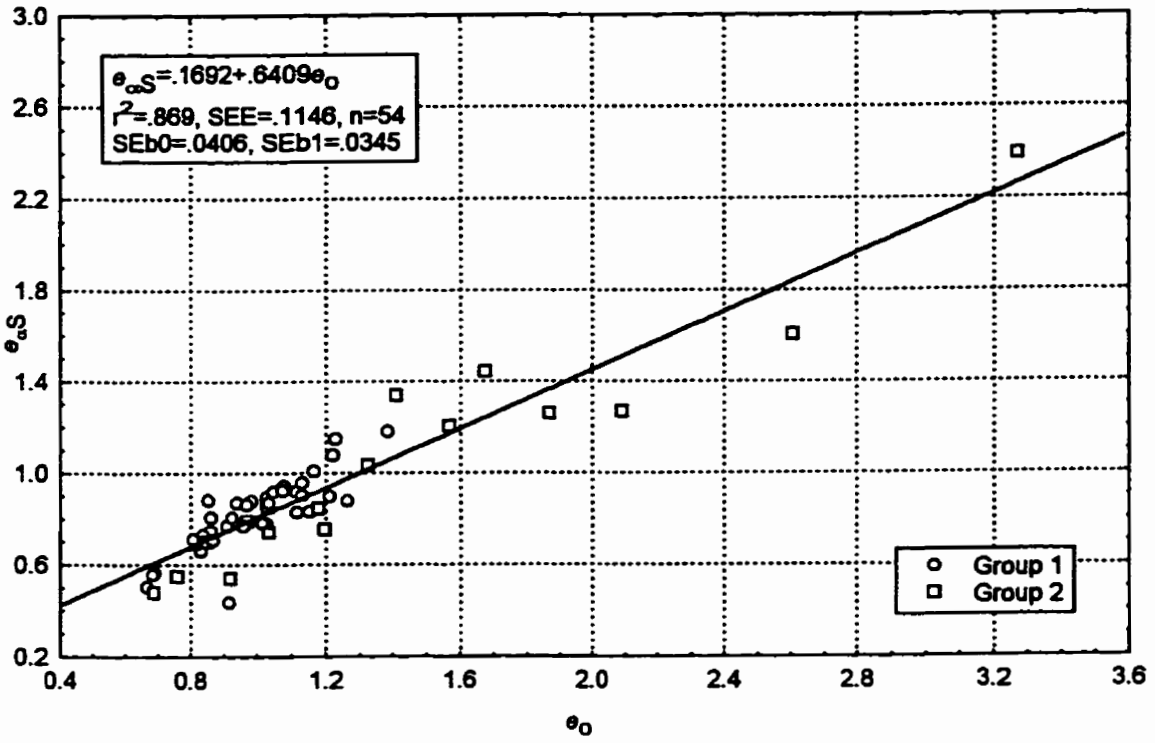

Figure 4.8. $e_{\alpha S}$ **versus** e_o.

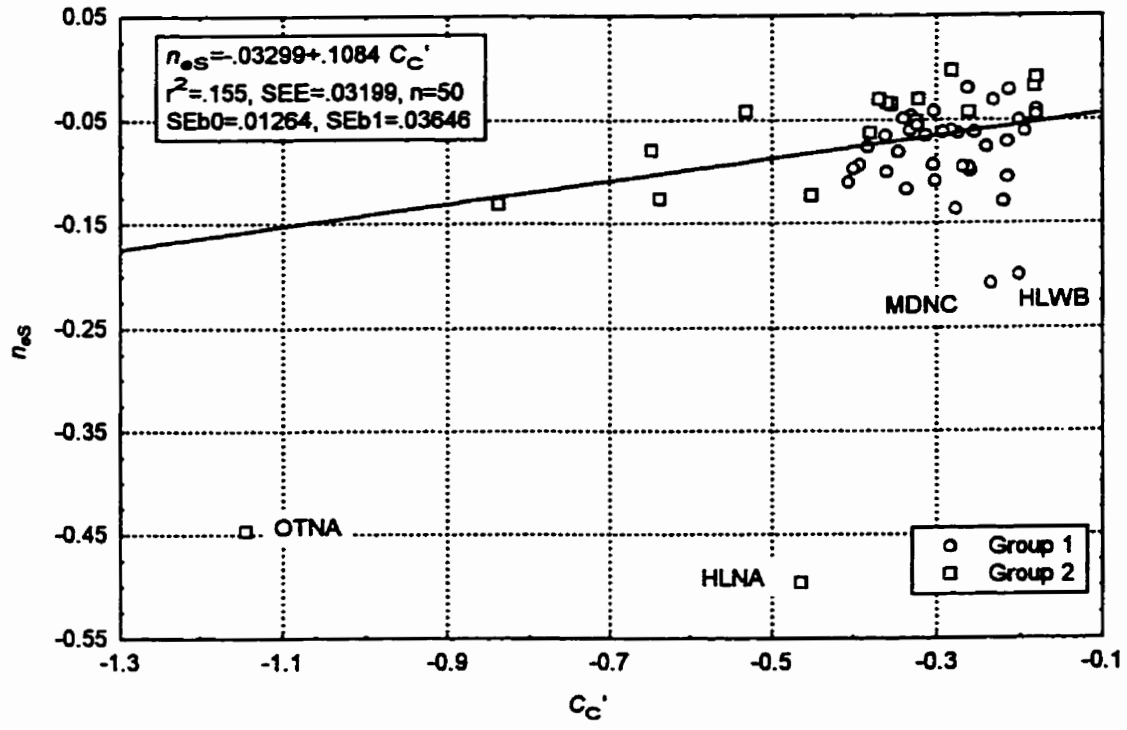

Figure 4.9. n_{eS} **versus** C_C'.

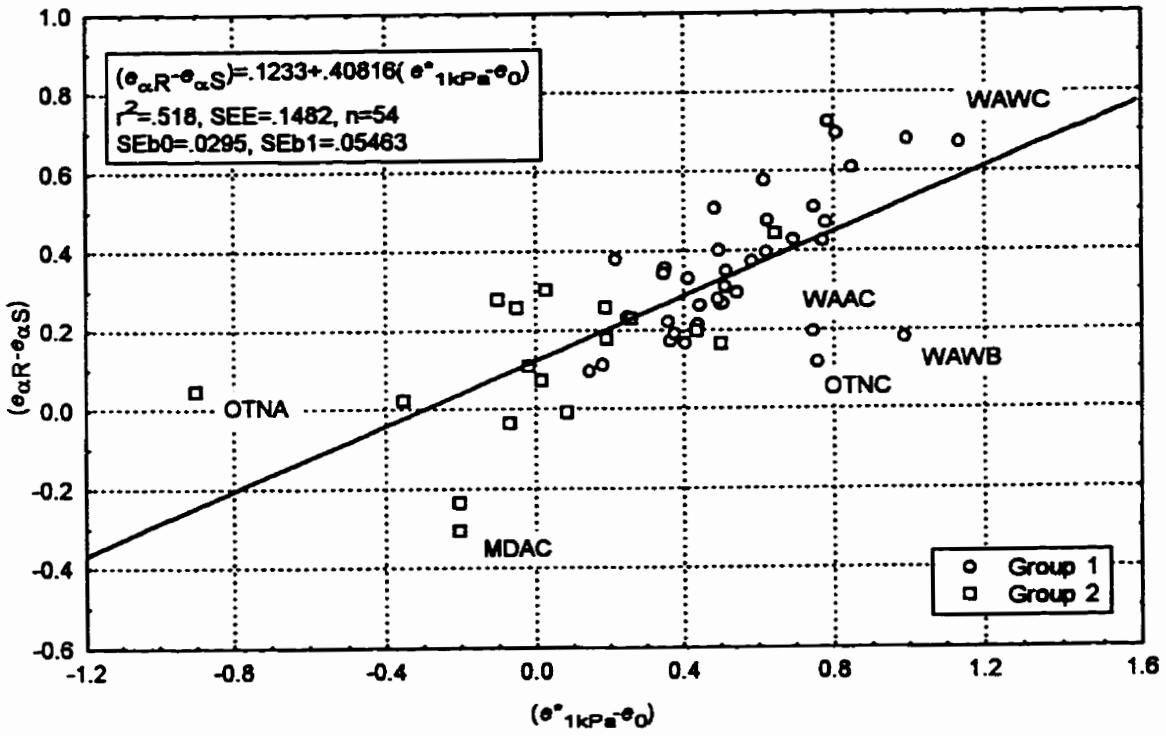

Figure 4.10. ($e_{\alpha R}$- $e_{\alpha S}$) versus (e^*_{1kPa}- e_0).

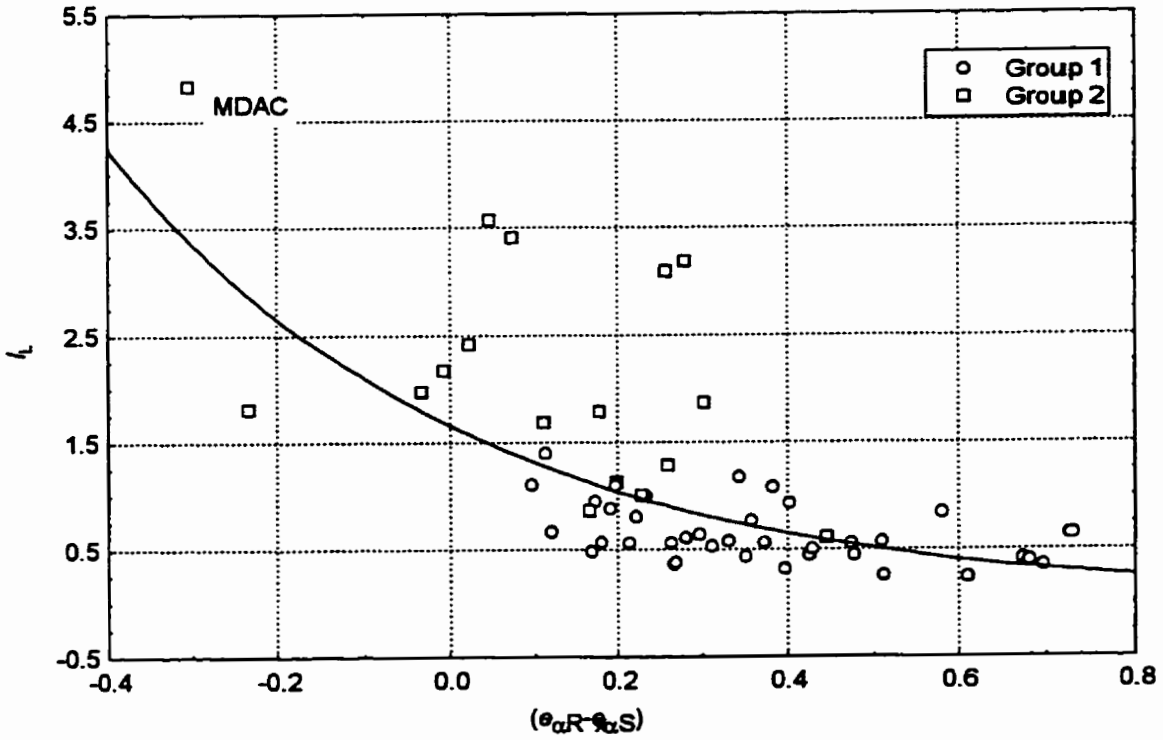

Figure 4.11. I_L versus ($e_{\alpha R}$- $e_{\alpha S}$).

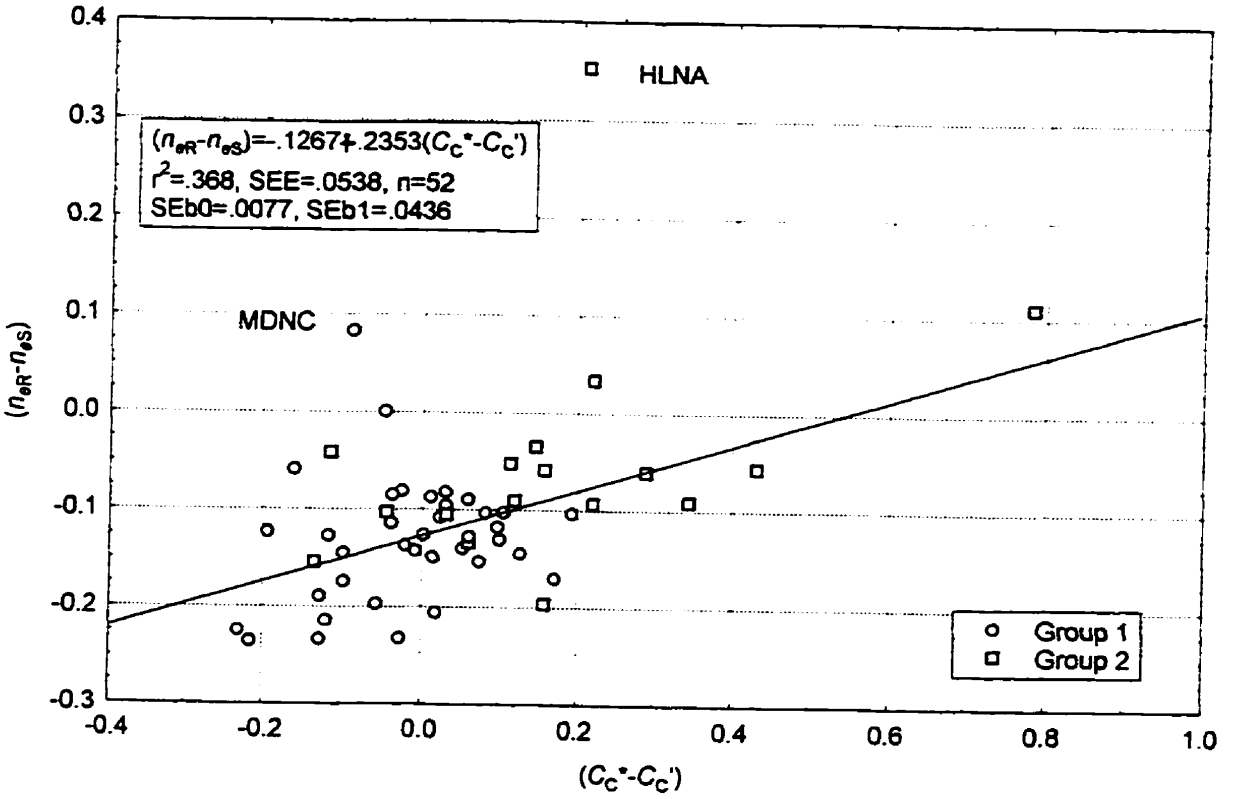

Figure 4.12. $(n_{\sigma R}- n_{\sigma S})$ **versus** $(C_C^*- C_C')$.

similar to that for the compression parameter (Figure 4.11).

There is a significant relationship, with normally distributed residuals if 2 outliers (HLNA and MDNC) are removed, between the relative difference slope parameters for the shrinkage and compression (Figure 4.12). These are the 2 outliers from the shrinkage data which had the structured shrinkage limit stress at incredibly low values (under -10 kPa) and so the portion of the shrinkage curve being measured is questionable; as well the actual shrink swell potential of these horizons is low (MDNC had a negative $COLE_{Struc}$ value). For all but 4 horizons the remoulded shrinkage slope was steeper than the structured while the compression slope differences were split.

It is difficult to use shrinkage parameters to measure structural quality because of the variety of pore-size distributions and their effect on the distribution of stress throughout the sample and the shape of the shrinkage characteristic curve. Figure 4.13 illustrates the increasing variability in the structured "normal" slope parameter away from a value of 1 as the size of the pores, as measured by plant available water content, increases. Above 10% AWC the under- and normally consolidated soils dominate and it is these soils which do not have a consistent "normal" structural phase as predicted by several researchers (Stirk, 1954). The role of the structural and residual shrinkage phases becomes more important in well structured soils. The difficulty in creating conditions to consistently measure these phases (D. McGarry, personal communication) means that shrinkage indices are unlikely to replace other accepted measures of structural quality such as water retention/pore size distributions, wet aggregate stability, and least limiting water range. Figure 4.14 presents the same information divided by the 2 shrinkage groups which illustrates the role of clay and organic carbon content in determining the shrinkage and consolidation behaviour of soil as the 2 figures are very similar. Thus the information contained in soil survey data is potentially useful for predicting the shrinkage and compression behaviour in the field.

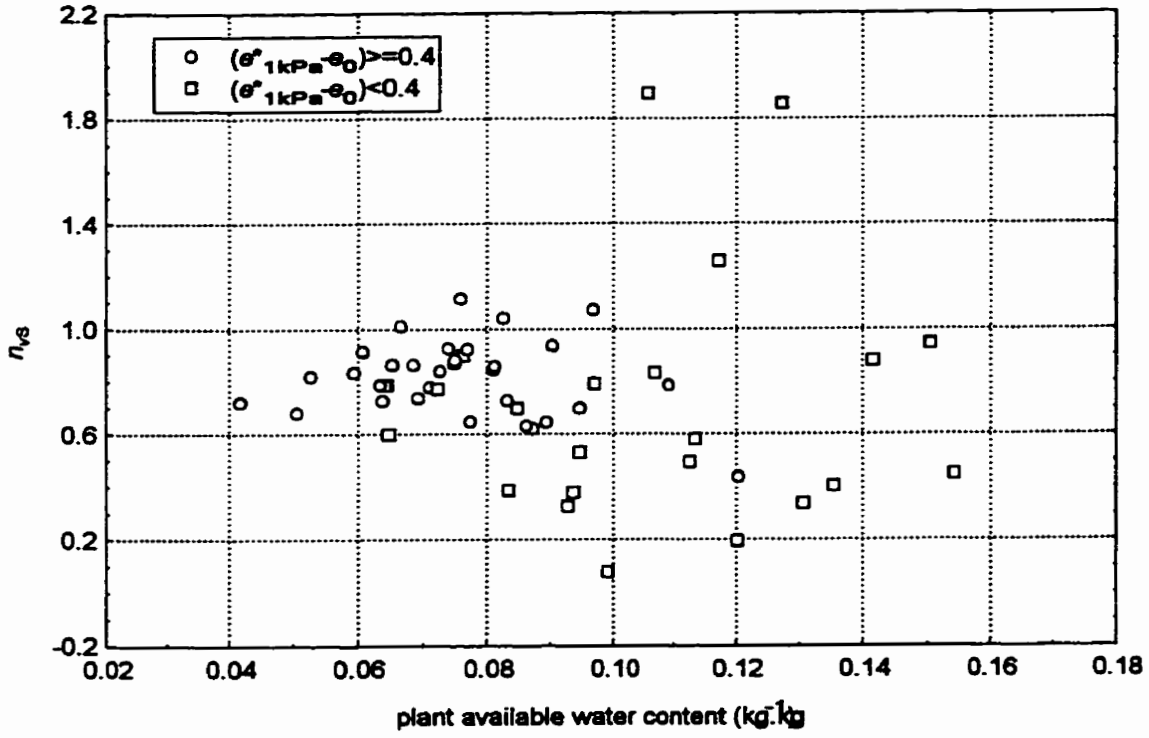

Figure 4.13. n_{vs} versus available water content (Threshold $(e^*_{1kPa}-e_0)$ values).

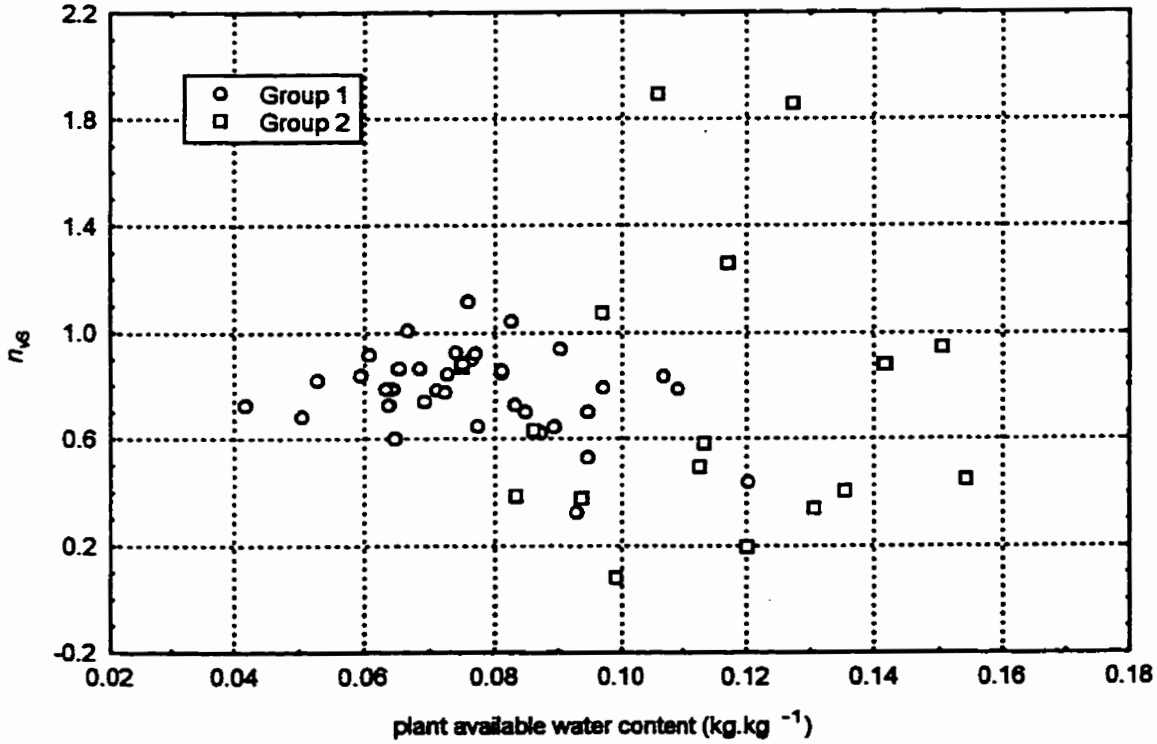

Figure 4.14. n_{vs} versus available water content (Shrinkage Group 1 and Group 2).

4.3 Conclusions

In many ways the compression and shrinkage tests and parameters were analogous. Both compression and shrinkage plots in $e(\sigma')$ co-ordinates showed converging behaviour of remoulded and structured samples. Almost all structured shrinkage curves were displaced below the remoulded curves and there was a greater displacement when the soils were severely overconsolidated. A threshold of 0.40 for $(e^*_{1kPa}-e_0)$ or 0.25 for $(e_{\alpha R}-e_{\alpha S})$ indicated severely overconsolidated soils with severe plant growth limitations for all mineralogies and land use treatments. The smaller threshold for the shrinkage parameters reflected the observation that the shrinkage void ratios were ≈65% of the compression void ratios.

The remoulded samples had generally overlapping ranges in volume change ratio (C_C* and $n_{\alpha R}$) although the corresponding $n_{\alpha R}$ were 0.36 times the C_C*. The structured samples had mutually exclusive shrinkage ($n_{\alpha S}$) and compression (C_C) volume change ratios. There also appear to be differences between the Group 1 and 2 soils as the slopes for the structured Group 1 soils had no relationship between the shrinkage and compression tests. Thus remoulded soils behave more similarly under mechanical or effective stresses, while structured soils resist effective stress deformation to a larger extent than compressive forces because of the gradual drainage of stable pores of various sizes and the presence of stable aggregates which inhibit shrinkage.

The linear relationships between the corresponding mechanical intercepts, slopes and relative indicators for compression and shrinkage tests suggest, at least partially, a scaling of structural quality through all structural aggregate sizes which resists both applied and internal stresses due to similar structural properties, even though the absolute values are smaller for shrinkage. There is still a large amount of variability unaccounted for in many of these linear relationships, with r^2 often around .50-.60, likely due to the heterogeneity of structured soils and the wide variety of soils sampled. Thus the analogy between the two types of stresses is not complete.

4.4 References

Bruand, A. and I. Cousin. 1995. Variation of textural porosity of a clay-loam soil during compaction. Eur. J. Soil Sci. 46:377-385.

Bruand, A. and R. Prost. 1987. Effect of water content on the fabric of a soil material: an experimental approach. J. Soil Sci. 38:461-472.

Chang, R.K. and B.P. Warkentin. 1968. Volume change of compacted clay soil aggregates. Soil Sci. 105(2):106-111.

Craig, R.F. 1992. Soil Mechanics. 5th ed. Chapman and Hall, New York.

Derdour, H., D.A. Angers et M.R. Laverdière. 1994. Comportement méchanique d'un sol argileux: Effets de la taille des agrégats, de la teneur en eau et de la pression appliquée. Can J. Soil Sci. 74:185-191.

Greene-Kelly, R. 1974. Shrinkage of clay soils: a statistical correlation with other soil properties. Geoderma. 11:243-257.

Guérif, J. 1982. Compactage d'un massif d'agrégats: effet de la teneur en eau et de la pression appliquée. Agronomie. 2:287-294.

Hettiaratchi, D.R.P. 1987. A critical state soil mechanics model for agricultural soils. Soil Use and Management. 3(3):94-105.

Hettiaratchi, D.R.P. and J.R. O'Callaghan. 1980. Mechanical behaviour of agricultural soils. J. Agr. Eng. Res. 25:239-259.

Ho, D.Y.F., D.G. Fredlund and H. Rahardjo. 1992. Volume change indices during loading and unloading of an unsaturated soil. Can. Geotech. J. 29:195-207.

Horn, R. 1988. Compressibility of arable land. p. 53-71. *In* J. Drescher et al., (ed.) Impact of water and external forces on soil structure. Catena Supplement 11. Catena-Verlag, Cremlingen-Destedt, Germany.

Kirby, J.M. 1989. Measurements of the yield surfaces and critical state of some unsaturated agricultural soils. J. Soil Sci. 40:167-182.

Kirby, J.M. 1991. Critical-state soil mechanics parameters and their variation for vertisols in eastern Australia. J. Soil Sci. 42:487-499.

Leeson, J.J. and D.J. Campbell. 1983. The variation of soil critical state parameters with water content and its relevance to the compaction of two agricultural soils. J. Soil Sci. 34:33-44.

McGarry, D. 1988. Quantification of the effects of zero and mechanical tillage on a Vertisol by using shrinkage curve indices. Aust. J. Soil Res. 26:537-542.

Newman, A.C.D. and A.J. Thomasson. 1979. Rothamsted studies of soil structure III: Pore size distribution and shrinkage processes. J. Soil Sci. 30:415-439.

O'Sullivan, M.F., D.J. Campbell, and D.R.P. Hettiaratchi. 1994. Critical state parameters derived from constant cell volume triaxial test. Eur. J. Soil Sci. 45:249-256.

Petersen, C.T. 1993. The variation of critical-state parameters with water content for two agricultural soils. J. Soil Sci. 44:397-410.

Rahardjo, H. and D.G. Fredlund. 1995. Experimental verification of the theory of consolidation for unsaturated soils. Can. Geotech. J. 32:749-766.

Toll, D.G. 1990. A framework for unsaturated soil behaviour. Géotechnique. 40(1):31-44.

Towner, G.D. 1983. Effective stresses in unsaturated soils and their applicability in the theory of critical state soil mechanics. J. Soil Sci. 34:429-435.

Wires, K.C., W.D. Zebchuk and G.C. Topp. 1987. Pore volume changes in a structured silt-loam soil during drying. Can. J. Soil Sci. 67:905-917.

5. Image Analysis of Clay Orientation in Structured Samples

5.1 Introduction

Micromorphological studies which investigate the pattern or fabric of the matrix, as opposed to pattern and orientation of the pore space, are relatively rare in the soil science literature (McGarry, 1989; Terrible and Fitzpatrick, 1995), and are found more commonly in geologic/sedimentary literature where it has long been recognized that particle orientation plays a key role in defining depositional and stress patterns, as well as influencing the engineering properties of the soil (Collins and McGown, 1974; Smart and Tovey, 1982; Bennett et al., 1991). Important properties such as porosity, permeability and stress-strain behaviour are intimately tied to microfabric and physicochemical characteristics (Bennett et al., 1991).

It is the orientation of clay particles (phyllosilicate minerals < 2 μm in diameter) which is particularly informative in soil or geological studies because the platy morphology gives a clear major and minor axis with which to define random vs. parallel fabrics. In soils with > 30% clay content, any clast or grain material is essentially embedded individually in the clay matrix so the physicochemical nature of the clays determines the physical behaviour of the soil (Derbyshire, 1978; Dalrymple and Jim, 1984). Clay fabric is defined as the orientation and arrangement or spatial distribution of the solid particles and the particle-to-particle relationships (Bennett et al., 1991).

Numerous authors have put forward the concept of increased orientation of clay with various indices of soil structural degradation, eg. increased massive structure, decreased plant available water-holding capacity, increased bulk density, decreased porosity and decreased soil-shrinkage/swelling (Aitchison and Holmes, 1953; Stirk, 1954; Chang and Warkentin, 1968). McGarry (1989) found differences in size, location and orientation pattern of zones of striated clay in vertisols both 'never' cultivated and cultivated at contrasting water contents, with a view to indexing soil structural

degradation. Conversely, Oleschko et al. (1993) found no difference in the pattern of birefringence of the fine material among three management systems on vertisols in Mexico. Knowledge on how clay fabric may influence the mechanical behaviour of structured surface soils is less understood and this link between form and process is necessary to improve our understanding of natural soil systems.

In this work, and in previous work by Veenhof (1993), there was considerable displacement of the structured VCL and shrinkage characteristic below that of the remoulded NCL and shrinkage characteristic, respectively, for clay-rich (>35% clay content) and structurally degraded soils. Typically, a structured soil is expected to have void ratios greater than its remoulded counterpart at the same loading stress due to increased strength from organic and chemical bonds, within and between aggregates (Quigley and Thompson, 1966). The finding of structured soil void ratios less than their remoulded counterparts at similar stresses led to overestimation of the compressibility and preconsolidation stress of soils based on PTF2 (McBride and Joosse, 1996). Veenhof (1993) proposed that particle alignment (orientation) due to wetting and drying cycles, secondary consolidation or trafficking was maintained in the structured condition and was absent in the remoulded state which would have flocculated particles. It was not known at the time if the positioning of the structured compression curve below the remoulded curve occured naturally or only in cultivated soils.

Most of the studies involving image analysis of clay orientation have involved monomineralic (kaolin), saturated clays in carefully controlled stress conditions in triaxial apparatus or shear boxes (McKeyes and Yong, 1971; McConnachie, 1974; Morgenstern and Tchalanko, 1976; Smart and Leng, 1993; Bai and Smart, 1997). Collins and McGown (1974) found that natural soil microfabric was much more complex than previously reported. Single clay platelet arrangements of any form were rarely seen, whereas groups of clay platelets interacting in various forms and multi-level assemblages were commonly found (Collins and McGown, 1974; McConnachie, 1974). These 'partly discernible particle arrangements' are common in natural soils where it is difficult to discern the exact nature of particle

interaction and orientation, due to the aggregation of particles with clay, silt and chemical or organic compounds (Collins and McGown, 1974).

As soil dries, pore water films become thinner, and clay particles that were in suspension become oriented in the smallest possible volumes (domains) as the surface tension forces them against pore walls and mineral grains. Domains are groups of particles in which adjacent particles have approximately the same orientation, and which cannot be broken down into smaller groups on the basis of differences in the orientation of its constituent particles (McConnachie, 1974). The anisotropy of a clay is due mainly to these domains which appear to behave as a single anisotropic unit because of parallel orientation of the component individual grains (Morgenstern and Tchalanko, 1976). The domains do not appear to change in size with deformation (Bai and Smart, 1997). As stresses are applied, domains orient themselves perpendicular to the major principle stress and become more closely packed, suggesting rotations rather than rupture at points of contact (Quigley and Thompson, 1966; McConnachie, 1974; Bai and Smart, 1997). Increasing pressure is not accompanied by continuously increasing preferred orientation of the soil fabric elements; above a pressure of 10 kPa, increases in parallelism, if occurring, are reversible. Particle reorientation in the presence of a loading stress during the secondary compression phase may not be reversible (Craig, 1992; Quigley and Thompson, 1966). Quigley and Thompson (1966) found an aburpt increase in particle parallelism when the preconsolidation pressure was exceeded in a sensitive marine (Leda) clay. Bai and Smart (1997) found the oriented fabric due to shear in a kaolin to be limited to a narrow zone (.47 mm) and that there was little reorientation of the fabric in the rest of the sample.

Groenevelt and Parlange (1974), Sposito and Giraldez (1976) and Ferry and Olsen (1975) indicated that increased particle parallelism occurs as a result of soil drying and crusting in swelling soil. Sposito and Giraldez (1976) also suggested that the small domains of orientated particles may be arranged essentially parallel to the soil surface because of overburden pressure and limitations to lateral

swelling. Dalrymple and Jim (1984) used isotropic wetting and drying stresses on laboratory prepared samples of montomorillonite with various proportions of sand:silt and found that only skelsepic microfabrics, those associated with coarse/sand particles, can develop from wetting and drying stresses and that plasma separations in the matrix must either be inherited or caused by anisotropic stresses. Bui and Mermut (1988) quantified the amout of vosepic plamsic fabric (porostriated birefringent fabric) of smectitic soils from Saskatchewan and found the amount related to the fine clay content and to stress-strain forces in the solum due to wetting, drying and overburden pressures. Studies of oriented clay in naturally occurring illite/vermiculite mineralogy soils was not found except for references to illuviated clay features (McKeague et al., 1978; Stolt and Rabenhorst, 1991)

It is hypothesized that the proportion of oriented matrix present would, therefore, depend on the type, frequency, magnitude and duration of stresses, whether external forces or internal pore water pressures, as well as the amount and type of clay minerals present.

Scanning electron and transmission electron microscopes permit observation of individual clay particles and their orientation on a large scale (<0.01 mm^2) (Smart and Tovey, 1982). Polarized transmitted light microscopy of a resin impregnated sample has been found to yield the best integral view of shear zones, compared to SEM and TEM, and may be the best method to use for determining the direction of shear movement or other larger scale features (up to 4 mm^2) (McKeyes and Yong, 1971). Digital image analysis of both optical and scanning electron micrographs gave similar results for measured directions and degree of anisotropy (Bai and Smart, 1997). Optical microscopy takes advantage of the birefringence of the oriented clay minerals, which causes the incoming polarized light to be split into components parallel to the mineral optical axes. The resultant light intensity observed in the polarizing microscope is a maximum when the *c* axes of particles are oriented at an angle of about 45° to the direction of incoming polarized light and a minimum when the axes are parallel to the direction of light travel (McKeyes and Yong, 1971). Observation of this extinction phenomenon allows for the

determination of the orientation of individual clay particles as well as domains of oriented clay particles which can exhibit various patterns (McKeyes and Yong, 1971; McGarry, 1989; Bui and Mermut, 1988). Circularly polarized light has been preferred to crossed polars for micromorphological studies because it is not affected by orientation of the optical anisotropy (Fitzpatrick, 1984; Terrible and Fitzpatrick, 1995). The characteristic of extinction has been exploited in studies using different angles of crossed polarizers to determine domain orientation in kaolin(Bai et al., 1994; Bai and Smart, 1997) and to identify pores in alfisols, spodisols and mollisols (Xu et al., 1994).

Improvement of computer hardware systems to attach to microscopes and to handle the vast quantities of data generated, and the development of image analysis software in the last 20 years, have together made the automatic analysis of images possible. Most work has been done with grey-level images in which the image is segmented into binary images based on solids and pore space using fluorescent dyes (Koppi et al., 1992;Moran and McBratney, 1992; Mermut et al., 1992; McBratney et al., 1992). Increasingly, the importance of colour and different light polarizations and conditions in distinguishing micromorphological characteristics is being used to distinguish features other than pores (Protz et al., 1992; Terrible and Fitzpatrick, 1992,1995; Protz and VandenBygaart, 1998). These features are defined using multispectral or multilayer images in combination with remote sensing digital image processing software. Terrible and Fitzpatrick (1995) were able to classify strong, moderate and weak matrix anisotropism using supervised classification algorithms. Terrible and Fitzpatrick (1992) found unsupervised classification unsatisfactory due to limitations of the software (ERDAS) and possibly because they only allowed 6 classes, to correspond to the supervised classification, which could have led to misclassification. Other users of remote sensing software for micromorphological analysis have tended to use a large number of classes (>16) and then amalgamate classes for simplification (Protz and VandenBygaart, 1998).

The objective of the study was to determine if there was a relationship between the orientation of

the clay microfabric and the mechanical behaviour of the soils studied. There was displacement of the VCL below the NCL for B and C horizons in natural as well as agricultural and workspace conditions. This led to the hypothesis that natural drying/wetting and consolidation cycles of clay soils creates effective stresses which are equal to or greater than those imposed by anthropogenic sources or uniaxial compression, and that this "natural consolidation" imparts similar clay fabric orientation and mechanical properties as anthropogenic sources, leading to displacement below the NCL.

5.2 Materials and Methods

5.2.1 Sample Preparation

Structurally intact cores (5 cm high x 8 cm diam.) from 36 soil horizons were selected for image analysis. These horizons were from 5 of the 7 sites (described in Chapter 2) where there was most similarity in texture between profiles, there was a high enough clay content (>30%) to have a predominantly clay matrix, and which represented the different treatments and mineralogies sampled.

The soil cores were saturated for 2 weeks in deaired, distilled water similar to preparation for soils which were subjected to compression. Corresponding cores were compressed to 1 MPa and 1.25X the measured average preconsolidation pressure for the horizon prior to resin impregnation. Saturated samples were then prepared for thin sectioning following the methods of Fox et al. (1993). Samples where soaked in acetone for up to 3 weeks until water replacement was at least 99% complete as measured by the specific gravity of the acetone solution. Samples were impregnated under vacuum with a polyester resin and allowed to harden for 3 months.

Using a rock saw, impregnated samples were cut vertically and horizontally in a 1 cm thick slice. Samples of 4 cm x 6 cm (3 cm x 5 cm for compressed samples) were cut and polished from these slices (Figure 5.1). These were larger samples than typically used for geological likely

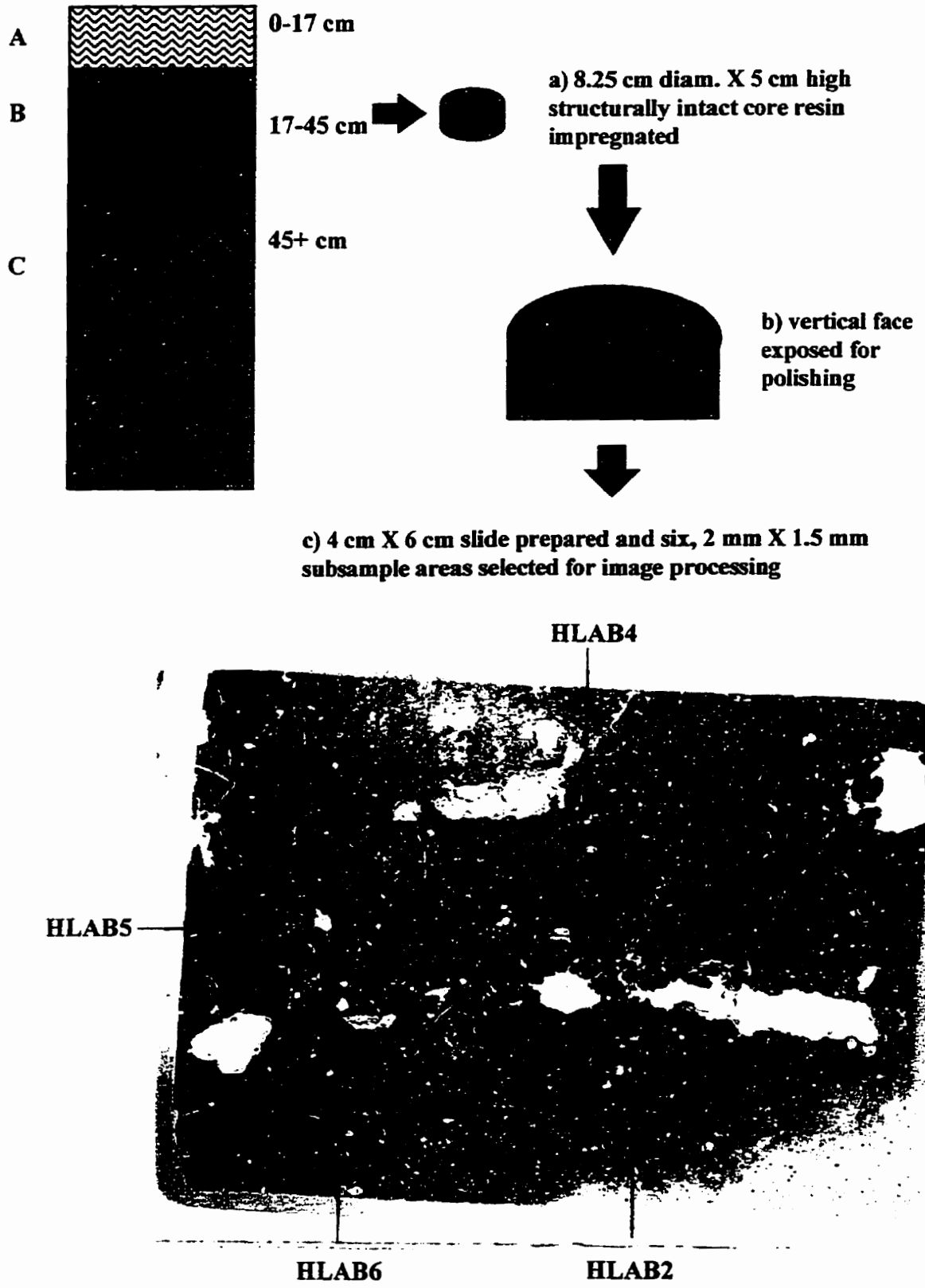

Figure 5.1 Sampling procedure for acquiring images (e.g. Chinguacousy Agricultural B horizon (HLAB)).

examination (2 cm X 2 cm). The sample size was intended to be representative of the soil horizon and comparable to the samples used for compression and shrinkage tests. Additional resin was added to the cut surface for those soils where the initial impregnation was poor, particularly for the compressed samples. The large size did pose some difficulty in preparation of the thin sections and resulted in only partial thin sections for some horizons. Thin sections were polished to 30-40 micron thickness, polished with diamond paste and cleaned with an ultrasonic cleaner. The thin sections were left uncovered.

5.2.2 Image Capture and Analysis

The method chosen for measuring the amount of optically anisotropic matrix was similar to that used by Terrible and Fitzpatrick (1995). The technique utilized a commonly available petrological light microscope equipped for plane and circularly polarized light illumination, a colour video camera and GIS software run on a desktop PC. This method of employing different light illumination/polarization, colour imagery and image analysis software to measure the amount of optically anisotropic matrix and other pedofeatures has gained acceptance in the soil micromophology community (Protz et al., 1992; Terrible and Fitzpatrick, 1995; Protz and Vandenbygaart, 1998). Additional benefits of this method were its economic feasibility and time efficiency which make it widely adaptable for most soil laboratories.

All thin sections were first observed and described under plane and cross polarized light using a petrological microscope. These preliminary observations revealed very little difference in the amount of matrix orientation between the different compression states as compared to between horizons and land use treatments. The decision was made to only study samples from the non-compressed state and the vertical orientation for this study to maximize the amount of information gained and minimize the amount of time needed. Lack of visual differences between stress states is

related to the complex nature of natural fabrics as compared to remoulded and monomineralic studies which have found increased parallelism with increased consolidation pressures (Collins and McGown, 1974; Quigley and Thompson, 1966; McConnachie, 1974).

Six subsample areas from each of the 36 slides were selected based on finding portions of the slide with similar/adequate thickness, minimum amount of pores and mineral grains, and maximum amount of matrix (Figure 5.1). It was attempted to avoid areas near pores and cracks where birefringence could be due to pedogenic processes such as illuviation of clay particles, weathering and biological activity. The goal was to measure the amount of orientation in the matrix and so those areas with a maximum amount of matrix were found. All potential areas were located and mapped on a scanned image of the slide for later reference. The scanned image was visually divided into 6 areas and a subsample image was taken, where possible, from each sixth of the slide to represent the variability.

Subsample areas were digitally captured as 24-bit colour (RGB) images using an optical petrological microscope (Zeiss Ultraphot II, Carl Zeiss) and video camera (COHU Inc., 8280 NTSC, San Diego, CA) under both plane polarized (PPL) and circularly polarized light (CPL) conditions. Light intensity was measured and maintained using a voltmeter on the filament at 4.6 ± 0.5V for the plane polarized images and 6.0 ± 0.5V for the circularly polarized images. Although the images were fairly dark, these light intensities were found to best illuminate all soil samples for full use of the 0-255 brightness scale without distortion around pore and grain edges.

Selection of magnification for the images was a compromise between the pixel size and the total area which could be covered. A 2.5 X objective and 1.6 X optivar were used. The camera head had 768 x 493 active picture elements which corresponded well with the 640 x 480 resolution TIFF file collected by the video digitizer (Snappy video snapshot, Play Incorporated, Rancho Cordova, CA). This produced a 3.1 x 3.1 micron pixel allowing a 1.99 x 1.49 mm area (≈3 mm^2) to be imaged at one time (Figure 5.2). Although this resolution does not identify individual clay

particles, it was deemed sufficient to capture interference colours from oriented clay domains overa sufficient portion of the matrix to be considered arising from stress patterns. The "highest quality still" setting amalgamated 8 fields of the incoming video signal to create the image.

Before each imaging session, the illuminating light was allowed to warm up for 1/2 hour. The light source, illuminator, condensers and objectives were centred using the Koehler principle (Inoué, 1986). Brightness and contrast levels on the video camera were kept constant by switching to manual settings. To eliminate any noise or shading, correction images were produced for background subtraction using a blue filter on the stage and capturing under plane and circularly polarized conditions prior to the daily imaging (Inoué, 1986; Terrible and Fitzpatrick, 1995). A single polarizer below the slide (vertically oriented to the image) was used to produce plane polarized light (PPL). Circularly polarized light (CPL) was used to identify all areas of anisotropy at one time since it eliminates the extinction which usually occurs with cross polarized light as the stage is rotated (Fitzpatrick, 1984). Two 1/4 wavelength mica plates were inserted below and above the slide at opposite 45 degree angles to polarizers above and below the slide to produce this light condition (Fitzpatrick, 1984).

The two colour images, PPL and CPL, were imported into IDRISI for Windows (IfW v.2, Clark University, Worcester, MA), a widely available and comparably affordable image analysis and geographic information system software package. The 24-bit TIFF files were imported as 3 band interleaved files with no georegistration as individual red, green and blue band images. The light correction image bands were histogram shifted so that 95% of the intensity difference was represented, and were subtracted from the corresponding image band. This minimized the absolute intensity value subtracted, so that the widest range of intensity values as possible was retained. No software image enhancements were done in order to maintain the integrity of the original data. The

a) Plane polarized light (PPL)-1.35 X 1.84 mm

b) Circularly polarized light (CPL) -1.35 X 1.84 mm

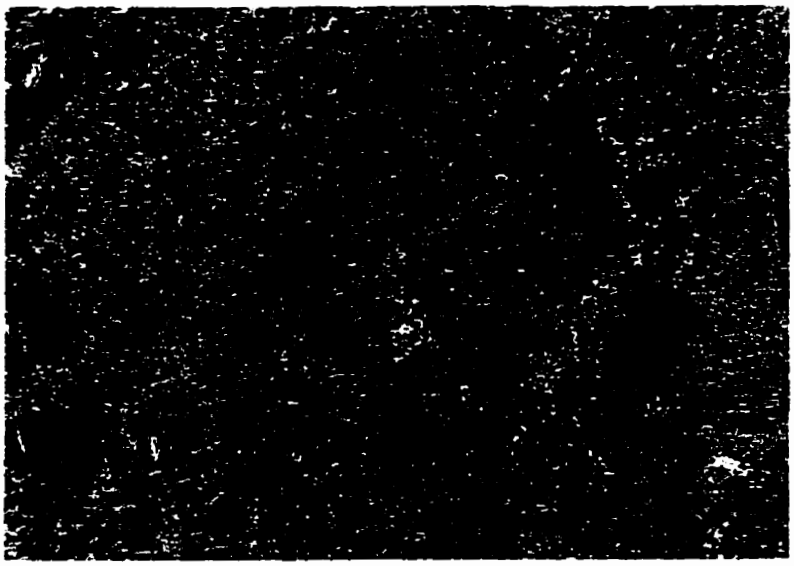

c) Unsupervised classified image from ISOCLUS procedure

d) Pedological features assigned using RECLASS function

Figure 5.2 Example of images used for feature analysis. Chinguacousy Agricultural B horizon (HLAB4).

2 sets of corrected image bands were then georectified by "windowing" the corresponding areas of the images so that they directly overlay each other (Figure 5.2). There was no circular or elliptical distortion as determined by selecting matching points of mineral grains on both images after cropping. The amount needed to shift for rectification varied from 0 to 40 pixels in the x or y directions which was later found to be due to a loose top polarizer. This made the resulting images slightly smaller than the original 640X480 pixels. These techniques are similar to those used by Terrible and Fitzpatrick (1995).

The ISOCLUS procedure in IfW 2 was used for unsupervised classification of the images. This procedure uses a 3 channel composite image from which initial signature clusters from the histogram CLUS algorithm are used to begin a Maximum Likelihood iterative procedure. From preliminary principal component analysis on diverse samples, it was decided to use the PPL blue and green channels and the CPL red channel to make the composite image for the ISOCLUS procedure for all images. These channels encompassed the most variability and had the lowest correlations to each other. In particular the PPL blue channel helps to identify pores while the CPL red channel reflects the grains and oriented matrix in circularly polarized light. The composite image is the signature class "seed" image and was composed using linear stretch with 1% saturation enhancement as suggested by the manufacturers. In the actual iterative cluster assignment process, the full set of 6 raw channels was used. Three iterations were recommended and found to be adequate to produce an image where all desired features could be identified visually using 20 classes. The histogram produced in the ISOCLUS procedure verified that 20 classes always encompassed 99% of the image. The 20 classes were then assigned using the RECLASS function to 1 of 9 pedological features (Table 5.1) (Figure 5.2). The PPL, CPL and classified images were all displayed at one time on the screen to aid in assigning classes to the various clusters. It was relatively easy to assign pore space, oxides and mineral grains. Portions of the image which were then matrix and appeared to have some birefringence in the CPL image were

classified as either weakly or strongly anisotropic depending on their brightness. The number of pixels in each feature class was then counted using the AREA function and these data were exported to Excel. The area of each feature as a proportion of the total area and the amount of anisotropic material as a proportion of the matrix only (total pixels- grains and pore pixels) were calculated in Excel.

Table 5.1. Feature classes used in assigning micromorphological features.

Class	Code	Feature
1	PORE	Void Space
2	MATRIX	Matrix (reduced)
3	MINERAL	Mineral grains
4	OXIDE	Oxides (oxidized matrix)
5	WEAK	Weakly anisotropic matrix
6	STRONG	Strongly anisotropic matrix
7	RESIN	Void space (coloured by resin)
8	BRIGHT	Bright minerals, thin matrix, edges
9	DARK	Dark matrix, organic materials, nodules

5.3 Results and Discussion

The feature proportions for the individual subsamples are presented in the Appendix. Presented here is a summary of data for all subsamples (Table 5.2) indicating the range in values for features found in the different soil horizons. The data are presented for each horizon as box plots utilizing median and quartile values, as the distribution for all horizons (n=216) or on a horizon basis (n=6) was rarely normal for any measured feature. The outlier values are 1.5X the difference between the 75% and 25% quartiles and extremes are 3X the difference. The wide variability in any one horizon also precluded the use of traditional statistics to determine significant differences.

Of primary interest was the percentage of the matrix occupied by oriented material. This information is presented in Figure 5.3. The data is arranged by horizon and by increasing clay

Table 5.2. Descriptive statistics and distribution for entire population.

Proportion of total area	Valid N	Mean	Confid. -95%	Confid. +95.0%	Median	Min.	Max.	Std.Dev.	Skewness	Kurtosis	Distribution (p<0.05)
PORES	216	.028028	.025032	.031024	.022619	0.000000	.151553	.022338	2.042875	5.98869	lognormal
MATRIX	216	.547233	.525649	.568817	.583857	.071023	.806449	.160937	-.900620	.25714	-
GRAINS	216	.041584	.037556	.045612	.034694	.003152	.201148	.030034	1.935271	5.77298	lognormal
OXIDES	216	.240344	.228522	.252167	.235666	.011132	.502436	.088154	.443652	.33988	normal
WEAK	216	.022793	.017782	.027803	.006632	0.000000	.232454	.037358	2.561379	8.09626	-
STRONG	216	.002897	.001759	.004036	0.000000	0.000000	.062226	.008488	3.750720	16.33283	-
RESIN	216	.021759	.019254	.024263	.017598	0.000000	.087972	.018675	1.085986	.74027	lognormal
BRIGHT	216	.043420	.038619	.048221	.035639	0.000000	.219152	.035799	1.699668	4.38541	lognormal
DARK	216	.051942	.033213	.070672	0.000000	0.000000	.653186	.139653	2.709216	6.31829	-
PORE+RESIN	216	.049786	.045525	.054048	.042197	.002432	.195511	.031777	1.167145	1.86454	lognormal
WEAK+STRONG	216	.025690	.019934	.031446	.006632	0.000000	.294680	.042920	2.652916	9.26434	-
Proportion of Matrix											
WEAK	216	.027695	.021158	.034233	.007149	0.000000	.376008	.048745	3.298877	15.62541	-
STRONG	216	.003560	.002069	.005052	0.000000	0.000000	.100654	.011119	4.757902	30.28404	-
WEAK+STRONG	216	.031256	.023683	.038828	.007149	0.000000	.476662	.056462	3.588769	19.76043	-

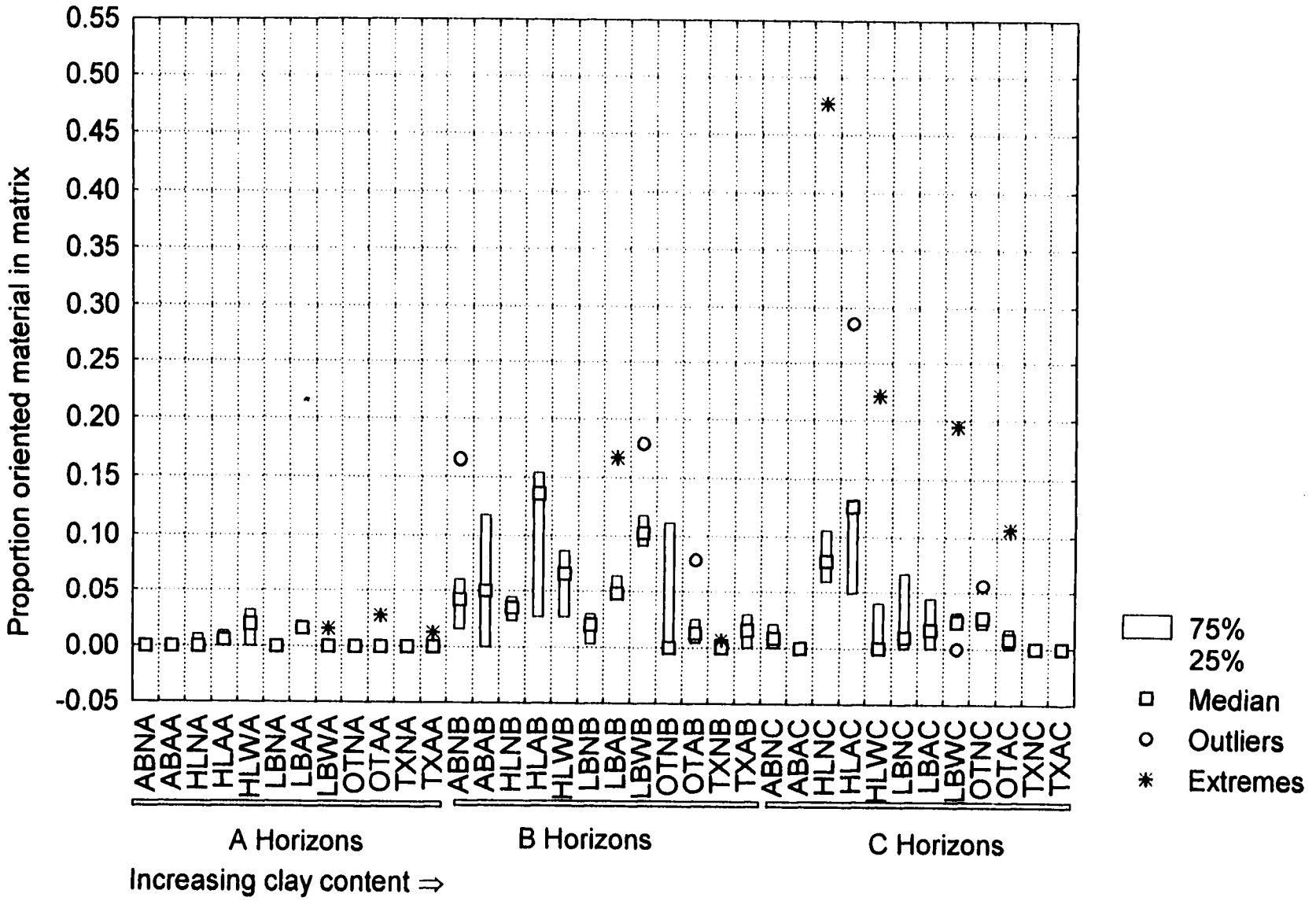

Figure 5.3. Proportion of matrix occupied by optically anisotropic material.

content by site to aid in visualizing trends. The median values are also summarized in Table 5.3.

Table 5.3. Median values for proportion of oriented material in matrix by horizon and land use.

Median (n)	Land Use			
Horizon	Natural	Agricultural	Workspace	All Land Uses
A	.0000 (30)	.0000 (30)	.0000. (12)	.0000 (72)
B	.0182 (30)	.0324 (30)	.0889 (12)	.0300 (72)
C	.0172 (30)	.0000 (30)	.0218 (12)	.0100 (72)
All Horizons	.0000 (90)	.0073 (90)	.0239(36)	

It can be seen that the Natural A horizons had virtually no orientation in the matrix. These were the soils which were under- or normally consolidated, except for TXNA which had an (e^*_{1kPa}-e_0) value of 0.543, and for which the VCL was below the NCL. The B horizon proportion medians are higher than the A or C proportion medians in any one profile, except for HLNB and OTNB where the C horizons have higher median values; the OTNB variability, however, encompasses that of the OTNC horizon. The higher proportion of oriented matrix suggests that the B horizons receive greater natural and anthropogenic stresses than those experienced by the C horizon, and that stress induced orientation is preserved in the B horizon due to lack of bioturbation or tillage as would occur in the A horizon. The greater amount of oriented matrix in the B horizons could also be due to pedogenic, illuviated clay features although pores were attempted to be avoided while sampling. Inclusion of some illuviated clay was not of great concern as it was the amount of clay oriented in the tightest possible arrangement which was expected to influence mechanical behaviour regardless of its origin.

An ANOVA utilizing the log transformed proportions and TRT and HOR factors found no interaction term. HOR was significant at the 5% level and TRT at the 10% level; Table 5.4 presents the results. Log transformation resulted in the omission of several horizons with zero

values, so Tukey's HSD for unequal sample sizes was used for mean separation.

Table 5.4. Results of ANOVA for log(Proportion of oriented material in matrix).

HOR	Back transformed Mean	TRT	Back transformed Mean
A	.0167 a	N	.0227 a
B	.0477 b	A	.0308 ab
C	.0400 b	W	.0457 b

Optically anisotropic material occurs in the Natural B horizons which may be due to naturally occurring wetting and drying cycles, illuviation, weathering or biological activity. The proportion of oriented matrix for the Nat B horizon at any one site has a lower median compared to the Agricultural and Workspace B horizons suggesting there are likely anthropogenic in addition to natural factors at work. The only horizons with medians > 0.05 are LBAB, LBWB, HLNC, HLAB, HLAC, HLWB, ABAB, indicating there is additional orientation of domains caused by applied anisotropic anthropogenic stresses.

The HLNC horizon is a curiosity since it had a high amount of oriented matrix yet had not experienced anthropogenic stresses. All Halton (Chinguacousy) horizons also represent the highest and most widely varying proportions of oriented material found (Figure 5.3). It is the only soil imaged with till parent material and imperfect drainage. It is probably a combination of these two factors which impart more anisotropic material in addition to anthropogenic stresses. The imperfect drainage would allow frequent wetting and drying cycles throughout the profile to induce the orientation of domains. The other two till sites were not imaged.

The Chinguacousy and Brookston B and C horizons tended to have the highest and more extreme values for orientation and both had till parent material. It is only the B horizons of the smectite containing soils which exhibit any significant (>1%) microfabric orientation. The agricultural B horizons have slightly higher values than the natural horizons. Overall the Texas

soil had very little orientation evident which was surprising given the potential for the presence of slickensides. The microscopic view revealed a fine pore network and a grainy appearance because of the many small aggregates in the swollen state. It was likely that slickenside faces were not included in the sampling of cores as major pressure induced movements occurred at depths greater than that sampled for the B horizon (35-40 cm) (SSSA, 1997; C. Coulombe, personal communication) and cracks (evidence of movement) were avoided when subsampling. It is also commonly thought that stress or illuvial oriented material would be mixed and incorporated into the matrix of soils of high shrink-swell potential (McKeague et al., 1978). An additional possibility is that since the thickness of the slides (25-30 μm) is about 10 times greater than the size of a pixel (3.1 μm) there may be overlapping of oriented domains in layers which act to extinguish each other when viewed through in circularly polarized light. The fact that smectites tend to occupy a greater portion of the fine clay fraction (<0.2 μm) only serves to magnify this possibility. Thus there may be more optically anisotropic material in the TX soils in particular than is measurable with this technique.

Although there is evidence of increased orientation due to anthropogenic stresses, it does not necessarily translate directly into the relative placement of the remoulded and structured compression and shrinkage curves. For the A and the B horizons from southern Ontario, increased orientation from Natural to Agricultural and Workspace land uses corresponded to increased displacement below the NCL. For the Alberta and Texas soils and most of the C horizons, the displacement below the NCL did not correspond to increased orientation as there was little measured. Also there was relatively consistent mechanical behaviour for the Halton C horizons but there was widely varying measurements of oriented microfabric.

The proportion of pore space could also influence consolidation characteristics and these values are portrayed in Figure 5.4. There were fewer outliers and no extreme values as the pore

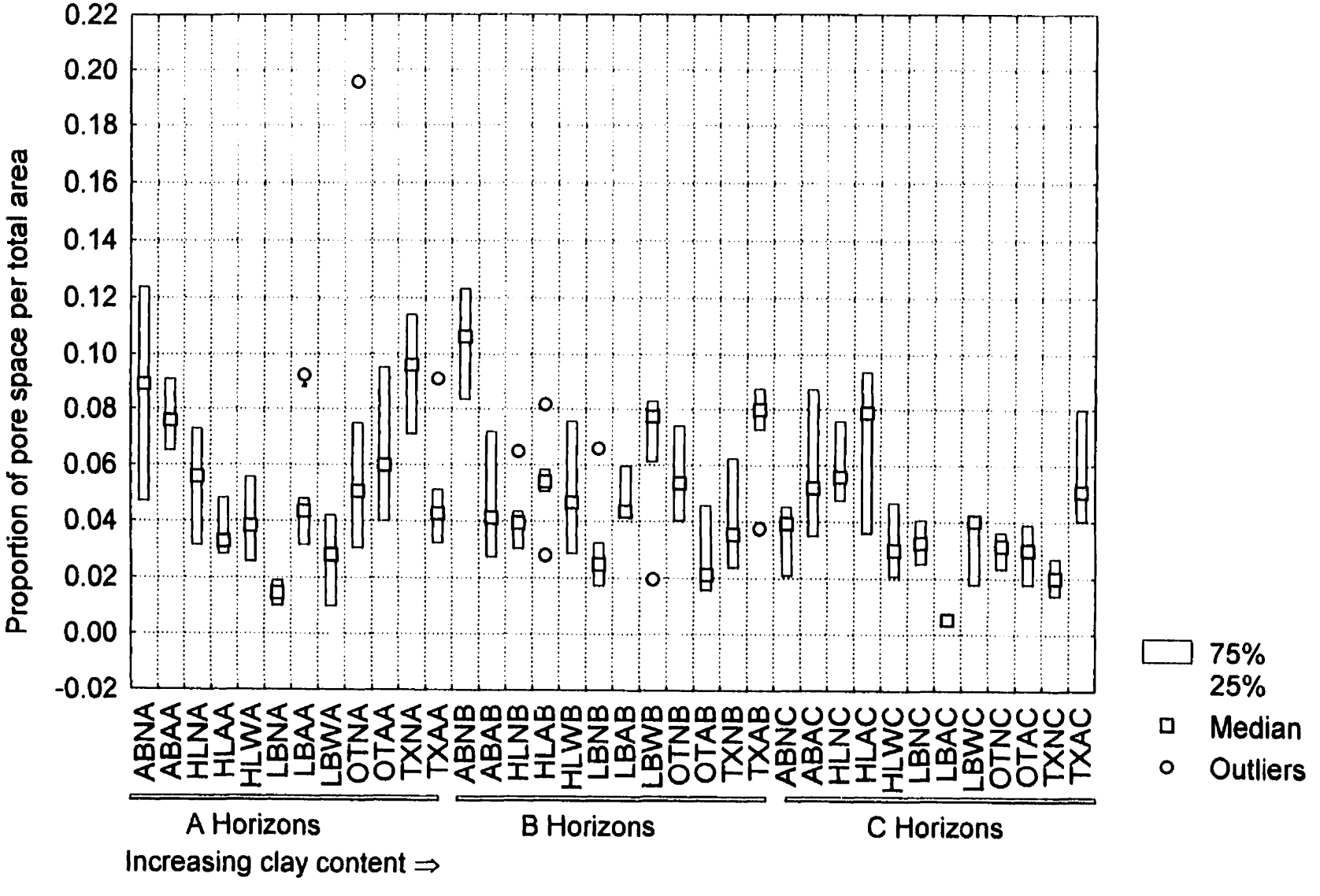

Figure 5.4. Proportion of total area occupied by pore space.

space was log normally distributed. The overall low values, most less than 10%, reflects the attempt to avoid pore space and concentrate on imaging the matrix. It was surprising that the A horizons from each site did not necessarily have the higher proportion of pore space. In particular the southern Ontario sites had lower porosities for A horizons compared to B and C horizons within profiles, and compared to the OT, TX and AB sites. This is likely a reflection of being able to sample from within an entire, dense aggregate in these A horizons while the fine pore network and aggregates of the smectitic soils was included in the field of view. Differences in pore size distribution, with more macropores being present in the LB A than TX A horizons, were also measured which could explain why more but smaller pores were measured in the TX soils. The AB horizons tended to have higher pore space and they also had the most coarse texture. The high proportion of pore space for the LB and HL B and C horizons may be an indication that the subsamples were not necessarily able to be selected away from pores and that the oriented clay found is associated with pores or cracks and may not necessarily have been independent of natural processes. The relatively low proportions (<0.04) of pore space for ABNC, TXNC, TXNB, OTAC, OTAB, OTNC may help to explain their overconsolidated behaviour since there is a lack of oriented microfabric. Again the use of pore space alone cannot account for displacement of the VCL below the NCL as many overconsolidated B horizons had relatively high pore space.

The proportion of grains in the sample was also analyzed (Figure 5.5). Halton and Alberta soils had slightly more mineral grains, particularly in the C horizons, which reflected their coarser texture. The amount of orientation in the matrix was better explained by the proportion of grains than the proportion of pores although both relationships were highly significant ($p<.001$) (Figure 5.6 and Figure 5.7). This suggests that rigid materials, such as grains or till stones, aid in aligning particles under stress. If regression equations are calculated for each site in Figure 5.6 separately, significant equations only result for OT and ON (LB and HL). This finding suggests that oriented

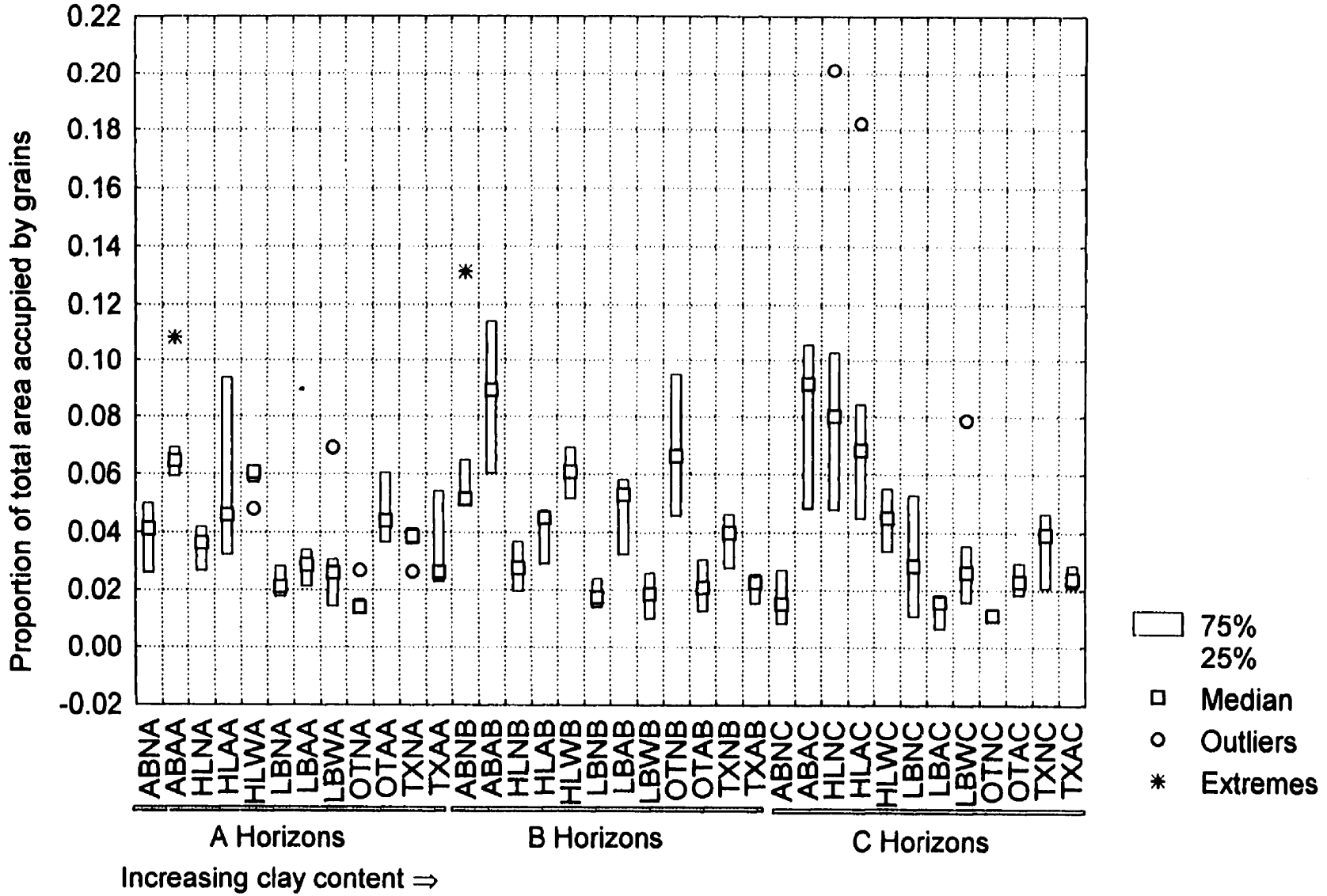

Figure 5.5. Proportion of total area occupied by grains.

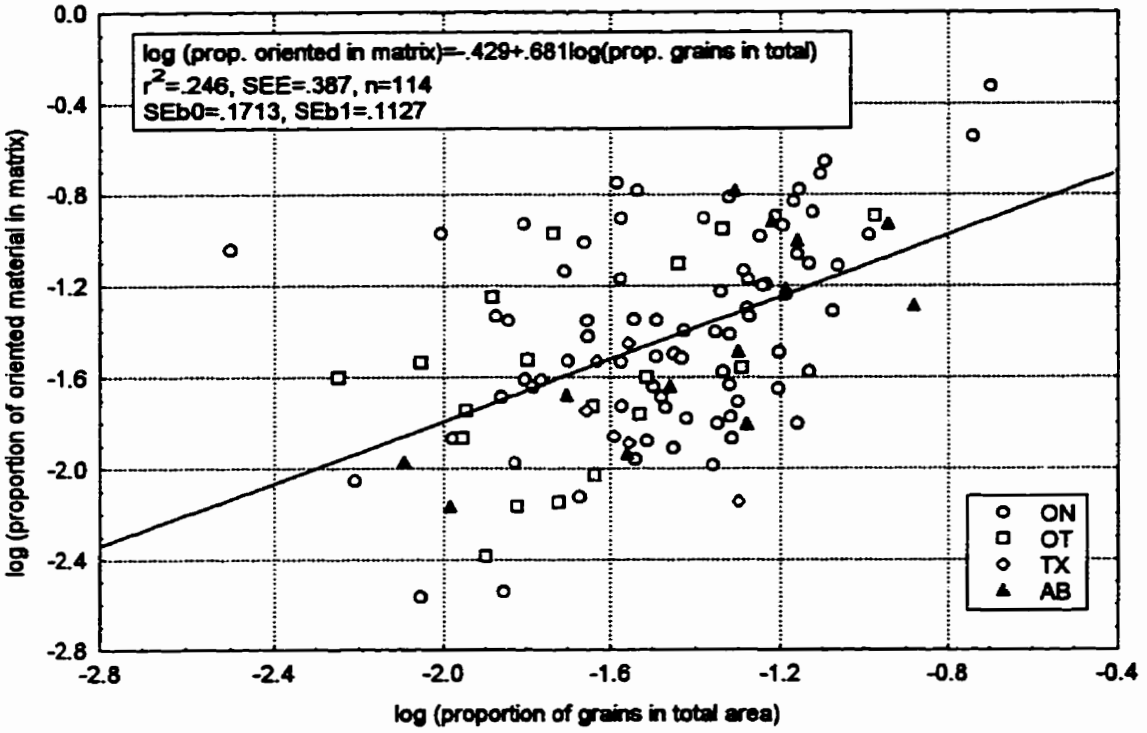

Figure 5.6. Relationship between orientation in matrix and proportion of grains.

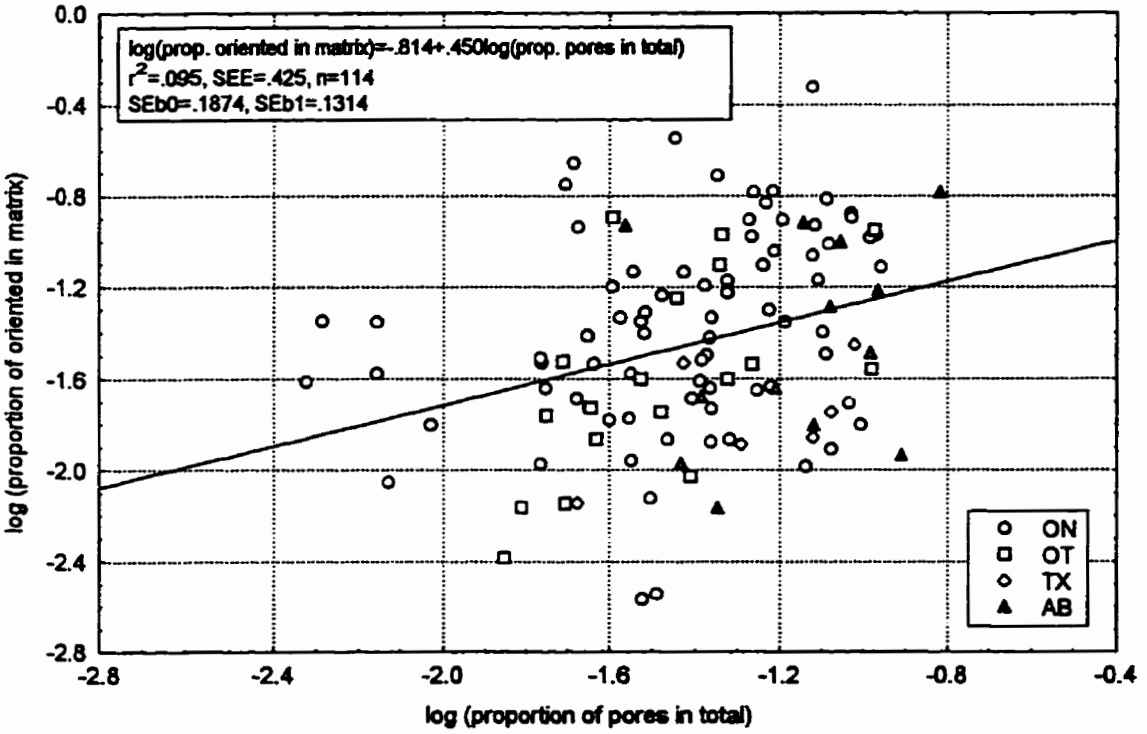

Figure 5.7. Relationship between orientation in matrix and proportion of pores.

matrix in smectitic soils is not related to wetting and drying around grains and/or that grain argillans can be disturbed by turbational processes in high shrink-swell soils. Pore space accommodates particle movement without alignment and organic and cementing agents absorb some of the energies which would be applied to particles, making microfabric patterns in natural soils much more complex than controlled laboratory experiments. Log transformations were required for all variables to achieve normally distributed residuals, thus only subsample images with measured orientation are included (n=114).

Dalrymple and Jim (1984) found that significant reorganization and orientation of the fabric occurred for laboratory soils with 20-40% clay content. The sand:silt ratio was important in determining the amount and expression of clay orientation. The presence of sand grains in a shrinking mass of clay offers a large non-deformable volume and hence a greater disruption of the otherwise uniform spatial distribution of strain than the presence of silt grains, allowing greater concentration of strain and thicker embedded grain argillans (>2.5 um). In a coarse matrix, unidirectional stress caused by a receding air-water interface resulted in strong free grain argillans, while in a fine matrix the unidirectional stress is replaced by an overall homogeneous compressive stress which is disrupted by mechanically inert grains to cause embedded grain argillans. This trend also continued at 60% clay but there was also the weak development of masepic fabrics (elongated plasma separations). A weak expression of masepic fabric was expected from a non-shearing development of plasma separation by isotropic compression. A sufficient amount of clay and skeletal grains were required for the development of masepic fabric by isotropic compression.

The current findings may also be explained by the results of Dalrymple and Jim (1984). All the sites sampled had sufficient clay content (27-65%) to exhibit oriented fabrics due to natural wetting and drying cycles. The southwestern Ontario sites were the only 2 with significant amounts of gravel (>1%) in all horizons which may explain their higher proportion of oriented

matrix. AB had a much higher proportion of sand to silt and clay than TX which may explain the greater orientation in this smectitic soil. The OT and TX soils had little sand or gravel, except OTNB and OTAA, which may explain the small amount of orientation present. Inherited microfabric from marine deposition may explain the orientation in OT C horizons where significant layering, varving and platy structure were noted when sampling.

Figure 5.8 illustrates that there is a partial relationship between overconsolidation and the amount of optically anisotropic material in the sample. The amount of oriented material tends to peak just after the threshold value of 0.40. There remain several horizons however which have no oriented matrix which are severely overconsolidated, particularly the TX soils, suggesting that there are additional mechanisms other than particle alignment which contribute to the displacement of the VCL below the NCL. These mechanisms may include the swelling potential of soils, the nature of particle contacts (any cementation) and the degree of structural development. Figure 5.9 illustrates that orientation and overconsolidation occur in all land use treatments. Thus naturally occurring effective stresses are able to generate oriented pedofeatures, as measured by the areal amount of oriented matrix, and mechanical characteristics similar to those imposed by external anthropogenic sources.

The proportion of oriented matrix (mean values) is linearly related to PTF2 (Figure 5.10), but not to any of the other compression parameters (i.e. preconsolidation stress, compression index). This further suggests that the amount of orientation is an indicator of past stress history but not necessarily the relative placement of the two compression curves.

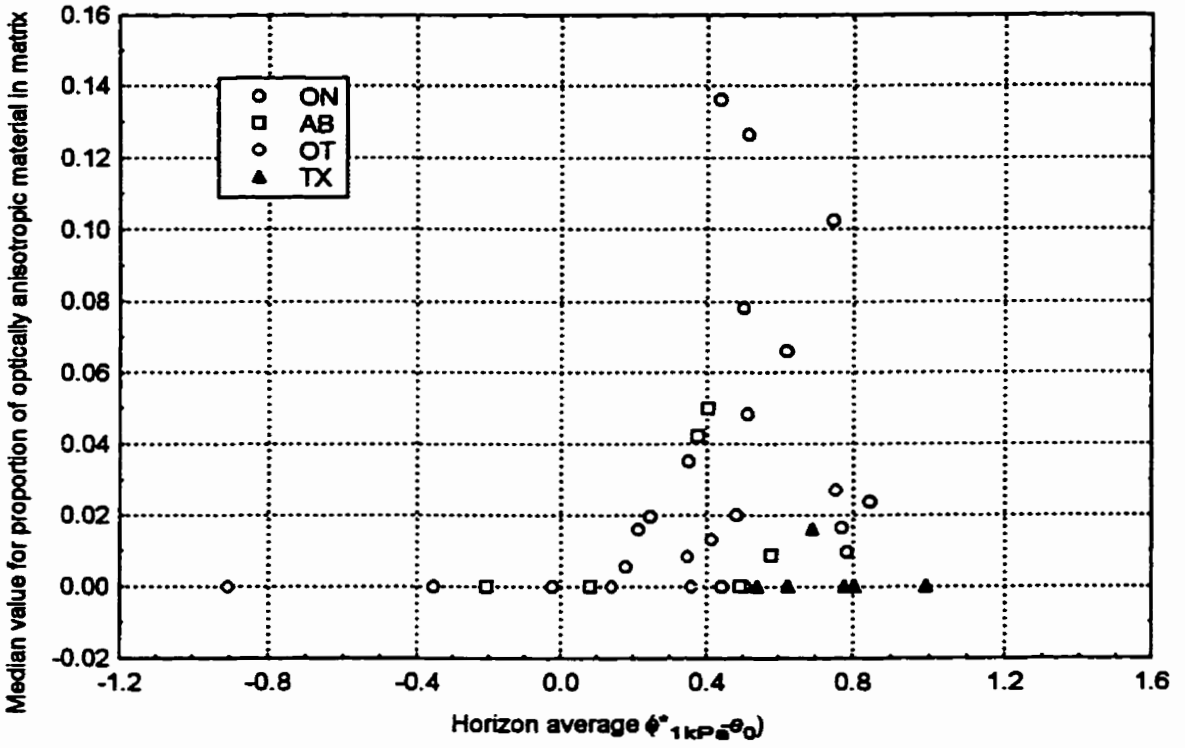

Figure 5.8. Comparison of amount of orientation and overconsolidation.

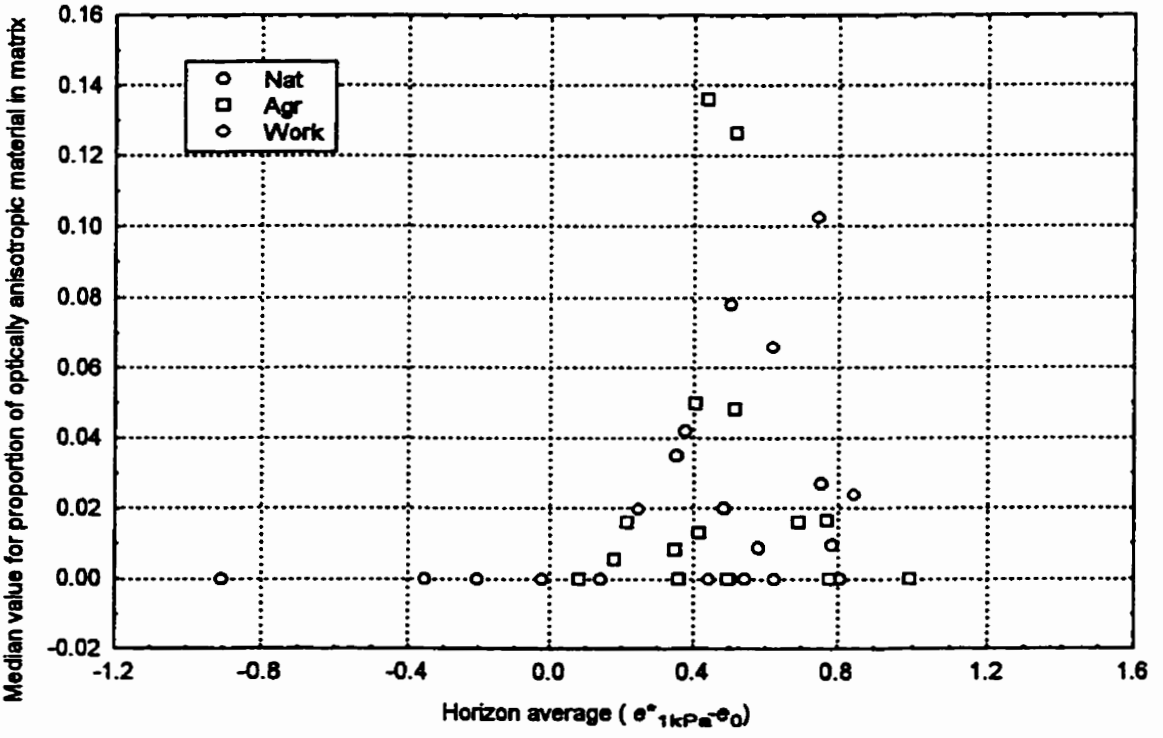

Figure 5.9. Comparison of amount of orientation and overconsolidation.

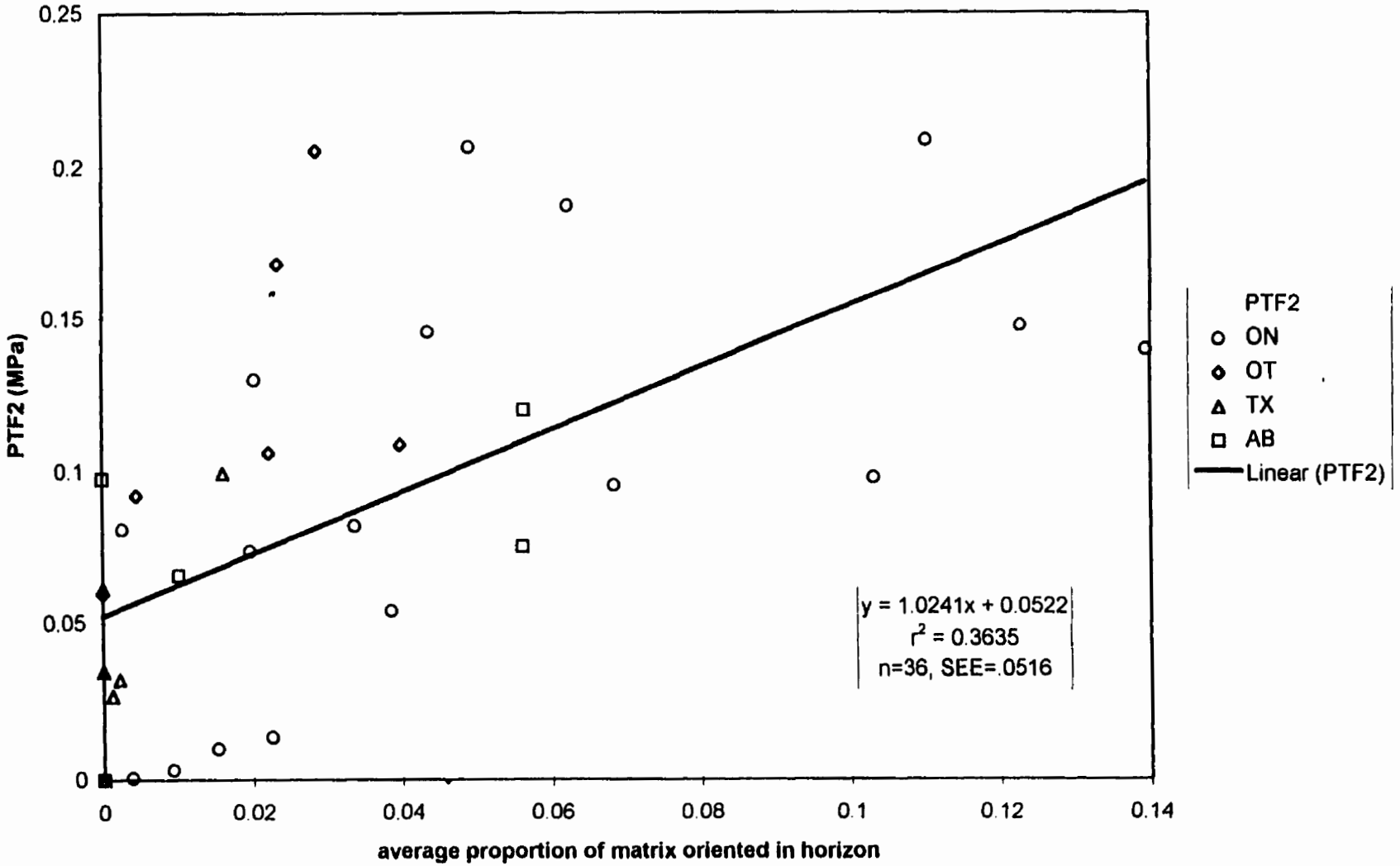

Figure 5.10. Proportion of oriented matrix in relation to PTF2.

5.4 Conclusions

This study was able to utilize a relatively quick and inexpensive image analysis system to generate informative data about optically anisotropic material in naturally occurring soils. The use of unsupervised classification algorithms means that those with relatively little micromorphological background can use image analysis to make quantitative measurements to apply to other areas of study. Obviously study of the literature is required to understand the behaviour and genesis of soils and the imaging conditions necessary to capture the features of interest. A more detailed study would need to be undertaken to determine if the classes determined by this method could be confirmed with other techniques before it is widely adopted.

In regard to the objective, the study confirmed that orientation and overconsolidation occur in natural land use as in agricultural or workspace conditions, although not always to the same degree. There seems to be additional orientation, at least for southern Ontario, for soils subjected to applied, anisotropic mechanical stresses. Although there is some relationship between the amount of orientation and overconsolidation indicated by displacement of the VCL below the NCL, there is significant variability not explained by areal coverage of oriented matrix or pore space alone. Likely some of the other morphometric measurements made on pores, such as shape, perimeter and orientation factors, could be applied to the anisotropic matrix and may be useful in differentiating the relationship between overconsolidation and orientated clay fabric. The usefulness of GIS capabilities for determining associations between different classes (shared boundaries, proximity to one another) in particular have not been explored in this or other studies. These "associations" between micromorphological features, as indicated by the relationship between oriented matrix and mineral grains, likely hold much promise in elucidating micromorphological and mechanical relationships in naturally occurring, structured soils.

5.5 References

Aitchison, G.D. and J.W. Holmes. 1953. Aspects of swelling in the soil profile. Aust. J. Applied Sci. 4:244-259.

Bai, X., P. Smart and X. Leng. 1994. Polarizing micro-photometric analysis. Géotechnique. 44(4):175-180.

Bai, X. and P. Smart. 1997. Change in microstructure of kaolin in consolidation and undrained shear. 47(5):1009-1017.

Bennett, R.H., N.R. O'Brien and M.H. Hulbert. 1991. Determinants of clay and shale microfabric signatures: Processes and mechanisms. pp. 5-32 *In* Microstructure of Fine-Grained Sediments: From Mud to Shale. (R.H. Bennet, W.R. Bryant and M.H. Hulbert eds.) Springer Verlag: New York. 582 pp.

Bui, E.N. and A.R. Mermut. 1988. Orientation of planar void in vertisols and soils with vertic properties. Soil Sci. Soc. Am. J. 52:171-178.

Chang, R.K. and B.P. Warkentin. 1968. Volume change of compacted clay soil aggregates. Soil Science 105:106-111.

Collins, K. and A. McGown. 1974. The form and function of microfabric features in a variety of natural soils. Géotechnique. 24(2):223-254.

Craig, R.F. 1992. Soil Mechanics - Fourth Edition. Van Nostrand Reinhold (International). 410 pp.

Dalrymple, J.B. and C.Y. Jim. 1984. Experimental study of soil microfabrics induced by isotropic stresses of wetting and drying. Geoderma. 34:43-68.

Derbyshire, E. 1978. A pilot study of till microfabrics using the scanning electron microscope. pp. 41-59 *In* Scanning Electron Microscopy in the Study of Sediments. (ed.) W.B. Whalley. Geo Abstracts: Norwich, England.

Ferry, D.M. and R.A. Olsen. 1975. Orientation of clay particles as it relates to crusting of soil. Soil Sci. 120(5):367-375.

Fitzpatrick, E.A. 1984. Micromorphology of soils. Chapmane and Hall, London.

Fox, C.A., R.K. Guertin, E. Dickson, S. Sweeney, R. Protz and A.R. Mermut. 1993. Micromorphological methodology for inorganic soils. pp 683-709. *In* M.R. Carter (ed.) Soil Sampling and Methods of Analysis. Can. Soc. Soil Sci. Lewis Publishers, Boca Raton.

Groenevelt, P.H. and J.Y. Parlange. 1974. Thermodynamic stability of swelling soils. Soil Sci. 118:1-5.

Inoué, S. 1986. Video Microscopy. Plenum Press, NewYork, NY.

Koppi, A.J., J.T. Douglas and C.J. Moran. 1992. An image analysis evaluation of soil compaction in grassland. J. Soil Sci. 43:15-25.

McBratney, A.B., C.J. Moran, J.B. Stewart, S.R. Cattle and A.J. Koppi. 1992. Modifications to a method of rapid assessment of soil macropore structure by image analysis. Geoderma. 53:255-274.

McBride, R.A. and P.J. Joosse. 1996. Overconsolidation in agricultural soils: II. Pedotransfer functions for estimating preconsolidation stress. Soil Sci. Soc. Am. J. 60:373-380.

McConnachie, I. 1974. Fabric changes in consolidated kaolin. Géotechnique. 24(2):207-222.

McGarry, D. 1989. The effect of wet cultivation on the structure and fabric of a Vertisol. J. Soil Sci. 40:199-207.

McKeague, J.A., R.K. Guertin, F. Page and K.W.G. Valentine. 1978. Micromorphological evidence of illuvial clay in horizons designated Bt in the field. Can. J. Soil Sci. 58:179-186.

McKeyes, E. and R.N. Yong. 1971. Three techniques for fabric viewing as applied to shear distortion of a clay. Clay and Clay Minerals. 19:289-293.

Mermut, A.R., M.C.J. Grevers and E. De Jong. 1992. Evaluation of pores under different management systems by image analysis of clay soils in Saskatchewan, Canada. Geoderma 53:357-372.

Moran, C.J. and A.B. McBratney. 1992. Acquisition and analysis of three-component digital images of soil pore structure. I. Method. J. Soil Sci. 43:541-549.

Morgenstern, N.R. and J.S. Tchalenko. 1967. The optical determination of preferred oriantation in clays and its application to the study of microstructure in consolidated kaolin. Proc. Royal Soc. London. A300:214-250.

Oleschko, K., J.D. Etchevers B. and L. Osorio J. 1993. Pedological features as indicators of the tillage effectiveness in vertisols. Soil & Tillage Res. 26:11-31.

Protz, R. and A.J. VandenBygaart. 1998. Towards systematic image analysis in the study of soil micromorphology. Sciences of Soils 3:4. http://www.hintze-online.com/SOS/1998/Articles/Art 4

Protz, R., Sweeney and C.A. Fox. 1992. An application of spectral image analysis to soil micromorphology. 1. Methods of analysis. Geoderma. 53:275-287.

Quigley, R.M. and C.D. Thompson. 1966. The fabric of anisotropically consolidated sensitive marine clay. Can. Geotech. J. 3(2):61-73.

Smart, P. and X. Leng. 1993. Present developments in image analysis. Scanning Microscopy. 7(1):5-16.

Smart, P. and N.K. Tovey. 1982. Electon microscopy of soils and sediments: techniqes. Oxford University Press, Oxford, UK.

Soil Science Society of America (SSSA). 1997. Glossary of Soil Science Terms. SSSA, Madison, WI.

Sposito, G. and J.V. Giraldez. 1976. Thermodynamic stability and the law of corresponding states in swelling soils. Soil Sci. Soc. Am. J. 40:352-358.

Stirk, G.B. 1954. Some aspects of soil shrinkage and the effect of cracking upon water entry into the soil. Australian J. of Agr. Res. 5:279-290.

Stolt, M.H. and M.C. Rabenhorst. 1991. Micromorphology of argillic horizons in an upland/tidal marsh catena. Soil Sci. Soc. Am. J. 55:443-450.

Terrible, F. and E.A. Fitzpatrick. 1992. The application of multilayer digital image processing techniques to the description of soil thin sections. Geoderma. 55:159-174.

Terrible, F. and E.A. Fitzpatrick. 1995. The application of some image-analysis techniques to recognition of soil micromorphological features. Eur. J. Soil Sci. 46:29-45.

Veenhof, D. 1993. The compression characteristics and susceptibility to compaction of agricultural soils from the Regional Municipality of Haldimand-Norfolk. Unpublished M.Sc. Thesis. University of Guelph, Guelph, Canada.

Xu, J.G., Y. Feng, D.H. McNabb and R.L. Johnson. 1994. A method of distinguishing mineral from pores in soil thin sections. Soil Science. 158(3):224-227.

6. Research Summary and Recommendations for Further Research

6.1 Research Summary

The study of compression and shrinkage mechanical tests on both remoulded and structurally intact samples provided insight into the influence of structural quality on the mechanical behaviour of soils. There was unification of mechanical concepts in that both compression and shrinkage plots in $e(\sigma')$ co-ordinates showed converging behaviour of remoulded and structured samples. This enabled the use of the difference of the remoulded and structured intercepts to be used as indicators of physical soil quality. A threshold of 0.40 for $(e^*_{1kPa}-e_0)$ and 0.25 for $(e_{\alpha R}-e_{\alpha S})$ separated normally from overconsolidated soils and soils with severe plant growth limitations for all mineralogies and land use treatments. The smaller threshold for the shrinkage parameters reflected the observation that the shrinkage void ratios were ≈65% of the compression void ratios. The relationship of both these relative indicators with an $I_L < 1$ suggests I_L may be an important indicator of structural condition itself.

The void ratio change in the compression tests was much larger than in the shrinkage tests due to the inclusion of larger inter-aggregate pores which reduced the strength of the soil mass and which provided room for crushed aggregates. The initial and resulting void ratios were much lower in the shrinkage tests indicating the measurement of intra-aggregate porosities to much higher stresses than could be imposed in the Rowe cell. The remoulded samples had generally overlapping ranges in volume change ratio (C_C^* and n_{eR}) although the corresponding n_{eR} were 0.36 times the C_C^*. The structured shrinkage samples had mutually exclusive shrinkage (n_{eS}) and compression (C_C) volume change ratios. There also appear to be differences between the Group 1 and 2 soils as the slopes for the structured Group 1 soils had no relationship between the shrinkage and compression tests. Thus remoulded soils behave more similarly under mechanical and

effective stresses due to the homogenizing of soil constituents, while structured soils resist effective stress deformation to a larger extent than compressive forces because of the gradual drainage of stable pores of various sizes and the presence of coarse particles which inhibit shrinkage. Decreasing matric potential was efficient in removing water from the sample but generally not as effective in inducing volume change as compressive forces. This may be due to the increasing strength of smaller aggregates being able to resist deformation to a greater degree.

The linear relationships between the corresponding mechanical intercepts, slopes and relative indicators for compression and shrinkage tests suggest, at least partially, a scaling of structural quality through all structural aggregate sizes which resists both applied and internal stresses due to similar structural properties even though the absolute values are smaller for shrinkage. There is still a large amount of variability unaccounted for in many of these linear relationships, with r^2 often around .50-.60, likely due to the heterogeneous nature of structured soils and the wide variety of soils sampled.

The remoulded compression and shrinkage parameters were highly related to the constitutive properties of the soil, primarily the liquid limit, clay and sand content, carbonate content and organic carbon content. Clay mineralogy differences were accounted for if %fine clay was used for estimating volume change ($COLE_{rem}$ or n_{aR}) for shrinkage tests. Generally, the remoulded soils provide a good mechanical reference point for agricultural soils and their parameters can be predicted well from existing soil survey information.

It was originally anticipated that mechanical parameters which integrate behaviour over a stress range as a dynamic quality would be most revealing of structural quality and it is rather fortuitous that the behaviour can generally be anticipated from static void ratios at 1kPa. It appears, at least for regional soil quality assessment, that laborious tests such as determining the preconsolidation stress are not warranted. The intercept of the remoulded soils is highly related to

the liquid limit and the intercept of the saturated, structurally intact soils was partially related to the plastic limit so that the Atterberg limits which have been widely used to provide guidelines for mechanical behaviour continue to have an important role in assessing structural quality.

Soils with greater than 36% clay content will continue to be naturally susceptible to overconsolidation and structural degradation due to plastic deformation, normal shrinkage and permanent orientation of clay particles. Lower clay content or high organic matter content soils may exhibit more volume change under stress but much of this volume change is reversible by bioturbation and swelling. It is soils with >36% clay content which will require management systems which include intensive biological activity or other loosening methods in conjunction with raising organic matter contents to overcome the natural tendency for structural deterioration. All soils become more susceptible to structural degradation as organic matter content levels are lowered and overconsolidation can still occur in coarse textured soils if excessive stresses are applied, as in a pipeline workspace.

The relative displacement of the structured soils below the remoulded soil for compression or shrinkage curves was not entirely explained by the amount of area occupied by optically anisotropic material in the matrix. Clay orientation was maintained in the saturated, structured condition, but the proportion of oriented matrix was linked to the inclusion of coarse fragments in the matrix and the drainage conditions necessary for wetting and drying cycles. Thus the presence of oriented matrix was an indicator of previous stress history in the soil but not a causative factor in the present mechanical behaviour of the soil. Several overconsolidated soils exhibited high amounts of oriented matrix while many did not exhibit any at all, as in the TX soils. The displacement may be related more to the simple packing and bonding of particles in a structured state rather than the proportion of orientation, even though this represents the closest packing state of fine grained material. Clay is only a portion of the constituents making up the structured soil.

The void ratio of the remoulded state is that much higher for clayey soils because clay domains are flocculated rather than tightly packed, as hypothesized by Veenhof (1993), which allow films of water to develop around each domain separately, creating a much higher surface area for water adsorption than packed domains, to reach a higher water content which the remoulded void ratio is based on.

This study provided some basic information for future attempts at deriving structural quality indicators from mechanical parameters and confirmed that remoulded soils can have void ratios above their structured counterparts at the same stress. It also showed that there is potential "universality" using relative physical soil quality parameters based on mechanical principals to indicate structural quality, but that estimation of these indicators might require different PTFs for different mineralogies.

6.2 Recommendations for Further Research

There were several questions raised through this thesis that warrant further investigation or comment.

1. There was sufficient evidence that those soils outside of the physiographic region of southwestern Ontario have different relationships between soil properties and mechanical parameters that the existing PTF functions cannot be routinely applied outside of this physiographic/climatic region. In particular, effective stresses at the Atterberg limits for smectitic soils were not related to organic carbon in the same way as illitic soils and TX was often different from the other soils. Although the OT and AB soils often followed the ON models, they also contained outliers on occasion. There was not enough variability from within one soil series of the different mineralogies to derive significant models with the current data. Also, the smectites tested here were of relatively low activity for comparable

mineralogies. It is therefore recommended that a more extensive sampling of soil series representing different mineralogies for a variety of particle size and organic carbon contents, plasticities and structural conditions be conducted similar to that for southwestern Ontario. It is promising that more specific PTFs could be developed for other areas given that all mineralogies exhibited converging behaviour, had universal thresholds for distinguishing structurally degraded soils and showed relationships with clay and/or organic carbon content.

2. There were several covariate analyses with either clay or organic carbon where there were significant TRT interactions with the covariate, indicating different responses to changes in the covariate by land use rather than simply separations in TRT by differences in the intercept. There were conditions for the compression tests such that the Workspace often behaved differently from the other two treatments and for the shrinkage tests such that the Agricultural horizons often had different behaviour with the covariate from the other treatments. Some of these differences were removed when Group 1 and 2 soils were analyzed separately. These treatment differences need to be better understood (i.e. if they were real or simply due to the soils and sampling and testing methods used), because it would determine if pedotransfer functions can be applied to all land uses simultaneously or if models have to be derived separately for extremes in land use based on soil properties.

This was an observational study where there was no control over the conditions during or following stress inducing periods. A controlled experiment which imitated stress conditions of various land uses but identically for each texture, mineralogical and organic content combination may elucidate if there are truly different covariate responses by land use. This study has revealed the importance of the structurally intact state and so if there is to be any ability of replicating a naturally occurring soil it would probably be best to begin with structurally intact samples, treat them similarly with imposed stress conditions and then repeat

the testing as in this study. Similar results to these, using artificially constructed soils from dried and sieved samples, would not be expected because subsoils in particular have never been subjected to this kind of disruption.

3. The relative indicators were able to distinguish Natural A horizons and Workspace B and C horizons from other horizons but these represent the extremes of land use impact and structural quality. They were also generally able to distinguish the A horizons from the B and C horizons of the same treatment, again representing the most structurally diverse conditions. Only one threshold has been established, distinguishing severely overconsolidated soils, while further testing may reveal potentially 1 or 2 more thresholds for structural quality monitoring on a regional basis. The sensitivity of the relative indicators needs to be tested more rigorously using different land management treatments to determine if they can distinguish to a finer degree the impact on structural quality of varying agricultural management systems in particular. The range of initial void ratios associated with a particular land use for a set of soil properties needs to be established. This could be tested by using these pedotransfer functions on existing data sets or including measurement of the indicator parameters in ongoing management studies.
4. The shrinkage parameters did not vary as systematically with soil properties as the compression parameters and there was a large amount of variability. Shrinkage testing was complicated by differences in behaviour because of texture and pore drainage, and in difficulties in assessing when equilibrium matric potentials had been achieved. The 3 line model was not really adequate for fitting the data and producing useful parameters because of the varying interpretation of the line segments to various shrinkage stages. The shrinkage tests results do indicate some resemblance or scaling of the compression test results. Although it was originally thought the natural ped size of aggregates would resemble that used for

compression, the low shrinkage void ratios indicate that much larger samples and a method such as the Saran coating which could potentially better capture structural shrinkage would produce a more direct relationship to the compression tests. This would limit tests to more cohesive soils and there may be difficulty in reusing a clod for different matric potentials (i.e. cutting away a patch of Saran and recoating for each tension). Because of these difficulties, compression tests likely hold more future for wide spread use in developing physical soil quality indicators based on mechanical parameters.

5. Computer image analysis has reached a level of technology which is accessible to many researchers and applications. One future possibility is using the technique devised here, or a similar technique on larger samples, to measure the amount of oriented matrix in existing soil thin section collections. This study would aid in characterizing the type and amount of clay orientation occurring naturally under various land uses of different soil orders and series so that some expectation of a "normal" occurrence could be made. Also a theory of development of oriented matrix based on horizon, mineralogy and particle size distribution could be refined. Then amounts or patterns of matrix orientation that arise outside of this normal expectation could be more reliably attributed to anthropogenic causes.

7. APPENDICES

7.1 Appendix to Chapter Two

7.1.1 ANOVA and ANCOVA Analysis

The experimental design used to analyse the significance of mineralogy (MNR), land use (TRT) and horizon (HOR) treatments is an unbalanced split plot design. There are 4 mineralogies based on the clay mineralogical analysis and geographical location denoted as AB, TX, OT and ON. The 4 southern Ontario sites are considered random effects and are nested within the ON mineralogy. Land use treatments (TRT-Natural, Agricultural or Workspace) are the whole plots and horizons are the sub-plots (HOR-A, B or C) as the horizons are necessarily sampled non-randomly within each pit.

The model factors included in the ANOVA analysis were then:

Fixed Effects
Whole Plot
MNR
TRT
MNR*TRT
Subplot
TRT*HOR
MNR*HOR
MNR*TRT*HOR
Random Effects
LOC(MNR)
TRT*LOC(MNR)
HOR*LOC(MNR)
TRT*HOR*LOC(MNR) (not possible for n=54, horizons without subsamples)

During the analysis it became evident that there was a wide variation in clay content and organic content (i.e. OTNA and the natural A horizons often were the only significant terms) and that this variation may mask the effects of mineralogy or land use or completely explain some of the compression results since organic carbon had a large influence on mechanical behaviour. An ANCOVA analysis was undertaken in which the % organic carbon or clay was used as a surrogate for the HOR factor (as there was only 1 value per horizon) and treated as a covariate in the

analysis. Linear as well as quadratic terms for the covariate slope were included. Organic carbon is not a true covariate (to increase precision or remove bias) because it is not independent of the treatments (horizon or land use) but is a result of or influenced by the treatments being imposed. A covariate can be used however to help reveal the nature of treatment effects and clarify the causal mechanisms present between treatment, covariate and response (Cochran and Cox, 1957). The model factors included in this ANCOVA analysis were then:

Fixed Effects
Whole Plot
MNR
TRT
MNR*TRT
COV
COV*COV
COV*MNR
COV*TRT
COV*COV*MNR
COV*COV*TRT
COV*MNR*TRT
COV*COV*MNR*TRT
Random Effects
LOC(MNR)
TRT*LOC(MNR)
HOR*LOC(MNR)
TRT*HOR*LOC(MNR) (not possible for n=54, horizons without subsamples)

The PROC MIXED procedure in SAS 6.12 was used to analyze these designs (SAS Institute, 1985). The MIXED model is particularly good at deriving appropriate standard errors of means and appropriate tests of Fixed effects for an unbalanced design such as this (ie. there are no workspace treatments in 3 locations) because it uses restricted maximum likelihood (REML) estimates of variance components.

Analysis of the residuals was conducted to determine if normality and homoscedasticity assumptions held and to identify outliers. If assumptions were violated, log, square root and 1/x transformations of the y variable were tried as well as addition or subtraction of small amounts under transformation, until assumptions were best met. Identification and removal of outliers if

appropriate also provided insight into the underlying structure of the data. Results are presented with and without the outliers where the model differed significantly with removal of the outlier.

Once the normality assumptions were best met the error terms were analyzed for the potential of pooling. The MIXED procedure is conservative in determining which random effects/variance components are significant and so the confidence limits in conjunction with actual values and p-values were used to determine which variance components to keep in the model. Elimination of variance components which were not significant allowed pooling of errors and more powerful tests (i.e. more df) of the fixed effects.

Once the error structure of the model was determined, the fixed effects were analyzed. Terms were removed one at a time, retaining lower order terms or interactions where appropriate, starting with the largest p-values. These p-values were usually over 0.15 and always over .05 for removal. This removal allowed simplification of the model and estimation of differences using paired t-tests (pdiff procedure) especially where there were confounding results (eg. could not estimate a MNR*TRT difference if MNR*TRT*HOR was still in the model even if it was not significant since there were no workspace samples from 3 of the mineralogies). LSMEANS and PDIFF procedures as well as ESTIMATE statements were then used to determine significant differences among the treatments.

ANCOVA equations are presented in the text where they were significant. The predictive equations generated by the ANCOVA approach have one mean square error (MSE) and correlation coefficient (R) for either a single equation or a series of equations (numbered as one equation) depending on the form of the model. The MSE is the residual error term estimated via restricted maximum likelihood iterations in PROC MIXED; there may be additional error terms in the model used to test higher order factors in the split plot design. The R value is derived from a simple correlation using PROC CORR, comparing the predicted and observed values. Asymptotic

standard errors (SEE) for the equation parameters and variance estimates are estimated from the first derivative found during the Newton-Raphson iterations (SAS Institute, 1996; W. Matthes-Sears, personal communication).

7.1.2 Description of pedal structure by horizon

Horizon Label	Primary structure	Secondary structure
LBNA		strong, fine granular
LBNB	strong, very coarse subangular blocky	strong, coarse subangular blocky
LBNC	strong, very coarse angular blocky	strong, coarse angular blocky
LBAA	moderate, massive	moderate, medium granular
LBAB	moderate, coarse prismatic	strong, coarse subangular blocky
LBAC	strong, coarse subangular blocky	strong, fine subangular blocky
LBWA	moderate, very coarse subangular blocky	moderate, medium granular
LBWB	moderate, massive	strong, medium prismatic
LBWC	strong, coarse angular blocky to prismatic	strong, medium subangular blocky
HLNA		strong, medium granular
HLNB	strong, coarse angular blocky	moderate, very fine subangular blocky
HLNC	moderate, medium angular blocky	moderate, very fine subangular blocky
HLAA	moderate, coarse subangular blocky	moderate, medium granular
HLAB	strong, very coarse angular blocky	strong, medium subangular blocky
HLAC	weak, coarse subangular blocky	moderate, medium subangular blocky
HLWA	moderate, coarse subangular blocky	moderate, medium granular
HLWB	strong, coarse angular blocky	moderate, fine subangular blocky
HLWC	moderate, coarse angular blocky	strong, medium subangular blocky
MDNA	strong, coarse subangular blocky	strong, very fine subangular blocky
MDNB	strong, coarse subangular blocky	strong, very fine subangular blocky
MDNC	strong, coarse subangular blocky	strong, fine subangular blocky
MDAA	weak, coarse subangular blocky	weak, fine granular
MDAB	moderate, coarse angular blocky	moderate, fine subangular blocky
MDAC	weak, massive to coarse subangular blocky	weak, medium granular
MDWA	moderate, coarse angular blocky	strong, medium subangular blocky
MDWB	moderate, massive to coarse angular blocky	weak, fine subangular blocky
MDWC	weak, coarse subangular blocky	weak, medium platy
WANA	weak, coarse subangular blocky	moderate, medium granular
WANB	moderate, coarse subangular blocky	moderate, fine subangular blocky
WANC	strong, coarse angular blocky	strong, medium angular blocky

Horizon Label	Primary structure	Secondary structure
WAAA	weak, coarse subangular blocky	weak, fine granular
WAAB	strong, very coarse angular blocky	strong, fine angular blocky
WAAC	strong, very coarse angular blocky	moderate, fine angular blocky
WAWA	weak, coarse subangular blocky	weak, medium granular
WAWB	strong, coarse angular blocky	strong, medium angular blocky
WAWC	strong, very coarse angular blocky	strong, medium & coarse angular blocky
TXNA	strong, coarse prismatic	strong, medium granular
TXNB	strong, very coarse prismatic or columnar	strong, coarse angular blocky
TXNC	weak, prismatic to massive	weak, coarse subangular blocky
TXAA	weak, prismatic to massive	massive
TXAB	strong, very coarse columnar	strong, coarse angular blocky
TXAC	weak, prismatic to massive	weak, coarse subangular blocky
OTNA		strong, fine granular
OTNB	moderate, coarse subangular blocky	moderate, fine subangular blocky
OTNC	strong, coarse angular blocky	strong, medium angular blocky
OTAA	weak, coarse subangular blocky	strong, coarse granular
OTAB	weak, coarse subangular blocky	moderate, coarse granular
OTAC	moderate, medium platy	strong, very fine subangular blocky
ABNA	moderate, coarse angular blocky	weak, very fine granular
ABNB	strong, medium subangular blocky	moderate, very fine subangular blocky
ABNC	moderate, coarse subangular blocky	weak, coarse granular
ABAA	weak, coarse subangular blocky	weak, medium granular
ABAB	strong, coarse subangular blocky	moderate, fine subangular blocky
ABAC	strong, very coarse subangular blocky	moderate, coarse subangular blocky

7.1.3 Additional horizon physical data details

Horizon	Family particle size class	Overburden pressure (kPa)	VCS	CS	MS	FS	VFS	FC	CC	FSi	CSi	C_C*	e^*_{1kPa}
LBNA	FC	0.294	1.248	1.248	1.248	1.248	1.248	15.5	30.5	40.2	7.5	0.40781	2.2520
LBNB	FC	2.156	0.99	0.99	0.99	0.99	0.99	16.7	27.6	41	9.6	0.26331	1.6168
LBNC	FC	5.096	1.524	1.524	1.524	1.524	1.524	17.3	29.7	36.7	8.7	0.40209	1.8151
LBAA	FC	0.294	1.222	1.222	1.222	1.222	1.222	15.2	27	44.3	7.4	0.2349	1.4271
LBAB	FC	2.156	1.056	1.056	1.056	1.056	1.056	16.6	31.4	37.8	8.1	0.24646	1.5397
LBAC	FC	5.096	1.528	1.528	1.528	1.528	1.528	16.3	31.8	36.4	7.9	0.35195	1.7037
LBWA	FC	0.49	1.6	2.6	2.9	3.2	2.8	10	25	41.2	10.8	0.24878	1.3844
LBWB	FC	2.254	1.812	1.812	1.812	1.812	1.812	16	29.9	36.4	8.7	0.31109	1.5784
LBWC	FC	4.606	2	2.3	3	3.6	2.6	13.2	30.2	36	7	0.34329	1.6657
HLNA	FL	0.098	3.8	3.4	2.9	4.6	5.4	11.7	22.2	32.6	13.5	0.25599	1.5505
HLNB	FC	1.96	1.5	1.4	2.4	4.1	4.6	21	22.7	30.6	11.8	0.23011	1.3692
HLNC	FL	5.194	2.2	2.4	3.6	5.2	4.7	7.9	25.6	37.2	11.2	0.21003	1.1902
HLAA	FL	0.686	0.9	1.8	3.2	5.7	9.9	10.7	18.3	33.9	15.6	0.27253	1.3317
HLAB	FC	1.666	1.3	1.6	2.5	4.8	6.9	14.9	25.4	32.5	10.1	0.21172	1.2988
HLAC	FL	4.41	2.9	2.2	2.9	5.1	6.8	9.4	20.6	38.6	11.6	0.22159	1.1977
HLWA	FL	0.098	1.6	2.8	3.1	5.4	8.2	8.9	21.2	35.2	13.6	0.24942	1.3691
HLWB	FC	1.764	1	1.3	2.1	4.2	5.9	20.9	24.3	30.2	10.2	0.25032	1.4619
HLWC	FL	4.018	2.8	2.2	3	5.4	6.7	9	21.4	37.2	12.4	0.20652	1.1740
MDNA	FS	0.196	0.7	1.4	1.7	3.2	5	3.9	14.7	50.9	18.6	0.35923	2.0384
MDNB	FC	1.96	1.3	1	1.9	3.5	5.4	12.5	22.8	33.1	18.5	0.23559	1.4426
MDNC	FC	2.94	3.8	3	3.4	5.3	4.6	10	25.5	33.9	10.5	0.32422	1.4173
MDAA	CL	0.294	0.5	2.9	3.9	6.6	12.7	5.8	11.7	36.3	19.7	0.29473	1.7657
MDAB	FL	1.96	0.8	0.3	0.9	1.9	12.5	12.7	12.3	26.3	32.3	0.19685	1.1628
MDAC	CL	2.94	3.1	2.6	2.8	4.7	12.9	5.5	7.7	26.4	34.4	0.13914	0.8330
MDWA	FL	0.196	0.6	0.9	1.4	2.4	14.6	5.2	13.9	34.8	26.1	0.25746	1.3887
MDWB	FL	2.94	0.3	0.5	0.9	1.7	14.6	12.2	12.7	27	30	0.31651	1.4074
MDWC	CL	3.92	2.6	2	2	2.4	15.9	6.9	8.6	27.6	31.9	0.29448	1.1898
WANA	FL	0.49	0.4	1.6	6.1	13.4	15.3	9.8	14.5	19.6	19.2	0.23538	1.2608
WANB	FL	2.94	0.7	1.7	7.2	17.6	17.9	8.3	12.1	18.3	16.2	0.16473	0.9574
WANC	FC	5.88	1.76	1.76	1.76	1.76	1.76	13.3	43.3	22.1	12.5	0.36741	1.8856
WAAA	FL	0.49	0.7	1.3	4.3	11.1	18.2	8.2	14.3	20.8	21.2	0.26207	1.2918
WAAB	FL	2.94	1.3	1.2	2.5	6.4	14.3	11	15.3	22.5	25.5	0.30674	1.2843
WAAC	FC	5.39	1.264	1.264	1.264	1.264	1.264	14.6	28.8	25.4	24.9	0.5073	1.8632
WAWA	CL	0.49	0.6	1.3	6.6	20.6	22.7	5	11.7	16.8	14.7	0.29333	1.1947
WAWB	FC	2.94	0.3	0.9	3.8	9.6	8.8	14	27.9	19.9	14.8	0.43833	1.8397
WAWC	VFC	4.9	0.544	0.544	0.544	0.544	0.544	12.4	48.6	25.2	11.1	0.47737	2.0440
TXNA	FC	0.98	1.956	1.956	1.956	1.956	1.956	22	25	33.2	9.9	0.33204	1.7066
TXNB1	FC	3.43	1.558	1.558	1.558	1.558	1.558	21.1	25.3	36.1	9.6	0.3039	1.5548
TXNC	FC	14.7	0.716	0.716	0.716	0.716	0.716	27.7	23.8	35.5	9.5	0.33913	1.7904
TXAA	FC	0.98	0.4	0.4	1.7	2.5	6.2	26.8	21.9	26.3	13.8	0.36644	1.8273

Horizon	Family particle size class	Overburden pressure (kPa)	VCS	CS	MS	FS	VFS	FC	CC	FSi	CSi	C_c^*	e^*_{1kPa}
TXAB	FC	3.92	1.512	1.512	1.512	1.512	1.512	28.2	22	29.9	12.3	0.32323	1.7693
TXAC	FC	14.7	1.52	1.52	1.52	1.52	1.52	31.4	18.7	31.9	10.5	0.44736	2.0282
OTNA	FC	0.49	0.4	0.4	1	6.9	7	18.1	26	28	12.3	0.36133	2.4097
OTNB	FC	2.45	0.2	0.4	1.2	11.8	12.4	14.2	25	26.2	8.6	0.20909	1.3740
OTNC	VFC	7.84	0.318	0.318	0.318	0.318	0.318	19.2	46.4	29.7	3.1	0.4039	2.1386
OTAMA	FC	0.49	0.9	1.1	1.8	3.3	13.6	15	23.4	27.3	13.7	0.24234	1.3348
OTAMB	FC	2.94	1.066	1.066	1.066	1.066	1.066	16.9	40.4	32.1	5.2	0.21301	1.6338
OTAMC	FC	8.33	0.744	0.744	0.744	0.744	0.744	11.1	26	48.6	10.7	0.26056	1.4883
ABAA	FL	0.588	0.7	1.5	4.3	6.9	12.5	9	18.5	24	22.6	0.29572	1.4945
ABAB	FC	4.214	1	2.8	7.6	12	8.9	18.3	18.7	19.6	11.1	0.21925	1.2139
ABAC	FL	12.74	1	2.4	6.4	9.4	6.8	10.5	23.5	29.4	10.5	0.27857	1.3551
ABNA	FL	0.588	0.9	1.3	4.1	6.7	11.3	11.9	15	28.3	20.3	0.31183	1.4779
ABNB	FC	4.214	0.6	2.3	7.9	11.9	7.3	18.2	19.5	24.1	8	0.24159	1.3383
ABNC	FL	12.74	0.4	1.6	5.7	10.7	7.5	11.1	20.5	33.7	8.9	0.31939	1.4515

7.1.4 Graphs of Remoulded and Structured Compression Curves

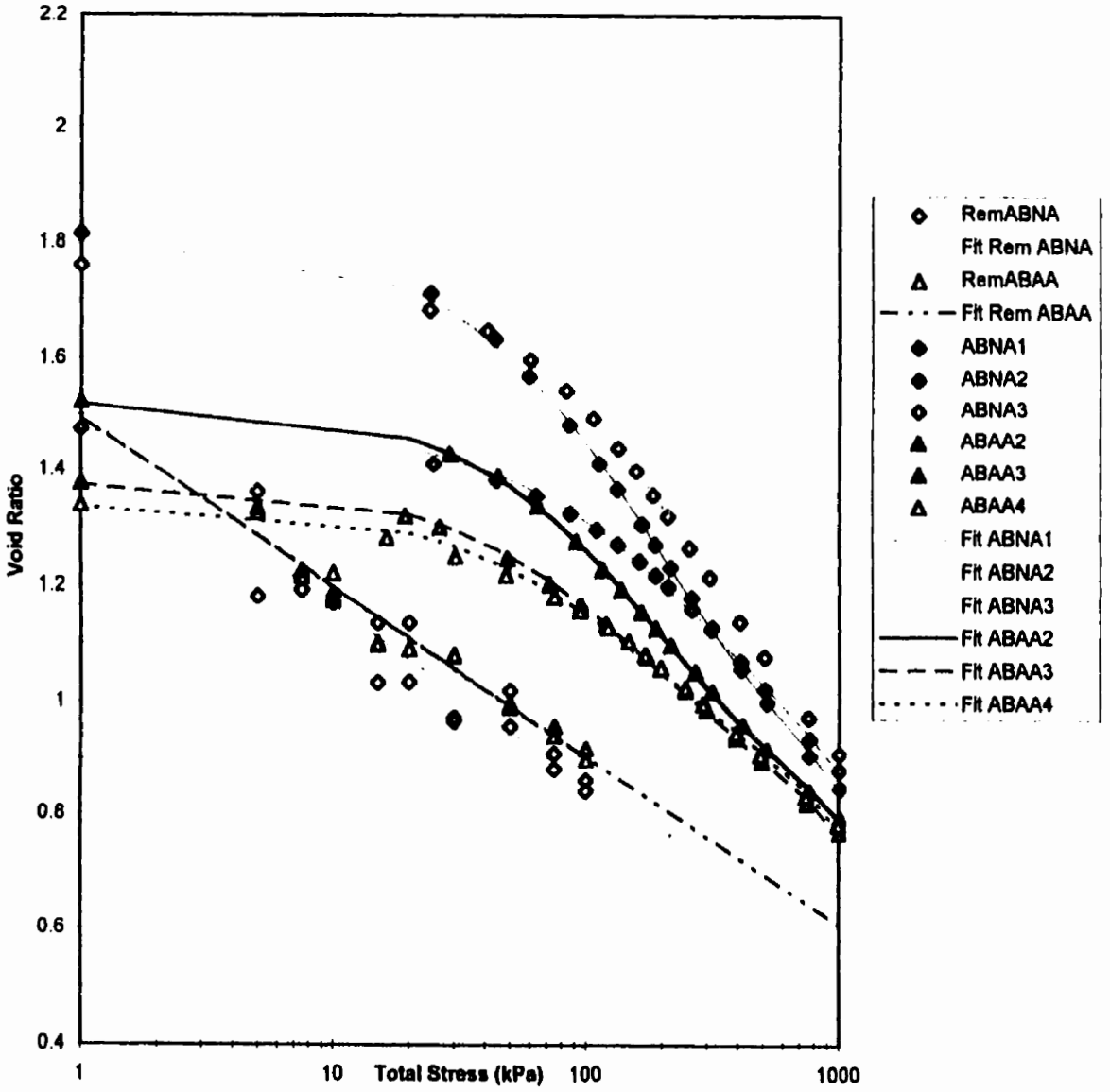

Total stress compression data for AB A horizon.

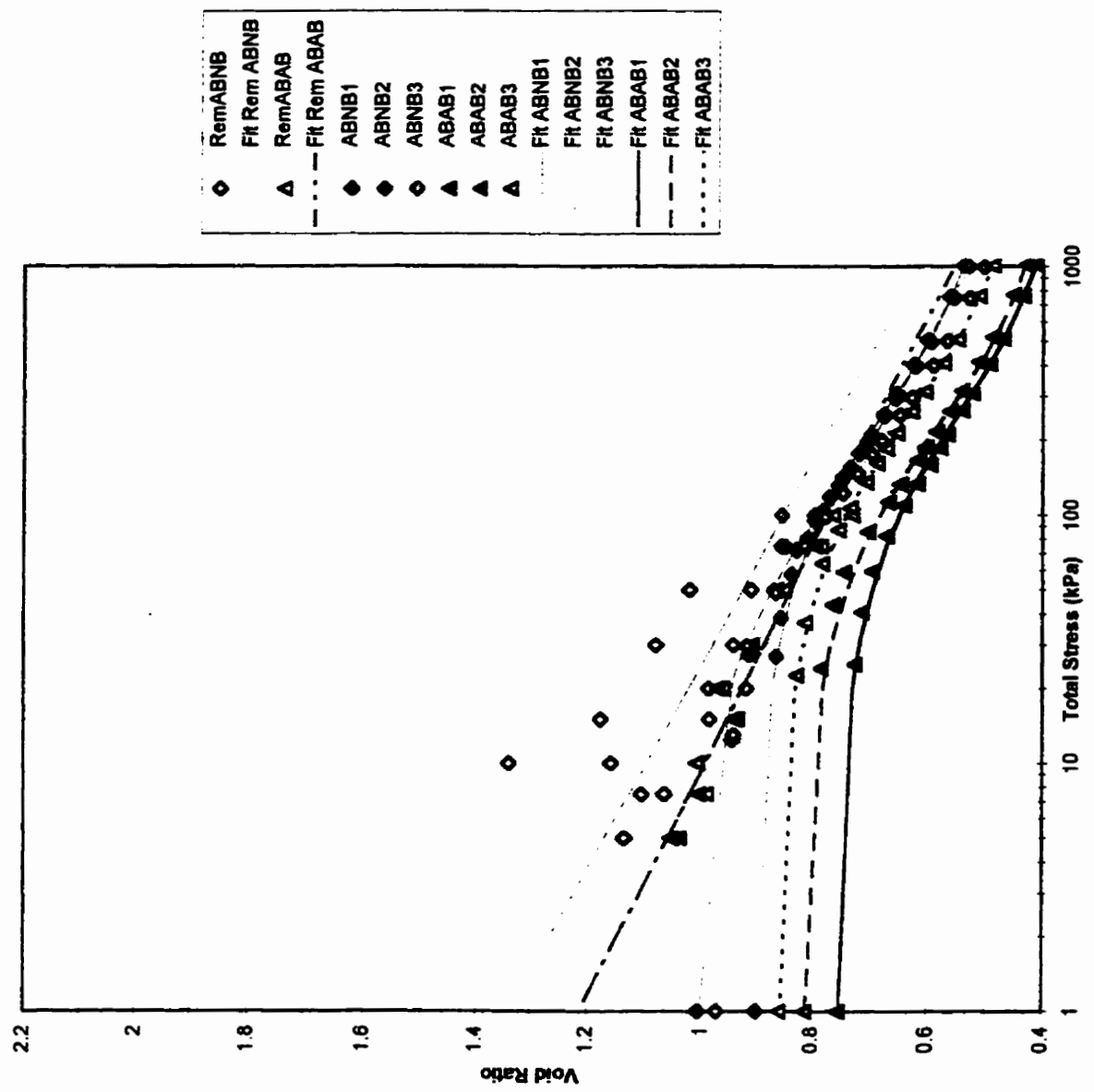

Total stress compression data for AB B horizon.

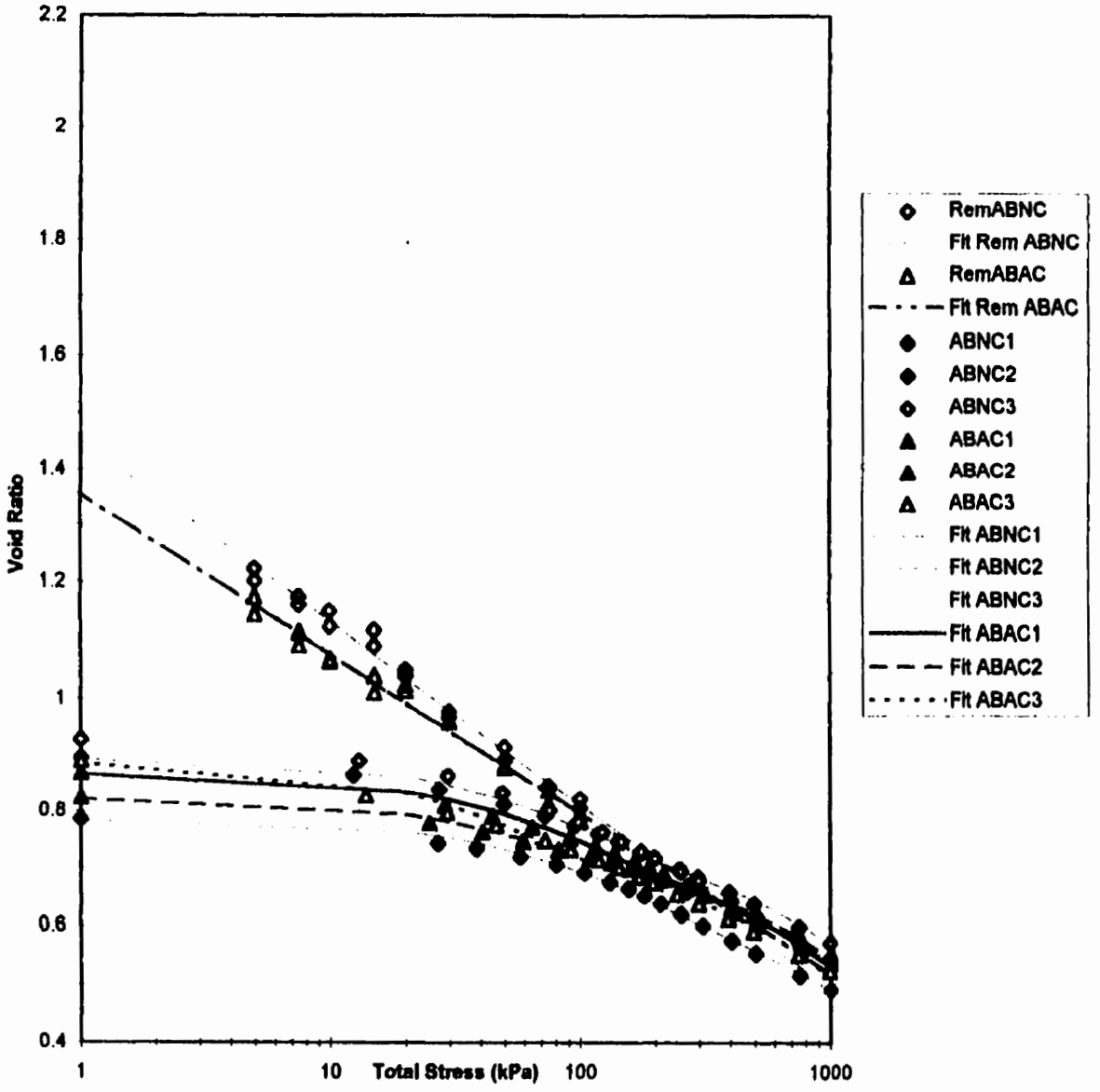

Total stress compression data for AB C horizon.

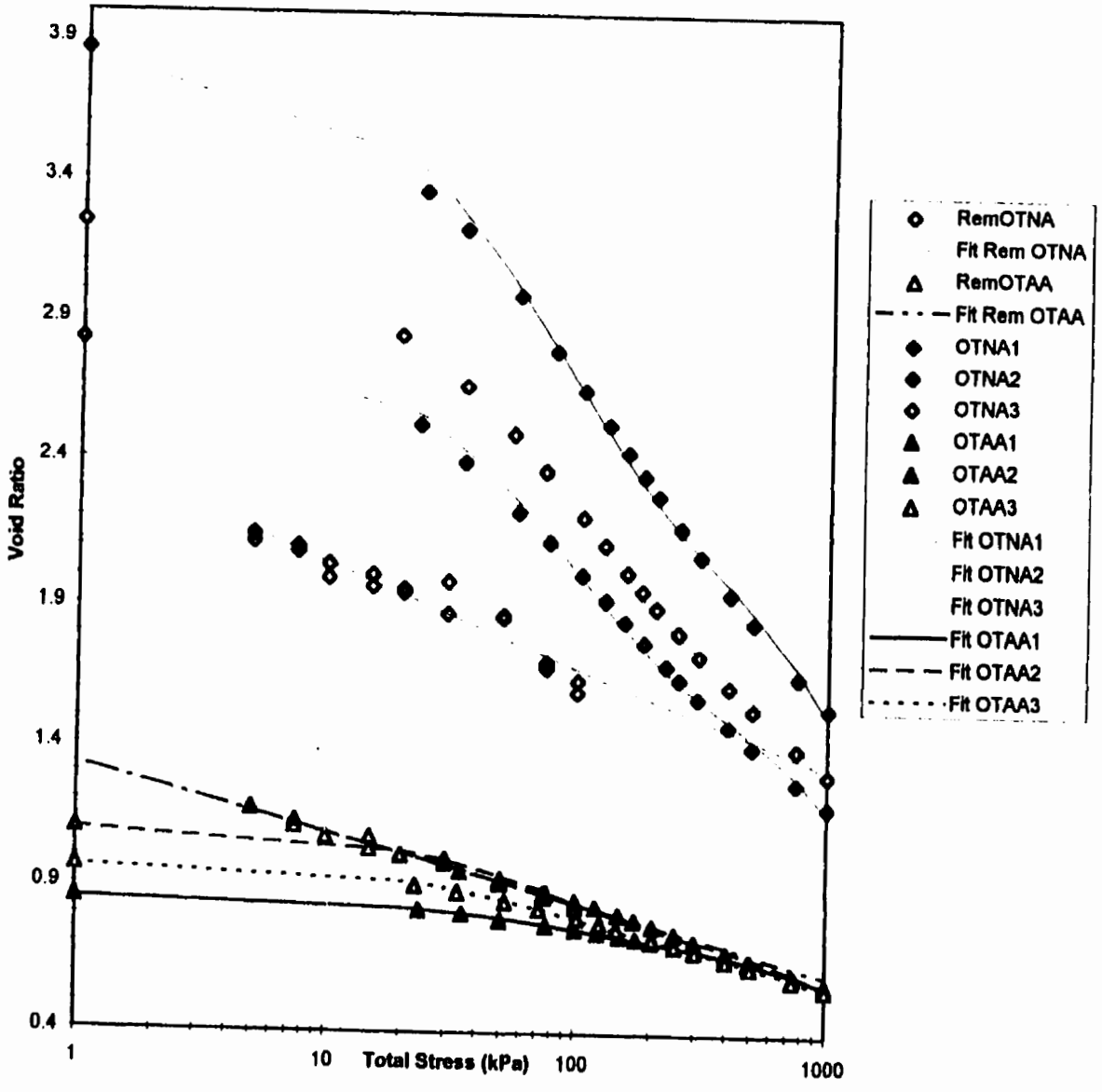

Total stress compression data for OT A horizon.

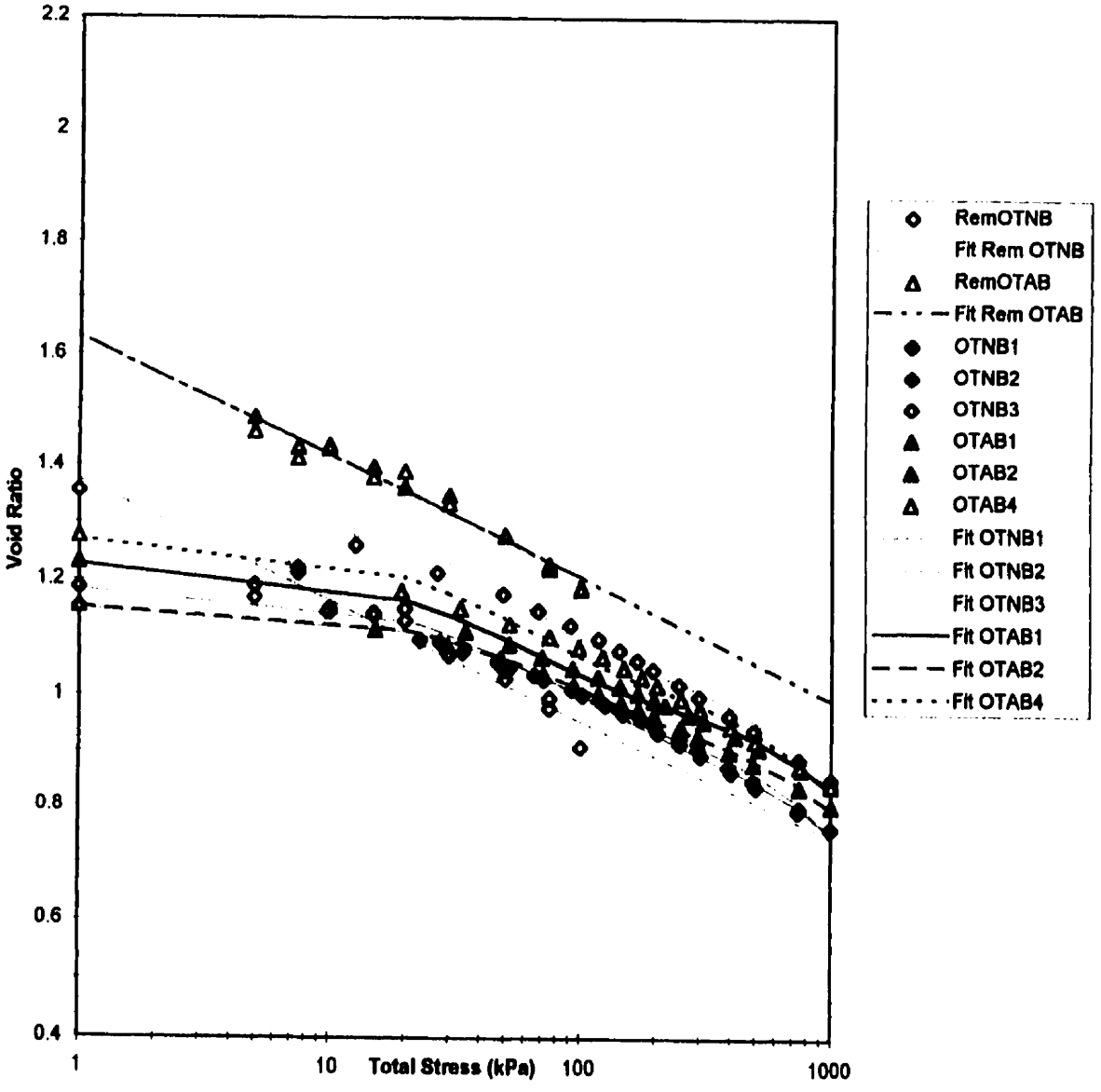

Total stress compression data for OT B horizon.

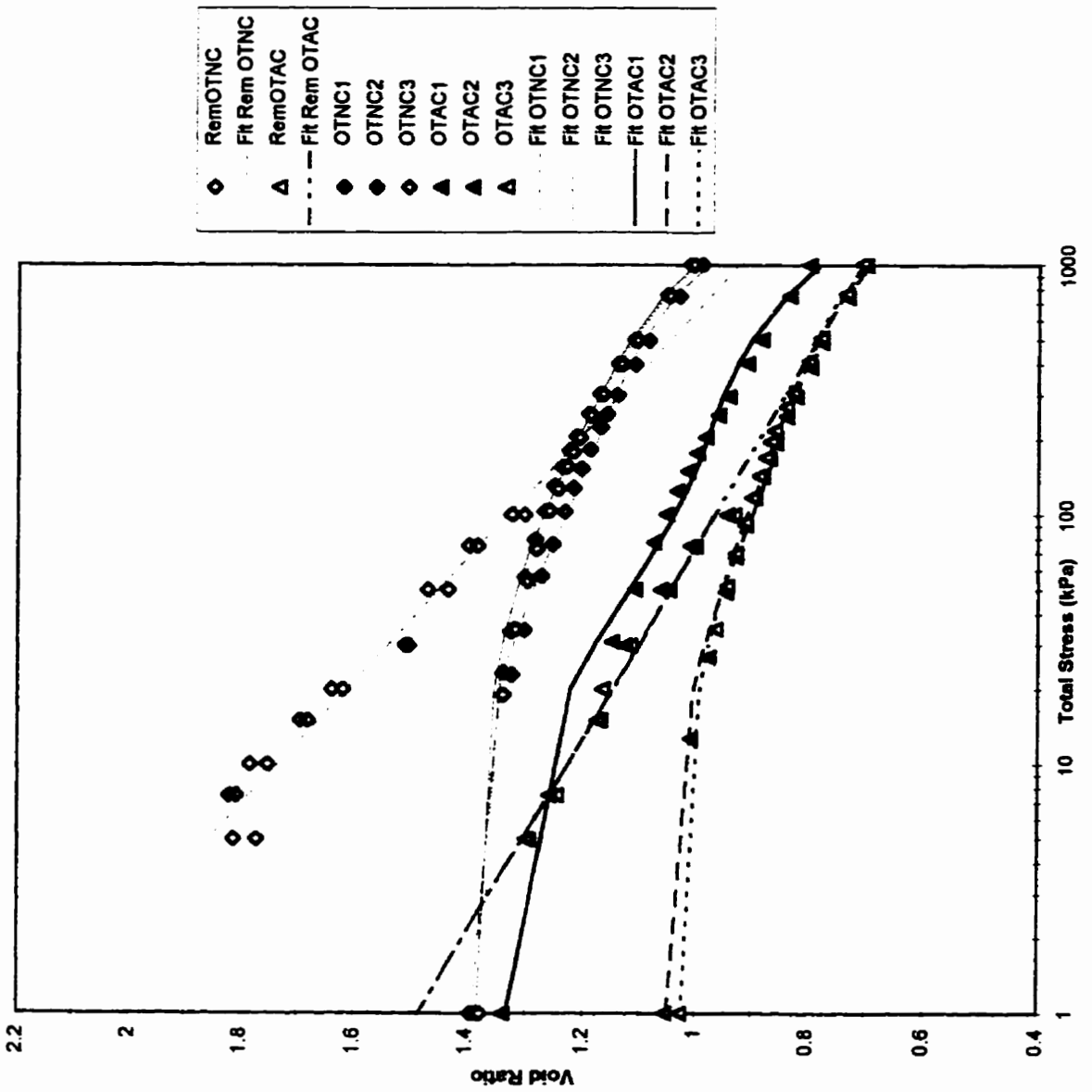

Total stress compression data for OT C horizon.

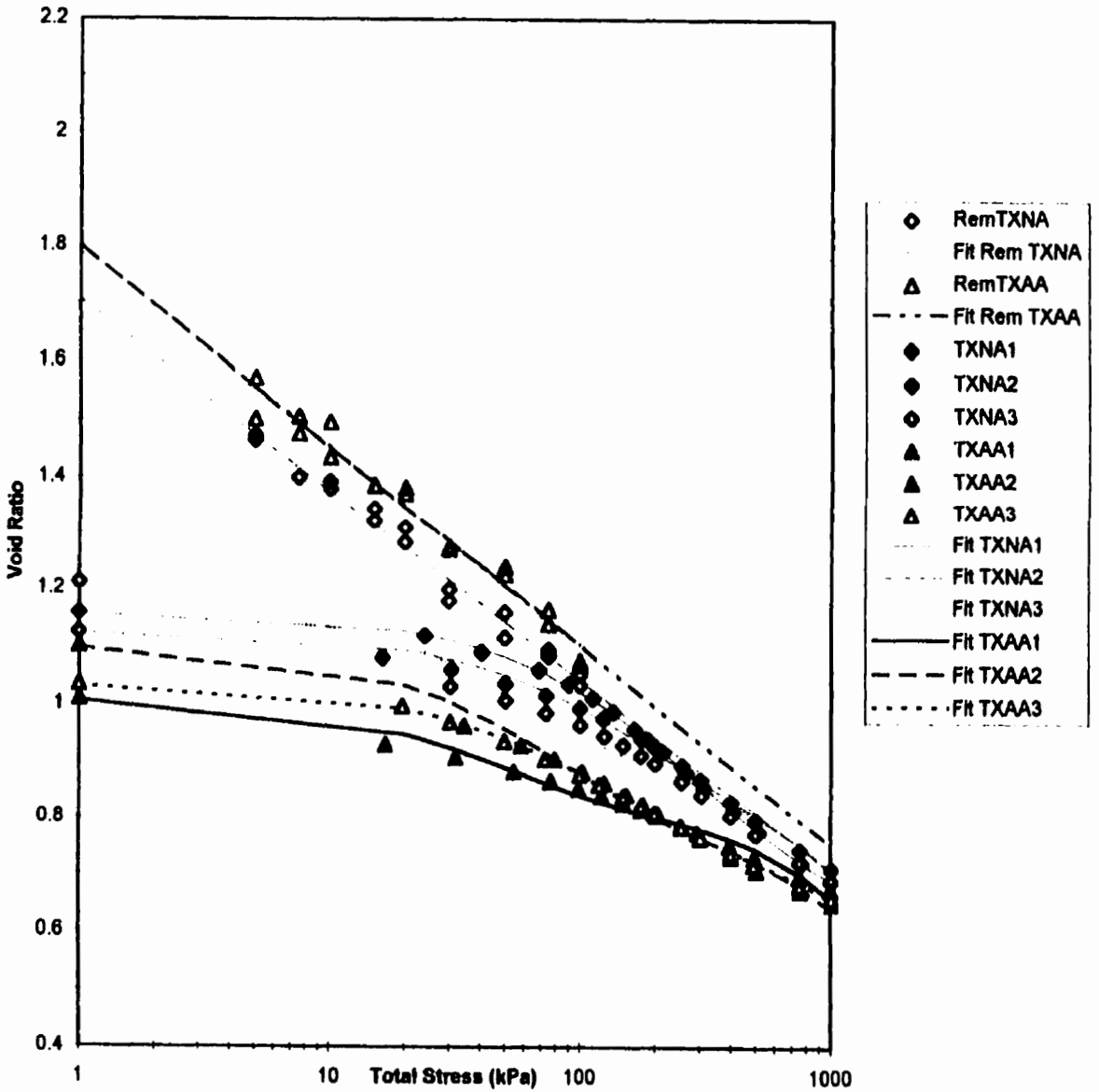

Total stress compression data for TX A horizons.

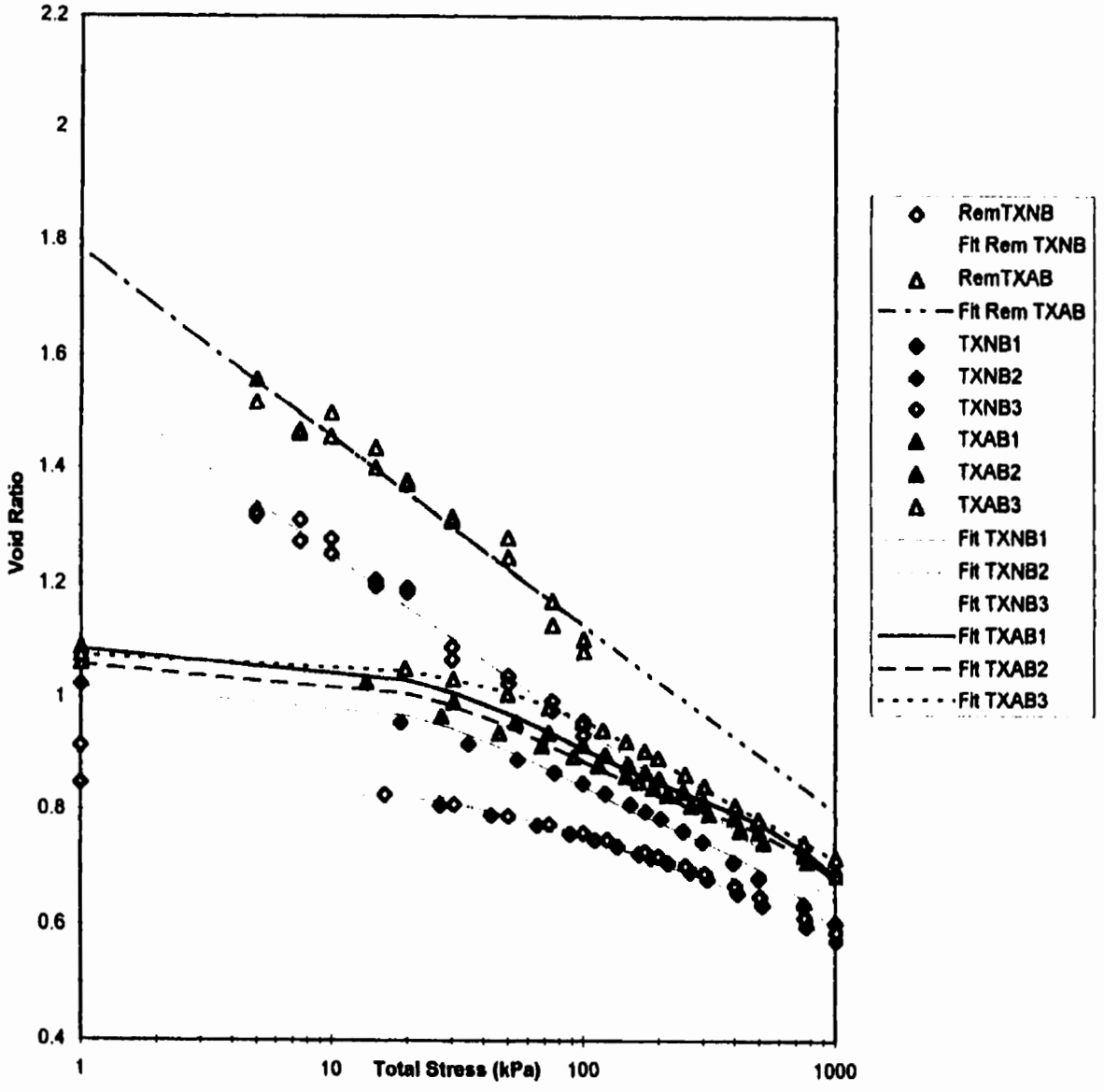

Total stress compression data for TX B horizons.

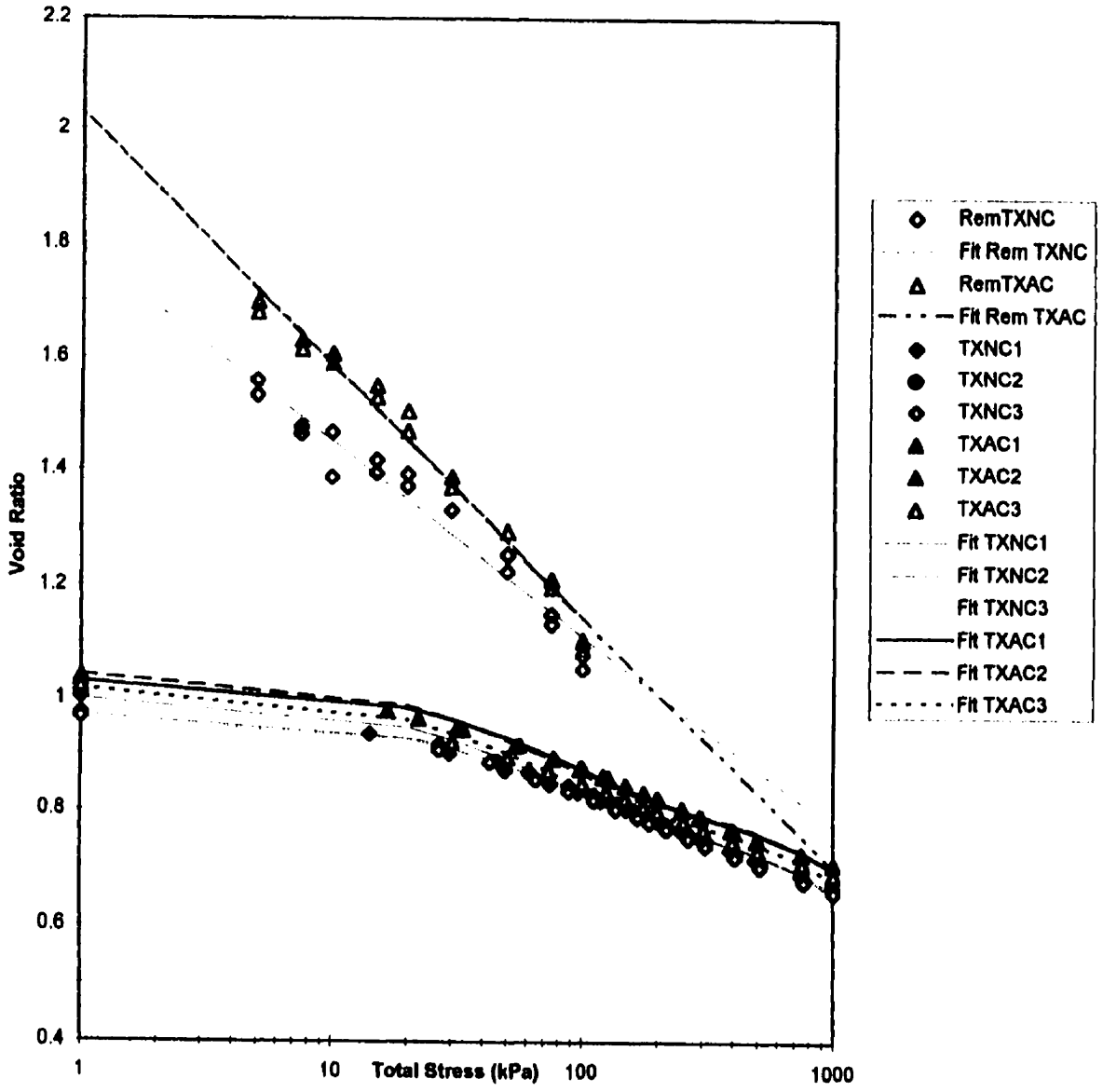

Total stress compression data for TX C horizons.

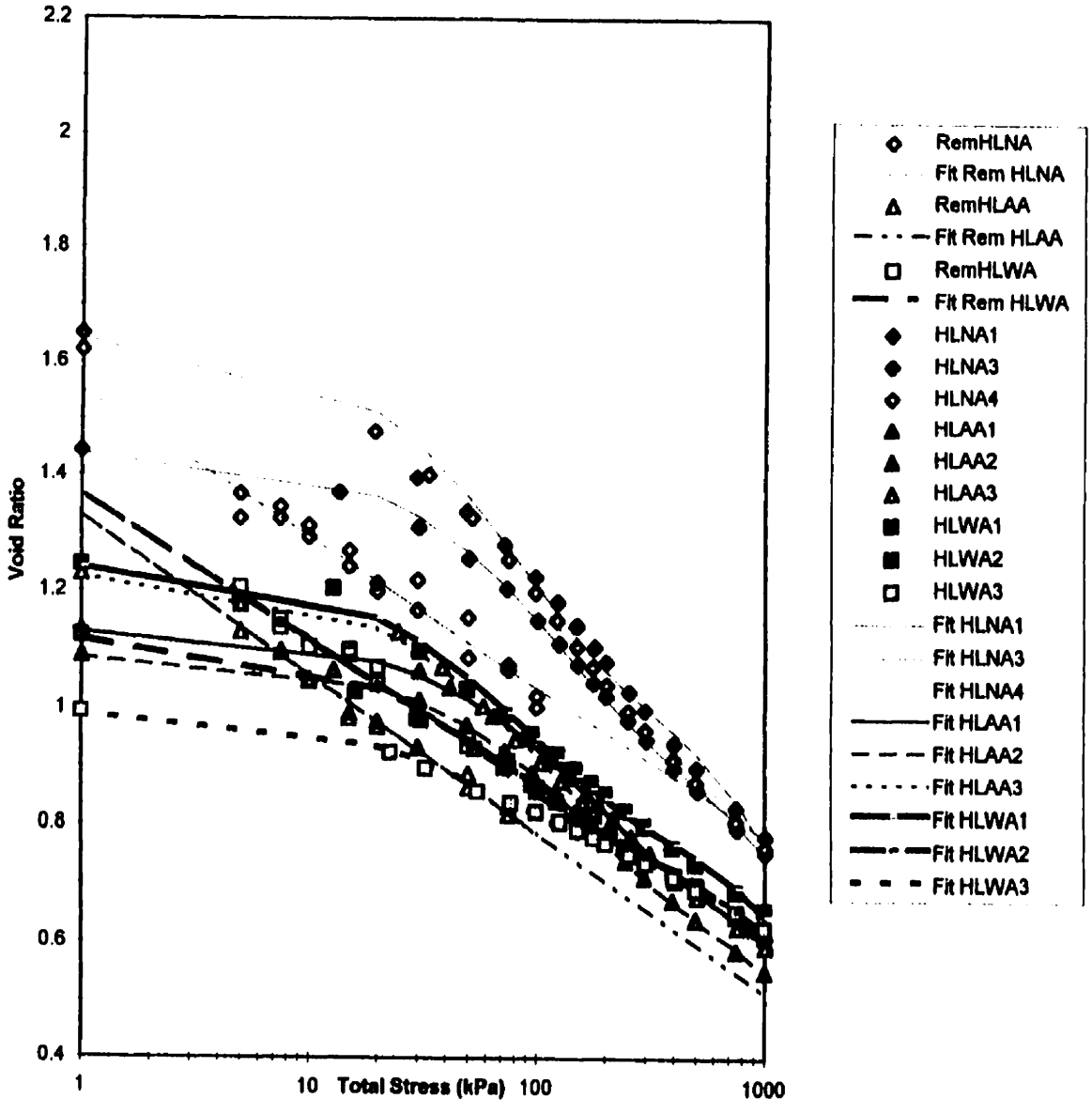

Total stress compression data for HL A horizons.

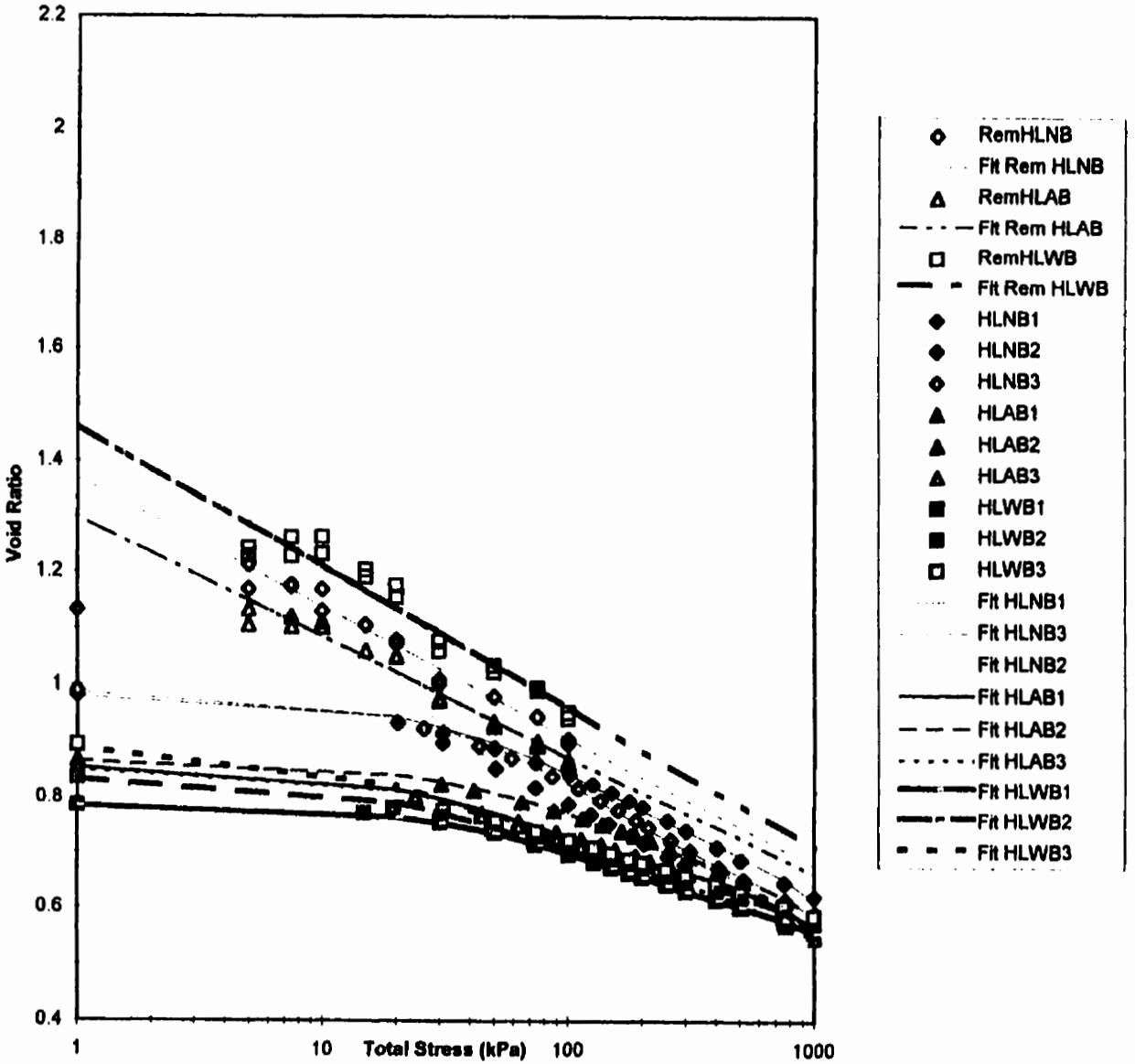

Total stress compression data for HL B horizons.

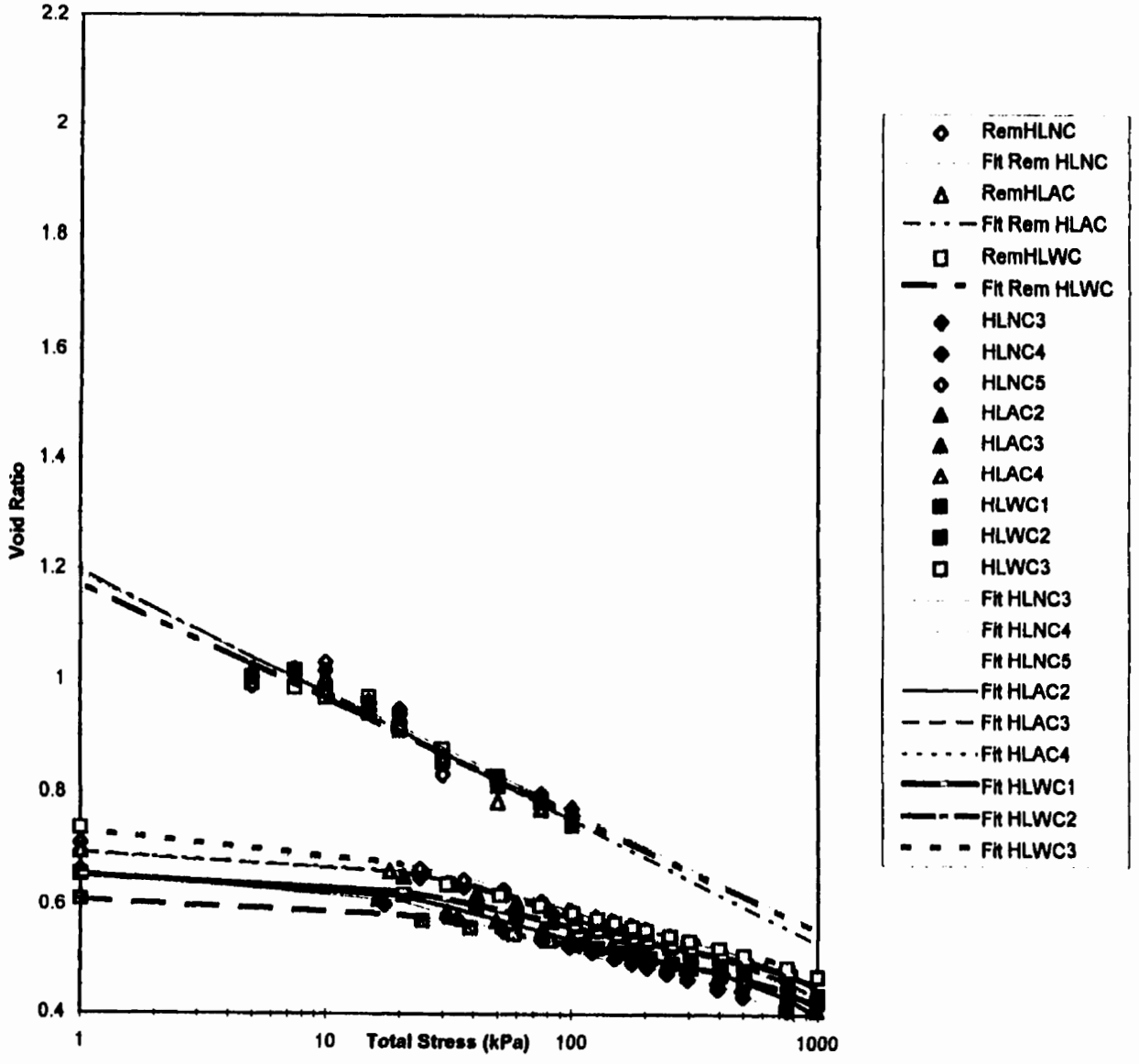

Total stress compression data for HL C horizons.

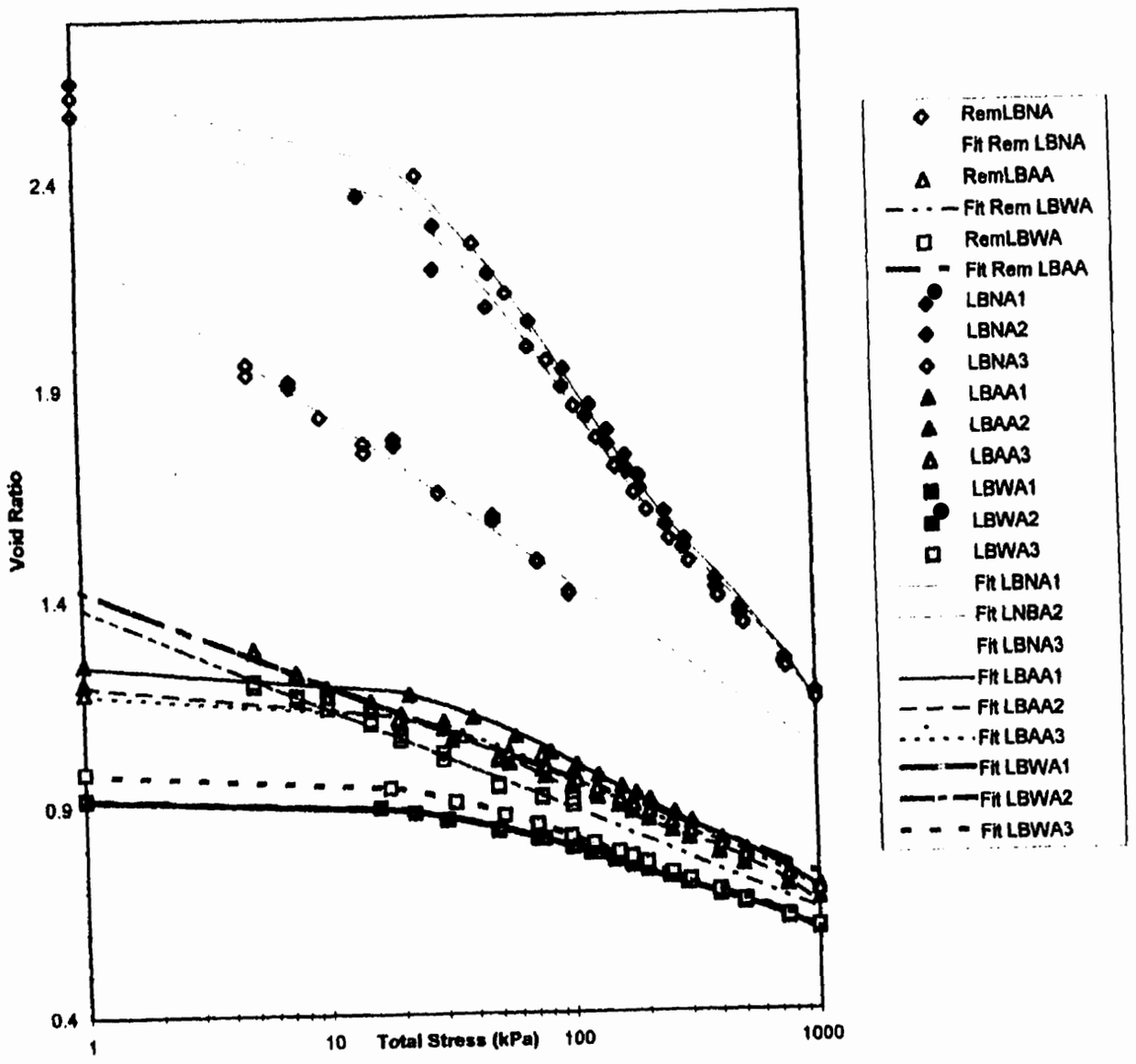

Total stress compression data for LB A horizons.

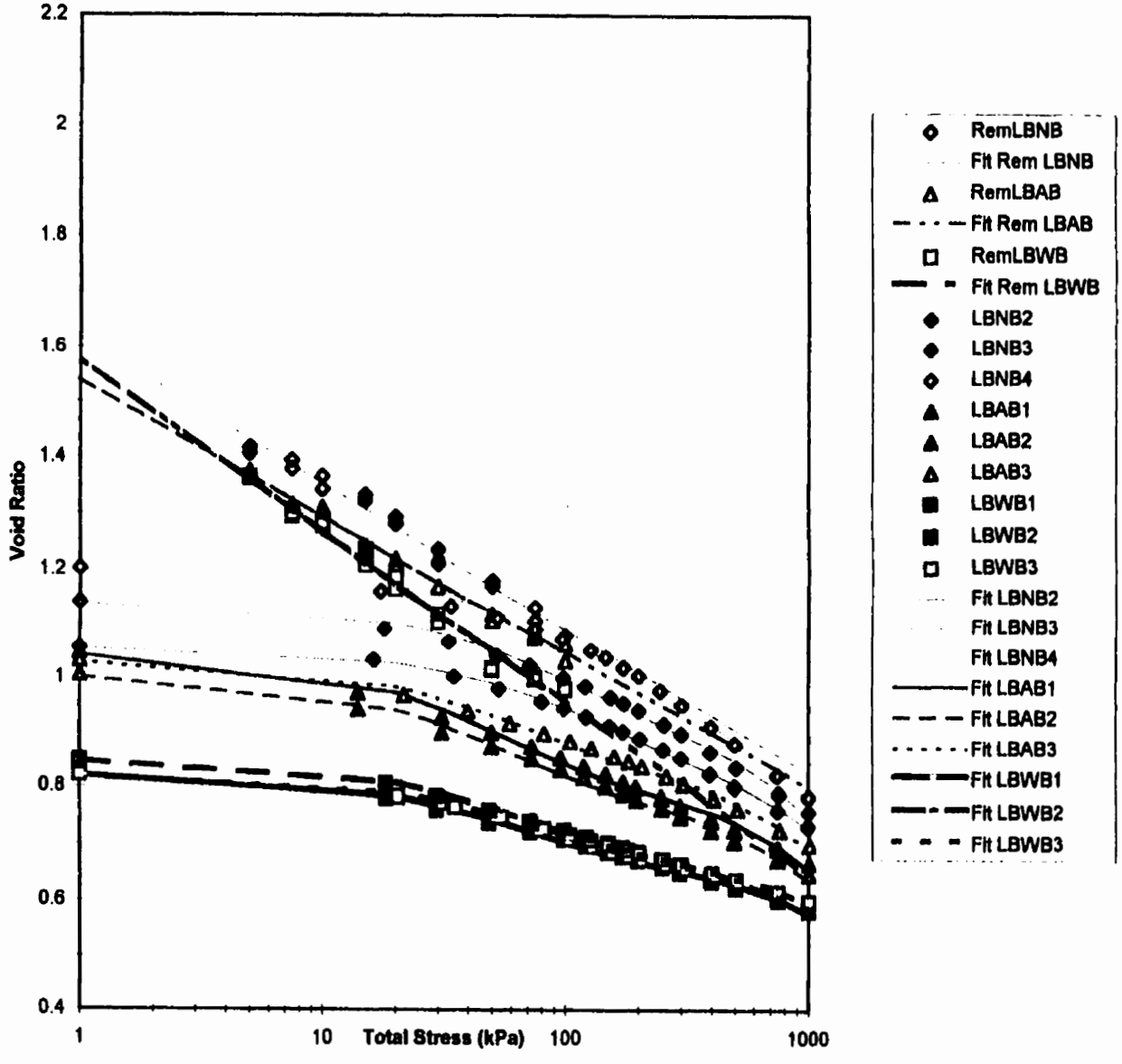

Total stress compression data for LB B horizons.

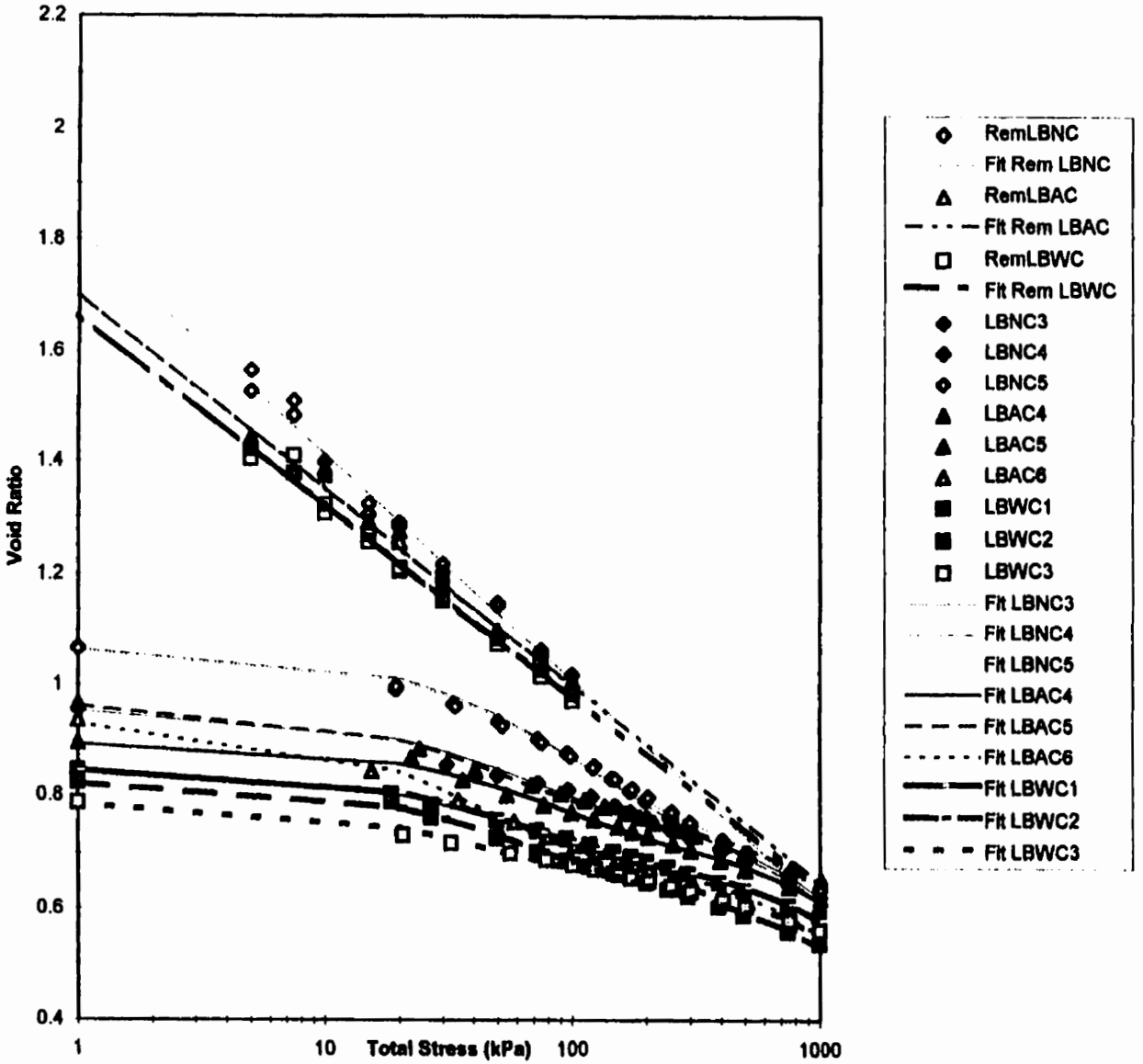

Total stress compression data for LB C horizons.

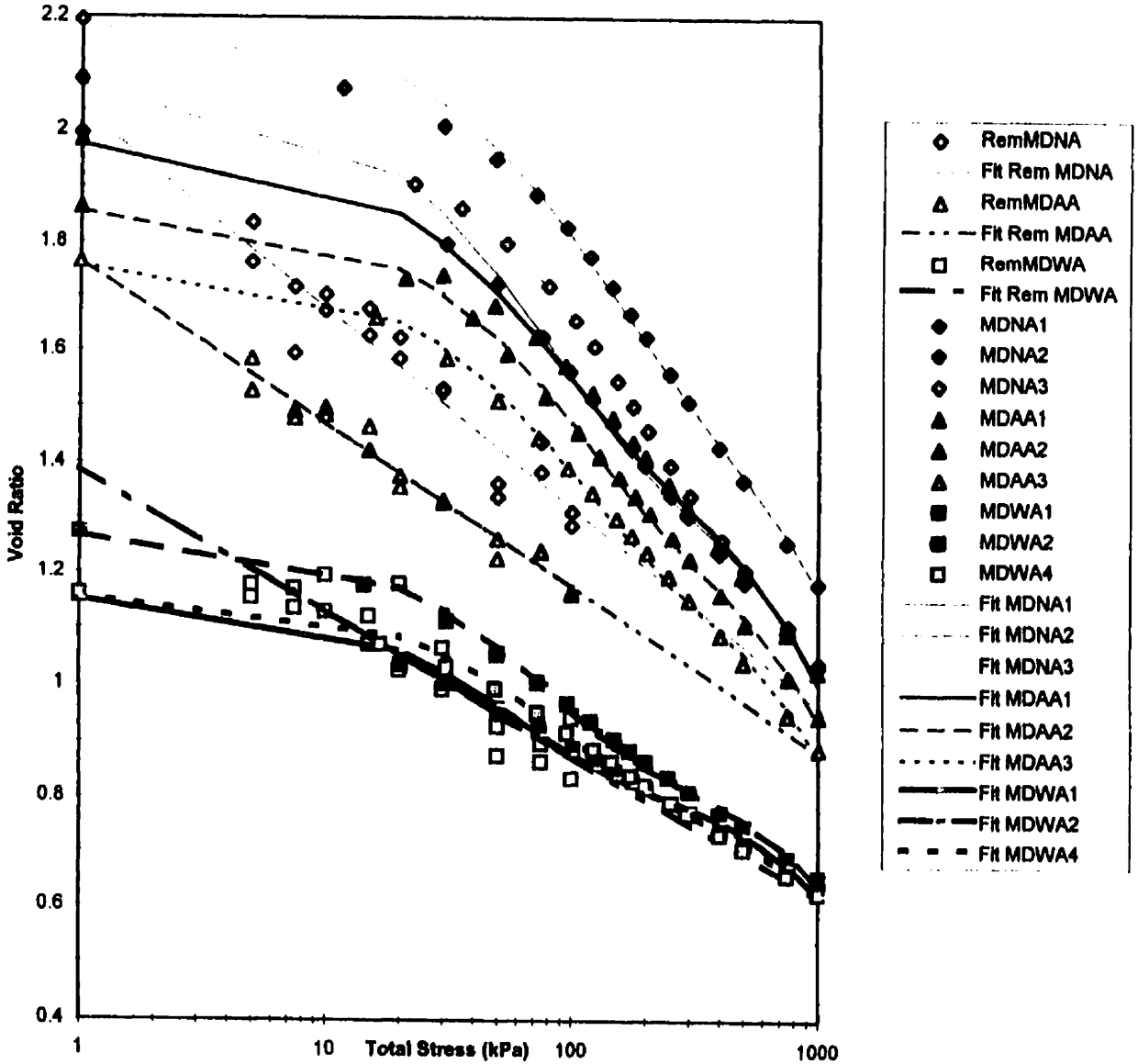

Total stress compression data for MD A horizons.

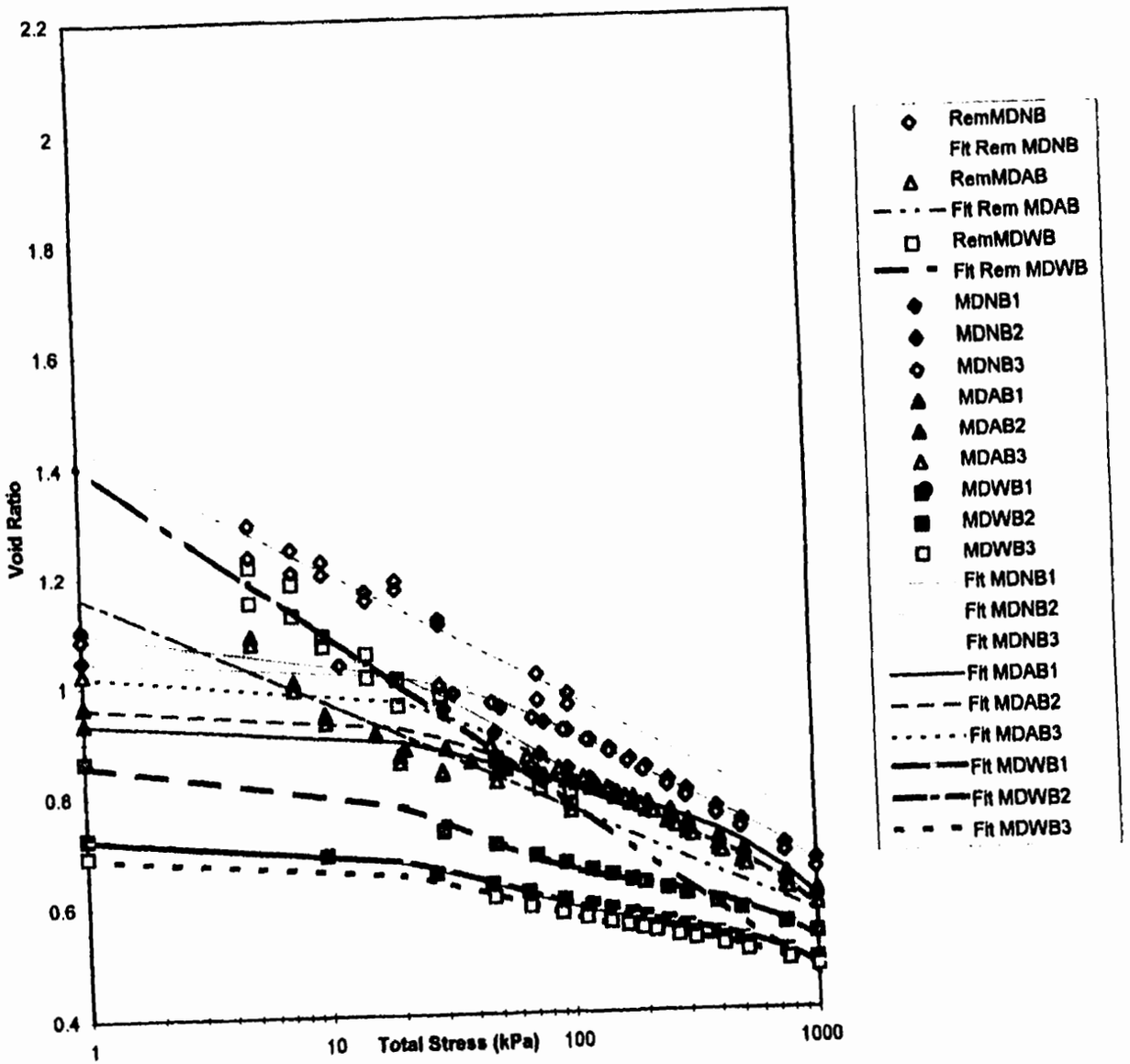

Total stress compression data for MD B horizons.

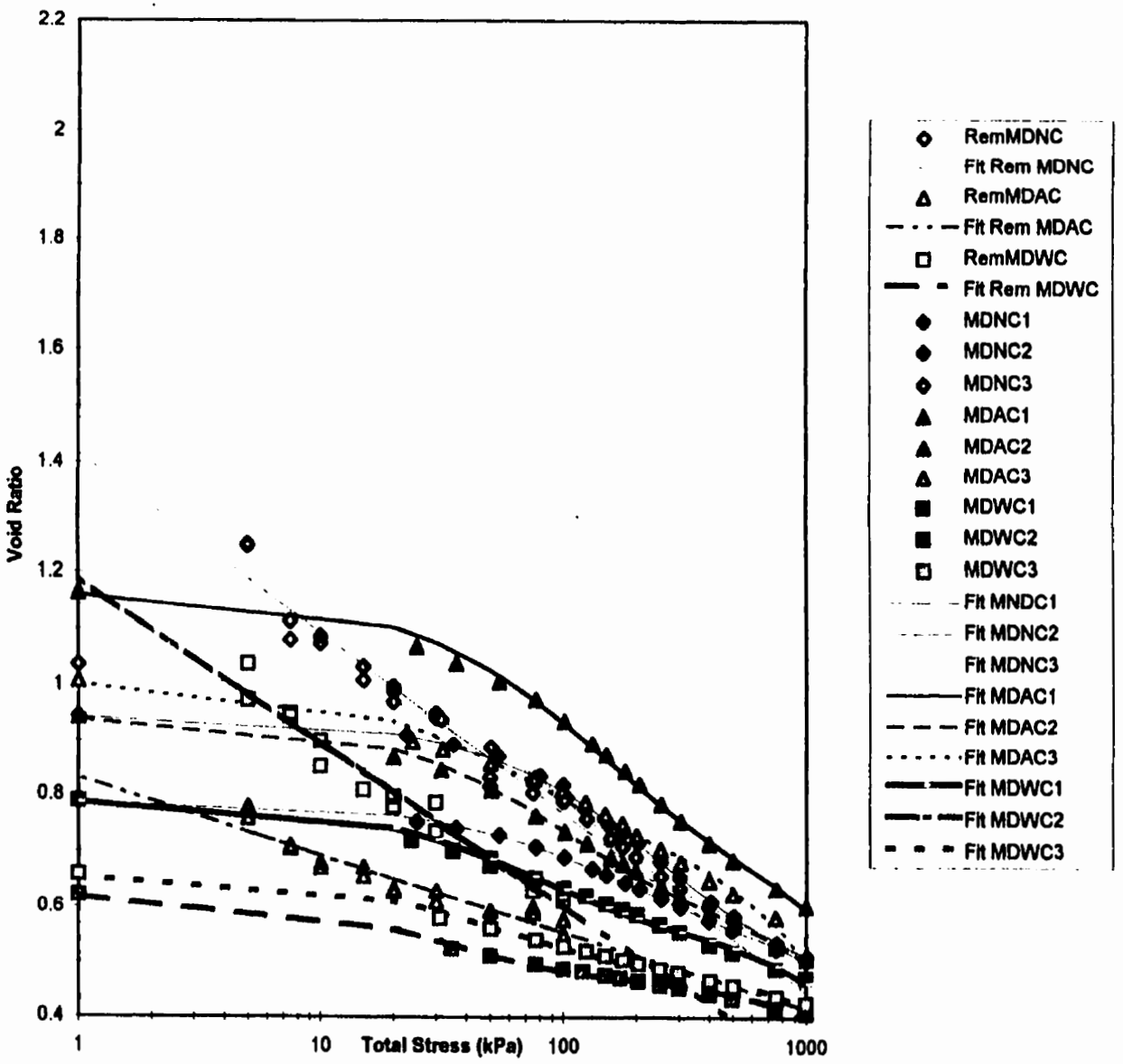

Total stress compression data for MD C horizons.

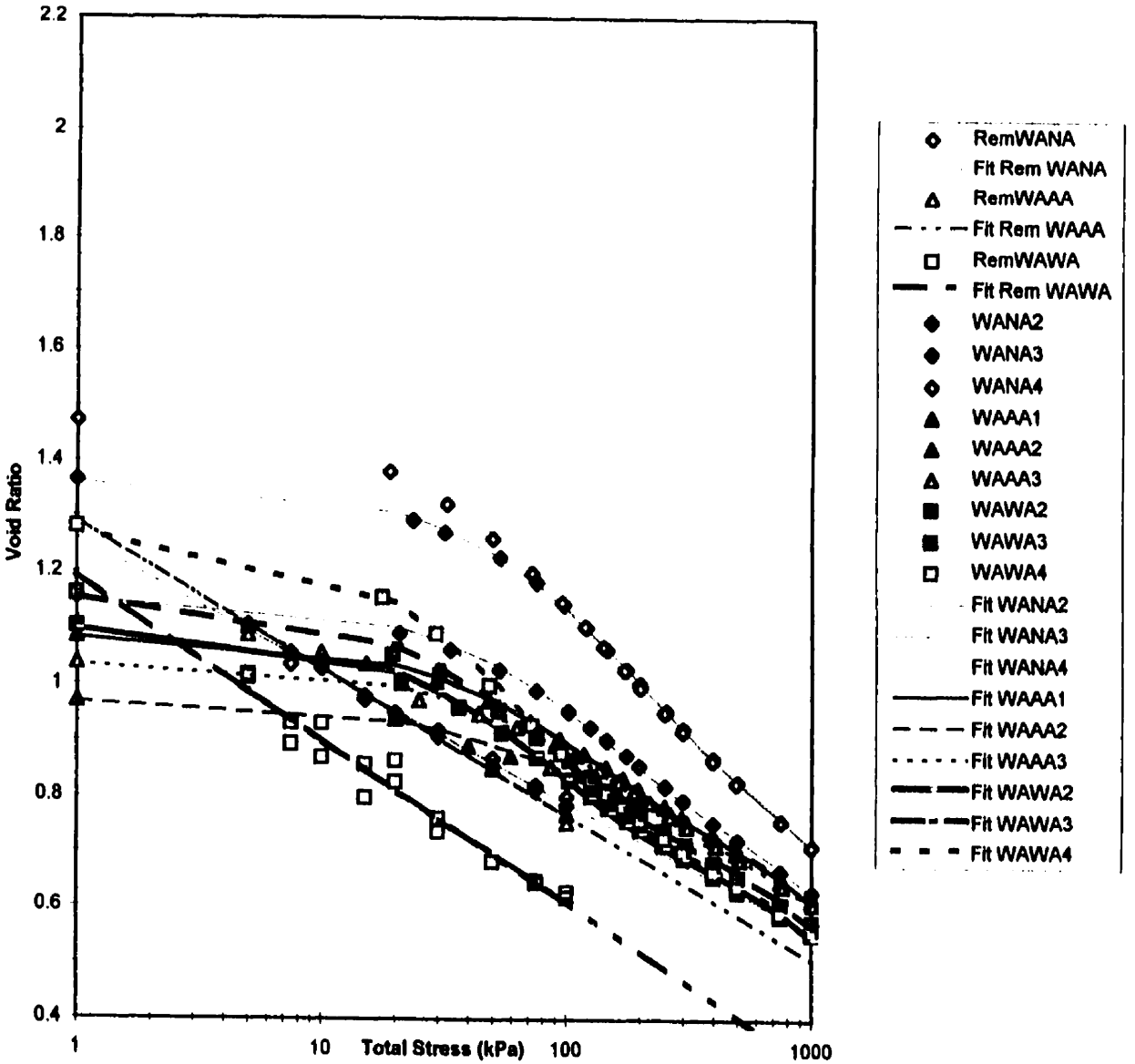

Total stress compression data for WA A horizons.

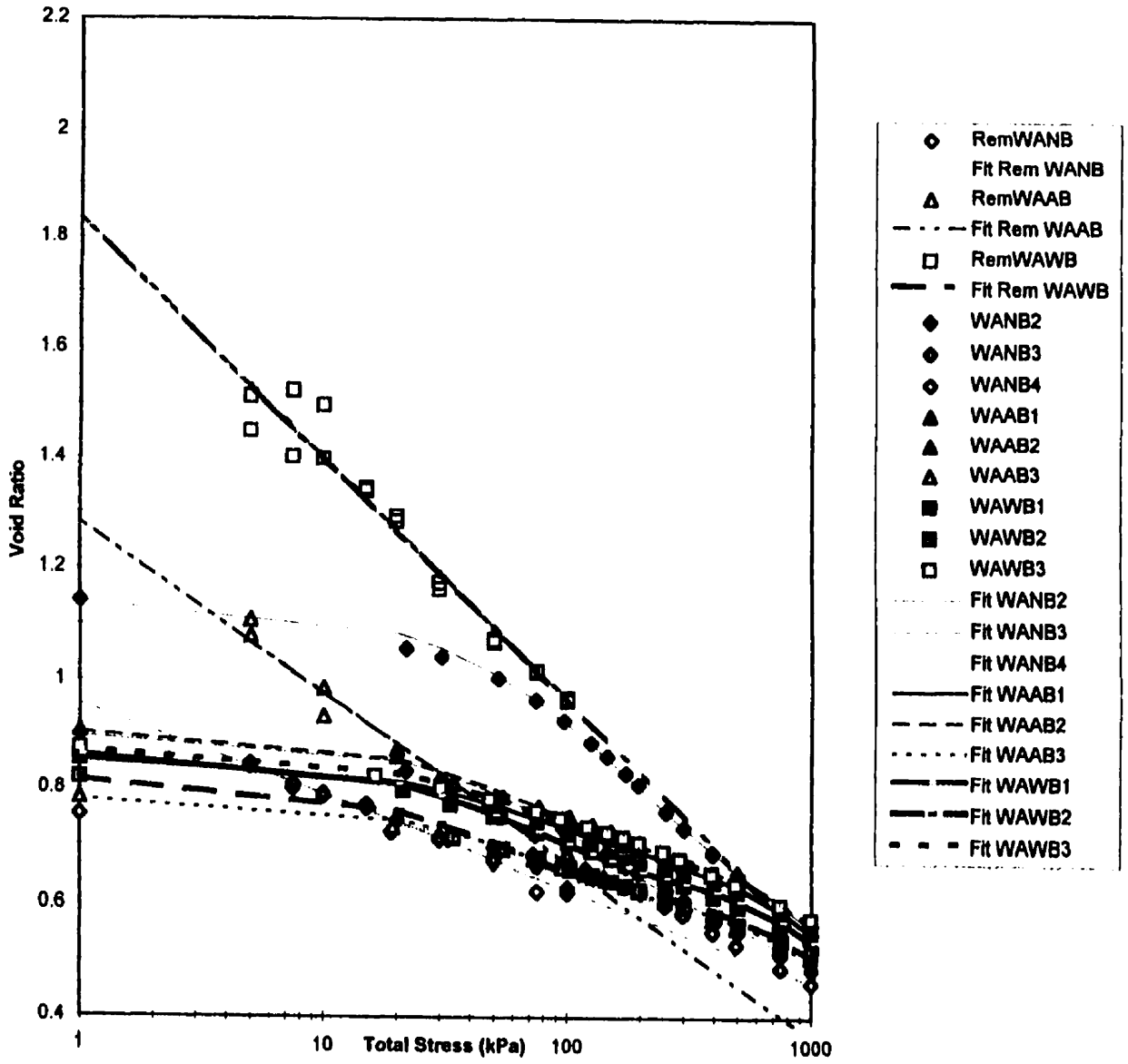

Total stress compression data for WA B horizons.

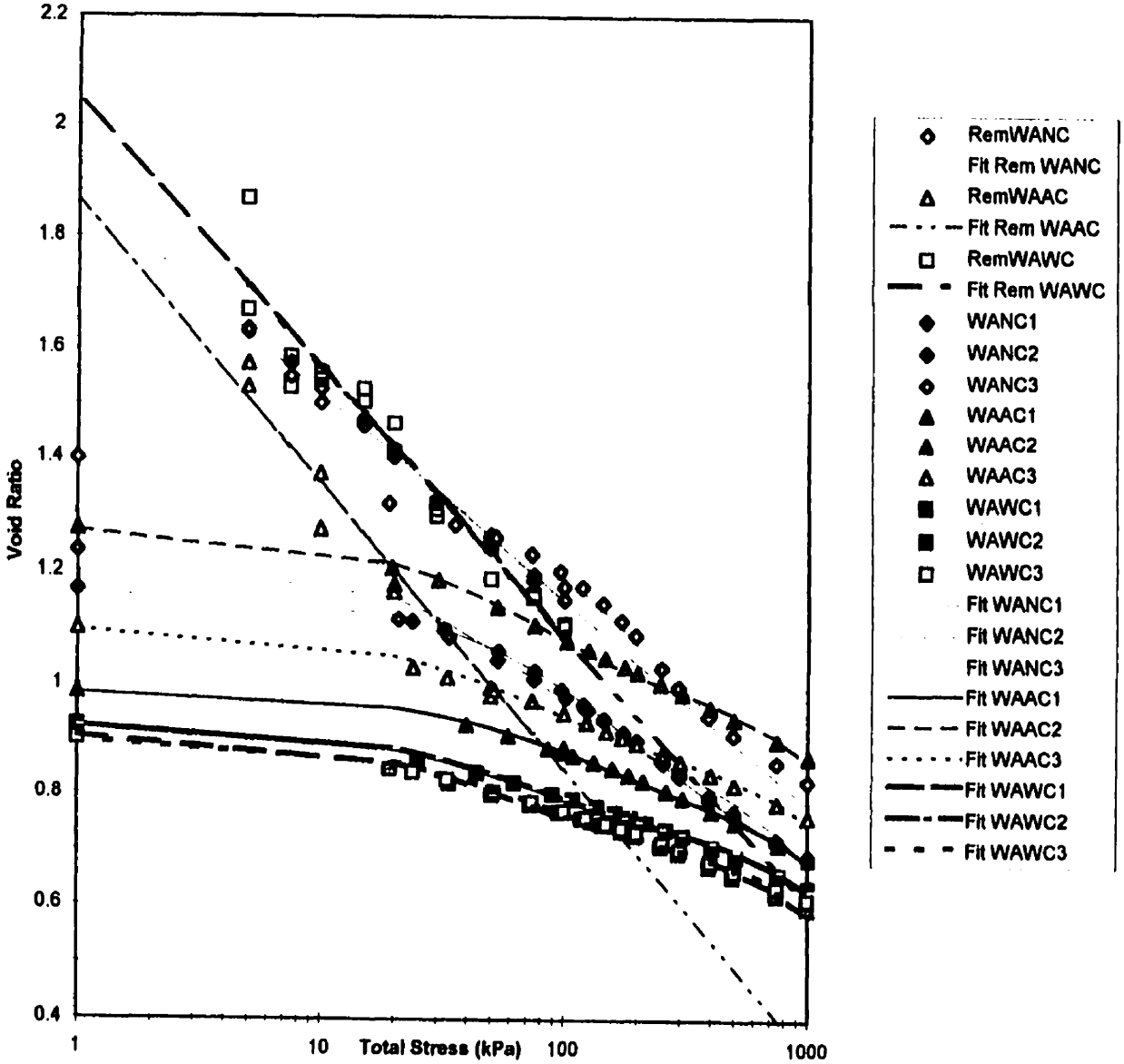

Total stress compression data for WA C horizons.

7.2 Appendix to Chapter Three

7.2.1 Graphs of Remoulded and Structured Shrinkage Curves

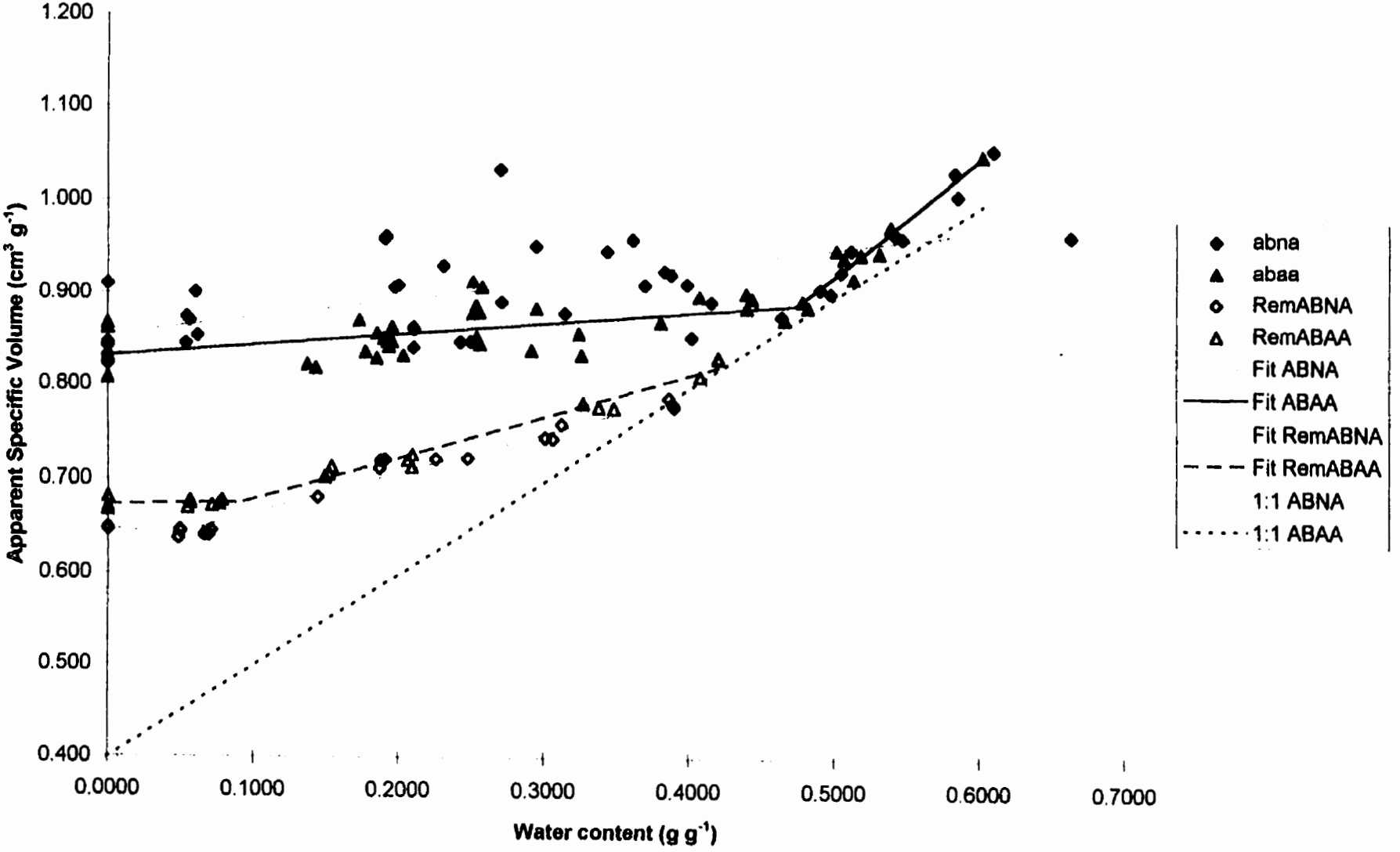

Shrinkage data for AB A horizons, *v* (*w*) coordinates.

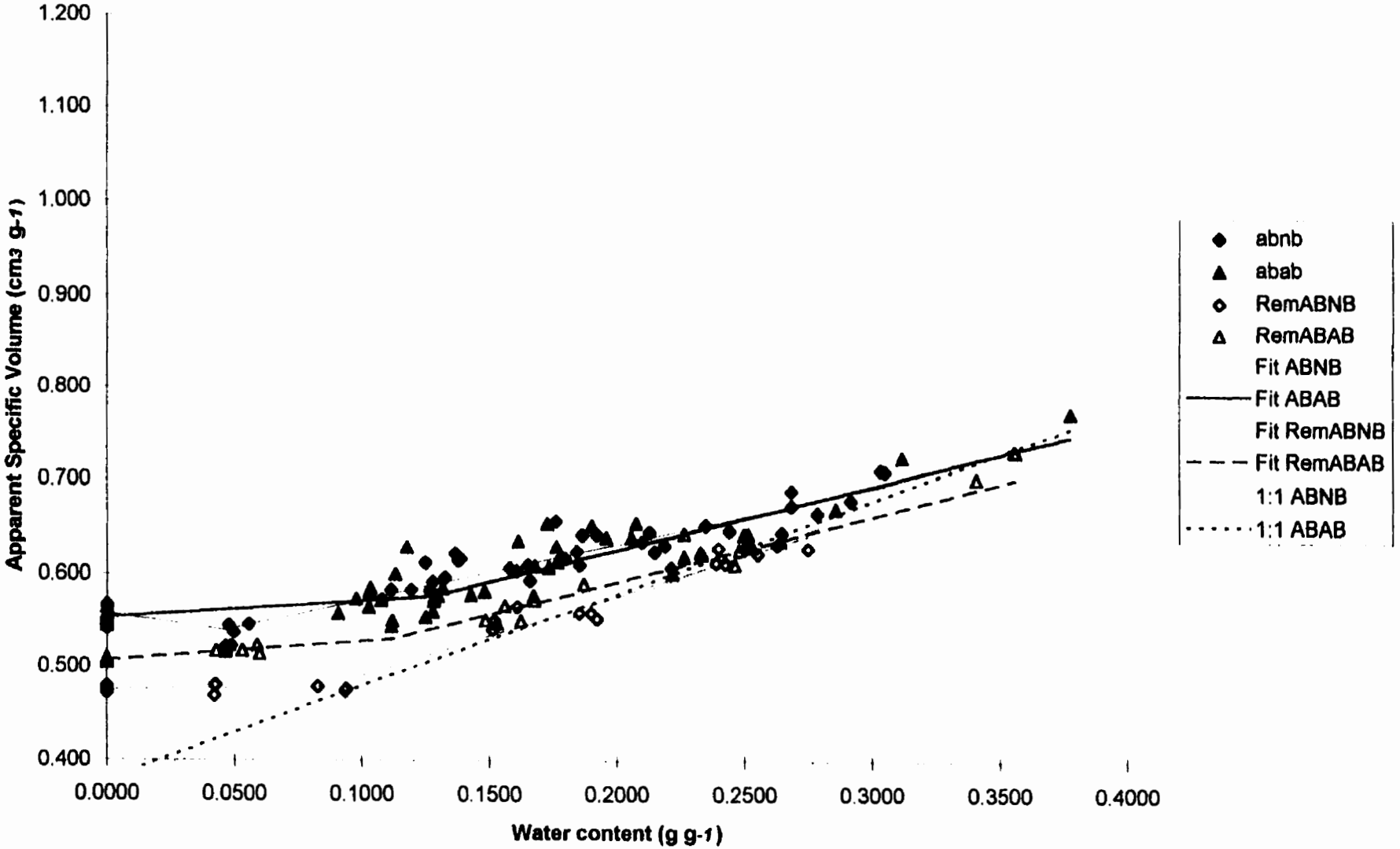

Shrinkage data for AB B horizons, $v(w)$ coordinates.

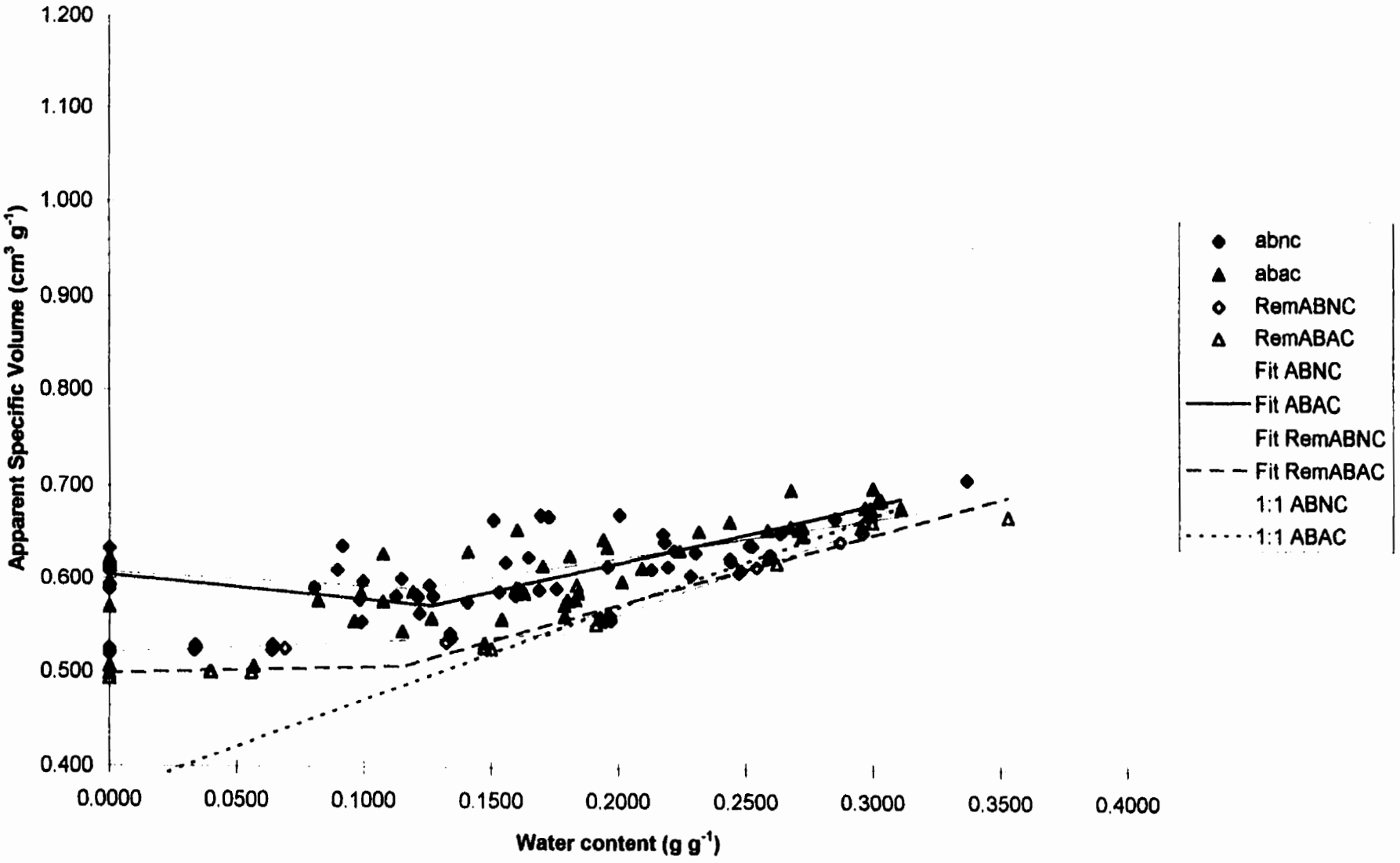

Shrinkage data for AB C horizons, *v* (*w*) coordinates.

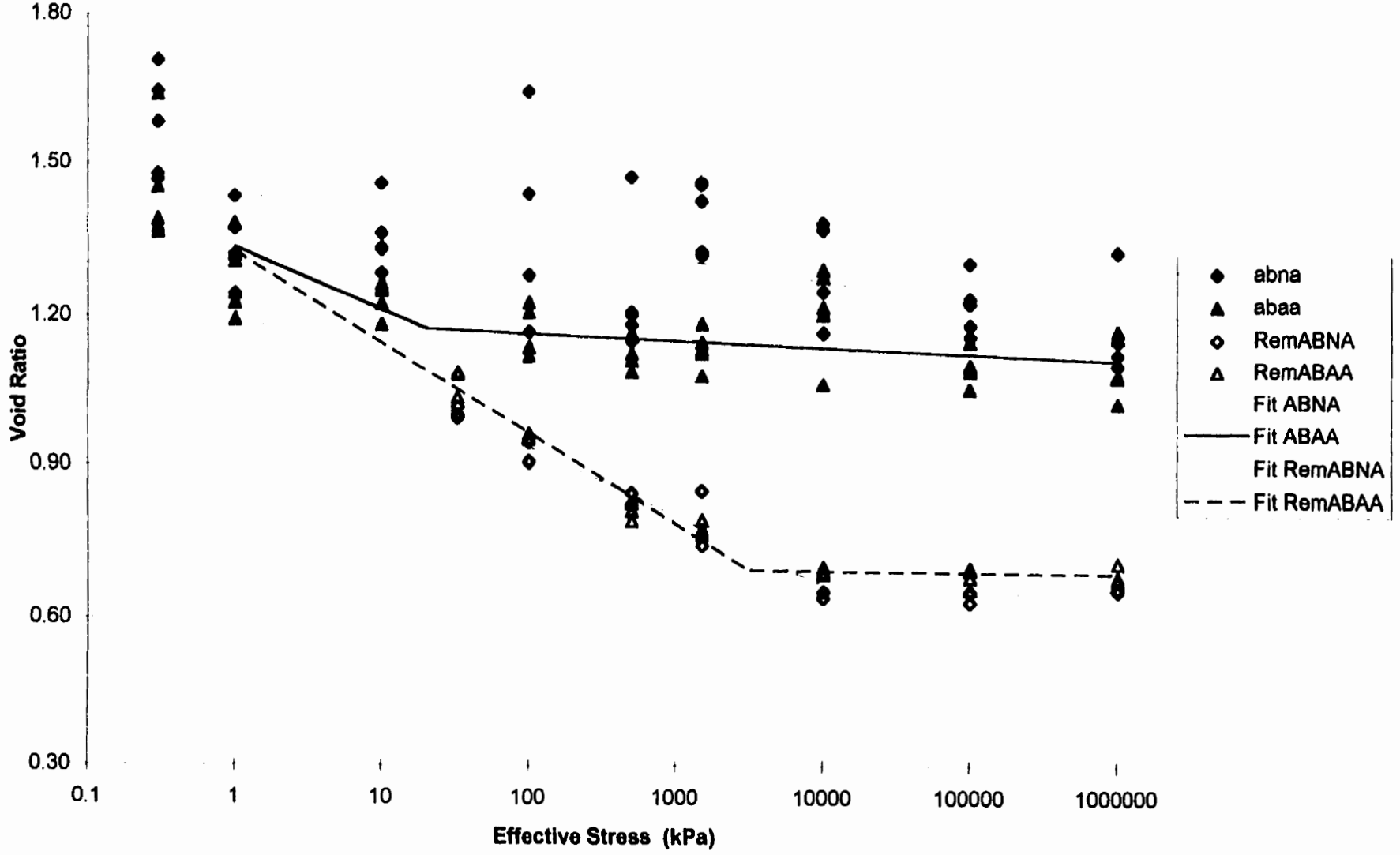

Shrinkage data for AB A horizons, $e(\sigma)$ co-ordinates.

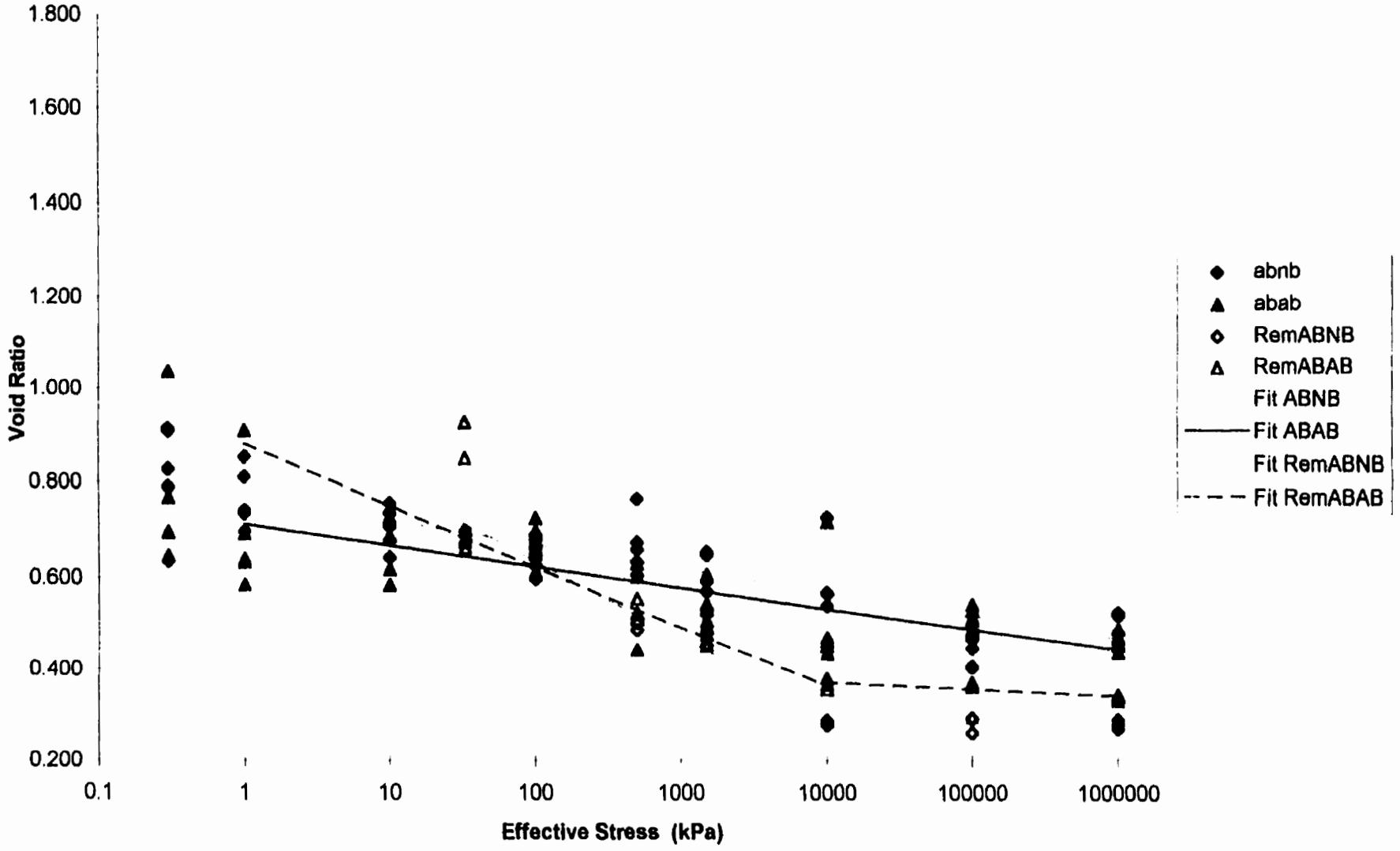

Shrinkage data for AB B horizons, $e(\sigma)$ co-ordinates.

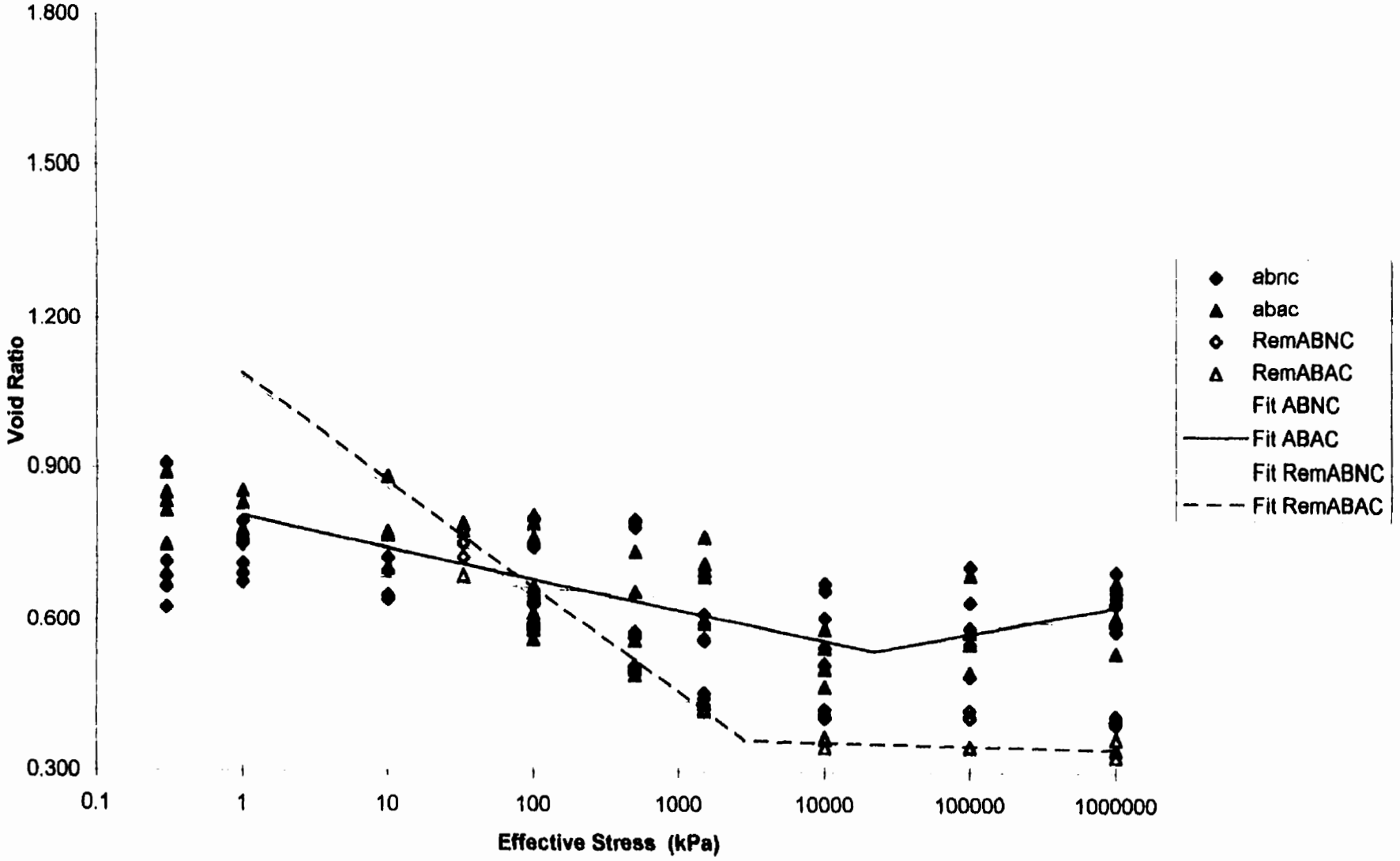

Shrinkage data for AB C horizons, $e(\sigma)$ co-ordinates.

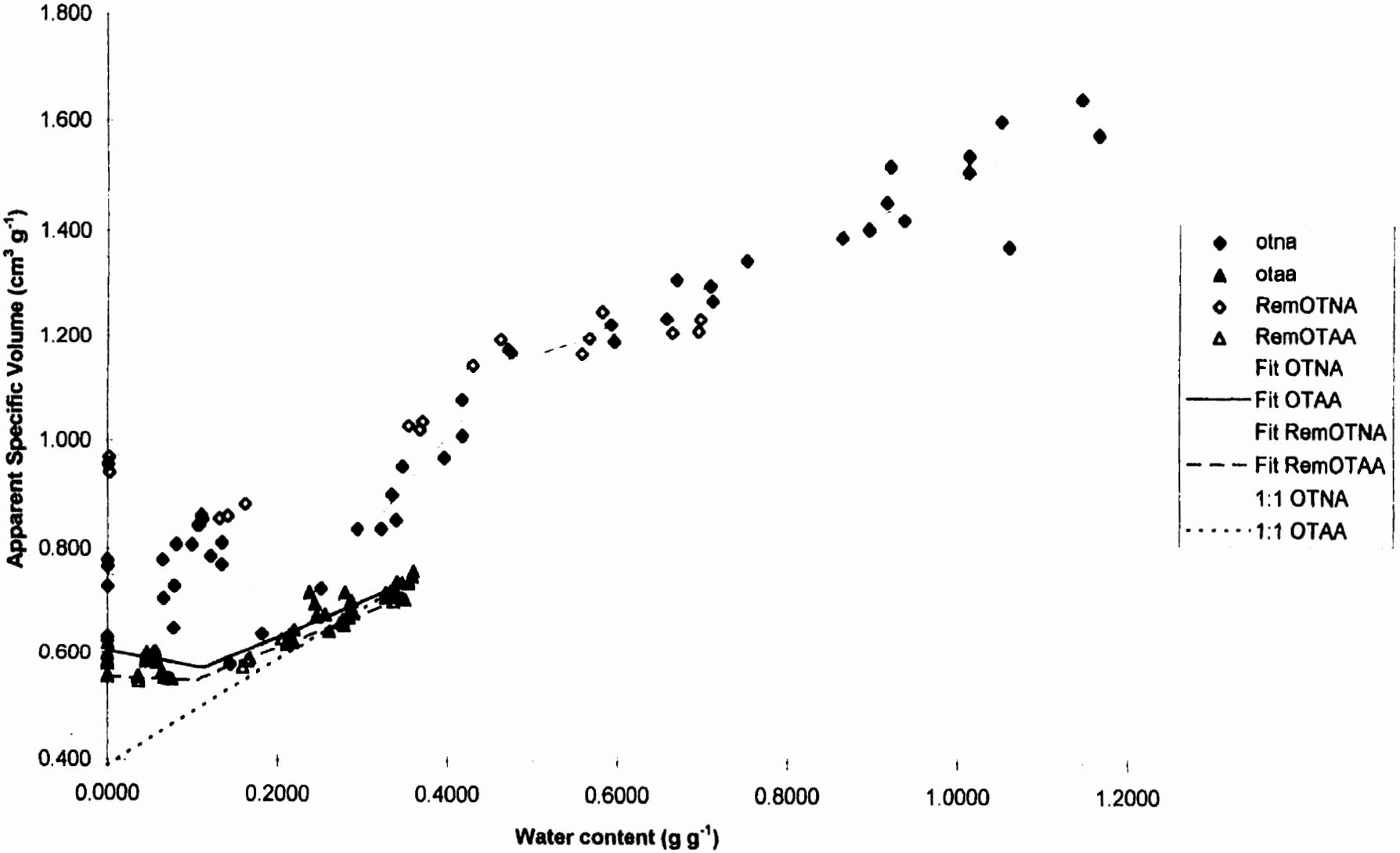

Shrinkage data for OT A horizons, $v(w)$ coordinates.

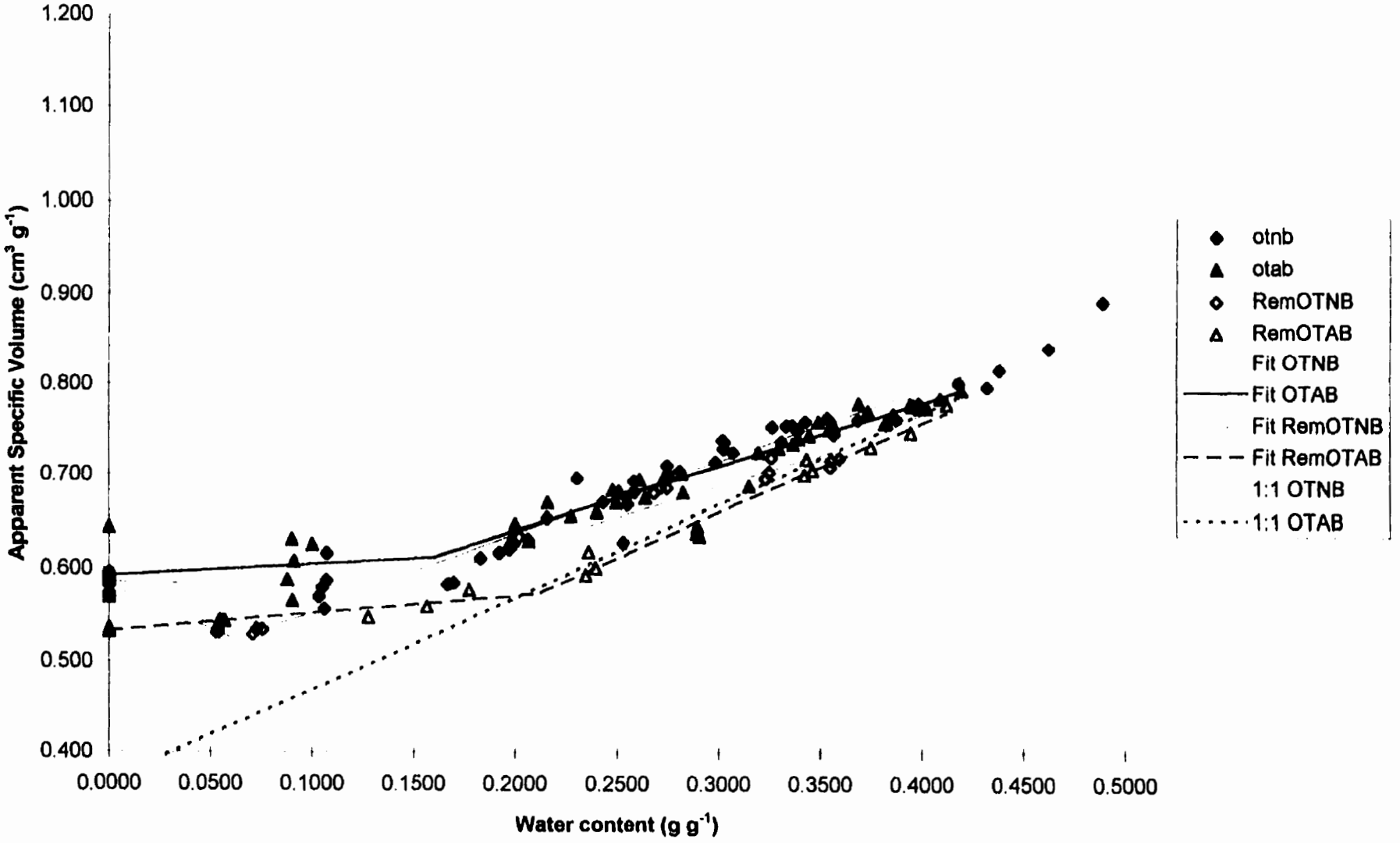

Shrinkage data for OT B horizons, $v(w)$ coordinates.

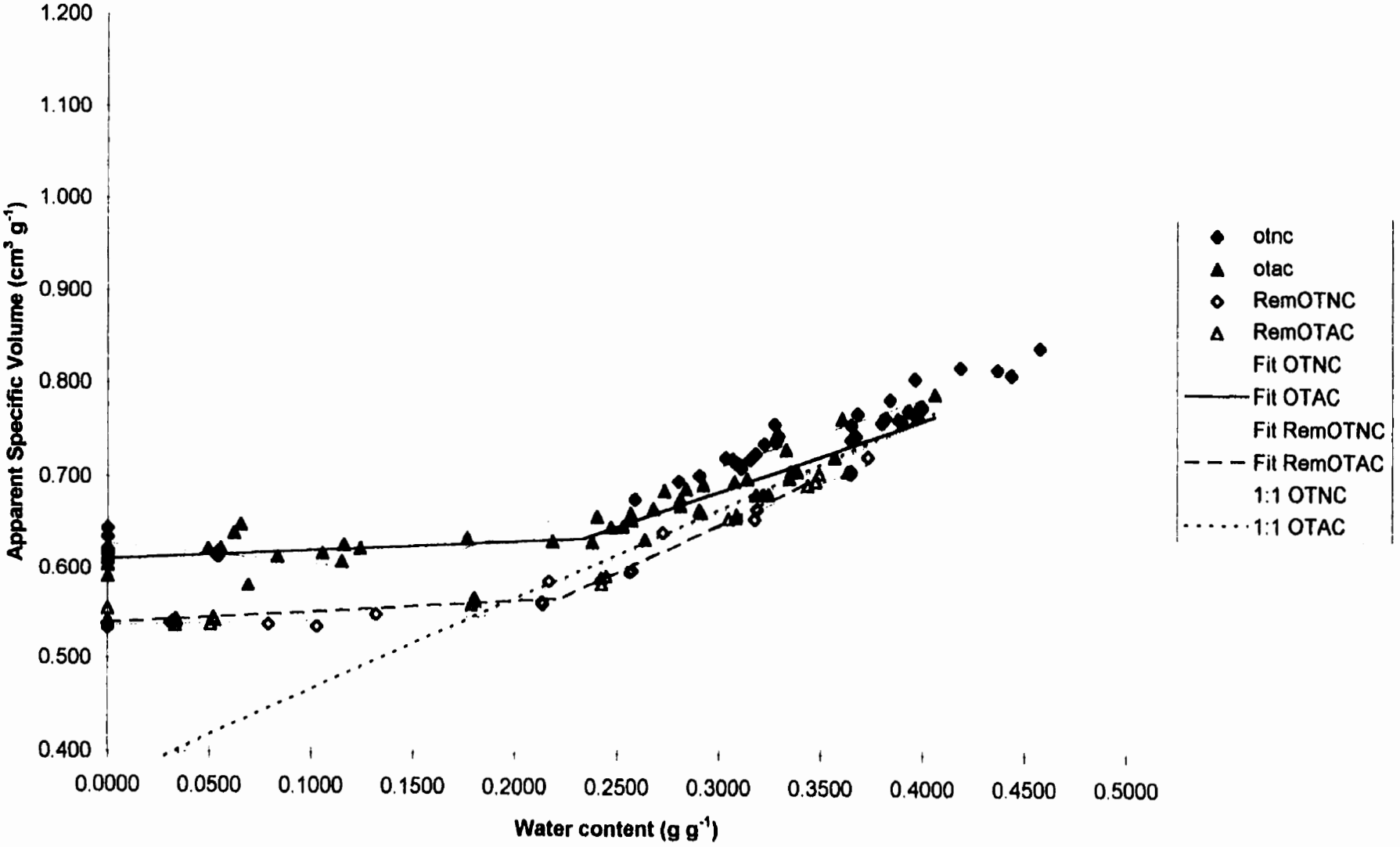

Shrinkage data for OT C horizons, *v* (*w*) coordinates.

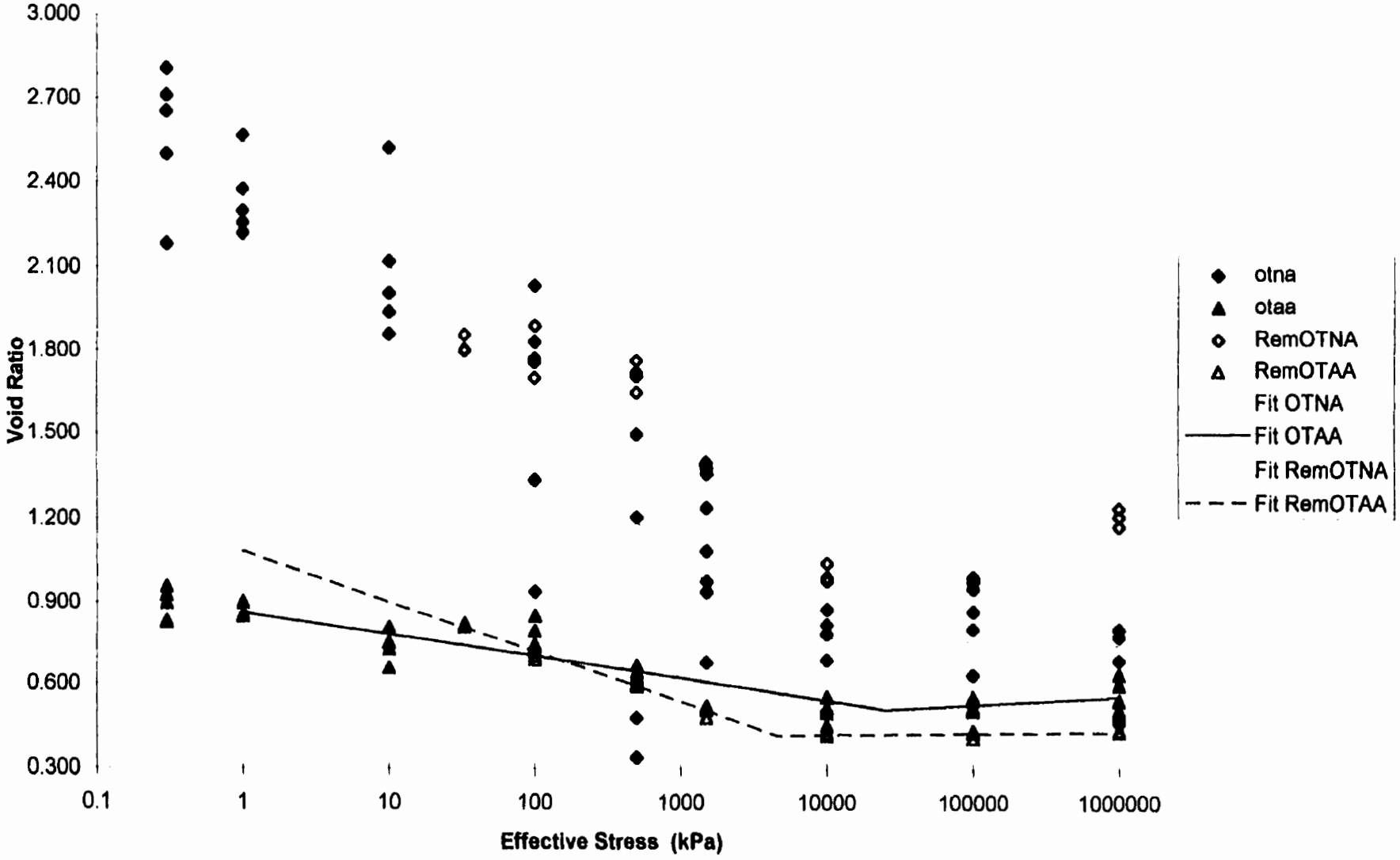

Shrinkage data for OT A horizons, $e(\sigma)$ co-ordinates.

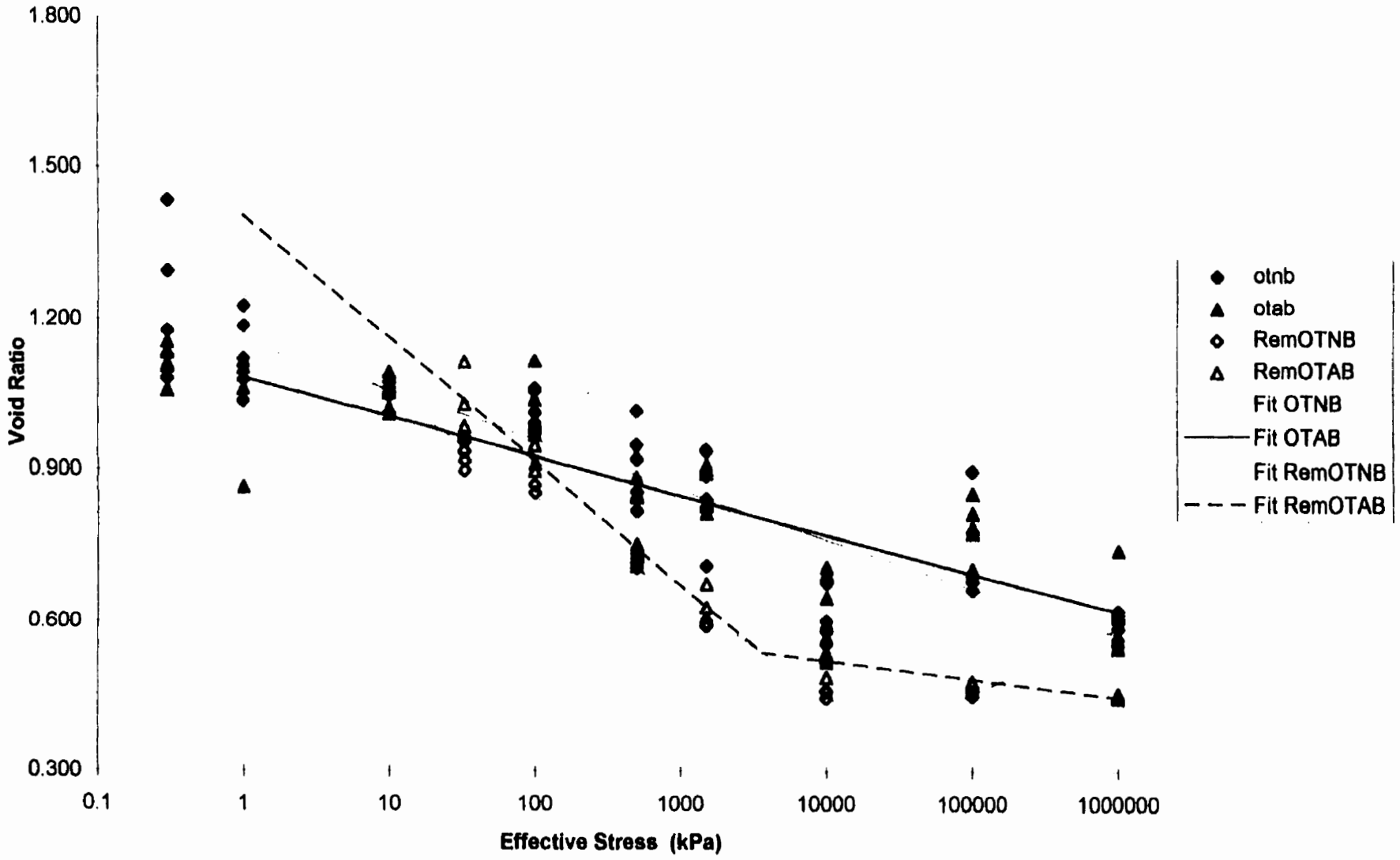

Shrinkage data for OT B horizons, e (σ) co-ordinates.

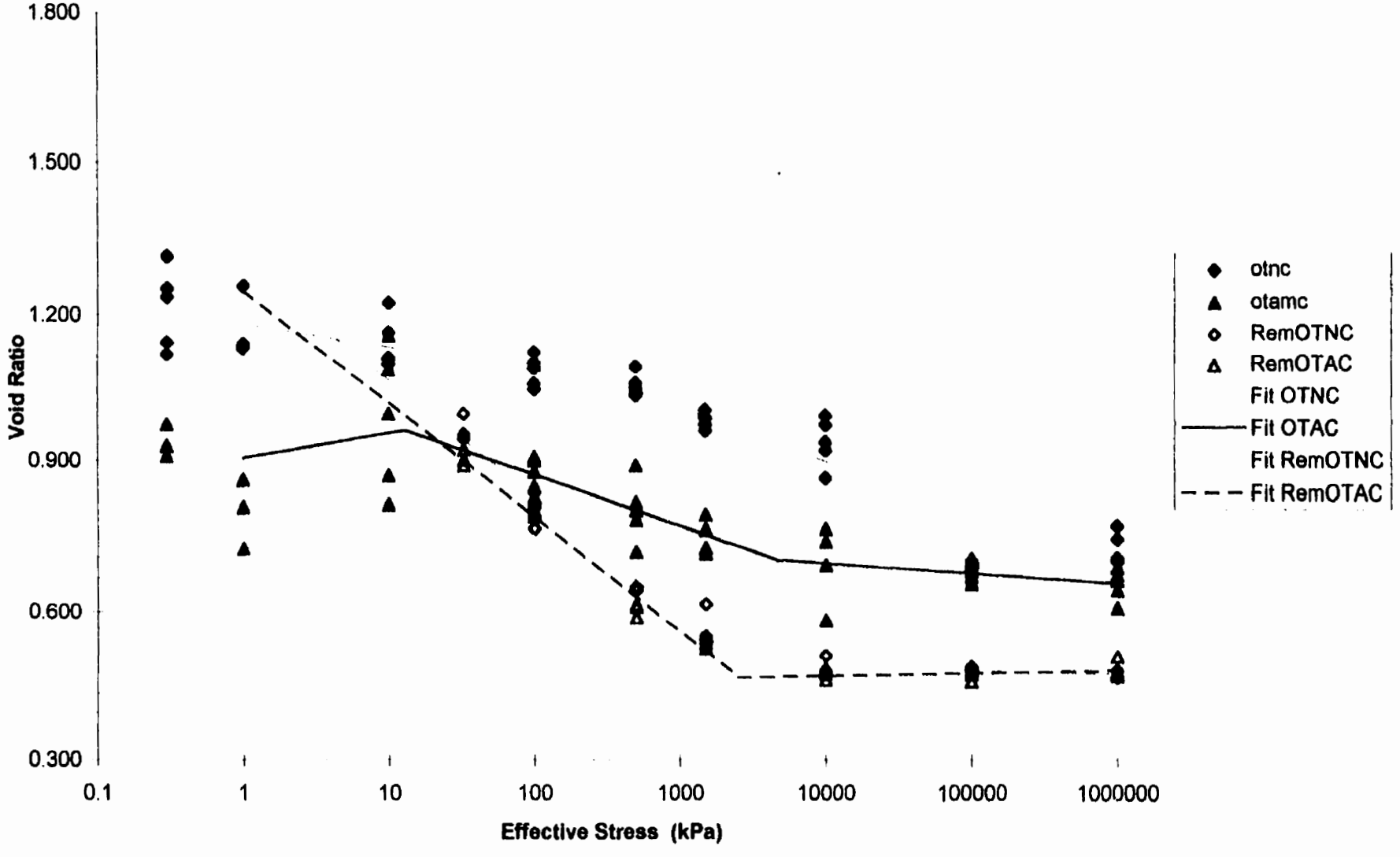

Shrinkage data for OT C horizons, $e(\sigma)$ co-ordinates.

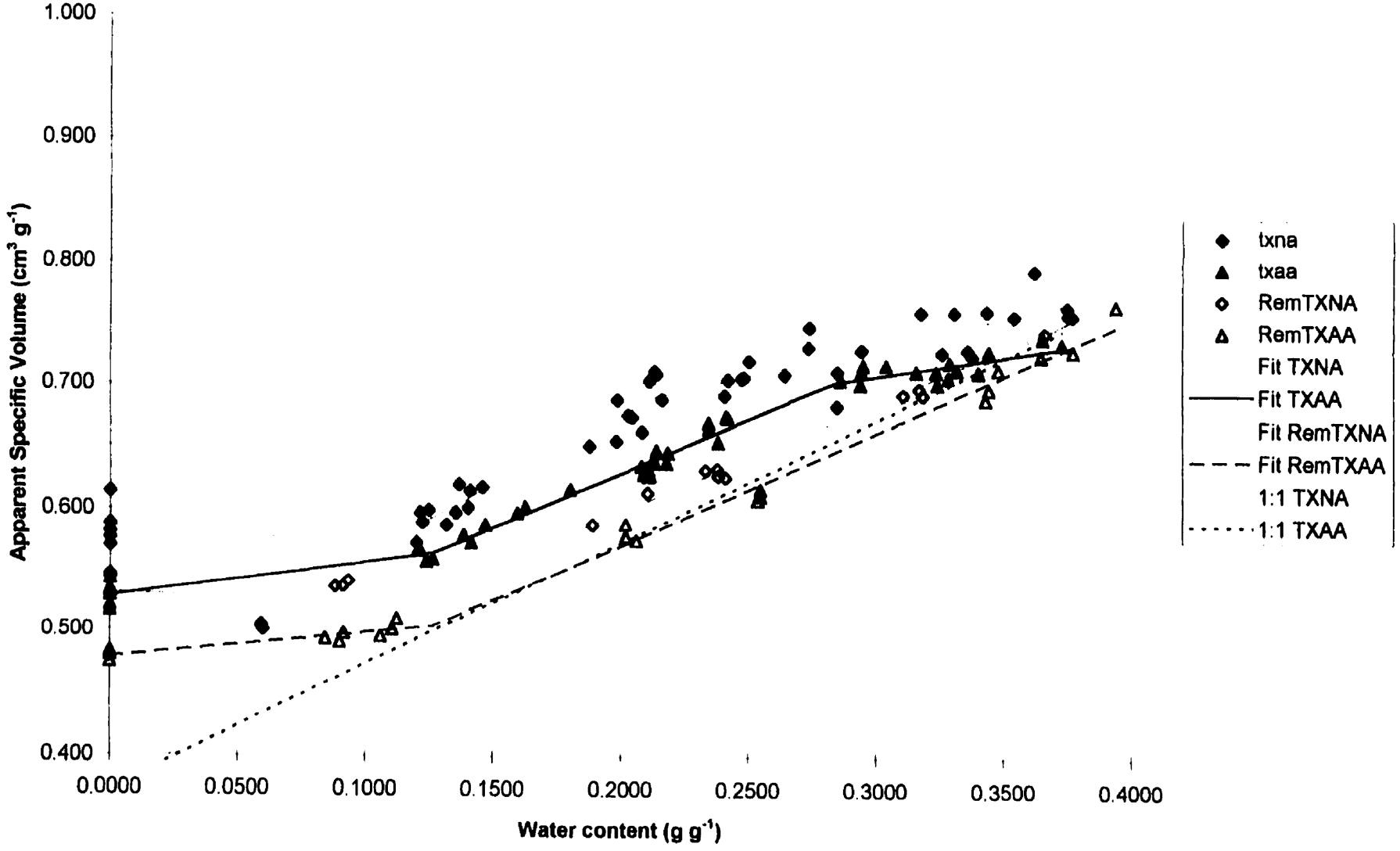

Shrinkage data for TX A horizons, $v(w)$ coordinates.

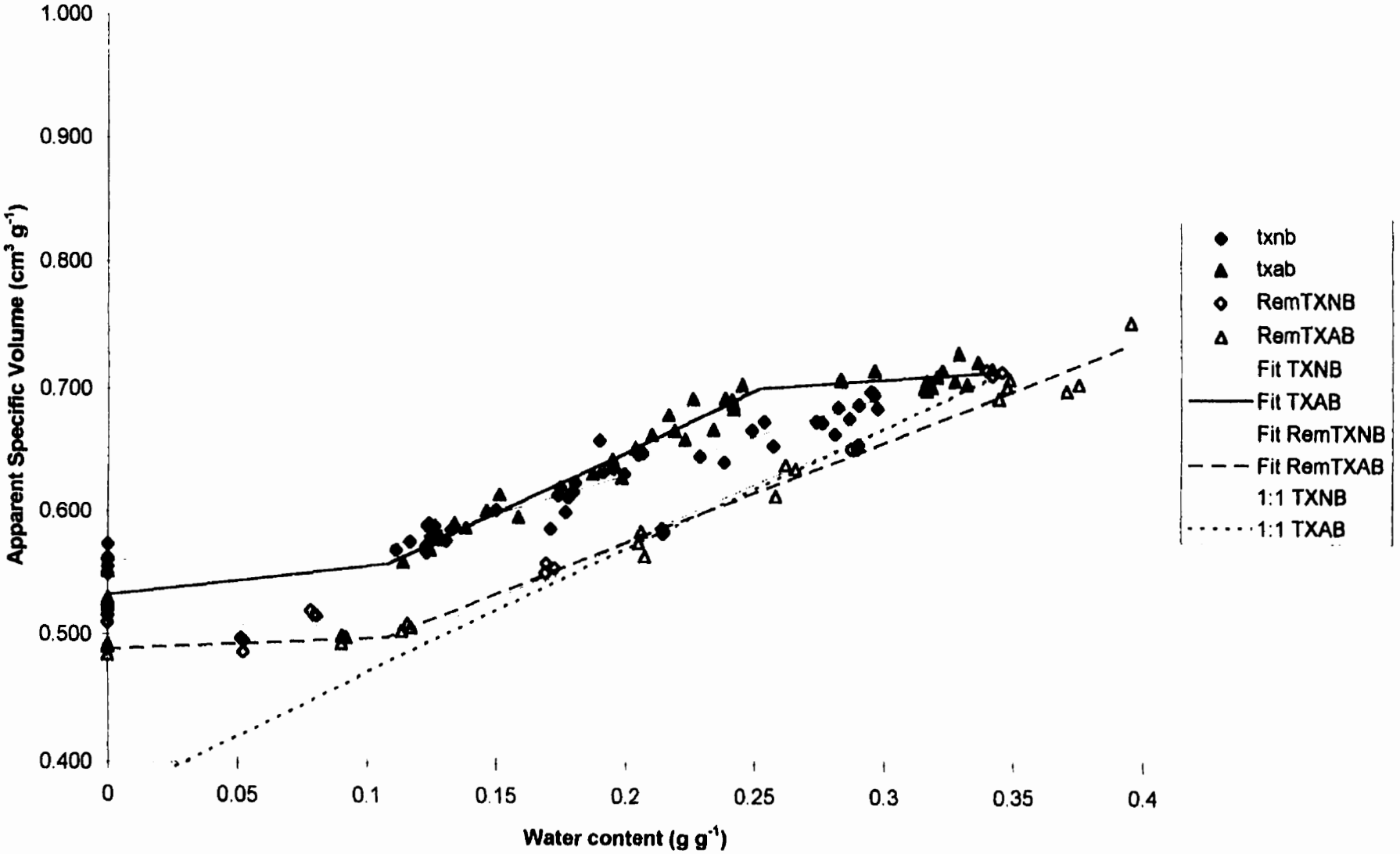

Shrinkage data for TX B horizons, $v(w)$ coordinates.

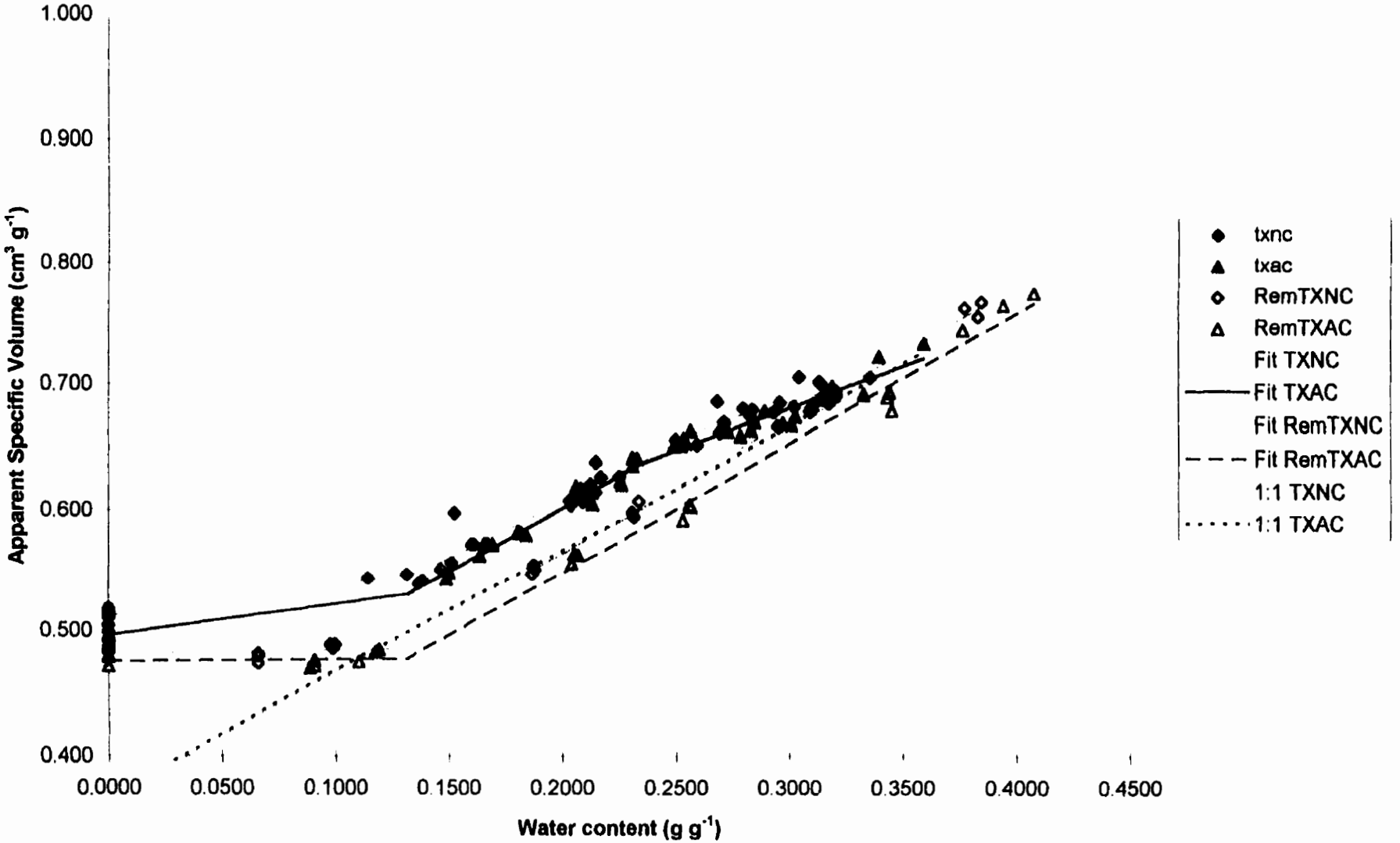

Shrinkage data for TX C horizons, $v(w)$ coordinates.

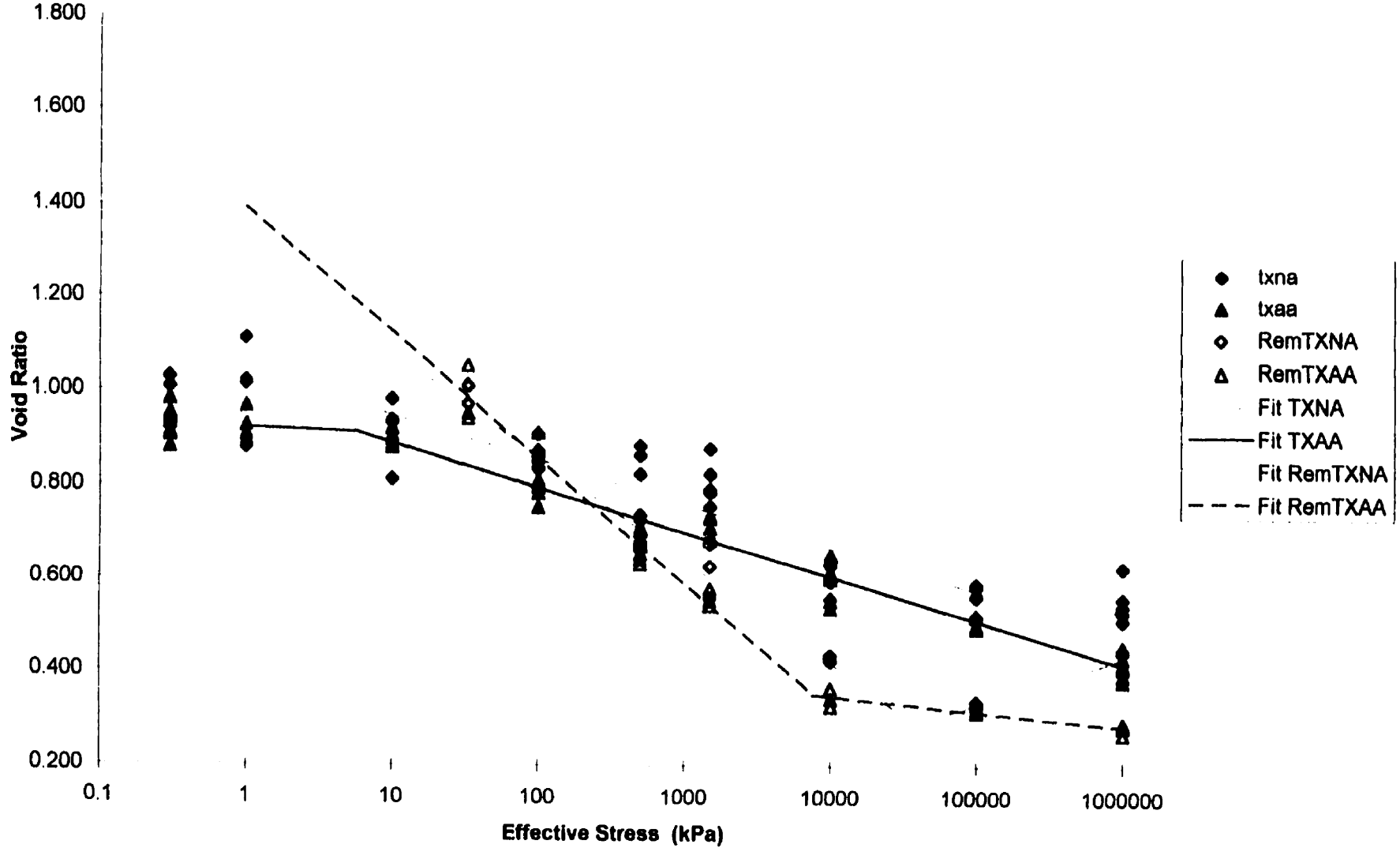

Shrinkage data for TX A horizons, $e(\sigma)$ co-ordinates.

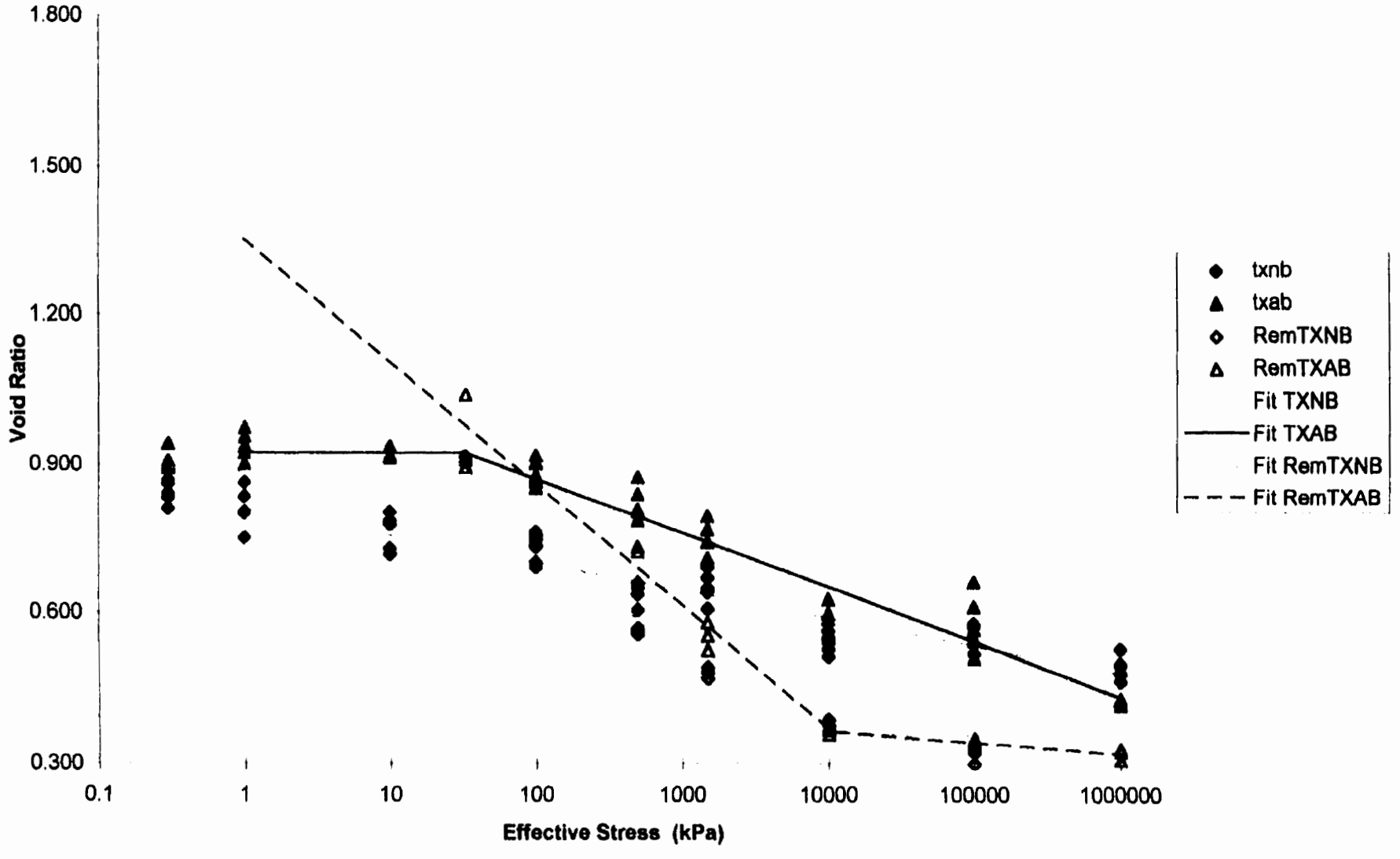

Shrinkage data for TX B horizons, $e(\sigma)$ co-ordinates.

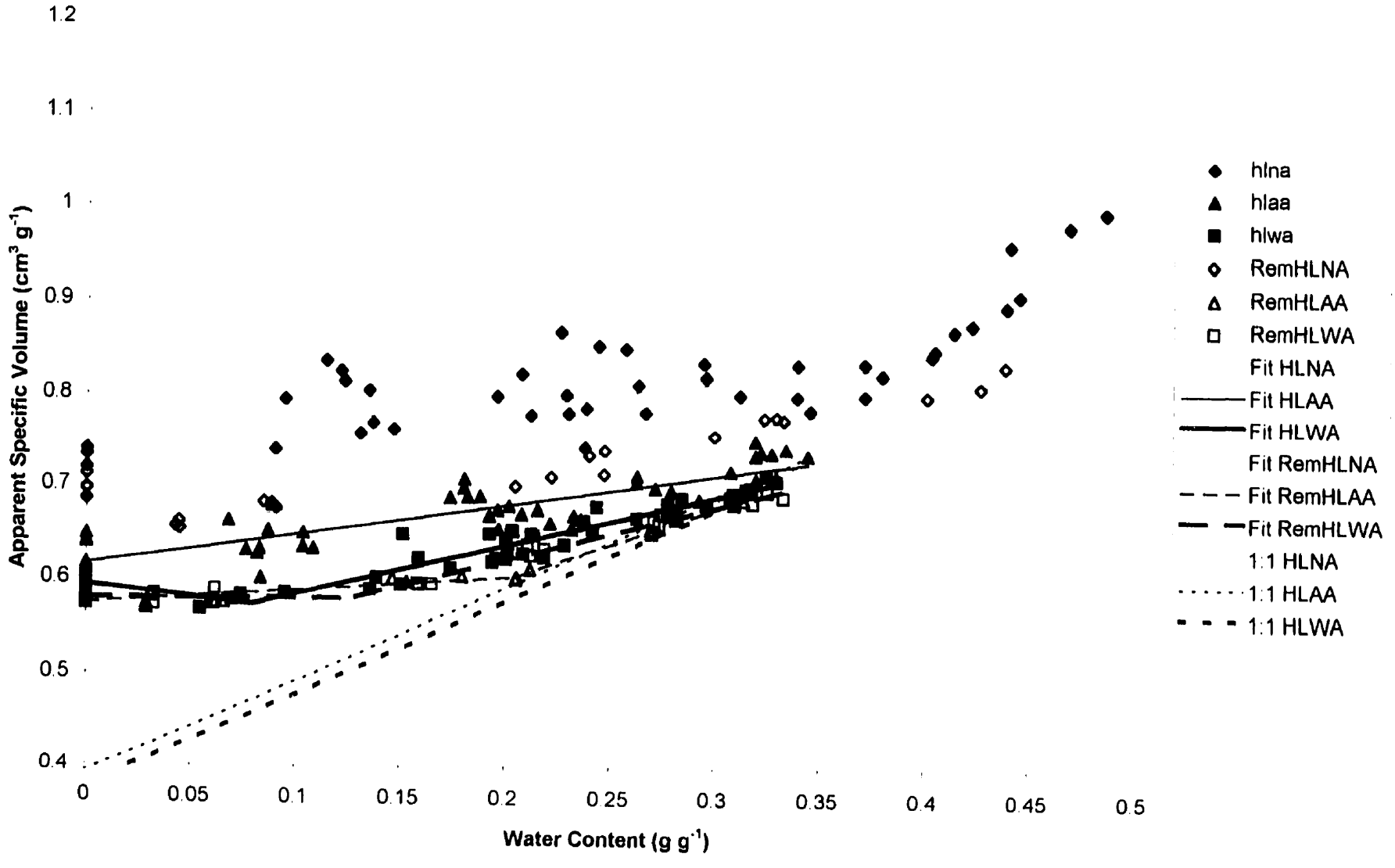

Shrinkage data for HL A horizons, $v(w)$ co-ordinates.

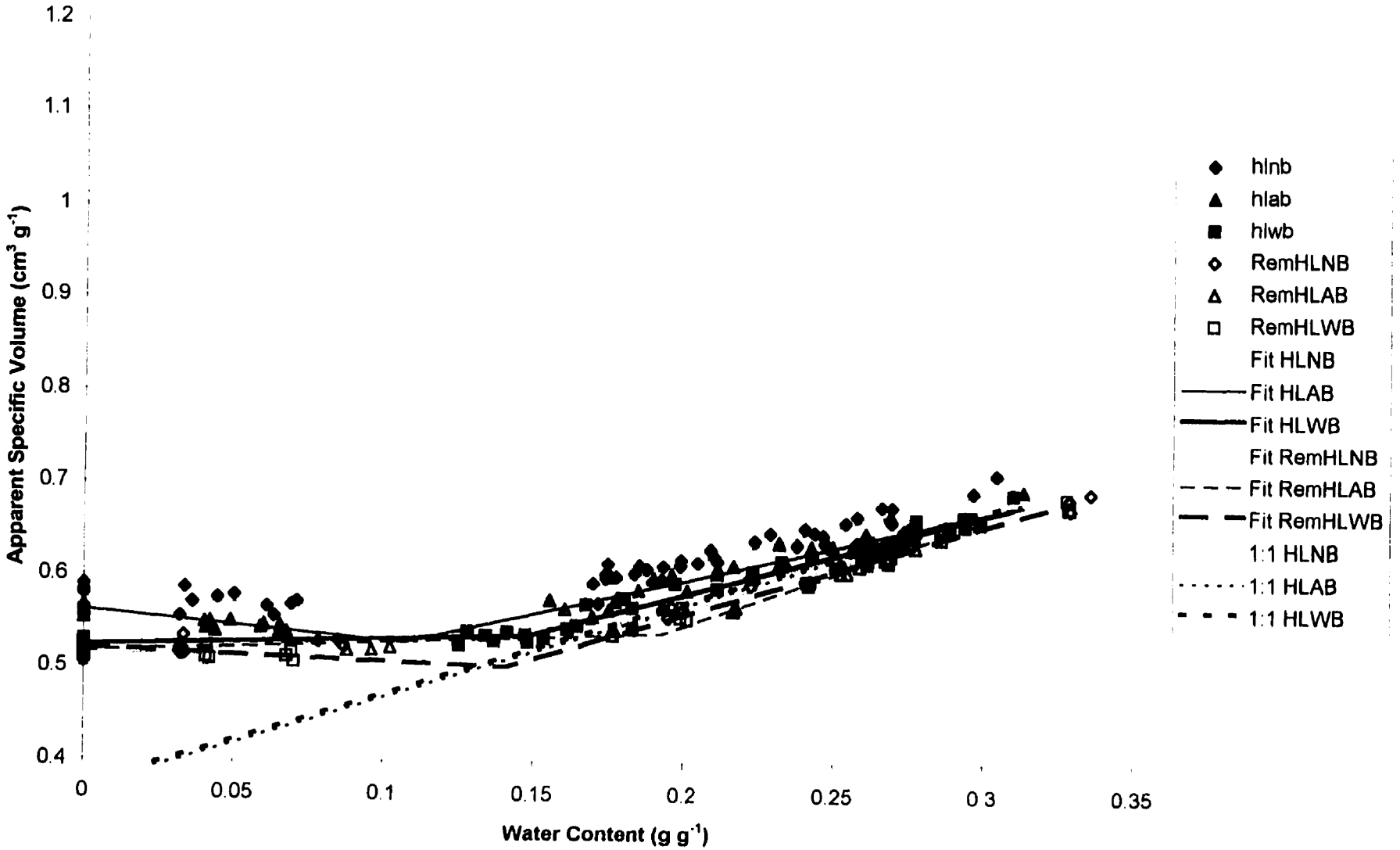

Shrinkage data for HL B horizons, $v(w)$ co-ordinates.

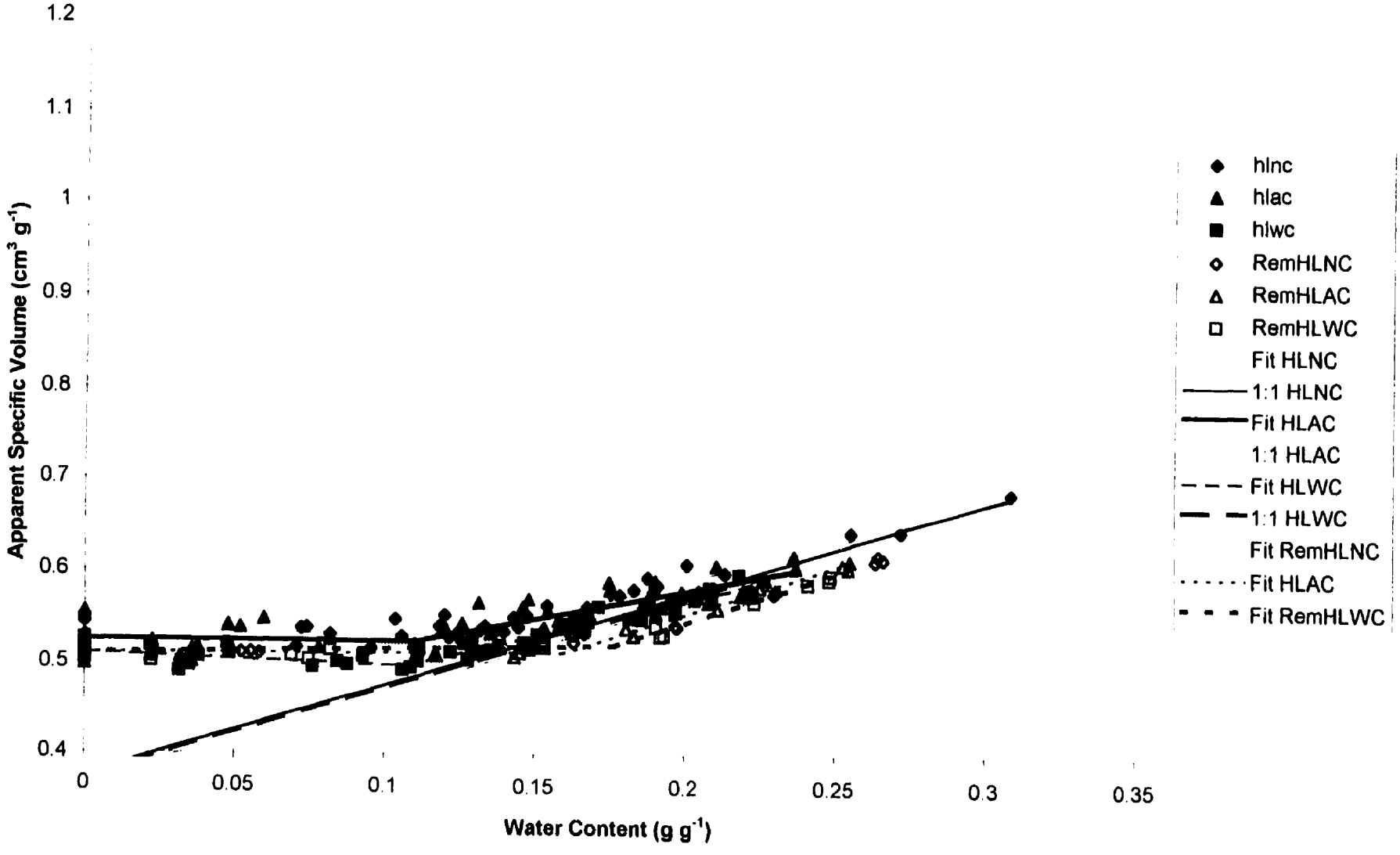

Shrinkage data for HL C horizons, $v(w)$ co-ordinates.

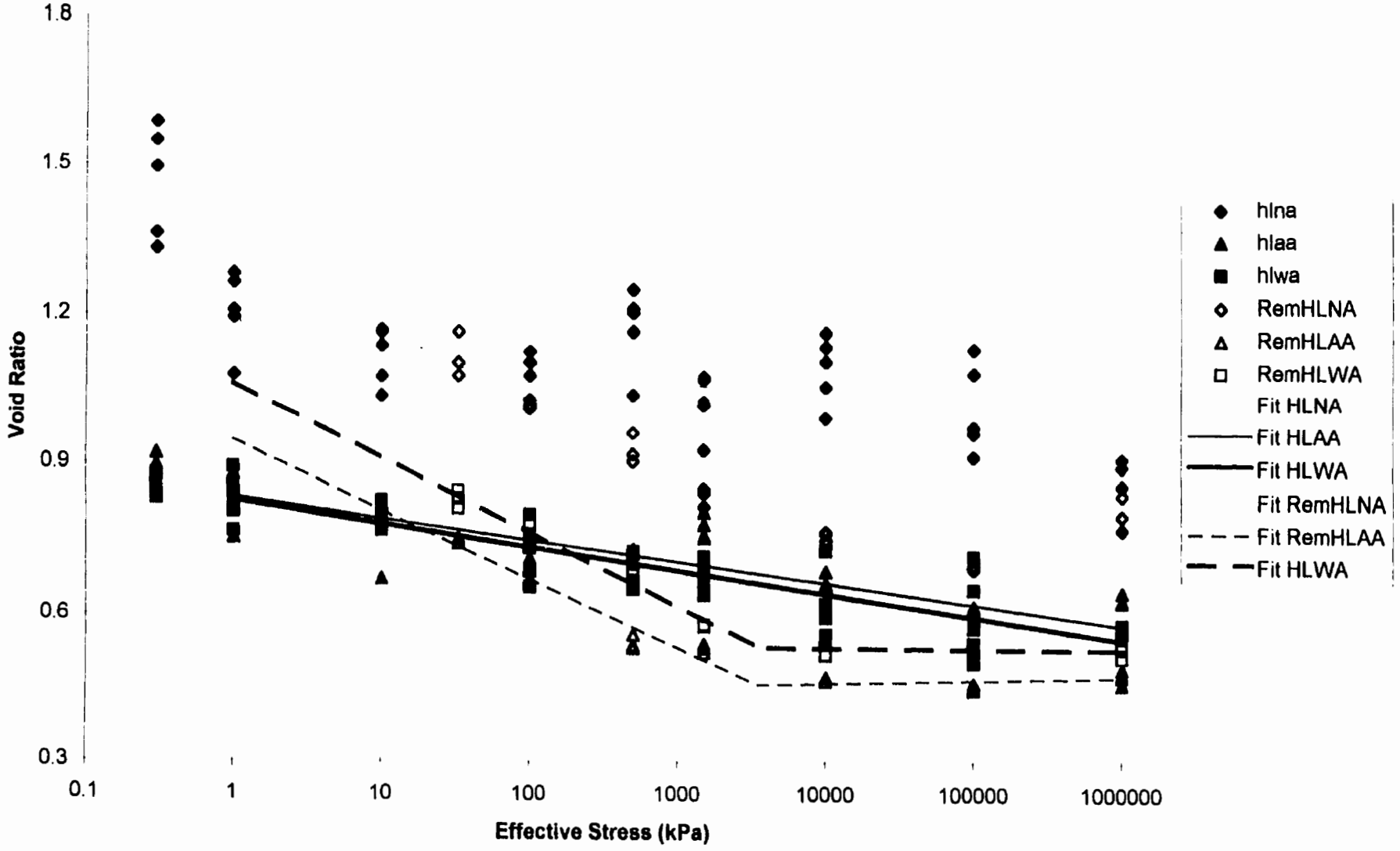

Shrinkage data for HL A horizons, $e(\sigma')$ co-ordinates.

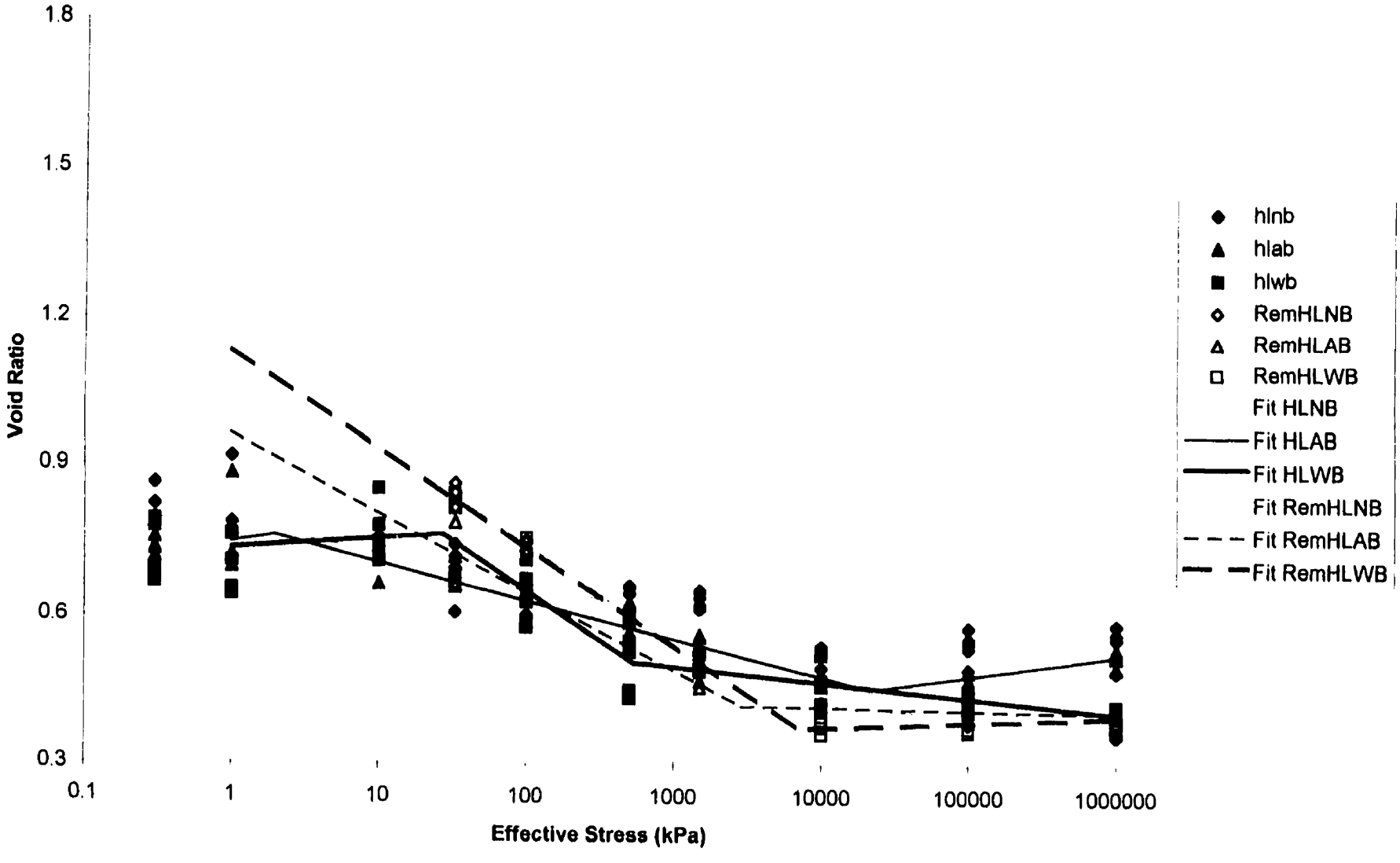

Shrinkage data for HL B horizons, $e(\sigma')$ co-ordinates.

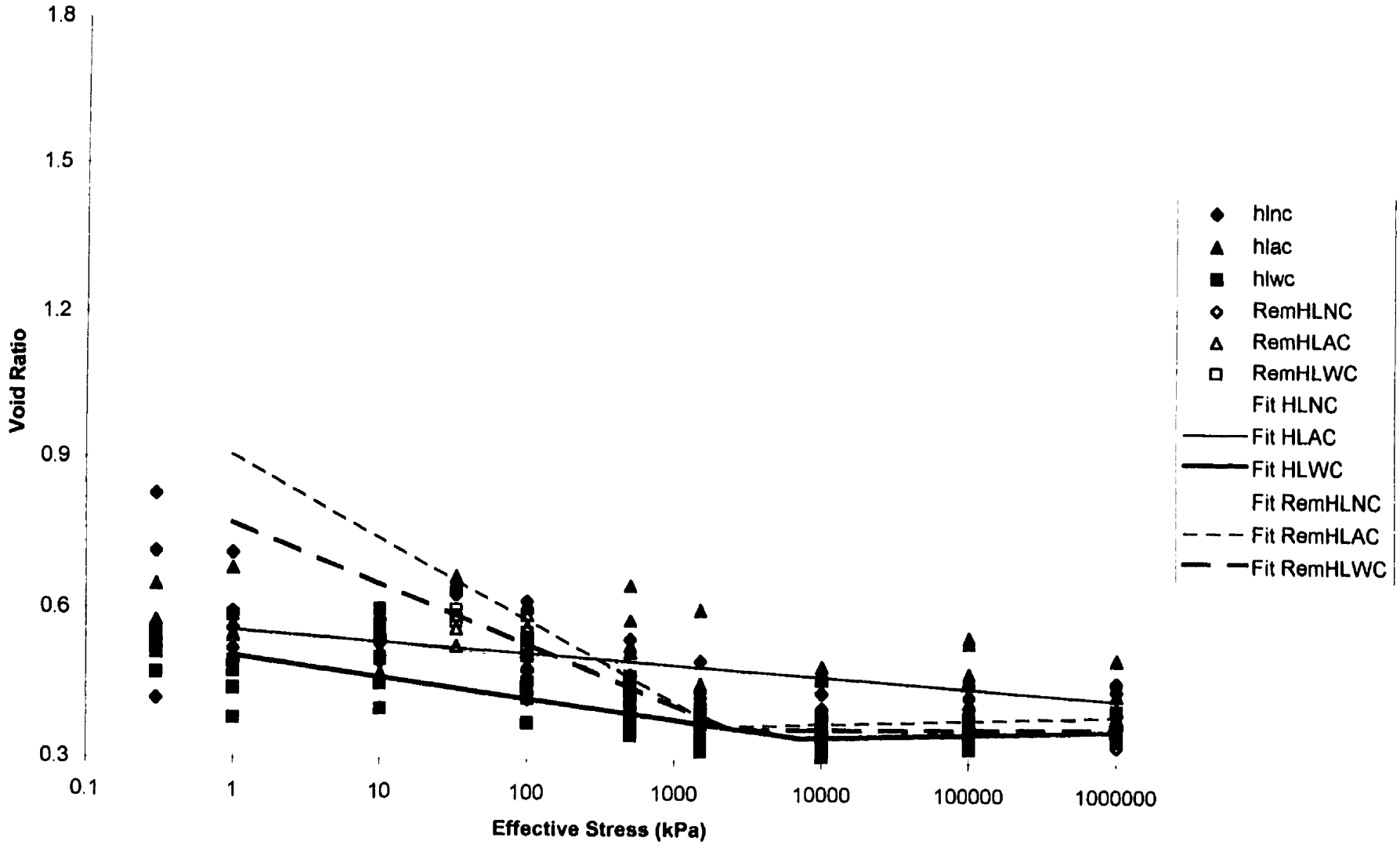

Shrinkage data for HL C horizons, $e(\sigma')$ co-ordinates.

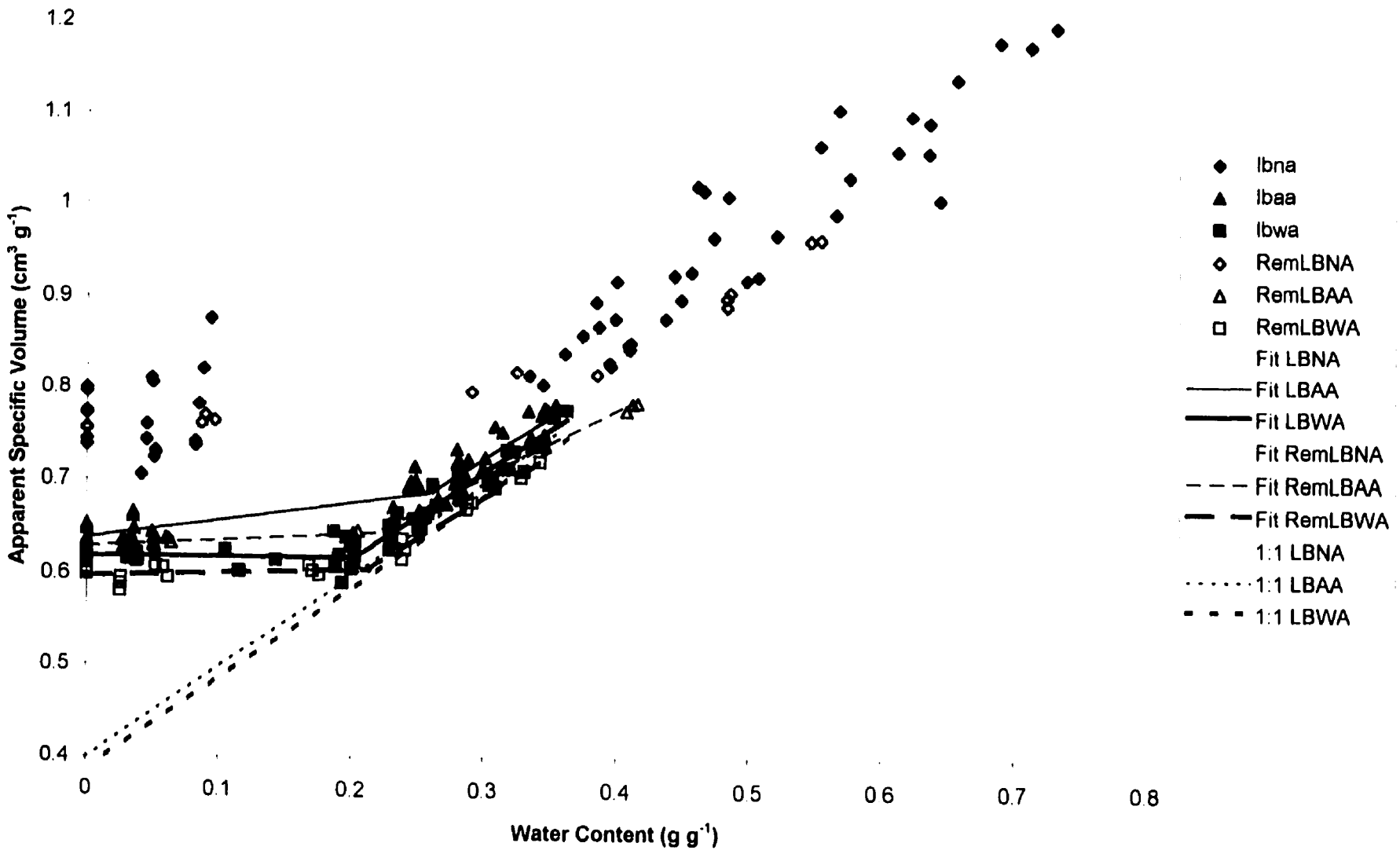

Shrinkage data for LB A horizons, *v* (*w*) co-ordinates.

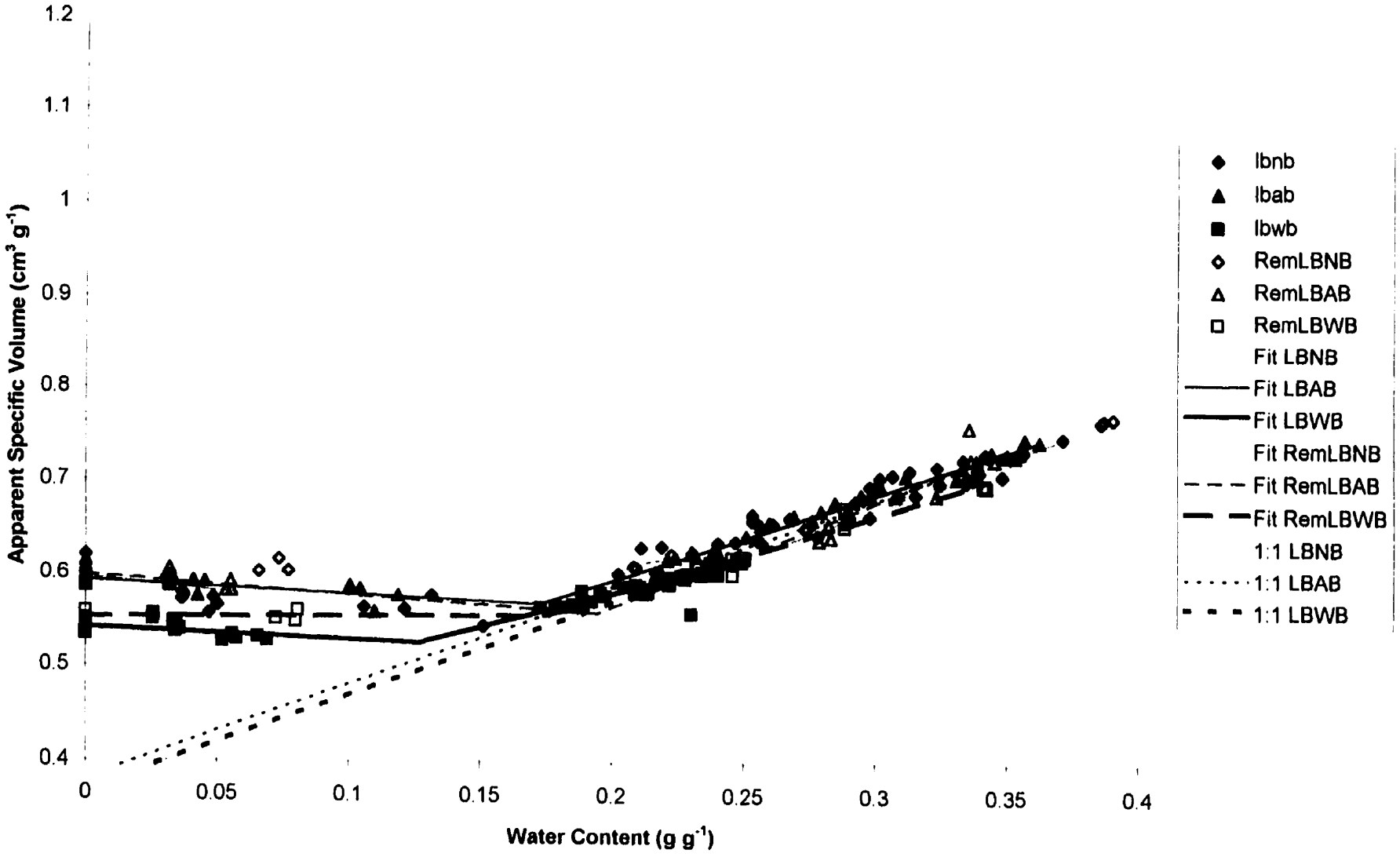

Shrinkage data for LB B horizons, *v* (*w*) co-ordinates.

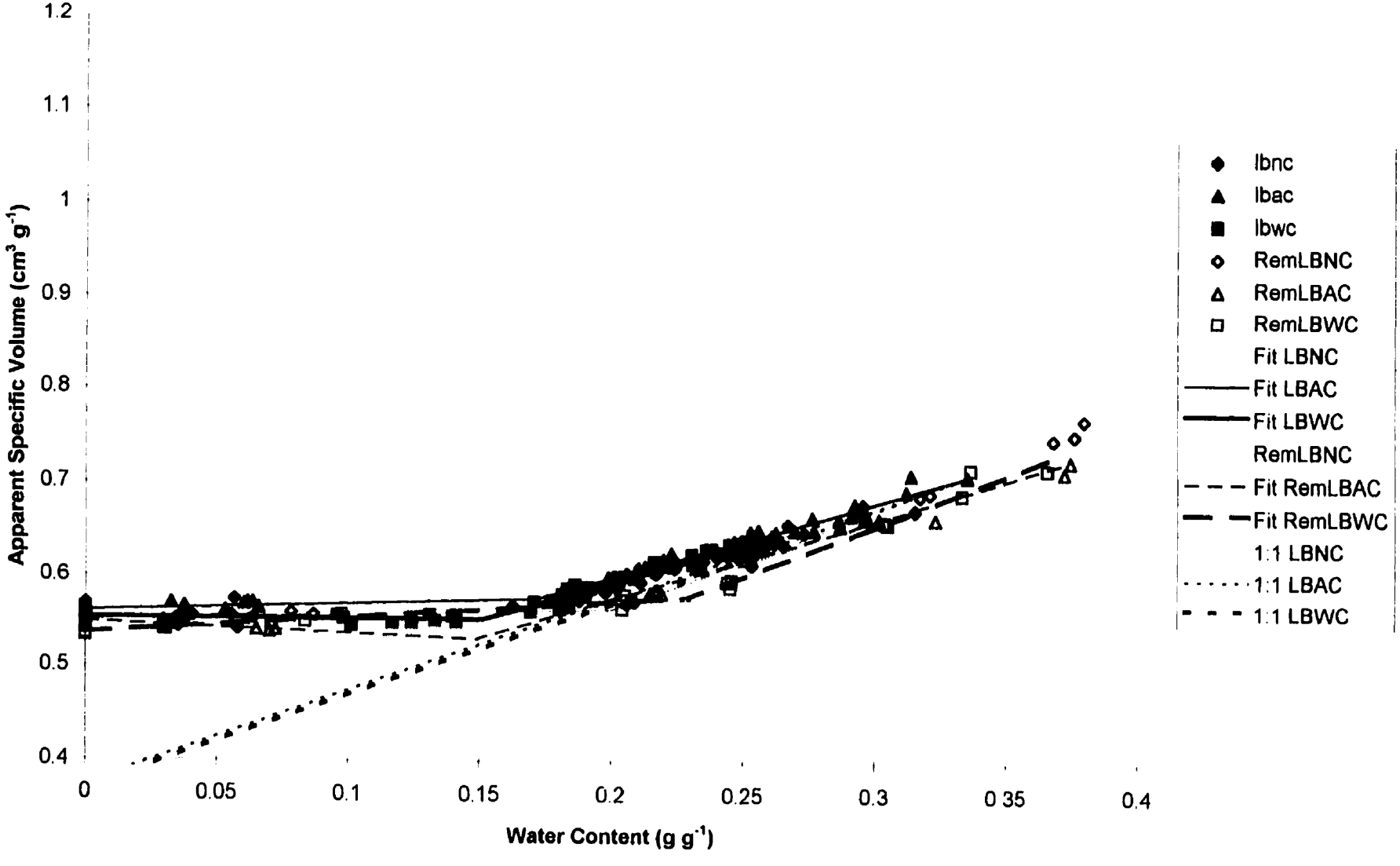

Shrinkage data for LB C horizons, *v* (*w*) co-ordinates.

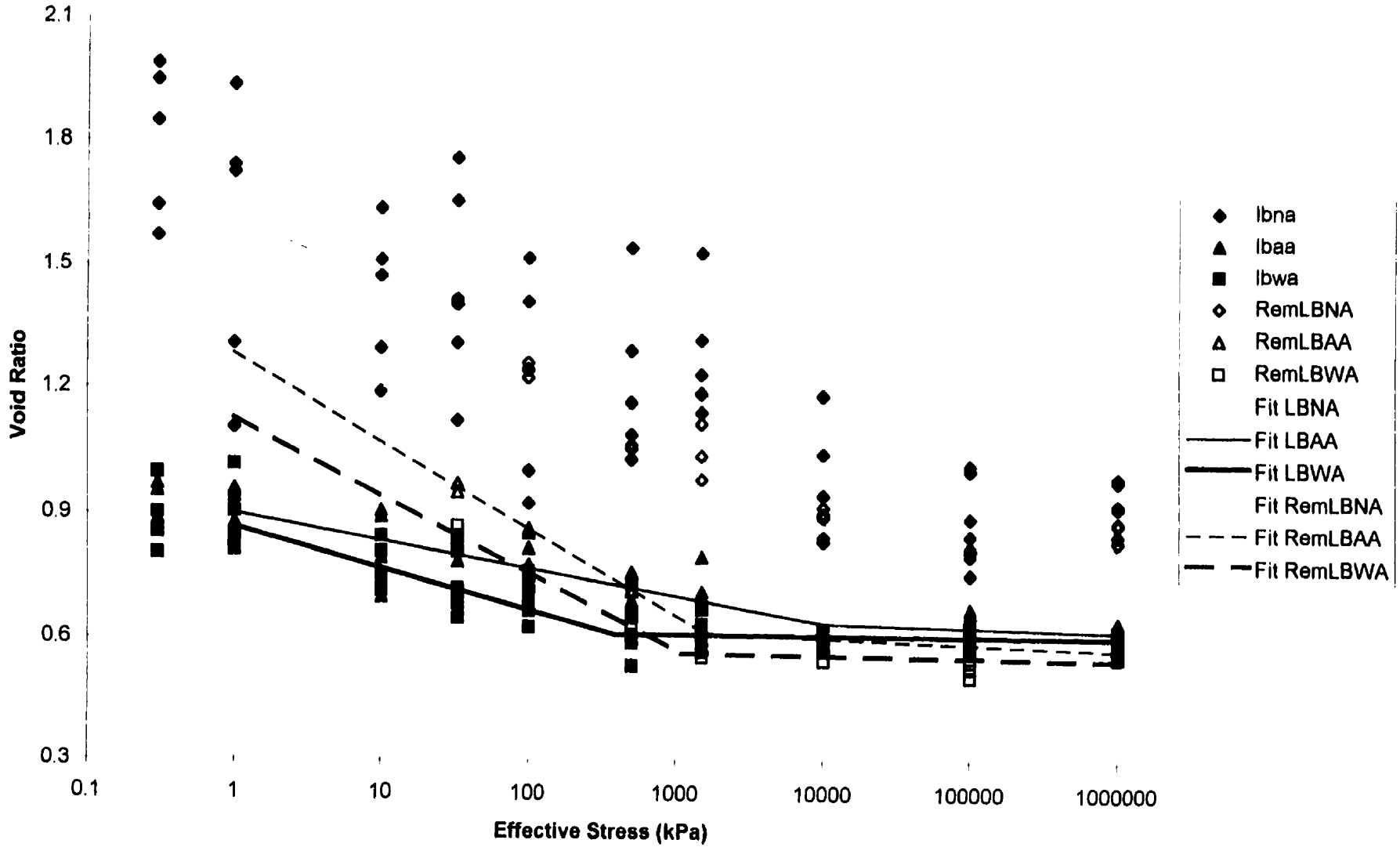

Shrinkage data for LB A horizons, e (σ') co-ordinates.

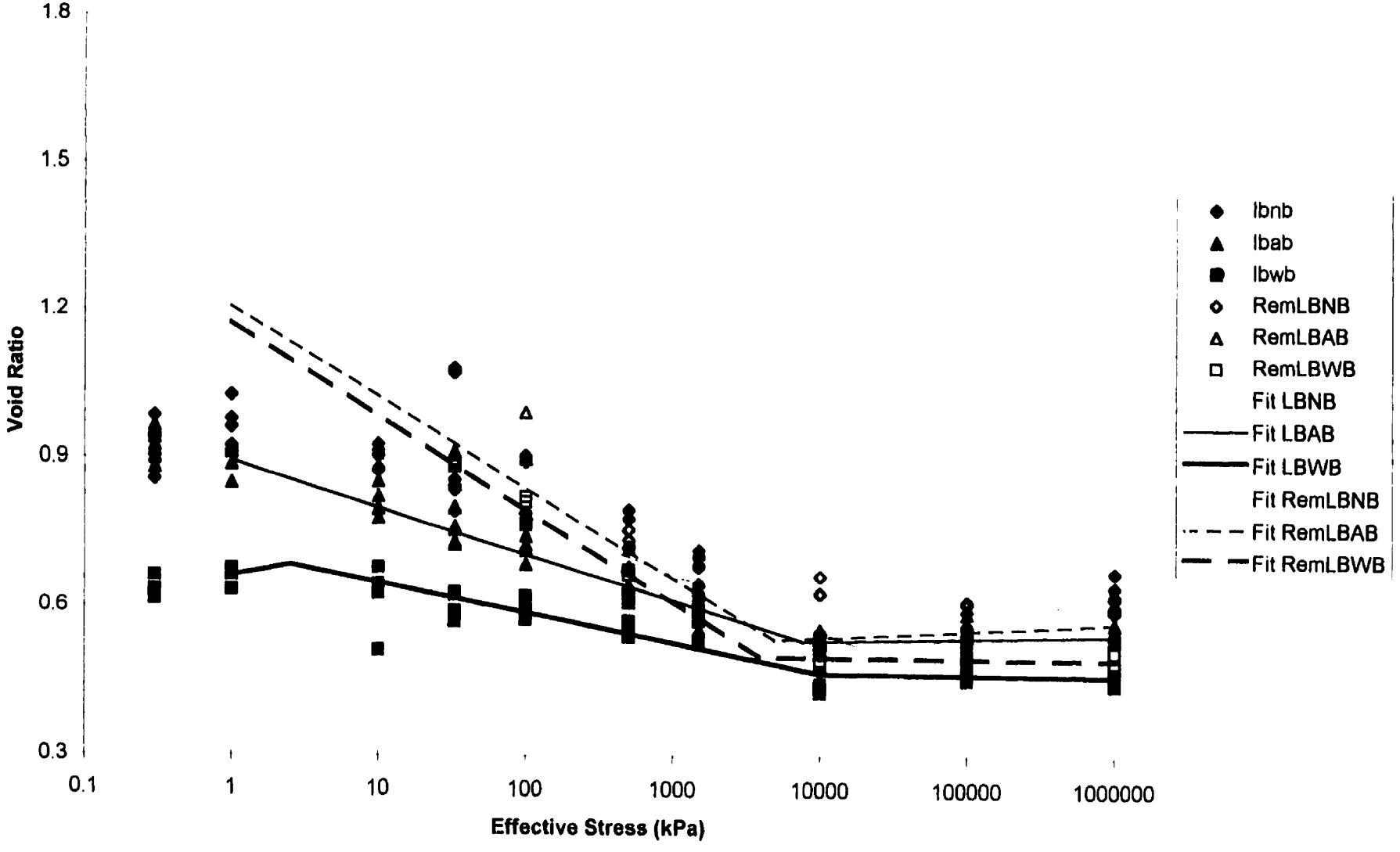

Shrinkage data for LB B horizons, $e(\sigma')$ co-ordinates.

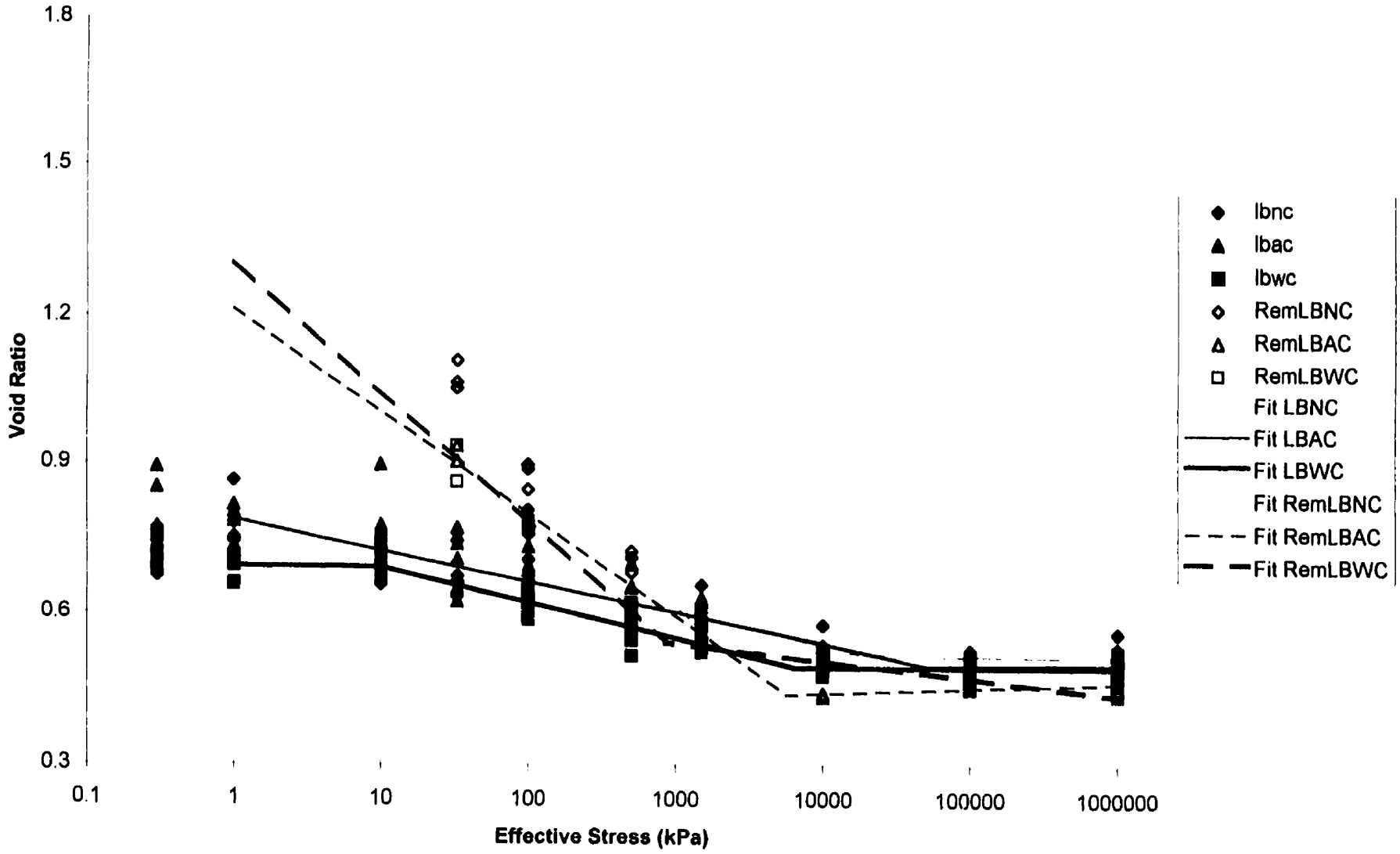

Shrinkage data for LB C horizons, $e(\sigma')$ co-ordinates.

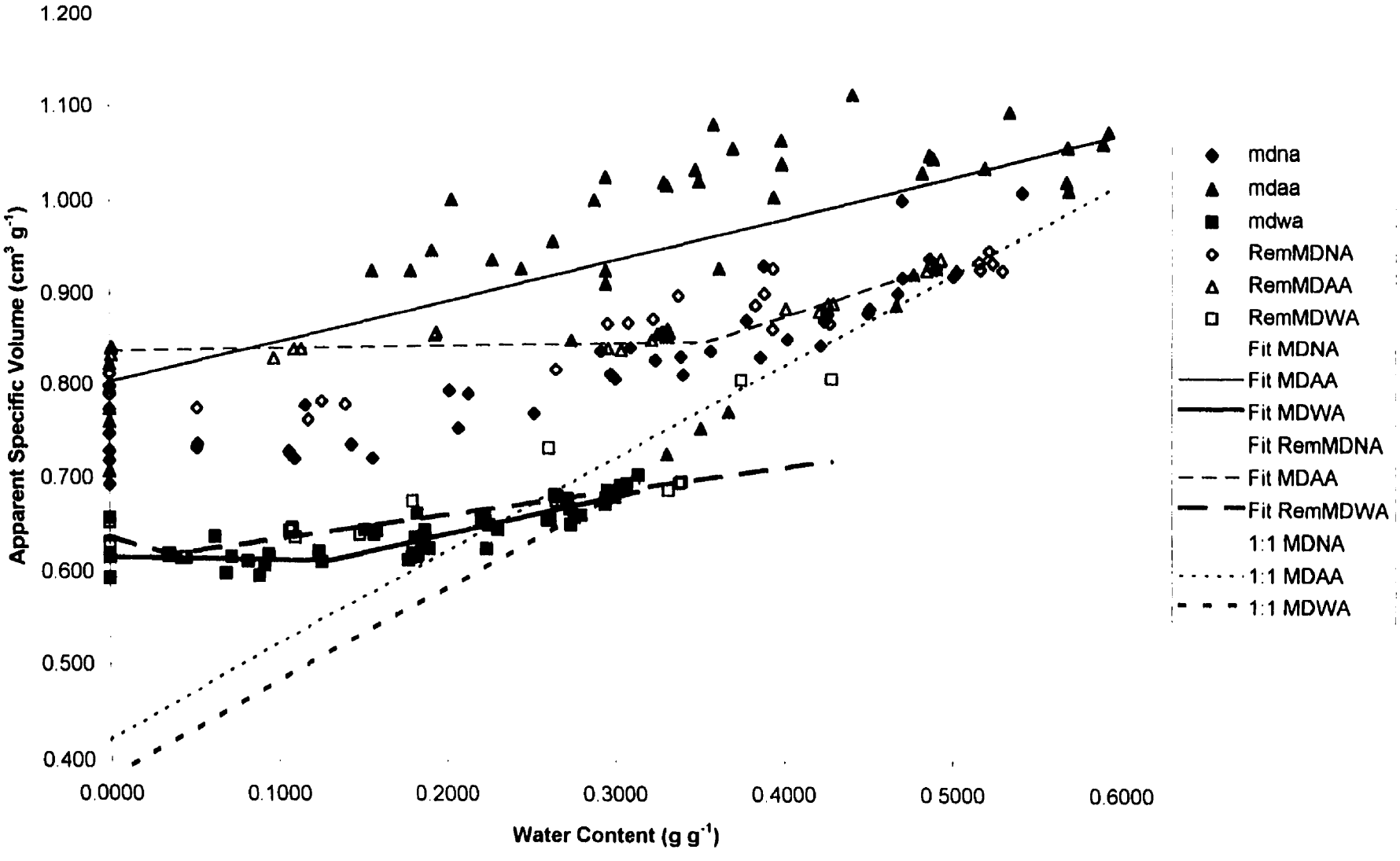

Shrinkage data for MD A horizons, $v(w)$ co-ordinates.

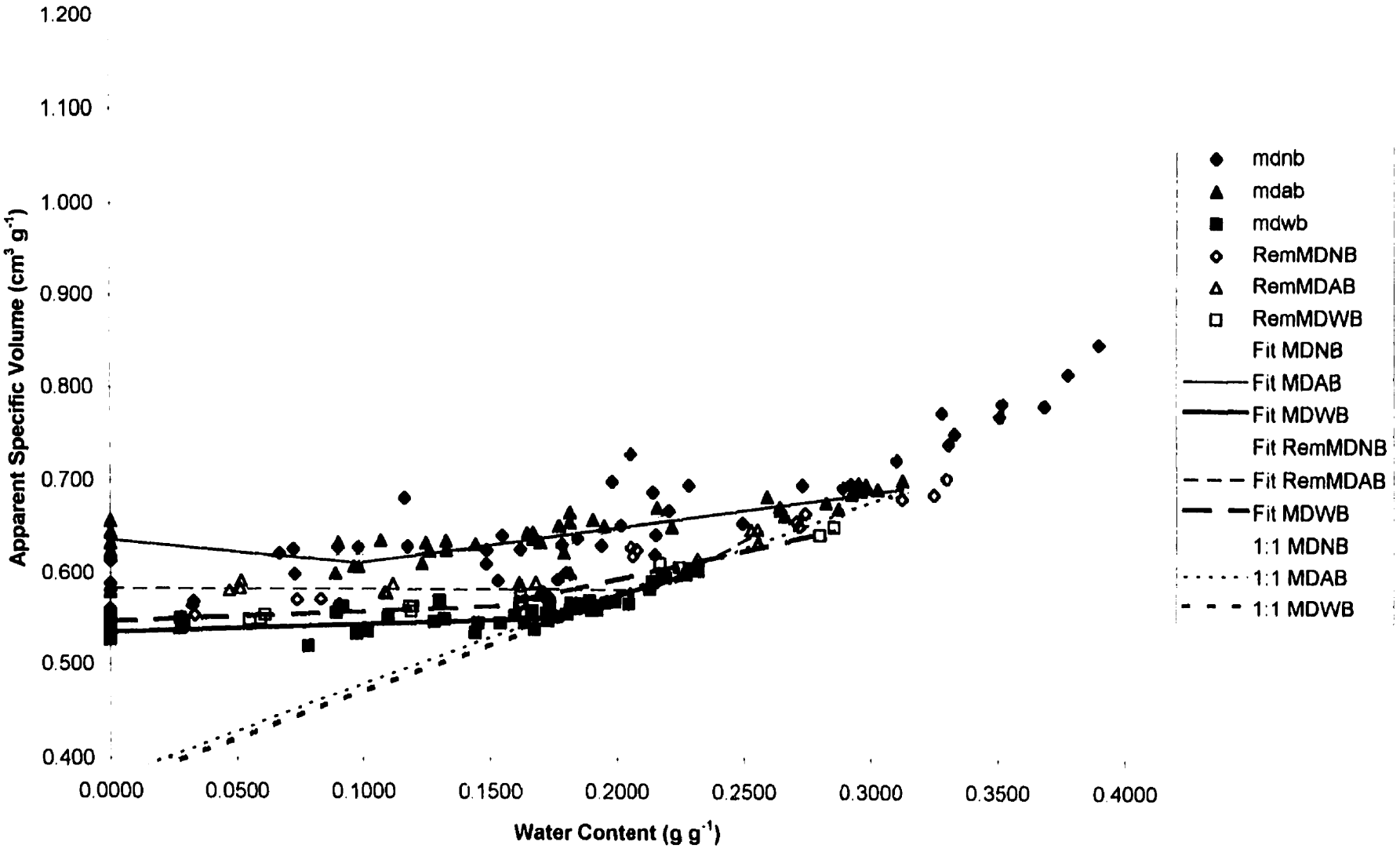

Shrinkage data for MD B horizons, $v(w)$ co-ordinates.

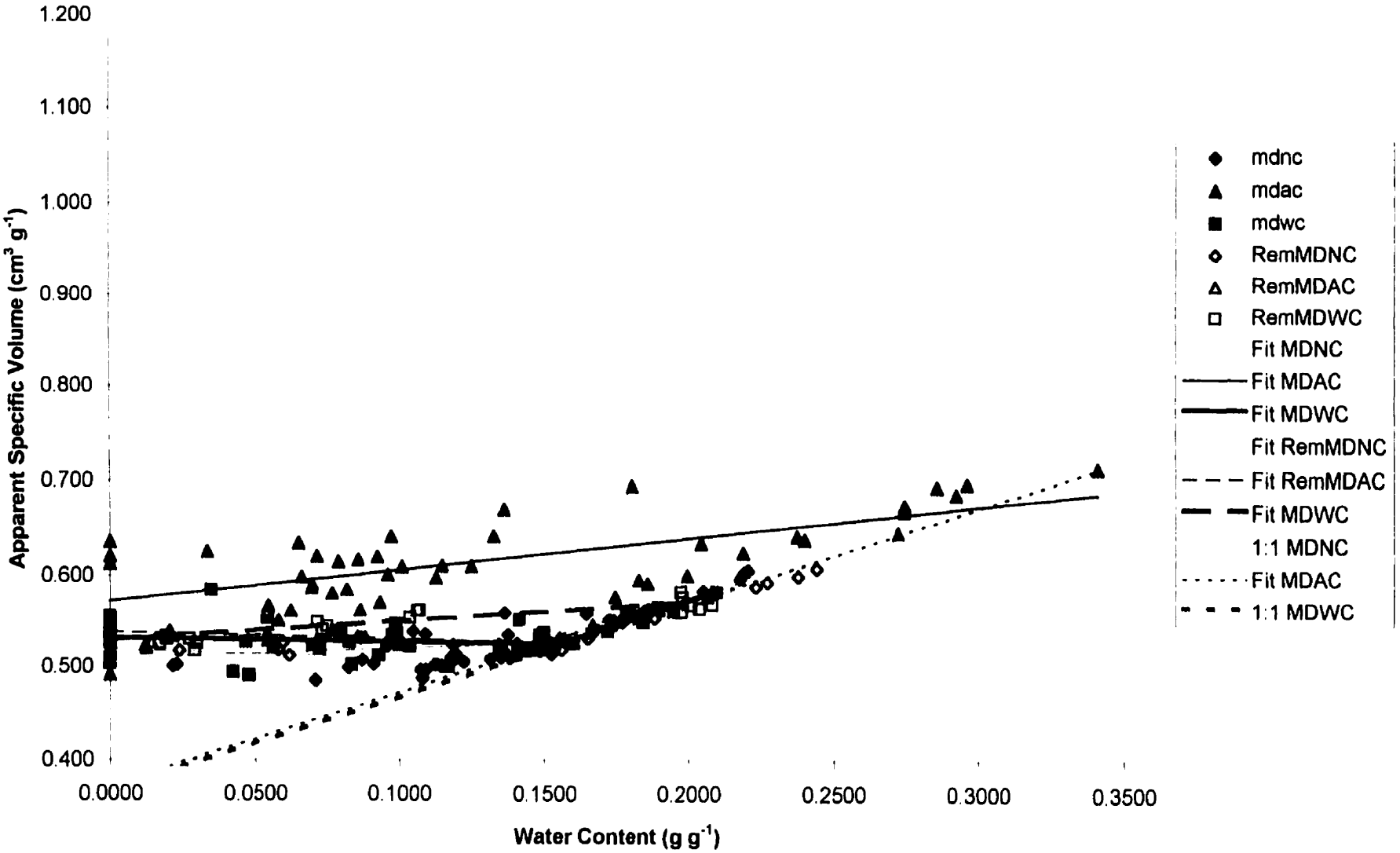

Shrinkage data for MD C horizons, $v(w)$ co-ordinates.

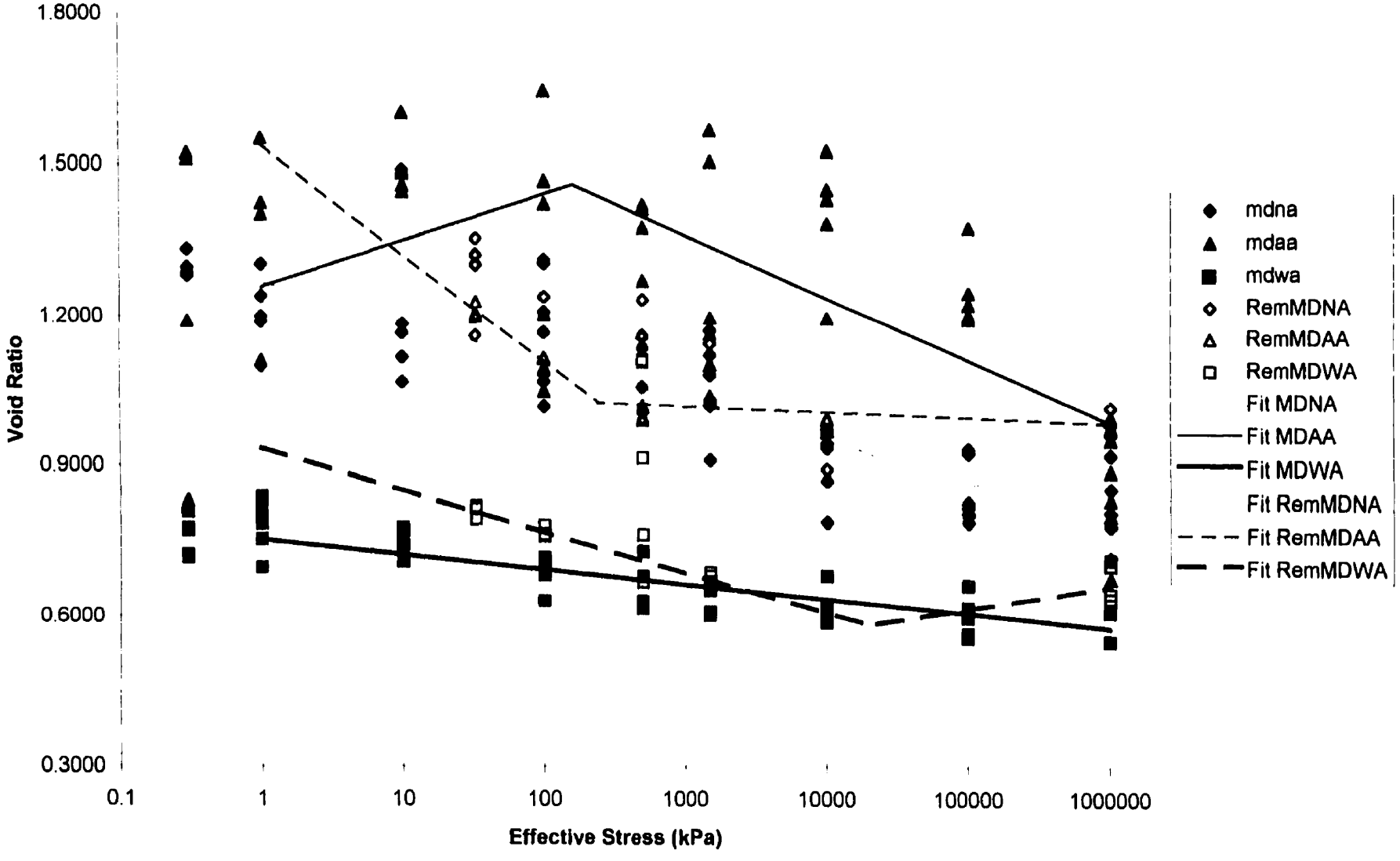

Shrinkage data for MD A horizons, e (σ') co-ordinates.

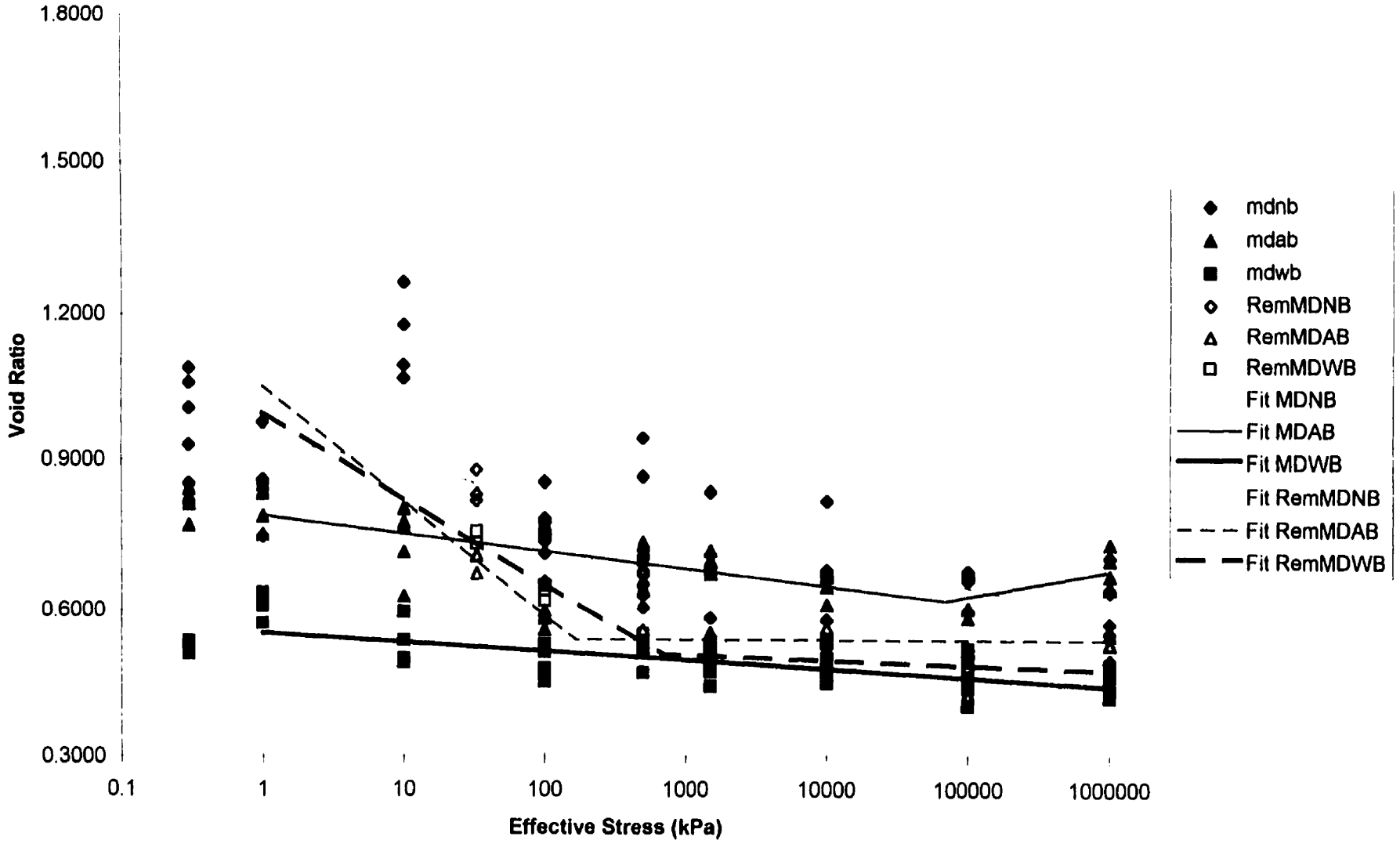

Shrinkage data for MD B horizons, $e(\sigma')$ co-ordinates.

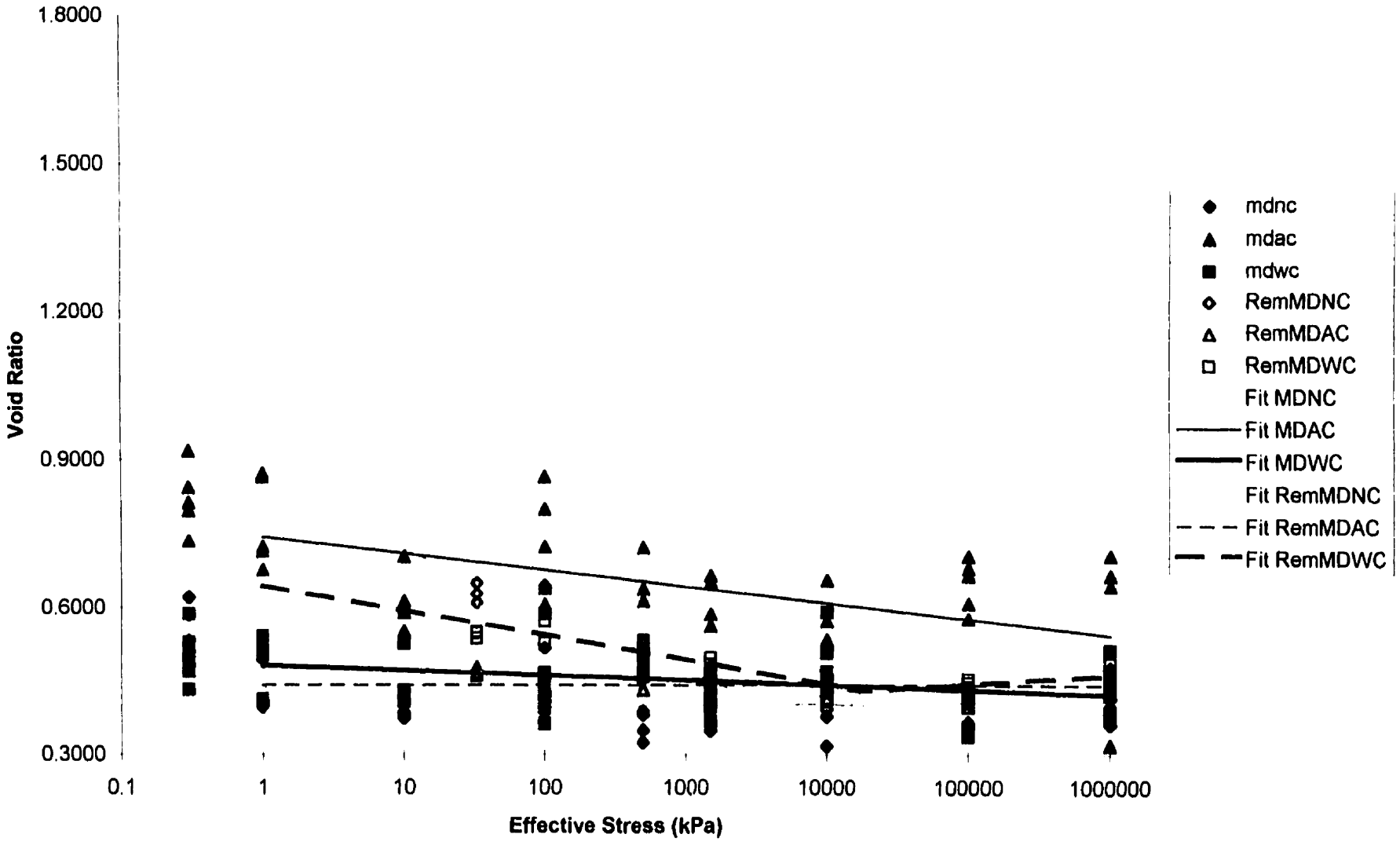

Shrinkage data for MD C horizons, e(σ') co-ordinates.

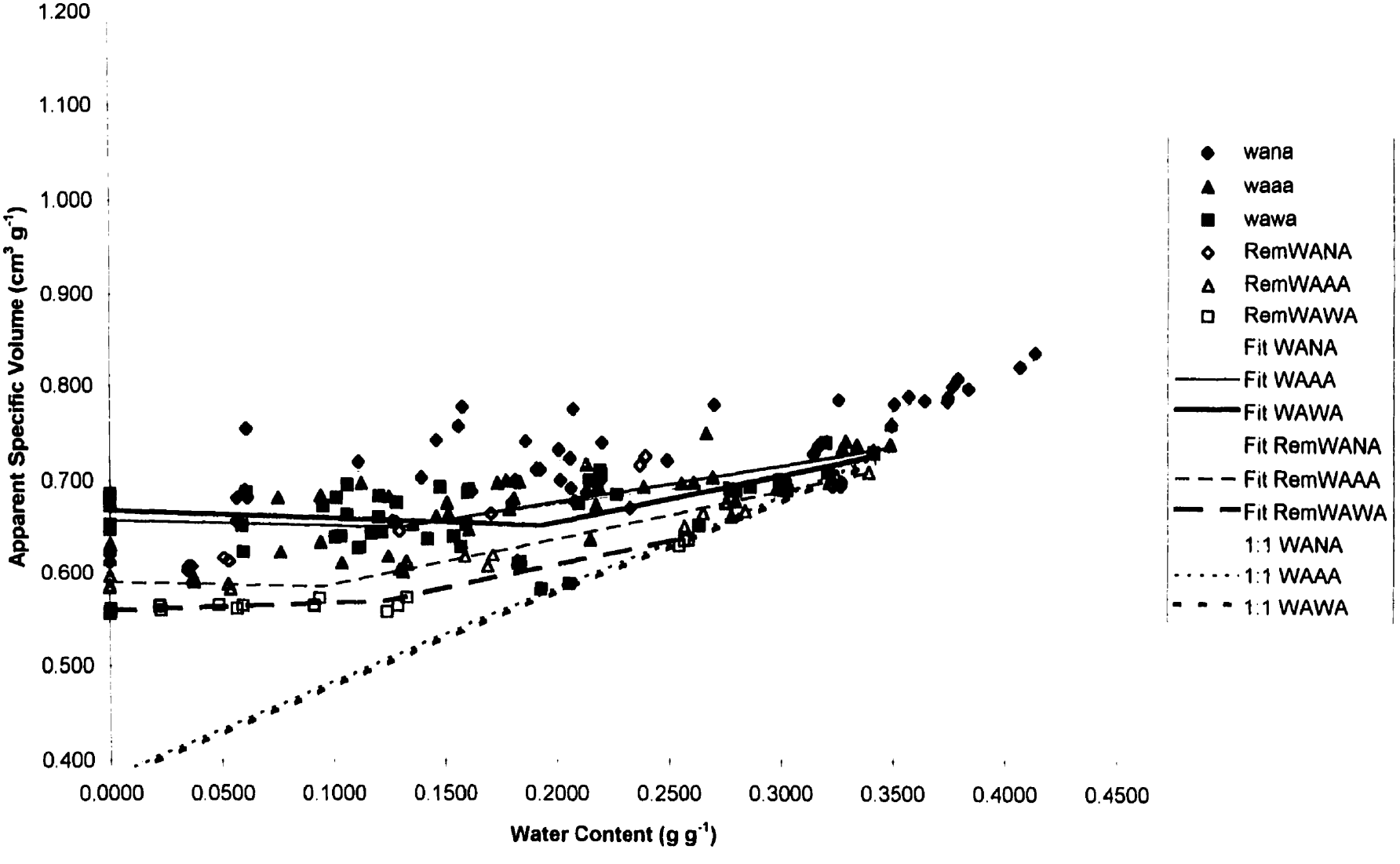

Shrinkage data for WA A horizons, *v* (*w*) co-ordinates.

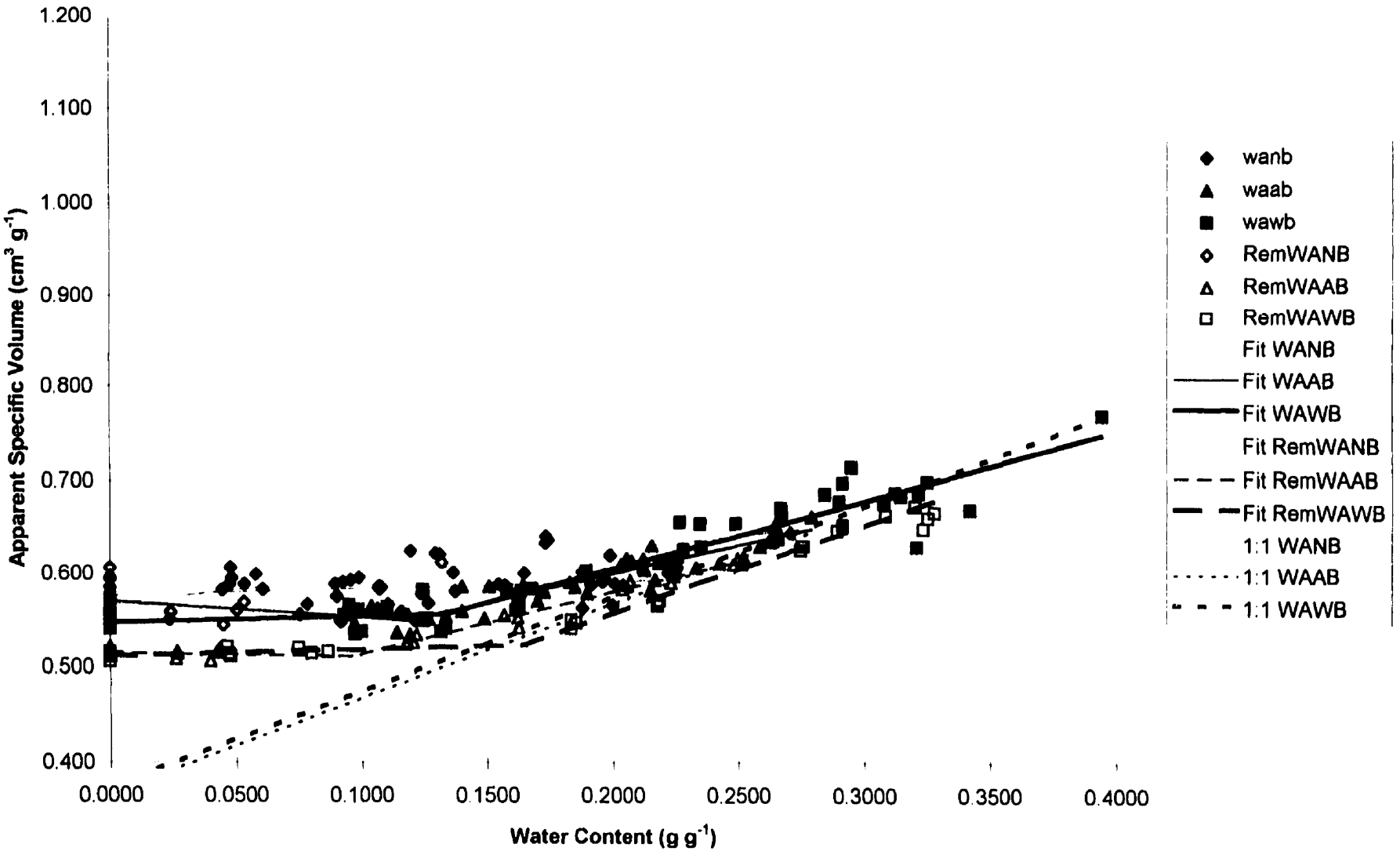

Shrinkage data for WA B horizons, *v* (*w*) co-ordinates.

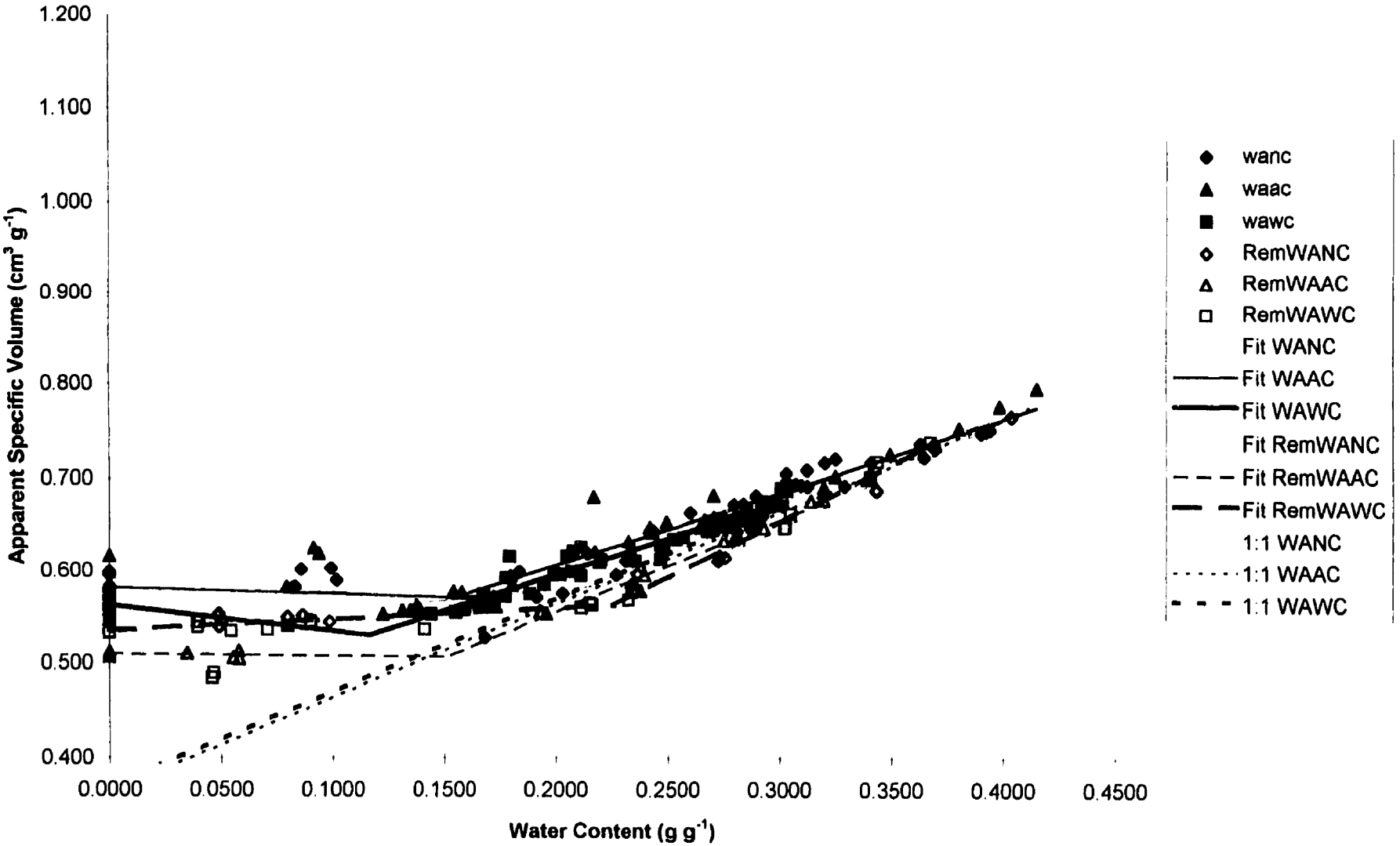

Shrinkage data for WA C horizons, *v* (*w*) co-ordinates.

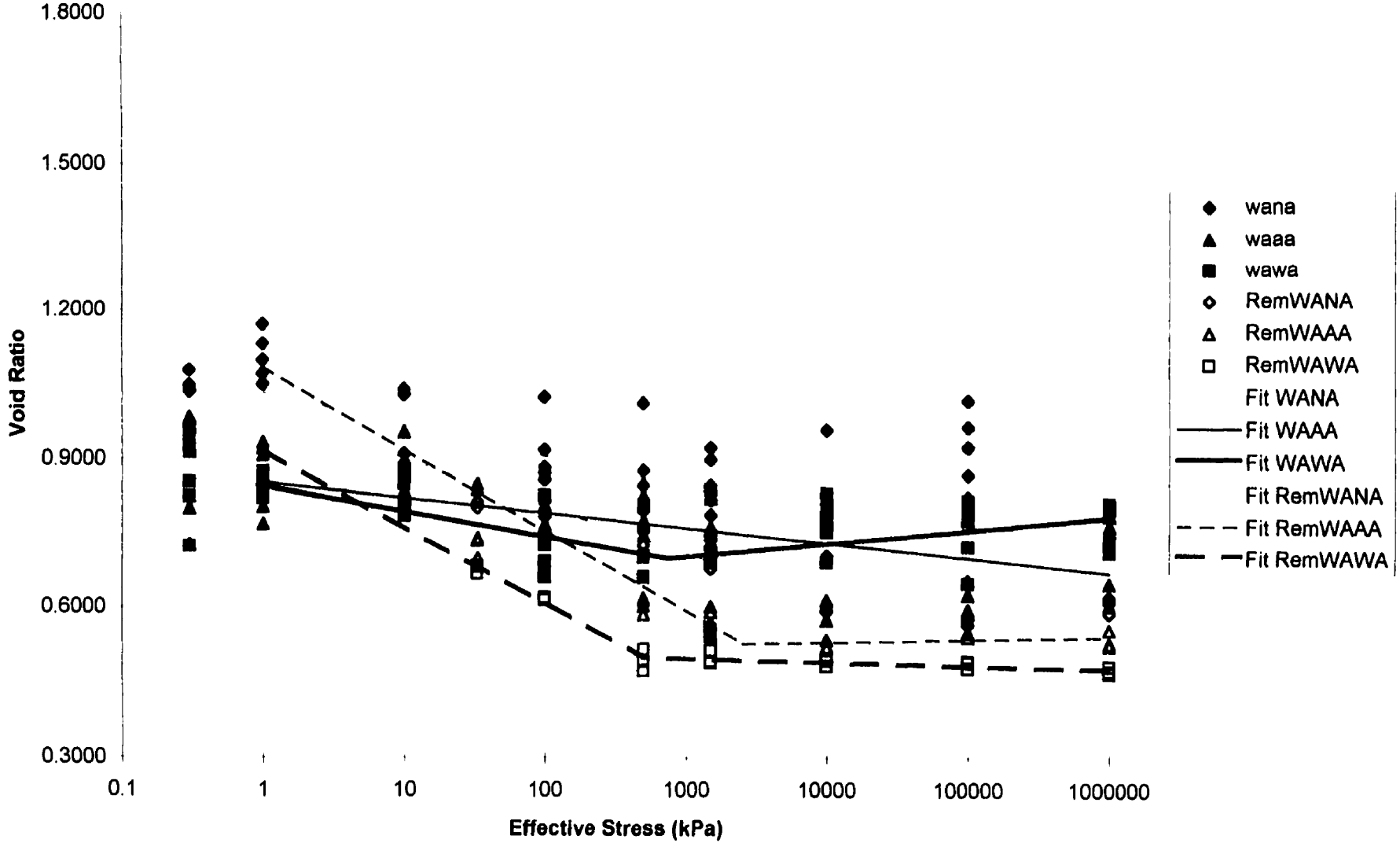

Shrinkage data for WA A horizons, e(σ') co-ordinates.

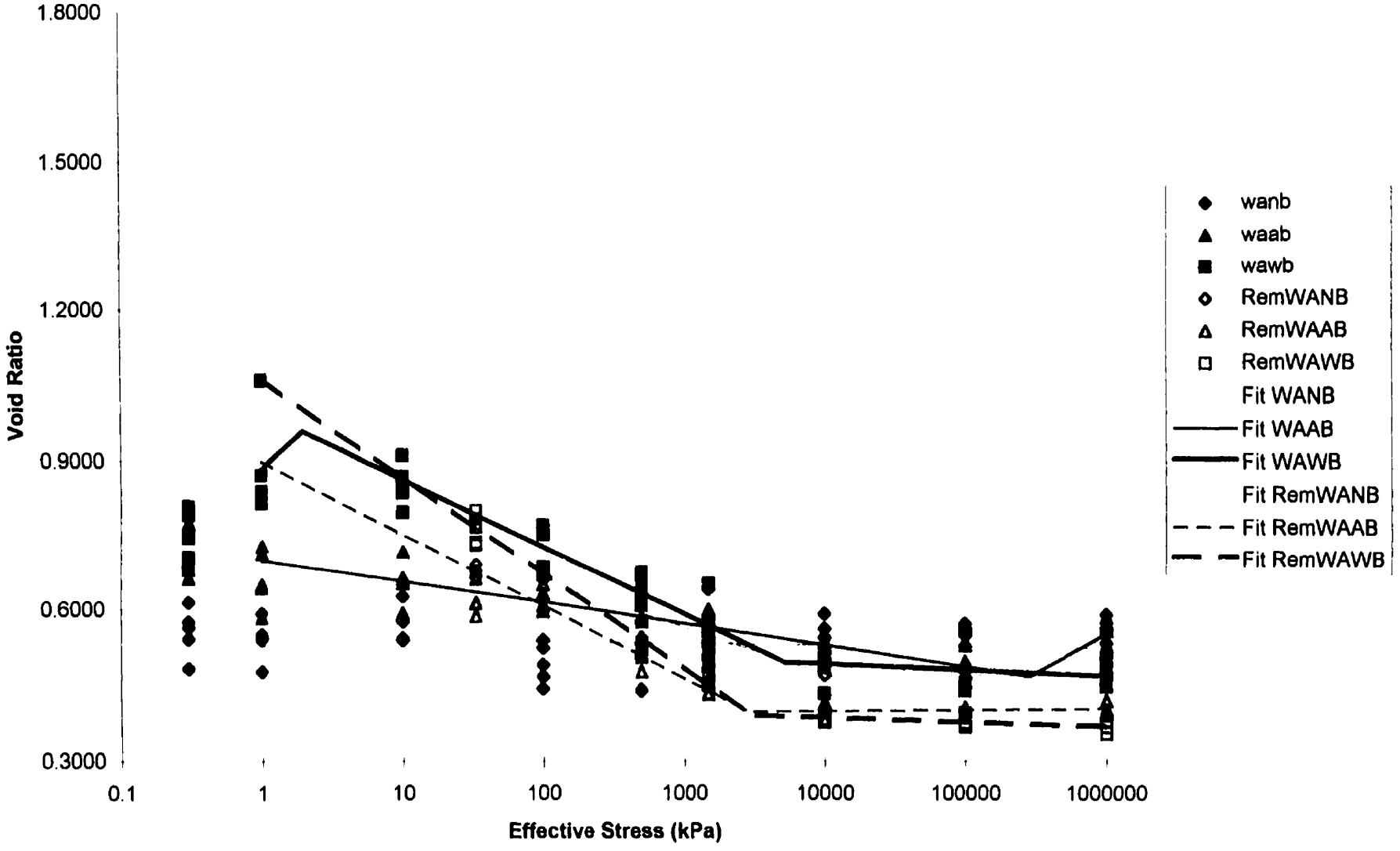

Shrinkage data for WA B horizons, $e(\sigma')$ co-ordinates.

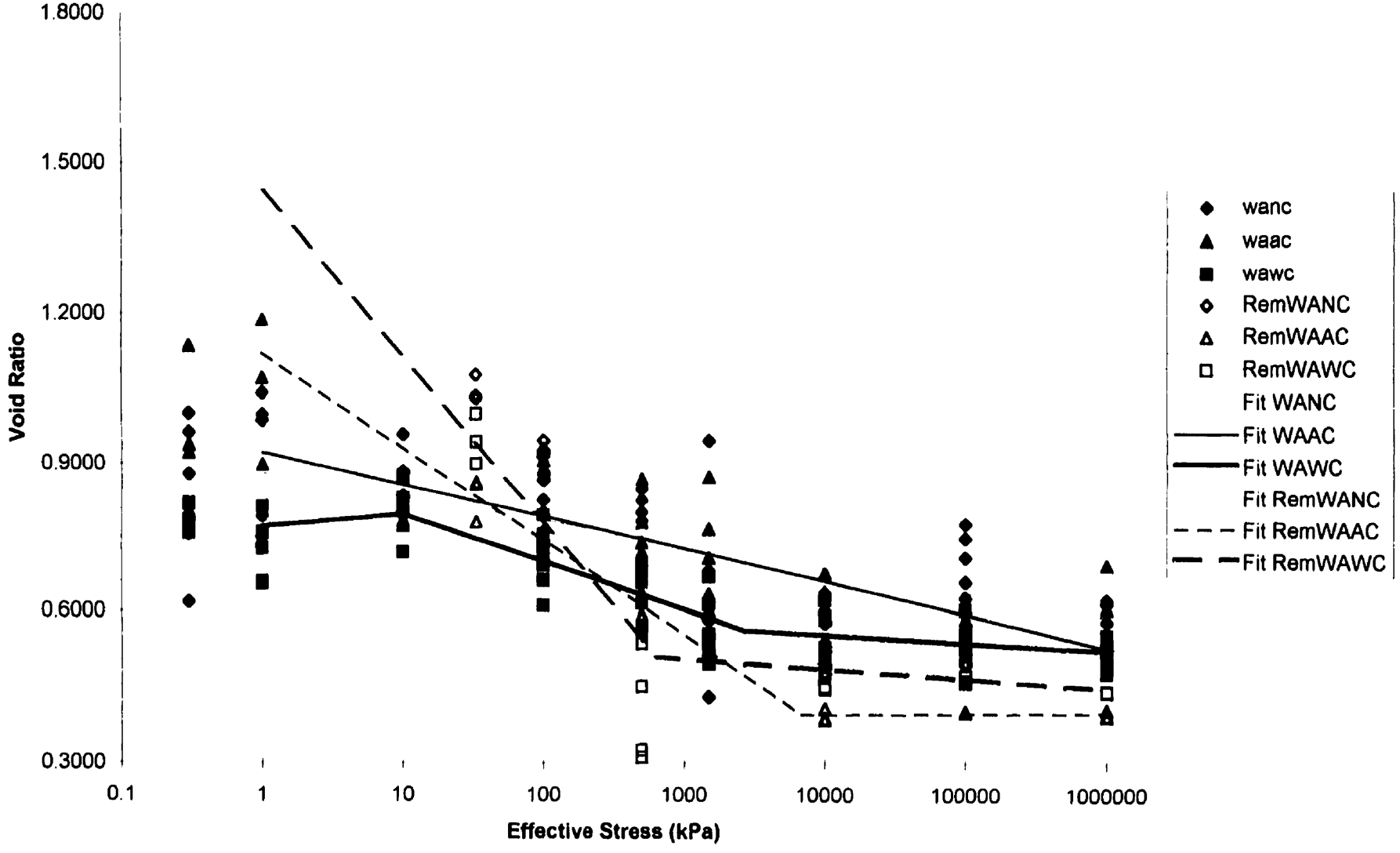

Shrinkage data for WA C horizons, $e(\sigma')$ co-ordinates.

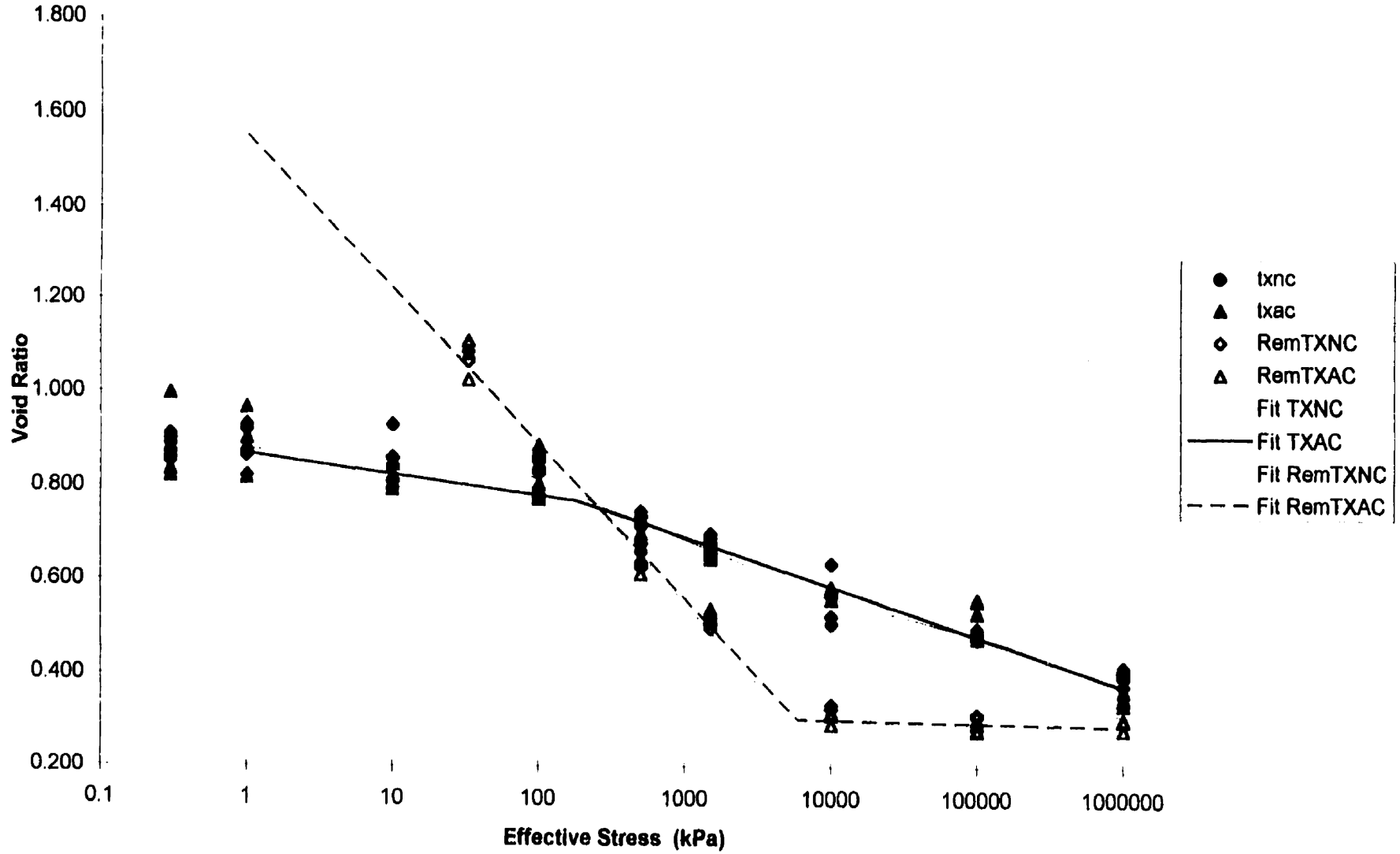

Shrinkage data for TX C horizons, e (σ) co-ordinates.

7.3 Appendix to Chapter Five

7.3.1 Areal results of image analysis for each subsample image

		Proportion of Total Area									Proportion of Matrix		
NAME	NO.	PORES	MATRIX	GRAINS	OXIDES	WEAK	STRONG	RESIN	BRIGHT	DARK	WEAK	STRONG	TOTAL
LBNA	1	0.010	0.704	0.030	0.234	0.000	0.000	0.000	0.022	0.000	0.000	0.000	0.000
LBNA	2	0.006	0.767	0.022	0.157	0.000	0.000	0.000	0.048	0.000	0.000	0.000	0.000
LBNA	3	0.009	0.581	0.017	0.212	0.000	0.000	0.005	0.018	0.159	0.000	0.000	0.000
LBNA	4	0.005	0.741	0.018	0.203	0.000	0.000	0.013	0.020	0.000	0.000	0.000	0.000
LBNA	5	0.009	0.323	0.020	0.152	0.000	0.000	0.017	0.043	0.436	0.000	0.000	0.000
LBNA	6	0.009	0.145	0.028	0.153	0.000	0.000	0.007	0.021	0.638	0.000	0.000	0.000
LBNB	1	0.015	0.699	0.014	0.238	0.003	0.000	0.017	0.013	0.000	0.003	0.000	0.003
LBNB	2	0.017	0.333	0.013	0.235	0.043	0.000	0.009	0.027	0.323	0.046	0.000	0.046
LBNB	3	0.017	0.328	0.020	0.132	0.028	0.000	0.000	0.005	0.470	0.030	0.000	0.030
LBNB	4	0.022	0.638	0.024	0.227	0.000	0.000	0.044	0.045	0.000	0.000	0.000	0.000
LBNB	5	0.021	0.620	0.027	0.279	0.027	0.000	0.002	0.024	0.000	0.029	0.000	0.029
LBNB	6	0.017	0.726	0.015	0.116	0.010	0.000	0.000	0.000	0.116	0.011	0.000	0.011
LBNC	1	0.025	0.680	0.011	0.262	0.000	0.000	0.010	0.012	0.000	0.000	0.000	0.000
LBNC	2	0.028	0.686	0.019	0.242	0.000	0.000	0.012	0.013	0.000	0.000	0.000	0.000
LBNC	3	0.016	0.483	0.009	0.467	0.003	0.000	0.014	0.009	0.000	0.003	0.000	0.003
LBNC	4	0.009	0.729	0.064	0.011	0.097	0.000	0.012	0.077	0.000	0.116	0.000	0.116
LBNC	5	0.010	0.583	0.038	0.260	0.014	0.000	0.015	0.080	0.000	0.017	0.000	0.017
LBNC	6	0.021	0.586	0.053	0.245	0.047	0.013	0.026	0.009	0.000	0.052	0.015	0.067
LBAA	1	0.009	0.424	0.027	0.473	0.017	0.000	0.013	0.037	0.000	0.019	0.000	0.019
LBAA	2	0.037	0.442	0.034	0.408	0.016	0.000	0.006	0.057	0.000	0.019	0.000	0.019
LBAA	3	0.028	0.277	0.031	0.195	0.012	0.000	0.015	0.000	0.441	0.013	0.000	0.013
LBAA	4	0.052	0.102	0.050	0.256	0.017	0.000	0.040	0.000	0.483	0.020	0.000	0.020
LBAA	5	0.014	0.197	0.021	0.392	0.007	0.000	0.018	0.024	0.327	0.008	0.000	0.008
LBAA	6	0.030	0.197	0.010	0.087	0.012	0.000	0.018	0.031	0.614	0.014	0.000	0.014
LBAB	1	0.033	0.451	0.053	0.298	0.045	0.000	0.026	0.000	0.094	0.050	0.000	0.050
LBAB	2	0.029	0.198	0.058	0.332	0.049	0.009	0.013	0.004	0.308	0.054	0.010	0.064
LBAB	3	0.041	0.393	0.070	0.315	0.142	0.000	0.020	0.020	0.000	0.167	0.000	0.167
LBAB	4	0.020	0.600	0.053	0.231	0.040	0.000	0.023	0.032	0.000	0.046	0.000	0.046
LBAB	5	0.013	0.417	0.032	0.412	0.039	0.000	0.017	0.071	0.000	0.045	0.000	0.045
LBAB	6	0.043	0.467	0.022	0.403	0.025	0.009	0.000	0.030	0.000	0.027	0.010	0.038

		Proportion of Total Area									Proportion of Matrix		
NAME	NO.	PORES	MATRIX	GRAINS	OXIDES	WEAK	STRONG	RESIN	BRIGHT	DARK	WEAK	STRONG	TOTAL
LBAC	1	0.002	0.655	0.006	0.315	0.000	0.000	0.000	0.022	0.000	0.000	0.000	0.000
LBAC	2	0.005	0.364	0.006	0.091	0.009	0.000	0.002	0.009	0.513	0.009	0.000	0.009
LBAC	3	0.003	0.784	0.018	0.181	0.000	0.000	0.003	0.011	0.000	0.000	0.000	0.000
LBAC	4	0.007	0.743	0.014	0.150	0.034	0.008	0.000	0.044	0.000	0.036	0.008	0.044
LBAC	5	0.005	0.646	0.028	0.263	0.034	0.008	0.000	0.014	0.000	0.036	0.009	0.045
LBAC	6	0.000	0.707	0.017	0.212	0.023	0.000	0.005	0.036	0.000	0.024	0.000	0.024
LBWA	1	0.009	0.675	0.069	0.224	0.014	0.000	0.000	0.008	0.000	0.016	0.000	0.016
LBWA	2	0.005	0.650	0.013	0.322	0.000	0.000	0.004	0.004	0.000	0.000	0.000	0.000
LBWA	3	0.024	0.734	0.031	0.148	0.000	0.000	0.018	0.045	0.000	0.000	0.000	0.000
LBWA	4	0.015	0.707	0.014	0.233	0.000	0.000	0.006	0.025	0.000	0.000	0.000	0.000
LBWA	5	0.033	0.690	0.027	0.198	0.000	0.000	0.019	0.034	0.000	0.000	0.000	0.000
LBWA	6	0.027	0.708	0.025	0.195	0.000	0.000	0.009	0.036	0.000	0.000	0.000	0.000
LBWB	1	0.010	0.678	0.026	0.105	0.149	0.021	0.010	0.002	0.000	0.157	0.022	0.178
LBWB	2	0.042	0.343	0.010	0.425	0.055	0.037	0.066	0.022	0.000	0.064	0.043	0.107
LBWB	3	0.024	0.445	0.026	0.369	0.047	0.012	0.054	0.022	0.000	0.054	0.014	0.068
LBWB	4	0.021	0.332	0.022	0.460	0.073	0.013	0.061	0.017	0.000	0.083	0.015	0.098
LBWB	5	0.010	0.413	0.016	0.351	0.085	0.017	0.066	0.041	0.000	0.098	0.020	0.118
LBWB	6	0.018	0.484	0.003	0.344	0.060	0.023	0.043	0.025	0.000	0.066	0.026	0.091
LBWC	1	0.037	0.434	0.079	0.218	0.119	0.038	0.008	0.067	0.000	0.148	0.047	0.195
LBWC	2	0.023	0.570	0.035	0.293	0.019	0.009	0.019	0.030	0.000	0.022	0.010	0.032
LBWC	3	0.030	0.755	0.016	0.060	0.015	0.005	0.011	0.107	0.000	0.018	0.007	0.025
LBWC	4	0.007	0.661	0.032	0.228	0.021	0.000	0.010	0.041	0.000	0.023	0.000	0.023
LBWC	5	0.006	0.770	0.021	0.172	0.000	0.000	0.010	0.022	0.000	0.000	0.000	0.000
LBWC	6	0.024	0.541	0.014	0.299	0.013	0.005	0.015	0.089	0.000	0.015	0.005	0.021
HLNA	1	0.054	0.594	0.035	0.202	0.010	0.000	0.030	0.074	0.000	0.012	0.000	0.012
HLNA	2	0.027	0.661	0.037	0.239	0.000	0.000	0.036	0.000	0.000	0.000	0.000	0.000
HLNA	3	0.049	0.688	0.027	0.203	0.000	0.000	0.000	0.033	0.000	0.000	0.000	0.000
HLNA	4	0.073	0.622	0.044	0.213	0.009	0.000	0.000	0.040	0.000	0.010	0.000	0.010
HLNA	5	0.014	0.631	0.019	0.262	0.000	0.000	0.000	0.059	0.016	0.000	0.000	0.000
HLNA	6	0.007	0.723	0.042	0.187	0.000	0.000	0.025	0.017	0.000	0.000	0.000	0.000
HLNB	1	0.037	0.213	0.020	0.296	0.049	0.014	0.000	0.088	0.283	0.057	0.016	0.073
HLNB	2	0.025	0.408	0.016	0.293	0.015	0.006	0.019	0.022	0.196	0.016	0.007	0.023
HLNB	3	0.010	0.509	0.044	0.314	0.027	0.007	0.020	0.068	0.000	0.032	0.008	0.040
HLNB	4	0.015	0.557	0.037	0.155	0.022	0.000	0.026	0.188	0.000	0.030	0.000	0.030
HLNB	5	0.008	0.664	0.033	0.198	0.018	0.000	0.013	0.065	0.000	0.021	0.000	0.021

		Proportion of Total Area									Proportion of Matrix		
NAME	NO.	PORES	MATRIX	GRAINS	OXIDES	WEAK	STRONG	RESIN	BRIGHT	DARK	WEAK	STRONG	TOTAL
HLNB	6	0.020	0.317	0.022	0.488	0.025	0.013	0.045	0.070	0.000	0.029	0.015	0.044
HLNC	1	0.028	0.367	0.046	0.394	0.040	0.008	0.020	0.098	0.000	0.050	0.010	0.060
HLNC	2	0.015	0.169	0.201	0.154	0.232	0.062	0.061	0.105	0.000	0.376	0.101	0.477
HLNC	3	0.031	0.333	0.074	0.420	0.064	0.000	0.026	0.052	0.000	0.079	0.000	0.079
HLNC	4	0.110	0.395	0.087	0.296	0.058	0.000	0.000	0.055	0.000	0.077	0.000	0.077
HLNC	5	0.039	0.422	0.103	0.286	0.061	0.023	0.016	0.051	0.000	0.076	0.029	0.106
HLNC	6	0.014	0.630	0.048	0.213	0.034	0.000	0.008	0.054	0.000	0.039	0.000	0.039
HLAA	1	0.013	0.681	0.043	0.202	0.000	0.000	0.019	0.042	0.000	0.000	0.000	0.000
HLAA	2	0.030	0.604	0.103	0.102	0.000	0.000	0.020	0.140	0.000	0.000	0.000	0.000
HLAA	3	0.002	0.659	0.032	0.228	0.028	0.000	0.015	0.035	0.000	0.031	0.000	0.031
HLAA	4	0.011	0.750	0.029	0.182	0.010	0.000	0.017	0.000	0.000	0.011	0.000	0.011
HLAA	5	0.012	0.638	0.048	0.229	0.012	0.000	0.022	0.039	0.000	0.014	0.000	0.014
HLAA	6	0.021	0.599	0.094	0.103	0.000	0.000	0.027	0.157	0.000	0.000	0.000	0.000
HLAB	1	0.018	0.512	0.068	0.168	0.118	0.000	0.041	0.076	0.000	0.148	0.000	0.148
HLAB	2	0.025	0.505	0.029	0.217	0.143	0.000	0.030	0.051	0.000	0.165	0.000	0.165
HLAB	3	0.021	0.591	0.044	0.269	0.000	0.000	0.029	0.047	0.000	0.000	0.000	0.000
HLAB	4	0.026	0.260	0.048	0.411	0.086	0.036	0.055	0.077	0.000	0.109	0.045	0.154
HLAB	5	0.019	0.268	0.027	0.502	0.068	0.041	0.034	0.039	0.000	0.078	0.047	0.125
HLAB	6	0.005	0.578	0.046	0.274	0.023	0.000	0.023	0.051	0.000	0.027	0.000	0.027
HLAC	1	0.033	0.266	0.075	0.327	0.067	0.023	0.061	0.147	0.000	0.098	0.034	0.132
HLAC	2	0.057	0.568	0.045	0.275	0.014	0.000	0.042	0.000	0.000	0.016	0.000	0.016
HLAC	3	0.045	0.271	0.061	0.427	0.089	0.014	0.048	0.045	0.000	0.111	0.017	0.128
HLAC	4	0.018	0.292	0.182	0.226	0.207	0.000	0.018	0.057	0.000	0.286	0.000	0.286
HLAC	5	0.030	0.461	0.084	0.336	0.041	0.000	0.000	0.048	0.000	0.049	0.000	0.049
HLAC	6	0.038	0.487	0.042	0.276	0.084	0.025	0.026	0.023	0.000	0.096	0.029	0.125
HLWA	1	0.013	0.622	0.062	0.240	0.020	0.000	0.043	0.000	0.000	0.022	0.000	0.022
HLWA	2	0.013	0.608	0.059	0.250	0.000	0.000	0.036	0.034	0.000	0.000	0.000	0.000
HLWA	3	0.030	0.256	0.063	0.153	0.028	0.000	0.052	0.000	0.419	0.032	0.000	0.032
HLWA	4	0.021	0.694	0.048	0.186	0.015	0.000	0.007	0.029	0.000	0.017	0.000	0.017
HLWA	5	0.006	0.617	0.066	0.251	0.000	0.000	0.020	0.040	0.000	0.000	0.000	0.000
HLWA	6	0.025	0.252	0.057	0.254	0.026	0.030	0.000	0.028	0.327	0.030	0.034	0.064
HLWB	1	0.043	0.163	0.048	0.223	0.013	0.006	0.017	0.089	0.398	0.016	0.007	0.023
HLWB	2	0.020	0.351	0.069	0.385	0.053	0.017	0.056	0.049	0.000	0.065	0.021	0.087
HLWB	3	0.011	0.559	0.052	0.253	0.065	0.000	0.018	0.044	0.000	0.074	0.000	0.074
HLWB	4	0.007	0.517	0.074	0.262	0.021	0.000	0.000	0.119	0.000	0.027	0.000	0.027

		Proportion of Total Area									Proportion of Matrix		
NAME	NO.	PORES	MATRIX	GRAINS	OXIDES	WEAK	STRONG	RESIN	BRIGHT	DARK	WEAK	STRONG	TOTAL
HLWB	5	0.016	0.548	0.056	0.158	0.082	0.000	0.088	0.052	0.000	0.104	0.000	0.104
HLWB	6	0.011	0.491	0.065	0.260	0.046	0.000	0.022	0.104	0.000	0.058	0.000	0.058
HLWC	1	0.005	0.732	0.029	0.218	0.000	0.000	0.007	0.010	0.000	0.000	0.000	0.000
HLWC	2	0.013	0.762	0.053	0.084	0.000	0.000	0.008	0.080	0.000	0.000	0.000	0.000
HLWC	3	0.011	0.610	0.033	0.278	0.000	0.000	0.027	0.040	0.000	0.000	0.000	0.000
HLWC	4	0.021	0.497	0.080	0.134	0.150	0.029	0.000	0.088	0.000	0.185	0.036	0.221
HLWC	5	0.069	0.545	0.037	0.270	0.034	0.000	0.011	0.034	0.000	0.040	0.000	0.040
HLWC	6	0.026	0.643	0.055	0.228	0.000	0.000	0.021	0.028	0.000	0.000	0.000	0.000
OTNA	1	0.017	0.308	0.011	0.110	0.000	0.000	0.013	0.079	0.461	0.000	0.000	0.000
OTNA	2	0.056	0.681	0.014	0.185	0.000	0.000	0.000	0.065	0.000	0.000	0.000	0.000
OTNA	3	0.017	0.692	0.027	0.179	0.000	0.000	0.013	0.072	0.000	0.000	0.000	0.000
OTNA	4	0.066	0.663	0.012	0.198	0.000	0.000	0.008	0.051	0.000	0.000	0.000	0.000
OTNA	5	0.038	0.563	0.017	0.339	0.000	0.000	0.007	0.036	0.000	0.000	0.000	0.000
OTNA	6	0.152	0.553	0.014	0.153	0.000	0.000	0.044	0.085	0.000	0.000	0.000	0.000
OTNB	1	0.017	0.117	0.095	0.195	0.000	0.000	0.033	0.017	0.526	0.000	0.000	0.000
OTNB	2	0.057	0.538	0.086	0.223	0.000	0.000	0.000	0.096	0.000	0.000	0.000	0.000
OTNB	3	0.041	0.527	0.046	0.173	0.088	0.000	0.066	0.059	0.000	0.112	0.000	0.112
OTNB	4	0.046	0.596	0.046	0.244	0.000	0.000	0.028	0.041	0.000	0.000	0.000	0.000
OTNB	5	0.034	0.635	0.045	0.236	0.000	0.000	0.006	0.044	0.000	0.000	0.000	0.000
OTNB	6	0.000	0.487	0.106	0.217	0.103	0.000	0.026	0.061	0.000	0.127	0.000	0.127
OTNC	1	0.029	0.422	0.009	0.252	0.026	0.000	0.025	0.052	0.185	0.029	0.000	0.029
OTNC	2	0.024	0.370	0.011	0.205	0.017	0.000	0.009	0.033	0.332	0.018	0.000	0.018
OTNC	3	0.015	0.356	0.013	0.359	0.052	0.000	0.021	0.025	0.158	0.056	0.000	0.056
OTNC	4	0.000	0.351	0.016	0.370	0.029	0.000	0.019	0.000	0.215	0.030	0.000	0.030
OTNC	5	0.014	0.380	0.006	0.324	0.022	0.000	0.016	0.079	0.160	0.025	0.000	0.025
OTNC	6	0.017	0.347	0.011	0.332	0.012	0.000	0.006	0.049	0.226	0.014	0.000	0.014
OTAA	1	0.018	0.620	0.060	0.258	0.000	0.000	0.005	0.039	0.000	0.000	0.000	0.000
OTAA	2	0.027	0.526	0.065	0.259	0.000	0.000	0.030	0.093	0.000	0.000	0.000	0.000
OTAA	3	0.021	0.628	0.032	0.217	0.000	0.000	0.042	0.060	0.000	0.000	0.000	0.000
OTAA	4	0.022	0.585	0.037	0.338	0.000	0.000	0.018	0.000	0.000	0.000	0.000	0.000
OTAA	5	0.044	0.071	0.051	0.206	0.020	0.000	0.061	0.127	0.420	0.028	0.000	0.028
OTAA	6	0.031	0.113	0.036	0.198	0.000	0.000	0.064	0.040	0.518	0.000	0.000	0.000
OTAB	1	0.009	0.779	0.019	0.155	0.007	0.000	0.011	0.020	0.000	0.007	0.000	0.007
OTAB	2	0.023	0.430	0.036	0.357	0.067	0.000	0.023	0.063	0.000	0.079	0.000	0.079
OTAB	3	0.009	0.806	0.013	0.158	0.004	0.000	0.005	0.005	0.000	0.004	0.000	0.004

		Proportion of Total Area									Proportion of Matrix		
NAME	NO.	PORES	MATRIX	GRAINS	OXIDES	WEAK	STRONG	RESIN	BRIGHT	DARK	WEAK	STRONG	TOTAL
OTAB	4	0.017	0.650	0.023	0.240	0.017	0.000	0.006	0.048	0.000	0.019	0.000	0.019
OTAB	5	0.019	0.629	0.030	0.203	0.021	0.000	0.029	0.069	0.000	0.025	0.000	0.025
OTAB	6	0.012	0.721	0.007	0.238	0.000	0.000	0.003	0.018	0.000	0.000	0.000	0.000
OTAC	1	0.015	0.569	0.039	0.332	0.000	0.000	0.018	0.028	0.000	0.000	0.000	0.000
OTAC	2	0.005	0.542	0.023	0.382	0.009	0.000	0.034	0.005	0.000	0.009	0.000	0.009
OTAC	3	0.007	0.723	0.015	0.226	0.007	0.000	0.008	0.014	0.000	0.007	0.000	0.007
OTAC	4	0.031	0.446	0.018	0.312	0.073	0.018	0.015	0.087	0.000	0.086	0.021	0.107
OTAC	5	0.027	0.763	0.023	0.136	0.000	0.000	0.000	0.051	0.000	0.000	0.000	0.000
OTAC	6	0.012	0.730	0.029	0.148	0.015	0.000	0.006	0.060	0.000	0.017	0.000	0.017
TXNA	1	0.026	0.708	0.043	0.185	0.000	0.000	0.013	0.025	0.000	0.000	0.000	0.000
TXNA	2	0.038	0.637	0.026	0.256	0.000	0.000	0.033	0.009	0.000	0.000	0.000	0.000
TXNA	3	0.042	0.527	0.039	0.298	0.000	0.000	0.047	0.047	0.000	0.000	0.000	0.000
TXNA	4	0.066	0.622	0.041	0.201	0.000	0.000	0.048	0.022	0.000	0.000	0.000	0.000
TXNA	5	0.068	0.580	0.038	0.235	0.000	0.000	0.079	0.000	0.000	0.000	0.000	0.000
TXNA	6	0.076	0.646	0.036	0.180	0.000	0.000	0.027	0.036	0.000	0.000	0.000	0.000
TXNB	1	0.026	0.688	0.035	0.217	0.000	0.000	0.013	0.021	0.000	0.000	0.000	0.000
TXNB	2	0.026	0.733	0.028	0.203	0.000	0.000	0.006	0.005	0.000	0.000	0.000	0.000
TXNB	3	0.054	0.617	0.045	0.254	0.000	0.000	0.008	0.022	0.000	0.000	0.000	0.000
TXNB	4	0.018	0.729	0.020	0.202	0.000	0.000	0.006	0.025	0.000	0.000	0.000	0.000
TXNB	5	0.041	0.626	0.046	0.245	0.000	0.000	0.025	0.017	0.000	0.000	0.000	0.000
TXNB	6	0.013	0.739	0.050	0.156	0.006	0.000	0.008	0.027	0.000	0.007	0.000	0.007
TXNC	1	0.009	0.417	0.075	0.423	0.000	0.000	0.007	0.068	0.000	0.000	0.000	0.000
TXNC	2	0.016	0.593	0.044	0.301	0.000	0.000	0.011	0.035	0.000	0.000	0.000	0.000
TXNC	3	0.015	0.675	0.035	0.238	0.000	0.000	0.009	0.028	0.000	0.000	0.000	0.000
TXNC	4	0.009	0.751	0.021	0.179	0.000	0.000	0.005	0.036	0.000	0.000	0.000	0.000
TXNC	5	0.007	0.773	0.011	0.198	0.000	0.000	0.003	0.008	0.000	0.000	0.000	0.000
TXNC	6	0.016	0.718	0.046	0.148	0.000	0.000	0.016	0.056	0.000	0.000	0.000	0.000
TXAA	1	0.016	0.625	0.067	0.224	0.000	0.000	0.014	0.053	0.000	0.000	0.000	0.000
TXAA	2	0.010	0.605	0.025	0.288	0.000	0.000	0.030	0.042	0.000	0.000	0.000	0.000
TXAA	3	0.022	0.647	0.015	0.254	0.000	0.000	0.023	0.038	0.000	0.000	0.000	0.000
TXAA	4	0.018	0.625	0.023	0.310	0.000	0.000	0.014	0.010	0.000	0.000	0.000	0.000
TXAA	5	0.037	0.137	0.054	0.049	0.000	0.000	0.054	0.016	0.653	0.000	0.000	0.000
TXAA	6	0.031	0.659	0.028	0.197	0.011	0.000	0.020	0.054	0.000	0.013	0.000	0.013
TXAB	1	0.061	0.600	0.028	0.214	0.030	0.000	0.034	0.033	0.000	0.035	0.000	0.035
TXAB	2	0.032	0.630	0.022	0.237	0.016	0.000	0.052	0.012	0.000	0.018	0.000	0.018

		Proportion of Total Area									Proportion of Matrix		
NAME	NO.	PORES	MATRIX	GRAINS	OXIDES	WEAK	STRONG	RESIN	BRIGHT	DARK	WEAK	STRONG	TOTAL
TXAB	3	0.038	0.561	0.026	0.305	0.012	0.000	0.038	0.020	0.000	0.014	0.000	0.014
TXAB	4	0.043	0.606	0.011	0.261	0.000	0.000	0.030	0.049	0.000	0.000	0.000	0.000
TXAB	5	0.017	0.543	0.015	0.337	0.000	0.000	0.070	0.018	0.000	0.000	0.000	0.000
TXAB	6	0.023	0.561	0.023	0.327	0.027	0.000	0.015	0.023	0.000	0.030	0.000	0.030
TXAC	1	0.028	0.710	0.022	0.220	0.000	0.000	0.012	0.008	0.000	0.000	0.000	0.000
TXAC	2	0.051	0.563	0.021	0.266	0.000	0.000	0.053	0.046	0.000	0.000	0.000	0.000
TXAC	3	0.043	0.529	0.029	0.391	0.000	0.000	0.009	0.000	0.000	0.000	0.000	0.000
TXAC	4	0.050	0.542	0.030	0.368	0.000	0.000	0.000	0.009	0.000	0.000	0.000	0.000
TXAC	5	0.024	0.701	0.019	0.250	0.000	0.000	0.007	0.000	0.000	0.000	0.000	0.000
TXAC	6	0.067	0.535	0.026	0.321	0.000	0.000	0.013	0.038	0.000	0.000	0.000	0.000
ABAA	1	0.101	0.540	0.068	0.195	0.000	0.000	0.000	0.096	0.000	0.000	0.000	0.000
ABAA	2	0.022	0.623	0.054	0.191	0.000	0.000	0.026	0.085	0.000	0.000	0.000	0.000
ABAA	3	0.045	0.585	0.059	0.240	0.000	0.000	0.037	0.034	0.000	0.000	0.000	0.000
ABAA	4	0.039	0.550	0.108	0.187	0.000	0.000	0.030	0.085	0.000	0.000	0.000	0.000
ABAA	5	0.023	0.600	0.069	0.244	0.000	0.000	0.042	0.022	0.000	0.000	0.000	0.000
ABAA	6	0.058	0.594	0.061	0.196	0.000	0.000	0.033	0.059	0.000	0.000	0.000	0.000
ABAB	1	0.011	0.636	0.037	0.251	0.000	0.000	0.031	0.034	0.000	0.000	0.000	0.000
ABAB	2	0.023	0.570	0.109	0.265	0.000	0.000	0.000	0.033	0.000	0.000	0.000	0.000
ABAB	3	0.039	0.529	0.060	0.168	0.096	0.000	0.032	0.076	0.000	0.121	0.000	0.121
ABAB	4	0.028	0.517	0.116	0.264	0.000	0.000	0.012	0.062	0.000	0.000	0.000	0.000
ABAB	5	0.027	0.543	0.114	0.145	0.092	0.000	0.000	0.078	0.000	0.118	0.000	0.118
ABAB	6	0.088	0.582	0.069	0.149	0.081	0.000	0.000	0.031	0.000	0.100	0.000	0.100
ABAC	1	0.018	0.623	0.101	0.115	0.000	0.000	0.017	0.126	0.000	0.000	0.000	0.000
ABAC	2	0.022	0.569	0.149	0.151	0.000	0.000	0.025	0.084	0.000	0.000	0.000	0.000
ABAC	3	0.031	0.599	0.082	0.077	0.000	0.000	0.026	0.186	0.000	0.000	0.000	0.000
ABAC	4	0.021	0.728	0.048	0.167	0.000	0.000	0.011	0.025	0.000	0.000	0.000	0.000
ABAC	5	0.041	0.509	0.106	0.079	0.000	0.000	0.046	0.219	0.000	0.000	0.000	0.000
ABAC	6	0.026	0.569	0.045	0.262	0.000	0.000	0.070	0.028	0.000	0.000	0.000	0.000
ABNA	1	0.055	0.720	0.026	0.097	0.000	0.000	0.068	0.034	0.000	0.000	0.000	0.000
ABNA	2	0.115	0.649	0.024	0.144	0.000	0.000	0.026	0.041	0.000	0.000	0.000	0.000
ABNA	3	0.025	0.766	0.036	0.127	0.000	0.000	0.022	0.024	0.000	0.000	0.000	0.000
ABNA	4	0.014	0.738	0.047	0.141	0.000	0.000	0.024	0.036	0.000	0.000	0.000	0.000
ABNA	5	0.068	0.575	0.051	0.292	0.000	0.000	0.007	0.007	0.000	0.000	0.000	0.000
ABNA	6	0.082	0.659	0.050	0.162	0.000	0.000	0.020	0.028	0.000	0.000	0.000	0.000
ABNB	1	0.100	0.556	0.027	0.251	0.010	0.000	0.023	0.032	0.000	0.012	0.000	0.012

		Proportion of Total Area									Proportion of Matrix		
NAME	NO.	PORES	MATRIX	GRAINS	OXIDES	WEAK	STRONG	RESIN	BRIGHT	DARK	WEAK	STRONG	TOTAL
ABNB	2	0.073	0.311	0.065	0.357	0.043	0.000	0.035	0.116	0.000	0.061	0.000	0.061
ABNB	3	0.048	0.524	0.050	0.248	0.026	0.000	0.056	0.048	0.000	0.032	0.000	0.032
ABNB	4	0.084	0.412	0.049	0.255	0.108	0.024	0.068	0.000	0.000	0.135	0.030	0.165
ABNB	5	0.041	0.432	0.131	0.288	0.039	0.000	0.042	0.026	0.000	0.052	0.000	0.052
ABNB	6	0.035	0.613	0.053	0.184	0.013	0.000	0.041	0.062	0.000	0.016	0.000	0.016
ABNC	1	0.011	0.436	0.005	0.104	0.000	0.000	0.000	0.027	0.418	0.000	0.000	0.000
ABNC	2	0.024	0.440	0.008	0.106	0.010	0.000	0.013	0.014	0.385	0.011	0.000	0.011
ABNC	3	0.030	0.562	0.035	0.244	0.019	0.000	0.031	0.079	0.000	0.023	0.000	0.023
ABNC	4	0.018	0.593	0.020	0.303	0.019	0.000	0.024	0.024	0.000	0.021	0.000	0.021
ABNC	5	0.011	0.627	0.027	0.293	0.000	0.000	0.010	0.032	0.000	0.000	0.000	0.000
ABNC	6	0.026	0.684	0.010	0.241	0.006	0.000	0.019	0.013	0.000	0.007	0.000	0.007

IMAGE EVALUATION
TEST TARGET (QA-3)

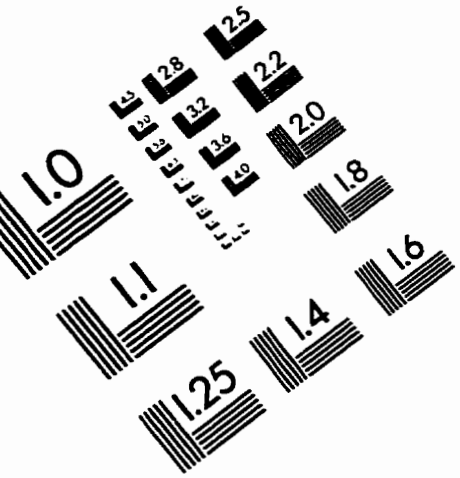

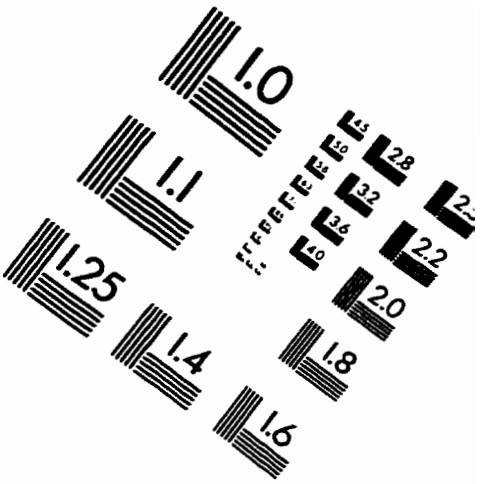

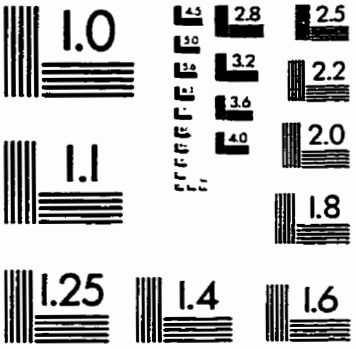

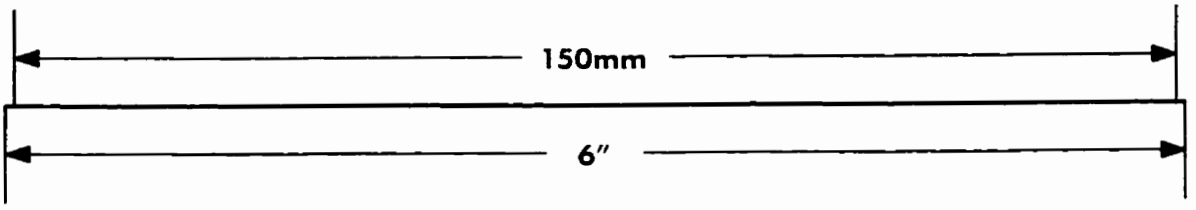

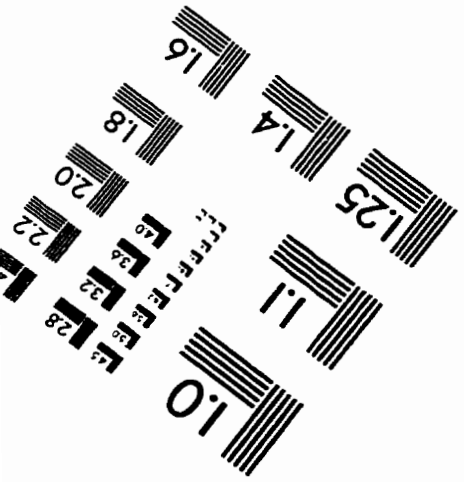

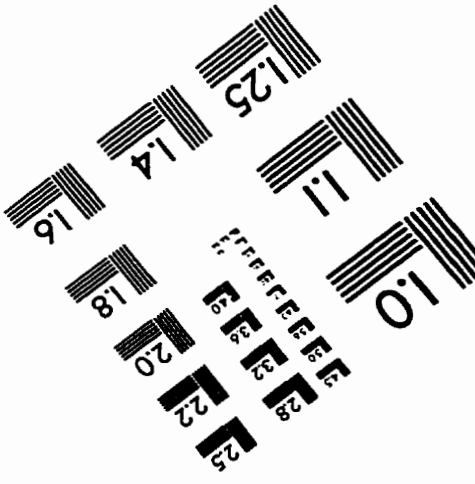

APPLIED IMAGE, Inc
1653 East Main Street
Rochester, NY 14609 USA
Phone: 716/482-0300
Fax: 716/288-5989